Control of sensory axon conduction by primary afferent depolarization

by

Krista Metz

A thesis submitted in partial fulfillment of the requirements for the degree of

Doctor of Philosophy

Neuroscience

University of Alberta

Abstract

Ia afferents conveying proprioceptive information to the spinal cord, and the regulation of action potential conduction along these afferents, are vital for motor function. After injury to the central nervous system (CNS), hyperexcitability in proprioceptive and other afferent pathways to the motoneuron is partly involved in the development of spasticity and motor dysfunction; however, the mechanisms are poorly understood. In this thesis, we explore how spinal networks involving gamma-aminobutyric acid (GABA) control conduction along Ia afferents before and after spinal cord injury (SCI). Sensory and cortical pathways activate GABAergic interneurons with axo-axonic contacts on Ia afferents that activate $GABA_A$ receptors near proximal branch points. Activation of $GABA_A$ receptors on Ia afferents results in an efflux of chloride ions and a depolarization of the afferent (primary afferent depolarization, PAD). PAD brings the afferent membrane closer to threshold, facilitating action potential conduction across branch points where failure is likely to occur, ultimately increasing the size of excitatory postsynaptic potentials (EPSPs) in the motoneuron. In chapter 2 we sought evidence of facilitation in the conduction of Ia afferents involved in the human H-reflex by inputs known to activate PAD in animals. Cutaneous afferent and corticospinal tract (CST) inputs produced H-reflex facilitation without direct facilitatory effects on the test motoneurons. The profile of H-reflex facilitation was akin to animal experiments showing $GABA_A$ receptor activation on Ia afferents facilitates monosynaptic reflexes (MSR)/EPSPs with a time course similar to PAD recorded from the Ia afferent (100-200 ms). We also observed longer-lasting (10's of seconds) H-reflex facilitation when trains of cutaneous input were used to condition the H-reflex. The long-lasting H-reflex facilitation was similar to animal experiments showing that trains of cutaneous stimulation produced a long-lasting tonic PAD and facilitation of MSRs/EPSPs, likely via GABA spillover activating

extrasynaptic $GABA_A$ receptors. After SCI in humans, the same trains of cutaneous stimulation to putatively evoke tonic PAD did not produce long-lasting H-reflex facilitation like it had in controls (chapter 4).

In addition to the facilitatory effects of PAD on Ia afferent conduction and H-reflexes, PAD can also produce inhibition of H-reflexes. PAD evoked in the proximal Ia afferent is often strong enough to reach sodium spiking threshold, producing action potentials that travel orthodromically to the Ia afferent terminal as evidenced by evoking a monosynaptic EPSPs in the motoneuron. Following these PAD-evoked spikes, Ia activation of the motoneuron is inhibited for a long period of time (up to 2500 ms) due to post-activation depression. In light of PAD-evoked spikes causing post-activation depression, in chapter 3 we re-examined experiments showing that extensor H-reflexes are inhibited by a prior activation of flexor afferents that were previously, and likely incorrectly, attributed to PAD-mediated presynaptic inhibition at the Ia afferent terminal. Similar to previous experiments, we found that antagonist flexor afferent conditioning, to putatively evoke PAD, inhibited the soleus H-reflex. The flexor afferent conditioning stimulation also evoked an early excitatory response in the soleus EMG, a response that has been noted in previous studies but largely ignored. A larger early reflex response in the soleus EMG from the flexor afferent conditioning was associated with larger H-reflex inhibition. Moreover, the profile of H-reflex inhibition from flexor afferent conditioning was also similar to the profile of H-reflex suppression from repetitive activations of the same H-reflex, a test of post-activation depression called rate dependent depression (RDD). Therefore, we propose that H-reflex inhibition from flexor afferent conditioning is due to post-activation depression and not PAD-mediated presynaptic inhibition of the Ia afferent terminal as speculated in many previous studies. In participants with SCI, the amount of H-reflex suppression from flexor afferent

conditioning and from RDD were similarly reduced compared to controls, likely mediated by a reduced post-activation depression whose mechanism requires further study (chapter 4).

Preface

This thesis is an original work by Krista Metz. The research project, of which this is a part, received research ethics approval from the University of Alberta Human Research Ethics Board (Pro 00078057 and 00031413) and performed with informed consent of the participants. Animal experimental procedures were approved by University of Alberta Animal Care and Use Committee, Health Sciences division (Protocol AUP 00000224).

Chapter 2 of this thesis has been submitted for preprint as K. Metz, I. Concha-Matos, Y. Li, B. Afsharipour, C.K. Thompson, F. Negro, DJ. Bennett, MA. Gorassini., 2021 "Facilitation of sensory axon conduction to motoneurons during cortical or sensory evoked primary afferent depolarization (PAD) in humans," *bioRxiv,* doi: 10.1101/2021.04.20.440509. Chapter 3 has been submitted for preprint as Metz K., Concha-Matos I., Hari K., Bseis O., Afsharipour B., Lin S, Singla R., Fenrich K., Bennett D.J. & Gorassini MA. 2022. "Post-activation depression produces extensor H-reflex suppresion following flexor afferent conditioning," *bioRxiv*, doi: 10.1101/2022.03.28.486118. Figure numbers have been changed in this thesis to conform with formatting requirements. Chapters 2-4 of this thesis will be submitted for peer-reviewed publication at a later date.

Along with my supervisor Gorassini M.A., I was involved in the human experimental design, data collection, analysis, and interpretation as well as the manuscript composition for Chapters 2-4. Concha-Matos I., Bseis O., Sun Y. and Yang J.F. were also involved in human data collection and analysis. Afsharipour B., Thompson C.K. and Negro F. were involved in human data analysis. Bennett D. was my co-supervisor, along with Hari K. and Lin S. they designed, collected and analyzed the animal data. Bennet D. was also involved in the manuscript composition for chapters 2-4.

Dedication

In loving memory of my brother, Paul.

Acknowledgments

I wish to express my sincerest appreciation to my supervisor, Dr Monica Gorassini. Her leadership and support throughout my thesis has truly meant the world to me. I am forever grateful that I was a part of her lab and under her guidance.

I would like to thank my co-supervisor, Dr Dave Bennett. His insight and feedback has been instrumental in directing me throughout my project. His passion for his work is truly remarkable.

I wish to show my gratitude to our lab technician, Jennifer Duchcherer. She has been an amazing support throughout my time at the U of A. I cannot thank her enough for the time and energy she has put towards me and my project.

To my committee members, Dr Jaynie Yang and Dr Kelvin Jones, thank you for taking time out of your incredibly busy schedules to support and be there for me.

To my summer students, Omayma Bseis and Isabel Concha-Matos, thank you for all your help and friendship.

Thank you to First Steps Wellness Centre for allowing us to come setup for a week and complete experiments. My passion for neuroscience started there as an undergraduate and I loved returning as a graduate student.

Thank you to every participant who took part in my study and made this research possible.

To my Mom and Dad, thank you from the bottom of my heart for supporting me and encouraging me to following my dreams. Thank you to my brothers, Nic and Paul, you have both supported and inspired me in different but very important ways.

Finally, thank you to my husband-to-be Colton. Thank you for putting up with the distance and driving so that I could pursue my dream. Thank you for being my rock, my best friend and encouraging me every step of the way.

Table of Contents

List of Tables

List of Figures

Chapter 1

Chapter 2

Chapter 3

Chapter 4

List of Symbols and Abbreviations

ABHal – abductor hallucis

AD – autonomic dysreflexia

AMT – active motor threshold

ASIA – American Spinal Injury Association impairment scale

BDNF – brain-derived neurotrophic factor

Ca - calcium

cDPN – medial (cutaneous) branch of the deep peroneal nerve

CFN – common fibular nerve

Cl – chloride

CNS – central nervous system

CPN – common peroneal nerve

CSAP – compound sensory nerve action potential

CST – corticospinal tract

DR – dorsal root

DRR – dorsal root reflex

EMG – electromyography

EPSP – excitatory post-synaptic potential

FRA – flexor reflex afferent

GABA – gamma aminobutyric acid

GAD – glutamate decarboxylase

GAT – GABA transporter

H-reflex – Hoffmann's reflex

IPSP – inhibitory post-synaptic potential

ISI – interstimulus interval

K – potassium

MEP – motor evoked potential

MG – medial gastrocnemius

MSR – monosynaptic reflex

MT – motor threshold

M-wave – motor wave

NA – noradrenaline

Na - sodium

PAD – primary afferent depolarization

PBST – posterior biceps semitendinosus

PICs – persistent inward current

PSF – peristimulus frequencygram

PSTH – peristimulus time histogram

PMR – posterior-root muscle reflex

Quad – quadriceps (vastus lateralis)

RDD – rate dependent depression

SCI – spinal cord injury

SD – standard deviation

SFN – superficial fibular nerve

SOL – soleus

T – threshold

TA – Tibialis anterior

TMS – transcranial magnetic stimulation

TN – Tibial Nerve

α – alpha

γ – gamma

Chapter 1: Introduction

Spinal Cord Injury

Spinal cord injury (SCI) is a life changing, debilitating injury that affects many aspects of a person's life. In 2010 43,964 Canadians were living with a traumatic SCI (51%) and 37,313 were living with a non-traumatic SCI (49%) (Noonan *et al.*, 2012). While people living with traumatic and nontraumatic SCI are almost equally prevalent in Canada, this thesis will mainly discuss traumatic SCI because all of the recruited participants and animal models used to understand mechanisms had a traumatic SCI. Traumatic SCI is the result of an external impact that damages the spinal cord, such as a motor vehicle accident, fall or violence (Noonan *et al.*, 2012). There are between 2 and 3 million people living with traumatic SCI around the world with 250,000 to 500,000 new injuries each year (Quadri *et al.*, 2018). Accurate data concerning the incidence (number of new cases of SCI over a period of time) and prevalence (number of people living with SCI at a point in time) is lacking and largely estimated, especially in Canada (Noonan *et al.*, 2012); however, general trends are known and can be estimated from data from other countries such as the United States (US). Canada and the US have a higher incidence than other countries with motor vehicles accidents being the most common cause (Devivo, 2012; Silva *et al.*, 2014; Chen *et al.*, 2016; Quadri *et al.*, 2018), resulting in 38.1% of new SCIs in the US from 2010 to 2014 (Chen *et al.*, 2016). In North America the incidence of traumatic SCI is estimated at 39 cases per million individuals, which is higher compared to other developed regions such as western Europe where the incidence is 15 cases per million (Ahuja *et al.*, 2017). In Canada, the incidence rate of traumatic SCI in 2010 was estimated at 53 cases per million (1,785 injuries) with a discharge incidence of 41 cases per million (1,389 injuries) (Devivo, 2012; Noonan *et al.*, 2012). The discharge incidence rate of nontraumatic SCI in Canada in 2010

was estimated to be 68 cases per million (2,286 injuries) (Noonan *et al.*, 2012). Possible reasons for higher incidence rates in the US and Canada compared to other regions may be because of higher motor vehicle related injuries due to more miles travelled, less use of seatbelts, unsafe driving habits and worse road conditions compared to other regions (Devivo, 2012). Alternatively, higher incidence in the US could result from increased survival rates after accidents compared to other regions (Devivo, 2012). The higher incidence rates in the US could also be a result of poorer reporting in other countries, making the incidence in other regions appear lower than it actually is (Devivo, 2012). However, no study has addressed the reason for SCI incidence variance across countries (Devivo, 2012).

Traumatic SCI is 2-5 times more common in males than females and historically incidence peaks in young adulthood (age 15-29), largely due to lifestyle related injuries (Quadri *et al.*, 2018); however, there has recently been a shift in the incidence of SCI to older individuals (>50 years of age) (Devivo, 2012; Ahuja *et al.*, 2017). In the US, the average age at the time of injury has increased from 28.7 years in the 1970s to 42.2 years between 2010 and 2014 (DeVivo & Chen, 2011; Chen *et al.*, 2016). The rate of increasing age at the time of injury is more dramatic than the increasing age of the general population, likely due to an increasing incidence rate in the elderly population, paralleled by a decreasing incidence rate in the younger population (i.e. 144 cases per million in 1993 to 87 cases per million in 2012 for ages 16-24 years), possibly due to prevention measures that reduce the risk of SCI in younger adults (Chen *et al.*, 2016). As the population ages the risk of fall-related injury increases, making falls the leading cause of SCI in adults over 60 years (Devivo, 2012), accounting for almost 60% of new traumatic SCIs in adults over 60 years of age (Chen *et al.*, 2016). In 2010 in Canada, 62% of individuals living with nontraumatic SCI were over the age of 60 years (Noonan *et al.*, 2012).

The sequelae of SCI

The progression of injury after traumatic SCI occurs in multiple stages. The first acute stage consists of the injury itself, an immediate mechanical injury caused by a permanent or temporary compression of the spinal cord that usually causes a contusion (Quadri *et al.*, 2018). This initial insult causes immediate damage to the neurons and oligodendrocytes in the central nervous system (CNS), disrupts vasculature and compromises the blood-spinal cord barrier (Ahuja *et al.*, 2017). Compromise of the cellular membrane (Simon *et al.*, 2009) and disruption of Ca^{2+} homeostasis from the initial injury result in a progression of injury and cell death (Schanne *et al.*, 1979; Choo *et al.*, 2007). A subacute phase lasting hours to weeks after the initial injury is characterized by destructive and self-propagating neuronal and glial cell death that leads to further dysfunction, sometimes in excess of that caused by the original injury (Schanne *et al.*, 1979; Crowe *et al.*, 1997; Oyinbo, 2011; Liu *et al.*, 2015; Ahuja *et al.*, 2017; Quadri *et al.*, 2018). Inflammatory responses and ischemia, combined with the disruption of the blood-spinal cord barrier, add to spinal cord swelling and further compression and damage of the cord (Senter & Venes, 1979; Ahuja *et al.*, 2017). As the injury progresses further over the course of days and years it enters the chronic phase. This is characterized by the return of spinal reflexes and alleviation of spinal shock, development of spasticity, pain disorders and mood disorders such as depression (Silva *et al.*, 2014). During the chronic phase there continues to be a cascade of cell death and alterations within the spinal cord (Oyinbo, 2011). Therefore, SCI is not as simple as the injury itself and is further complicated by the progression of dysfunction associated with it.

A variety of neuroplastic changes occur after SCI including neuronal reorganization, synaptic rearrangements, changes in neuronal activation patterns and intact or lesioned axon

collateral sprouting (Krenz & Weaver, 1998; Ballermann & Fouad, 2006; Silva *et al.*, 2014). These plastic changes in the CNS extend from the spinal cord to the brainstem and to the brain, where cortical plasticity in the sensorimotor cortex of chronic human SCI participants has been recorded (Cramer *et al.*, 2005; Baker, 2011; Baker & Perez, 2017). During the months to years following SCI, it is possible to harness this plasticity with rehabilitation. For example, under experimental conditions paralyzed cats can be trained to walk (de Leon *et al.*, 1998; Rossignol *et al.*, 1999). In humans, novel treatment strategies such as treadmill and exoskeleton training are employed to harness this plasticity (Wernig *et al.*, 1995; Behrman & Harkema, 2000; Khan *et al.*, 2016; Angeli *et al.*, 2018); however, the specific biological mechanisms behind plasticity remain largely unknown (Silva *et al.*, 2014).

While plasticity can be harnessed for rehabilitation purposes, maladaptive plasticity occurring from afferent inputs to motoneurons often prevails after SCI as outlined below. Reorganization of spinal circuitry, including sprouting of primary afferent fibres below the level of injury, may lead to the development of central pain (Ondarza *et al.*, 2003). Primary afferent sprouting may also lead to spasticity and autonomic dysreflexia by increasing the excitatory inputs to interneurons, which in turn increase excitatory input to motoneurons (Krenz & Weaver, 1998). Spinal neurons, such as wide dynamic range neurons, have exaggerated responses to innocuous and noxious mechanical stimuli after SCI, which has been associated with allodynia (Drew *et al.*, 2001). Motoneurons of humans (Gorassini *et al.*, 2004) and animals (Li & Bennett, 2003; Heckmann *et al.*, 2005) with chronic SCI have been shown to activate for long periods of time after brief sensory activation, recruiting slowly activating persistent inward currents that in part mediate motoneuron activation during involuntary muscle spasms.

The host of complications surrounding SCI, including motor and sensory impairment or loss, spasticity, pain, cardiovascular and respiratory impairment, and bladder, bowel and sexual dysfunction, makes SCI complicated to treat and, unfortunately, very few effective treatment options are available and typically only deliver modest effects (Silva *et al.*, 2014; Quadri *et al.*, 2018). There are currently no effective pharmacological treatments for the motor and sensory loss associate with SCI and few advances in the treatment of secondary issues (Rabchevsky & Kitzman, 2011; Silva *et al.*, 2014). When asked, individuals living with SCI reported that the alleviation of secondary issues such as autonomic dysreflexia, pain and spasticity was more important to them than walking in respect to quality of life (Anderson, 2004; Rabchevsky & Kitzman, 2011).

Spasticity after SCI

Many definitions exist for spasticity; however, the most commonly accepted was developed by Lance in 1980, which defines spasticity as a "motor disorder characterized by a velocity-dependent increase in tonic stretch reflexes (muscle tone), with exaggerated tendon jerks, resulting from hyperexcitability of the stretch reflex" (Schindler-Ivens & Shields, 2000; Voerman *et al.*, 2005; Grey *et al.*, 2008). Spasticity is also often characterized by intermittent or sustained involuntary somatic reflexes, clonus and painful muscle spasms in response to stretch and innoxious cutaneous stimuli (Voerman *et al.*, 2005; Rabchevsky & Kitzman, 2011; Silva *et al.*, 2014). Spasticity can be extremely debilitating and can profoundly impact activities of daily living such as transferring, independent dressing, management of bowel and bladder and can increase the risk of falls (i.e. during walking or out of wheelchairs and beds) (Rabchevsky & Kitzman, 2011). Spasticity can also cause pain, fatigue, disturbances during sleep, contribute to the development of contractures, pressure ulcers, infections, negative self-image and impede

rehabilitation efforts (Adams & Hicks, 2005). There are cases when spasticity can be helpful, for example maintaining an upright posture, during transferring, to increase or maintain muscle bulk and increase venous return, making decisions around the management of spasticity difficult (Adams & Hicks, 2005). Approximately 12 million people around the world have spasticity and 80% of people who suffer from SCI acquire spasticity (Voerman *et al.*, 2005).

Spasticity is not present during acute SCI and develops over the course of days or weeks after the initial injury, with the gradual development of involuntary muscle spasms, increased muscle tone and exaggerated tendon reflexes (Dietz, 2000; Adams & Hicks, 2005). The exact spinal pathophysiology of spasticity remains unclear and is likely the result of many mechanisms, making it difficult to fully understand and treat (Dietz, 2000; Adams & Hicks, 2005). Potential mechanisms involved in spasticity could include increased glutamatergic signaling to uninhibited motoneurons below the level of injury (Nacimiento *et al.*, 1995; Rabchevsky & Kitzman, 2011). For example, there may be increased glutamate release from primary afferents onto motoneurons due to reduced presynaptic inhibition of their terminals as proposed in a large number of studies (Ashby *et al.*, 1974; Ashby & Verrier, 1975, 1976; Nielsen *et al.*, 1993b; Faist *et al.*, 1994; Nielsen *et al.*, 1995; Aymard *et al.*, 2000; Hultborn, 2006; Grey *et al.*, 2008). Normal modulatory mechanisms that alter transmission of Ia input during the various phases of gate, such as presynaptic inhibition, appear to be deficient in SCI, pointing to dysfunction in the control of Ia conduction or transmission after SCI (Fung & Barbeau, 1994). Tremor and clonus associated with spasticity could be related to unstable oscillators in the agonist-antagonist system, which would normally be stabilized by intact presynaptic inhibitory mechanisms (Nielsen & Kagamihara, 1993).

There also appears to be partial loss of axosomatic (mainly inhibitory) inputs onto motoneurons with a parallel increase in excitatory input (M-type axon terminals derived from Ia afferents, which mediate the monosynaptic reflex), resulting in a disruption of the balance of inputs onto motoneurons and subsequent increased excitation caudal to the injury (Nacimiento *et al.*, 1995). After SCI, sensory inputs also recruit functional interneuron pathways that further excite motoneurons and appear be involved in the generation of persistent excitatory activity and spasticity (Bellardita *et al.*, 2017). Interestingly, studies have shown that both inhibitory (expressing vesicular inhibitory amino acid transporter [VIAAT]) and excitatory (expressing vesicular glutamate transporter 2 [Vglut2]) interneurons in the spinal cord increase their activity following SCI and increased excitatory interneuron activity appears to largely contribute to muscle spasms (Bellardita *et al.*, 2017). Persistent premotor activity, especially interneuron activity, appears to have a pivotal role in driving sustained motoneuron activity after chronic SCI (Bellardita *et al.*, 2017) although there is also a role of motoneurons in the production of spasticity as described below.

Increased motoneuron activity in response to sensory input also plays a role in the generation of spasticity after SCI. For example, there is a loss or reduction in brief inhibitory post-synaptic potentials (IPSPs) and a prolongation of excitatory post-synaptic potentials (EPSPs) in response to brief, sensory stimuli after SCI (Baker & Chandler, 1987; Bennett *et al.*, 2004; Norton *et al.*, 2008). A reduction in the KCC2 cotransporter on motoneurons after SCI results in a small depolarization of the Cl^- equilibrium potential and reduced efficacy of postsynaptic inhibition (Murray *et al.*, 2011b). Excessive motoneuron excitability from voltage-dependent calcium and sodium persistent inward currents (PICs) facilitate motoneuron firing during prolonged muscle spasms (Gorassini *et al.*, 2004; D'Amico *et al.*, 2014). As a result of

decreased descending monoamines from the brainstem after SCI, 5-$HT_{2B/C}$ (Murray *et al.*, 2011a) and NAα1 (Rank *et al.*, 2011) receptors on motoneurons, which facilitate PICs, become constitutively active, contributing to the recovery of self-sustained motoneuron firing and the development of spasticity after SCI.

Changes in the efficacy of spinal inhibitory circuits, such as reduced reciprocal inhibition (Crone *et al.*, 1994; Crone *et al.*, 2003), reduced or even reversed Ib inhibition (Pierrot-Deseilligny *et al.*, 1979; Delwaide & Oliver, 1988), reduced recurrent inhibition (Shefner *et al.*, 1992a) and reduced rate dependent depression (RDD) (Schindler-Ivens & Shields, 2000) have all been observed following SCI. However, studies in animals have shown that inhibitory input to motoneurons increases after chronic SCI and observed reduced inhibition may be a result of increased excitatory input that sways the balance towards excitation (Bellardita *et al.*, 2017).

Changes in muscle properties after SCI, including a transition from slower (type I) to faster (type IIb(x)) fibre types (Edstrom, 1970; Biering-Sorensen *et al.*, 2009) and muscle stiffness (Mirbagheri *et al.*, 2001) may decrease the threshold and increase the gain of the stretch reflex pathway, also contributing to spasticity (D'Amico *et al.*, 2014). Many mechanisms contribute to spasticity and hyperexcitability, but the cause vs the result of this hyperexcitability is less known (Bellardita *et al.*, 2017).

Treatment options for spasticity following SCI are typically either pharmacological or physical therapy. Pharmacological treatments typically involve either baclofen, tizanidine and/or botulinum neurotoxin (Rabchevsky & Kitzman, 2011). Pharmacological treatments may also involve benzodiazepine, dantrolene sodium, gabapentin and pregabalin, clonidine and/or cannabis (Rabchevsky & Kitzman, 2011); however, baclofen is the most common treatment for spasticity following SCI. Baclofen is a $GABA_B$ receptor agonist, and likely binds to presynaptic

$GABA_B$ receptors in lamina I-IV and IX in the spinal cord where sensory fibres terminate (Kangrga *et al.*, 1991; Hari *et al.*, 2021). Baclofen appears to reduce the influx of Ca^{2+} into the presynaptic terminal, reducing the amount of neurotransmitter released (Kangrga *et al.*, 1991). However, baclofen ingestion is accompanied by many adverse effects including sedation, fatigue, drowsiness, ataxia and mental confusion and it becomes less effective at reducing spasticity over long-term use (Rabchevsky & Kitzman, 2011).

Unfortunately, because the mechanisms of spasticity are not fully understood, all potential pharmacological treatments have not been explored and current drugs only give modest results for the treatment of spasticity. To understand spasticity and its pathophysiology and to develop more effective treatments, we must consider and understand normal sensory transmission and control.

Normal Sensory transmission / Ia afferent control

Sensory input conveying proprioceptive and kinematic information is crucial to shaping motor behavior, as evidenced by the devastating effect that peripheral sensory loss has on motor function (Rothwell *et al.*, 1982; Akay *et al.*, 2014). Peripheral sensory loss makes daily tasks such as using a pen, fastening buttons on a shirt, holding a cup or walking nearly impossible (Rothwell *et al.*, 1982). Similarly, abnormal sensory perception, such as after a spinal cord injury, can be devastating and reduce quality of life (Silva *et al.*, 2014). While it has long been observed that afferent signals are imperative for the generation of purposeful movement (Mott & Sherrington, 1895), how sensory conduction and transmission is controlled is not fully understood.

Reflexive systems within the spinal cord are crucial in controlling normal movement and are highly controlled in both a phase and context dependent manner. The ability of the CNS to regulate the barrage of incoming sensory information and produce meaningful movement is truly remarkable (Prochazka, 2015). Control mechanisms, specifically inhibitory control mechanisms, are needed to control the mass amounts of afferent impulses from various sense organs that would otherwise exceed the overall computing capacity of the CNS (Rudomin & Schmidt, 1999). These control mechanism allows the CNS to focus on the relevant afferent impulses based on a given task (Rudomin & Schmidt, 1999). Amazingly, at a spinal level this information control system works in a coordinated and highly regulated manner to harmonize sensory information and motor output.

A major finding of this elaborate control system is that presynaptic inhibition Ia afferents and postsynaptic inhibition of second-order cells are the prime targets of inhibitory control of sensory information (Rudomin & Schmidt, 1999). An important and well-studied mechanism of presynaptic inhibition is the activation of $GABA_A$ receptors on Ia afferents (Rudomin, 1999). Historically, studies have pointed towards an inhibitory action of $GABA_A$ receptor activation on Ia afferent terminals, leading to a reduction in neurotransmitter release and subsequent reduced motoneuron activation (Rudomin, 1999; Willis, 2006). However, recent animal experiments have pointed to an additional facilitatory role of $GABA_A$ receptor activation on Ia afferents, which cause a depolarization of the afferent at vulnerable branch points where action potentials tend to fail, helping to increase afferent conduction (Lucas-Osma *et al.*, 2018b) and subsequent motoneuron excitation (Hari *et al.*, 2021). Thus, even well studied aspects of sensory control, like presynaptic inhibition, appear to be more complicated than what was first thought and need to be re-addressed. The focus of this thesis is to better understand how the GABAergic system

presynaptically controls action potential propagation along Ia afferents and how this control changes after spinal cord injury.

GABA system is highly involved in the control of sensory information

In his 1999 review "Presynaptic selection of afferent inflow in the spinal cord" Rudomin wrote, "The mechanisms involved in the selective control of information have not been fully elucidated; however, activation of $GABA_A$ receptors appears to play a part in the control of transmitter release. The role of $GABA_B$ is less understood but it is not unreasonable to assume that activation of the $GABA_B$ receptor is also involved in the long term changes of synaptic effectiveness." (Rudomin, 1999). As Rudomin elaborated, the GABA system is highly involved in the transmission of sensory information, as will be discussed below.

Primary afferent depolarization (PAD) effects the excitability of monosynaptic reflexes evoked by primary afferents and is produced when gamma-aminobutyric acid-A ($GABA_A$) receptors on primary afferents are activated. Because afferents have a high concentration of intracellular chloride, activation of $GABA_A$ receptors results in chloride leaving the axon to produce a depolarization or PAD (Gallagher *et al.*, 1978b; Willis, 2006). Stimulation of low-threshold proprioceptive afferents is well known to elicit a depolarization in other primary afferents lasting ~100 ms (synaptic $\alpha 1GABA_A$-receptor mediated phasic PAD) that is widely distributed across many primary afferents (Eccles *et al.*, 1962b; Willis, 2006). Typically, PAD recorded from afferents has a latency of about 4 ms attributed to transmission along a central pathway with two interposed interneurons (marked by red and blue interneurons in Fig. 1.1) (Jankowska *et al.*, 1981c). The depolarization peaks at 15-20 ms, which has been attributed to the repetitive firing of the PAD interneurons, and has a total duration of approximately 100-300 ms, which has been attributed to prolonged transmitter action on the $GABA_A$ receptor (Eccles *et*

al., 1962b; Willis, 2006). Historically, this depolarization was thought to only occur at the afferent terminal (see Ventral phasic PAD circuit in Fig. 1.1), producing a shunting of current and/or inactivation of Na^+ channels to then reduce neurotransmitter release (Willis, 2006). Recent evidence has revealed a faciliatory role for PAD along Ia afferents, discussed below in *Presynaptic Facilitation: Dorsal GABAA receptor activation*.

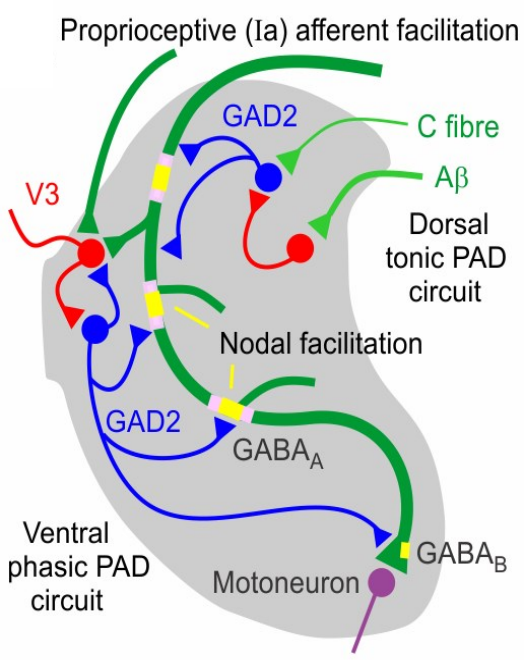

Figure 1.1. PAD schematic. A) Schematic of PAD GABA Circuit. Ia afferents (green), afferent nodes (yellow), GABA interneurons (blue), putative glutamatergic pre-GABA 1st order interneurons (red).

GABAaxo circuitry

$GABA_A$ receptors on proprioceptive afferents are activated by a trisynaptic pathway where cutaneous (Aβ), pain (C fibre) or proprioceptive (Ia) afferents disynaptically activate GABAergic neurons (blue, referred to as GABAaxo) which then activate synapses on proprioceptive afferents (dark green afferents in Fig. 1.1) (Jankowska *et al.*, 1981b; Rudomin,

1999; Lucas-Osma *et al.*, 2018b). A minimum latency of 1.7-2.0 ms to the onset of the PAD suggests a trisynaptic pathway with two interposed interneurons, a first order glutaminergic interneuron (red) and a second order GABAaxo interneuron (blue) (Jankowska *et al.*, 1981b). However, parallel polysynaptic pathways other than this short trisynaptic pathway may also be involved in the generation and/or maintenance of PAD, especially considering the latency of PAD in group I afferent is often estimated closer to 4 or 5 ms (Jankowska *et al.*, 1981c). Early recordings revealed the location of the first and last order interneurons involved in the generation of PAD of group I afferents to be located in laminae V-VI of the spinal cord (Jankowska *et al.*, 1981c). Recent recordings of extracellular field potentials, which reflect the intracellular recording of group I afferents, revealed a maximum response dorsal in laminae II-V which by far dominated the neuronal response in that region (Lucas-Osma *et al.*, 2018b). Therefore, the projections of the interneurons located in laminae V-VI appear to have strong depolarizing effect on the dorsal part of the Ia afferents.

$GABA_A$ receptor characteristics

$GABA_A$ receptors are coupled to anion channels permeable mainly to Cl^- ions but also to those anions whose hydrated diameter is no larger than that of ClO^-_3 (Gallagher *et al.*, 1978b). Two or three molecules of GABA are required to activate the receptor and open the anion channel (Gallagher *et al.*, 1978b). Cl^- ions are concentrated intracellularly in the dorsal root ganglion soma with an equilibrium potential of about -20 to -35mV. The equilibrium potential for GABA induced PAD was also found to be -23.5 $\pm$ 6.1 mV and dependent on $[Cl^-]_o$ but independent of $[Na^+]_o$, $[K^+]_o$ or $[Ca^{2+}]_o$ (Gallagher *et al.*, 1978b). The equilibrium potential of Cl^- is maintained by the NKCC1 cotransporter that carries two Cl^-, one Na^+ and one K+ into the cell/axon (Rudomin & Schmidt, 1999; Willis, 1999, 2006). Activation of $GABA_A$ receptors on

primary afferents therefore results in the net efflux of Cl^- ions and a depolarization of the primary afferent (Rudomin & Schmidt, 1999; Willis, 2006). This depolarization can be eliminated by the $GABA_A$ receptor antagonist bicuculine (refer to Figure 6E in Lucas-Osma *et al*., 2018) (Levy & Anderson, 1972; Curtis & Lodge, 1982).

GABAergic changes after SCI

Interestingly, after SCI, there is a loss of GABA/GAD+ neurons with a paradoxical hyperexcitability of remaining GABAergic function. The vesicular enzyme involved in *synaptic* GABA (GAD65 encoded by the GAD2 gene) decreases with SCI, consistent with the reported loss of presynaptic inhibition and rate dependent depression with SCI potentially associated with $GABA_B$ receptor activation as we propose in Chapter 4 (Kapitza *et al.*, 2012; Russ *et al.*, 2013). In contrast to synaptic GABA, the cytoplasmic enzyme associated with *extrasynaptic* GABA (GAD67 encoded by the GAD1 gene) increases with SCI, suggesting possible increased extrasynaptic GABA produced by surviving neurons (Tillakaratne *et al.*, 2000). Similar changes occur in stroke and possibly other brain injuries, where phasic synaptic GABA innervation is lost and tonic extrasynaptic GABA is increased, the latter due to loss of extra-synaptic glial GABA transporters (GAT-3) (Clarkson *et al.*, 2010).

The expression of GAD1 and GAD2 is highly dependent on the expression of BDNF and glutamate expression (Mende *et al.*, 2016). Therefore, reduced movement and sensory feedback from muscle paralysis after injury, and subsequent reduced expression of BDNF and glutamate in the spinal cord, could cause decreased expression of GAD1 and GAD2 in GABAaxo terminals (Mende *et al.*, 2016; Lalonde & Bui, 2021).

Classic Presynaptic Inhibition – Ventral $GABA_A$ receptor activation

Primary afferent depolarization has long been associated with presynaptic inhibition of primary afferents. Presynaptic inhibition was first discovered by Frank and Fuortes in 1957 when they noticed that the monosynaptic EPSP in the motoneuron could be depressed without any changes in its time course (onset/offset time), baseline potential or in the excitability of the motoneuron (Rudomin & Schmidt, 1999; Willis, 1999; Hultborn, 2006). The original findings of Frank and Fuortes were extensively expanded by Eccles, Lundberg and colleagues who painted the picture of classical $GABA_A$ mediated presynaptic inhibition with over 29 papers being published between 1961 and 1965 concerning the mechanisms of presynaptic inhibition and spinal cord organization (Rudomin & Schmidt, 1999; Hultborn, 2006; Willis, 2006). Eccles attributed presynaptic inhibition of primary afferents to a putative conductance increase in presynaptic terminals and shunting of the presynaptic action potential caused by the primary afferent depolarization created by $GABA_A$ receptor activation (Willis, 2006). That is, activation of $GABA_A$ receptors caused a depolarization of the afferent terminal, producing a shunting of current (Rudomin & Schmidt, 1999; Willis, 2006). This assumed depolarization of the afferent terminal would block or reduce action potential invasion into the terminal, resulting in a smaller influx of Ca^{2+} ions into the afferent terminal and, therefore, less neurotransmitter release (Rudomin & Schmidt, 1999). Eccles postulated that presynaptic inhibition was due to a depolarization of the afferent terminals (PAD) and a subsequent decrease in neurotransmitter release to ultimately reduce the Ia activation of the motoneuron EPSP (Ventral phasic PAD circuit, Fig. 1.1).

Eccles recorded this phenomena by stimulating a variety of afferent species to evoke PAD and putative presynaptic inhibition in other afferents, showing that PAD is wide spread and

readily evoked in almost all afferent types (refer to Fig. 12 in Willis, 2006) (Willis, 2006). PAD is evoked in virtually all flexor and extensor Ia afferents from flexor muscle Ia and Ib afferents of the ipsilateral limb but only a minor extent from extensor muscles. The strength of evoked PAD is indicated by the thickness of the arrows in Figure 12 in Willis, 2006 (Hultborn, 2006; Willis, 2006). PAD recorded from dorsal roots was also found to be controlled by supraspinal centers, with the pyramidal tract and rubrospinal tract decreasing putative presynaptic inhibition (Hultborn, 2006).

Eccles' work confirmed that of Frank and Fuortes showing that the monosynaptic EPSP could be depressed in parallel with the recorded PAD, with a depression latency as little as 5 ms after the arrival of a conditioning muscle afferent volley, reaching a maximum depression at 15-20 ms and lasting more than 200 ms (refer to Fig. 2 in Eccles *et al*., 1961a) (Willis, 2006), a time-course similar to $GABA_A$ receptor mediated PAD (refer to Figure 6B in Lucas-Osma *et al*., 2018). He also showed that the inhibition of the monosynaptic EPSP (refer to Fig. 2 in Eccles *et al*., 1961a) (Eccles *et al.*, 1961a) and monosynaptic reflex [refer to Fig. 1 in (Eccles *et al.*, 1962c)] of extensors could be prolonged when trains of high frequency conditioning stimuli of flexor nerves (4 pulses, 300 Hz) were used to evoke PAD (Willis, 2006).

Testing presynaptic inhibition in human participants

Based on the findings in animals described above, researchers set out to find evidence of $GABA_A$ receptor and PAD mediated presynaptic inhibition in human Ia afferents (Mizuno *et al.*, 1971; El-Tohamy & Sedgwick, 1983; Hultborn *et al.*, 1987a; Hultborn *et al.*, 1987b). A variety of methods have been used to investigate that a reduction in the size of the H-reflex from a prior

putative PAD-evoking stimulation is due to PAD-mediated presynaptic inhibition of the Ia afferent terminal; however, sufficient direct evidence is lacking to support this claim. Since this conclusion is likely incorrect in these human papers, we will only present the results of these papers and restate potential mechanisms in the final discussion of chapter 5.

The H-reflex, analogous to the monosynaptic reflex but with potential polysynaptic components, was utilized in human participants to study the effect of a variety of conditioning stimulations that activated PAD networks in animals. One method involved evoking PAD networks by stimulating Ia afferents from flexor muscles (either by electrical stimulation of the nerve or tendon vibration) and recording the long-lasting inhibition of the H-reflex mediated by extensor afferents receiving the potential presynaptic inhibition (El-Tohamy & Sedgwick, 1983; Hultborn *et al.*, 1987a; Hultborn *et al.*, 1987b; Capaday *et al.*, 1995).

Inhibition of the extensor soleus H-reflex from multiple pulses of common peroneal nerve (CPN, supplying the antagonist tibialis anterior muscle) stimulation has been described having 2 phases. First, D1 inhibition which has been associated with PAD-mediated presynaptic inhibition, occurs at conditioning intervals beginning at 5-7 ms, increases to a maximum around 15-20 ms, and is only present when more than 1.0xMT of CPN conditioning stimulation is used for multiple pulses (i.e. 3 pulses, 200 Hz) (refer to Fig. 2 in El-Tohamy & Sedgwick, 1983) (Mizuno *et al.*, 1971; El-Tohamy & Sedgwick, 1983). However, it is important to note that although the early profile of D1 inhibition follows the profile of $GABA_A$-receptor mediated PAD in the Ia afferent, it does not last as long, ending near 40 ms (compare to phasic PAD in Figure 6B in Lucas-Osma *et al*., 2018*).* The early D1 inhibition is then followed by a later D2 inhibition that has an onset of approximately 60 ms and lasts for up to 500 ms. D2 inhibition was thought to be mediated by afferent activity produced from the muscle twitch evoked by the conditioning CPN stimulation in

addition to PAD [refer to Fig. 1 in (Mizuno *et al.*, 1971)]. Again, the profile of D2 H-reflex inhibition does not match the profile of $GABA_A$ receptor mediated PAD as D2 inhibition lasts for much longer (i.e., 500 ms vs 100-200 ms PAD).

Hultborn and colleagues were the first to perform parallel animal and human studies to examine if D1 and D2 H-reflex inhibition were both produced by PAD-mediated presynaptic inhibition. To examine possible presynaptic inhibition from PAD, the flexor tibialis anterior (TA) tendon was vibrated (3 pulses, 200Hz), 0-500 ms before evoking an extensor soleus H-reflex [refer to Fig. 5A in (Hultborn *et al.*, 1987a)]. The soleus H-reflex was inhibited from approximately 40 to 500 ms after the conditioning flexor vibration (refer to Fig. 4B in Hultborn *et al.,* 1987a) with the idea that the flexor TA Ia afferents activated GABAaxo interneurons to the terminal soleus Ia afferents to produced presynaptic inhibition (red pathway). Because the H-reflex can potentially be activated by polysynaptic pathways, they used another method to ensure they were examining the suppression of a pure monosynaptic reflex. Here, the amount of soleus H-reflex facilitation from a prior stimulation of the heteronymous (quadriceps) Ia afferent at strict monosynaptic latencies was used to assess presynaptic inhibition in the quadriceps Ia afferents (refer to Fig 5A in Hultborn *et al.,* 1987a). Any decrease in the heteronymous facilitation of the soleus H-reflex by the conditioning flexor vibration was then attributed to an increase in presynaptic inhibition of the quadriceps Ia afferents (refer to Fig 5A J and K in Hultborn *et al.,* 1987a) (Hultborn *et al.*, 1987a). It was also assumed that direct postsynaptic inhibitory effects on the soleus motoneurons from the flexor tendon vibration would not last long enough (> 10 ms) or be strong enough to account for the reduction in the facilitation of the soleus H-reflex by the heteronymous quadriceps Ia stimulation.

The validity of this method was tested in cats, showing that a pure postsynaptic inhibitory input to soleus motoneurons from Ib afferents from the gastrocnemius medialis muscle had peak inhibition around 5 ms (onset at 2 ms and over by 10 ms) and did not suppress the heteronymous facilitation of the soleus H-reflex; therefore, any decrease in the heteronymous facilitation had to be presynaptic in origin (Hultborn *et al.*, 1987a). With this, it was also assumed that any inhibition that fell outside of this postsynaptic inhibitory window (longer than 10 ms) had to be presynaptic (Hultborn *et al.*, 1987a). These assumptions became the bases for years of research that assumed a presynaptic role of inhibition in human experiments where H-reflexes were suppressed with conditioning intervals > 10-40 ms (Burke *et al.*, 1992; Nielsen & Kagamihara, 1993; Capaday *et al.*, 1995; Faist *et al.*, 1996; Iles, 1996; Rudomin & Schmidt, 1999). The direct effect of the conditioning input (TA tendon vibration) on the soleus motoneuron or quadriceps Ia afferent was never tested, leaving the exact mechanism of the H-reflex inhibition/reduced heteronymous facilitation largely speculative.

Despite the conclusions from the above experiments being largely assumed, the methods developed by Hultborn and colleagues to test presynaptic inhibition were extended to test presynaptic inhibition during a variety of tasks, such as at the onset of voluntary contractions (Hultborn *et al.*, 1987b), during gait (Faist *et al.*, 1996) and to compare walking vs standing (Capaday *et al.*, 1995). The results of these experiments will not be discussed here as more attention needs to be taken in understanding the mechanisms behind H-reflex suppression from a prior putative PAD-evoking stimulation in the resting state before it can be properly studied during movement and tasks.

In many experiments exploring putative presynaptic inhibition in human participants, the effect of the conditioning stimulation on the test motoneurons during the period of H-reflex

suppression was not examined. Despite this, the methods and assumptions described above have been used in a number of studies (Burke *et al.*, 1992; Nielsen & Kagamihara, 1993; Capaday *et al.*, 1995; Faist *et al.*, 1996; Iles, 1996; Rudomin & Schmidt, 1999) to assume presynaptic inhibition and the original Hultborn paper (Hultborn *et al.*, 1987a) has been cited over 417 times. The few studies where postsynaptic effects of the conditioning stimulation were tested using the ongoing EMG from the test muscle (Roby-Brami & Bussel, 1990; Capaday *et al.*, 1995) or cortically evoked muscle action potentials (Berardelli *et al.*, 1987; Iles & Pisini, 1992; Faist *et al.*, 1996) with the conditioning stimulation alone often did not consider methods other than $GABA_A$ receptor mediated terminal presynaptic inhibition, despite recording postsynaptic effects from the conditioning stimulation alone in the test motoneurons. Capaday and colleagues noted an early response recorded in the test (soleus) muscle from a CPN conditioning stimulation alone, even at intensities as low as 1.0xMT and a definite response at 1.5xMT (refer to Fig. 4 and 5 in Capaday *et al*., 1995), therefore a postsynaptic response has been recorded in the soleus muscle (at the 50-120 ms interval, refer to Fig 4 and 5 in Capaday *et al.,* 1995), but it was assumed that post-synaptic effects do not contribute to H-reflex suppression beyond this. The role of an earlier post-synaptic response on prolonged H-reflex suppression is discussed below in "*Post activation depression in human participants*".

Presynaptic Inhibition after SCI

Based on findings in control participants, various methods have been used to assess putative presynaptic inhibition after CNS injury. In SCI, these experiments have led to the long-standing assumption that $GABA_A$ receptor and PAD-mediated presynaptic inhibition of Ia afferent terminals is reduced following injury and could account for some hyperexcitability along

the Ia – motoneuron pathway (Ashby *et al.*, 1974; Ashby & Verrier, 1975, 1976; Nielsen *et al.*, 1993b; Faist *et al.*, 1994; Nielsen *et al.*, 1995; Aymard *et al.*, 2000; Hultborn, 2006; Grey *et al.*, 2008). Given that there is deficient evidence proving a role for PAD-mediated presynaptic inhibition of Ia afferent terminals in control participant [reviewed below in *Inconsistencies linking GABAA receptor mediated PAD at the afferent terminal with presynaptic inhibition* and in (Hari *et al.*, 2021)] there is a need to re-evaluate these findings after injury. Below is a summary of some of the experiments used to assess putative presynaptic inhibition after SCI and how the interpretations of these findings may be misleading. Many of these studies have been cited many times for providing evidence of supposed decreased presynaptic inhibition after SCI; however, the evidence for such a claim is lacking.

The methods developed by Hultborn to assess presynaptic inhibition using heteronymous facilitation (explained above) (Hultborn *et al.*, 1987a) were applied to assess presynaptic inhibition of Ia afferents in patients with spasticity, notably those with SCI (Faist *et al.*, 1994). Here, the amount of facilitation of the soleus H-reflex from a heteronymous (quadriceps) input was compared to controls to assess basal (tonic) levels of putative presynaptic inhibition, with smaller amounts of heteronymous facilitation indicating larger basal levels of presynaptic inhibition of the soleus Ia afferent. Individuals with SCI (refer to Faist *et al*., 1994) showed increased soleus H-reflex facilitation from the quadriceps conditioning stimulation compared to controls (left bars). The larger soleus H-reflex facilitation evoked in participants with SCI was taken as evidence for supposed reduced basal, tonic PAD and presynaptic inhibition after SCI (Faist *et al.*, 1994). This was in contrast to participants who had suffered a stroke (refer to Fig. 1 in Faist *et al*., 1994) who showed no difference in the amount of soleus H-reflex facilitation from a heteronymous (quadriceps) input compared to controls. Even though examining presynaptic

inhibition more directly by using a conditioning stimulation to evoke PAD or assessing changes at other levels (such as the excitability of the motoneurons or interneurons) was not used, this paper has been cited over 237 times and has helped established the misconception that $GABA_A$ receptor mediated inhibition of the Ia afferent terminal is reduced after SCI.

Other researchers have also used the heteronymous Ia facilitation methods described by Hultborn (Hultborn *et al.*, 1987a) to examine presynaptic inhibition after complete SCI (Roby-Brami & Bussel, 1990). Roby-Brami & Bussel (1990), stimulated the sural nerve to activate the flexor reflex afferent (FRA) pathway as a conditioning input to evoke PAD and examined the effect of this input on the facilitation of the soleus H-reflex by heteronymous (quadriceps) Ia inputs. This method was similar to the TA tendon vibration conditioning used by Hultborn (Hultborn *et al*., 1987a, described above) whereby the FRA stimulation was used to evoked PAD. They also combined the FRA conditioning stimulation with TA tendon vibration to theoretically produce faciliatory convergence on to the GABAaxo interneurons that produce PAD. These authors showed that the FRA stimulation reduced the amount of soleus H-reflex heteronymous facilitation in participant with complete SCI. The TA tendon vibration alone did not always reduce the amount of soleus H-reflex heteronymous facilitation in participants with complete SCI, but when the FRA stimulation and TA tendon vibration were combined, the amount of soleus H-reflex heteronymous facilitation was significantly reduced. They equated the reduction in soleus H-reflex facilitation from the FRA stimulation to evidence of supposed presynaptic inhibition in complete SCI, something that was not observed when just TA tendon vibration was used to conditioning the soleus H-reflex heteronymous facilitation. However, there were no control participants recruited in this study to provide comparable uninjured data. The FRA stimulation alone also produced large reflex responses in both the TA and soleus muscles

and was evoked at high stimulation intensities (ranging from 5 to 50 mA), recruiting many afferent species. While these results are interesting, it seems unlikely that only presynaptic inhibition of Ia afferents would account for the reduction in heteronymous H-reflex facilitation and there is insufficient evidence to prove a role for presynaptic inhibition in these experiments.

To further examine putative presynaptic inhibition after complete and incomplete SCI, the ratio of the maximum soleus H-reflex response with and without TA tendon vibration has also been assessed [refer to Fig 2 in (Ashby & Verrier, 1975)]. In theory, conditioning inputs to evoked PAD (i.e. TA tendon vibration) would reduce the maximum size of the soleus H-reflex and could therefore be used as a simple way to assess putative presynaptic inhibition. The ratio of the maximum H-reflex with vibration/the maximum H-reflex without vibration was plotted against the time since injury, where 100% would mean that both H-reflexes are the same size and 0% would mean that the vibration completely wipes out the soleus H-reflex. In uninjured controls, the average ratio was 41.5% (refer to Fig 2 in Ashby & Verrier, 1975). After *complete* SCI, vibration almost completely abolishes the H-reflex to produce an average H vib/H no vib ratio of 2.2 % (refer to Fig 2 in Ashby & Verrier, 1975). In this case, the non-vibrated (test) maximum H-reflex was just as large, or even larger, than non-injured controls (Ashby & Verrier, 1975).

After *incomplete* spinal cord injury, vibration reduced the size of the Hvib/Hno vib ratio but only to an average of 29% (not shown) (Ashby & Verrier, 1975). As the SCI progresses from the acute, sub-acute to chronic stages over the course of several months and years, the Hvib/H no vib ratio in *complete* SCI increased to an average of 47% (refer to Fig 2 in Ashby & Verrier, 1975), which is slightly higher than the average healthy control ratio of 41.5% (Ashby & Verrier, 1975). The greater ratio in chronic *complete* SCI compared to controls was taken as evidence for

reduced presynaptic inhibition after SCI but this measurement alone does not provide sufficient evidence to support that claim. No measurements were made to assess the direct post-synaptic response from the TA tendon vibration on to the soleus motoneurons or Ia afferents.

Other studies have assessed the modulation of the H-reflex during walking to further examine presynaptic inhibition after SCI (Fung & Barbeau, 1994). In the uninjured CNS, the H-reflex is modulated during walking; however, after SCI H-reflex modulation is diminished or completely absent, which has been attributed, likely incorrectly, to inadequate control of presynaptic inhibition of Ia afferent terminals (Fung & Barbeau, 1994). In SCI, the H-reflex is larger during active gate compared to similar joint angles and motor output during sitting, which is opposite of what is observed in uninjured control participants, again suggesting that the H-reflex is not being modulated properly after SCI (Fung & Barbeau, 1994). The inability of the CNS to modulate and control sensory input effects normal movements and may lead to exaggerated reflexes, spasticity and clonus (Fung & Barbeau, 1994). This inadequate control of sensory input has been attributed to a reduction of presynaptic inhibition of Ia afferent terminals; however, there is insufficient direct evidence to support this.

Reduced presynaptic inhibition has been proposed to be a major contributor to hyperexcitable reflexes and spasticity; however, direct evidence for this is lacking and many other mechanisms contribute to this hyperexcitability (refer to *Spasticity after SCI* above). Without specific measurements to dissociate pre (Ia afferent) vs postsynaptic (motoneuron) effects or the kind of presynaptic inhibitory mechanism (discussed below), caution must be taken when ascribing any mechanism to the altered control of H-reflexes after injury.

Inconsistencies linking $GABA_A$ receptor mediated PAD at the afferent terminal with presynaptic inhibition

There is a correlation between the occurrence and time course of $GABA_A$ receptor mediated PAD and EPSP suppression; however, there are many inconsistencies as well. The classic $GABA_A$ mediated primary afferent depolarization is too short (<100ms) (refer to Figure 6B in Lucas-Osma *et al.,* 2018) to account for the long lasting inhibition of EPSPs and monosynaptic reflexes that can last >200 ms in cats [refer to Fig. 2 in (Eccles *et al.*, 1961a)] and the suppression of H-reflexes in humans that can last >500 ms (Mizuno *et al.*, 1971; El-Tohamy & Sedgwick, 1983; Hultborn *et al.*, 1987a) produced by conditioning flexor nerve stimulation. Therefore, longer-lasting mechanisms, such as post-activation depression from $GABA_B$ receptor activation on the Ia afferent terminal, are also likely involved as described below.

One of the other inconsistencies linking $GABA_A$ receptor mediated PAD at the Ia afferent terminal with presynaptic inhibition is the location of $GABA_A$ receptors on Ia afferents. $GABA_A$ receptors have been difficult to locate on afferent terminals, which is where they need to be for shunting inhibition to occur, and instead appear to be located more dorsally near branch points (Lucas-Osma *et al.*, 2018b; Hari *et al.*, 2021). The role of these more proximally located $GABA_A$ receptors is discussed below in *Presynaptic Facilitation: Dorsal $GABA_A$ receptor activation.* Further, when PAD was recorded in the spinal cord using extracellular field potentials, the strongest response was found in the dorsal horn compared to the ventral horn, making it less likely that PAD could produce appreciable presynaptic inhibition at afferent terminals (Lucas-Osma *et al.*, 2018b). There are GABAergic synapses that contact the afferent terminals, likely activating $GABA_B$ receptors (discussed below), and these contacts often make both pre- and post-synaptic contacts at the same time (Pierce & Mendell, 1993; Hughes *et al.*, 2005), making

the distinction between pre- and postsynaptic mechanisms difficult to dissociate. Since little was known about the location of axo-axonic contacts along axons in the spinal cord, which have been attributed to producing PAD and presynaptic inhibition, many of the mathematical models used to understand impulse conduction/transmission and shunting inhibition had to estimate some of the electrophysiological parameters at the afferent terminal because empirical measures were not available (Rudomin & Schmidt, 1999). In many models, the depolarization needed to produce a complete block of the action potential would need to be very large and likely not physiologically relevant or realistic, and would need to be combined with other mechanisms such as a leak conductance (Rudomin & Schmidt, 1999). As a result, concepts of $GABA_A$ receptor mediated presynaptic inhibition have recently been reexamined (Hari *et al.*, 2021).

$GABA_B$ receptor activation

Other mechanisms have been suggested for the presumptive $GABA_A$ mediated presynaptic inhibition observed, although less attention has been paid to them. For example, Curtis and Lacey have suggested that presynaptic inhibition could also be caused by the activation of $GABA_B$ receptors located on the afferent terminals, which inhibits neurotransmitter release by blocking or reducing voltage-gated Ca^{2+} channels (Curtis & Lacey, 1994) or by increasing K^+ conductance, although the latter is less likely (Willis, 1999). $GABA_B$ receptors are metabotropic, activating second messengers that cause a longer lasting effect than $GABA_A$ receptors. Activation of $GABA_B$ receptors on presynaptic afferents terminals may therefore account for the long-lasting (up to 2 s) presynaptic inhibition observed in many studies (Eccles *et al.*, 1961a; Curtis & Lacey, 1994, 1998).

Baclofen (a $GABA_B$ receptor agonist) reduces the amount of transmitter release from presynaptic afferent terminals by presumably reducing Ca^{2+} influx into the afferent terminal

(Curtis *et al.*, 1997) without effecting the motoneuron at clinically relevant doses (Li *et al.*, 2004c). In humans, baclofen is a common antispastic medication (Adams & Hicks, 2005) that could reduce spasms by facilitating long-lasting presynaptic inhibition of Ia afferent terminals (Robertson & Taylor, 1986; Rudomin & Schmidt, 1999).

PAD-evoked spikes

$GABA_A$ receptor mediated depolarization in primary afferents is often strong enough for the afferent to reach spiking threshold (Rudomin & Schmidt, 1999), resulting in an action potential that propagates antidromically to be recorded as a dorsal root reflex (DRR) and orthodromically to excite motoneurons (Eccles *et al.*, 1961b; Willis, 1999). Under certain experimental conditions, orthodromic PAD-evoked spikes can evoke large reflex discharges in motoneurons; however, very little attention has been paid to this (Duchen, 1986; Willis, 1999). Recent evidence, and evidence drawn from previous studies, demonstrates that inhibition of the extensor monosynaptic/H-reflex could be due to post-activation depression caused by PAD-evoked spikes in extensor Ia afferents evoked from a prior conditioning (flexor) nerve stimulation (Curtis & Eccles, 1960; Willis, 2006; Hari *et al.*, 2021) and this will be explored further in Chapter 3.

DRRs have been recorded in awake, behaving animals during locomotion and appear to be physiologically relevant during movement, although their exact purpose remains largely unknown (Rudomin & Schmidt, 1999). What appears to be DRRs has also been recorded in humans using near-nerve needle electrodes and compound sensory nerve action potentials (CSAP) recorded at the calf (Shefner *et al.*, 1992b). Late antidromic components (distinguished from earlier orthodromic reflex responses) of the CSAP (30 to 80 ms) were suggested to arise

from PAD in the spinal cord and subsequent DRRs that propagate back down the afferent (Shefner *et al.*, 1992b).

Post-activation depression

Post-activation depression is another form of presynaptic inhibition different from the concept of PAD-mediated presynaptic inhibition at the Ia afferent terminal. Simply put, post-activation depression is suppression along the Ia – motoneuron pathway following repetitive activations of that pathway. It has also been referred to as "homosynaptic depression", "frequency depression" or "rate dependent depression (RDD)" and has been well documented in humans (Crone & Nielsen, 1989; Hultborn *et al.*, 1996a) and animals (Curtis & Eccles, 1960; Ashby *et al.*, 1974; Hultborn *et al.*, 1996a). For example, when multiple volleys are evoked in one afferent, the second EPSP evoked in the cat motoneuron is depressed compared to the first EPSP when the interval between the volleys is greater than 20 ms (refer to Fig 2 in Curtis & Eccles, 1960). During repetitive stimulation of the same afferents at these same intervals, the average size of the second, third and fourth EPSPs remain inhibited at a relatively steady state compared to the first EPSP (refer to Fig 2 in Curtis & Eccles, 1960). When the interval is less than 20 ms, facilitation of the EPSP is often observed (refer to Fig 2 in Curtis & Eccles, 1960), depression of the second EPSP is regularly observed (Curtis & Eccles, 1960).

Each presynaptic impulse theoretically exerts two opposing actions on the transmitter membrane, the depletion of available transmitter and the mobilization of transmitter stores (Curtis & Eccles, 1960). Depending on the time between impulses, the availability of transmitter will change. At longer intervals the depletion of transmitter may dominate the mobilization of transmitter, leading to a depression of the second volley (Curtis & Eccles, 1960). The recovery

time constant from maximal transmitter depletion is approximately 300-400 ms (Neher & Sakaba, 2001), so any subsequent activations of the afferent terminal occurring within 400 ms could be inhibited because transmitter levels have not been restored. $GABA_B$ receptor activation at the afferent terminal may also play a role in long-lasting suppression of neurotransmitter release (lasting 800 ms or longer) (Curtis & Lacey, 1994, 1998). At shorter intervals (<20 ms) it has been theorized that transmitter is mobilized in the presynaptic terminal by repetitive stimulation so that more transmitter is liberated by a test volley, leading to facilitation of the second volley (Eccles & Rall, 1951). Temporal summation of motoneuron EPSPs at shorter intervals also enhances subsequent volleys (Cushing *et al.*, 2005).

Examining post-activation depression in human participants

Post-activation depression can be examined in human participants by activating Ia afferents and recording the effect on subsequent activations along that same pathway. For example, the size of the soleus H-reflex is reduced following a passive dorsiflexion to stretch and presumably activate the soleus afferents (Hultborn *et al.*, 1996a). The inhibition in the soleus H-reflex caused by passive dorsiflexion is less pronounced in patients with spasticity compared to healthy controls (Nielsen *et al.*, 1993a; Hultborn *et al.*, 1996a).

Post-activation depression can also be induced by evoking pairs of H-reflexes, similar to the pairs of volleys used in intracellular recordings in animals. The size of the second H-reflex compared to the first H-reflex is tested and plotted at intervals anywhere from 1 ms to 10 s, referred to as the H-reflex recovery curve. Magladery was the first investigator to study the recovery cycle of the H-reflex, using pairs of H-reflexes at varying intervals, noting inhibition of the second H-reflex with an interposed reduction in inhibition (hump) when the interval was around 200-300 ms when pairs of homonymous H-reflexes were evoked (Magladery *et al.*,

1952). Further investigations provided more detail to the H-reflex recovery cycle, revealing the depressed state of the H-reflex was strong out to the 400 ms intervals (Goulart *et al.*, 2000) and lasted to approximately 1200 ms (Taborikova & Sax, 1969; Spaulding *et al.*, 1987; Schindler-Ivens & Shields, 2000). Even when the first H-reflex (conditioning pulse) was just below threshold to evoke a recordable H-reflex in the muscle, the second H-reflex continued to be depressed at intervals out to 1000 ms (8% inhibition at 1000 ms, furthest interval tested) (refer to Fig. 2 in Taborikova & Sax, 1969). Therefore, prior activation of the homonymous afferent has a strong and long-lasting inhibitory effect on subsequent reflex activations, even when the first activation is below threshold for a recordable response in the muscle.

Other inhibitory mechanisms to consider

There are several other mechanisms which could account for H-reflex inhibition from a prior conditioning stimulation previously attributed to PAD-mediated presynaptic inhibition. If the conditioning stimulation produces a small twitch in the muscle this could activate Ib (non-reciprocal) inhibition around the 15 ms interval (Masland, 1972); however, this would not account for the long-lasting inhibition observed. Activation of motoneurons by the conditioning volley could also lead to recurrent (Renshaw Cell) inhibition around the 5-15 ms interval (Masland, 1972). Renshaw cells activated by antidromic stimulation are widely distributed to motoneuron pools (Fisher, 1992). Again, this would not account for the long-lasting inhibition observed. Finally, if the conditioning stimulation produces a twitch in the test muscle, the shortening of the muscle will unload muscle spindles and diminish the excitatory Ia afferent activity (Masland, 1972); however this is also unlikely to account for the long-lasting inhibition.

Post-activation depression and spasticity

Post-activation depression is decreased in individuals with spasticity compared to healthy controls (Ashby *et al.*, 1974; Nielsen *et al.*, 1993a; Aymard *et al.*, 2000; Schindler-Ivens & Shields, 2000). Observations of this include soleus H-reflexes that are less depressed and for shorter periods of time following a passive plantarflexion in spastic traumatic SCI (returns to baseline after 9 s) compared to healthy controls (returns to baseline after 16 s) (refer to Fig. 2 in Nielsen *et* al., 1993b). H-reflex inhibition from vibration to activate antagonist Ia afferents is reduced in patients with spasticity and has also been suggested to be mediated by a decrease in post-activation depression (Nielsen *et al.*, 1993b), similar to that shown by Ashby and colleagues (refer to Fig 2 in Ashby & Verrier, 1975) who instead proposed the reduced H-reflex inhibition was due to reduce presynaptic inhibition at the Ia afferent terminal.

Time after spinal cord injury also plays a role in post-activation depression. When RDD of the H-reflex was tested (at 0.1, 0.2, 1, 5 and 10 Hz) in healthy controls, acute SCI and chronic SCI, the H-reflex amplitude decreased with increasing stimulation frequency in all three groups but H-reflexes were more suppressed in the healthy controls and acute SCI compared to the chronic SCI group (refer to Fig. 2 in Schindler-Ivens & Shields, 2000). The authors attributed the reduce amount of H-reflex inhibition in the chronic SCI group to a decrease in presynaptic inhibition; however, no direct evidence supported this (Schindler-Ivens & Shields, 2000).

Post-activation depression of the H-reflex is also influenced by the severity of SCI. Eight weeks after injury, rats with mild and moderate SCI had less post-activation depression of H-reflexes at 5Hz (~25% reduction) compared to complete spinal transected rats (~60% reduction) and uninjured controls (~80% reduction) (Lee *et al.*, 2005). This was in contrast to previous assumptions that more severe SCI leads to more abnormal H-reflex post-activation depression

and suggests that even in the absence of supraspinal influence, H-reflexes recover some sensitivity to repetitive afferent stimulation (Lee *et al.*, 2005).

H-reflex inhibition from repetitive activation of the same H-reflex at varying intervals (H-reflex recovery curve described above) in humans with SCI is also different based on severity of injury but not level of injury (Kumru *et al.*, 2015). For example, at early intervals (<150 ms) participants with incomplete SCI (ASIA C and D) had H-reflex recovery curves similar to control participants, unlike participants with complete SCI (ASIA A) who had reduced inhibition compared to controls (refer to Fig. 3 in Kumru *et al*., 2015). At longer intervals all participants with SCI showed less inhibition in their H-reflex recovery curve compared to controls (Kumru *et al.*, 2015).

Hofstoetter and colleagues (2019) showed no significant change in the recovery cycle of the H-reflex between participants with SCI and controls, although this may have been due to a higher number of ASIA D participants recruited in this study (5 ASIA D, 3 ASIA C and 2 ASIA A). Interestingly, there was less suppression in the recovery cycle of the posterior-root muscle reflex (PMR), a short latency reflex evoked by epidural or transcutaneous spinal cord stimulation, in participants with SCI compared to controls (Hofstoetter *et al.*, 2019). In the control group, the PMR recovery cycle was more depressed compared to the H-reflex recovery cycle, but the two cycles showed no difference in the SCI group. The spinal cord stimulation used to evoke the PMR likely recruited more posterior roots than the peripheral nerve stimulation used to evoke an H-reflex, activating more afferents and more post-activation depression. The PMR recovery cycle may be a more sensitive measure of post-activation depression, making small changes seen in the H-reflex recovery curve more pronounced in the SCI group.

Studies looking at the firing probability of a soleus single motor unit in patients with spinal lesions also showed a decrease in the amount of inhibition on the soleus motoneuron from two successive soleus afferent volleys (30 ms interval) compared to uninjured controls (Mailis & Ashby, 1990). The single motor unit measures provided evidence that post-activation depression involves inhibition along a single Ia – motoneuron pathway.

Changes in homosynaptic depression, postsynaptic inhibition and GABAergic circuits following SCI all appear to play a role in the development of spasticity and hyperexcitability in the spinal cord. Historically, attention has been paid to the reduction of $GABA_A$ receptor mediated presynaptic inhibition at afferent terminals with little direct evidence. Caution needs to be taken when studying these circuits in healthy controls and participants with SCI to understand what is happening at a pre- and post-synaptic level, especially considering new evidence for an alternative facilitatory role for $GABA_A$ receptors on Ia afferents.

Presynaptic Facilitation: Dorsal $GABA_A$ receptor activation

The sparsity of $GABA_A$ receptors and GABA-mediated depolarization at the afferent terminal has put into question the mechanism of presynaptic inhibition mediating the reduction of monosynaptic and H-reflexes described above. Based on 2 recent papers (Lucas-Osma *et al*. 2018 and Hari *et al.*, 2021 in Appendix), intracellular recordings in afferents have revealed that a short-lasting (80-100 ms), bicuculline-sensitive phasic PAD can also depolarize the afferents at nodes far from the afferent terminal and help save failing action potentials at branch points (see Fig. 1.1, described further below). This dorsal, $GABA_A$-receptor mediated depolarization is readily activated by cutaneous (Aβ) or pain afferents (C fibre) and produces facilitation, rather than inhibition, of the Ia-mediated monosynaptic reflex in both animals and humans (Hari *et al.*,

2021). This short-duration (phasic) depolarization lasts for 100-200 ms and is mediated by the activation of synaptic α1 and α2$GABA_A$ receptors (refer to Figure 6 in Lucas-Osma *et al*., 2018).

There is also a long-lasting tonic PAD that is readily activated by a train of cutaneous (Aβ) or pain (C fibre) afferent stimulation (Lucas-Osma *et al.*, 2018b) (refer to Figure 10B in Lucas-Osma *et al*., 2018). This second type of $GABA_A$ -mediated PAD is a long-duration (tonic) depolarization that lasts for 10's of seconds and is mediated by extra-synaptic α5$GABA_A$ receptors and presumable GABA spillover (Lucas-Osma *et al.*, 2018b; Hari *et al.*, 2021). The α5$GABA_A$ receptors involved in tonic PAD are largely absent from the unmyelinated afferent terminals on proprioceptive afferents but are largely and widely distributed near or on branch points on Ia afferents throughout the spinal cord (Lucas-Osma *et al.*, 2018b). Tonic PAD starts slowly (approximately 20 ms after stimulation), can last for seconds to minutes and is blocked by L655708, an α5$GABA_A$ receptor antagonist (Lucas-Osma *et al.*, 2018b). Trains of fast stimulation increase the tonic PAD recorded in afferents (Eccles *et al.*, 1962a) and only at intervals of 10 s or longer did the PAD cease to build up with repeated stimulations (Lucas-Osma *et al.*, 2018b).

Dorsal $GABA_A$ receptor activation reduces branch-point failure

Once afferents, including proprioceptive Ia afferents, enter the spinal cord, they branching extensively with large en passant boutons and nodal regions, especially just proximal to branch points (Lucas-Osma *et al.*, 2018b). Action potentials often fail at these branch points due to their large conductance, leaving silent branches where action potentials fail to propagate (Henneman *et al.*, 1984b; Lucas-Osma *et al.*, 2018b). Unlike the small classic Ia afferent terminal boutons, the nodes at branch points receive synaptic contacts (Nicol & Walmsley, 1991; Pierce & Mendell, 1993; Vincent *et al.*, 2017; Lucas-Osma *et al.*, 2018b) and sodium channels

and $GABA_A$ receptors are often clustered there or on nearby boutons (Lucas-Osma *et al.*, 2018b; Hari *et al.*, 2021). $GABA_A$ mediated depolarization (PAD) at the branch points facilitates action potential propagation by bringing the afferent closer to threshold, saving failing action potentials (Lucas-Osma *et al.*, 2018b; Hari *et al.*, 2021). For example, stimulation of a dorsal root (DR2) evokes an action potential in the homonymous (recorded) Ia afferent that sometimes fails to propagate, leaving a failed spike (refer to Fig. 4 in Hari *et* al., 2021). Stimulation of an adjacent dorsal root evokes a PAD in the recorded afferent (refer to Fig. 4 in Hari *et* al., 2021). Activation of PAD in the recorded afferent from DR1 stimulation brings the afferent closer to threshold and rescues the failed spike from DR2 stimulation (refer to Fig. 4 in Hari *et* al., 2021

Summary and Motivations

$GABA_A$ receptor mediated facilitation represents a fundamental shift in our thinking of how sensory conduction is controlled by other sensory afferents, central pattern locomotor networks and descending pathways. Considering the new evidence for the facilitatory role of $GABA_A$ receptors on Ia afferents, we examined potential presynaptic facilitation in Ia afferents mediating the H-reflex in human participants. Previous studies examining presynaptic inhibition have noted a reduction in the amount of H-reflex suppression from a putative PAD-producing conditioning input when cutaneous and corticospinal tract (CST) pathways are activated prior to the conditioning inputs, which has been associated with inhibition of GABA interneurons in the PAD pathway (Berardelli *et al.*, 1987; Hultborn *et al.*, 1987a; Hultborn *et al.*, 1987b; Iles & Roberts, 1987; Nakashima *et al.*, 1990; Iles, 1996; Meunier & Pierrot-Deseilligny, 1998b; Aimonetti *et al.*, 2000a). Thus, in Chapter 2 we explore the concept of presynaptic facilitation of Ia afferent in humans using cutaneous and CST conditioning inputs, given new evidence that

these conditioning inputs evoke a PAD that facilitates afferent conduction in animals (rather than simply disinhibiting presynaptic inhibition) (Lucas-Osma *et al.*, 2018b; Hari *et al.*, 2021).

In Chapter 3 we revisit classical experiments examining suppression of extensor H-reflexes produced by flexor afferent conditioning to determine if mechanisms other than PAD-mediated presynaptic inhibition at the afferent terminal, such as post-activation depression, may account for some of the H-reflex suppression observed by others. Finally, in Chapter 4, we explored possible Ia afferent conduction in human participants with SCI. Specifically, we examined potential presynaptic facilitation from tonic PAD and extensor H-reflex suppression from post-activation depression

With a better understanding of how normal Ia sensory transmission in controlled in the spinal cord and how this control changes after injury to the CNS, more targeted treatment approaches can be developed for the treatment of spasticity and motor dysfunction. These treatment approaches have the potential to target spasticity more specifically without diminishing, or could even enhance, preserved general motor function and limit the number of adverse side effects such as sedation, fatigue and nausea that are commonly associated with currently available pharmacological treatments.

References

Adams MM & Hicks AL. (2005). Spasticity after spinal cord injury. *Spinal Cord* **43,** 577-586.

Ahuja CS, Wilson JR, Nori S, Kotter MRN, Druschel C, Curt A & Fehlings MG. (2017). Traumatic spinal cord injury. *Nat Rev Dis Primers* **3,** 17018.

Aimonetti JM, Vedel JP, Schmied A & Pagni S. (2000). Distribution of presynaptic inhibition on type-identified motoneurones in the extensor carpi radialis pool in man. *The Journal of physiology* **522 Pt 1,** 125-135.

Akay T, Tourtellotte WG, Arber S & Jessell TM. (2014). Degradation of mouse locomotor pattern in the absence of proprioceptive sensory feedback. *Proc Natl Acad Sci U S A* **111,** 16877-16882.

Anderson KD. (2004). Targeting recovery: priorities of the spinal cord-injured population. *J Neurotrauma* **21,** 1371-1383.

Angeli CA, Boakye M, Morton RA, Vogt J, Benton K, Chen Y, Ferreira CK & Harkema SJ. (2018). Recovery of Over-Ground Walking after Chronic Motor Complete Spinal Cord Injury. *N Engl J Med* **379,** 1244-1250.

Ashby P & Verrier M. (1975). Neurophysiological changes following spinal cord lesions in man. *Can J Neurol Sci* **2,** 91-100.

Ashby P & Verrier M. (1976). Neurophysiologic changes in hemiplegia. Possible explanation for the initial disparity between muscle tone and tendon reflexes. *Neurology* **26,** 1145-1151.

Ashby P, Verrier M & Lightfoot E. (1974). Segmental reflex pathways in spinal shock and spinal spasticity in man. *J Neurol Neurosurg Psychiatry* **37,** 1352-1360.

Aymard C, Katz R, Lafitte C, Lo E, Penicaud A, Pradat-Diehl P & Raoul S. (2000). Presynaptic inhibition and homosynaptic depression: a comparison between lower and upper limbs in normal human subjects and patients with hemiplegia. *Brain* **123 (Pt 8),** 1688-1702.

Baker LL & Chandler SH. (1987). Characterization of postsynaptic potentials evoked by sural nerve stimulation in hindlimb motoneurons from acute and chronic spinal cats. *Brain Res* **420,** 340-350.

Baker SN. (2011). The primate reticulospinal tract, hand function and functional recovery. *J Physiol* **589,** 5603-5612.

Baker SN & Perez MA. (2017). Reticulospinal Contributions to Gross Hand Function after Human Spinal Cord Injury. *J Neurosci* **37,** 9778-9784.

Ballermann M & Fouad K. (2006). Spontaneous locomotor recovery in spinal cord injured rats is accompanied by anatomical plasticity of reticulospinal fibers. *Eur J Neurosci* **23,** 1988-1996.

Behrman AL & Harkema SJ. (2000). Locomotor training after human spinal cord injury: a series of case studies. *Phys Ther* **80,** 688-700.

Bellardita C, Caggiano V, Leiras R, Caldeira V, Fuchs A, Bouvier J, Low P & Kiehn O. (2017). Spatiotemporal correlation of spinal network dynamics underlying spasms in chronic spinalized mice. *Elife* **6**.

Bennett DJ, Sanelli L, Cooke CL, Harvey PJ & Gorassini MA. (2004). Spastic long-lasting reflexes in the awake rat after sacral spinal cord injury. *J Neurophysiol* **91,** 2247-2258.

Berardelli A, Day BL, Marsden CD & Rothwell JC. (1987). Evidence favouring presynaptic inhibition between antagonist muscle afferents in the human forearm. *J Physiol* **391,** 71-83.

Biering-Sorensen B, Kristensen IB, Kjaer M & Biering-Sorensen F. (2009). Muscle after spinal cord injury. *Muscle Nerve* **40,** 499-519.

Burke D, Gracies JM, Meunier S & Pierrot-Deseilligny E. (1992). Changes in presynaptic inhibition of afferents to propriospinal-like neurones in man during voluntary contractions. *J Physiol* **449,** 673-687.

Capaday C, Lavoie BA & Comeau F. (1995). Differential effects of a flexor nerve input on the human soleus H-reflex during standing versus walking. *Can J Physiol Pharmacol* **73,** 436-449.

Chen Y, He Y & DeVivo MJ. (2016). Changing Demographics and Injury Profile of New Traumatic Spinal Cord Injuries in the United States, 1972-2014. *Arch Phys Med Rehabil* **97,** 1610-1619.

Choo AM, Liu J, Lam CK, Dvorak M, Tetzlaff W & Oxland TR. (2007). Contusion, dislocation, and distraction: primary hemorrhage and membrane permeability in distinct mechanisms of spinal cord injury. *J Neurosurg Spine* **6,** 255-266.

Clarkson AN, Huang BS, Macisaac SE, Mody I & Carmichael ST. (2010). Reducing excessive GABA-mediated tonic inhibition promotes functional recovery after stroke. *Nature* **468,** 305-309.

Cramer SC, Lastra L, Lacourse MG & Cohen MJ. (2005). Brain motor system function after chronic, complete spinal cord injury. *Brain* **128,** 2941-2950.

Crone C, Johnsen LL, Biering-Sorensen F & Nielsen JB. (2003). Appearance of reciprocal facilitation of ankle extensors from ankle flexors in patients with stroke or spinal cord injury. *Brain* **126,** 495-507.

Crone C & Nielsen J. (1989). Methodological implications of the post activation depression of the soleus H-reflex in man. *Experimental brain research* **78,** 28-32.

Crone C, Nielsen J, Petersen N, Ballegaard M & Hultborn H. (1994). Disynaptic reciprocal inhibition of ankle extensors in spastic patients. *Brain* **117 (Pt 5),** 1161-1168.

Crowe MJ, Bresnahan JC, Shuman SL, Masters JN & Beattie MS. (1997). Apoptosis and delayed degeneration after spinal cord injury in rats and monkeys. *Nat Med* **3,** 73-76.

Curtis DR & Eccles JC. (1960). Synaptic action during and after repetitive stimulation. *The Journal of physiology* **150,** 374-398.

Curtis DR, Gynther BD, Lacey G & Beattie DT. (1997). Baclofen: reduction of presynaptic calcium influx in the cat spinal cord in vivo. *Exp Brain Res* **113,** 520-533.

Curtis DR & Lacey G. (1994). GABA-B receptor-mediated spinal inhibition. *Neuroreport* **5,** 540-542.

Curtis DR & Lacey G. (1998). Prolonged GABA(B) receptor-mediated synaptic inhibition in the cat spinal cord: an in vivo study. *Exp Brain Res* **121,** 319-333.

Curtis DR & Lodge D. (1982). The depolarization of feline ventral horn group Ia spinal afferent terminations by GABA. *Exp Brain Res* **46,** 215-233.

Cushing S, Bui T & Rose PK. (2005). Effect of nonlinear summation of synaptic currents on the input-output properties of spinal motoneurons. *J Neurophysiol* **94,** 3465-3478.

D'Amico JM, Condliffe EG, Martins KJ, Bennett DJ & Gorassini MA. (2014). Recovery of neuronal and network excitability after spinal cord injury and implications for spasticity. *Front Integr Neurosci* **8,** 36.

de Leon RD, Hodgson JA, Roy RR & Edgerton VR. (1998). Locomotor capacity attributable to step training versus spontaneous recovery after spinalization in adult cats. *J Neurophysiol* **79,** 1329-1340.

Delwaide PJ & Oliver E. (1988). Short-latency autogenic inhibition (IB inhibition) in human spasticity. *J Neurol Neurosurg Psychiatry* **51,** 1546-1550.

Devivo MJ. (2012). Epidemiology of traumatic spinal cord injury: trends and future implications. *Spinal Cord* **50,** 365-372.

DeVivo MJ & Chen Y. (2011). Trends in new injuries, prevalent cases, and aging with spinal cord injury. *Arch Phys Med Rehabil* **92,** 332-338.

Dietz V. (2000). Spastic movement disorder. *Spinal Cord* **38,** 389-393.

Drew GM, Siddall PJ & Duggan AW. (2001). Responses of spinal neurones to cutaneous and dorsal root stimuli in rats with mechanical allodynia after contusive spinal cord injury. *Brain Res* **893,** 59-69.

Duchen MR. (1986). Excitation of mouse motoneurones by GABA-mediated primary afferent depolarization. *Brain Res* **379,** 182-187.

Eccles JC, Eccles RM & Magni F. (1961a). Central inhibitory action attributable to presynaptic depolarization produced by muscle afferent volleys. *J Physiol* **159,** 147-166.

Eccles JC, Kozak W & Magni F. (1961b). Dorsal root reflexes of muscle group I afferent fibres. *J Physiol* **159,** 128-146.

Eccles JC, Magni F & Willis WD. (1962a). Depolarization of central terminals of Group I afferent fibres from muscle. *The Journal of physiology* **160,** 62-93.

Eccles JC, Magni F & Willis WD. (1962b). Depolarization of central terminals of Group I afferent fibres from muscle. *J Physiol* **160,** 62-93.

Eccles JC & Rall W. (1951). Effects induced in a monosynaptic reflex path by its activation. *Journal of neurophysiology* **14,** 353-376.

Eccles JC, Schmidt RF & Willis WD. (1962c). Presynaptic inhibition of the spinal monosynaptic reflex pathway. *J Physiol* **161,** 282-297.

Edstrom L. (1970). Selective changes in the sizes of red and white muscle fibres in upper motor lesions and Parkinsonism. *J Neurol Sci* **11,** 537-550.

El-Tohamy A & Sedgwick EM. (1983). Spinal inhibition in man: depression of the soleus H reflex by stimulation of the nerve to the antagonist muscle. *J Physiol* **337,** 497-508.

Faist M, Dietz V & Pierrot-Deseilligny E. (1996). Modulation, probably presynaptic in origin, of monosynaptic Ia excitation during human gait. *Exp Brain Res* **109,** 441-449.

Faist M, Mazevet D, Dietz V & Pierrot-Deseilligny E. (1994). A quantitative assessment of presynaptic inhibition of Ia afferents in spastics. Differences in hemiplegics and paraplegics. *Brain* **117 (Pt 6),** 1449-1455.

Fisher MA. (1992). AAEM Minimonograph #13: H reflexes and F waves: physiology and clinical indications. *Muscle Nerve* **15,** 1223-1233.

Fung J & Barbeau H. (1994). Effects of conditioning cutaneomuscular stimulation on the soleus H-reflex in normal and spastic paretic subjects during walking and standing. *Journal of neurophysiology* **72,** 2090-2104.

Gallagher JP, Higashi H & Nishi S. (1978). Characterization and ionic basis of GABA-induced depolarizations recorded in vitro from cat primary afferent neurones. *The Journal of physiology* **275,** 263-282.

Gorassini MA, Knash ME, Harvey PJ, Bennett DJ & Yang JF. (2004). Role of motoneurons in the generation of muscle spasms after spinal cord injury. *Brain* **127,** 2247-2258.

Goulart F, Valls-Sole J & Alvarez R. (2000). Posture-related changes of soleus H-reflex excitability. *Muscle Nerve* **23,** 925-932.

Grey MJ, Klinge K, Crone C, Lorentzen J, Biering-Sorensen F, Ravnborg M & Nielsen JB. (2008). Post-activation depression of soleus stretch reflexes in healthy and spastic humans. *Exp Brain Res* **185,** 189-197.

Hari K, Lucas-Osma AM, Metz K, Lin S, Pardell N, Roszko D, Black S, Minarik A, Singla R, Stephens MJ, Fouad K, Jones KE, Gorassini M, Fenrich KK, Li Y & Bennett DJ. (2021). Nodal GABA facilitates axon spike transmission in the spinal cord. *BioRxiv*.

Heckmann CJ, Gorassini MA & Bennett DJ. (2005). Persistent inward currents in motoneuron dendrites: implications for motor output. *Muscle Nerve* **31,** 135-156.

Henneman E, Luscher HR & Mathis J. (1984). Simultaneously active and inactive synapses of single Ia fibres on cat spinal motoneurones. *The Journal of physiology* **352,** 147-161.

Hofstoetter US, Freundl B, Binder H & Minassian K. (2019). Recovery cycles of posterior root-muscle reflexes evoked by transcutaneous spinal cord stimulation and of the H reflex in individuals with intact and injured spinal cord. *PLoS One* **14,** e0227057.

Hughes DI, Mackie M, Nagy GG, Riddell JS, Maxwell DJ, Szabo G, Erdelyi F, Veress G, Szucs P, Antal M & Todd AJ. (2005). P boutons in lamina IX of the rodent spinal cord express high levels of glutamic acid decarboxylase-65 and originate from cells in deep medial dorsal horn. *Proc Natl Acad Sci U S A* **102,** 9038-9043.

Hultborn H. (2006). Spinal reflexes, mechanisms and concepts: from Eccles to Lundberg and beyond. *Prog Neurobiol* **78,** 215-232.

Hultborn H, Illert M, Nielsen J, Paul A, Ballegaard M & Wiese H. (1996). On the mechanism of the post-activation depression of the H-reflex in human subjects. *Experimental brain research* **108,** 450-462.

Hultborn H, Meunier S, Morin C & Pierrot-Deseilligny E. (1987a). Assessing changes in presynaptic inhibition of I a fibres: a study in man and the cat. *J Physiol* **389,** 729-756.

Hultborn H, Meunier S, Pierrot-Deseilligny E & Shindo M. (1987b). Changes in presynaptic inhibition of Ia fibres at the onset of voluntary contraction in man. *J Physiol* **389,** 757-772.

Iles JF. (1996). Evidence for cutaneous and corticospinal modulation of presynaptic inhibition of Ia afferents from the human lower limb. *J Physiol* **491 (Pt 1),** 197-207.

Iles JF & Pisini JV. (1992). Cortical modulation of transmission in spinal reflex pathways of man. *J Physiol* **455,** 425-446.

Iles JF & Roberts RC. (1987). Inhibition of monosynaptic reflexes in the human lower limb. *J Physiol* **385,** 69-87.

Jankowska E, McCrea D, Rudomin P & Sykova E. (1981a). Observations on neuronal pathways subserving primary afferent depolarization. *J Neurophysiol* **46,** 506-516.

Jankowska E, McCrea D, Rudomin P & Sykova E. (1981b). Observations on neuronal pathways subserving primary afferent depolarization. *Journal of neurophysiology* **46,** 506-516.

Kangrga I, Jiang MC & Randic M. (1991). Actions of (-)-baclofen on rat dorsal horn neurons. *Brain Res* **562,** 265-275.

Kapitza S, Zorner B, Weinmann O, Bolliger M, Filli L, Dietz V & Schwab ME. (2012). Tail spasms in rat spinal cord injury: changes in interneuronal connectivity. *Exp Neurol* **236,** 179-189.

Khan AS, Patrick SK, Roy FD, Gorassini MA & Yang JF. (2016). Training-Specific Neural Plasticity in Spinal Reflexes after Incomplete Spinal Cord Injury. *Neural Plast* **2016,** 6718763.

Krenz NR & Weaver LC. (1998). Sprouting of primary afferent fibers after spinal cord transection in the rat. *Neuroscience* **85,** 443-458.

Kumru H, Albu S, Valls-Sole J, Murillo N, Tormos JM & Vidal J. (2015). Influence of spinal cord lesion level and severity on H-reflex excitability and recovery curve. *Muscle Nerve* **52,** 616-622.

Lalonde NR & Bui TV. (2021). Do spinal circuits still require gating of sensory information by presynaptic inhibition after spinal cord injury? *Current Opinion in Physiology* **19,** 113-118.

Lee JK, Emch GS, Johnson CS & Wrathall JR. (2005). Effect of spinal cord injury severity on alterations of the H-reflex. *Exp Neurol* **196,** 430-440.

Levy RA & Anderson EG. (1972). The effect of the GABA antagonists bicuculline and picrotoxin on primary afferent terminal excitability. *Brain Res* **43,** 171-180.

Li Y & Bennett DJ. (2003). Persistent sodium and calcium currents cause plateau potentials in motoneurons of chronic spinal rats. *J Neurophysiol* **90,** 857-869.

Li Y, Li X, Harvey PJ & Bennett DJ. (2004). Effects of baclofen on spinal reflexes and persistent inward currents in motoneurons of chronic spinal rats with spasticity. *J Neurophysiol* **92,** 2694-2703.

Liu M, Wu W, Li H, Li S, Huang LT, Yang YQ, Sun Q, Wang CX, Yu Z & Hang CH. (2015). Necroptosis, a novel type of programmed cell death, contributes to early neural cells damage after spinal cord injury in adult mice. *J Spinal Cord Med* **38,** 745-753.

Lucas-Osma AM, Li Y, Lin S, Black S, Singla R, Fouad K, Fenrich KK & Bennett DJ. (2018). Extrasynaptic proportional, variant5GABAA receptors on proprioceptive afferents produce a tonic depolarization that modulates sodium channel function in the rat spinal cord. *J Neurophysiol*.

Magladery JW, Teasdall RD, Park AM & Languth HW. (1952). Electrophysiological studies of reflex activity in patients with lesions of the nervous system. I. A comparison of spinal motoneurone excitability following afferent nerve volleys in normal persons and patients with upper motor neurone lesions. *Bull Johns Hopkins Hosp* **91,** 219-244; passim.

Mailis A & Ashby P. (1990). Alterations in group Ia projections to motoneurons following spinal lesions in humans. *J Neurophysiol* **64,** 637-647.

Masland WS. (1972). Facilitation during the H-reflex recovery cycle. *Arch Neurol* **26,** 313-319.

Mende M, Fletcher EV, Belluardo JL, Pierce JP, Bommareddy PK, Weinrich JA, Kabir ZD, Schierberl KC, Pagiazitis JG, Mendelsohn AI, Francesconi A, Edwards RH, Milner TA, Rajadhyaksha AM, van Roessel PJ, Mentis GZ & Kaltschmidt JA. (2016). Sensory-Derived Glutamate Regulates Presynaptic Inhibitory Terminals in Mouse Spinal Cord. *Neuron* **90,** 1189-1202.

Meunier S & Pierrot-Deseilligny E. (1998). Cortical control of presynaptic inhibition of Ia afferents in humans. *Experimental brain research* **119,** 415-426.

Mirbagheri MM, Barbeau H, Ladouceur M & Kearney RE. (2001). Intrinsic and reflex stiffness in normal and spastic, spinal cord injured subjects. *Exp Brain Res* **141,** 446-459.

Mizuno Y, Tanaka R & Yanagisawa N. (1971). Reciprocal group I inhibition on triceps surae motoneurons in man. *J Neurophysiol* **34,** 1010-1017.

Mott FW & Sherrington CS. (1895). Experiments upon the influence of sensory nerves upon movements and nutrition of the limbs. *Proceedings of the Royal Society* **B,** 481-488.

Murray KC, Stephens MJ, Ballou EW, Heckman CJ & Bennett DJ. (2011a). Motoneuron excitability and muscle spasms are regulated by 5-HT2B and 5-HT2C receptor activity. *J Neurophysiol* **105,** 731-748.

Murray KC, Stephens MJ, Rank M, D'Amico J, Gorassini MA & Bennett DJ. (2011b). Polysynaptic excitatory postsynaptic potentials that trigger spasms after spinal cord injury in rats are inhibited by 5-HT1B and 5-HT1F receptors. *J Neurophysiol* **106,** 925-943.

Nacimiento W, Sappok T, Brook GA, Toth L, Schoen SW, Noth J & Kreutzberg GW. (1995). Structural changes of anterior horn neurons and their synaptic input caudal to a low thoracic spinal cord hemisection in the adult rat: a light and electron microscopic study. *Acta Neuropathol* **90,** 552-564.

Nakashima K, Rothwell JC, Day BL, Thompson PD & Marsden CD. (1990). Cutaneous effects on presynaptic inhibition of flexor Ia afferents in the human forearm. *J Physiol* **426,** 369-380.

Neher E & Sakaba T. (2001). Estimating transmitter release rates from postsynaptic current fluctuations. *J Neurosci* **21,** 9638-9654.

Nicol MJ & Walmsley B. (1991). A serial section electron microscope study of an identified Ia afferent collateral in the cat spinal cord. *J Comp Neurol* **314,** 257-277.

Nielsen J & Kagamihara Y. (1993). The regulation of presynaptic inhibition during co-contraction of antagonistic muscles in man. *J Physiol* **464,** 575-593.

Nielsen J, Petersen N, Ballegaard M, Biering-Sorensen F & Kiehn O. (1993a). H-reflexes are less depressed following muscle stretch in spastic spinal cord injured patients than in healthy subjects. *Experimental brain research* **97,** 173-176.

Nielsen J, Petersen N, Ballegaard M, Biering-Sorensen F & Kiehn O. (1993b). H-reflexes are less depressed following muscle stretch in spastic spinal cord injured patients than in healthy subjects. *Exp Brain Res* **97,** 173-176.

Nielsen J, Petersen N & Crone C. (1995). Changes in transmission across synapses of Ia afferents in spastic patients. *Brain* **118 (Pt 4),** 995-1004.

Noonan VK, Fingas M, Farry A, Baxter D, Singh A, Fehlings MG & Dvorak MF. (2012). Incidence and prevalence of spinal cord injury in Canada: a national perspective. *Neuroepidemiology* **38,** 219-226.

Norton JA, Bennett DJ, Knash ME, Murray KC & Gorassini MA. (2008). Changes in sensory-evoked synaptic activation of motoneurons after spinal cord injury in man. *Brain* **131,** 1478-1491.

Ondarza AB, Ye Z & Hulsebosch CE. (2003). Direct evidence of primary afferent sprouting in distant segments following spinal cord injury in the rat: colocalization of GAP-43 and CGRP. *Exp Neurol* **184,** 373-380.

Oyinbo CA. (2011). Secondary injury mechanisms in traumatic spinal cord injury: a nugget of this multiply cascade. *Acta Neurobiol Exp (Wars)* **71,** 281-299.

Pierce JP & Mendell LM. (1993). Quantitative ultrastructure of Ia boutons in the ventral horn: scaling and positional relationships. *J Neurosci* **13,** 4748-4763.

Pierrot-Deseilligny E, Katz R & Morin C. (1979). Evidence of Ib inhibition in human subjects. *Brain Res* **166,** 176-179.

Prochazka A. (2015). Sensory control of normal movement and of movement aided by neural prostheses. *J Anat* **227,** 167-177.

Quadri SA, Farooqui M, Ikram A, Zafar A, Khan MA, Suriya SS, Claus CF, Fiani B, Rahman M, Ramachandran A, Armstrong IIT, Taqi MA & Mortazavi MM. (2018). Recent update on basic mechanisms of spinal cord injury. *Neurosurg Rev*.

Rabchevsky AG & Kitzman PH. (2011). Latest approaches for the treatment of spasticity and autonomic dysreflexia in chronic spinal cord injury. *Neurotherapeutics* **8,** 274-282.

Rank MM, Murray KC, Stephens MJ, D'Amico J, Gorassini MA & Bennett DJ. (2011). Adrenergic receptors modulate motoneuron excitability, sensory synaptic transmission and muscle spasms after chronic spinal cord injury. *J Neurophysiol* **105,** 410-422.

Robertson B & Taylor WR. (1986). Effects of gamma-aminobutyric acid and (-)-baclofen on calcium and potassium currents in cat dorsal root ganglion neurones in vitro. *Br J Pharmacol* **89,** 661-672.

Roby-Brami A & Bussel B. (1990). Effects of flexor reflex afferent stimulation on the soleus H reflex in patients with a complete spinal cord lesion: evidence for presynaptic inhibition of Ia transmission. *Exp Brain Res* **81,** 593-601.

Rossignol S, Drew T, Brustein E & Jiang W. (1999). Locomotor performance and adaptation after partial or complete spinal cord lesions in the cat. *Prog Brain Res* **123,** 349-365.

Rothwell JC, Traub MM, Day BL, Obeso JA, Thomas PK & Marsden CD. (1982). Manual motor performance in a deafferented man. *Brain* **105 (Pt 3),** 515-542.

Rudomin P. (1999). Presynaptic selection of afferent inflow in the spinal cord. *J Physiol Paris* **93,** 329-347.

Rudomin P & Schmidt RF. (1999). Presynaptic inhibition in the vertebrate spinal cord revisited. *Exp Brain Res* **129,** 1-37.

Russ JB, Verina T, Comer JD, Comi AM & Kaltschmidt JA. (2013). Corticospinal tract insult alters GABAergic circuitry in the mammalian spinal cord. *Front Neural Circuits* **7,** 150.

Schanne FA, Kane AB, Young EE & Farber JL. (1979). Calcium dependence of toxic cell death: a final common pathway. *Science* **206,** 700-702.

Schindler-Ivens S & Shields RK. (2000). Low frequency depression of H-reflexes in humans with acute and chronic spinal-cord injury. *Exp Brain Res* **133,** 233-241.

Senter HJ & Venes JL. (1979). Loss of autoregulation and posttraumatic ischemia following experimental spinal cord trauma. *J Neurosurg* **50,** 198-206.

Shefner JM, Berman SA, Sarkarati M & Young RR. (1992a). Recurrent inhibition is increased in patients with spinal cord injury. *Neurology* **42,** 2162-2168.

Shefner JM, Buchthal F & Krarup C. (1992b). Recurrent potentials in human peripheral sensory nerve: possible evidence of primary afferent depolarization of the spinal cord. *Muscle Nerve* **15,** 1354-1363.

Silva NA, Sousa N, Reis RL & Salgado AJ. (2014). From basics to clinical: a comprehensive review on spinal cord injury. *Prog Neurobiol* **114,** 25-57.

Simon CM, Sharif S, Tan RP & LaPlaca MC. (2009). Spinal cord contusion causes acute plasma membrane damage. *J Neurotrauma* **26,** 563-574.

Spaulding SJ, Hayes KC & Harburn KL. (1987). Periodicity in the Hoffmann reflex recovery curve. *Exp Neurol* **98,** 13-25.

Taborikova H & Sax DS. (1969). Conditioning of H-reflexes by a preceding subthreshold H-reflex stimulus. *Brain* **92,** 203-212.

Tillakaratne NJ, Mouria M, Ziv NB, Roy RR, Edgerton VR & Tobin AJ. (2000). Increased expression of glutamate decarboxylase (GAD(67)) in feline lumbar spinal cord after complete thoracic spinal cord transection. *J Neurosci Res* **60,** 219-230.

Vincent JA, Gabriel HM, Deardorff AS, Nardelli P, Fyffe REW, Burkholder T & Cope TC. (2017). Muscle proprioceptors in adult rat: mechanosensory signaling and synapse distribution in spinal cord. *J Neurophysiol* **118,** 2687-2701.

Voerman GE, Gregoric M & Hermens HJ. (2005). Neurophysiological methods for the assessment of spasticity: the Hoffmann reflex, the tendon reflex, and the stretch reflex. *Disabil Rehabil* **27,** 33-68.

Wernig A, Muller S, Nanassy A & Cagol E. (1995). Laufband therapy based on 'rules of spinal locomotion' is effective in spinal cord injured persons. *Eur J Neurosci* **7,** 823-829.

Willis WD. (2006). John Eccles' studies of spinal cord presynaptic inhibition. *Prog Neurobiol* **78,** 189-214.

Willis WD, Jr. (1999). Dorsal root potentials and dorsal root reflexes: a double-edged sword. *Exp Brain Res* **124,** 395-421.

Chapter 2: Facilitation of Ia afferent axon conduction to motoneurons during cortical or sensory evoked primary afferent depolarization (PAD) in humans

Krista Metz[1,6], Isabella Concha-Matos[1,6], Yaqing Li[5,6], Babak Afsharipour[1,6], Christopher K. Thompson[2], Francesco Negro[3], Kathrina Quinlan[4], David J. Bennett[5,6], and Monica A. Gorassini[1,6]

[1] Biomedical Engineering, Faculty of Medicine and Dentistry, University of Alberta, Edmonton Canada

[2] Health and Rehabilitation Sciences, Temple University, Philadelphia United States

[3] Clinical and Experimental Sciences, Universita degli Studi di Brescia, Brescia Italia

[4] Biomedical and Pharmaceutical Sciences, College of Pharmacy, University of Rhode Island, Kingston United States

[5] Faculty of Rehabilitation Medicine, University of Alberta, Edmonton Canada

[6] Neuroscience and Mental Health Institute, University of Alberta, Edmonton Canada

Running title: Facilitation of sensory axon conduction during PAD in humans.

Key words: presynaptic inhibition, proprioceptive afferents, H-reflex

Table of Contents category: Neuroscience

Preprint link: https://www.biorxiv.org/content/10.1101/2021.04.20.440509v1

Figures: 8

Corresponding Author: Monica Gorassini, monica.gorassini@ualberta.ca; ORCID: 0000-0003-3079-6129; 5005-A Katz Group Building, University of Alberta, Edmonton, AB, (Canada) T6G 2E1

Current address for Y Li:

Department of Physiology, School of Medicine, Emory University, Atlanta Georgia

Key Points Summary

- Controlled execution of posture and movement requires continual and adjusted feedback from peripheral sensory pathways, especially those that carry information about body position, movement, and effort.
- It was previously thought that the flow of this proprioceptive feedback was only reduced by GABAergic neurons in the spinal cord that sent projections to the terminal endings of sensory axons.
- Based on new findings in rodents, we provide complimentary evidence in humans that sensory and corticospinal pathways that are known to activate these GABAergic neurons can also increase the flow of proprioceptive feedback to motoneurons in the spinal cord.
- These findings can be applied to investigate how changes in spinal GABA neurons from brain and spinal cord injury, and their activation by spared sensory and descending pathways, control the flow of proprioceptive feedback and its effects on residual motor function and involuntary muscle spasticity.

Figure 2.0: Abstract Figure Legend

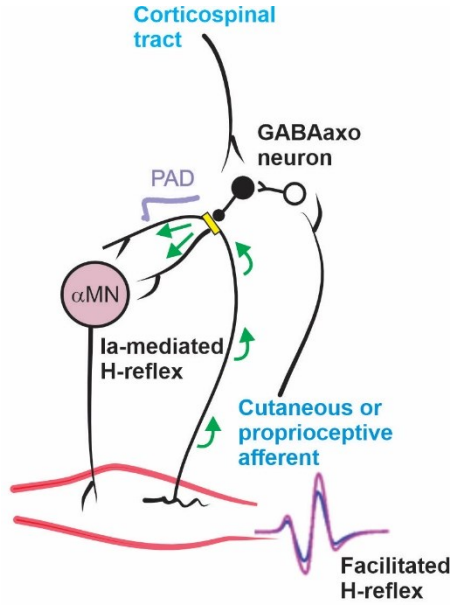

Activation of gamma-aminobutyric-acid (GABA) receptors on or near the nodes of Ranvier in Ia afferents (nodes, yellow) cause a net efflux of chloride ions to produce primary afferent depolarization (PAD, purple). PAD increases action potential conduction along the Ia afferent (green arrows) by facilitating sodium channels at the nodes, which reduces commonly occurring failure of action potentials at myelinated axon branchpoints, resulting in a larger and more secure activation of spinal motoneurons (aMN) by the Ia afferents. In humans we show that corticospinal and sensory pathways, that are known from animal studies to activate GABA neurons with axoaxonic connections to the Ia afferent (PAD $GABA_{axo}$ neurons), can facilitate conduction in Ia afferents as assessed by the H-reflex, with a time course similar to phasic and tonic PAD. These results support the idea that activation of corticospinal and sensory pathways help to secure Ia afferent activation of spinal motoneurons important for voluntary and reflex control of movement.

Abstract

Sensory and corticospinal (CST) pathways activate spinal GABAergic interneurons with axo-axonic connections onto proprioceptive (Ia) afferents that depolarize them (termed primary afferent depolarization, PAD). In rodents sensory-evoked PAD is produced by $GABA_A$ receptors at nodes of Ranvier in Ia-afferents, rather than at presynaptic terminals, and facilitates spike propagation to motoneurons by preventing branch point failures, rather than causing presynaptic inhibition. Here we examined if activation of Ia-PAD by sensory and CST pathways can also facilitate Ia-afferent activation of human motoneurons via the H-reflex. H-reflexes in several lower limb muscles were facilitated by prior conditioning from low-threshold proprioceptive,

cutaneous or CST pathways, with a similar time course (~200 ms) to phasic PAD measured in rodent Ia-afferents. Long trains of repeated cutaneous or proprioceptive afferent stimulation produced long-lasting facilitation of the H-reflex for up to 2 minutes, consistent with tonic PAD in rodent Ia-afferents mediated by nodal α5-$GABA_A$ receptors for similar stimulation trains. Facilitation of the conditioned H-reflexes was not mediated by direct facilitation of the motoneurons because isolated stimulation of sensory or CST pathways did not modulate the firing rate of tonically activated motor units in tested muscles. Furthermore, cutaneous conditioning increased the firing probability of a single motor unit (motoneuron) during the H-reflex without increasing its firing rate at this time, indicating that the underlying excitatory postsynaptic potential (EPSP) was more probable, but not larger. These results are consistent with sensory and CST pathways activating nodal $GABA_A$ receptors that reduce intermittent failure of action potentials propagating into Ia-afferent branches.

Introduction

Peripheral sensory pathways in the spinal cord regulate the transmission of action potentials in other sensory axons through a network of interneurons that release gamma-aminobutyric-acid (GABA) onto these axons. Specifically, proprioceptive or cutaneous afferents activate excitatory glutamatergic interneurons, which in turn synapse onto specialized GABAergic interneurons (termed $GABA_{axo}$ neurons; GAD2+) with axo-axonic contacts onto other afferents, forming the classic tri-synaptic pathway described in (Jankowska *et al.*, 1981b; Alvarez, 1998; Lalonde & Bui, 2021). The activation of $GABA_A$ receptors on these sensory axons produces a local depolarization of the afferent due to an outward flow of chloride ions (Gallagher *et al.*, 1978a) [also reviewed in (Rudomin & Schmidt, 1999; Willis, 1999)]. Although paradoxically excitatory, this $GABA_A$ receptor-mediated depolarization (referred to as primary afferent depolarization, PAD) was previously thought to shunt or inactivate action potentials invading the afferent terminal, thereby inhibiting neurotransmitter release to produce presynaptic inhibition (Willis, 2006). This inhibitory role was postulated because the PAD evoked by a flexor afferent followed a similar time course to the suppression of Ia-mediated excitatory postsynaptic potentials (EPSP) in an extensor motoneuron when conditioned by the same flexor afferent (Frank & Fortes, 1957; Eccles *et al.*, 1961a; Willis, 1999). Because there appeared to be no direct effects of the conditioning flexor nerve stimulation on the motoneuron a presynaptic, inhibitory mechanism of PAD on afferent transmission was assumed and this idea has prevailed over the past 60 years (Willis, 2006; Zimmerman *et al.*, 2019). However, recent studies reveal that $GABA_A$ receptors are generally not found on Ia afferent terminals (Alvarez *et al.*, 1996; Lucas-Osma *et al.*, 2018b; Hari *et al.*, 2021) and do not depolarize the Ia afferent terminals during PAD (Lucas-Osma *et al.*, 2018b; Hari *et al.*, 2021), conflicting with the concept of

presynaptic inhibition. Instead, $GABA_A$ receptors are found mostly at or within 100 mm of the nodes of Ranvier (nodes) in the many large, myelinated branches of Ia afferents throughout the dorsal and ventral spinal cord. Accordingly, a novel role of GABA in facilitating, rather than inhibiting, afferent conduction has been proposed where the activation of $GABA_A$ receptors in the afferent nodes produces a local depolarization that facilitates adjacent sodium channels to secure action potential propagation and decreases downstream branch point failure (termed nodal facilitation) (Hari *et al*., 2022). In rodents, these $GABA_A$ receptors on the dorsal Ia afferents are readily activated by cutaneous or pain afferent pathways and produce nodal facilitation, rather than presynaptic inhibition, of the Ia-mediated monosynaptic reflex (Lucas-Osma *et al.*, 2018b; Hari *et al.*, 2021). Our preliminary data from the soleus muscle suggests that this may also occur in humans following cutaneous afferent conditioning to evoke PAD (Hari *et al.*, 2021). In this paper we expand these studies to provide further evidence for nodal facilitation in human Ia afferents by examining additional muscle groups with various forms of conditioning stimuli to induce PAD. The conditioning included stimulation of proprioceptive and cutaneous afferents and descending corticospinal (CST) motor pathways, the latter which directly synapse onto $GABA_{axo}$ neurons (Ueno *et al.*, 2018) and thus, should produce a PAD as previously shown for afferents in the dorsal horn following trains of motor cortex stimulation (Carpenter *et al.*, 1963).

Previous studies in humans have suggested that cutaneous and CST pathways reduce inhibition in Ia afferents produced by a conditioning proprioceptive stimulation, and this was argued to be mediated by dis-facilitating the $GABA_{axo}$ interneurons within the classic tri-synaptic PAD pathway (Rudomin *et al.*, 1983), effectively causing a reduction of presynaptic inhibition (Berardelli *et al.*, 1987; Iles & Roberts, 1987; Nakashima *et al.*, 1990; Iles, 1996; Meunier & Pierrot-Deseilligny, 1998a; Aimonetti *et al.*, 2000b). Specifically, as in animal experiments,

conditioning by a proprioceptive antagonist nerve was used to suppress the agonist H-reflex and this was assumed (likely incorrectly) to be a demonstration of $GABA_A$ receptor-mediated presynaptic inhibition of the Ia afferents mediating the H-reflex. Then, a prior activation of cutaneous or CST pathways before the conditioning antagonist nerve stimulation was found to reduce this H-reflex suppression. It was proposed that these cutaneous and CST pathways reduced PAD and presynaptic inhibition of the Ia afferent terminals (H-reflexes) by decreasing activity in the $GABA_{axo}$ interneurons. However, recent direct recordings from Ia afferents indicate that a cutaneous conditioning stimulation increases, rather than decreases, $GABA_{axo}$ activity and PAD (Lucas-Osma *et al.*, 2018b; Hari *et al.*, 2021). Thus, we propose a simpler mechanism whereby cutaneous and CST pathways *facilitate* conduction in Ia afferents (and H-reflexes) by activating the $GABA_{axo}$ interneurons that mediate nodal depolarizations to reduce action potential failure at dorsally located branch points. This would not only explain the older data that show cutaneous and CST conditioning causes a reduced inhibition of the H-reflex, but also accounts for the direct facilitation of the Ia afferents mediating the H-reflex by these conditioning pathways. Here we provide further evidence to support this view.

There are two types of PAD that have been measured in proprioceptive and cutaneous afferents (Rudomin & Schmidt, 1999; Willis, 1999; Delgado-Lezama *et al.*, 2013; Lucas-Osma *et al.*, 2018b; Hari *et al.*, 2021). The first is a short-duration (phasic) depolarization lasting for 100 to 200 ms that is evoked from a brief stimulation train (1-3 pulses at 200 Hz) of low threshold proprioceptive, cutaneous or pain afferents (Eccles *et al.*, 1962a; Willis, 2006; Lucas-Osma *et al.*, 2018b). This phasic PAD is mediated by synaptic $GABA_A$ receptors with α1, α2 and γ2 subunits that are located adjacent to sodium channels in afferent nodes (Hari *et al.*, 2021). The second type of PAD is a longer-duration (tonic) depolarization that lasts for 10's of seconds

(Eccles *et al.*, 1962b) and is activated by longer trains of stimulation, most effectively from a fast stimulation train (0.5 s at 200 Hz) or from a relatively slower but longer frequency train (20 s at 0.2 to 2 Hz) (Lucas-Osma *et al.*, 2018b). This tonic PAD is mediated by the activation of extra-synaptic $GABA_A$ receptors with α5 subunits (α5 $GABA_A$ receptors) that are also located near nodal sodium channels and is specifically reduced by the α5 $GABA_A$ receptor antagonist L655708 (Lucas-Osma *et al.*, 2018b; Hari *et al.*, 2021).

Importantly, the time course of phasic PAD (100-200 ms), and the reduction in branch point failure it produces in the Ia afferent, is reflected in the time course of motoneuron EPSP potentiation mediated by the facilitated Ia afferents (Hari *et al.*, 2021). Thus, in the present study we first examined in human participants if the facilitation of Ia-mediated H-reflexes had a similar time course to the phasic PAD measured in rodent Ia afferents. To do this we measured the facilitation of the H-reflex (as a measure of Ia afferent conduction) produced by a brief, peripheral sensory or CST conditioning stimulation at interstimulus intervals (ISIs) between 0 to 200 ms. Second, to determine if we could induce long-lasting increases in H-reflexes indicative of tonic PAD in the Ia afferents, we used long trains of cutaneous stimulation (0.5 to 10 s) to produce tonic PAD, which is thought to result from GABA spillover in the dorsal horn and subsequent long-lasting activation of extra-synaptic α5 $GABA_A$ receptors and tonic PAD (Lucas-Osma *et al.*, 2018b). Since Lucas-Osma *et al*., 2018 found that faster cutaneous stimulation trains were more effective in inducing tonic PAD, we examined if fast, compared to slower, trains produced more long-lasting H-reflex facilitation.

In all experiments, special attention was given to ensure there were no direct postsynaptic effects on the motoneuron produced by the sensory or CST conditioning stimulation to ensure that any facilitation of H-reflexes was likely presynaptic in origin. To rule out direct

effects on the motoneuron pool, we examined if the conditioning stimulation itself modulated the firing rate of tonically firing motor units in the test muscle, because the generation of action potentials in a motoneuron is very sensitive to small changes in synaptic inputs, even at distal dendrites, making firing rate a sensitive measure of postsynaptic effects on the motoneuron (Powers & Binder, 2001).

Lastly, we measured changes in the firing rate and discharge probability of single motor units (motoneurons) activated during the H-reflex to estimate the underlying Ia-EPSP by using the peristimulus frequencygram (PSF) method (Turker & Powers, 2005). This allowed us to examine whether spontaneous failures in Ia branch point conduction and EPSP activation decreased with PAD. Remarkably, with the PSF method we found that increases in H-reflex amplitude from cutaneous conditioning (and likely PAD) were not associated with an increase in the underlying unitary Ia-EPSP size, ruling out changes in presynaptic neurotransmitter release and/or postsynaptic effects, where both should produce *graded* changes in the size of the EPSP. Instead, the all-or-none probability of motor unit firing during the EPSP increased, suggesting that the underlying EPSP was more probable, but not larger. This is consistent with results from the rat where cutaneous-evoked PAD increased the probability of Ia afferent conduction through branch points and the resultant unitary EPSPs (Hari *et al.*, 2021). Taken together, these experiments provide evidence for nodal facilitation in the Ia primary afferent by sensory and CST pathways overcoming intermittent branchpoint failure.

Methods

Ethical Approval

Experiments were approved from the Human Research Ethics Board at the University of Alberta (Pro 00078057), performed with informed consent of the participants, and adhered to the *Declaration of Helsinki*. Our sample comprised of 35 participants (18 male) with no known neurological injury or disease, ranging in age from 18 to 57 years [27.0 (9.5), mean (standard deviation)].

Experimental Set up

Participants were seated in a reclined, supine position on a padded table. The right leg was bent slightly to access the popliteal fossa and padded supports were added to facilitate complete relaxation of all leg muscles because CST activation could potentially activate spinal GABA circuits (Ueno *et al.*, 2018). For the transcranial magnetic stimulation (TMS) experiments, participants sat in a padded chair with the right leg slightly extended to 100° at both the knee and ankle joint and the foot was strapped to a supporting platform. The upper leg was also supported with straps and padding as above. The head was supported by a headrest to allow minimal movement during TMS. During H-reflex recordings, participants were asked to rest completely with no talking, hand or arms movements.

Surface EMG recordings

To measure M-wave and H-reflexes, a pair of Ag-AgCl electrodes (Kendall; Chicopee, MA, USA, 3.2 cm by 2.2 cm) was used to record surface EMG from the soleus, tibialis anterior (TA), abductor hallucis (AbHal), biceps femoris, medial gastrocnemius and vastus lateralis

(Quad) muscles with a ground electrode placed just below the knee. The EMG signals were amplified by 200 to 1000 and band-pass filtered from 10 to 1000 Hz (Octopus, Bortec Technologies; Calgary, AB, Canada) and digitized at 5000 Hz using Axoscope 10 hardware and software (Digidata 1400 Series, Axon Instruments, Union City, CA). To examine if the conditioning inputs had any direct effects on the motoneuron pool, the surface electrodes were also used to record single motor unit activity in the soleus and AbHal muscles by placing them on the border of the muscle as per (Matthews, 1996).

Motor unit activity from the soleus muscle was also recorded at higher levels of contraction using a High-Density surface EMG (HDsEMG) electrode (OT Bioelettronica, Torino, Italy, Semi-disposable adhesive matrix, 64 electrodes, 5x13, 8 mm inter-electrode distance) with differential and ground electrodes wrapped above the ankle and below the knee respectively. Signals were amplified (150 times), filtered (10 to 900 Hz) and digitized (16 bit at 5120 Hz) using the Quattrocento Bioelectrical signal amplifier and OTBioLab+ v.1.2.3.0 software (OT Bioelettronica, Torino, Italy). The EMG signal was decomposed into single motor units using a convolutive blind source separation algorithm implemented in MatLab R2020b with additional quality assessment and accuracy improvement of the automatically decomposed motor unit action potential spike (pulse) trains as described previously (Negro *et al.*, 2016; Martinez-Valdes *et al.*, 2017; Afsharipour *et al.*, 2020). Single motor units that were measured from standard surface and intramuscular EMG were discriminated visually.

Nerve Stimulation to evoke homonymous and heteronymous H-reflexes

The tibial nerve (TN) was stimulated using a constant current stimulator (1 ms rectangular pulse width, Digitimer DS7A, Hertfordshire, UK) to evoke a homonymous H-reflex in the soleus

and AbHal muscles. After searching for the TN with a surface probe, an Ag-AgCl cathode electrode (Kendall; Chicopee, MA, USA, 2.2 cm by 2.2 cm) was placed in the popliteal fossa, with the anode electrode (Axelgaard; Fallbrook, CA, USA, 5 cm by 10 cm) placed on the patella. If an AbHal H-reflex was not readily evoked from TN stimulation behind the knee, the posterior TN was stimulated below the medial malleolus. A heteronymous H-reflex (> 100 □V) was evoked in the biceps femoris muscle by stimulating the nerve to medial gastrocnemius (MG) in the popliteal fossa (1 ms pulse width, ~3.3 x M-wave threshold measured in MG muscle). A homonymous H-reflex was evoked in the vastus lateralis (Quad) muscle by stimulating the femoral nerve in the femoral triangle, also with a 1 ms pulse width. Stimulation intensity for the homonymous H-reflexes was set to evoke a test (unconditioned) H-reflex below half maximum on the ascending phase of the H-reflex recruitment curve (~30% of the maximum H-reflex) to reduce the possibility of evoking polysynaptic reflexes and observing increases in Ia conduction (Hari *et al.*, 2021). H-reflexes were evoked every 5 seconds to minimize post-activation depression of the Ia afferents (Hultborn *et al.*, 1996a). At least 20 test H-reflexes were evoked before conditioning to establish a steady baseline since the Ia afferent activation itself could also activate spinal GABA networks and facilitate H-reflexes (i.e., self-priming, Hari *et al*., 2021). All H-reflexes were recorded at rest except during the firing probability experiments described below.

Sensory and CST conditioning of H-reflexes to produce phasic PAD

Cutaneous and proprioceptive conditioning stimulation: To condition the H-reflex by mainly cutaneous afferents, the medial (cutaneous) branch of the superficial fibular nerve (SFN) was stimulated on the dorsal surface of the ankle using a bipolar arrangement (Ag-AgCl

electrodes, Kendall; Chicopee, MA, USA, 2.2 cm by 2.2 cm). A short train (3 pulses, 200 Hz for 10 ms) of SFN stimulation was applied at intensities corresponding to perception threshold but below radiating threshold (3.0 to 7.4 mA) to avoid direct activation of motoneurons as assessed below. A train of pulses was used for the cutaneous nerve stimulation because it evokes larger phasic PAD in Ia afferents compared to single pulse stimulation (Eccles *et al.*, 1962c). Approximately 20 baseline soleus H-reflexes were elicited to ensure the H-reflex was stable, followed by 7 conditioned H-reflexes at one of the ISIs (0, 30, 60, 80, 100, 150 or 200 ms). Following this, 7 unconditioned H-reflexes were evoked to re-establish baseline and another run of 7 conditioned H-reflexes was applied at another randomly chosen ISI. This was repeated until all ISIs were applied. To condition the H-reflex by mainly low-threshold proprioceptive afferents, the common fibular nerve (CFN) was stimulated in a bipolar arrangement just below the head of the fibula (3 pulses at 200 Hz) at 1.0 x motor threshold measured in the TA muscle, being careful to elicit a pure dorsiflexion response.

CST conditioning stimulation: The CST to the soleus, AbHal or Quad motoneuron pool was activated by applying TMS to the contralateral motor cortex using a custom made figure-of-eight batwing coil [(P/N 15857; 90 mm diameter, (Nielsen & Petersen, 1994)] that was connected to a Magstim 200 stimulator (Magstim; Dyfed, UK). The coil was typically positioned 2 cm lateral to vertex to target the lower leg muscles. Active motor threshold (AMT) was determined by the lowest-intensity TMS pulse that produced a discernable and reproducible motor evoked potential (MEP) in the tested muscle while the participant held a small voluntary contraction. The TMS intensity was set to 0.9 x AMT in the resting muscle to avoid direct activation of the motoneuron. H-reflexes were conditioned by TMS at the same ISIs as for the

sensory conditioning experiment above, in addition to the 250 and 300 ms ISIs given the longer duration of facilitation in some participants.

Data analysis: For both the sensory and CST conditioning experiments, the unrectified, peak-to-peak amplitude of the 7 test H-reflexes immediately preceding the 7 conditioned H-reflexes for a given ISI were averaged together because test H-reflexes could grow over time (self-priming, Hari *et al.*, 2021). The effect of the conditioning stimulation on the test H-reflex was measured using the formula: % change H-reflex = ([(conditioned H - test H)/test H] *100%). Data was also analyzed by averaging the amplitude of all test H-reflexes in a trial and this provided similar results throughout so only calculations of % change using the immediately preceding test H-reflexes are reported here. The mean % change H-reflex for each ISI was averaged across participants. Because the profile of H-reflex facilitation could be variable between participants, the maximum or peak % change H-reflex, irrespective of ISI, was also averaged across participants.

Postsynaptic effects of conditioning stimuli: To determine if there were any direct effects on the motoneurons from the conditioning stimulation at the time the H-reflexes were evoked, we measured if the sensory or CST stimulation applied alone produced any changes in the tonic firing rate of single motor units or changes in the amplitude of the rectified surface EMG. Single motor units were activated in the soleus or AbHal muscle while the participant held a small voluntary contraction around 5% of maximum. Both auditory and visual feedback was used to keep the firing rates of the units steady while the conditioning cutaneous or CST stimulation was applied every 3 to 5 seconds. The firing rate profiles from many stimulation trials were superimposed and time-locked to the onset of the conditioning stimulation to produce a peri-stimulus frequencygram (PSF) as done previously (Turker & Powers, 2005; Norton *et al.*, 2008).

A mean PSF was produced by averaging the frequency values into 20 ms bins. The mean rate in each 20 ms bin was compared to the mean rate measured in a 100 ms window before the conditioning stimulation and expressed as: % change PSF = ([(mean bin rate - mean pre-stimulus rate)/mean pre-stimulus rate] *100%). A similar binning process and averaging was done for the rectified surface EMG using a 100 ms window before the conditioning stimulation to measure the pre-stimulation background EMG.

Motoneuron and Ia afferent excitability during conditioned H-reflex: We wanted to estimate both the excitability of the motoneuron (as reflected in the PSF and rectified EMG), and the predicted amplitude of PAD in the Ia afferent, at the time the conditioned Ia afferents activated the motoneurons at the spinal cord to ensure any increase in H-reflex size was not due to an increase in motoneuron excitability from the conditioning stimulation but due to an increased conduction in the Ia afferents mediating the H-reflex (Fig. 1). First to align motoneuron excitability, the conditioned H-reflex values, as a function of the various ISIs (see bottom graph, Fig. 1), were shifted to the right of the onset of the conditioning (SFN) stimulation in the PSF (light blue trace) and EMG profiles (not shown) by an amount equivalent to the latency of the H-reflex (~30 ms, solid black arrows in Fig. 1). The rightward shift accounted for the time it takes the Ia afferent volley to reach the spinal cord plus the time it takes the motoneuron response to reach the muscle where the H-reflex is measured (grey arrows). Thus, the PSF (or EMG) values occurring near the shifted conditioned H-reflexes can be used as an estimate of the motoneuron excitability at the time the conditioned H-reflexes were activated at the spinal cord. Second, plotting the estimated time course of PAD in a Ia afferent after the conditioning stimulation helps to predict when the Ia afferents mediating the H-reflexes should be facilitated by the conditioning PAD. Because the conditioned-evoked PAD in the Ia afferent

is activated at the cord with a similar delay as the Ia EPSP mediating the H-reflex (top two traces in Fig. 1), a 0 ms ISI corresponds to just before the conditioning afferent stimulation can influence the H-reflex. In contrast, at the 80 ms ISI while PAD is activated in the Ia afferent, the H-reflex can be facilitated (Fig. 1; compare pink and blue dots representing H-reflexes in inset at 0 and 80 ms ISI respectively). Moreover, if the mean firing rate of the motor units (PSF, light blue line) near the 80 ms ISI is at or below the pre-conditioned level (below red line at red double arrow), this would indicate that the facilitation of the conditioned H-reflex at this ISI was not mediated by a depolarization of the motoneurons from the conditioning stimulation.

Figure 1. Time course of predicted phasic PAD and its relationship to H-reflex facilitation. **Top three traces:** *Trace 1*) Theoretical example of phasic afferent depolarization (PAD) recorded in Ia afferent (top dark blue trace, profile taken from a rat Ia afferent recording). *Trace 2*) EPSP recorded in spinal motoneuron and H-reflex recorded in muscle (pink traces) from simultaneous SPN and TN stimulation to produce a conditioned H-reflex as measured for the 0 ms ISI (pink dot, bottom trace). Time of stimulation marked by rectangular pulses on left. PAD profile

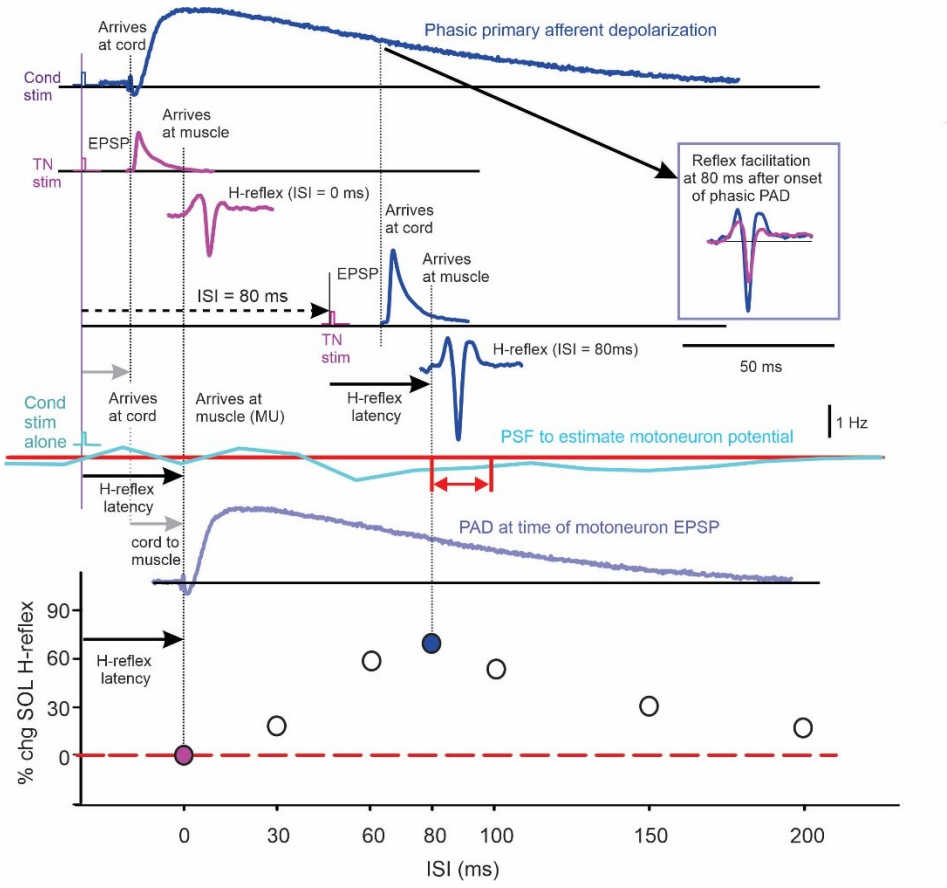

taken from intracellular recording in rat afferent (sacral S3) in response to stimulation of an adjacent dorsal root (S4: 1.1 x threshold, 0.1 ms pulse, Hari et al., 2022). *Trace 3*) EPSP (upper) and H-reflex (lower dark blue traces) in response to TN stimulation applied 80 ms after the SPN stimulation (ISI of 80 ms, dashed arrow). **Bottom three traces**: *Trace 4*) Example mean PSF (light blue trace) to represent profile of motoneuron excitability in response to conditioning SPN stimulation alone. Red trace represents mean firing rate before SPN stimulation was applied. Double red arrow marks the excitability of the motoneuron (potential estimated from the PSF) during activation of the H-reflex. *Trace 5*) Violet trace is profile of PAD shifted to the right by the conduction time from the spinal cord to the muscle to visually line up the excitability of the Ia afferents at the time the motoneuron is being activated during the H-reflex and how this affects the resulting amplitude of the H-reflex recorded at the muscle. *Trace 6*) Percent change in H-reflex amplitude [(conditioned H – test H)/test H x 100%] at the various ISIs, highlighting the 0 and 80 ms ISIs. H-reflex values shifted to the right of the onset of the conditioning stimulation by an amount equal to the H-reflex latency (solid black arrows) plus the ISI interval (e.g., dashed line for 80 ms ISI).

Cutaneous and proprioceptive facilitation of H-reflexes during tonic PAD

a) Slow (0.2 Hz) vs moderate (2 Hz) cutaneous frequency trains: A slow (0.2 Hz) and moderate (2 Hz) frequency train of SFN stimulation was applied as per animal studies (Lucas-Osma *et al.*, 2018b). A higher stimulation intensity at 2 times perception threshold [10.6 (1.6) mA, n = 16 participants] was used to induce GABA spillover. Following a baseline of 20 test H-reflexes (delivered every 5 s), the slow or moderate SFN stimulation train was applied along with the test H-reflexes for 10 s, with each SFN stimulation occurring 500 ms before any H-reflex. Test H-reflexes were evoked for another 120 s to examine aftereffects from the SFN trains. This stimulation protocol was repeated 3 times for both the 0.2 Hz and 2 Hz stimulation trains in each participant, waiting at least 1 minute at rest between each trial.

b) Fast (200 Hz) cutaneous frequency train: A faster (200 Hz) but shorter (500 ms) train of SFN stimulation was also used to condition the H-reflex as per (Hari *et al.*, 2021) using a protocol similar to the slower 10 s trains. Here, the cDPN train was applied 700 ms before the test H-reflex and following this, H-reflexes continued to be evoked for another 90 to 120 s. A very low intensity of stimulation below radiating threshold (3.0 to 4.5 mA, n = 15 participants) was used to ensure the high frequency stimulation was not painful.

c) Slow (0.2 Hz) proprioceptive frequency train: Because repetitive activation of Ia afferents also produces tonic PAD (Hari *et al.*, 2021), we examined if there was a buildup of test H-reflexes from repetitive stimulation of the TN afferents alone. In rodents, activation of Ia afferent collaterals activate PAD networks that connect back to the same afferent to produce self-facilitation, which is revealed during low-intensity, repetitive stimulation of Ia afferents (1.1 x afferent threshold, 0.1 Hz, ~ 30% of maximum EPSP). Thus, we measured the amplitude of test H-reflexes activated every 5 seconds (0.2 Hz) at a low intensity of TN stimulation (~30% of maximum H-reflex) in 19 participants before any conditioning (cutaneous or CST) stimulation was applied.

Data analysis: H-reflexes following the cutaneous conditioning train in experiments *a* and *b* (post-train H) were compared to the average amplitude of the 20 baseline H-reflexes (pre-train H) using the % change formula: [(post-train H - pre-train H)/pre-train H] *100%. The resulting % change H-reflex values were plotted against time and divided into 10 s bins (2 H-reflexes per bin). H-reflexes from all 3 trial runs were grouped together (2 H-reflexes per bin x 3 trials = 6 H-reflexes per bin). The average % change H-reflex in each bin was then averaged across all 16 participants. In experiment *c* the amplitude of each of the 14 test H-reflexes measured at baseline before any conditioning stimulation was applied (set 1 in Experimental

Protocol, Fig. 2) was expressed as a percentage of the average of the 7 test H-reflexes following the first conditioning run (in set 2) where the H-reflexes reached a stable state using the formula: (set 1 $H_{1\text{-}14)}$ /avg set 2 H) * 100%. Each 1st to 14th %H-reflex was then averaged across the 19 participants and plotted against stimulation number (and time).

Firing probability of single motor units during the H-reflex ẁ cutaneous conditioning

The firing probability of single motor units during the H-reflex window (approximately 30 to 45 ms post TN stimulation) was measured with and without cDPN conditioning in 13 participants. In 12 participants, single motor units were identified from HDsEMG and in 1 participant with intramuscular EMG to verify the HDsEMG recordings. The size of the H-reflex was set to just above motor threshold [5.2 (3.9)% Mmax] during a small plantarflexion so that single motor units at the time of the H-reflex could be distinguished from the compound H-reflex potential (Yavuz *et al.*, 2015; Nielsen *et al.*, 2019a). In a single trial run, test H-reflexes were evoked every 3-5 s for the first 100 s followed by cDPN-conditioned H-reflexes for the next 100 s using a 200 Hz, 50 ms pulse train (3.0 to 4.5 mA, below radiating threshold) applied 500 ms before each H-reflex. Approximately 40-50 usable test and conditioned firing rate profiles (PSFs) were produced for a single trial run where the motor units had a steady discharge rate 400 ms before and 600 ms after the cDPN stimulation. Trial runs were repeated 3-6 times to obtain a sufficient number of frequency profiles to construct the PSF (~200) (Norton *et al.*, 2008).

Data analysis: For each test or conditioned PSF, the probability that a motor unit discharged during the ~15 ms H-reflex window was measured using the following formula: [(number of discharges during the H-reflex window) / (total number of sweeps) *100%]. The mean background firing rate 100 ms before the TN stimulation with and without conditioning was also

measured. For both the test and conditioned trials, the average firing probability during the H-reflex window and the mean background rate were measured for each participant and then averaged across the 13 participants. The mean firing rate during the H-reflex window was also measured as an estimate of EPSP size (Norton *et al.*, 2008), and expressed as a % change between the test and conditioned H-reflex trials ([(conditioned rate-test rate)/test rate]*100).

Statistical Analysis

Statistical analysis was performed in Sigma Plot 11. The % change of various measures (conditioned H-reflex, PSF and rectified EMG) across the different ISIs were compared to a 0% change using either a one-way ANOVA for repeated measures for normally distributed data (determined by the Equal Variance test) or by a Friedman Repeated Measures Analysis of Variance on Ranks for data that was not normally distributed. Post hoc Tukey tests for the ANOVA and Friedman were used to determine which ISIs were significantly different from a 0% change. A two-way ANOVA for repeated measures was used to compare the % change in H-reflexes from the 2 Hz and 0.2 Hz conditioning cutaneous stimulation trains, with frequency and time as factors. Post hoc Tukey tests were used to determine which time bins were significantly different between the two stimulation frequencies. A Mann-Whitney U Test was used to compare group values that were not normally distributed and Student's t-tests for normally distributed data. Data are presented in figures and in the text as mean (standard deviation). Significance was set as $p < 0.05$ and n refers to the number of participants tested in each experiment.

Results

Cutaneous and proprioceptive facilitation of H-reflexes during phasic PAD

To explore whether conduction in Ia afferents was facilitated during the relatively long duration of phasic PAD (100 - 200 ms, Hari *et al.,* 2022), we started by examining whether the soleus H-reflex was facilitated by a cutaneous conditioning stimulation [SFN: 4.1 (1.1) mA at perception threshold] at interstimulus intervals (ISI) between 0 and 200 ms (see schematic of experimental protocol, top of Fig. 2). Consistent with the time course of phasic PAD, the soleus H-reflex was facilitated when the brief SFN train was applied between 60 to 150 ms earlier, as shown for two participants in Figures 2A-C & B-D respectively. The change in the conditioned H-reflex with respect to the test H-reflex is plotted as a function of the ISI (Figs. 2C and D) to evaluate how the facilitation changes with the expected time course of phasic PAD (up to 200 ms; see below). For this analysis, the H-reflex and conditioning SFN volley are expected to have a similar latency in reaching the spinal cord (see Methods, Fig. 1) and thus, an ISI of 0 ms corresponds to a time just before the expected onset of PAD where appreciable H-reflex facilitation is not expected. Longer ISIs correspond to times during the activation of PAD where Ia afferent and reflex facilitation is expected, as highlighted for the H-reflexes at the 60 and 80 ms ISIs in the two participants (see insets in Figs. 2A-B with corresponding %change values shown between the grey dashed lines in Figs. 2 C-D).

The facilitation of the soleus H-reflex occurred even though the conditioning SFN stimulation itself (when applied alone) did not facilitate the soleus motoneuron pool as reflected in the mean motor unit firing profile (PSF, light blue line in Figs. 2E and F), remaining close to or slightly below the mean firing rate before the SFN stimulation was applied (red line), and thus

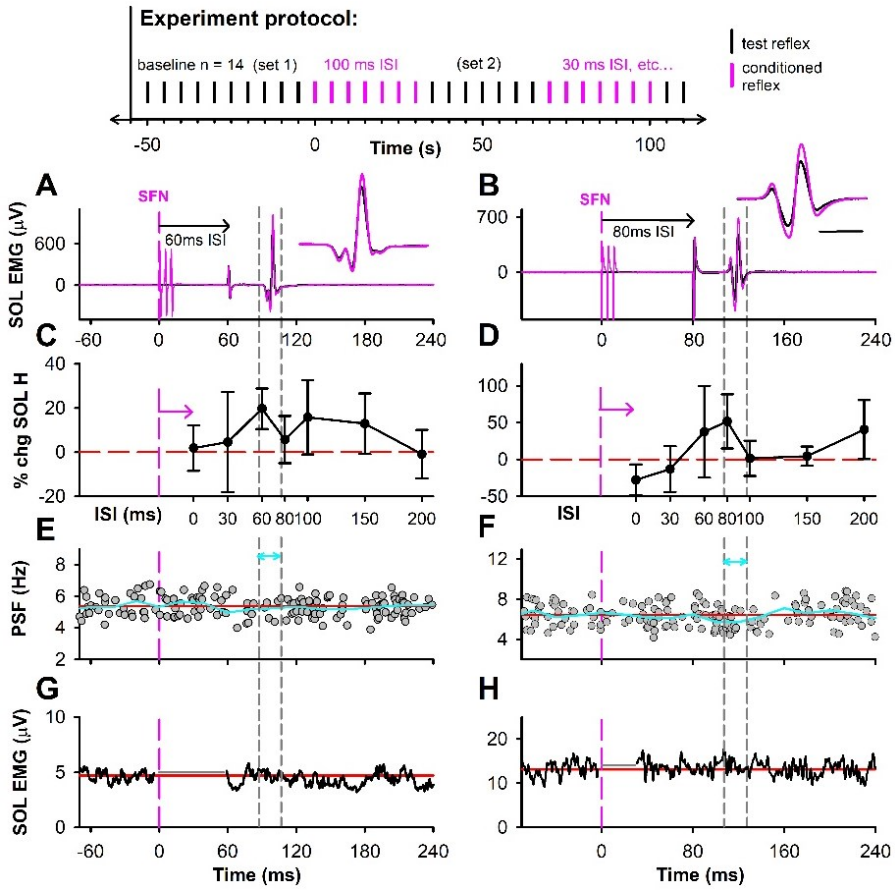

Figure 2. Short-duration H-reflex facilitation by cutaneous inputs. **Top:** Experiment protocol showing alternating sequence of applying test (black) and conditioned (pink) H-reflexes at the various ISIs. **A&B)** Soleus (SOL) H-reflex modulation from SFN conditioning stimulation in 2 representative participants. Average of 7 test (black) and 7 SFN-conditioned (pink) SOL H-reflexes (200 Hz, 10 ms, 3.5mA and 4.0mA respectively) with TN stimulation at 60 ms in A and 80 ms in B (expanded time scale for H-reflex in insets, 10 ms time bar in B). **C&D)** % change of the SOL H-reflex at each ISI [mean (SD)]. Peak % change marked by dashed vertical lines. Data points are shifted to the right with respect to the onset of SFN stimulation in E&F as marked by the pink vertical dashed line. The amount of shift is equal to the onset latency of the H-reflex (length of pink arrow). **E&F**) PSF of a SOL single motor unit, time-locked to the time of the SFN conditioning stimulation alone at 0 ms (vertical pink line) with 110 sweeps in E and 180 sweeps in F. Firing rate averaged into 20 ms bins (blue trace) for comparison to the average pre-stimulus firing rate (red line). **G&H)** Averaged rectified SOL EMG recorded with the SFN conditioning stimulation alone with 112 sweeps in G and 82 sweeps in H. Stimulation artifact removed (grey horizontal line). Average pre-stimulus EMG marked by the horizontal red line. Note x-axis in A-B, E-H is in time (ms) and C-D in ISI (ms).

ruling out postsynaptic facilitation of the H-reflex. Likewise, the SFN stimulation did not produce an increase in the mean rectified EMG, representing the activity of a larger number of motor units and ruling out the addition of newly recruited units from the conditioning input (Figs. 2G and H). For comparing the PSF or EMG after the SFN stimulation (Figs. 2E-H) to the conditioned H-reflex changes (Figs. 2C-D), the H-reflex-ISI plots were shifted to the right by the latency of the H-reflex, to determine how the SFN stimulation affected the excitability of the soleus motoneurons at the time the H-reflex was activated (if at all; see Methods, Fig. 1). As highlighted for the maximally facilitated H-reflexes at the 60 and 80 ms ISIs (between grey dashed lines in Fig. 2), both the PSF and EMG remained close to or slightly below the pre-stimulus values indicating an unfacilitated soleus motoneuron pool when the conditioned H-reflexes were evoked and facilitated.

Overall from the 16 participants, the mean profile of soleus H-reflex facilitation from the conditioning SFN stimulation resembled the profile of afferent depolarization (PAD) evoked by a cutaneous afferent stimulation (Hari *et al.*, 2021), lasting for ~150 ms but with a later peak at 80 ms (Figs. 3Ai) and with a significant facilitation of the reflex at the 80 and 100 ms ISIs (see legend for statistics). In contrast, there was no change in the mean PSF or EMG for all ISIs tested, again indicating a lack of direct effect from the conditioning SFN stimulation on the soleus motoneurons. The maximal facilitation of the soleus H-reflex across the different condition-test ISIs in each participant was 42.0 ± 27.4% ($p < 0.001$, Fig. 3B left bar), whereas the average firing rate during the PSF when the maximal H-reflex was evoked at the spinal cord (e.g., within the grey dashed lines in Figs. 2E and F) was reduced slightly compared to the firing rate before the SFN stimulation (-3.4 ± 4.8%, $p = 0.020$, Fig. 3B middle bar). Although there was no change in the overall rectified EMG (Fig. 3B right bar), in 3 participants the rectified EMG

was increased compared to the mean pre-stimulus level but this was likely in response to motor unit synchronization following a preceding EMG suppression, highlighting that caution should be used when using EMG to estimate motoneuron depolarization levels (Turker & Powers, 2005). In summary, the facilitation of the H-reflex by the SFN stimulation was likely not produced by a direct facilitation of the soleus motoneuron pool at the time of Ia activation based on the PSF and EMG. Rather, facilitation likely occurred at a pre-motoneuron level, potentially due to facilitation of spike propagation on the Ia afferents mediating the H-reflex as demonstrated in the motor unit firing probability experiment detailed below.

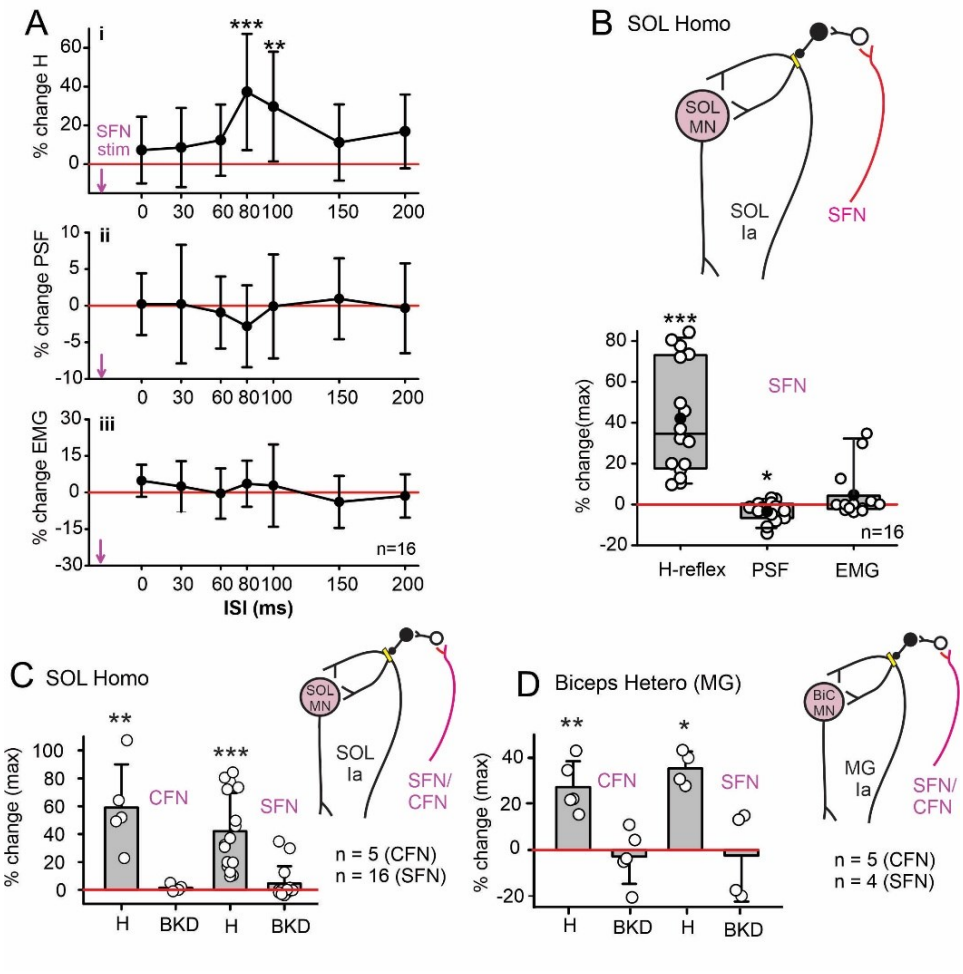

Figure 3. Short-duration H-reflex facilitation by sensory inputs: group data. A) Average % change in (i) soleus H-reflex, (ii) motor unit firing rate (PSF) and (iii) rectified EMG from a prior cutaneous SFN conditioning stimulation (3 pulses, 200 Hz) at each ISI across the group (n=16 participants). Error bars represent standard deviation about the mean. The

average size of the test (unconditioned) SOL H-reflex was 0.86 (0.76) mV [or 11.4 (9.2) % of Mmax]. There was an effect of the conditioning-test ISI on the H-reflex [$F(15,7) = 4.3$, $P < 0.001$, one-way ANOVA], being significantly greater than a 0% change at the 80 ($p < 0.001$, Tukey) and 100 ms ($p < 0.008$, Tukey) but no effect of ISI for both the mean PSF (Chi-square, DF 7, $p = 0.520$) and EMG [$F (13,7) = 1.1$, $p = 0.351$], one way ANOVA). **B)** Left bar: Maximum (peak) % change of the conditioned SOL H-reflex for each participant (white circles, n = 16 participants), mean represented by black circle and median by horizontal line, 25th and 75th percentiles by the box bounds, and the 95th and 5th percentiles by whiskers (median greater than a 0% change, $p < 0.001$). Middle bar: % change PSF at the time bin where the peak conditioned H-reflex would have been activated at the spinal cord (n=16 units, one unit measured in each participant with 5 units recorded using intramuscular or surface EMG, 11 units decomposed from HDsEMG, median smaller than a 0% change, $p = 0.018$). Right bar: % change of rectified surface EMG as in PSF (median not different from 0 %change, $p = 0.507$). **C)** Maximum % change in soleus H-reflex (H) from conditioning of CFN (n = 5 participants: median greater than 0% change, $p = 0.008$) and corresponding % change in EMG (median not greater than 0% change, $p = 0.556$). Data for conditioning of soleus H-reflex by SFN is replotted from B for comparison. Length of vertical bar represents mean and whiskers SD. **D)** Same as in C but for maximum % change from CFN conditioning in biceps femoris (BiC) H-reflex (median greater than 0% change, $p = 0.008$) and associated in EMG (median not greater than 0% change, $p = 0.690$) and for SFN conditioning of biceps femoris H-reflex (median greater than a 0% change, $p = 0.029$) and associated %change EMG (median not greater than a 0% change, $p = 1.000$) (n = 5 participants for CFN, n = 4 participants for SFN). Mann-Whitney U test used for all pairwise comparisons (B-D) to a 0 %change with * $p < 0.05$, ** $p < 0.01$, *** $p < 0.001$.

Conditioning with proprioceptive afferents also produced facilitation of both homonymous and heteronymous H-reflexes. A low intensity of stimulation to the common fibular nerve (CFN, 1.0 x MT), mainly to recruit proprioceptive afferents from the TA muscle (antagonist to the soleus), produced a maximum facilitation of soleus H-reflexes of 59.1 ± 30.9% in 5 participants ($p = 0.008$), with no corresponding increase in EMG activity ($p > 0.50$, Fig. 3C).

Like the cutaneous SFN stimulation (replotted in Fig. 3C), the maximum facilitation of the soleus H-reflex from the antagonist CFN conditioning occurred between the 60 and 80 ms ISIs (average 68.0 ± 11.0 ms, not shown). The conditioning CFN stimulation also facilitated a heteronymous H-reflex in the biceps femoris muscle (Biceps Hetero) activated by the MG nerve, with a maximum facilitation of 27.4 ± 11.2% ($p < 0.001$, n = 5 participants) that occurred between the 60 and 80 ms ISIs (64.0 ± 8.9 ms, Fig. 3D). Likewise, the cutaneous SFN stimulation facilitated the heteronymous biceps femoris H-reflex by 35.4 ± 7.4% at an average ISI of 60.0 ± 14.1 ms ($p < 0.001$, Fig. 3D, n = 5 participants), with both low-intensity conditioning stimuli producing no change in the surface EMG reflecting the excitability of the motoneuron pool at the time the H-reflex was evoked ($p > 0.65$, Fig. 3D). Thus, the facilitation of the H-reflex by sensory conditioning not only follows the time course of phasic PAD, but also spatially mimics the widespread distribution of PAD in Ia afferents across many spinal segments from both flexor and extensor muscles (Rudomin & Schmidt, 1999; Willis, 2006).

CST facilitation of the H-reflex during phasic PAD

Similar to the action of sensory conditioning, the H-reflex was also facilitated by prior conditioning from the CST activated by TMS to the contralateral motor cortex, which should produce PAD (Carpenter *et al.*, 1963). This occurred for both the soleus and AbHal H-reflexes (representative AbHal H-reflex data shown for two participants in Figs. 4A and B, inset). A very weak TMS intensity (0.9 x AMT applied at rest) was used to condition the resting H-reflex to avoid direct facilitation of the motoneuron pool. The profile of AbHal H-reflex facilitation from TMS conditioning at the different ISIs was similar to the cutaneous conditioning, lasting for ~ 150 ms and peaking near 80 and 60 ms in the two participants (Figs. 4C and D). When applied

alone, the conditioning TMS did not produce an increase in the mean firing rate of the tonically active motor units (PSF in Figs. 4E and F) or in the rectified surface EMG (Figs. 4G and H), again suggesting that the facilitation of the H-reflex was not due to postsynaptic changes in the motoneurons.

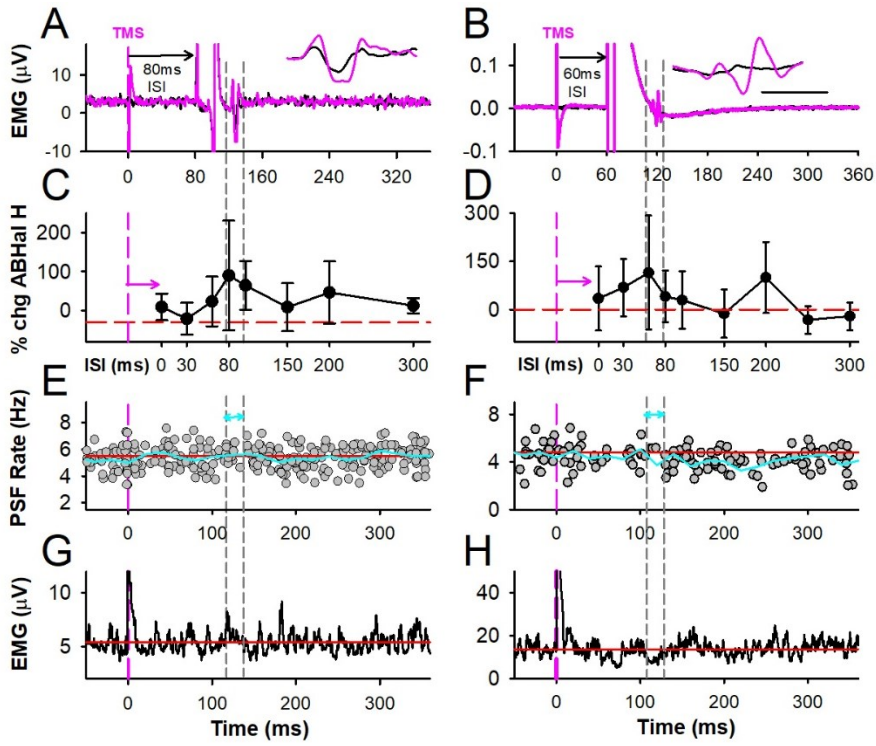

Figure 4. Short-duration H-reflex facilitation by CST inputs. A&B) Similar format to Figure 2 with example of test (black) and conditioned (pink) AbHal unrectified EMG illustrating conditioned H-reflex from TMS (0.9xAMT) in two participants at the 80 ms ISI in A and 60 ms ISI in B. **C&D)** Mean (± SD) % change of conditioned AbHal H-reflex at each ISI. **E&F)** PSF of a AbHal single motor unit, time-locked to TMS at 0 ms (vertical pink line) with 139 sweeps in E and 86 sweeps in F. **G&H)** Averaged rectified AbHal EMG recorded with TMS conditioning stimulation alone with 71 sweeps in G and 37 sweeps in H. Stimulation artifact removed (grey horizontal line).

In the group average (n = 9 participants), the AbHal H-reflex was facilitated across the various ISIs with TMS conditioning (Fig. 5Ai, see statistics in legend), similar to the sensory afferent conditioning of the H-reflex, being significant at the 80 ms ISI (51.1 ± 41.8%, $p = 0.033$, Tukey), and similar in duration to the expected CST-evoked phasic PAD (Carpenter *et al.*, 1963). In contrast, the PSF and background EMG was not altered by the conditioning TMS (Figs.

5Aii&Aiii), indicating a lack of direct effect from the TMS on the AbHal motoneurons, like the low intensity CPN and cDPN stimulation. The maximum facilitation of the AbHal H-reflex across the various ISIs in each participant was 71.2 (33.7)% ($p < 0.001$, Fig. 5B, Mann-Whitney U test), with no change in the firing rate of the AbHal motor units or rectified EMG at time points when the maximal conditioned H-reflex occurred at the spinal cord. The soleus H-reflexes were also facilitated by a low intensity TMS pulse (Fig. 5C). The peak facilitation of the soleus H-reflex was 37.6 (29.5)% ($p < 0.001$, n = 9 participants) at an average ISI of 78.0 (24.4) ms (not shown), with no corresponding change in PSF or EMG (see legend for statistics).

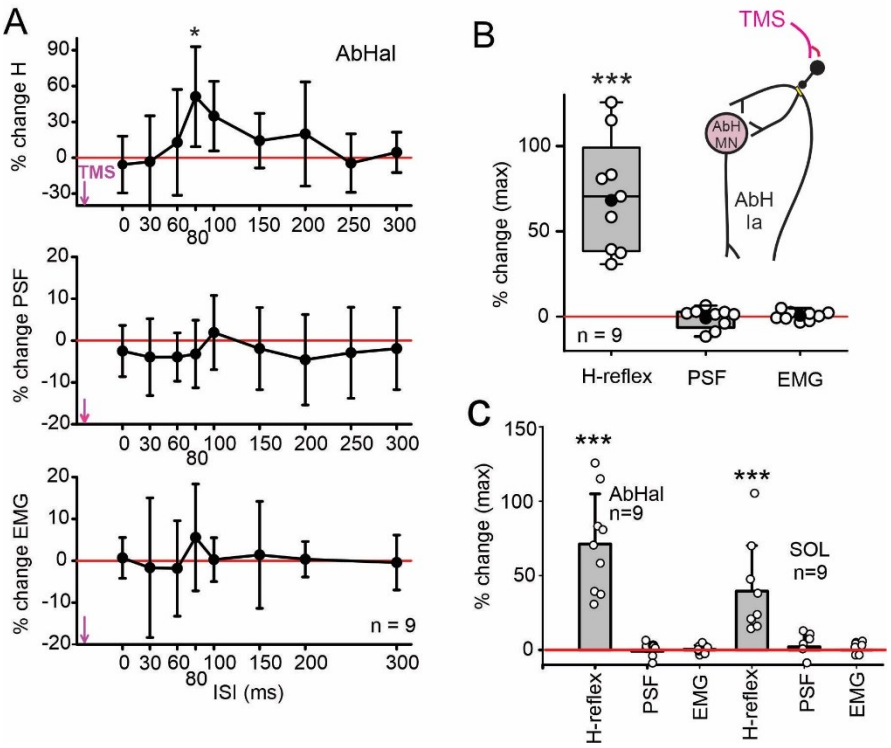

Figure 5. Short-duration H-reflex facilitation by CST inputs. Group data. **A)** Same format to Figure 3. Mean % change in (i) AbHal H-reflex (ii), motor unit firing rate (PSF) and (iii) rectified EMG from a prior TMS conditioning (0.9xAMT) at each ISI across the group (n=9 participants). The average size of the test AbHal H-reflex was 0.11 (0.82) mV (Mmax was not recorded in this muscle). There was an effect of the condition-test ISI on the AbHal H-reflex [$F(8,9) = 3.345$, $p = 0.002$, one-way ANOVA] but not for the PSF [$F(8,7) = 0.630$, $p = 0.731$, one-way ANOVA] or EMG [$F(8,7) = 0.501$, $p < 0.830$), one-way ANOVA]. **B)** Left bar: Peak % change of the TMS-conditioned AbHal H-reflex (median greater than 0% change, $p < 0.001$). Middle bar: % change PSF at the ISI time bin where the peak conditioned H-reflex would have been activated at the spinal cord (all units were recorded using surface EMG,

median not different from 0% change, p = 0.220). Right bar: % change of rectified surface EMG as in PSF (median not different from 0% change, p = 0.706). **C)** Maximal % change in TMS-conditioned AbHal H-reflex, PSF and EMG (n = 9 participants, replotted from B) and maximal % change in soleus H-reflex (median greater than 0% change, $p < 0.001$), % change PSF (median not different from 0% change, p = 0.129) and % change EMG (median not different from 0% change, p = 0.706) (SOL, n = 9 participants). Mann-Whitney U test used for pairwise comparisons to 0% change (B-C) with * = $p < 0.05$ and *** = $p < 0.001$.

Cutaneous and proprioceptive facilitation of H-reflexes to produce tonic PAD

Slow (0.2 Hz) vs moderate (2 Hz) speed of cutaneous afferent trains: We next examined if a more intense and longer duration of cutaneous SFN stimulation could produce a longer-lasting facilitation of the H-reflex indicative of the tonic PAD in Ia afferents produced by such stimuli (Lucas-Osma *et al.*, 2018b; Hari *et al.*, 2021). The SFN intensity was increased to 2 x radiating threshold (10.6 ± 1.7mA) to potentially produce GABA spillover and applied for 10 s at either 2 Hz or 0.2 Hz to determine if there was a frequency-dependent effect, as previously shown for tonic PAD mediated by □5 $GABA_A$ receptors (Lucas-Osma *et al.*, 2018b). During both of the 10-s stimulation trains (2 or 0.2 Hz), the soleus H-reflex was facilitated (pink circles at 0-s time bin, Fig. 6A) compared to the unconditioned test H-reflexes (< 0-s time bins), with direct motoneuron depolarization occurring during the period of SFN stimulation (not shown). The H-reflexes following the 0.2 Hz or 2 Hz conditioning SFN stimulation trains (> 0-s time bins) increased across all binned time points (see statistics in legend) with post-hoc analysis revealing that H-reflexes were significantly larger at all time points for the 2 Hz train only ($p < 0.05$). The facilitation of the H-reflex was greater following the 2 Hz stimulation train compared to the 0.2 Hz train at several of the condition-test ISIs ($p < 0.05$, marked by *'s in Fig. 6A).

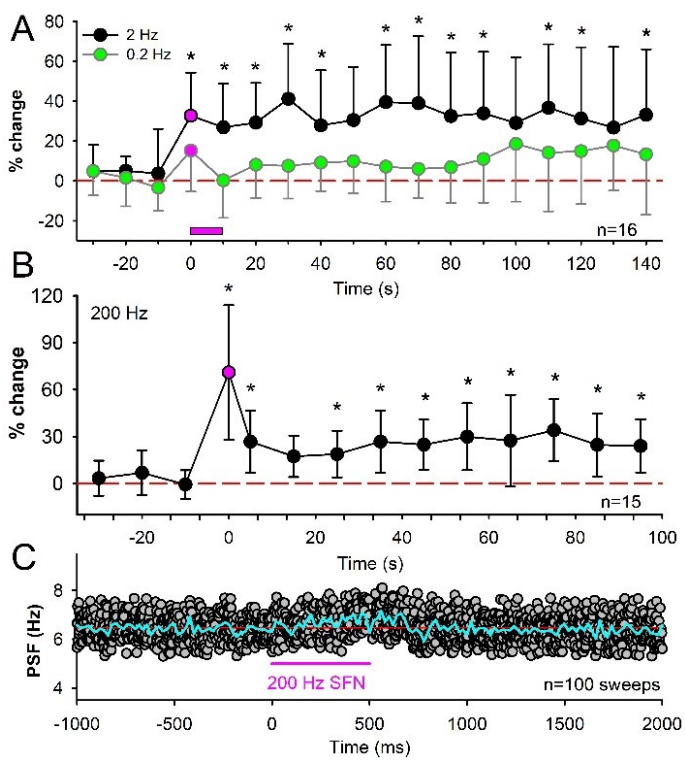

Figure 6. Long-duration H-reflex facilitation. A) Mean (SD error bars) of SOL H-reflexes before (< 0 s) and after (> 0 s) a 10 s train of 2 Hz (black circles) or 0.2 Hz (green circles) SFN stimulation as shown by pink bar (n = 16 participants). H-reflexes that occurred during the SFN stimulation train are marked in pink at 0 ms. H reflexes were evoked every 5 seconds and data were averaged into 10-s bins. Dashed red line indicates 0 %change. H-reflexes were larger across all time points for both the 0.2 Hz ($F(15,18)=2.56$, $p = 0.007$) and 2.0 Hz ($F(15,18) = 6.39$, $p <0.001$) stimulation trains (one-way ANOVA) with H-reflexes after the 2 Hz stimulation greater than a 0 %change at all time points (not shown, $p < 0.05$, Tukey). The increase in H-reflex was larger for the 2 Hz stimulation compared to the 0.2 Hz stimulation [$F(1, 17) = 2.2$, $p = 0.005$, two-way repeated measures ANOVA] with * indicating post-hoc analysis where 2 Hz values > 0.2 Hz values ($p < 0.05$, Tukey). **B**) Same format in A but in response to a fast cDPN train (200 Hz for 500 ms, n=15 participants). Pink circle represents conditioned H-reflex where start of SFN stimulation preceded the H-reflex by 700 ms. There was an effect of time on the H-reflex [Chi-square = 100.6, DF = 14 ($p <0.001$)] with * indicating significant difference from a 0 %change ($p < 0.05$, Tukey). **C)** PSF of soleus motor unit in response to fast SFN stimulation used in B (note different time scale). Overlay of 100 stimulation trials from one participant. Blue line is binned average of frequency points (20 ms bin width). Red line is pre-stimulus rate.

Fast (200 Hz) cutaneous afferent train: Given the larger sustained facilitation of H-reflexes by the faster conditioning stimulation train of 2 Hz, we also examined a much higher frequency conditioning stimulation train of the SFN at 200 Hz, but of shorter duration (500 ms).

This was very effective in facilitating the H-reflex, consistent with the long-lasting tonic PAD and facilitation of monosynaptic reflexes evoked by this stimulation in animals, lasting for upwards of a minute after the train was terminated (Lucas-Osma *et al.*, 2018b; Hari *et al.*, 2021). Because high frequency stimuli can be painful, we used an intensity of SFN stimulation that was below radiating threshold [3.6 (0.3) mA]. The 500 ms, 200 Hz SFN stimulation produced a large facilitation of the H-reflex immediately after the stimulus train (pink circle at 0-s time bin, Fig. 6B) compared to the unconditioned H-reflexes (black circles, at time bins < 0-s). This large H-reflex facilitation was associated with a ~ 1 s increase in the PSF of the soleus motor units following the SFN train (Fig. 6C, note different time scale in ms) and thus, was partly produced by direct facilitation of the soleus motoneurons. However, after the PSF returned to baseline by 1 s, the H-reflex continued to be facilitated for at least 95 s after the high frequency train ended. The H-reflexes were facilitated at many time points following the conditioning SFN train (at time bins > 0-s, marked by *, $p < 0.05$, Tukey) relative to any of the H-reflexes evoked before the SFN train (at time bins < 0-s).

Slow (0.2 Hz) proprioceptive afferent train: The small gradual increase in H-reflexes from the 0.2 Hz cDPN stimulation was likely produced by a small tonic PAD from cutaneous afferent pathways with a buildup in extra-synaptic GABA (Lucas-Osma *et al.*, 2018; Hari *et al.*, 2021). Similarly, a tonic PAD may also have been produced by the repeated activation of the soleus Ia afferents themselves. During repetitive stimulation of Ia afferents in the rodent, tonic PAD can be produced in other Ia afferents via the classic tri-synaptic pathway, and also in the stimulated Ia afferent itself, the latter termed self-facilitation (Hari *et al.,* 2022). Thus, we predicted that repeated activation of Ia afferents by TN stimulation alone may also produce long-

lasting facilitation of the soleus H-reflex via self-facilitation from tonic PAD (see schematic in Fig. 7). To examine this, we measured if there was any buildup of *test* H-reflexes during baseline measures before any conditioning stimulation was applied. The repetition rate of every 5 s of TN stimulation likely produces a small amount of post-activation depression (Hultborn *et al*., 1996), but the self-facilitation of Ia afferents from tonic PAD may override this. In the 19 participants tested, H-reflexes evoked from the 1st to the 14th TN stimulation (set 1, Fig. 2) gradually increased in amplitude over a period of 1 minute compared to the test H-reflexes that reached a steady state after the first run of conditioning stimuli (set 2, see statistics in legend). Post-hoc, the 6th to 14th H-reflexes were each larger than the 1st H-reflex, suggesting self-facilitation of the Ia afferents arising from the repeated TN stimulation.

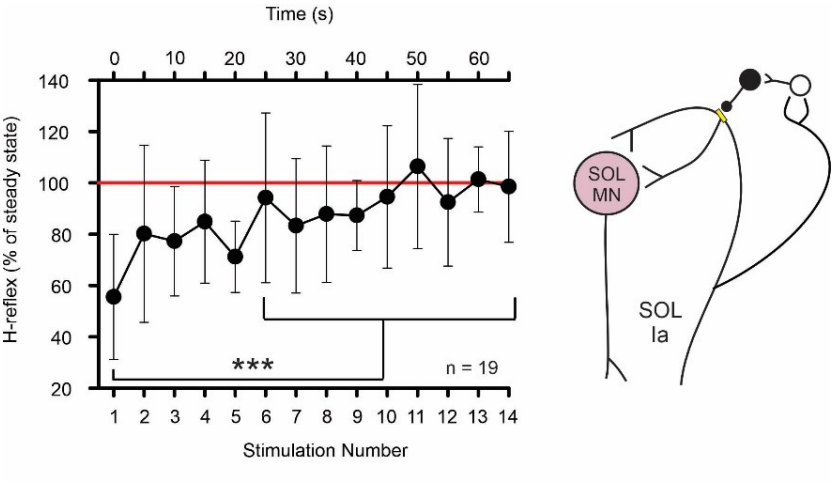

Figure 7. Self-facilitation of H-reflex during tonic PAD. Left: Mean (SD) of first 14 test SOL H-reflexes before any conditioning stimulation was applied averaged across 19 participants. H-reflexes were evoked every 5 seconds at ~ 30% of maximum H-reflex. H-reflexes were expressed as a % of the average of the 7 H-reflexes following the first run of conditioned H-reflexes in set 2 (see Fig. 2, set 2 average = 100% as marked by red horizontal line). The test H-reflexes increased over the 14 TN stimulations ($F(18,13) = 3.93$, $p < 0.001$, one way ANOVA) with H-reflexes 6 to 14 all larger than the first H-reflex (all $p < 0.001$, Tukey). Right: schematic of SOL Ia afferent collateral activating PAD circuit that synapses back onto its own branchpoint node to produce tonic PAD and self-facilitation.

Cutaneous facilitation of single motor unit discharge probability

To provide stronger evidence that a conditioning cutaneous stimulus facilitates the soleus H-reflex by preventing intermittent failure in Ia afferent conduction and generation of the EPSP on the motoneuron, we examined whether the firing *probability* of soleus motor units within the H-reflex (Ia-EPSP) window was increased without producing an increase in the *amplitude* of the motoneuron EPSP estimated by the PSF method. The PSF requires many motor unit firing trials to be averaged and thus, we used cutaneous stimulation trains that produced long-duration increases in afferent depolarization (tonic PAD), where we repeatedly tested the H-reflex before and then after conditioning. The intensity of the TN stimulation used to evoke the H-reflex was adjusted to produce a firing probability of the motor units near or below 50%, since intermittent failure in afferent branch points are more readily seen at low stimulation intensities (Hari *et al.*, 2021). Participants held a weak plantarflexion to recruit a motor unit with a steady background firing rate, upon which we could evaluate changes in firing rate with TN stimulation (PSF, Fig. 8A). At the onset of the H-reflex window (marked by vertical grey line, representative data from a single participant in Fig. 8A), the PSF increased with a profile consistent with the underlying Ia EPSP that produces the H-reflex (PSF in light blue), as previously detailed (Turker & Powers, 2005). A brief duration (50 ms), low intensity SFN stimulation train [4.0 (0.55) mA, 200 Hz] was applied 500 ms

before each TN stimulation to avoid any postsynaptic effects on the motoneuron at the time of Ia activation and allow motor units to be reliably followed. By ~200 ms after the conditioning SFN train, any depolarization of the SOL motoneuron subsided as reflected in the PSF returning to baseline before the H-reflex was evoked (light blue trace near red line, Fig. 8Aii). In this participant, the probability of motor unit discharge within the H-reflex window (15 ms in

duration) increased from 58% during the test-alone trials (Fig. 8Ai) to 71% during the SFN-conditioning trials (Fig. 8Aii). The increased probability of motor unit discharge occurred even though the PSF, representing the profile of the Ia-evoked EPSP (~ 15 ms in duration in rats, Hari et al., 2022), was not altered by the cutaneous conditioning stimulation (note overlay of blue test PSF and pink conditioned PSF, inset of Fig. 8Aii).

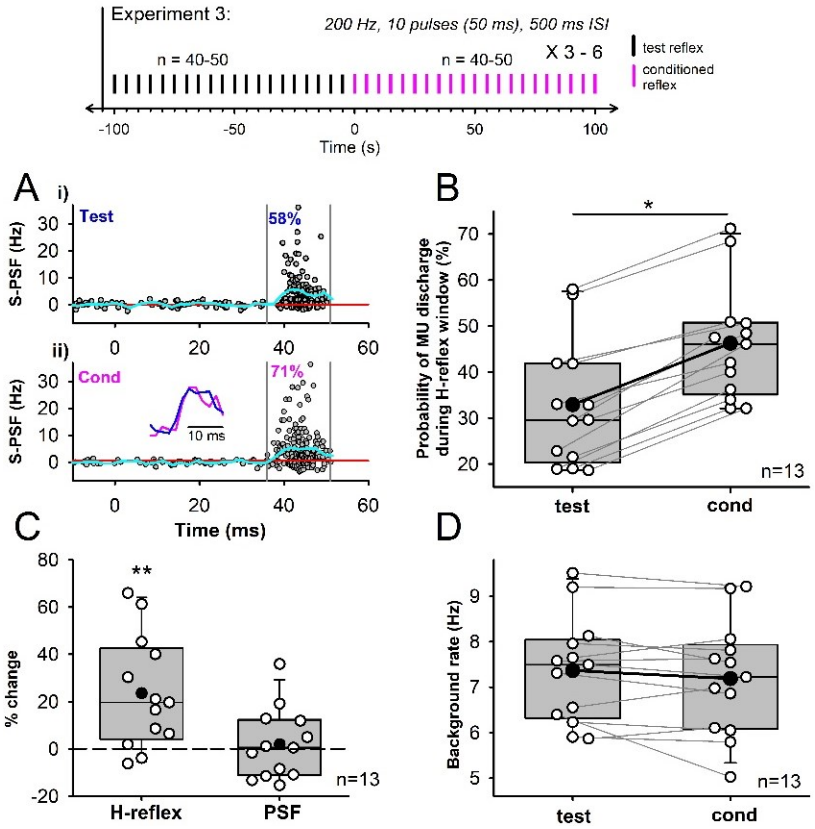

Figure 8. Probability of Single Motor Unit Discharge. A) A representative PSF of SOL motor units recorded from a single male participant using HDsEMG, time-locked to the TN stimulation (at 0 ms) without (i, test) and with (ii, cond) SFN conditioning (10 pulses, 200 Hz, 500 ms ISI). Activity of 11 units are superimposed over 302 sweeps in i (test H-reflexes) and 311 sweeps in ii (conditioned H-reflexes). To reduce variability across units, the mean pre-stimulus firing rate was subtracted from each unit (S-PSF). The mean S-PSF (blue line) is plotted over the mean pre-stimulus rate (red line). The firing probability of the units were measured within the H-reflex window between the grey vertical lines. *Inset:* estimated EPSP from the test (blue) and conditioned (pink) S-PSF. **B)** Probability of motor unit (MU) discharge during H-reflex window before (test) and after (cond) SFN conditioning for each participant (white circles, n = 13 participants, p = 0.014, Mann-Whitney U test), mean represented by the black circle and median by the horizontal line, 25th and 75th percentiles by the box bounds, and the 95th and 5th percentiles by whiskers. Unit activity was measured with HDsEMG in 12 PSFs and with intramuscular EMG in 1 PSF. **C)** % change of the conditioned

SOL H-reflex (left bar) and % change of the PSF within the H-reflex window (right bar), with the H-reflex greater than a 0 % change ($p = 0.001$) but no change in the PSF ($p = 0.74$), both using Mann Whitney U test. **D)** Average firing rate of the SOL motor units measured 100 ms before TN nerve stimulation from the test (left bar) and conditioned (right bar) stimulation trials, with no difference between the two ($p = 0.710$, Student's t-test). * = $p < 0.05$, ** = $p < 0.01$).

Across the group (n = 13), the firing probability of the motor units within the test H-reflex window was 32.9 (14.2) % and increased to 46.3 (12.8) % during the cutaneous conditioning trials (Fig. 8B, see statistics in legend). Importantly, the average firing rate of the PSF within the H-reflex window [13.6 (4.6) ms in duration; reflecting the EPSP size] did not change in response to the cutaneous conditioning (Fig. 8C, right bar), suggesting that an increase in firing probability of the soleus motoneurons activated by the Ia afferents occurred without an increase in the amplitude of the EPSP. In 8 of the 13 participants, the mean PSF was unchanged or even decreased in response to the cutaneous conditioning (Fig. 8C), ruling out changes in motoneuron facilitation (postsynaptic) accounting for the increased motor unit firing probability. The overall soleus H-reflex measured from the surface EMG also increased with conditioning (Fig. 8C left bar), as expected from Figure 6, consistent with the increased probability of the EPSP(s) dominating over any changes in EPSP size and leading to a net increase in the H-reflex. Across the group, the mean background firing rate of the motor unit PSF 100 ms before the TN stimulation with cutaneous conditioning (cond, right bar Fig. 8D) was not different compared to without conditioning (test, left bar) in all participants, further supporting the conclusion that changes in firing probability of the units were not mediated by postsynaptic facilitation of the soleus motoneurons.

Discussion

Over the past 60 years, GABA and the depolarization it produces in peripheral afferents (PAD) was thought to inhibit sensory transmission in the spinal cord by reducing action potential size at the afferent terminal and subsequent neurotransmitter release. However, in the brainstem (Calix of Held), cerebellum (Purkinje cells) and cortex (basket cells) where it is sometimes possible to record directly from presynaptic boutons, the depolarization of the axon terminal from $GABA_A$ or glycine receptors can facilitate neurotransmitter release (typically by increasing intracellular calcium) and subsequent excitatory postsynaptic currents [reviewed in (Trigo *et al.*, 2008; Zorrilla de San Martin *et al.*, 2017)]. We do not think that this terminal facilitation accounts for the facilitation of the monosynaptic reflex detailed here or in the related animal studies (Hari *et al.*, 2021), because $GABA_A$ receptors are mostly absent from proprioceptive afferent terminals in this reflex pathway. Instead, facilitation of Ia mediated EPSPs in the motoneuron likely occurs when axon nodes are depolarized from the activation of nodal $GABA_A$ receptors, which helps to bring sodium channels closer and more rapidly to threshold to reduce branch point failure in the Ia afferent (Hari *et al.*, 2021). This depolarization, or PAD, measured in rodent Ia afferents is readily activated by other Ia afferents or cutaneous and pain afferents demonstrating a facilitatory, rather than inhibitory, role of sensory inputs on the conduction of action potentials in proprioceptive axons. In agreement with this animal study, we provide evidence that the conduction in Ia afferents is similarly facilitated by proprioceptive, cutaneous and CST inputs in the human.

Short-duration facilitation of H-reflexes by sensory and CST pathways.

The profile of H-reflex facilitation from a brief conditioning stimulation of sensory or CST pathways lasted for about 100-200 ms and peaked near the 60 or 80 ms ISI. A similar

profile of monosynaptic reflex facilitation was produced in rodents following either a brief cutaneous stimulation or from direct light activation of $GABA_{axo}$ interneurons (Hari *et al.*, 2021). In both cases, we propose that the time course of monosynaptic reflex facilitation follows the time course of the evoked phasic PAD in the Ia afferent. An illustration of the general profile of H-reflex facilitation in relation to the estimated PAD evoked in the Ia afferents is provided in Figure 1. For instance, at the 0 ms ISI, the phasic PAD from the conditioning stimulation was not yet activated in the Ia afferents when the afferent was activated by the TN stimulation for the H-reflex. This likely produces a motoneuron EPSP and H-reflex that is uninfluenced by PAD. However, when the TN stimulation followed the conditioning stimulation by 60 to 80 ms, the activation of the TN Ia afferents occurs during the presence of the PAD, allowing the TN stimulation to activate more Ia afferent branches and produce more or larger EPSPs and a larger H-reflex (H-reflex at 60 to 80 ms ISI > at 0 ms ISI). An axonal (nodal) mechanism of H-reflex facilitation is likely because when the conditioning stimulation was applied alone, the PSF was slightly below the mean pre-stimulus rate, indicating that the conditioning stimulation itself did not depolarize the motoneuron to facilitate the H-reflex.

Although the mean profile of H-reflex facilitation closely follows the estimated profile of phasic PAD from the 60 to 80 ms ISI onwards, the facilitation of the H-reflex at the earlier ISIs are smaller than expected based on the PAD profile. This may be due to direct effects on the motoneuron from the conditioning stimulation that mask the facilitation of Ia transmission by PAD. For example, any excitatory or inhibitory activation of the motoneuron may have prevented full H-reflex facilitation at these earlier ISIs due to postsynaptic shunting or direct inhibition of the motoneuron as shown in rodents (Hari *et al.*, 2021). Small decreases in the PSF during these earlier ISIs provide some evidence that the motoneuron may have been slightly

inhibited by the conditioning sensory and CST stimulation. In the rodent, when the direct effects on the motoneuron from the conditioning stimulation are removed with voltage clamp, the full effect of the PAD facilitation on monosynaptic reflexes is unmasked. Thus if anything, subtle postsynaptic effects on the motoneuron from the conditioning stimulation tend to decrease the Ia EPSP, strengthening the conclusion that any H-reflex facilitation occurred from facilitation of the Ia afferent conduction.

Both cutaneous and CST inputs have the majority of their terminations in the dorsal horn as measured from anatomical tracings (Lucas-Osma *et al.*, 2018b; Ueno *et al.*, 2018). These inputs may activate the tri-synaptic GABA pathway, possibly including activating the first order glutamatergic interneurons that synapse onto the $GABA_{axo}$ interneurons in this pathway, which in turn activate $GABA_A$ receptors on dorsal nodes of the Ia afferent (Hari *et al.*, 2022). Similar to pain afferents (Hayes & Carlton, 1992), terminals of the CST also synapse directly onto the $GABA_{axo}$ interneurons (identified as d14: GAD2+/Ptf1a+ neurons) that in turn project onto Ia afferents (Ueno *et al.*, 2018). As a descending regulator of sensory inflow to the brain and spinal cord (Liu *et al.*, 2018), our results indicate that CST projections that activate $GABA_{axo}$ interneurons directly facilitate Ia afferent conduction and reflex activation of motoneurons during movement.

The net facilitating action of GABA on afferent conduction is likely due to the relatively greater expression of $GABA_A$ receptors on the dorsally located nodes of the myelinated segments of Ia afferents, compared to the sparser receptor expression found on the unmyelinated terminals of these Ia afferents (Lucas-Osma *et al.*, 2018b; Hari *et al.*, 2021). The few $GABA_A$ receptors at the terminals could, in principle, provide a graded shunting of current to produce presynaptic inhibition of Ia inputs onto the motoneuron. However, mathematical models demonstrate that

this shunting is not sufficient to reduce the size of the action potential invading the terminal (Walmsley *et al.*, 1995; Hari *et al.*, 2021). Moreover, PAD measured at the terminal is small (Lucas-Osma *et al.*, 2018b), likely owing to the small number of terminal $GABA_A$ receptors (Alvarez *et al.*, 1996; Betley *et al.*, 2009; Fink *et al.*, 2014) compared to dorsal parts of the afferent (Lucas-Osma *et al.*, 2018b) and the large electrotonic attenuation of current from the last node to the terminal (Hari *et al.*, 2021). However, GABA may also activate $GABA_B$ receptors on the afferent terminal and $GABA_A$ receptors on the motoneuron to reduce the size of the monosynaptic reflex (Pierce & Mendell, 1993; Hughes *et al.*, 2005; Hari *et al.*, 2021). Thus, the net increase in monosynaptic reflexes from the activation of $GABA_{axo}$ interneurons is likely mediated by the activation of $GABA_A$ receptors on the dorsal regions of the Ia afferent that have a stronger facilitatory effect on Ia afferent conduction compared to the inhibitory effect of $GABA_B$ receptors activated on afferent terminals and the $GABA_A$ receptors on the motoneurons. This balance may favor the facilitation of reflexes when the conditioning stimuli are moderate or small and instead favor a suppression of H-reflexes when higher intensity conditioning stimuli are applied, which may have stronger effects on $GABA_B$ receptor-mediated presynaptic inhibition and/or direct motoneuron inhibition (Hari *et al.*, 2021). It remains to be determined if the same or separate $GABA_{axo}$ neurons innervate nodes ($GABA_A$) and terminals ($GABA_B$). For example, perhaps a separate group of GABAergic neurons innervate the terminals (and $GABA_B$ receptors) and are driven by homonymous nerve stimulation, causing the strong depression of the H-reflex with repeated stimulation (i.e., rate dependent or post-activation depression), and another more dorsal group of GABAergic neurons mediate nodal facilitation (via $GABA_A$ receptors) that are driven by more diverse afferent (e.g., cutaneous) and descending inputs.

Long-lasting facilitation of Ia afferents by cutaneous and proprioceptive inputs

Our results demonstrate that trains of cutaneous stimulation (2 Hz and 200 Hz) facilitate the soleus H-reflex for up to 2 minutes, similar to the duration of long-lasting (tonic) PAD recorded in rodent Ia afferents in response to identical stimulation trains applied to a dorsal root (Lucas-Osma *et al.*, 2018b; Hari *et al.*, 2021). The long duration of PAD evoked in Ia afferents from the multiple, especially high frequency, sensory inputs is produced by the activation of extra-synaptic α5 $GABA_A$ receptors on the Ia afferent nodes, potentially from GABA spillover produced by the repeated activation of $GABA_{axo}$ interneurons (Lucas-Osma *et al.*, 2018b). It is unlikely that the motoneuron is continually facilitated for 2 minutes by these high frequency stimulation trains given that the membrane potential of the motoneuron in the rat, and the motor unit firing rates in the human (PSF), return to pre-stimulation baseline by less than 1 second after the stimulation train. The trains of low frequency (0.2 Hz) cutaneous stimulation produce a smaller sustained facilitation of the H-reflex, comparable to the low-amplitude tonic PAD produced from the same stimulation train in the rodent (Lucas-Osma *et al.*, 2018b), and thus this small facilitation is likely due to a small tonic PAD. It is likewise possible that the gradual increase in H-reflexes over the 2-minute recording is produced by tonic PAD evoked by the repeated (0.2 Hz) activation of the soleus Ia afferents themselves when evoking the H-reflex (repetitive TN stimulation). The gradual increase in test H-reflexes with TN stimulation alone (Fig. 7) supports this hypothesis of self-facilitation where collaterals of the Ia afferent activate a PAD network that synapses back onto its own branch point nodes. Self-facilitation of the Ia afferents is most readily revealed when we use low intensities of TN stimulation that produced an H-reflex of ~30% of maximum, giving headroom for recruiting new afferent branches with tonic PAD (Hari *et al.*, 2021).

Probability of motor unit firing

To strengthen the conclusion that the facilitation of the H-reflex by the sensory or CST conditioning is mediated by facilitation of the Ia afferents, we found it useful to measure single motor unit (motoneuron) activity before and during the H-reflex (Ia-EPSP) window. This allows us to: 1) examine whether the conditioning stimulation alone changes the motoneuron depolarization by examining baseline motor unit firing rates just before the H-reflex (postsynaptic actions), 2) examine whether the conditioning changes the EPSP size in a graded manner by measuring the PSF during the Ia-EPSP (H-reflex) window since graded changes in EPSP would be mediated by changes in either presynaptic inhibition or postsynaptic facilitation and 3) examine the probability of the evoked Ia-EPSP (all-or-nothing failure) reflected in whether the motor unit participated in the H-reflex or not. Overall, we found that the conditioning-evoked PAD was not associated with an increase in baseline motor unit firing or the size of the estimated EPSP, consistent with a lack of postsynaptic facilitation or decrease in presynaptic inhibition that would otherwise grade the EPSP size. If anything, conditioning tended to slightly slow motor unit firing or hyperpolarize motoneurons, as in rats (Hari *et al.*, 2021), which would decrease the probability of the motor unit contribution to the H-reflex. In contrast, we found that the conditioning consistently increased the probability of the motor unit participating in the H-reflex, in agreement with conclusions from rats that PAD prevents branch point failure and reduces the probability of intermittent, all-or-nothing EPSP failures.

Low amplitude TN stimulation intensities were used with the intention of evoking monosynaptic soleus H-reflexes only and not polysynaptic reflexes. Thus, the PSF within the 15 ms H-reflex window likely reflected motor unit discharge during the monosynaptic EPSP and its increased probability by increases in Ia afferent conduction. In support of this, mechanical

cutaneous conditioning of the H-reflex in a forearm muscle also increased the discharge probability of motor units measured during the first 0.5 ms of the reflex window (i.e., during the early monosynaptic component of the EPSP), without increases in integrated EMG and motor unit firing rates, again showing that the motoneuron was not facilitated by cutaneous conditioning but the firing probability of the Ia afferents were (Aimonetti *et al.*, 2000b). In addition, the Aimonetti *et al.,* 2000 results were obtained using single motor unit recordings from intramuscular EMG and corroborates our findings using decomposition of single motor units from HDsEMG during reflex activity (see also Yavuz et al. 2015).

Outside of sensory-evoked PAD preventing branch point failure, there are a few other possible explanations for the increased probability of motor unit discharge contributing to the facilitated H-reflex during conditioning which we must rule out. The conditioning input might somehow increase the probability of quantal transmitter release at the Ia afferent terminal, thereby increasing the probability of the EPSP. This could occur by a yet undescribed non-GABAergic innervation of the Ia afferent terminal that may facilitate intracellular calcium and neurotransmitter release. GABAergic effects on the afferent terminal seem unlikely to increase firing probability because imaging in rodents indicate that Ia afferent terminals mainly only express $GABA_B$ receptors (Hari *et al.*, 2021) which decrease, rather than increase, transmitter release via its inhibitory Gi protein coupled pathways (Curtis & Lacey, 1998). Even if a few $GABA_A$ receptors were on the terminals, these have little practical depolarizing action as shown from direct terminal recordings (Lucas-Osma *et al.*, 2018b) and, if anything, likely inhibits transmitter release (although see Trigo *et al.*, 2008). Thus, we conclude that the most likely explanation for the increased H-reflex and motor unit discharge probability during conditioning is a PAD-mediated facilitation of branch point conduction in the afferents mediating the H-

reflex. Further work is needed to confirm this, including showing that when the motor unit fires during the H-reflex window, there is a uniformly bigger H-reflex than when the motor unit fails to fire during the reflex, consistent with recruitment of unitary EPSPs that result from an afferent branch that is recruited into action.

Relation to previous animal and human studies

The idea that cutaneous and CST pathways facilitate H-reflexes by increasing Ia afferent excitability from PAD is not at odds with previous cat data (Rudomin *et al.*, 1983), but is at odds with the previous conclusion that these pathways reduced PAD measured in extensor afferents (Rudomin *et al.*, 1983). In the cat studies, the size of PAD was indirectly measured by quantifying the threshold current needed to maintain a set level of antidromic firing probability of the Ia afferent when activated by extracellular stimulation in the intermediate or ventral motor nucleus in the spinal cord (Wall, 1958; Carpenter *et al.*, 1963; Willis *et al.*, 1976; Rudomin *et al.*, 1983). Cutaneous and CST inputs reversed the lowering of the threshold current produced by tonic flexor afferent stimulation, leading to the conclusion that cutaneous and CST inputs reduced PAD and hence, the assumed presynaptic inhibition. However, this indirect measure of inhibition of PAD may have been misinterpreted, since it is in contrast to the large PAD directly observed following cutaneous afferent stimulation measured intra-axonally in more dorsal regions of the Ia afferent (Lucas-Osma *et al.*, 2018b; Hari *et al.*, 2021) and the dorsal root potentials evoked from low threshold stimulation of the dorsal cutaneous nerve in mice (Zimmerman *et al.*, 2019). To reconcile these differences, it may be that cutaneous and CST inputs activate $GABA_{axo}$ interneurons to produce PAD in dorsal portions of the Ia afferent but at the same time, inhibit $GABA_{axo}$ interneurons with connections to more ventral portions of the

afferent (i.e., again two separated populations of interneurons). This is supported by the finding that antidromic potentials activated by stimulation of afferents in the dorsal horn are strongly facilitated by cortical stimulation in contrast to antidromic potentials evoked from stimulation of afferent terminals in the ventral horn (Carpenter *et al.*, 1963). In this way, cutaneous pathways (and potentially CST pathways) may enhance dorsal nodes to secure (facilitate) action potential transmission and at the same time, reduce PAD at more ventral nodes to reduce any lowering of threshold currents. Direct measurements of PAD in dorsal and ventral parts of the Ia afferent and its modulation from cutaneous and CST inputs are needed to sort out this discrepancy (though see Lucas-Osma *et al*., 2018).

Based on the cat work, human studies have also proposed that cutaneous and CST inputs reduce the amount of PAD and presynaptic inhibition in agonist Ia afferents, the latter measured from the suppression of H-reflexes by antagonist afferents (Berardelli *et al.*, 1987; Iles & Roberts, 1987; Nakashima *et al.*, 1990; Iles, 1996; Meunier & Pierrot-Deseilligny, 1998a; Aimonetti *et al.*, 2000b). In these studies, it has been proposed that the suppression of H-reflexes by antagonist afferents is reduced by cutaneous and CST pathways via dis-facilitation of the $GABA_{axo}$ interneurons mediating PAD, which would then result in a decrease of presynaptic inhibition. However, recent evidence in rodents shows that the suppression of monosynaptic reflexes by afferents is not mediated by presynaptic inhibition of Ia afferents by PAD (Hari *et al.*, 2021). Rather, inhibition of monosynaptic reflexes by afferent conditioning is produced by other mechanisms such as terminal $GABA_B$ receptor activation, post-activation depression and/or postsynaptic shunting on the motoneuron (Curtis & Lacey, 1994; Walmsley *et al.*, 1995; Trigo *et al.*, 2008; Howell & Pugh, 2016; Zbili & Debanne, 2019; Hari *et al.*, 2021). Thus, the reduced H-reflex inhibition from cutaneous and CST conditioning in previous human studies is likely

explained by facilitating action potential propagation in the Ia afferents by reducing branch point failure to counteract the inhibition of the monosynaptic reflex from these other inhibitory mechanisms.

Functional implications

Activation of GABAergic networks in the spinal cord can have both facilitating and inhibitory actions on afferent transmission within the spinal cord. We demonstrate here that proprioceptive, cutaneous and CST pathways have a net excitatory influence on Ia afferents and this Ia facilitation may also be produce by other afferent modalities as well, such as touch and pain (Lucas-Osma *et al.*, 2018b; Hari *et al.*, 2021). Thus, the drive from the CST during volitional movements and the coincident activation of movement-related proprioceptive and cutaneous inputs may help to secure propagation of action potentials in sensory axons toward both the brain and spinal cord to facilitate the use of this sensory information in movement generation and control. Such regulation of afferent conduction may be affected by brain or spinal cord injury given the known changes to GABAergic networks following these insults (Faist *et al.*, 1994; Tillakaratne *et al.*, 2000; Kapitza *et al.*, 2012; Mende *et al.*, 2016; Khalki *et al.*, 2018; Lalonde & Bui, 2021). Perhaps some of the problems with movement control and development of spasticity from injury may be produced by alterations in GABAergic control of nodal facilitation in afferents, a topic we are currently exploring.

References

Afsharipour B, Manzur N, Duchcherer J, Fenrich KF, Thompson CK, Negro F, Quinlan KA, Bennett DJ & Gorassini MA. (2020). Estimation of self-sustained activity produced by persistent inward currents using firing rate profiles of multiple motor units in humans. *J Neurophysiol* **124,** 63-85.

Aimonetti JM, Vedel JP, Schmied A & Pagni S. (2000). Mechanical cutaneous stimulation alters Ia presynaptic inhibition in human wrist extensor muscles: a single motor unit study. *The Journal of physiology* **522 Pt 1,** 137-145.

Alvarez FJ. (1998). Anatomical basis for presynaptic inhibition of primary sensory fibers. In *Presynaptic Inhibition and Neuron Control*, ed. Rudmon P, Romo R & Mendell LM, pp. 13-41. Oxford University Press, New York.

Alvarez FJ, Taylor-Blake B, Fyffe RE, De Blas AL & Light AR. (1996). Distribution of immunoreactivity for the beta 2 and beta 3 subunits of the GABAA receptor in the mammalian spinal cord. *J Comp Neurol* **365,** 392-412.

Berardelli A, Day BL, Marsden CD & Rothwell JC. (1987). Evidence favouring presynaptic inhibition between antagonist muscle afferents in the human forearm. *J Physiol* **391,** 71-83.

Betley JN, Wright CV, Kawaguchi Y, Erdelyi F, Szabo G, Jessell TM & Kaltschmidt JA. (2009). Stringent specificity in the construction of a GABAergic presynaptic inhibitory circuit. *Cell* **139,** 161-174.

Carpenter D, Lundberg A & Norrsell U. (1963). Primary Afferent Depolarization Evoked from the Sensorimotor Cortex. *Acta Physiol Scand* **59,** 126-142.

Curtis DR & Lacey G. (1994). GABA-B receptor-mediated spinal inhibition. *Neuroreport* **5,** 540-542.

Curtis DR & Lacey G. (1998). Prolonged GABA(B) receptor-mediated synaptic inhibition in the cat spinal cord: an in vivo study. *Exp Brain Res* **121,** 319-333.

Delgado-Lezama R, Loeza-Alcocer E, Andres C, Aguilar J, Guertin PA & Felix R. (2013). Extrasynaptic GABA(A) receptors in the brainstem and spinal cord: structure and function. *Curr Pharm Des* **19,** 4485-4497.

Eccles JC, Eccles RM & Magni F. (1961). Central inhibitory action attributable to presynaptic depolarization produced by muscle afferent volleys. *J Physiol* **159,** 147-166.

Eccles JC, Magni F & Willis WD. (1962a). Depolarization of central terminals of Group I afferent fibres from muscle. *J Physiol* **160,** 62-93.

Eccles JC, Magni F & Willis WD. (1962b). Depolarization of central terminals of Group I afferent fibres from muscle. *The Journal of physiology* **160,** 62-93.

Eccles JC, Schmidt RF & Willis WD. (1962c). Presynaptic inhibition of the spinal monosynaptic reflex pathway. *J Physiol* **161,** 282-297.

Faist M, Mazevet D, Dietz V & Pierrot-Deseilligny E. (1994). A quantitative assessment of presynaptic inhibition of Ia afferents in spastics. Differences in hemiplegics and paraplegics. *Brain* **117 (Pt 6),** 1449-1455.

Fink AJ, Croce KR, Huang ZJ, Abbott LF, Jessell TM & Azim E. (2014). Presynaptic inhibition of spinal sensory feedback ensures smooth movement. *Nature* **509,** 43-48.

Frank K & Fortes MGF. (1957). Presynaptic and postsynaptic inhibition of monosynaptic reflexes. . *Fed Proc* **16,** 39-40.

Gallagher JP, Higashi H & Nishi S. (1978). Characterization and ionic basis of GABA-induced depolarizations recorded in vitro from cat primary afferent neurones. *J Physiol* **275,** 263-282.

Hari K, Lucas-Osma AM, Metz K, Lin S, Pardell N, Roszko D, Black S, Minarik A, Singla R, Stephens MJ, Fouad K, Jones KE, Gorassini M, Fenrich KK, Li Y & Bennett DJ. (2022). Nodal GABA facilitates axon spike transmission in the spinal cord. *Nature Neuroscience* In press.

Hayes ES & Carlton SM. (1992). Primary afferent interactions: analysis of calcitonin gene-related peptide-immunoreactive terminals in contact with unlabeled and GABA-immunoreactive profiles in the monkey dorsal horn. *Neuroscience* **47,** 873-896.

Howell RD & Pugh JR. (2016). Biphasic modulation of parallel fibre synaptic transmission by co-activation of presynaptic GABAA and GABAB receptors in mice. *J Physiol* **594,** 3651-3666.

Hughes DI, Mackie M, Nagy GG, Riddell JS, Maxwell DJ, Szabo G, Erdelyi F, Veress G, Szucs P, Antal M & Todd AJ. (2005). P boutons in lamina IX of the rodent spinal cord express high levels of glutamic acid decarboxylase-65 and originate from cells in deep medial dorsal horn. *Proc Natl Acad Sci U S A* **102,** 9038-9043.

Hultborn H, Illert M, Nielsen J, Paul A, Ballegaard M & Wiese H. (1996). On the mechanism of the post-activation depression of the H-reflex in human subjects. *Experimental brain research* **108,** 450-462.

Iles JF. (1996). Evidence for cutaneous and corticospinal modulation of presynaptic inhibition of Ia afferents from the human lower limb. *J Physiol* **491 (Pt 1),** 197-207.

Iles JF & Roberts RC. (1987). Inhibition of monosynaptic reflexes in the human lower limb. *J Physiol* **385,** 69-87.

Jankowska E, McCrea D, Rudomin P & Sykova E. (1981). Observations on neuronal pathways subserving primary afferent depolarization. *J Neurophysiol* **46,** 506-516.

Kapitza S, Zorner B, Weinmann O, Bolliger M, Filli L, Dietz V & Schwab ME. (2012). Tail spasms in rat spinal cord injury: changes in interneuronal connectivity. *Exp Neurol* **236,** 179-189.

Khalki L, Sadlaoud K, Lerond J, Coq JO, Brezun JM, Vinay L, Coulon P & Bras H. (2018). Changes in innervation of lumbar motoneurons and organization of premotor network following training of transected adult rats. *Exp Neurol* **299,** 1-14.

Lalonde NR & Bui TV. (2021). Do spinal circuits still require gating of sensory information by presynaptic inhibition after spinal cord injury? *Current Opinion in Physiology* **19,** 113-118.

Liu Y, Latremoliere A, Li X, Zhang Z, Chen M, Wang X, Fang C, Zhu J, Alexandre C, Gao Z, Chen B, Ding X, Zhou JY, Zhang Y, Chen C, Wang KH, Woolf CJ & He Z. (2018). Touch and tactile neuropathic pain sensitivity are set by corticospinal projections. *Nature* **561,** 547-550.

Lucas-Osma AM, Li Y, Lin S, Black S, Singla R, Fouad K, Fenrich KK & Bennett DJ. (2018). Extrasynaptic proportional, variant5GABAA receptors on proprioceptive afferents produce a tonic depolarization that modulates sodium channel function in the rat spinal cord. *J Neurophysiol*.

Martinez-Valdes E, Negro F, Laine CM, Falla D, Mayer F & Farina D. (2017). Tracking motor units longitudinally across experimental sessions with high-density surface electromyography. *J Physiol* **595,** 1479-1496.

Matthews PB. (1996). Relationship of firing intervals of human motor units to the trajectory of post-spike after-hyperpolarization and synaptic noise. *The Journal of physiology* **492 (Pt 2),** 597-628.

Mende M, Fletcher EV, Belluardo JL, Pierce JP, Bommareddy PK, Weinrich JA, Kabir ZD, Schierberl KC, Pagiazitis JG, Mendelsohn AI, Francesconi A, Edwards RH, Milner TA, Rajadhyaksha AM, van Roessel PJ, Mentis GZ & Kaltschmidt JA. (2016). Sensory-Derived Glutamate Regulates Presynaptic Inhibitory Terminals in Mouse Spinal Cord. *Neuron* **90,** 1189-1202.

Meunier S & Pierrot-Deseilligny E. (1998). Cortical control of presynaptic inhibition of Ia afferents in humans. *Exp Brain Res* **119,** 415-426.

Nakashima K, Rothwell JC, Day BL, Thompson PD & Marsden CD. (1990). Cutaneous effects on presynaptic inhibition of flexor Ia afferents in the human forearm. *J Physiol* **426,** 369-380.

Negro F, Muceli S, Castronovo AM, Holobar A & Farina D. (2016). Multi-channel intramuscular and surface EMG decomposition by convolutive blind source separation. *J Neural Eng* **13,** 026027.

Nielsen J & Petersen N. (1994). Is presynaptic inhibition distributed to corticospinal fibres in man? *J Physiol* **477,** 47-58.

Nielsen JB, Morita H, Wenzelburger R, Deuschl G, Gossard JP & Hultborn H. (2019). Recruitment gain of spinal motor neuron pools in cat and human. *Experimental brain research*.

Norton JA, Bennett DJ, Knash ME, Murray KC & Gorassini MA. (2008). Changes in sensory-evoked synaptic activation of motoneurons after spinal cord injury in man. *Brain* **131,** 1478-1491.

Pierce JP & Mendell LM. (1993). Quantitative ultrastructure of Ia boutons in the ventral horn: scaling and positional relationships. *J Neurosci* **13,** 4748-4763.

Powers RK & Binder MD. (2001). Input-output functions of mammalian motoneurons. *Rev Physiol Biochem Pharmacol* **143,** 137-263.

Rudomin P, Jimenez I, Solodkin M & Duenas S. (1983). Sites of action of segmental and descending control of transmission on pathways mediating PAD of Ia- and Ib-afferent fibers in cat spinal cord. *Journal of neurophysiology* **50,** 743-769.

Rudomin P & Schmidt RF. (1999). Presynaptic inhibition in the vertebrate spinal cord revisited. *Exp Brain Res* **129,** 1-37.

Tillakaratne NJ, Mouria M, Ziv NB, Roy RR, Edgerton VR & Tobin AJ. (2000). Increased expression of glutamate decarboxylase (GAD(67)) in feline lumbar spinal cord after complete thoracic spinal cord transection. *J Neurosci Res* **60,** 219-230.

Trigo FF, Marty A & Stell BM. (2008). Axonal GABAA receptors. *Eur J Neurosci* **28,** 841-848.

Turker KS & Powers RK. (2005). Black box revisited: a technique for estimating postsynaptic potentials in neurons. *Trends Neurosci* **28,** 379-386.

Ueno M, Nakamura Y, Li J, Gu Z, Niehaus J, Maezawa M, Crone SA, Goulding M, Baccei ML & Yoshida Y. (2018). Corticospinal Circuits from the Sensory and Motor Cortices Differentially Regulate Skilled Movements through Distinct Spinal Interneurons. *Cell Rep* **23,** 1286-1300 e1287.

Wall PD. (1958). Excitability changes in afferent fibre terminations and their relation to slow potentials. *J Physiol* **142,** i3-21.

Walmsley B, Graham B & Nicol MJ. (1995). Serial E-M and simulation study of presynaptic inhibition along a group Ia collateral in the spinal cord. *J Neurophysiol* **74,** 616-623.

Willis WD. (2006). John Eccles' studies of spinal cord presynaptic inhibition. *Prog Neurobiol* **78,** 189-214.

Willis WD, Jr. (1999). Dorsal root potentials and dorsal root reflexes: a double-edged sword. *Exp Brain Res* **124,** 395-421.

Willis WD, Nunez R & Rudomin P. (1976). Excitability changes of terminal arborizations of single Ia and Ib afferent fibers produced by muscle and cutaneous conditioning volleys. *J Neurophysiol* **39,** 1150-1159.

Yavuz US, Negro F, Sebik O, Holobar A, Frommel C, Turker KS & Farina D. (2015). Estimating reflex responses in large populations of motor units by decomposition of the high-density surface electromyogram. *J Physiol* **593,** 4305-4318.

Zbili M & Debanne D. (2019). Past and Future of Analog-Digital Modulation of Synaptic Transmission. *Front Cell Neurosci* **13,** 160.

Zimmerman AL, Kovatsis EM, Pozsgai RY, Tasnim A, Zhang Q & Ginty DD. (2019). Distinct Modes of Presynaptic Inhibition of Cutaneous Afferents and Their Functions in Behavior. *Neuron* **102,** 420-434 e428.

Zorrilla de San Martin J, Trigo FF & Kawaguchi SY. (2017). Axonal GABAA receptors depolarize presynaptic terminals and facilitate transmitter release in cerebellar Purkinje cells. *J Physiol* **595,** 7477-7493.

Additional Information

Competing Interests

The authors have no competing interests to declare.

Author contributions

K.M., Y.L., D.J.B and M.A.G. conceived and designed research; K.M., I.C-M., Y.L., D.J.B. and M.A.G. performed experiments; K.M., I.C-M. and M.A.G. analyzed data; K.M., B.A., C.T. and F.N. decomposed the HDsEMG data; K.M., Y.L., D.J. B. and M.A.G. interpreted results of experiments; K.M., I.C-M and M.A.G. prepared figures; K.M.. D.J.B. and M.A.G. drafted, edited and revised manuscript.

All authors approve the final version of the article and agree to be accountable for all aspects of the work. The authors confirm that all persons designated as authors are qualified.

Funding

This work was supported by a National Science and Engineering Grant 05205 to M.A.G. and studentship funding to K.M. from the Neuroscience and Mental Health Institute and Faculty of Medicine and Dentistry at the University of Alberta.

Acknowledgments

We thank Ms. Jennifer Duchcherer for technical assistance.

Chapter 3: Post-activation depression from primary afferent depolarization (PAD) produces extensor H-reflex suppression following flexor afferent conditioning

Krista Metz[1,3], Isabel Concha Matos[1,3], Krishnapura Hari[2,3], Omayma Bseis[1,3], Babak Afsharipour[1,3], Shihao Lin[2,3], Rahul Singla[2,3], Keith Fenrich[2,3], Li Y[2,3], David J. Bennett[2,3], and Monica A. Gorassini[1,3]

[1] *Biomedical Engineering, Faculty of Medicine and Dentistry, University of Alberta, Edmonton Canada*

[2] *Faculty of Rehabilitation Medicine, University of Alberta, Edmonton Canada*

[3] *Neuroscience and Mental Health Institute, University of Alberta, Edmonton Canada*

Running title: Post-activation depression and H-reflex suppression from primary afferent depolarization

Key words: presynaptic inhibition, GABA, Ia afferents

Table of Contents category: Neuroscience

Preprint link: https://www.biorxiv.org/content/10.1101/2021.04.20.440509v1

Figures: 11

Corresponding Author: Monica Gorassini, monica.gorassini@ualberta.ca; ORCID: 0000-0003-3079-6129; 5005-A Katz Group Building, University of Alberta, Edmonton, AB, (Canada) T6G 2E1

Current address for Y Li:

Department of Physiology, School of Medicine, Emory University, Atlanta Georgia

Key Points Summary

- For many years, suppression of extensor H-reflexes by flexor afferent conditioning was thought to be mediated by $GABA_A$ receptor-mediated primary afferent depolarization (PAD) shunting action potentials in the Ia afferent terminal.
- In line with recent findings that PAD has a facilitatory role in Ia afferent conduction, we show here that when PAD is large enough, it can evoke orthodromic spikes that travel to the Ia afferent terminal to evoke excitatory postsynaptic potentials in the motoneuron.
- These PAD-evoked spikes also produce post-activation depression of Ia afferent terminals and likely mediate the short and long-lasting suppression of extensor H-reflexes in response to flexor afferent conditioning.
- Our findings bring into question that presynaptic inhibition of Ia afferent terminals from $GABA_A$ receptor-mediated PAD is reduced following nervous system injury or disease and highlights that we must reexamine how changes in the activation of PAD affects the regulation of afferent transmission to spinal neurons and ultimately spasticity in these disorders.

Figure 3.0: Abstract Figure Legend

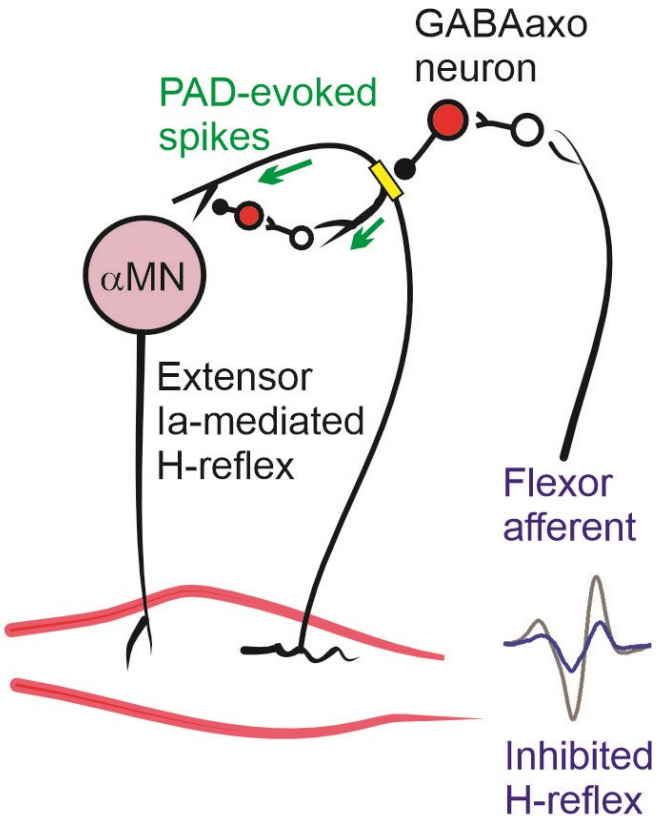

We propose that stimulation of flexor afferents activate GABAergic interneurons ($GABA_{axo}$, red) with axoaxonic connections to or near dorsal nodes of Ranvier (yellow) in extensor Ia afferents. The ensuing activation of $GABA_A$ receptor-mediated PAD at the nodes, if large enough, will activate spikes in the extensor Ia afferent (green arrows) that travel to the extensor motoneuron to produce an excitatory postsynaptic potential. We also hypothesize that PAD-evoked spikes in other branches of the extensor Ia afferent activate more ventral $GABA_{axo}$ interneurons with projections to the Ia afferent terminal. This in turn will activate $GABA_B$ receptors at the Ia afferent terminal to produce post-activation depression and suppression of subsequently activated extensor H-reflexes.

Abstract

Suppression of the extensor H-reflex by flexor afferent conditioning is thought to be produced by a long-lasting inhibition of extensor Ia-afferent terminals via $GABA_A$ receptor-activated primary afferent depolarization (PAD). Considering the recent finding that PAD does not produce presynaptic inhibition of Ia-afferent terminals, we examined if H-reflex suppression is instead mediated by post-activation depression of the test extensor Ia-afferents triggered by PAD-evoked spikes and/or by a long-lasting inhibition of the extensor motoneurons. A brief conditioning vibration of the flexor tendon suppressed both the extensor soleus H-reflex and the tonic discharge of soleus motor units for 300 ms, indicating that part of the H-reflex suppression was

mediated by a long-lasting inhibition of the extensor motoneurons. When activating the flexor afferents electrically to produce conditioning, the soleus H-reflex was also suppressed for 300 ms, but only when a short-latency reflex was evoked in the soleus muscle by the conditioning input itself. In mice, a similar short-latency reflex was evoked when optogenetic or afferent activation of GABAergic ($GAD2^{+}$) neurons produced a large enough PAD to evoke orthodromic spikes in the test Ia-afferents, causing post-activation depression of subsequent monosynaptic excitatory-post-synaptic potentials. The time course of this post-activation depression and related H-reflex suppression (lasting 2 s) was similar to rate-dependent depression that is also due to post-activation depression. We conclude that extensor H-reflex inhibition by brief flexor afferent conditioning is produced by both post-activation depression of extensor Ia-afferents and long-lasting inhibition of extensor motoneurons, rather than from PAD inhibiting Ia-afferent terminals.

Introduction

The suppression of the H-reflex following a conditioning stimulation to an antagonist nerve was until recently thought to be mediated by the activation of a primary afferent depolarization (PAD) in the Ia afferent terminal (Hultborn *et al.*, 1987a; Stein, 1995; Misiaszek, 2003; Hultborn, 2006). Since the 1960's, PAD was thought to be activated by $GABA_A$ receptors at the Ia afferent terminal, resulting in a shunting of terminal currents, depression of neurotransmitter release and ultimately a reduction in the excitatory postsynaptic potential (EPSP) evoked in the motoneuron, as reviewed in (Willis, 2006). However, the role of PAD and $GABA_A$ receptors in producing presynaptic inhibition in the Ia afferent terminal has recently been disproven by multiple lines of evidence (Hari *et al.*, 2021). For example, there is a sparsity of $GABA_A$ receptors on the Ia afferent terminal (Alvarez *et al.*, 1996; Hari *et al.*, 2021) and correspondingly, PAD measured at the unmyelinated Ia afferent terminal is small-to-nonexistent and brief, lasting for 20 ms compared to more proximal, myelinated regions of the Ia afferent that contain nodes of Ranvier where PAD lasts for 100-200 ms (Lucas-Osma *et al.*, 2018b). Further, computer simulations confirm that PAD at the Ia afferent terminal is too weak and brief to produce a physiologically *relevant* decrease in action potential size to reduce EPSP activation in the motoneuron (Hari *et al.*, 2021). In contrast, Ia afferent terminals are densely covered by $GABA_B$ receptors that contribute to terminal presynaptic inhibition (Curtis & Lacey, 1994; Fink, 2013b; Hari *et al.*, 2021).

PAD and $GABA_A$ receptors have instead been shown to facilitate sodium channels at the nodes of Ranvier in Ia afferents, helping spike propagation through branch points to facilitate motoneuron EPSPs (Hari *et al.*, 2021; Metz *et al.*, 2021). This is mediated by axoaxonic connections from GABAergic neurons ($GABA_{axo}$ neurons) onto $GABA_A$ receptors at or near

nodes producing PAD that brings sodium spikes closers to threshold (Hari *et al.*, 2021). Despite its minor influence at the Ia afferent terminal, $GABA_A$ receptors have repeatedly been shown to contribute to the inhibition of the monosynaptic reflex in extensor motoneurons following conditioning of an antagonist flexor nerve to evoke PAD, since this inhibition is partly decreased by $GABA_A$ receptor blockers (Eccles *et al.*, 1963; Stuart & Redman, 1992; Curtis & Lacey, 1994; Curtis, 1998a). This raises the question of how can the activation of $GABA_A$ receptors be inhibitory in some instances (i.e., reduce reflexes) and excitatory in other (i.e., facilitate afferent nodal conduction), and how is this related to the observations that the extensor H-reflex is sometimes inhibited by an antagonist afferent conditioning stimulation (Mizuno *et al.*, 1971; El-Tohamy & Sedgwick, 1983; Berardelli *et al.*, 1987; Hultborn *et al.*, 1987a; Nakashima *et al.*, 1990; Burke *et al.*, 1992; Capaday *et al.*, 1995; Faist *et al.*, 1996; Iles, 1996; Aymard *et al.*, 2000; Howells *et al.*, 2020) and at other times, the same H-reflex is facilitated by this conditioning stimulation (Hari *et al.*, 2021; Metz *et al.*, 2021).

One intriguing possibility recently proposed is that PAD can induce post-activation depression in the Ia afferent terminals mediating the H-reflex (Hari *et al.*, 2021). Here, we broadly define post-activation depression as a reduction in a monosynaptic EPSP caused by a prior activation of the same EPSP, where the first and second EPSPs are evoked by the same Ia afferent population each time, regardless of how the afferents are activated. Post-activation depression can be caused by numerous mechanisms, including transmitter depletion in the Ia afferents following the first EPSP, decreased afferent excitability from the post-spike refractory period that follows the first Ia afferent spike, and even inhibition of the afferent terminals by $GABA_B$ receptors indirectly activated by the test afferents that activated the first EPSP ($GABA_B$

mediated presynaptic inhibition) (Curtis & Eccles, 1960; Eccles *et al.*, 1961a; Hultborn *et al.*, 1996a).

But how would PAD evoked from a conditioning stimulation to an antagonist afferent produce an EPSP in the agonist motoneurons and subsequent post-activation depression of EPSPs and related H-reflexes? Superficially this seems contrary to the conventional understanding that antagonist afferents generally produce reciprocal postsynaptic inhibition of agonist motoneurons (Sherrington, 1908). However, it is well known that PAD can produce antidromic action potentials in sensory axons that are recorded as dorsal root reflexes in the proximal afferent (termed dorsal root reflexes, DRRs), and PAD is strongest when evoked in extensor Ia afferents by antagonist flexor afferent conditioning (Eccles *et al.*, 1961b; Rudomin & Schmidt, 1999). Further, since the early work of Eccles, it has been known that PAD in Ia afferents can also evoke *orthodromic* action potentials, as evidenced by the generation of motoneuron EPSPs from these PAD-evoked spikes (Eccles *et al.*, 1961b; Duchen, 1986; Willis, 1999). Theoretically, this orthodromic action potential evoked in the Ia afferent terminal should reduce subsequent neurotransmitter release for seconds via post-activation depression and thus, may result in a depression of subsequent EPSPs evoked by directly stimulating this same Ia afferent, just as the motoneuron EPSP is reduced by direct, repetitive activation of the Ia afferent. The latter EPSP depression with repetitive activation of the Ia afferent is termed rate dependent depression (RDD) and is caused by post-activation depression of the Ia afferent, and not terminal $GABA_A$ receptor-mediated presynaptic inhibition (Hultborn *et al.*, 1996a). This led us to speculate that H-reflexes following a conditioning stimulation of an antagonist nerve may be suppressed if the antagonist afferents activate PAD and orthodromic action potentials in the Ia afferents mediating the H-reflex, as suggested for the suppression of motoneuron EPSPs in the

rodent when followed by PAD-evoked spikes (Duchen, 1986; Hari *et al.*, 2021). To examine this, we first sought confirmation in mice that when orthodromic action potentials are activated in the Ia afferent from PAD circuits (PAD-evoked spikes), then subsequent direct activation of the Ia afferent produces a smaller EPSP in the motoneuron when tested within the time course of post-activation depression and related RDD (between 20 ms to 2s). For this we activated PAD either through optogenetic activation of specific GABA neurons with axo-axonic connections to Ia afferents and their nodes (light activation of GAD2+ neurons in GAD2-cre//ChR2 mice), or from a separate, heteronymous sensory pathway (Hari et al., 2022). The former optogenetic method is especially powerful because any direct action of GABAergic neurons on motoneurons is inhibitory and so observations of monosynaptic EPSPs that are evoked by light unequivocally demonstrate that the PAD-evoked spikes drive these EPSPs.

We also examined in humans if a conditioning stimulation of the antagonist flexor nerve to the extensor soleus muscle, the common fibular nerve (CFN), could likewise produce a short latency response in the soleus muscle indicative of activating an orthodromic, PAD-evoked spike in the soleus Ia afferent, as directly shown in sural and median afferents with microneurography (Shefner *et al.*, 1992b). We then examined if the suppression of subsequently activated H-reflexes was related to the presence or size of this putative PAD-evoked reflex at stimulation delays previously and incorrectly attributed to the time-course of PAD-mediated presynaptic inhibition (30 to 400 ms). We also examined the time course of this antagonist-evoked H-reflex suppression at much longer delays within the post-activation depression window (500 ms to 2.5 s). The profile of the antagonist (flexor) H-reflex suppression was compared to the profile of RDD, and associated post-activation depression, produced from repeated and direct activation of the soleus Ia afferents mediating the H-reflex at similar delays. We hypothesized that a similar

long-lasting profile of H-reflex suppression from CFN conditioning or RDD would indicate that both were mediated by post-activation depression of the Ia afferents.

A more obvious, but rarely measured, mechanism of long-lasting (300 - 400 ms) H-reflex suppression by antagonist conditioning stimulation is postsynaptic inhibition of the motoneuron given the well-known *glycinergic,* Ia-reciprocal postsynaptic inhibition on the motoneuron and the less well known inhibition caused by *GABA*, where 70-80% of GABAergic interneurons with projections to afferent terminals ($GABA_{axo}$) also have projections onto the postsynaptic motoneuron (Pierce & Mendell, 1993; Hughes *et al.*, 2005). Thus, we first examined if a brief conditioning stimulation of antagonist afferents directly inhibits the motoneuron with a time course similar to the long-lasting suppression of the H-reflex previously attributed to PAD. Inhibition of the soleus H-reflex from a brief vibration to the antagonist tibialis anterior (TA) tendon, or from percutaneous electrical stimulation to the common fibular nerve (CFN), was measured at interstimulus intervals (ISIs) between 0 and 500 ms. Direct effects of the conditioning stimulation onto the test motoneuron(s) were measured from changes in the firing rate of tonically discharging single motor units in response to the conditioning stimulation alone. Changes in the firing rate of the tonically discharging motor units were taken as evidence of a postsynaptic effect on the motoneuron (Powers & Binder, 2001). We hypothesized that if the profile of suppression in the firing rate of the motor unit was similar to the profile of inhibition of the H-reflex from the same conditioning stimulation, then postsynaptic inhibition of the test motoneuron mediated a part of the H-reflex inhibition.

Parts of the data from the human vibration experiments (Hari *et al.*, 2021) and the low-intensity CFN stimulation (Metz *et al.*, 2021) have been published and are expanded upon here.

Methods

Ethics approvals, participants and animals

Human experiments were approved by the Human Research Ethics Board at the University of Alberta (Protocol 00078057), conformed to the *Declaration of Helsinki*, and conducted with informed consent of the participants. Our sample comprised of 19 participants (7 male) with no known neurological injury or disease, ranging in age from 21 to 57 years [26.4 (10.2), mean (standard deviation]. *In vitro* recordings were made from adult mice (2.5 – 6.0 months old, both female and male equally) without (control) and with Cre expressed under the endogenous *Gad2* promotor region (*Gad2tm1(cre/ERT2)Zjh* mice abbreviated to Gad2-CreER mice, The Jackson Laboratory, Stock # 010702) as per Hari *et al.,* 2022. These GAD2-CreER mice were crossed with mice containing flx-stop-flx-ChR2 expressed under the ubiquitous promotor Rosa, to yield mice with GAD2+ neurons expressing light sensitive ChR2 after they were injected with tamoxofin (abbreviated Gad2//ChR2 mice, as detailed in Hari *et al.,* 2021). *In vivo* recordings were made from adult rats (3 - 8 months old, female only, Sprague-Dawley) as per Hari *et al.,* 2022. All experimental procedures were approved by the University of Alberta Animal Care and Use Committee, Health Sciences division (Protocol AUP 00000224).

Animal experimental setup

In vitro recordings in mice

Following extraction of the sacrocaudal spinal cord, dorsal and ventral roots (DR and VR) were mounted on silver-silver chloride wires above the nASCF of the recording chamber and covered with grease for monopolar stimulation and recording (see Hari *et al.,* 2022 for details). Dorsal roots were stimulated with a constant current stimulator (Isoflex, Israel) with

short pulses (0.1 ms) at 1.1 – 1.5 x threshold (T) to specifically activate proprioceptive afferents to evoke both PAD in Ia afferents and monosynaptic EPSPs in motoneurons. This grease gap method was also used to record the composite intracellular response of many sensory axons or motoneurons where the high impedance seal on the dorsal or ventral roots reduces extracellular currents, allowing the recording to reflect intracellular potentials (Luscher *et al.*, 1979; Leppanen & Stys, 1997b; Lucas-Osma *et al.*, 2018b). Return and ground wires were placed in the bath and likewise made of silver-silver chloride. Specifically for sensory axons, we recorded from the central ends of dorsal roots cut within about 2 - 4 mm of their entry into the spinal cord, to give the compound potential from all afferents in the root (dorsal root potential, DRP), which has previously been shown to correspond to PAD (Lucas-Osma *et al.*, 2018b). The dorsal root recordings were amplified (2,000 times), high-pass filtered at 0.1 Hz to remove drift, low-pass filtered at 10 kHz, and sampled at 30 kHz (Axoscope 8; Axon Instruments /Molecular Devices, Burlingame, CA). These grease gap recordings of PAD on sensory afferents reflect only the response of the largest diameter axons in the dorsal root, mainly group I proprioceptive afferents, as detailed previously (Hari *et al.*, 2021). The composite EPSPs in many motoneurons were likewise recorded from the central cut end of ventral roots mounted in the grease gap, which has also previously been shown to yield reliable estimates of the EPSPs (Fedirchuk *et al.*, 1999). The EPSPs were identified as monosynaptic by their rapid onset (first component, ~1 ms after afferent volley arrives in the ventral horn), lack of variability in latency (< 1 ms jitter), persistence at high rates (10 Hz) and appearance in isolation at the threshold for DR stimulation (< 1.1xT), unlike polysynaptic reflexes which vary in latency, disappear at high rates, and mostly need stronger DR stimulation to activate.

Light was used to evoke PAD in the GAD2//ChR2 mice and dorsal root stimulation was used to evoke PAD in control mice as described previously (Lin *et al.*, 2019). Light was derived from a laser with a 447 nm wavelength (D442001FX lasers from Laserglow Technologies, Toronto) and was passed through a fibre optic cable (MFP_200/220/900-0.22_2m_FC-ZF1.25, Doric Lenses, Quebec City). A half cylindrical prism the length of about two spinal segments (8 mm; 3.9 mm focal length, Thor Labs, Newton, USA,) collimated the light into a narrow long beam (200 mm wide and 8 mm long). This narrow beam was focused longitudinally on the left side of the spinal cord roughly at the level of the dorsal horn, to target the epicentre of $GABA_{axo}$ neurons, which are dorsally located. ChR2 rapidly depolarizes neurons (Zhang *et al.*, 2011), and thus we used 5 - 10 ms light pulses to activate $GABA_{axo}$ neurons, as confirmed by direct recordings from these neurons (Hari *et al.*, 2021). Light was always kept at a minimal intensity, 1.1x T, where T is the threshold to evoke a light response in sensory axons, which made local heating from light unlikely.

Intracellular recordings of Ia afferent branches in the dorsal horn of rats were performed as in (Hari *et al.*, 2021). Briefly, glass capillary tubes (1.5 mm and 0.86 mm outer and inner diameters, respectively; with filament; 603000 A-M Systems; Sequim, USA) with a bevelled hypodermic-shaped point of < 100 nm, were filled through their tips with 1 M K-acetate and 1 M KCl. Intracellular recording and current injection were performed with an Axoclamp2B amplifier (Axon Inst. and Molecular Devices, San Jose, USA). Recordings were low pass filtered at 10 kHz and sampled at 30 kHz (Clampex and Clampfit; Molecular Devices, San Jose, USA). Electrodes were advanced into myelinated afferents of the sacrocaudal spinal cord with a stepper motor (Model 2662, Kopf, USA, 10 μm steps at maximal speed, 4 mm/s), usually at the boundary between the dorsal columns and dorsal horn gray matter. Upon penetration, afferents

were identified with direct orthodromic spikes evoked from DR stimulation. The lowest threshold proprioceptive group Ia afferents were identified by their direct response to DR stimulation, very low threshold (< 1.5 x T, T: afferent volley threshold), short latency (group Ia latency, coincident with onset of afferent volley), and antidromic response to micro stimulation of the afferent terminal in the ventral horn [~ 10 μA stimulation via tungsten microelectrode as per (Lucas-Osma *et al.*, 2018b)]. Post hoc these were confirmed to be large proprioceptive Ia afferents by their unique extensive terminal branching around motoneurons, unlike large cutaneous Aβ afferents that do not project to the ventral horn. Clean axon penetrations without injury occurred abruptly with a sharp pop detected on speakers attached to the recorded signal, the membrane potential settling rapidly to near – 70 mV, and > 70 mV spikes usually readily evoked by DR stimulation or brief current injection pulses (1 – 3 nA, 20 ms, 1 Hz). Sensory axons also had a characteristic >100 ms long depolarization following stimulation of a dorsal root (primary afferent depolarization, PAD, at 4 - 5 ms latency) and short spike afterhyperpolarization (AHP ~ 10 ms), which further distinguished them from other axons or neurons. Injured axons had higher resting potentials (> - 60 mV), poor spikes (< 60 mV) and low resistance (to current pulse; Rm < 10 MΩ) and were discarded.

In vivo recordings in rats

The influence of evoking PAD in Ia afferents on the monosynaptic reflex (MSR) was performed in awake rats with percutaneous tail EMG recording and nerve stimulation as per Hari et al., 2022. Here, PAD was evoked by a cutaneous conditioning stimulation of the tip of the tail (0.2 ms pulses, 3xT, 40 - 120 ms prior to MSR testing) using an additional pair of fine Cooner wires implanted at the tip of the tail (separated by 8 mm). In rats the MSR latency is later than in

mice due to the larger peripheral conduction time, ~12 ms (as again confirmed by a similar latency to the F wave). This MSR was thus quantified by averaging the rectified EMG over a 12 - 20 ms window. Also, to confirm the $GABA_A$ receptor involvement in regulating the MSR, the antagonist L655708 was injected systemically (1 mg/kg i.p., dissolved in 50 µl DMSO and diluted in 900 µl saline). Again, the MSR was tested at matched background EMG levels before and after conditioning (or L655708 application) to rule out changes in postsynaptic inhibition.

Human experimental setup

Participants were seated in a reclined, supine position on a padded table. The right leg was bent slightly to access the popliteal fossa and padded supports were added to facilitate complete relaxation of all leg muscles because descending activation could potentially activate $GABA_{axo}$ circuits within the spinal cord (Jankowska *et al.*, 1981c; Rudomin, 1990; Eguibar *et al.*, 1997; Ueno *et al.*, 2018). During H-reflex recordings, participants were asked to rest completely with no talking, hand or arm movements.

Surface EMG recordings

A pair of Ag-AgCl electrodes (Kendall; Chicopee, MA, USA, 3.2 cm by 2.2 cm) was used to record surface EMG from the soleus and tibialis anterior (TA) muscles with a ground electrode placed just below the knee. The EMG signals were amplified by 1000 and band-pass filtered from 10 to 1000 Hz (Octopus, Bortec Technologies; Calgary, AB, Canada) and then digitized at a rate of 5000 Hz using Axoscope 10 hardware and software (Digidata 1400 Series, Axon Instruments, Union City, CA). To examine the postsynaptic effects of the conditioning inputs alone on the soleus motoneurons, surface EMG electrodes were also used to record single motor

units during weak contractions by placing the surface electrodes on the lateral border of the muscle as done previously (Matthews, 1996). Single motor units were also recorded using a high-density surface EMG electrode (HDsEMG, OT Bioelettronica, Torino, Italy, Semi-disposable adhesive matrix, 64 electrodes, 5x13, 8 mm inter-electrode distance) with ground and differential electrodes wrapped around the ankle and below the knee. Signals were amplified (150 times), filtered (10 to 900 Hz) and digitized (16 bit at 5120 Hz) using the Quattrocento Bioelectrical signal amplifier and OTBioLab+ v.1.2.3.0 software (OT Bioelettronica, Torino, Italy). The EMG signal was decomposed into single motor units using custom MatLab software as per (Negro *et al.*, 2016; Afsharipour *et al.*, 2020).

Nerve stimulation to evoke an H-reflex

The tibial nerve (TN) was stimulated in a bipolar arrangement using a constant current stimulator (1 ms rectangular pulse width, Digitimer DS7A, Hertfordshire, UK) to evoke an H-reflex in the soleus muscle. After searching for the TN with a probe to evoke a pure plantarflexion, an Ag-AgCl electrode (cathode: Kendall; Chicopee, MA, USA, 2.2 cm by 2.2 cm) was placed in the popliteal fossa, with the anode (Axelgaard; Fallbrook, CA, USA, 5 cm by 10 cm) placed on the patella. Stimulation intensity was set to evoke a test H-reflex of approximately half maximum on the ascending phase of the H-reflex recruitment curve to allow for both facilitatory and inhibitory effects of the conditioning input to be revealed (Crone *et al.*, 1990). H-reflexes recorded at rest were evoked every 5 seconds to minimize post-activation depression from RDD (Hultborn *et al.*, 1996a) and at least 10 H-reflexes were evoked before conditioning to establish a steady baseline. All H-reflexes were recorded at rest.

Antagonist TA tendon vibration

In 8 participants, the soleus H-reflex was conditioned by a prior vibration of the TA tendon (3 pulses, 200 Hz) to preferentially activate Ia afferents as done previously (Hultborn *et al.*, 1987a). A 7 mm diameter probe attached to an audio amplifier was pressed gently against the TA tendon at the base of the leg. Approximately 10 baseline soleus H-reflexes were elicited to ensure the H-reflex was stable, followed by 7 conditioned H-reflexes at a single ISI (0, 30, 60, 100, 150, 200, 300, 400 or 500 ms). Following this, 3 to 4 unconditioned H-reflexes were evoked to reestablish baseline and another run of 7 conditioned H-reflexes was applied at a randomly chosen interval. This was repeated until all ISI intervals were applied (Fig. 1A).

Modulation in the tonic firing rate of single soleus motor units was used to determine if the TA tendon vibration had any postsynaptic actions on the soleus motoneurons. A small voluntary isometric contraction (~5% of maximum) was used to produce a steady discharge of the single unit(s) using both auditory and visual feedback, while the vibration was delivered every 3 seconds. Seven units from 5 participants were isolated from the surface EMG and 12 units from 3 participants were decomposed from the HDsEMG. Modulation of the whole-muscle surface EMG was also measured while participants held a stronger isometric voluntary contraction at approximately 10% of maximum.

Antagonist CFN stimulation

In a separate experiment on a different day in 13 participants (2 participants from the vibration experiment), the CFN supplying the antagonist TA muscle was stimulated to condition the ipsilateral soleus H-reflex as done previously (Mizuno *et al.*, 1971; El-Tohamy & Sedgwick, 1983; Capaday *et al.*, 1995). The CFN was stimulated using a bipolar arrangement (Ag-AgCl

electrodes, Kendall; Chicopee, MA, USA, 2.2 cm by 2.2 cm) with the anode placed anterior and slightly distal to the fibular head on the right leg and the cathode 2-3 cm more proximal. Care was taken to elicit a pure dorsiflexion response without foot eversion. Three pulses (200 Hz, 1-ms pulse width) were applied to the CFN at an intensity of 1.0 and 1.5 x motor threshold (MT) at the 3, 15, 30, 60, 80, 100, 150, 200, 300 and 400 ms ISIs using a similar protocol as in the vibration experiment (Fig. 1A). Motor threshold was determined by the lowest-intensity, single-pulse stimulation of the CFN that produced a small (< 10 □V) but reproducible direct motor response (M wave) in the TA muscle at rest. In a separate trial, CFN stimulation was applied at longer ISI intervals (500, 1000, 1500, 2000 and 2500 ms) at both the 1.0 and 1.5 x MT stimulation intensities with the same protocol as for the shorter ISIs.

The effect of the 1.0 and 1.5 x MT conditioning CFN stimuli on the firing rate of tonically discharging soleus motor units and whole muscle EMG were also measured as done for the vibration stimuli described above. In 12 participants, 44 units were isolated from the surface EMG and in 1 participant, 2 units were decomposed from the HDsEMG.

Post-activation depression of the soleus H-reflex during RDD

In 8 of the 13 participants from the CFN-conditioning experiment, we examined the suppression of the soleus H-reflex in response to repetitive stimulation of the TN to directly assess post-activation depression and compare it to the long-lasting depression evoked from a conditioning heteronymous CFN stimulation. To measure post-activation depression during RDD, the first H-reflex (H1) of a stimulation trial was evoked at approximately 50% of maximum on the ascending part of the H-reflex recruitment curve. A run of at least 10 H-reflexes were repetitively evoked at the same conditioning-test intervals as for the CFN

stimulation at 500, 1000, 1500, 2000 and 2500 ms. Three trials were performed for each stimulation frequency with at least 30 to 40 s in between each trial.

Data analysis

EPSP modulation: Similar to Hari *et al.,* 2022, the amplitude of the EPSP recorded in the ventral root evoked from dorsal root stimulation was compared with and without action potentials evoked in the Ia afferent from optogenetic or sensory activated PAD. The average EPSP from ~10 trials evoked every 10 s just before conditioning and 10 trials during conditioning was used to compute the change in the peak size of the monosynaptic EPSP with conditioning. The background motoneuron potential, membrane resistance (Rm) and time constant just prior to the EPSP was also assessed before and after conditioning to examine whether there were any postsynaptic changes that might contribute to changes in the EPSP with conditioning. The latency of the direct EPSPs evoked by dorsal root stimulation was also compared to the latency of the EPSPs from PAD-evoked spikes. Along with the ventral root recordings, PAD was simultaneously recorded from the dorsal roots by a similar averaging method (10 trials of conditioning), to establish the relation of changes in EPSPs with associated PAD.

H-reflex modulation: For a given trial run, the average, unrectified peak-peak amplitude of all test (unconditioned) soleus H-reflexes was compared to the average peak-peak amplitude of the 7 conditioned soleus H-reflexes (vibration and CFN stimulation) for each of the ISIs tested. The conditioned H-reflexes were expressed as a % change from the test reflex using the formula: % change H-reflex = ([(condition H - test H)/test H]*100%). The mean % change of the soleus H-reflex at each ISI was then averaged across participants.

Effect of conditioning stimulation on soleus motoneurons: The firing rate profile of soleus motor units in response to the conditioning TA tendon vibration or CFN stimulation were superimposed and time-locked to the time of the stimulation (set to 0 ms) to produce a peri-stimulus frequencygram (PSF), as done previously (Norton *et al.*, 2008). The PSF was divided into 10 ms bins and the mean of each bin was expressed as a percentage of the mean, pre-stimulus firing rate measured from a 100 ms window before the conditioning stimulation using the formula: % change PSF = ([(post-stimulus rate - pre-stimulus rate)/pre-stimulus rate]*100%). The mean % change in each bin was then averaged across participants to produce the group mean PSF. The cumulative sum (CUSUM) of the mean PSF was measured by subtracting the mean pre-stimulus values and integrating over time. A significant increase or decrease in the mean PSF CUSUM was considered when it fell above or below, respectively, 2 standard deviations (SD) of the mean pre-stimulus value. For group changes in EMG activity, a similar bin analysis was done for the rectified surface EMG. The mean pre-stimulus EMG measured between -300 to 0 ms was subtracted from each of the mean bin values to measure the net increase or decrease in EMG activity. The artifact from the CFN stimulation (typically from 0 to 20 ms) was manually removed from the soleus EMG.

Post-activation depression of H-reflexes: To quantify the amount of post-activation depression during the RDD trials, the average peak-peak amplitude of the second to eighth H-reflex (H2-H8) was compared to the peak-peak amplitude of the first H-reflex (H1) in each trial run using the formula: % change post-activation depression = ([(H2-H8)/H1]*100%). The % change post-activation depression value for the three trials at each stimulation frequency was averaged together and this value was then averaged across the 8 participants. The resulting %

change in post-activation depression at each stimulation frequency was compared to the % change of the CFN-conditioned soleus H-reflex at the corresponding ISI.

Statistical Analysis

All statistics were performed with SigmaPlot 11 software. To determine if the suppression of the H-reflex across the various conditioning stimulation intervals was different from a 0% change, a One-Way Repeated Measure ANOVA was used because the data was normally distributed. The F value was reported and post hoc Tukey Tests were used to determine which ISIs were significantly different from a 0% change. A Two-Way Repeated Measure ANOVA was used to compare if the H-reflex suppression using antagonist CFN stimulation was different across the various ISIs compared to the repetitive TN conditioning stimulation during RDD. Student t-tests and Pearson Product-Moment Correlation were used to compare the two groups of normally distributed data. Data are presented in the figures and in the text as means and standard deviation (SD). Significance was set as $P < 0.05$.

Results

Antagonist TA tendon vibration.

We started by examining the action of tendon vibration, as this was the classic method of examining presynaptic inhibition of Ia afferents in humans (Morin *et al.*, 1984; Hultborn *et al.*, 1987a; Hultborn *et al.*, 1987b; Roby-Brami & Bussel, 1990; Rossi *et al.*, 1999). The suppression of the soleus H-reflex from a prior vibration (3 cycles at 200 Hz) to the antagonist TA tendon was examined in 8 participants (schematic of experimental protocol in Fig. 1A). Similar to earlier studies, the soleus H-reflex was suppressed between 60 to 400 ms following the brief tendon vibration, as shown for participant 1 (Fig. 1B-C) and participant 2 (Fig. 1G-H). Across the 8 participants, the amplitude of the conditioned soleus H-reflex was modulated across the various ISIs, with the H-reflex being significantly suppressed at the 100, 150 and 200 ms ISIs (marked by white circles, Fig. 2A, see statistics in legend).

To determine if the profile of H-reflex suppression was mediated, in part, from a postsynaptic inhibition of the soleus motoneurons, the firing rate of a voluntarily activated soleus motor unit was measured in response to the conditioning tendon vibration applied alone. Following the conditioning stimulus, the mean firing rate of the soleus motor unit measured from the peristimulus frequencygram (PSF) decreased below the mean pre-stimulus rate, with a time course similar to the soleus H-reflex inhibition (between 80 and 400 ms in Figs. 1D & I, red trace). Note that the H-reflex data plotted at the various ISIs are shifted to the right of the PSF by ~ 30 ms, the latency of the H-reflex, to estimate the excitability of the spinal motoneurons at the time they were activated by Ia afferents in the H-reflex (see also Metz *et al*., 2022). The decrease in the PSF is an indication of a prolonged inhibitory postsynaptic potential (IPSP) (Turker & Powers, 1999), with the duration of the IPSP marked by the lowest point in the blue PSF

CUSUM line (Figs 1D and I). On average, the PSF was suppressed out to 270 ms (red arrow in PSF CUSUM, Fig. 2C) at time points when the H-reflex was also suppressed. There was also a decrease in the number of motor unit action potentials compared to the mean pre-stimulus count during the early decrease in the PSF, as assessed from the PSTH (Figs. 1E&J, Fig. 2D), that was also reflected in the decreased surface EMG during this period (Figs. 1 F&K, 2E). In some cases, the IPSP was large enough to produce a synchronous resetting of the tonic motor unit discharge, as marked by repetitive clusters of increased firing in the PSTH following the reduced firing periods (near 230 and 360 ms in Fig. 1E). Taken together, our results provide evidence for prolonged inhibition of the soleus motoneurons from the conditioning TA tendon vibration, which likely contributed to the profile of H-reflex suppression.

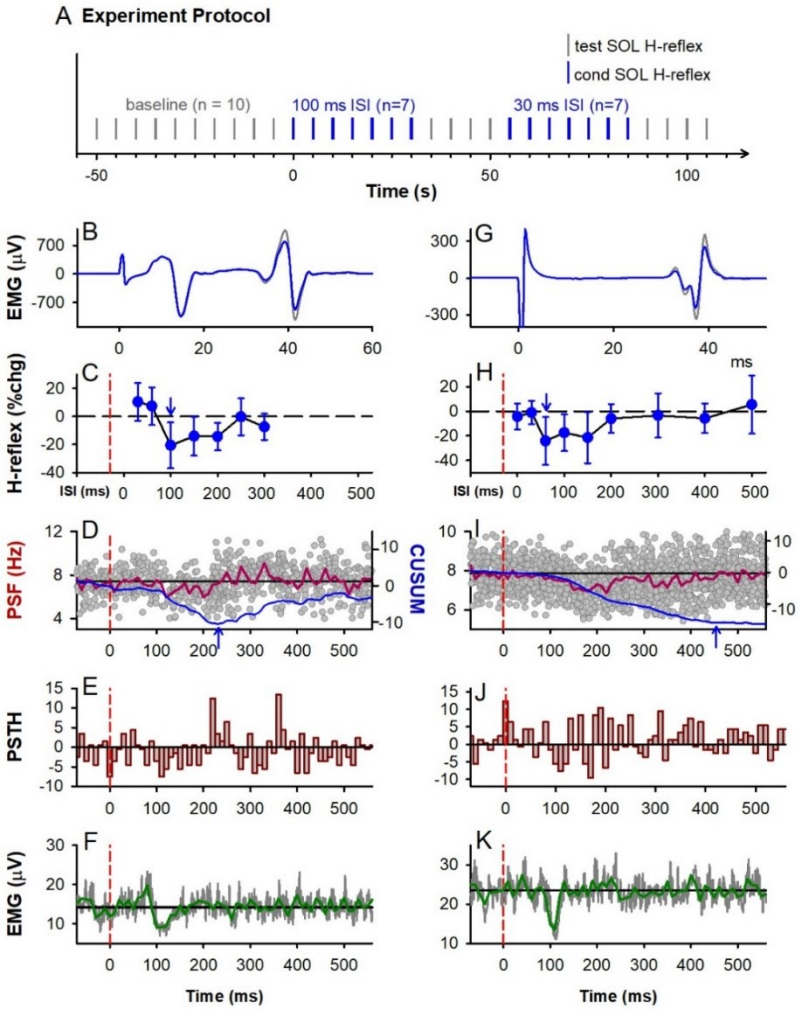

Figure 1: TA tendon vibration. **A)** General experiment schematic: vertical bars mark application of unconditioned test (grey) and conditioned (blue) H-reflexes to the soleus (SOL) muscle, evoked every 5 s with random application of the various conditioning ISIs interposed with a run of test H-reflexes. **B-F** & **G-K**: Representative data from 2 participants. **B,G)** Average of 7 test (grey) and 7 conditioned (blue) soleus H-reflexes (unrectified EMG) at the 100 ms (B) and 60 ms (G) ISI respectively. TN stimulation to

evoke H-reflex applied at 0 ms. **C,H)** % change (chg) of the soleus H-reflex (mean ± SD) plotted at each ISI with peak % change indicated by the arrow. Time of vibration indicated by red dashed line, occurring to the left of the 0 ms ISI by the latency of H-reflex. **D,I)** Superimposed firing rates (grey dots, PSF) of soleus motor units in response to TA tendon vibration alone (185 and 340 sweeps respectively), with a 10-ms binned average rate (red line, mean PSF) and mean PSF CUSUM (blue line). **E,J)** Post-stimulus time histogram (PSTH) showing motor unit count per each 10 ms bin with mean pre-vibration count subtracted. **F,K)** Rectified soleus EMG (grey lines, 31 and 68 sweeps respectively), with 10-ms binned average (green line). Vertical dashed red lines in C to K mark onset of TA tendon vibration (at time 0). Horizontal black lines mark the average pre-vibration values (from -100 to 0 ms).

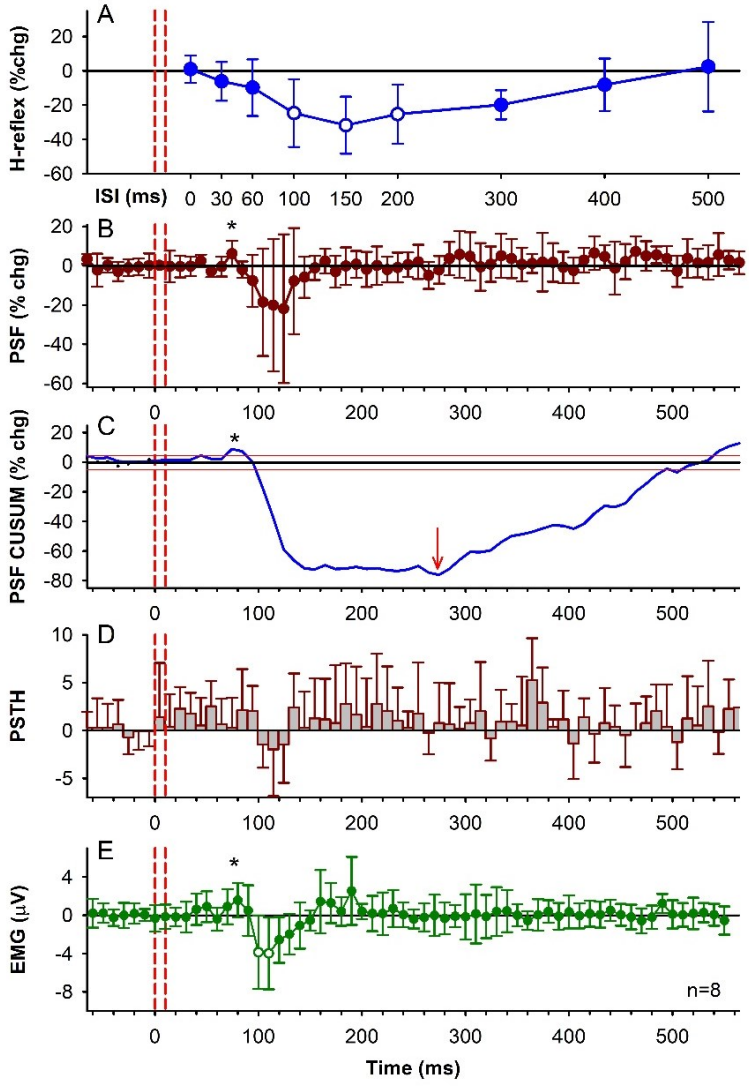

Figure 2: TA tendon vibration, group data. **A)** % change (chg) of the soleus H-reflex from TA tendon vibration at each ISI averaged across the group (n=8 participants). The average size of the unconditioned test soleus H-reflex was 1581 (648) μV [50.3 (15.5)% of H-Max]. There was an effect of ISI on the conditioned H-reflexes [$F(7, 9)=45.2$, $P < 0.001$, one-way RM ANOVA] with post-hoc analysis showing the 100 ms ($P = 0.015$), 150 ms ($P = 0.005$) and 200 ms ($P = 0.012$) ISIs significantly different from a 0% change (white symbols, Tukey Tests). The 0 ms ISI is

shifted to the right of the vibration onset (first dashed red line) by the average latency of the H-reflex. **B)** % change of the PSF averaged across the group (10-ms bins) in response to TA tendon vibration alone. There was an effect of time on the % change PSF ($F[71,64] = 2.02$, $P < 0.001$, one-way RM ANOVA), but no single value was significantly different than a 0% change (post hoc Tukey Test, all $P > 0.05$). **C)** CUSUM of mean PSF in B, plotted with the mean pre-vibration value (horizontal black line) and 2 SD values above and below the mean line (red lines). **D)** Number of soleus motor unit action potentials averaged across the group in each 10-ms bin (PSTH) with the mean pre-vibration number subtracted. The count per bin did not significantly change across the time bins ($F[71,64] = 1.10$, $P = 0.288$, one-way RM ANOVA). **E)** Rectified soleus EMG (mean EMG - pre-stimulus EMG) in each 10-ms bin averaged across the group. The EMG was significantly different across the tested time bins ($F[7,56] = 2.85$, $P < 0.001$, one-way RM ANOVA), being significantly different from 0 mV at the 100 ms ($P = 0.015$) and 110 ms ($P = 0.009$, Tukey Test, white symbols) bins. Vertical red dashed lines indicate the onset and offset of TA tendon vibration. Error bars indicate ± SD. * indicates small increases in motor unit or EMG activity shortly after the vibration.

Unexpectedly, in some participants there was a clear early excitation of the extensor soleus EMG (abbreviated *early soleus reflex*) following the vibration to the *antagonist TA* tendon applied alone (e.g., Fig. 1F). This excitation was evident in the group EMG averages and in the PSF and PSF CUSUM (at *, Figs. 2B,C and E), occurring at about 50 -70 ms after the tendon vibration. The relevance of this early soleus excitation evoked by the antagonist afferent conditioning in suppressing the H-reflex was investigated further below in mice and rats.

Post-activation depression of afferent transmission in mice and rats

The early soleus reflex following the TA tendon vibration raised the possibility that the antagonist TA afferents evoked a PAD in the soleus Ia afferents that produced orthodromic action potentials (PAD-evoked spikes) to subsequently activate a monosynaptic reflex (MSR),

causing post-activation depression of soleus Ia afferent transmission, as we detail in the Introduction. Thus, we examined if GABAergic neurons with axo-axonic connections to afferents ($GABA_{axo}$ neurons) could, in principle, evoke PAD and orthodromic spikes in Ia afferents to produce such post-activation depression and a reduction of subsequent motoneuron EPSPs. To do this, grease gap recordings from sacral dorsal and ventral roots were made in adult spinal cords from GAD2//ChR2 positive mice (schematic in Fig. 3A). These recordings allowed simultaneous assessment of afferent PAD and motoneuron EPSPs, with PAD directly evoked by $GABA_{axo}$ ($GAD2^{+}$) neurons, which cannot themselves directly evoke EPSPs in motoneurons (Hari *et al.*, 2021). When light activation of $GABA_{axo}$ neurons produced a PAD without generating action potentials in the afferents (top light blue trace, Fig. 3A), the monosynaptic EPSP evoked from a dorsal root (DR 1) stimulation during this PAD was facilitated (bottom light blue trace) compared to when PAD was not present (pink trace, DR 1 stim alone). As we have recently shown, this EPSP facilitation is due to increased conduction in Ia afferents evoking the EPSP, via PAD facilitating spike generation at the nodes [nodal facilitation (Hari *et al.*, 2021; Metz *et al.*, 2021)]. However, when activation of the $GABA_{axo}$ neurons produced a larger and faster rising PAD that also generated an action potential in the Ia afferent (PAD-evoked spike, DRR; top black trace Fig. 3A), a fast transient EPSP was evoked in the motoneurons (middle black trace, Fig. 3A), indicating that the PAD-evoked spike traveled orthodromically to the Ia afferent terminal and evoked a monosynaptic EPSP, as Duchen (1986) has previously demonstrated. Indeed, this PAD-evoked spike in the Ia axon activates the motoneuron synchronously at a monosynaptic latency that is similar to the latency of EPSPs generated by direct activation of the Ia afferent by dorsal root stimulation (DR 1, Fig. 3F,G). Following these PAD-evoked spikes and EPSPs, subsequently tested monosynaptic EPSPs evoked by direct DR

stimulation were always depressed, regardless of whether the EPSP was evoked during or after PAD and the related PAD-evoked EPSPs (Figs. 3A and B respectively, black traces), demonstrating that PAD-evoked spikes cause post-activation depression of the Ia-mediated EPSP (see also Fig. 3C).

If the suppression of the monosynaptic EPSP following the PAD-evoked spike is indeed due to post-activation depression of the Ia afferent terminal, this suppression should last for many seconds (Curtis & Eccles, 1960; Hultborn *et al.*, 1996a). In support of this, we evaluated a very long interval between the PAD-evoked spikes and the test EPSP. When an EPSP was evoked during a tonic PAD produced by a long train of light pulses, the EPSP was facilitated by the PAD when no PAD-evoked spikes were produced, as previously reported (Hari *et al.,* 2022) (Fig. 3D and expanded in H, pink trace EPSP alone, blue trace EPSP with tonic PAD). In contrast, when the same long train of light pulses evoked a spike at the start of the tonic PAD (Fig. 3E and expanded in I), the test EPSP that was evoked 1.5 s later was instead depressed (Fig. 3E and expanded in J, black trace), especially compared to the expected facilitation at this time (blue trace overlayed from Fig. 3H). This is broadly similar to Fig. 3 of Duchen 1986, though in that case PAD was evoked indirectly by a DR stimulation, as we detail next.

A similar suppression of the monosynaptic EPSP occurred when PAD-evoked spikes in the Ia afferent were activated by sensory-evoked PAD, rather than light-evoked PAD, the former produced by stimulating a separate dorsal root (termed DR2) to that used to evoke the test EPSP (DR1). As shown from an intracellular (IC) axon recording of a proprioceptive Ia afferent (top, Fig. 3K), a single dorsal root pulse (DR2) sometimes produced a spike in the Ia afferent on the rising phase of the PAD evoked by this dorsal root stimulation (expanded view in bottom). The same DR2 stimulation produced multiple axon spikes in the afferent population recorded from

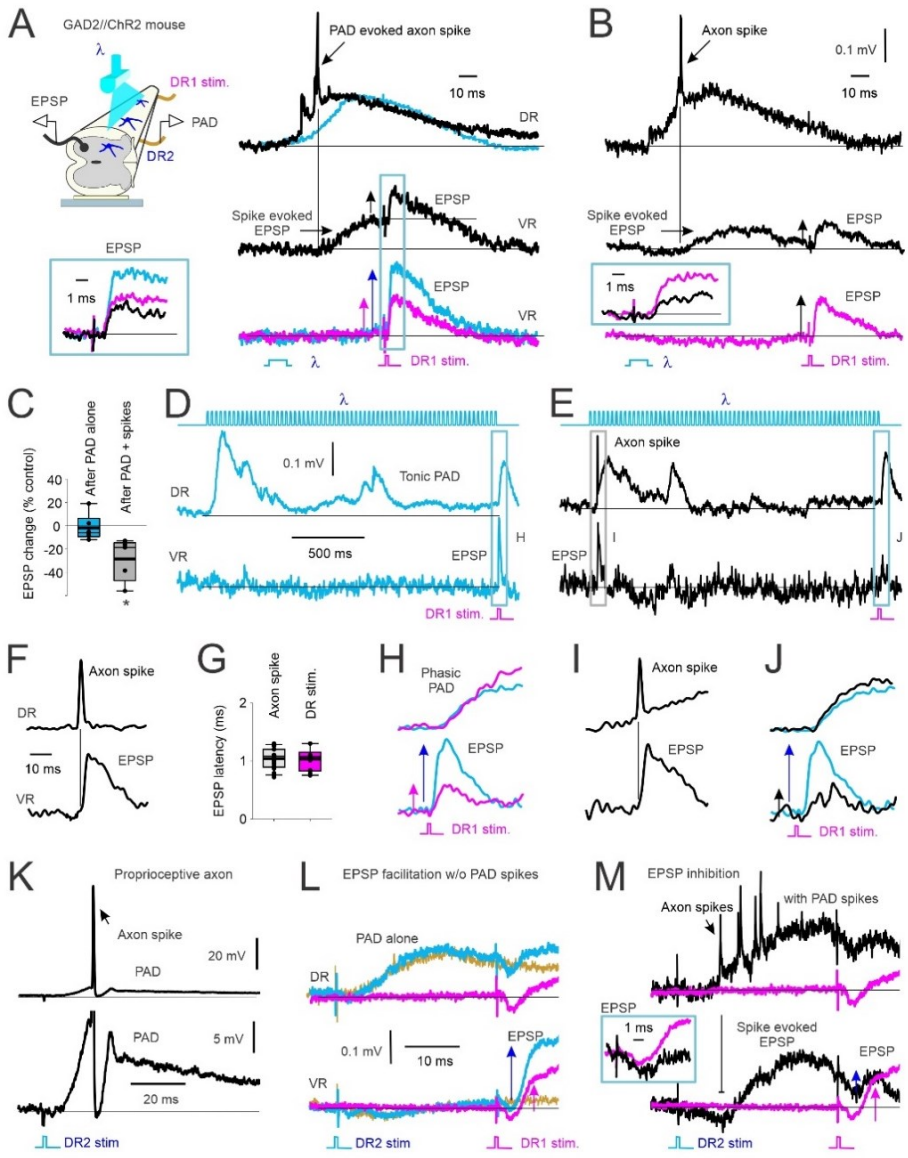

Figure 3: GABA$_A$ mediated PAD in Ia afferents with and without spiking and subsequent EPSPs. **A)** *Left*, In vitro experimental set up showing PAD recorded from dorsal root 2 (DR2) activated by light (λ) in a GAD2//ChR2 positive mouse. Monosynaptic reflex (MSR) activated by stimulation of DR1, subsequent EPSPs recorded from ventral root (VR). *Right, top*: PAD recorded from DR2 with (black) and without (blue) PAD-evoked axon spike. *Middle*: VR recording of evoked EPSP from the PAD-evoked axon spike in top trace. Subsequent test EPSP activation (DR1 stimulation) is reduced (vertical arrows indicate EPSP amplitude). *Bottom*: EPSP from DR1 stimulation alone (pink) compared to EPSP following the light-evoked, non-spiking PAD shown in top trace (blue). *Box*: Overlay of EPSPs from middle and bottom traces in A. **B)** Same as in A but test EPSP from DR1 stimulation delivered at a longer interval after the PAD spike-evoked EPSP returned to baseline. *Box:* Overlay of conditioned (black) and control (pink, DR1 stimulation only) EPSPs. **C)** Change in amplitude of light-conditioned EPSPs (100 - 150 ms ISI) after a non-spiking PAD (PAD alone) and after a PAD with spike(s) as a percentage of an EPSP evoked from DR1 stimulation alone (control).

Box plots: median, thin line; mean, thick line; interquartile range IQR, box bounds; most extreme data points within 1.5 x IQR, standard error bars. EPSPs after a PAD-evoked spike were smaller than a 0% change (* p = 0.021) but not after PAD alone (p = 0.151, Mann-Whitney U test, n=5 mice). **D-E)** *Top*: Light-evoked tonic PAD recorded from DR2 (middle trace) without (D, blue) and with (E, black) a PAD-evoked spike. *Bottom*: VR recordings of associated of monosynaptic EPSP from DR1 stimulation and PAD spike-evoked EPSP. **F)** Example DR and VR recording of PAD-evoked axon spike and resulting EPSP at a monosynaptic latency on expanded time scale. **G)** Comparison of EPSP latency following PAD evoked axon spike and DR 1 stimulation (not significantly different, p = 0.683, Student's t test, n = 6 mice). **H-J)** Expanded view of PAD (top) and EPSPs (bottom) evoked in D and E. Similar results observed in in n=6/6 mice. **K-M)** Same as in A and B but DR2 stimulation (1.5 x T) used to evoke PAD instead of light. Similar results in n = 5/5 rats. **K)** *Top*: Rat intracellular (IC) recording of proprioceptive (Ia) afferent with PAD-evoked axon spike from DR2 stimulation. *Bottom*: expanded vertical axis of top trace. **L-M)** PAD evoked with DR2 stimulation. *Top*: DR recording. *Bottom:* VR recording. **L)** PAD evoked without axon spikes. Pink: EPSP alone from DR1 stim. Blue: Non-spiking PAD evoked from DR2 stimulation and facilitated EPSP from DR1 stimulation. Yellow: PAD from DR2 stimulation applied alone. **M)** PAD, axon spikes and motoneuron EPSPs evoked from DR2 stimulation and test EPSP from DR1 stimulation without (pink) and with (black) spiking PAD (EPSPs expanded in box).

the dorsal root (top, Fig. 3M) that in turn evoked multiple compounded motoneuron EPSPs recorded in the ventral root (VR, bottom), as with the optogenetically-evoked PAD (Fig 3A). Following these PAD-evoked EPSPs, a direct test EPSP evoked by a DR1 stimulation was suppressed (inset in Fig. 3M), even though it was evoked when the membrane potential of the motoneuron returned to near baseline. Similar to light activation of $GABA_{axo}$ neurons when PAD did not produce axon spikes or associated depolarizations (EPSPs) of the motoneurons (DR2 stimulation only: yellow trace, Fig. 3L), then the test EPSP was facilitated by PAD (EPSP evoked by a DR 1 stimulation 1.5xT; blue trace, Fig. 3L) compared to the EPSP tested alone

without PAD (pink trace, Fig. 3L). This absence or presence of PAD-evoked spikes occurred randomly at a fixed DR2 stimulation intensity, as in Figures 3L or M, respectively, though these spikes could also be reduced in occurrence by reducing the stimulation intensity and again, the EPSP was inhibited only when they occurred (not shown). In summary, the same sensory conditioning stimulation can produce either suppression or facilitation of subsequent EPSPs depending on whether the associated PAD activates orthodromic spikes in the Ia afferent. Additionally, afferents from one nerve (e.g., DR 2) can produce widespread activation of PAD in afferents from other nerves (DR 1) (Lucas-Osma *et al.*, 2018b), reminiscent of reflex irradiation (Zehr & Stein, 1999).

To explore whether PAD-evoked spikes can produce motoneuron reflexes *in vivo*, we first examined the special characteristics of these spikes and the reflexes they evoke *in vitro* so they can be distinguished from polysynaptic reflexes activated from other sources and ultimately, be detected *in vivo.* We started by determining the origin of the PAD-evoked spikes by recording intracellularly from single group Ia afferents in the spinal cord near the dorsal root entry zone (Fig. 4A). A brief DR stimulation that was subthreshold to the Ia afferent being recorded (as indicated by a lack of an orthodromic spike at the green arrowhead in Fig. 4B) evoked a PAD in the recorded Ia afferent. In some of the trials, the DR stimulation produced one or more spikes starting on the rising phase of the PAD (dark blue Fig. 4B), which propagated antidromically toward the recording electrode and out the dorsal root and was recorded as a dorsal root reflex (DRR; Lucas-Osma *et al.*, 2018). In trials where the DR stimulation did not produce these antidromic spikes, there were underlying oscillations on top of the PAD at times where the spikes occurred in other trials (light blue, Fig. 4B). Previously, we have demonstrated that these oscillations represent spikes that are generated by PAD deep in the spinal cord (distal to the

recording electrode) that fail to propagate antidromically out the dorsal root, but likely propagate orthodromically toward the motoneurons (Lucas-Osma *et al.*, 2018b), and so have functional importance. One key characteristic of these PAD-evoked spikes and oscillations is that they are blocked by hyperpolarization, with a small hyperpolarization of the Ia afferent consistently eliminating the spikes (pink, Fig 4B) and a stronger hyperpolarization eliminating the underlying oscillations (Fig. 4D). Consistent with the recorded oscillations being mediated by distal sodium spikes, we found that inducing sodium spike inactivation by evoking a direct orthodromic spike in the Ia afferent via a supra-threshold stimulation to its DR (at green arrowhead, Fig. 4C) reduced the subsequent PAD-triggered oscillations measured in the DR (dark blue, Fig. 4C). Furthermore, after blocking these oscillations with a strong intracellular hyperpolarization, they resumed when the hyperpolarization was removed (Fig. 4D), the latter showing that they are mediated intrinsically to the axon and not by synaptic inputs. Another characteristic of the PAD-evoked spikes and oscillations is their unique timing, starting at about a 5-7 ms latency on the rising portion of a phasic PAD evoked by sensory stimulation (Fig. 4E, top left), and sometimes repeating at about 7-10 ms intervals, driving a characteristic oscillation in the population recording of afferents in the DRs, with a frequency (100 - 140 Hz) that is likely determined by the axon's refractory period and associated AHP (seen in Fig. 4B). Finally, as with direct hyperpolarization of the Ia afferent, indirect afferent hyperpolarization induced by blocking spontaneous tonic PAD on the afferents with either a low dose of the non-selective $GABA_A$ receptor antagonist bicuculline (Fig. 4E, top traces) or the selective extra-synaptic α5 $GABA_A$ receptor antagonist L655708 (Fig. 4F, top traces; see Lucas-Osma *et al.,* 2018 for details) reduced PAD-evoked spikes and oscillations. These same activation characteristics appear in the motoneurons (VR recordings, pink) when simultaneously recorded with the PAD, consistent

with these PAD-evoked spikes driving the motoneuron EPSPs. That is, the population of motoneuron EPSPs in the VR recording followed the oscillatory profile of the PAD measured on the DR recording with the same timing and were eliminated by hyperpolarizing the afferents with bicuculline (Fig. 4E, bottom) or L655708 (Fig. 4F, bottom), consistent with previous observations of Duchen (1986) in mice, also studied *in vitro*.

In the awake rat (Fig. 4G), cutaneous nerve stimulation known to evoke PAD caused reflexes with repeated bursts of activity (Fig. 4H, top), again separated by about 7-10 ms (140 to 100 Hz), similar to that seen *in vitro* (Fig. E, left), suggesting that they may be due to the oscillating PAD-evoked spikes driving the oscillating reflexes. Indeed, hyperpolarizing the afferents with L655708 reduced these reflex oscillations (Fig. 4H, bottom) without changing the postsynaptic activity of the motoneurons assessed by the background EMG (Bkg, Fig. 4J), consistent with an action on the Ia afferents rather than on the motoneurons. L655708 reduced both the small monosynaptic reflex (# in Fig. 4H), as previously reported (Hari *et al.*, 2021), and the repeated bursts of EMG at longer intervals. This is consistent with these long-latency reflexes being mediated by monosynaptic EPSPs triggered by PAD-evoked spikes, rather than polysynaptic reflexes from other sources, the latter which should be increased, rather than decreased, by reducing GABA action. Note that with L655708, the monosynaptic reflex (#) and some of the later putative PAD-evoked reflexes were facilitated with a prior brief cutaneous conditioning stimulation known to activate phasic PAD circuits and facilitate the monosynaptic EPSP by depolarizing the afferents (Fig. 4I), showing that the L655708 simply eliminated the EPSPs by hyperpolarizing the axons in Fig 4H, rather than indirectly acting to eliminate the EPSP by other pre- or postsynaptic pathways (e.g. via $GABA_B$ receptors).

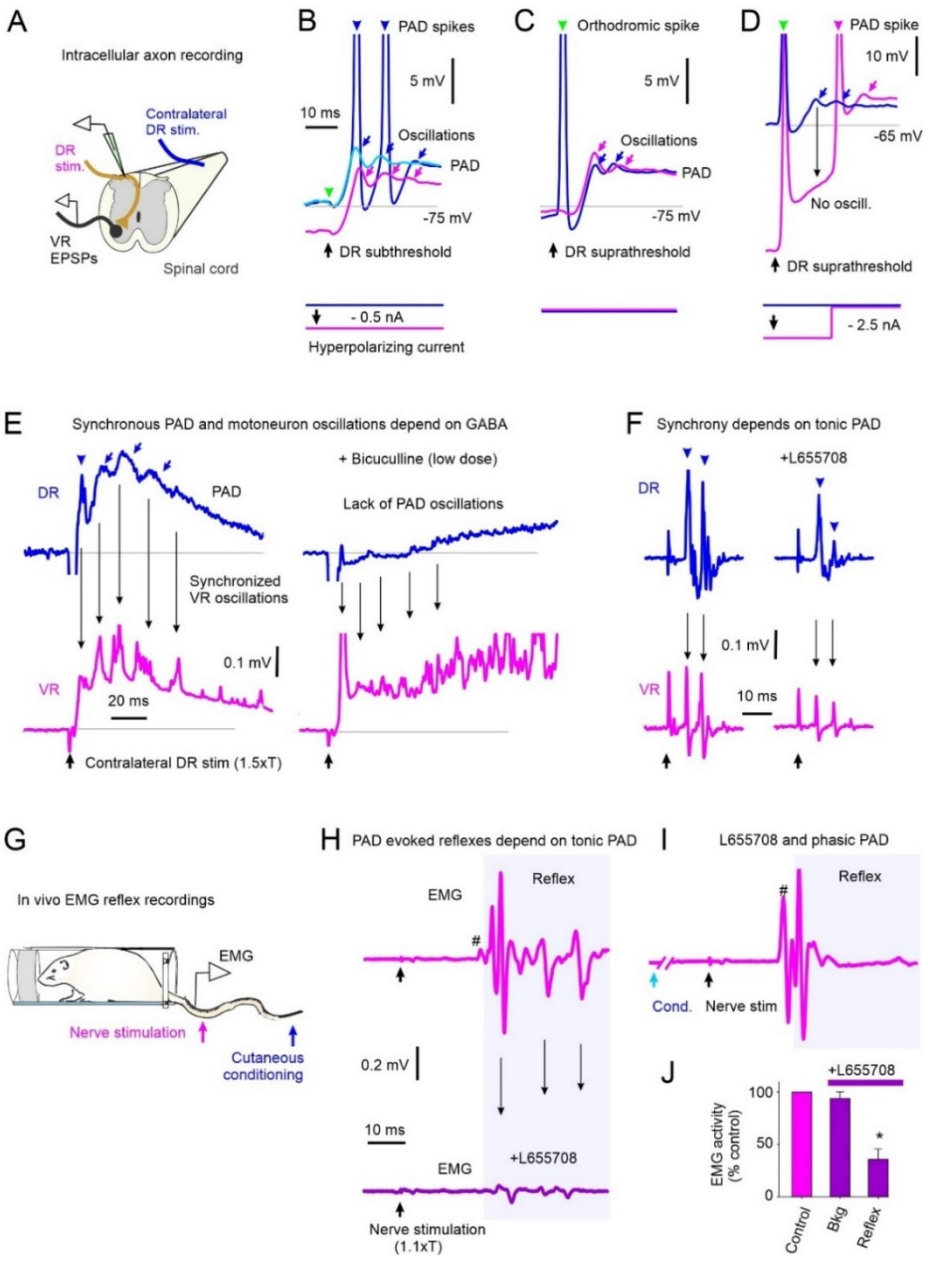

Figure 4. $GABA_A$ mediated synchronous PAD and motoneuron oscillations. A-D) PAD recorded intra-axonally from a rat Ia afferent. **A)** In vitro experimental set up. **B)** Stimulation of DR that is subthreshold to orthodromic spike for recorded Ia afferent without (blue & light blue traces) and with (pink) a small, applied hyperpolarization. PAD-evoked spikes and oscillations marked by arrowheads and arrows, respectively. Predicted timing of non-activated orthodromic spike indicated by green arrowhead. **C)** Suprathreshold DR stimulation producing orthodromic spike (green arrow and blue trace) compared to PAD oscillations produced with subthreshold DR stimulation in A (pink). **D)** Suprathreshold DR stimulation with strong hyperpolarization of Ia afferent to reduce PAD oscillations from distal spikes, n = 10/10 axons similar to results in B-D. **E-F)** *Left:* Synchronized PAD (DR recording, top) and motoneuron EPSP (VR recording, bottom) oscillations from PAD evoked by contralateral DR stimulation in rat. *Right:* Application of the wide spectrum $GABA_A$ receptor antagonist bicuculine **(E)** or the a5 $GABA_A$ receptor antagonist L655708 **(F)** to the recording bath, similar findings in 7/7 rats. **G)**

PAD evoked by stimulating cutaneous afferents in tip of tail in awake rat and MSR EMG recordings from more proximal tail nerve stimulation. **H)** *Top*: Small MSR (#) and oscillating EMG reflex responses from tail nerve stimulation (1.1xT) to recruit proprioceptive afferents. *Bottom*: EMG response to tail nerve stimulation following i.p. application of L655708. **I)** Facilitation of MSR and later reflex from prior (60 ms ISI) conditioning cutaneous stimulation of tip of tail. **J)** Pre-stimulus background (Bkd) EMG and post-MSR reflex activity (shaded window in I) following application of L655708 as a percentage of pre-drug (control). * = reflex significantly different from control (Mann Whitney U test, $p < 0.001$, $n = 6$ rats).

Soleus H-reflex inhibition following an antagonist-evoked early soleus reflex associated with post-activation depression.

Similar to mice and rats, a conditioning electrical stimulation to the human flexor CFN supplying the TA muscle often produced an early excitatory reflex response in the extensor soleus muscle (early soleus reflex), which is not expected from our classical understanding of the reciprocal organization of reflexes, but is similar to what we observed with vibration, as detailed above. As described below, this early soleus reflex is consistent with a CFN-evoked PAD causing extensor afferent spikes and associated reflexes based on its latency and frequency of oscillation. Moreover, when we observed an early soleus reflex from antagonist CFN stimulation, subsequent soleus H-reflexes were suppressed (Figs. 5 & 6). In contrast, soleus H-reflexes were facilitated when we did not observe an early soleus reflex from the CFN stimulation (Fig. 7), indicating a non-spiking PAD that facilitated Ia conduction and motoneuron EPSPs, similar to that seen in rodents detailed above.

In participants where CFN conditioning produced an early soleus reflex that may be due to PAD-evoked spikes (in 13/18 participants tested, Figs. 5 & 6), there was consistently an associated inhibition of the H-reflex. As shown for two of these participants, an early soleus

reflex was readily apparent in the surface EMG near 40 ms at both CFN stimulation intensities (see arrows in Figs. 5E and J) that was more readily observed at 1.0 x MT since there was no crosstalk from the TA M-wave between 10 to 30 ms (* in Fig. 5J). Overall, the average amplitude of the early reflex response was larger for the 1.5 x MT stimulation (Fig. 6J) compared to the 1.0 x MT stimulation (Fig. 6E). This consistent reflex response produced marked synchronization in the firing probability of the soleus motor units, as shown in the PSTH (Figs. 6D,I; see also Fig. 5I) that was not readily apparent in the surface EMG. Interestingly, power spectrum analysis of the soleus EMG during the predicted early PAD window (i.e., 30-80 ms after the first CFN stimulation) revealed a frequency spike at 161.9 (27.4) Hz (not shown, 1.5 x MT), similar to the frequency of the PAD oscillations recorded in the VR in the rodent (140 Hz, Fig. 4 E).

The early soleus reflex was also reflected in the firing rate profiles of the soleus motor units in response to the CFN stimulation applied alone (PSF and PSF CUSUM), which reflect the profile of the underlying motoneuron membrane potential (Turker & Powers, 1999). The PSF increased early near 40 ms as shown for the 1.0 x MT stimulation in Figure 5C and in the group data where at the 1.5 x MT intensity, the PSF increased above 2 SD near 40 ms (Fig. 6H), which was around 7 ms later than the onset latency of the H-reflex [32.3 (2.0) ms] evoked from direct TN stimulation. Unlike the surface EMG, the PSF and PSF CUSUM displayed a longer-lasting increase following the CFN stimulation, lasting out to 400 ms as illustrated by the PSF remaining above the baseline rate (Fig. 6B,G) and by the sustained increase in the PSF CUSUM (Figs. 6C,H). This is consistent with multiple PAD-evoked Ia-EPSPs or a polysynaptic reflex response (see multiple Ia spikes in Figs. 3M and 4B-F). Similar effects are seen in cat motoneurons, where the flexor-evoked EPSPs appear in antagonist extensor motoneurons, sometimes alone (Frank,

1959b) and sometimes riding on an IPSP (Stuart & Redman, 1992), and these too likely resulted from PAD-evoked spikes and caused post-activation depression of the Ia afferents (Hari *et al.,* 2021).

Following the early soleus reflex, the inhibition of the H-reflex had two phases, an early phase starting at the 15-30 ms ISI (D1) and a later, more sustained phase of inhibition (D2) starting at the 100 ms ISI that was larger with the higher intensity 1.5 x MT CFN stimulation (Fig. 5F,G) compared to the lower intensity 1.0 x MT CFN stimulation (Fig. 5A,B), similar to previous studies (Mizuno *et al.*, 1971; El-Tohamy & Sedgwick, 1983; Capaday *et al.*, 1995). When averaged across the 13 participants, the soleus H-reflex was suppressed at the 30 ms ISI when conditioned with the 1.0 x MT CFN stimulation (Fig. 6A, white circle) and at several ISIs starting at 15 ms when conditioned with the 1.5 x MT CFN stimulation (Fig. 6F, see legend for statistics). In summary, the CFN conditioning stimulation produced an early and prolonged excitation in the soleus muscle indicative of PAD-evoked spikes in the soleus Ia afferent producing soleus monosynaptic EPSPs, as we have seen in rodents, and this EPSP activation of the soleus is associated with the long-lasting inhibition of the H-reflex, likely via post-activation depression of the H-reflex.

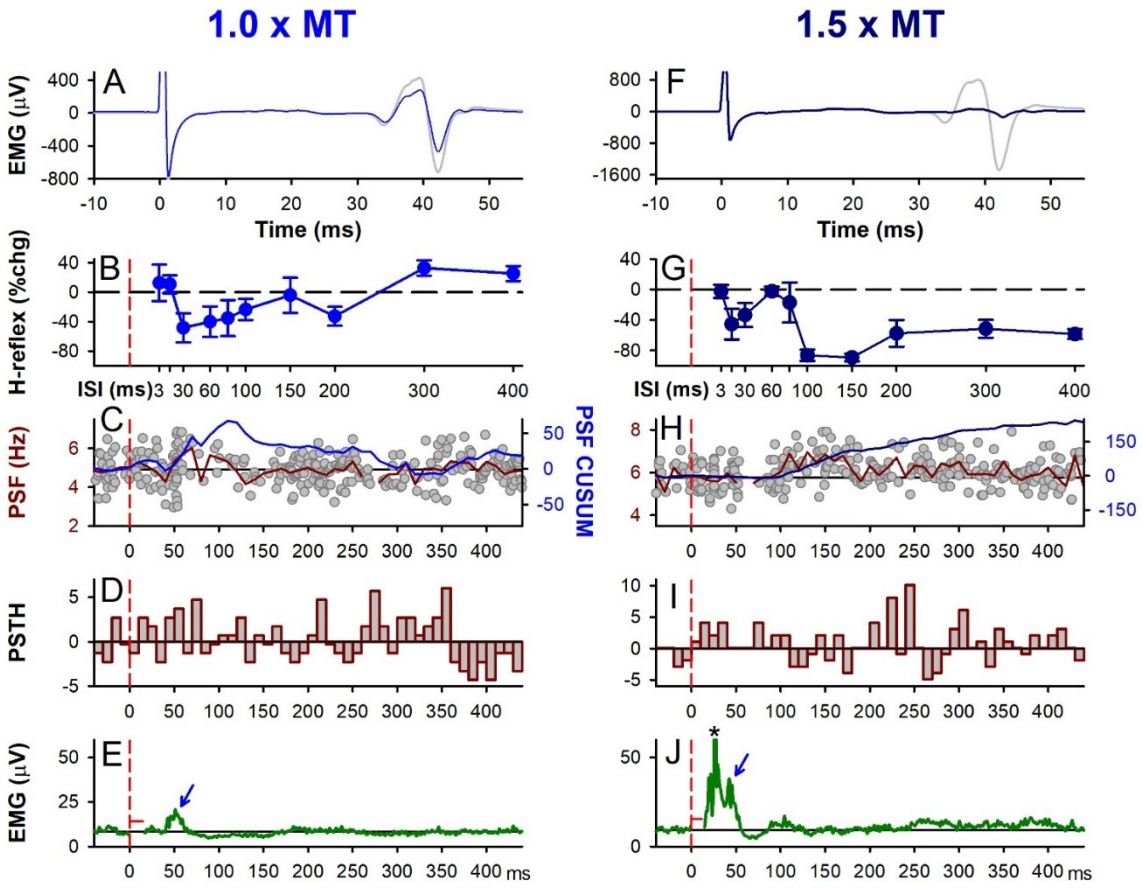

Figure 5: CFN stimulation: early H-reflex suppression. Same presentation as Figure 1 but for 1.0 x MT (A-E) and 1.5 x MT (F-J) electrical CFN conditioning stimulation, representative data from a single participant. A,F) Unrectified EMG of test (grey) and conditioned H-reflex (blue, 1.0 x MT at 30 ms ISI and dark blue, 1.5 x MT at 100 ms ISI). B,G) % change soleus H-reflex (Mean ± SD) plotted at each ISI tested. C,H) PSF (grey dots) with 108 sweeps in C and 98 sweeps in H, mean PSF (red line) and CUSUM of mean PSF (blue line). D,I) Number of motor unit counts per 10-ms time bin with average pre-stimulation count subtracted. E,J) Average rectified soleus EMG with 131 sweeps in E and 100 sweeps in J. Stimulation artifact has been removed (horizontal red line near 0 ms). B-J) Vertical dashed red lines indicate the onset of the CFN conditioning stimulation train (at time 0). * in J marks crosstalk from TA M-wave.

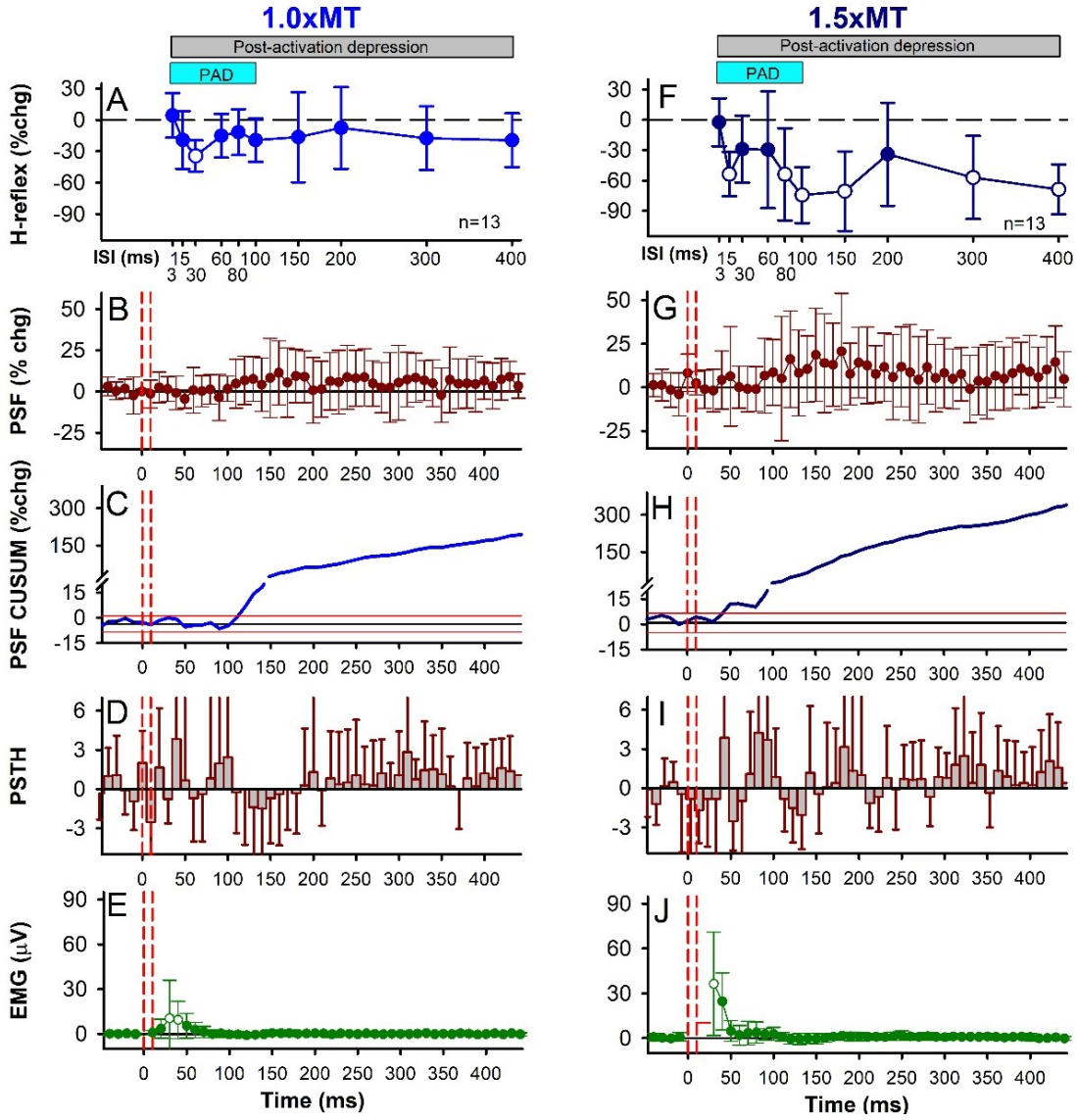

Figure 6: CFN stimulation: early H-reflex suppression, group data. Same presentation as Figure 2 but for the 1.0 x MT (A-E) and 1.5 x MT (F-J) CFN conditioning stimulation with data averaged across the 13 participants. The average size of the unconditioned H-reflex was 961.2 (454.1) μV [30.9 (13.8)% of Hmax; 16.6 (6.6)% of Mmax]. **A&F)** There was an effect of ISI on the % change of the H-reflex for both the 1.0 x MT ($F[12,10] = 2.392$, $P = 0.030$) and 1.5 x MT ($F[12,10] = 7.801$, $P < 0.001$, one-way RM ANOVAs) stimulus intensities, with the 30 ms ISI ($P = 0.017$, 1.0 x MT) and 15, 80, 100, 300 and 400 ms ISIs (P's < 0.01, 1.5 x MT) significantly different from a 0% change (Tukey Test, white symbols). Blue bar indicates predicted duration of PAD and grey bar the predicted duration of post-activation depression. **B,G)** There was no

effect of time on the % change PSF for the 1.0 x MT (F[12,61] = 1.094, $P = 0.298$**)** and 1.5 x MT (F[12,61] = 1.270, $P = 0.087$, CFN conditioning stimulation (one-way RM ANOVAs). **C,H)** % change CUSUM of the mean PSF averaged across participants. **D,I)** There was an effect of time on the count per bin (PSTH) for the 1.0 x MT (F[116,47] = 1.579, $P = 0.010$), but not the 1.5 x MT (F[116,47] = 1.352, $P = 0.064$), CFN conditioning stimulation (one-way RM ANOVAs). **E,J)** There was an effect of time on the EMG with the 1.0 x MT (F[12,46] = 3.361, $P < 0.001$) and 1.5 x MT (F[12,59] = 10.708, $P < 0.001$) CFN stimulation (one-way RM ANOVAs), with the 30 and 40 ms ($P < 0.001$, 1.0 x MT) and 30 ms ($P < 0.001$, 1.5 x MT) time bins significantly greater than 0 mV (Tukey Test, white symbols). Error bars ± SD.

Soleus H-reflex facilitation in the absence of an antagonist-evoked early soleus reflex

Based on the findings in the mice, if a flexor conditioning stimulation does *not* activate a PAD-evoked spike in the extensor Ia afferents and thus, does *not* pre-activate the monosynaptic extensor EPSPs (as evident by a lack of early soleus reflex), then the H-reflex should not be inhibited by post- activation depression, but if anything facilitated by PAD (Hari *et al.*, 2022). Indeed, we found that when there was a lack of an early soleus reflex (and putative PAD-evoked spikes) evoked by conditioning, the H-reflex was not inhibited, but instead facilitated by conditioning (seen in 5/18 participants in response to the 1.0 x MT CFN conditioning) [see also (Metz *et al.*, 2021)]. This is shown for one participant in Figure 7 where the CFN stimulation does not increase the PSF or PSF CUSUM (Fig. 7B and C respectively) or the rectified surface EMG (Fig. 7E), whereas the H-reflex was facilitated at the 80 and 100 ms ISIs within the predicted PAD window. When averaged across these 5 participants, the H-reflex was facilitated between the 30 and 250 ms ISIs (blue trace, Fig. 7F) compared to the H-reflex suppression that occurred in the other group of 13 participants where an early reflex response was present (grey trace replotted from Fig. 6A). The amplitude of the H-reflex was significantly modulated across the different ISIs but post hoc analysis revealed that no H-reflex at a given ISI was different than

a 0% change, likely due to the small number of participants [Fig. 7F, see legend for statistics]. However, this is consistent with our main conclusion that the lack of early reflex and associated PAD-evoked spikes prevents an inhibition of the H-reflex, due to a lack of post- activation depression. Further, when comparing the peak H-reflex facilitation that occurred at the 60 or 80 ms ISIs in each participant (during the predicted PAD window), the conditioned H-reflex was significantly greater than a 0% change (see also Fig. 3C in Metz *et al.*, 2021). Note that on average, there was a brief period of motoneuron inhibition from 30 to 100 ms after the 1.0 x MT CFN stimulation, as reflected in the PSF (Fig. 7G), PSF CUSUM (Fig. 7H) and clustering of motor unit firing probability in the PSTH starting at 60 ms (Fig. 7I). This early motoneuron inhibition may have reduced the early facilitation of the conditioned H-reflex between the 15 to 60 ms ISIs within the PAD window. Following this early inhibition, there was a period of motoneuron facilitation as shown in the PSF (Fig. 7G, red) and PSF CUSUM (Fig. 7H, blue), but it was much briefer compared to when there was an early excitatory reflex response in the other group (the latter again plotted in grey from Fig. 6). Like in the PSF, the amplitude of the early excitatory reflex response in the soleus EMG was much smaller or absent in these 5 participants (Fig. 7J, compare green and grey traces).

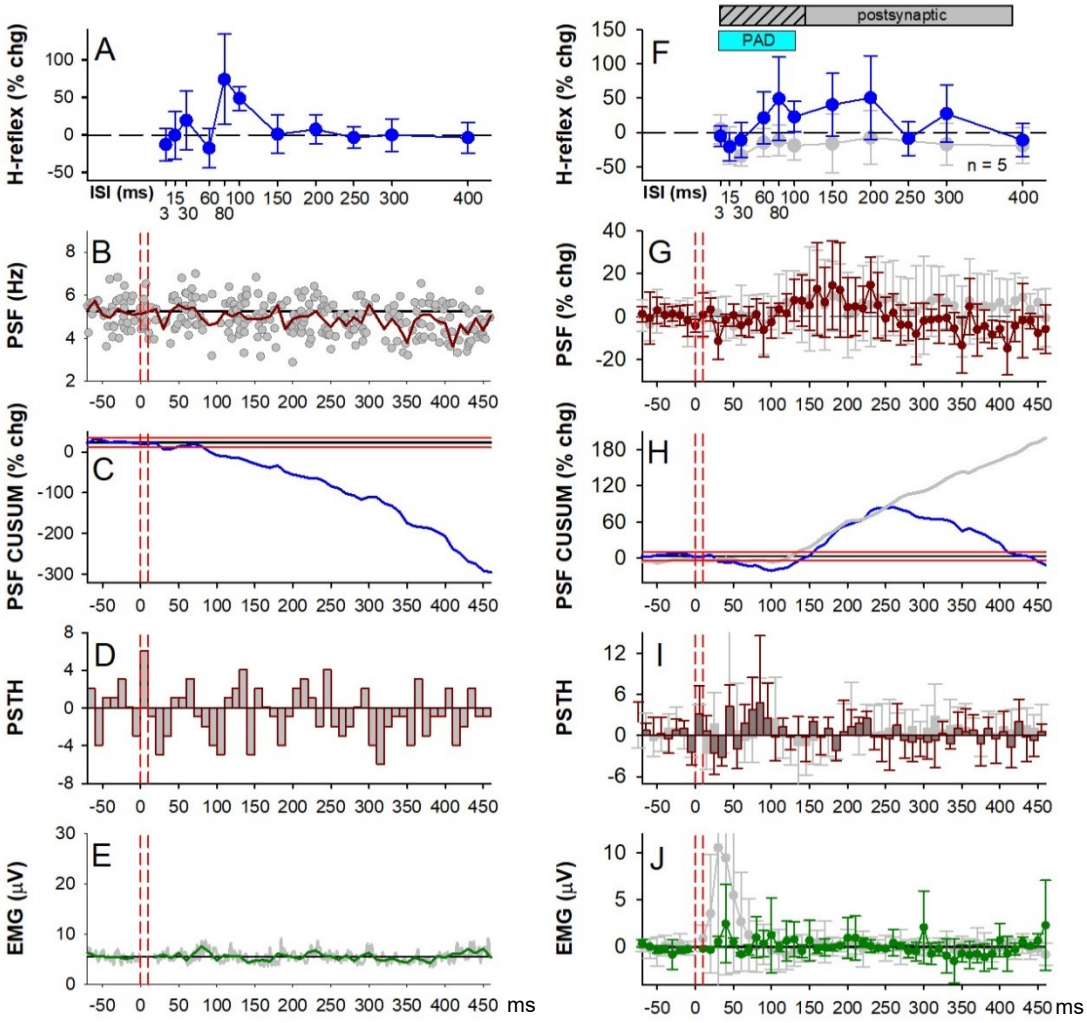

Figure 7: CFN stimulation: early H-reflex facilitation, individual and group data. Similar presentation as Figure 6 but with 1.0 x MT CFN conditioning stimulation that did not evoke an early reflex response in the soleus muscle. A-E data from an individual participant and F-J group data (n = 5 participants). Grey data points in F-J are replotted from Figs. 6A-E where 1.0 x MT CFN stimulation produced an early soleus reflex response. There was an effect of ISI on the % change H-reflex (F) ($F[4,11] = 2.113$, $P = 0.043$) and time on the % change PSF (G) ($F[3,61] = 1.673$, $P = 0.005$) but no effect of time on the count per bin in the PSTH (I) ($F[3,61] = 1.120$, $P = 0.281$) or EMG (J) ($F[3, 60] = 0.994$, $P = 0.498$), all one-way RM ANOVAs. Error bars ± SD.

As described above, our observed early excitatory reflex in the soleus EMG or PSF from the CFN conditioning stimulation may be indicative of PAD-evoked spiking in the soleus Ia afferents that produces long-lasting post-activation depression and subsequent H-reflex suppression. In contrast, when we observed no or very little early reflex activity, PAD evoked from the conditioning afferent input likely facilitates afferent conduction and thus, increases subsequent H-reflexes. In further support of this, we observed that the amount of H-reflex inhibition at the 100 ms ISI was greater when the amplitude of the early soleus reflex (measured between 30 - 50 ms) was also greater, as demonstrated by the negative correlation between these two measures (Fig. 8). Facilitation of the soleus H-reflex at the 100 ms ISI was typically produced only when there was no or very little (< 2 mV) early excitatory reflex activity in the soleus muscle.

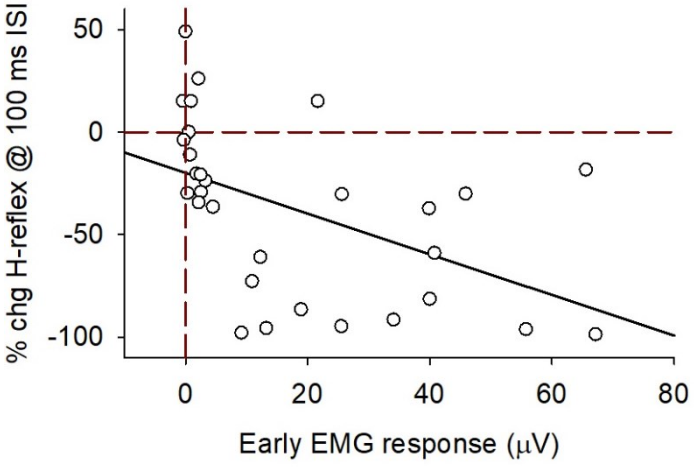

Figure 8: CFN stimulation: % change soleus H-reflex at the 100 ms ISI vs early soleus EMG response. % change (chg) H-reflex (100 ms ISI) plotted against the early EMG response (30-50 ms after CFN stimulation during slight contraction) for both the 1.0 and 1.5 x MT CFN stimulation for participants with and without an early soleus reflex (n = 18). Data fitted to a linear line (slope = 1.0 % chg /mV). There was a significant correlation between the % chg H-reflex and the early EMG response (r = -0.50, P = 0.005, Pearson Product-Moment Correlation). There are 30 data points: typically 2 values from each participant (from the 1.0 and 1.5 x MT trials). In some recordings (n = 6), the TA M-wave obscured the early soleus reflex and this data was not used. Red vertical dashed line marks no change in the soleus EMG from the CFN stimulation. Red horizontal dashed line marks 0 % change in the soleus H-reflex.

Long lasting soleus H-reflex inhibition consistent with post-activation depression

Given that conditioning of the flexor CFN may produce spikes in the extensor soleus Ia afferents and post-activation depression of the H-reflex, we examined this further by exploring the *duration* of H-reflex inhibition by the CFN conditioning, which should be similar to the associated rate-dependent depression (RDD) of the H-reflex that is mediated by post-activation depression, which can last seconds (Nielsen *et al.*, 1993b; Hultborn *et al.*, 1996a). Thus, we examined how long the H-reflex inhibition from the conditioning CFN stimulation lasted for in the same 13 participants that had the earlier suppression of the H-reflex presented above. As shown for two participants, the soleus H-reflex was maximally suppressed at the 500 ms ISI by a 1.5 x MT conditioning CFN stimulation and continued to be suppressed out to the 2500 ms ISI (Figs. 9Ai and Bi), which is similar in duration to the suppression of monosynaptic EPSPs seen in mice and rats when followed by a PAD-evoked spike and associated EPSP (Fig. 3E and Duchen, 1986). Across the group, the H-reflex was modulated at these very long ISIs, being significantly suppressed at all ISIs from 500 to 2500 ms (* Fig. 9Ci, see legend for statistics). By itself, the 1.5 x MT CFN stimulation increased the firing rate of the soleus motor units for at least 500 ms in some participants (PSF Fig. 9Bii) and for a briefer period in others (PSF Fig. 9Aii). Across the group, both the PSF (Fig. 9Cii) and the rectified surface EMG (Fig. 9Ciii) returned to pre-stimulus levels by 500 ms while the H-reflex continued to be suppressed (see statistics in legend). In contrast, the 1.0 x MT CFN stimulation intensity did not suppress the soleus H-reflex at these long ISIs as plotted for the 500 ms ISI (Fig. 9Di), consistent with it having a weaker or absent early soleus reflex that we take as evidence for PAD-evoked spikes (Fig. 9Dii). Thus, the suppressed H-reflex at these long ISIs was not likely related to any direct postsynaptic inhibition of the soleus motoneuron at the time the H-reflex was evoked but rather, may have been

produced by the earlier soleus reflex activation described above. In support of this, H-reflex suppression was significantly correlated to the early increase in PSF when data for the 1.0 and 1.5 x MT CFN stimulation intensities were plotted together (Fig. 9Diii) or when compared to the amplitude of the early EMG response to CFN stimulation (from 30 to 50 ms, r = -0.74, P <0.001, Pearson's Product, not shown).

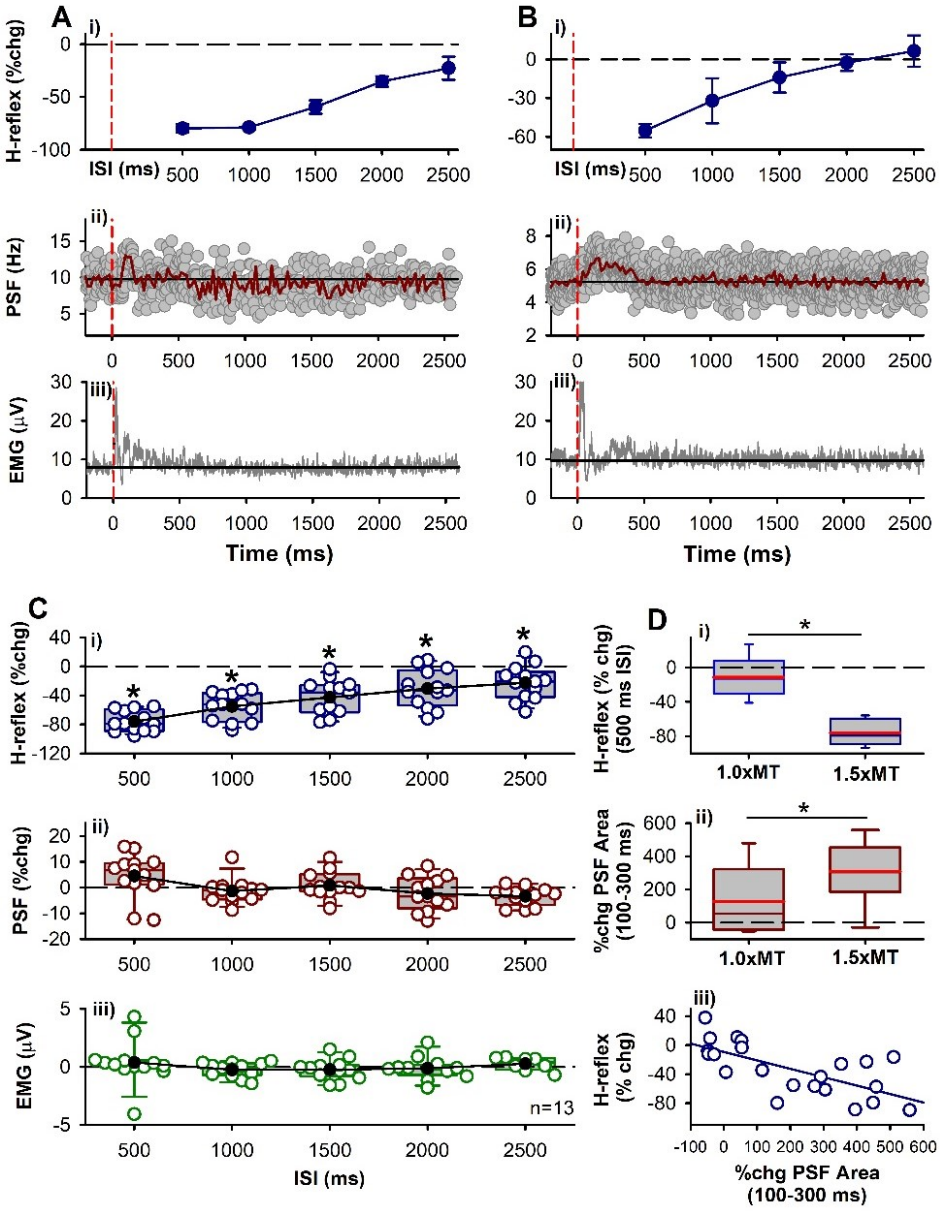

Figure 9: CFN stimulation: late H-reflex suppression. A-B) Representative data from two participants showing **i)** % change in H-reflex, **ii)** PSF (37 sweeps in A, 98 sweeps in B) and **iii)** rectified soleus EMG (40 sweeps in A, 30 sweeps in B). Vertical dashed red lines indicate time of 1.5 x MT CFN conditioning stimulation. **C)** Mean (black circles) and individual data

points (open circles) from the 13 participants tested. There was an effect of ISI on the % change in the soleus H-reflex **(i)** ($F[12,5] = 55.697$, $P < 0.001$, one-way RM ANOVA) with all ISI's significantly different from 0% change ($P < 0.001$, Tukey Test, marked by *). There was an effect of ISI on the % change PSF **(ii)** ($F[12,5] = 4.393$, $P = 0.002$) but not EMG ($F[12,5] = 0.716$, $P = 0.614$, one-way RM ANOVAs). The PSF and EMG data points occurred in the time bin that matched when the H-reflex was evoked at the various ISIs. **D)** Box plot (similar to Figs. 3C&G) of: **(i)** % change soleus H-reflex at the 500 ms ISI for the 1.0 and 1.5 x MT CFN conditioning stimulation, significantly different ($P = 0.040$, Student's t-test); **(ii)**, % change in area of the PSF measured 100-300 ms after the 1.0 and 1.5 x MT CFN stimulation, significantly different ($P < 0.001$, Student's t-test); **(iii)** % change H-reflex at 500 ms ISI plotted against % change PSF area (100 - 300 ms) with fitted linear line (blue, $r = -0.74$, $P < 0.001$, Pearson Product-Moment Correlation). Error bars ± SD.

Post-activation depression of the soleus H-reflex during RDD

We next investigated whether the early reflex activation in the soleus muscle by the antagonist CFN stimulation causes a similar long duration inhibition of the H-reflex to that expected from RDD, which has previously been demonstrated to be due to post-activation depression, thus providing further evidence that PAD-evoked spikes in the soleus Ia afferents produces a long-lasting post-activation depression of the soleus H-reflex. That is, in 8 of the 13 participants from above, we examined if the profile of long-lasting suppression of the soleus H-reflex from antagonist CFN conditioning (CFN→TN) was similar to the profile of H-reflex suppression evoked by repetitive TN stimulation during RDD (TN→TN), the latter used to quantify the duration and profile of post-activation depression. Like with the CFN conditioning, repetitive stimulation of the TN inhibited the H-reflex at all intervals tested out to 2500 ms, with the greatest suppression at the 500 ms ISI (compare Figs. 10Ai & Aii). Across all participants, the average profile of H-reflex inhibition at the different ISIs was not different between antagonist CFN (dark blue) or homonymous TN (pink) conditioning stimulation trials (Fig. 10B,

see legend for statistics), with both forms of inhibition lasting to 2500 ms. This suggested that the mechanism of H-reflex suppression was similar between the two stimulation protocols and likely due to post-activation depression.

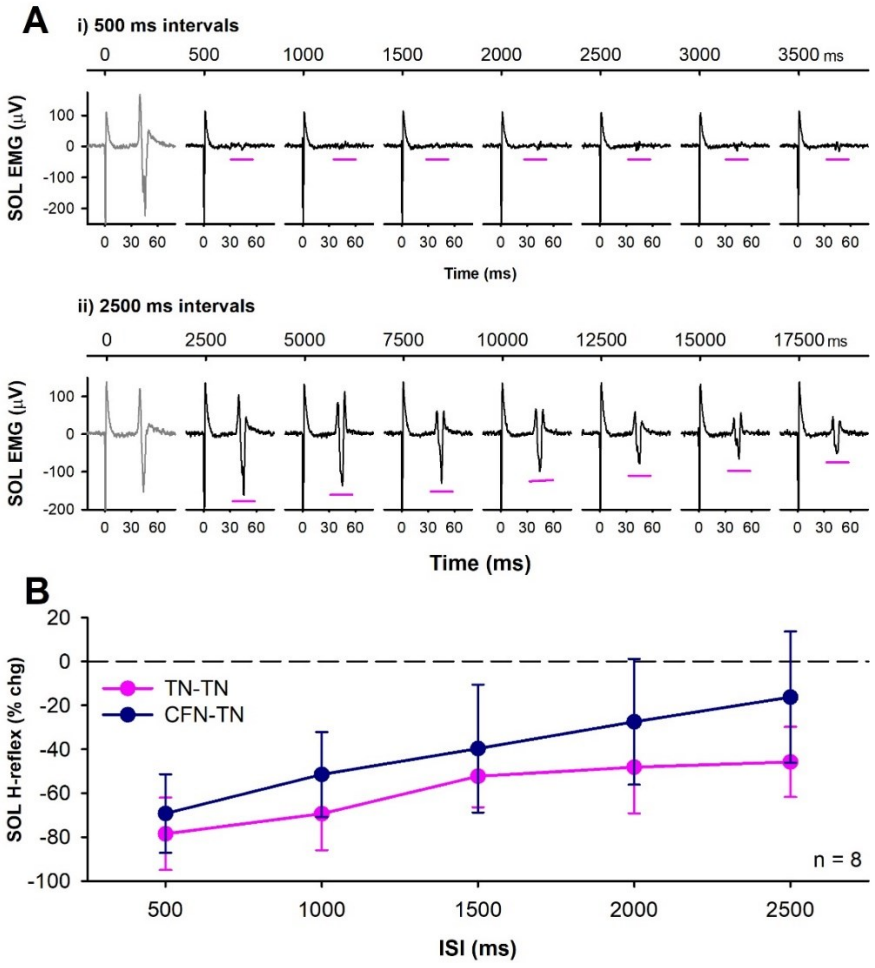

Figure 10: Post-activation depression of the soleus H-reflex. A) Example rate dependent depression (RDD) of unrectified soleus EMG evoked by repetitive TN stimulation every 500 ms (i) and 2500 ms (ii) in one participant. Continuous time displayed in top trace to show when TN stimulation was applied (marked by large stimulation artifact) and expanded time scale in bottom to display the H-reflex occurring in the time window marked by the pink horizontal lines (time reset to 0 ms when TN stimulation was applied). B) The % change in soleus H-reflex from repetitive TN stimulation (RDD, pink) averaged across the 8 participants at the different ISIs and % change H-reflex from CFN conditioning stimulation (dark blue), not significantly different ($F[1,4] = 1.860$, $P = 0.152$, two-way RM ANOVA). Error bars ± SD.

Discussion

Inhibitory control mechanisms within the spinal cord are needed to regulate the large influx of sensory information from the periphery that would otherwise exceed the computing capacity of the central nervous system (Rudomin & Schmidt, 1999). One way to reduce the flow of sensory information to spinal targets is through presynaptic inhibition of afferent terminals. To regulate the transmission of *proprioceptive* information, the depolarization of primary (Ia) afferents, or PAD, from the activation of $GABA_A$ receptors was historically thought to inactivate sodium channels and/or shunt current at the afferent terminal and reduce neurotransmitter release to spinal motoneurons as one form of presynaptic inhibition (Willis, 2006). To demonstrate this, antagonist afferents were used to activate PAD in Ia afferents via GABAergic interneurons and shown to be accompanied by a parallel suppression of monosynaptic EPSPs in the motoneuron, though direct evidence for presynaptic inhibition via activation of terminal $GABA_A$ receptors is lacking. For example, numerous studies have failed to find $GABA_A$ receptors on Ia afferent terminals (Alvarez *et al.*, 1996; Fink *et al.*, 2014; Lucas-Osma *et al.*, 2018b; Hari *et al.*, 2021). Instead these receptors are located more dorsally near the nodes of Ranvier near branch points where their activation facilitates afferent conduction and monosynaptic reflexes (Hari *et al.*, 2021; Metz *et al.*, 2021). We demonstrate here that the more likely mechanisms that produces the H-reflex suppression by antagonist afferents is both a direct long-lasting inhibition of the test motoneurons and an indirect post-activation depression of the Ia afferents mediating the H-reflex, two mechanisms that have been suggested previously but not tested explicitly (Eccles *et al.*, 1961a; Hultborn *et al.*, 1987a; Fink *et al.*, 2014; Hari *et al.*, 2021).

Postsynaptic inhibition of motoneurons from antagonist afferents

We demonstrate here that the extensor H-reflex is inhibited for up to a half second following vibration of the flexor tendon, consistent with previous findings in cats (Curtis, 1998a), which is too long to be explained by presynaptic inhibition from phasic PAD that only lasts for 100-200 ms, contrary to previous conclusions (Morin *et al.*, 1984; Hultborn *et al.*, 1987a; Hultborn *et al.*, 1987b; Iles & Roberts, 1987; Roby-Brami & Bussel, 1990; Rossi *et al.*, 1999). In humans, H-reflex suppression at ISIs of 40 to 500 ms was considered to be mediated primarily by PAD-induced presynaptic inhibition because it was thought that direct effects on the motoneuron from antagonist afferent conditioning did not last beyond the 40 ms ISI (Hultborn *et al.*, 1987a; Hultborn *et al.*, 1987b). However, as shown here and by others when using the PSF (Yavuz *et al.*, 2018), inhibition of soleus motoneurons from a brief antagonist stimulation can last up to 300 ms. On average, the profile of PSF suppression from tendon vibration closely followed the early profile of H-reflex suppression following vibration, out to the 100 ms ISI (Fig. 2), and this motoneuron inhibition likely contributes to the suppression H-reflexes during this period. In cats and rodents, similar long-duration IPSPs and reduced neuronal time constants (τ, indicating postsynaptic shunting) have been induced in motoneurons from heteronymous afferent conditioning that also produced long-duration EPSP suppression (McCrea *et al.*, 1990; Hari *et al.*, 2021).

The prolonged inhibition of the soleus motoneurons may have resulted from a single long-duration IPSP (Pierce & Mendell, 1993; Hughes *et al.*, 2005; Hari *et al.*, 2021) or from multiple shorter-duration IPSPs triggered by multiple afferent inputs (Desmedt & Godaux, 1978). Regardless of the source, when using a weak conditioning stimulation to suppress H-reflexes like brief tendon vibration, sensitive methods are needed to measure if there are any direct actions on

the motoneuron and for how long. The PSF provides a better representation of the IPSP evoked in the soleus motoneuron compared to the PSTH or surface EMG, the latter which better represent the occurrence of motoneuron discharge and are subject to synchronization artifact (Turker & Powers, 1999; Yavuz *et al.*, 2018). In addition, we tested the excitability of the soleus motoneurons while they were tonically active during a weak voluntary contraction, so that any subtle inhibition from the tendon vibration or low intensity CFN stimulation could be revealed, in contrast to a resting motoneuron. A hyperpolarization of the distal dendrites by a low-intensity conditioning stimulation, which might not be detectible from intracellular somatic recordings in a resting motoneuron (McCrea et al., 1990), may produce a greater influence on the firing rate response of the cell (Hari *et al.,* 2022). Thus, it is important to record single motor unit activity in a preactivated motoneuron to examine if the conditioning stimulation has any direct inhibitory effects on the motoneuron and the duration of its effect on the suppression of the H-reflex.

Post-activation depression by antagonist afferents.

Our finding that direct electrical stimulation to the flexor CFN, and sometimes even flexor tendon vibration, causes early extensor soleus reflexes led us to examine whether these unusual, excitatory reciprocal reflexes may contribute to subsequent post-activation depression of the soleus H-reflex. Consistent with previous findings, we found that H-reflexes are suppressed by the antagonist CFN conditioning (Mizuno *et al.*, 1971; El-Tohamy & Sedgwick, 1983; Capaday *et al.*, 1995). However, we demonstrate that this inhibition only occurred when short-latency reflexes to the soleus muscle are evoked by the conditioning electrical stimulation to the flexor CFN. The inhibition of the extensor H-reflex by electrical CFN stimulation occurred even though there was little evidence of postsynaptic inhibition of the soleus motoneurons

compared to conditioning with tendon vibration. We propose here that the H-reflex suppression following this early reflex response is likely mediated by post-activation depression of the soleus H-reflex induced by the antagonist CFN afferents activating PAD-evoked spikes in the soleus Ia afferents. In rodents we show that during a large and fast rising PAD, the membrane potential of the afferent can reach the sodium spiking threshold and produce action potentials that travel orthodromically down the Ia afferent to evoke monosynaptic EPSPs (early reflexes) in the motoneuron [see also (Duchen, 1986; Lucas-Osma *et al.*, 2018b)]. These monosynaptic EPSPs are likely produced by PAD-evoked spikes because: 1) the occurrence of the PAD-evoked spikes and the associated EPSPs are tightly linked in time with a monosynaptic latency [see also (Duchen, 1986)], 2) they repeat with a characteristic period of about the duration of the afferent AHP with a refractory period of 7-10 ms (140-100 Hz) in both rodent VR and human EMG recordings, and 3) both are reduced by specifically hyperpolarizing the afferent by blocking tonic PAD with L655708.

The PAD-evoked spike and the associated EPSP and excitatory soleus reflex likely cause post-activation depression that can have multiple underlying mechanisms, as detailed in the Introduction. These include the depletion of transmitter packaging and release from the Ia afferent, the afferent AHP and its refractory period (lasting up to 10 ms), and the indirect activation of $GABA_B$ receptors on the afferent terminals triggered by the PAD-evoked spike to ultimately produce $GABA_B$ mediated presynaptic inhibition (Fig. 11). Likely all these mechanisms are involved in the early inhibition of the extensor soleus H-reflex by flexor conditioning, but only the $GABA_B$ action can account for the very long, up to 2 s, inhibition seen in our study and others (Eccles *et al.*, 1961a; Curtis & Lacey, 1994, 1998) given that the recovery time constant from maximal transmitter depletion is around 300-400 ms (Neher &

Sakaba, 2001). This raises the question of how are the $GABA_B$ receptors on soleus afferent terminals activated by the flexor nerve stimulation? We do not favor the simple idea that flexor nerve stimulation directly activates the trisynaptic circuit that drives the GABAergic neurons that innervate the soleus afferent terminals and associated $GABA_B$ receptors for two reasons. First, the inhibition of the soleus H-reflex or related mice EPSPs only occurs when it is linked to PAD-evoked spikes and associated PAD-evoked EPSPs or early soleus reflexes and thus, must be somehow indirectly linked to the $GABA_A$ receptors that mediate PAD, as previously argued from the actions of $GABA_A$ receptor blockers on this inhibition (Stuart & Redman, 1992). Second, the profile of inhibition from conditioning is similar in timing to RDD caused by repeated H-reflex activation, which has been shown to be mostly confined to inhibition mediated by the activation of the same afferents that are stimulated to evoke the H-reflex (thus also called homosynaptic depression) (Hultborn *et al.*, 1996a). This RDD is likely mediated by a restricted trisynaptic circuit, where the extensor afferent activates private GABAergic neurons that only activate extensor afferent terminals (Fig. 11). Thus, we favor the more complex scenario where flexor nerve stimulation evokes a widespread PAD and PAD-evoked spikes in extensor soleus afferents, which then activate a restricted trisynaptic circuit with GABAegic neurons that activate $GABA_B$ receptors on the extensor afferent terminal (Fig. 11). This raises interesting questions about whether there are indeed subpopulations of different GABAergic neurons that innervate extensor vs flexor afferent terminals, which needs to be investigated in the future (Curtis & Eccles, 1960; Hultborn *et al.*, 1996a).

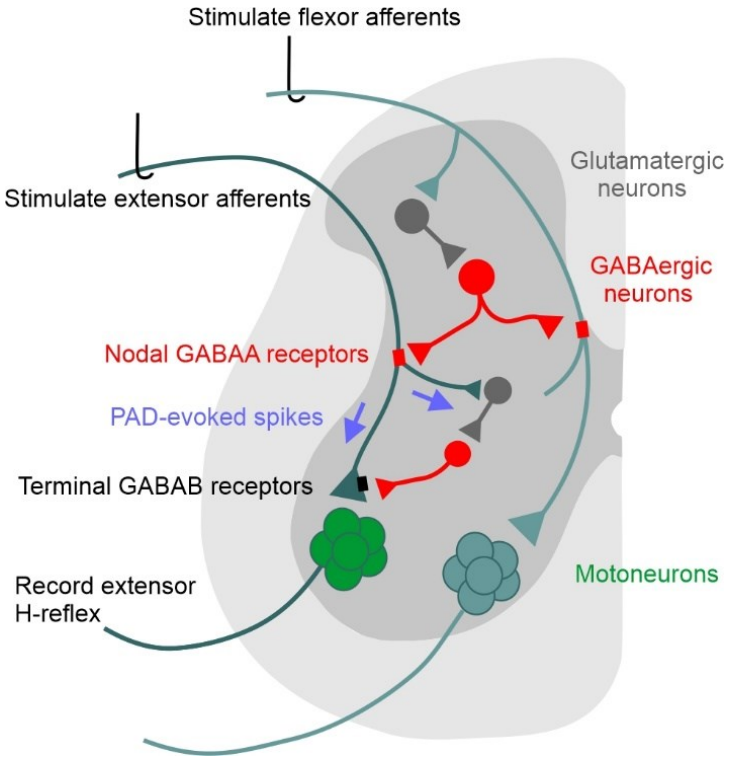

Figure 11. Schematic of PAD pathways mediating post-activation depression in the spinal cord. Activation of flexor afferents (cyan) activates a tri-synaptic dorsal PAD pathway (glutamatergic interneuron dark grey, $GABA_{axo}$ neuron red) with axo-axonic projections to an extensor afferent (dark green), activating nodal $GABA_A$ receptors (red) and PAD in the extensor afferent. If the resulting PAD in the extensor afferent reaches sodium spiking threshold, PAD-evoked spikes (purple arrows) travel orthodromically to: 1) depolarize extensor afferent terminals, evoking an EPSP in the extensor motoneurons and a subsequent MSR/H-reflex; 2) activate a trisynaptic circuit containing GABAergic neurons that activate $GABA_B$ receptors (black) on the extensor afferent terminal. Thus, the PAD-evoked spike in the extensor Ia afferent can produce early and late post-activation depression of subsequently activated MSRs/H-reflexes by: 1) transmitter depletion following the PAD-evoked spike entering the extensor Ia afferent; 2) decreased afferent excitability from the post-spike refractory period that follows the PAD-evoked spike, and/or 3) inhibition of the afferent terminals by $GABA_B$ receptors indirectly activated by the PAD-evoked spike ($GABA_B$ mediated presynaptic inhibition).

For the flexor CFN to evoke PAD in extensor afferents, they must activate a circuit that that has GABAergic interneurons with axo-axonic projections ($GABA_{axo}$ interneurons) onto extensor afferents, as just mentioned (Fig. 11). This arrangement is broadly consistent with our understanding of the widespread nature of PAD. That is, it has been known for many years in

both animals (Eccles *et al.*, 1961b; Willis, 1999) and humans (Shefner *et al.*, 1992b) that stimulation of afferents from one nerve can produce PAD and related PAD-evoked spikes (DRRs) in afferents from neighbouring nerves, since $GABA_{axo}$ interneurons are innervated by first order neurons with projections across many segments within the spinal cord (Jankowska *et al.*, 1981c; Willis, 2006; Lucas-Osma *et al.*, 2018b). Furthermore, flexor nerve stimulation produces the strongest PAD in extensor afferents, compared to in flexor afferents (Eccles *et al.*, 1961a; Rudomin & Schmidt, 1999). Here the new addition to this older concept is that PAD is likely mediated by $GABA_A$ receptors at nodes, rather than ventral terminals (Hari *et al.*, 2021), though this does not change the known distributions of PAD (Fig. 11). Thus, the amplitude or presence of the early reflex response in the soleus muscle evoked from the antagonist CFN stimulation can be used as a gross indicator of PAD-evoked spikes in the soleus Ia afferents. These Ia spikes likely produce post-activation depression in the soleus Ia afferent terminals to mediate the suppression of the conditioned H-reflexes, as we have discussed above. Indeed, the amplitude of the early soleus reflex activity is correlated with the amount of H-reflex suppression at the 100 ms ISI (Fig 8), an interval previously attributed to PAD-induced presynaptic inhibition of the Ia afferent terminal (Mizuno *et al.*, 1971; Burke *et al.*, 1992; Iles & Pisini, 1992; Capaday *et al.*, 1995; Iles, 1996; Knikou & Mummidisetty, 2014; Howells *et al.*, 2020). Moreover, when an early soleus reflex is not produced following low-intensity CFN stimulation, the conditioned H-reflexes are instead facilitated, likely due to a facilitation of spikes through the soleus Ia branch points by nodal PAD (Hari *et al.*, 2021; Metz *et al.*, 2021). Nodal depolarization and facilitation of Ia afferent conductance likely also occurs when H-reflexes were suppressed following the early soleus reflex and may account for the decrease in H-reflex suppression near the 30 to 60 ms ISIs during the rising phase of PAD that divide the D1 and D2 phases of

inhibition (Mizuno *et al.*, 1971; El-Tohamy & Sedgwick, 1983; Berardelli *et al.*, 1987; Faist *et al.*, 1996). However, this facilitation is probably masked by the stronger post-activation depression of the Ia afferents from the PAD-evoked Ia spike(s).

Further evidence to support the conclusion that the profile of H-reflex inhibition from antagonist CFN conditioning is mediated by post-activation depression of the Ia afferent terminals is provided by its resemblance to the seconds long profile of rate dependent depression (RDD) from repeated TN stimulation that directly activates spikes in the soleus Ia afferents. Similar to RDD at long repetition intervals, H-reflexes are also suppressed out to 2.5 s after a strong conditioning CFN stimulation, well after any direct effect on the soleus motoneurons from the CFN stimulation had subsided. This is consistent with the long-duration suppression of the Ia-EPSP in mice and rats when a PAD-evoked Ia spike occurred 1500 ms earlier, even though the motoneuron had long returned to its resting membrane potential (Fig 3 and Duchen, 1986). Suppression of the H-reflex at these long intervals after conditioning occurs only when there is an early reflex activation of the soleus motoneurons, as measured by both the PSF and rectified EMG. Alternatively, if this early-latency soleus reflex was solely mediated by a polysynaptic pathway from the CFN afferents that bypassed the soleus Ia afferents, the suppression of the H-reflex would likely not have lasted out to 2500 ms as we observe. Future studies using microneurography to measure PAD-evoked in humans, like in (Shefner *et al.*, 1992b), could provide more insight into the mechanism of post-activation depression. Likewise, it is important to examine if suppressing $GABA_A$ receptors in human participants, as with the α5 $GABA_A$ receptor neutral antagonist S44819 used in clinical stroke trials (Darmani *et al.*, 2016; Chabriat *et al.*, 2020), could reduce PAD evoked spikes and post-activation depression of H-reflexes.

GABAB receptor activation. Activation of $GABA_B$ receptors on Ia afferent terminals by the flexor CFN stimulation may be involved in the suppression of the H-reflex and post-activation depression as we discuss above, though we detail the mechanisms further here. Activation of $GABA_B$ receptors produces presynaptic inhibition of Ia afferents and reflex transmission to motoneurons (Curtis & Lacey, 1994; Fink, 2013; Hari *et al.,* 2022), likely by inhibiting voltage dependent calcium channels on the presynaptic boutons to reduce the calcium-dependent exocytosis of neurotransmitter following the arrival of an action potential at the afferent terminal (Curtis & Lacey, 1994; Curtis *et al.*, 1997; Howell & Pugh, 2016). In contrast to $GABA_A$ receptors, $GABA_B$ receptors are densely located on Ia afferent terminals (Hari *et al.*, 2021) and when activated by a brief train of conditioning afferent stimulation, they can suppress monosynaptic EPSPs for up to 800 ms (Curtis & Lacey, 1994, 1998) or more (Salio *et al.*, 2017; Hari *et al.*, 2021). This $GABA_B$ mediated presynaptic inhibition is blocked by selective $GABA_B$ receptor antagonists (Curtis & Lacey, 1994; Fink, 2013; Hari *et al.,* 2022), with evidence for a spontaneous amount of steady presynaptic inhibition at rest (Hari *et al*., 2022), demonstrating how long it can last. Thus, $GABA_B$ receptor activation on Ia afferent terminals could account for some of the long-lasting inhibition of the soleus H-reflex from the CFN conditioning stimulation or TA tendon vibration, requiring further study with specific antagonists to elucidate (Curtis *et al.*, 1997). As mentioned above, we argue that these receptors are activated secondarily to PAD, with PAD-evoked spikes activating circuits that drive GABAergic innervation of extensor afferent terminals, as detailed in Fig. 11.

Passive PAD current to Ia terminals. Finally, although there are sparse $GABA_A$ receptors at the afferent terminal, PAD from more proximal nodes may passively enter the afferent terminal to reduce the size of subsequent action potentials activated by the TN stimulation.

However, because of the long distance of the last node from the Ia terminal (Hari *et al.*, 2021) and the short space constant of the Ia axon, the amount of depolarization at the Ia afferent terminal is small (Lucas-Osma *et al.*, 2018b) and only reduces the size of the action potential by 1% even when nearby. This reduction is not likely to have a noticeable effect on neurotransmitter release and suppression of H-reflexes (Hari *et al.*, 2022).

Conclusion and clinical implications

We have provided several lines of evidence that H-reflex suppression from antagonist afferents is produced, in part, by direct effects on the motoneuron and from post-activation depression of Ia afferent transmission, the latter mediated by PAD-evoked Ia spikes triggered from the conditioning afferent input. These findings bring into question the interpretation of many human experiments claiming that H-reflex suppression by antagonist/heteronymous afferents are produced by PAD-mediated presynaptic inhibition of the Ia afferent terminal [reviewed in (Stein, 1995; Misiaszek, 2003; Hultborn, 2006; Willis, 2006)]. By extension, the idea that presynaptic inhibition of Ia afferents from PAD is reduced following nervous system injury or disease also needs to be reexamined, with examples including spinal cord injury (Ashby & Verrier, 1975; Mailis & Ashby, 1990; Roby-Brami & Bussel, 1990; Azouvi *et al.*, 1993; Calancie *et al.*, 1993; Faist *et al.*, 1994; Aymard *et al.*, 2000; Knikou & Mummidisetty, 2014; Caron *et al.*, 2020), cerebral palsy (Mizuno *et al.*, 1971; Achache *et al.*, 2010), brain injury (Koelman *et al.*, 1993; Faist *et al.*, 1994), stroke (Milanov, 1992; Koelman *et al.*, 1993) and multiple sclerosis (Azouvi *et al.*, 1993; Koelman *et al.*, 1993; Nielsen *et al.*, 1995). Because the amount of H-reflex suppression has been incorrectly equated to the amplitude of PAD, changes in the activation of $GABA_A$-receptor mediated PAD and its role in the regulation of afferent

conduction in these various disorders needs to be reexamined. This is important because drug therapies that enhance $GABA_A$ receptor activation, such as the benzodiazepine diazepam (Valium), have been used to treat spasticity in some of these conditions (Simon & Yelnik, 2010; Chang *et al.*, 2013). The greater use of $GABA_B$ antagonists, such as baclofen, to treat spasticity aligns better with our new understanding of the role of $GABA_B$ in presynaptic inhibition and post-activation depression. Interestingly, diazepam increases PAD measured in the dorsal part of the afferent and also reduces the monosynaptic reflex (Stratten & Barnes, 1971). Thus, drug therapies that enhance the activation of $GABA_A$ receptors could actually increase afferent transmission while paradoxically increasing post-activation depression through the triggering of PAD-evoked Ia spikes or by directly facilitating inhibitory $GABA_A$ receptors on the motoneuron (Cartlidge *et al.*, 1974; Simon & Yelnik, 2010; Chang *et al.*, 2013). In light of our new findings, we need to investigate how PAD evoked in dorsal parts of the Ia afferent is involved in the abnormal control of afferent conduction and transmission following injury or disease of the central nervous system in order to develop better methods to improve spared sensorimotor function and treat spasticity.

References

Achache V, Roche N, Lamy JC, Boakye M, Lackmy A, Gastal A, Quentin V & Katz R. (2010). Transmission within several spinal pathways in adults with cerebral palsy. *Brain* **133,** 1470-1483.

Afsharipour B, Manzur N, Duchcherer J, Fenrich KF, Thompson CK, Negro F, Quinlan KA, Bennett DJ & Gorassini MA. (2020). Estimation of self-sustained activity produced by persistent inward currents using firing rate profiles of multiple motor units in humans. *J Neurophysiol* **124,** 63-85.

Alvarez FJ, Taylor-Blake B, Fyffe RE, De Blas AL & Light AR. (1996). Distribution of immunoreactivity for the beta 2 and beta 3 subunits of the GABAA receptor in the mammalian spinal cord. *J Comp Neurol* **365,** 392-412.

Ashby P & Verrier M. (1975). Neurophysiological changes following spinal cord lesions in man. *Can J Neurol Sci* **2,** 91-100.

Aymard C, Katz R, Lafitte C, Lo E, Penicaud A, Pradat-Diehl P & Raoul S. (2000). Presynaptic inhibition and homosynaptic depression: a comparison between lower and upper limbs in normal human subjects and patients with hemiplegia. *Brain* **123 (Pt 8),** 1688-1702.

Azouvi P, Roby-Brami A, Biraben A, Thiebaut JB, Thurel C & Bussel B. (1993). Effect of intrathecal baclofen on the monosynaptic reflex in humans: evidence for a postsynaptic action. *J Neurol Neurosurg Psychiatry* **56,** 515-519.

Berardelli A, Day BL, Marsden CD & Rothwell JC. (1987). Evidence favouring presynaptic inhibition between antagonist muscle afferents in the human forearm. *J Physiol* **391,** 71-83.

Burke D, Gracies JM, Meunier S & Pierrot-Deseilligny E. (1992). Changes in presynaptic inhibition of afferents to propriospinal-like neurones in man during voluntary contractions. *J Physiol* **449,** 673-687.

Calancie B, Broton JG, Klose KJ, Traad M, Difini J & Ayyar DR. (1993). Evidence that alterations in presynaptic inhibition contribute to segmental hypo- and hyperexcitability after spinal cord injury in man. *Electroencephalogr Clin Neurophysiol* **89,** 177-186.

Capaday C, Lavoie BA & Comeau F. (1995). Differential effects of a flexor nerve input on the human soleus H-reflex during standing versus walking. *Can J Physiol Pharmacol* **73,** 436-449.

Caron G, Bilchak JN & Cote MP. (2020). Direct evidence for decreased presynaptic inhibition evoked by PBSt group I muscle afferents after chronic SCI and recovery with step-training in rats. *J Physiol*.

Cartlidge NE, Hudgson P & Weightman D. (1974). A comparison of baclofen and diazepam in the treatment of spasticity. *J Neurol Sci* **23,** 17-24.

Chabriat H, Bassetti CL, Marx U, Picarel-Blanchot F, Sors A, Gruget C, Saba B, Wattez M, Audoli ML & Hermann DM. (2020). Randomized Efficacy and Safety Trial with Oral S 44819 after Recent ischemic cerebral Event (RESTORE BRAIN study): a placebo controlled phase II study. *Trials* **21,** 136.

Chang E, Ghosh N, Yanni D, Lee S, Alexandru D & Mozaffar T. (2013). A Review of Spasticity Treatments: Pharmacological and Interventional Approaches. *Crit Rev Phys Rehabil Med* **25,** 11-22.

Crone C, Hultborn H, Mazieres L, Morin C, Nielsen J & Pierrot-Deseilligny E. (1990). Sensitivity of monosynaptic test reflexes to facilitation and inhibition as a function of the test reflex size: a study in man and the cat. *Exp Brain Res* **81,** 35-45.

Curtis DR. (1998). *Two types of inhibition in the spinal cord*. Oxford University Press, New York.

Curtis DR & Eccles JC. (1960). Synaptic action during and after repetitive stimulation. *The Journal of physiology* **150,** 374-398.

Curtis DR, Gynther BD, Lacey G & Beattie DT. (1997). Baclofen: reduction of presynaptic calcium influx in the cat spinal cord in vivo. *Exp Brain Res* **113,** 520-533.

Curtis DR & Lacey G. (1994). GABA-B receptor-mediated spinal inhibition. *Neuroreport* **5,** 540-542.

Curtis DR & Lacey G. (1998). Prolonged GABA(B) receptor-mediated synaptic inhibition in the cat spinal cord: an in vivo study. *Exp Brain Res* **121,** 319-333.

Darmani G, Zipser CM, Bohmer GM, Deschet K, Muller-Dahlhaus F, Belardinelli P, Schwab M & Ziemann U. (2016). Effects of the Selective alpha5-GABAAR Antagonist S44819 on Excitability in the Human Brain: A TMS-EMG and TMS-EEG Phase I Study. *J Neurosci* **36,** 12312-12320.

Desmedt JE & Godaux E. (1978). Mechanism of the vibration paradox: excitatory and inhibitory effects of tendon vibration on single soleus muscle motor units in man. *J Physiol* **285,** 197-207.

Duchen MR. (1986). Excitation of mouse motoneurones by GABA-mediated primary afferent depolarization. *Brain Res* **379,** 182-187.

Eccles JC, Eccles RM & Magni F. (1961a). Central inhibitory action attributable to presynaptic depolarization produced by muscle afferent volleys. *J Physiol* **159,** 147-166.

Eccles JC, Kozak W & Magni F. (1961b). Dorsal root reflexes of muscle group I afferent fibres. *J Physiol* **159,** 128-146.

Eccles JC, Schmidt R & Willis WD. (1963). Pharmacological Studies on Presynaptic Inhibition. *J Physiol* **168,** 500-530.

Eguibar JR, Quevedo J & Rudomin P. (1997). Selective cortical and segmental control of primary afferent depolarization of single muscle afferents in the cat spinal cord. *Experimental brain research* **113,** 411-430.

El-Tohamy A & Sedgwick EM. (1983). Spinal inhibition in man: depression of the soleus H reflex by stimulation of the nerve to the antagonist muscle. *J Physiol* **337,** 497-508.

Faist M, Dietz V & Pierrot-Deseilligny E. (1996). Modulation, probably presynaptic in origin, of monosynaptic Ia excitation during human gait. *Exp Brain Res* **109,** 441-449.

Faist M, Mazevet D, Dietz V & Pierrot-Deseilligny E. (1994). A quantitative assessment of presynaptic inhibition of Ia afferents in spastics. Differences in hemiplegics and paraplegics. *Brain* **117 (Pt 6),** 1449-1455.

Fedirchuk B, Wenner P, Whelan PJ, Ho S, Tabak J & O'Donovan MJ. (1999). Spontaneous network activity transiently depresses synaptic transmission in the embryonic chick spinal cord. *J Neurosci* **19,** 2102-2112.

Fink AJ. (2013). Exploring a behavioural role for presynaptic inhibition in spinal sensory-motor synapses. *PhD Thesis, Columbia University***,** 1-293.

Fink AJ, Croce KR, Huang ZJ, Abbott LF, Jessell TM & Azim E. (2014). Presynaptic inhibition of spinal sensory feedback ensures smooth movement. *Nature* **509,** 43-48.

Frank K. (1959). Basic mechanisms of synaptic transmission in the central nervous system. *Inst Radio Eng Trans Med Electron* **ME-6,** 85-88.

Hari K, Lucas-Osma AM, Metz K, Lin S, Pardell N, Roszko D, Black S, Minarik A, Singla R, Stephens MJ, Fouad K, Jones KE, Gorassini M, Fenrich KK, Li Y & Bennett DJ. (2022). Nodal GABA facilitates axon spike transmission in the spinal cord. *Nature Neuroscience* In press.

Howell RD & Pugh JR. (2016). Biphasic modulation of parallel fibre synaptic transmission by co-activation of presynaptic GABAA and GABAB receptors in mice. *J Physiol* **594,** 3651-3666.

Howells J, Sangari S, Matamala JM, Kiernan MC, Marchand-Pauvert V & Burke D. (2020). Interrogating interneurone function using threshold tracking of the H reflex in healthy subjects and patients with motor neurone disease. *Clin Neurophysiol* **131,** 1986-1996.

Hughes DI, Mackie M, Nagy GG, Riddell JS, Maxwell DJ, Szabo G, Erdelyi F, Veress G, Szucs P, Antal M & Todd AJ. (2005). P boutons in lamina IX of the rodent spinal cord express high levels of glutamic acid decarboxylase-65 and originate from cells in deep medial dorsal horn. *Proc Natl Acad Sci U S A* **102,** 9038-9043.

Hultborn H. (2006). Spinal reflexes, mechanisms and concepts: from Eccles to Lundberg and beyond. *Prog Neurobiol* **78,** 215-232.

Hultborn H, Illert M, Nielsen J, Paul A, Ballegaard M & Wiese H. (1996). On the mechanism of the post-activation depression of the H-reflex in human subjects. *Experimental brain research* **108,** 450-462.

Hultborn H, Meunier S, Morin C & Pierrot-Deseilligny E. (1987a). Assessing changes in presynaptic inhibition of I a fibres: a study in man and the cat. *J Physiol* **389,** 729-756.

Hultborn H, Meunier S, Pierrot-Deseilligny E & Shindo M. (1987b). Changes in presynaptic inhibition of Ia fibres at the onset of voluntary contraction in man. *J Physiol* **389,** 757-772.

Iles JF. (1996). Evidence for cutaneous and corticospinal modulation of presynaptic inhibition of Ia afferents from the human lower limb. *J Physiol* **491 (Pt 1),** 197-207.

Iles JF & Pisini JV. (1992). Cortical modulation of transmission in spinal reflex pathways of man. *J Physiol* **455,** 425-446.

Iles JF & Roberts RC. (1987). Inhibition of monosynaptic reflexes in the human lower limb. *J Physiol* **385,** 69-87.

Jankowska E, McCrea D, Rudomin P & Sykova E. (1981). Observations on neuronal pathways subserving primary afferent depolarization. *Journal of neurophysiology* **46,** 506-516.

Knikou M & Mummidisetty CK. (2014). Locomotor training improves premotoneuronal control after chronic spinal cord injury. *J Neurophysiol* **111,** 2264-2275.

Koelman JH, Bour LJ, Hilgevoord AA, van Bruggen GJ & Ongerboer de Visser BW. (1993). Soleus H-reflex tests and clinical signs of the upper motor neuron syndrome. *J Neurol Neurosurg Psychiatry* **56,** 776-781.

Leppanen L & Stys PK. (1997). Ion transport and membrane potential in CNS myelinated axons. II. Effects of metabolic inhibition. *J Neurophysiol* **78,** 2095-2107.

Lin S, Li Y, Lucas-Osma AM, Hari K, Stephens MJ, Singla R, Heckman CJ, Zhang Y, Fouad K, Fenrich KK & Bennett DJ. (2019). Locomotor-related V3 interneurons initiate and coordinate muscles spasms after spinal cord injury. *J Neurophysiol* **121,** 1352-1367.

Lucas-Osma AM, Li Y, Lin S, Black S, Singla R, Fouad K, Fenrich KK & Bennett DJ. (2018a). Extrasynaptic alpha-5GABAA receptors on proprioceptive afferents produce a tonic depolarization that modulates sodium channel function in the rat spinal cord. *J Neurophysiol*.

Lucas-Osma AM, Li Y, Lin S, Black S, Singla R, Fouad K, Fenrich KK & Bennett DJ. (2018b). Extrasynaptic proportional, variant5GABAA receptors on proprioceptive afferents produce a tonic depolarization that modulates sodium channel function in the rat spinal cord. *J Neurophysiol*.

Luscher HR, Ruenzel P, Fetz E & Henneman E. (1979). Postsynatpic population potentials recorded from ventral roots perfused with isotonic sucrose: connections of groups Ia and II spindle afferent fibers with large populations of motoneurons. *J Neurophysiol* **42,** 1146-1164.

Mailis A & Ashby P. (1990). Alterations in group Ia projections to motoneurons following spinal lesions in humans. *J Neurophysiol* **64,** 637-647.

Matthews PB. (1996). Relationship of firing intervals of human motor units to the trajectory of post-spike after-hyperpolarization and synaptic noise. *J Physiol* **492 (Pt 2),** 597-628.

McCrea DA, Shefchyk SJ & Carlen PL. (1990). Large reductions in composite monosynaptic EPSP amplitude following conditioning stimulation are not accounted for by increased postsynaptic conductances in motoneurons. *Neurosci Lett* **109,** 117-122.

Metz K, Concha Matos I, Li Y, Afsharipour B, Thompson CK, Negro F, Quinlan KA, Bennett DJ & Gorassini M. (2022). Facilitation of sensory axon conduction to motoneurons during cortical or sensory evoked primary afferent depolarization (PAD) in humans. Submitted *J. Physiol.*

Milanov I. (1992). A comparative study of methods for estimation of presynaptic inhibition. *J Neurol* **239,** 287-292.

Misiaszek JE. (2003). The H-reflex as a tool in neurophysiology: its limitations and uses in understanding nervous system function. *Muscle Nerve* **28,** 144-160.

Mizuno Y, Tanaka R & Yanagisawa N. (1971). Reciprocal group I inhibition on triceps surae motoneurons in man. *J Neurophysiol* **34,** 1010-1017.

Morin C, Pierrot-Deseilligny E & Hultborn H. (1984). Evidence for presynaptic inhibition of muscle spindle Ia afferents in man. *Neurosci Lett* **44,** 137-142.

Nakashima K, Rothwell JC, Day BL, Thompson PD & Marsden CD. (1990). Cutaneous effects on presynaptic inhibition of flexor Ia afferents in the human forearm. *J Physiol* **426,** 369-380.

Negro F, Muceli S, Castronovo AM, Holobar A & Farina D. (2016). Multi-channel intramuscular and surface EMG decomposition by convolutive blind source separation. *J Neural Eng* **13,** 026027.

Neher E & Sakaba T. (2001). Estimating transmitter release rates from postsynaptic current fluctuations. *J Neurosci* **21,** 9638-9654.

Nielsen J, Petersen N, Ballegaard M, Biering-Sorensen F & Kiehn O. (1993). H-reflexes are less depressed following muscle stretch in spastic spinal cord injured patients than in healthy subjects. *Experimental brain research* **97,** 173-176.

Nielsen J, Petersen N & Crone C. (1995). Changes in transmission across synapses of Ia afferents in spastic patients. *Brain* **118 (Pt 4),** 995-1004.

Norton JA, Bennett DJ, Knash ME, Murray KC & Gorassini MA. (2008). Changes in sensory-evoked synaptic activation of motoneurons after spinal cord injury in man. *Brain* **131,** 1478-1491.

Pierce JP & Mendell LM. (1993). Quantitative ultrastructure of Ia boutons in the ventral horn: scaling and positional relationships. *J Neurosci* **13,** 4748-4763.

Powers RK & Binder MD. (2001). Input-output functions of mammalian motoneurons. *Rev Physiol Biochem Pharmacol* **143,** 137-263.

Roby-Brami A & Bussel B. (1990). Effects of flexor reflex afferent stimulation on the soleus H reflex in patients with a complete spinal cord lesion: evidence for presynaptic inhibition of Ia transmission. *Exp Brain Res* **81,** 593-601.

Rossi A, Decchi B & Ginanneschi F. (1999). Presynaptic excitability changes of group Ia fibres to muscle nociceptive stimulation in humans. *Brain Res* **818,** 12-22.

Rudomin P. (1990). Presynaptic inhibition of muscle spindle and tendon organ afferents in the mammalian spinal cord. *Trends Neurosci* **13,** 499-505.

Rudomin P & Schmidt RF. (1999). Presynaptic inhibition in the vertebrate spinal cord revisited. *Exp Brain Res* **129,** 1-37.

Salio C, Merighi A & Bardoni R. (2017). GABAB receptors-mediated tonic inhibition of glutamate release from Abeta fibers in rat laminae III/IV of the spinal cord dorsal horn. *Mol Pain* **13,** 1744806917710041.

Shefner JM, Buchthal F & Krarup C. (1992). Recurrent potentials in human peripheral sensory nerve: possible evidence of primary afferent depolarization of the spinal cord. *Muscle Nerve* **15,** 1354-1363.

Sherrington CS. (1908). On reciprocal innervation of antagonist muscles. Twelfth Note - Proprioceptive reflexes. *Proc R Soc Lond B Biol Sci* **80,** 552-564.

Simon O & Yelnik AP. (2010). Managing spasticity with drugs. *Eur J Phys Rehabil Med* **46,** 401-410.

Stein RB. (1995). Presynaptic inhibition in humans. *Prog Neurobiol* **47,** 533-544.

Stratten WP & Barnes CD. (1971). Diazepam and presynaptic inhibition. *Neuropharmacology* **10,** 685-696.

Stuart GJ & Redman SJ. (1992). The role of GABAA and GABAB receptors in presynaptic inhibition of Ia EPSPs in cat spinal motoneurones. *J Physiol* **447,** 675-692.

Turker KS & Powers RK. (1999). Effects of large excitatory and inhibitory inputs on motoneuron discharge rate and probability. *J Neurophysiol* **82,** 829-840.

Ueno M, Nakamura Y, Li J, Gu Z, Niehaus J, Maezawa M, Crone SA, Goulding M, Baccei ML & Yoshida Y. (2018). Corticospinal Circuits from the Sensory and Motor Cortices

Differentially Regulate Skilled Movements through Distinct Spinal Interneurons. *Cell Rep* **23,** 1286-1300 e1287.

Willis WD. (2006). John Eccles' studies of spinal cord presynaptic inhibition. *Prog Neurobiol* **78,** 189-214.

Willis WD, Jr. (1999). Dorsal root potentials and dorsal root reflexes: a double-edged sword. *Exp Brain Res* **124,** 395-421.

Yavuz US, Negro F, Diedrichs R & Farina D. (2018). Reciprocal inhibition between motor neurons of the tibialis anterior and triceps surae in humans. *J Neurophysiol* **119,** 1699-1706.

Zehr EP & Stein RB. (1999). Interaction of the Jendrassik maneuver with segmental presynaptic inhibition. *Exp Brain Res* **124,** 474-480.

Zhang F, Vierock J, Yizhar O, Fenno LE, Tsunoda S, Kianianmomeni A, Prigge M, Berndt A, Cushman J, Polle J, Magnuson J, Hegemann P & Deisseroth K. (2011). The microbial opsin family of optogenetic tools. *Cell* **147,** 1446-1457.

Additional Information

Competing Interests

The authors have no competing interests to declare.

Author contributions

K.M., Y.L., D.J.B and M.A.G. conceived and designed research; K.M., I.C.M., O.B., Y.L., D.J.B. and M.A.G. performed human experiments; K.H., S.L., R.S., K.F., Y.L., and D.J.B. performed animal experiments; K.M., I.C.M., O.B., B.A., D.J.B. and M.A.G. analyzed the data; K.M., K.H., Y.L., D.J.B. and M.A.G. interpreted the results of experiments; K.M., I.C.M., D.J.B. and M.A.G. prepared figures; K.M., D.J.B. and M.A.G. drafted and revised the manuscript and all authors edited the manuscript.

All authors approved the final version of the article and agreed to be accountable for all aspects of the work. The authors confirm that all persons designated as authors are qualified.

Funding

This work was supported by a National Science and Engineering Grant 05205 to M.A.G. and studentship funding to K.M. from the Neuroscience and Mental Health Institute and Faculty of Medicine and Dentistry at the University of Alberta.

Acknowledgments

We thank Ms. Jennifer Duchcherer for technical assistance.

Chapter 4: Facilitated conduction and reduced post activation depression of proprioceptive afferents after spinal cord injury.

Metz K.[1,4], Concha-Matos I.[1,4], Sun Y. [2,3,4], Yang JF. [2,3,4], Bennett DJ [3,4] and Gorassini MA.[1,4]

[1] Department of Biomedical Engineering, Faculty of Medicine and Dentistry, [2] Department of Physical Therapy, [3] Faculty of Rehabilitation Medicine, [4] Neuroscience and Mental Health Research Institute, University of Alberta

Abstract: 250
Text: 6,172
Tables: 1
Figures: 6

Key words: H-reflex, presynaptic inhibition, primary afferent depolarization, GABA, afferent priming, proprioceptive afferents, sensory transmission

Corresponding Author:
Dr. Monica Gorassini, PhD
Department of Biomedical Engineering
Institute of Neuroscience and Mental Health
Faculty of Medicine and Dentistry
University of Alberta
Edmonton, AB CANADA T6G 0G2
monica.gorassini@ualberta.ca

Introduction

Controlling the flow of sensory information entering the spinal cord is essential to functional motor behaviour (Rothwell *et al.*, 1982; Fink *et al.*, 2014; Prochazka, 2015; Mayer *et al.*, 2018). After injury to the spinal cord (SCI), abnormal control over sensory transmission can lead to a host of devastating secondary complications like spasticity, which is characterized by muscle spasms, hyperreflexia, clonus and co-contraction (Rabchevsky & Kitzman, 2011; Silva *et al.*, 2014). Several animal and human studies have concluded that spasticity following SCI is mediated, in part, from an enhanced activation of spinal interneurons and motoneurons by Ia muscle afferents due to a decrease in presynaptic inhibition of the Ia axon terminal (reviewed in Lalonde & Bui, 2021). Presynaptic inhibition at the Ia afferent terminal has been thought to be mediated by primary afferent depolarization (PAD), produced by the activation of $GABA_A$ receptors and the efflux of chloride ions down its concentration gradient, resulting in the inactivation sodium channels and/or shunting of incoming action potentials to reduce the probability of neurotransmitter release (Gallagher *et al.*, 1978; Rudomin & Schmidt, 1999; Willis, 2006). The observation that sensory-evoked PAD measured in the proximal dorsal root was less excitable in chronic compared to acute injury was taken as evidence that presynaptic inhibition at the Ia afferent terminal was reduced and this contributes to the increase in Ia-mediated reflexes when spasticity develops in chronic SCI (Hancock *et al.*, 1973; Naftchi *et al.*, 1979; Quevedo *et al.*, 1993; Caron *et al.*, 2020). Likewise, the suppression of Ia-mediated monosynaptic reflexes (MSR) by a prior activation of sensory-evoked PAD is reduced after chronic SCI (Caron *et al.*, 2020) and this also has been taken as evidence of reduced PAD-mediated presynaptic inhibition [(Eccles *et al.*, 1962; Hultborn, 2006; Willis, 2006) reviewd in Hari *et al*., 2021].

Based on the animal findings described above, several human studies sought evidence of reduced presynaptic inhibition after SCI by quantifying how much sensory pathways that activate PAD could suppress the Ia-mediated H-reflex. In contrast to uninjured controls (Mizuno *et al.*, 1971; El-Tohamy & Sedgwick, 1983; Capaday *et al.*, 1995), the suppression of upper and lower limb H-reflexes by a conditioning antagonist nerve stimulation was minimal or non-existent in participants with chronic SCI (Kagamihara & Masakado, 2005; Knikou & Mummidisetty, 2014). Likewise, the amount of monosynaptic facilitation of the soleus H-reflex by quadriceps afferents was greater in SCI participants compared to controls, leading Faist et al. (1994) to conclude that there is a reduced basal tone of presynaptic inhibition in Ia afferents after chronic SCI. Taken together, the reduced suppression of H-reflexes by sensory pathways that activate $GABA_A$ receptor-mediated PAD was used as evidence that presynaptic inhibition of the Ia afferent terminal is reduced in chronic SCI.

We have recently shown that PAD does not produce presynaptic inhibition at the Ia afferent terminal. What then produces the suppression of H-reflexes by an antagonist sensory conditioning that is known to activate PAD networks and why is this suppression reduced after SCI? We have also recently shown that PAD can produce post-activation depression of H-reflexes if the sensory activation of PAD is large enough to evoke spikes in the Ia afferent (Hari *et al.*, 2021; Metz *et al.*, 2022). These PAD-evoked spikes travel orthodromically to the Ia afferent terminal and reduce transmission for several seconds via post-activation depression, resulting in the suppression of subsequent H-reflexes that are activated by the same Ia inputs (Metz *et al.*, 2022). The H-reflex suppression from PAD-evoked spikes is similar to the profile of H-reflex suppression from repeated activations of the same H-reflex, termed rate dependent depression (RDD), leading to the speculation that both are due to post-activation depression

(Metz *et al.*, 2022). After chronic SCI, RDD and post-activation depression are reduced (Ashby & Verrier, 1975; Thompson *et al.*, 1992; Calancie *et al.*, 1993; Nielsen *et al.*, 1993; Schindler-Ivens & Shields, 2000; Grey *et al.*, 2008; Kumru *et al.*, 2015; Hofstoetter *et al.*, 2019); however, the role of PAD-evoked spikes in H-reflex suppression has never been explored. We have recently shown that these PAD-evoked orthodromic spikes produce monosynaptic EPSPs in the motoneuron and early-latency reflexes in the test muscle, indicating that the PAD-evoked spikes indeed travelled to the afferent terminal (Metz *et al.*, 2022). Thus, in this study we examined if there were any early-latency reflex responses in the test soleus (extensor) motoneurons following a conditioning stimulation of antagonist (flexor) afferents, to indicate activation of PAD-evoked Ia spikes, and if their relationship to H-reflex suppression was modified after SCI. We hypothesized that H-reflexes conditioned by antagonist afferents would be suppressed if there is an early soleus reflex response reflecting PAD-evoked Ia spikes but this inhibition would be less after SCI given that post-activation depression is reduced after chronic injury (Ashby & Verrier, 1975; Thompson *et al.*, 1992; Calancie *et al.*, 1993; Nielsen *et al.*, 1993; Schindler-Ivens & Shields, 2000; Grey *et al.*, 2008; Kumru *et al.*, 2015; Hofstoetter *et al.*, 2019).

Besides evoking post activation depression, the function of PAD activated by $GABA_A$ receptors is to depolarize sodium channels located at or near the nodes of Ranvier between the myelinated parts of the afferent, which then facilitate afferent conduction by reducing action potential failure in downstream branch points. Evidence for facilitation of H-reflexes by sensory and corticospinal pathways that activate PAD with no, or even slight hyperpolarizing effects on the motoneuron, support these findings (Hari *et al.*, 2021; Metz *et al.*, 2021). Facilitation of Ia afferent conduction is readily seen following a low-intensity, conditioning stimulation of cutaneous sensory pathways that more readily activate a long-lasting, tonic PAD that is mediated

by extra-synaptic α5 $GABA_A$ receptors (Lucas-Osma *et al.*, 2018; Hari *et al.*, 2021). For example, a brief 0.5 s train of low-intensity, but high frequency (200 Hz) stimulation of cutaneous afferents produced a tonic PAD that lasted for several minutes and facilitated monosynaptic and H-reflexes for a similar duration in both rodents and humans without direct facilitation of the motoneuron (Lucas-Osma *et al.*, 2018; Hari *et al.*, 2021; Metz *et al.*, 2022). Here we examined if a similar long-lasting facilitation of H-reflexes can be evoked in participants with chronic SCI given the changes in GABA networks or receptors that occur after injury. For example, after corticospinal tract injury, extra-synaptic GABA that is produced by the enzyme GAD67 (encoded by the GAD1 gene) is increased (Russ *et al.*, 2013) and this may produce continual activation of extrasynaptic α5$GABA_A$ receptors and tonic PAD to produce secure action potential conduction in Ia afferents that would normally be subject to branch point failure. Indeed, our unpublished findings suggest that after SCI, Ia afferents are not as prone to branch point failure, potentially due to continual activation of $GABA_A$ receptors near branch points (Hari and Bennett personal communication). We hypothesized that after SCI Ia afferents, and H-reflexes by extension, would be less facilitated by a further release of extra-synaptic GABA from high frequency cutaneous stimulation compared to uninjured controls since afferent conduction after SCI is already secure and there is no room for further facilitation.

Portions of the control data were presented in Metz *et al*., 2021, 2022.

Methods

Participants and ethics

Experiments were approved by the Human Research Ethics Board at the University of Alberta (Protocols 000780557 and 00031413) and performed with informed consent of the

participants. Our sample comprised of 36 participants with a SCI (27 male) ranging in age from 20 to 67 years (40.6±16, mean ± SD, Table 1). The age of injury varied from 0.5 to 33.5 years (8.1±7.3 years) with neurologic injury levels ranging from C2 to T12 with 16 of the 36 participants with SCI unable to voluntarily activate one or more muscles of the leg (Table 1). Comparative data from 33 control participants (15 male) with no known neurological injury or disease were recruited. Ages of the control participants ranged from 20 to 58 years (29.8±12) and were significantly younger than the SCI group ($P<0.001$, Mann-Whitney Rank Sum).

Experimental procedures

Participants were typically seated in their wheelchairs with one leg slightly extended to access the popliteal fossa. The right leg was used in all control and SCI participants except in 4 SCI participants where the more spastic left leg was used. Padded supports were added to facilitate complete relaxation and minimal movement of the leg. Participants were asked to rest completely with no talking and no hand or arm movements, including participants with motor complete SCI as residual pathways may exist and movement of the upper body could stretch/shift the lower body, effecting H-reflex measurements.

EMG recordings. A pair of Ag-AgCl electrodes (Kendall; Chicopee, MA, USA, 3.2 cm by 2.2 cm) was used to record surface EMG from the soleus and tibialis anterior (TA) muscles with a ground electrode placed just below the knee. The EMG signals were amplified by 1000 and band-pass filtered from 10 to 1000 Hz (Octopus, Bortec Technologies; Calgary, AB, Canada) and then digitized at a rate of 5000 Hz using

Axoscope 10 hardware and software (Digidata 1400 Series, Axon Instruments, Union City, CA).

Percutaneous nerve stimulation to evoke an H-reflex: The tibial nerve (TN) was stimulated in a bipolar arrangement using a constant current stimulator (1 ms rectangular pulse width, Digitimer DS7A, Hertfordshire, UK) to evoke an H-reflex in the soleus muscle. After searching for the TN with a probe, an Ag-AgCl electrode (Kendall; Chicopee, MA, USA, 2.2 cm by 2.2 cm) was placed in the popliteal fossa, with the return electrode (Axelgaard; Fallbrook, CA, USA, 5 cm by 10 cm) placed on the patella. Stimulation intensity was set to evoke a test (unconditioned) H-reflex below half maximum on the ascending phase of H-reflex recruitment curve to reduce the potential for evoking polysynaptic reflexes or self-facilitation (Hari *et al.*, 2021). H-reflexes recorded at rest were evoked every 5 seconds to minimize post activation depression (Hultborn *et al.*, 1996) and at least 10 H-reflexes were evoked before conditioning to establish a steady baseline. All H-reflexes were recorded at rest.

H-reflex/M-wave recruitment curves were collected from each participant by gradually increasing the TN stimulation, starting at an intensity that did not elicit an H-reflex or M-wave and increasing the TN stimulation until the maximum M-wave was achieved. The maximum peak-peak amplitude of the H-reflex and M-wave was used to calculate an Hmax/Mmax ratio for each participant. The average peak-to-peak amplitude of the test (unconditioned) H-reflex was expressed as a percentage of the maximum H-reflex ([test H / Hmax]*100%).

Short-duration H-reflex suppression by antagonist CPN conditioning

In 23 participants with SCI (see Table 1), the soleus H-reflex was conditioned by stimulating the ipsilateral common peroneal nerve (CPN) supplying the antagonist TA muscle (a.k.a. the common fibular nerve) as done previously in uninjured controls [n = 13 from Metz *et*

al., 2022]. The CPN was stimulated using a bipolar arrangement (Ag-AgCl electrodes, Kendall; Chicopee, MA, USA, 2.2 cm by 2.2 cm) with the anode placed anterior and slightly distal to the fibular head on the right leg. The cathode was placed near the fibular head in a location that elicited pure dorsiflexion. Three pulses (200 Hz, 1-ms pulse width) were applied to the CPN at an intensity of 1.0 and 1.5 x motor threshold (MT). Motor threshold was determined by the lowest CPN stimulation intensity that produced a discernable and reproducible M-wave in the TA muscle at rest. Following a run of unconditioned (test) soleus H-reflexes, 7 conditioned H-reflexes at one of the randomly chosen ISIs (3, 15, 30, 60, 100 or 200 ms) were elicited with 3-4 unconditioned H-reflexes interposed between each run of conditioned H-reflexes to reestablish a steady baseline before the next set of conditioning stimuli.

Data analysis: The average peak-to-peak amplitude of the conditioned soleus H-reflexes at each ISI was compared to the average peak-to-peak amplitude of all the unconditioned (test) soleus H-reflexes evoked in a trial run. The % change H-reflex was expressed as: ([conditioned H-reflex – test H-reflex]/test H-reflex*100%). The % change at each ISI was then averaged across participants in each group. The effect of an isolated 1.0 and 1.5 x MT conditioning CPN stimulation on the soleus motoneurons was measured in the resting soleus EMG. The rectified EMG from 7 to 10 CPN stimulation trials were averaged into 20 ms bins and the mean pre-stimulus EMG (or noise) measured between -100 and 0 ms was subtracted from each of the mean bin values. Bins containing EMG with CPN stimulation artifact (typically from 0 to 20 ms) were removed. The mean EMG in each time bin was then averaged across participants in each group.

Long-duration H-reflex suppression by CPN and TN conditioning

To examine a longer time course of H-reflex suppression, soleus H-reflexes were conditioned with 1.5 x MT CPN stimulation as described above but at longer ISIs (500, 1000, 1500, 2000 and 2500 ms) in the same 23 participants with SCI (see Table 1) and compared to data from 13 controls from Metz *et al*., 2022. To examine if the long-duration suppression of soleus H-reflexes from CPN stimulation resembled the profile of repeated TN stimulation during RDD, in 33 participants with SCI (21 of whom also participated in the CPN experiment, Table 1) and in 16 controls (13 from Metz *et al*., 2022), repeated activation of the TN was examined at similar ISIs (500 to 2500 ms). During RDD, the first H-reflex (H1) of a stimulation trial of at least 10 H-reflexes was evoked just below 50% of maximum on the ascending part of the H-reflex recruitment curve (39.4$\pm$23.2% of Hmax). Each RDD interval was repeated 3 times.

Data analysis: The % change in the soleus H-reflex from the CPN stimulation applied at the longer ISIs was measured as above (% chg H-reflex$_{(CPN-TN)}$). To quantify the amount of H-reflex suppression during RDD, the average peak-to-peak amplitude of the second to eighth H-reflex (H2-8) was expressed as a percentage of the first H-reflex (H1) using the formula: % chg H-reflex$_{(TN-TN)}$ = [([avg H2-8] – H1) / H1]*100% for each stimulation frequency. In each participant, the resulting % chg H-reflex$_{(TN-TN)}$ was averaged across the 3 trials for each RDD frequency and then averaged across participants in each group.

Long-duration H-reflex facilitation by cutaneous conditioning

The long-duration facilitation of the soleus H-reflex by a brief, high frequency stimulation of cutaneous afferents was examined in 18 participants with SCI (Table 1) and in 16 uninjured controls [n = 15 controls from Metz *et al.,* 2021]. The soleus H-reflex was conditioned

by stimulating the lateral cutaneous branch of the deep peroneal nerve (cDPN) on the dorsal surface of the ankle using a bipolar arrangement. A 200 Hz (0.5 ms pulse width), 500 ms train of cDPN stimulation was applied at an intensity of 4 mA, which was below radiating threshold in control participants (Metz *et al.*, 2021). Following a baseline of 20 test H-reflexes (delivered every 5 s), the cDPN stimulation train was applied once, 700 ms before a further run of H-reflexes evoked for another 90-120 s. This stimulation protocol was repeated 3 times with at least 2 minutes in between each run.

Data analysis: Each H-reflex was expressed as a percentage of the average amplitude of the 20 baseline H-reflexes using the formula: % change H-reflex$_{(cDPN)}$ = (H-reflex – baseline H-reflex)/baseline H-reflex)*100%. The % change H-reflexes$_{(cDPN)}$ were plotted against time and divided into 10 s bins (2 H-reflexes per bin). H-reflexes from all 3 trial runs were grouped together in each bin (2 H-reflexes per bin x 3 trials = 6 H-reflexes per bin). The average % change H-reflex$_{(cDPN)}$ in each bin was then averaged across participants in each group.

Statistical Analysis

The % change of the conditioned H-reflex and binned EMG across the different ISIs were compared to a 0% change using a one-way ANOVA for repeated measures. Post hoc Tukey tests were used to determine which ISIs were significantly different from a 0% change. A mixed model, two-way ANOVA for repeated measures was used to compare values between the SCI and control participants with group and ISI (or time) as factors. A pairwise comparison (adjusted for multiple comparisons using Bonferroni) was used to compare the two groups (SCI vs control) at each ISI or timepoint. In cases where

H-reflexes were not collected at a specific ISI (40 of the 802 ISIs tested were missing, or 5% of data), the value from the closest ISI was used. For example, if the H-reflexes at the 60 ms ISI was missing for a given participant, the 30 ms ISI value was used. These substitutions did not change the average H-reflex at any ISI (tested using Student's t-test, not shown). Data are presented in figures and in the text as mean $\pm$ standard deviation (SD) unless otherwise stated, standard error (SE) was sometimes used for easier visualization of the estimated spread of the EMG data. Significance was set as $P < 0.05$.

ID	Age	Sex	Years post injury	Injury Level	Leg Muscle Contraction	CPN-TN Short/Long	TN-TN RDD	cDPN
1	25	M	.5	T5/6	No	✓	✓	✓
2	31	M	11	C5	Yes	✓	✓	✓
3	23	M	6	C2/3	No	✓	✓	✓
4	61	F	3	C4/5	Yes	✓	✓	✓
5	31	M	5.5	T6	No	✓	✓	✓
6	58	M	3.5	C3/4	No	✓	✓	✓
7	20	M	3.5	T8	No	✓	✓	✓
8	65	F	6.5	T12	Yes	✓	✓	✓
9	28	M	15	C4/5	Yes	✓	✓	✓
10	25	M	1.5	T5	Yes	✓	✓	✓
11	36	M	11.5	C4	No	✓	✓	✓
12	26	F	10	C4/5	No	✓	✓	✓
13	24	M	4	C5	No	✓	✓	✓
14	24	F	3	T5	No	✓	✓	✓
15	29	F	11	C4/5/6	No	✓	✓	✓
16	29	M	12	T4	Yes	✓	✓	✓
17	35	M	3	T7	No	✓	✓	
18	51	M	13.5	T12	Yes	✓	✓	
19	33	M	5.5	T2	No	✓	✓	
20	21	M	4	C4	No	✓	✓	
21	57	M	3.5	T2	No	✓	✓	
22	64	M	.5	C4	Yes	✓		✓
23	21	F	5	T6	No	✓		
24	28	M	4.5	T4	Yes		✓	
25	45	M	7	C6	Yes		✓	
26	54	F	11	T2	Yes		✓	
27	67	M	24.5	C4	Yes		✓	
28	64	M	33.5	T12	Yes		✓	
29	47	M	11	T12	Yes		✓	
30	55	M	18	C6-7	Yes		✓	
31	52	M	1.5	T10	Yes		✓	
32	47	M	1	T12	Yes		✓	
33	64	M	1	C3	Yes		✓	
34	57	F	10.5	C6	Yes		✓	
35	30	F	4.2	C6	Yes		✓	
36	44	F	22	T6/7	No			✓
36	**40.6± 15.0**	**26 M 10 F**	**8.1±7.3**	**C2-T12**	**16 No/20 Yes**	**23**	**33**	**18**

Table 1. Participant demographics, injury and experiment details. Age, sex, number of years post-injury, neurologic level of injury and whether a participant could voluntarily activate one or more muscles in their leg are listed for each participant with SCI. Checkmarks indicate if the participant participated in the CPN, cDPN and/or RRD conditioning experiments.

Results

M-wave/H-wave recruitment curves

The maximum peak-to-peak amplitude of the unrectified soleus M-wave and H-reflex, as measured from the largest response evoked during a run of increasing TN stimulation intensities (open symbols in Fig. 4.1A), were both ~30% smaller in participants with SCI compared to uninjured controls (Figs. 4.1Bi and Bii respectively, $P < 0.05$). Correspondingly, the median ratio of Hmax/Mmax was not different between the two groups, with both ratios ~50% (Fig. 4.1Biii, $P = 0.84$). For all subsequent experiments where the soleus H-reflex was conditioned by a prior stimulation to the CPN or cDPN, an intensity of TN stimulation that produced a test (unconditioned) H-reflex below ½ Hmax was used (arrows in Fig. 4.1A) to avoid self-facilitation of the soleus Ia afferents that can occur with high test stimulation intensities (Hari *et al.*, 2021). The average amplitude of the test H-reflex, expressed as a % of Hmax, used in the SCI participants (27.5 ± 21.3%) was not different from controls (30.9 ± 13.8%, $P = 0.30$).

Short-duration inhibition of H-reflexes by antagonist nerve stimulation

A low-intensity conditioning stimulation of the CPN at 1.0 x MT did not modulate the test soleus H-reflex across the various ISIs in participants with SCI (Fig. 4.2A individual and Fig. 4.2B group data) but did so in control participants (statistics described in legend), with post-hoc analysis revealing a greater suppression of the H-reflex in controls at the 30 ms ISI (* in Fig. 4.2Bi). As proposed in Metz *et al*., 2022, the suppression of the H-reflex may have been mediated by post-activation depression of the soleus Ia afferents due to the conditioning CPN stimulation producing an orthodromic,

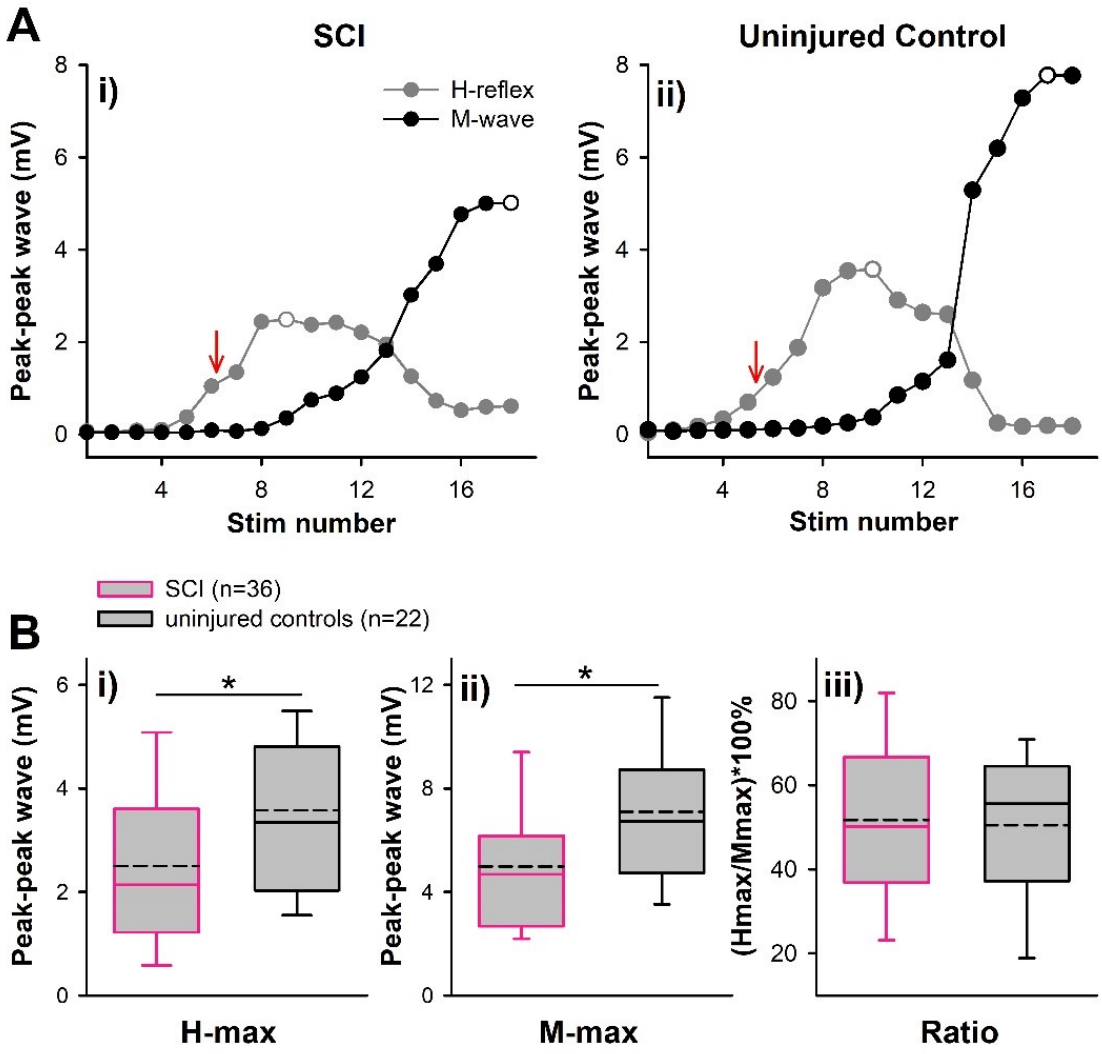

Figure 4.1: H-reflex/M-wave recruitment curves A) Peak-to-peak amplitude of the soleus H-reflex (grey circles) and M-wave (black circles) from a participant with SCI **(i)** and an uninjured control participant **(ii)** plotted against stimulation number during increasing stimulation intensities to the TN. Maximum H-reflex and M-wave marked with open circles and amplitude of H-reflex used as a test H-reflex in subsequent conditioning experiments marked by red arrows. **B)** Box plot of maximum H-reflex ($P < 0.05$, Mann-Whitney Rank Sum test) **(i)**, M-wave ($P < 0.05$, Mann-Whitney Rank Sum test) **(ii)** and H-reflex/M-wave ratio ($P = 0.84$, t-test) **(iii)** with mean represented by black dashed lines and median by solid lines, 25th and 75th percentiles by the box bounds, and the 95th and 5th percentiles by whiskers. * = $P < 0.05$.

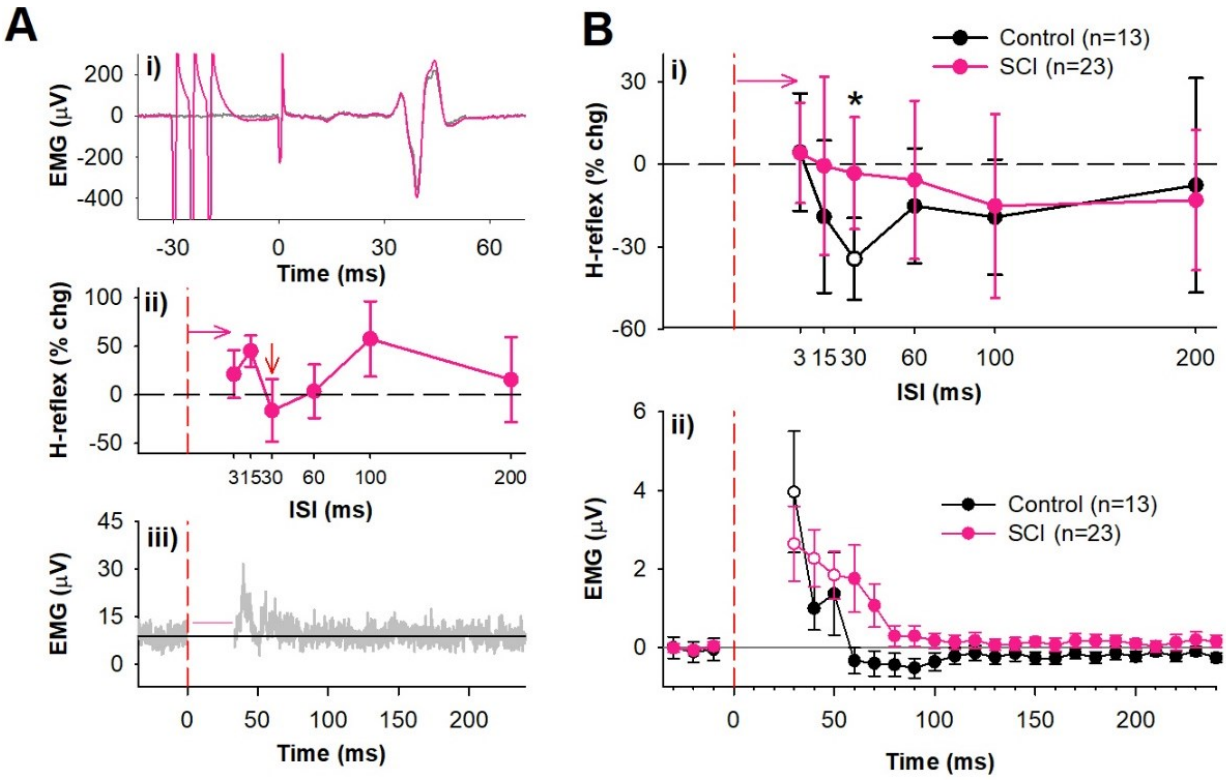

Figure 4.2: Conditioning soleus H-reflex by 1.0 x MT CPN stimulation at short ISIs. A) Representative data from a participant with SCI. **i)** Average of 7 conditioned (pink, 1.0 x MT CPN stimulation) and 7 test (grey) soleus H-reflexes (unrectified EMG) at the 30 ms ISI at rest. TN stimulation to evoke H-reflex applied at 0 ms. **ii)** Mean (±SD) % change of the H-reflex plotted at each ISI. Time of CPN stimulation marked by red dashed line. H-reflexes are shifted to the right of the time of CPN stimulation by the latency of the H-reflex (~30 ms, see Methods). **iii)** Average rectified soleus EMG (8 sweeps) measured at rest with CPN stimulation delivered alone. Stimulation artifact and TA M-wave cross talk has been removed as marked by pink horizontal line. **B)** Group data. **i)** Mean (±SD) % change soleus H-reflex averaged across the SCI (pink, n=23) and control (black, n=13) groups (control data from Metz et al., 2022). The conditioned H-reflex in the SCI group was not different across the tested ISIs ($F[22,6] = 2.095$, $P = 0.058$, observed power = 0.414, one-way RM ANOVA) but was in the control group ($F[12,6] = 4.679$, $P < 0.001$, observed power = 0.949, one-way RM ANOVA) being significantly different from 0% at the 30 ms ISI ($P = 0.003$, Tukey Test). The conditioned H-reflex was different between the SCI and control groups across the different ISIs ($F[1,34] = 4.04$, $P = 0.05$, observed power = 0.498, Mixed RM ANOVA], with greater H-reflex suppression in the control group at the 30 ms ISI ($P < 0.001$, pairwise comparison with Bonferroni adjustment). **ii)** Mean (±SE) soleus EMG from CPN stimulation alone

at rest, values averaged into 10 ms bins with the mean, pre-stimulus value (100 ms window just prior to stimulation) subtracted from each bin. The EMG in the SCI group was significantly different across the time bins ($F[22,21] = 5.535$, $P < 0.001$, observed power = 1.00, one-way RM ANOVA) being significantly different from 0 mV EMG at the 30 ($P < 0.001$), 40 ($P < 0.001$) and 50 ms bins ($P = 0.031$, Tukey Test). The EMG in the control group was also significantly different across the time bins ($F[12,21] = 5.128$, $P < 0.001$, observed power = 1.00, one-way RM ANOVA) being significantly different from 0 mV at the 30 ms bin ($P < 0.001$, tukey test). The modulation of the EMG was not different between the SCI and control groups across the different time bins ($F[1,34] = 2.279$, $P = 0.140$, observed power = 0.311, Mixed RM ANOVA]. White symbols mark H-reflexes or binned EMG that are significantly different than 0% change or 0 mV EMG, respectively. * indicates a significant difference between the SCI and control group.

PAD-evoked spike in the soleus Ia afferent, which is reflected in the presence of an early reflex response in the soleus EMG (e.g., Fig. 4.2Aiii). Although the amplitude of this early reflex response was broader in participants with SCI (Fig. 4.2Bii, see statistics in legend), unlike controls none of the H-reflexes that followed this early reflex response were suppressed in the participants with SCI (i.e., no open symbols in the SCI data of Fig. 4.2Bi). Although the average age of the participants with SCI was older than the controls (see values in "Participants" in Methods), there was no correlation between the amount of H-reflex suppression at the 30 ms ISI and the age of the participant in both the control ($r = -0.05$) or SCI group ($r = 0.07$, both $P > 0.05$, Pearson Product Moment Correlation, not shown). Therefore, the older age of the participants with SCI likely did not contribute to the reduced H-reflex suppression compared to the younger control group.

We next stimulated the CPN at 1.5 x MT to examine the effects of a stronger conditioning intensity on the suppression of the soleus H-reflex (Fig. 4.3). Although the

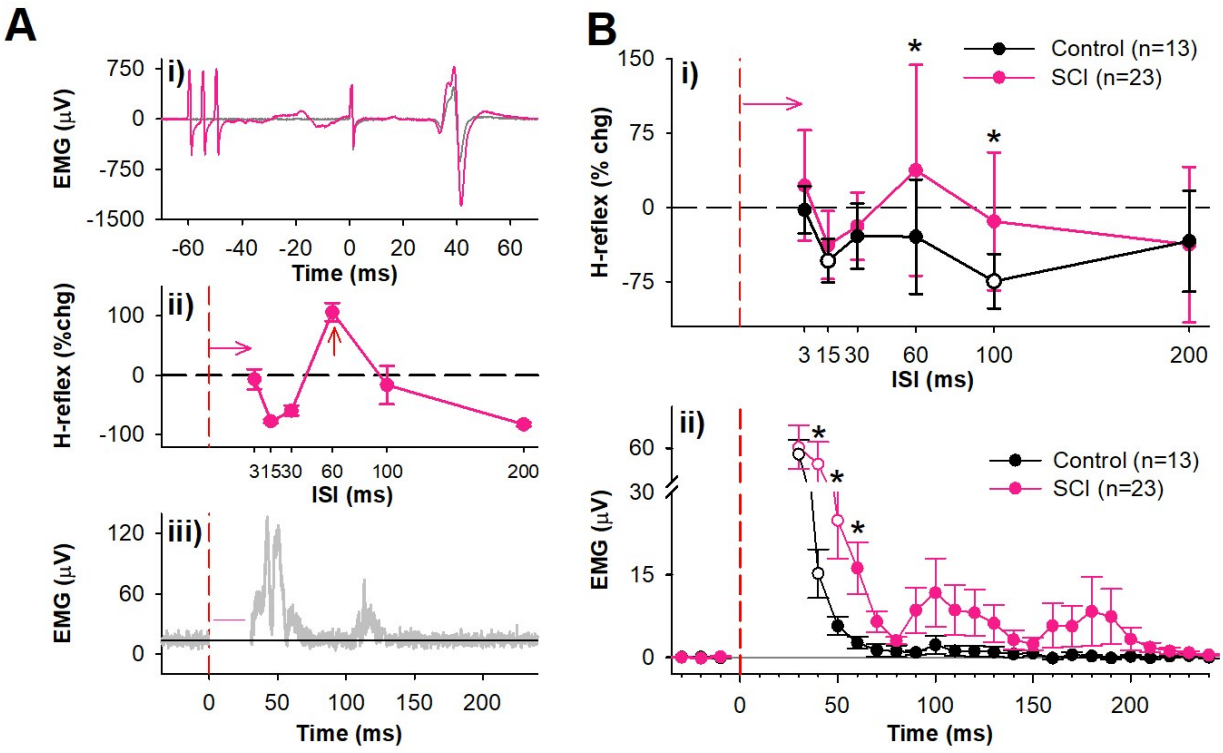

Figure 4.3: Conditioning soleus H-reflex by 1.5 x MT CPN stimulation at short ISIs. Same format as Figure 2 but with a 1.5 x MT CPN conditioning stimulation. **A)** Data from representative participant with SCI showing test and conditioned H-reflex at 60 ms ISI **(i)**, % change in conditioned H-reflex across all ISIs **(ii)** and rectified soleus EMG from CPN stimulation alone **(iii)**. **B)** Group data. **i)** Mean (±SD) % change of the soleus H-reflex averaged across the SCI (pink, n=23) and uninjured control (black, n=13) groups. The conditioned H-reflex in the SCI group was significantly different across the tested ISIs ($F[22,6] = 4.836$, $P < 0.001$, observed power = 0.965, one-way RM ANOVA); however, no ISIs were significantly different from 0 % chg ($P > 0.05$, Tukey Test). The conditioned H-reflex in the control group was significantly different across the tested ISIs ($F[12,6] = 8.765$, $P < 0.001$, observed power = 1.00, one-way RM ANOVA) being significantly different from 0% chg at the 15 ms ($P = 0.001$) and 100 ms ISIs ($P < 0.001$, Tukey Test). The modulation of the conditioned H-reflex was different between the SCI and control groups across the different ISIs ($F[1,33] = 6.576$, $P = 0.015$, observed power = 0.702, Mixed RM ANOVA], with greater H-reflex suppression in the control group at the 100 ms ISI ($P = 0.004$, pairwise comparison with Bonferroni adjustment). **ii)** The EMG in the SCI group was significantly different across the time bins ($F[22,21] = 11.062$, $P < 0.001$, observed power = 1.00, one-way RM ANOVA) being significantly different from 0 mV EMG at the 30 ($P < 0.001$), 40 ($P < 0.001$) and

50 ms bins (P = 0.015, Tukey Test). The EMG in the control group was also significantly different across the time bins (F[12,21] = 31.492, P < 0.001, observed power = 1.00, one-way RM ANOVA) being significantly different from 0 mV EMG at the 30 (P < 0.001) and 40 ms bin (P < 0.001, Tukey Test). The modulation of the EMG was not different between the SCI and control groups across the different time bins (F[1,33] = 3.847, P = 0.058, observed power = 0.478, Mixed RM ANOVA]; however, pairwise comparison did reveal a difference at the 40 (P = 0.042), 50 (P = 0.028) and 60 ms bin (P = 0.038, Bonferroni adjustment). White symbols mark H-reflexes or binned EMG that are significantly different than 0% change or 0 mV EMG, respectively. * indicates a significant difference between the SCI and uninjured control group.

higher intensity of CPN stimulation produced a larger early reflex in the participants with SCI (Fig. 4.3Bii, see legend for all statistics), the amount of H-reflex suppression was still larger in the control participants. At this higher conditioning stimulation intensity, there was significant modulation in the soleus H-reflex across all ISIs in both groups; however, only H-reflexes at the 15 and 100 ms were significantly smaller than a 0% change in the control participants (open symbols in Fig. 4.3Bi). Likewise, the amount of H-reflex suppression at the 60 and 100 ms ISIs was greater in the control participants compared to participants with SCI (* in Fig. 4.3Bi).

As proposed previously (Metz *et al.*, 2022), the early soleus reflex may reflect the activation of PAD-evoked spikes in the soleus Ia afferents by the CPN conditioning, which would then reduce subsequent H-reflexes via post-activation depression. Thus, we expect that a larger number of afferents with PAD-evoked spikes, as reflected in a larger amplitude of the early soleus reflex, would produce a larger suppression of subsequent soleus H-reflexes. In support of this, there was a significant correlation when plotting the amplitude of the early reflex EMG (between 30 and 50 ms post CPN stimulation) and the amount of soleus H-reflex suppression at the 100 ms ISI in controls (Fig. 4.4, right). A similar relationship was found for the participants with SCI but the slope of the straight line fit through the data was 2.5 times as

shallow (Fig. 4.4, left). This suggests that the early effects on the soleus Ia afferents (or motoneurons) from the CPN stimulation may have affected the suppression of the H-reflex less in participants with SCI compared to controls.

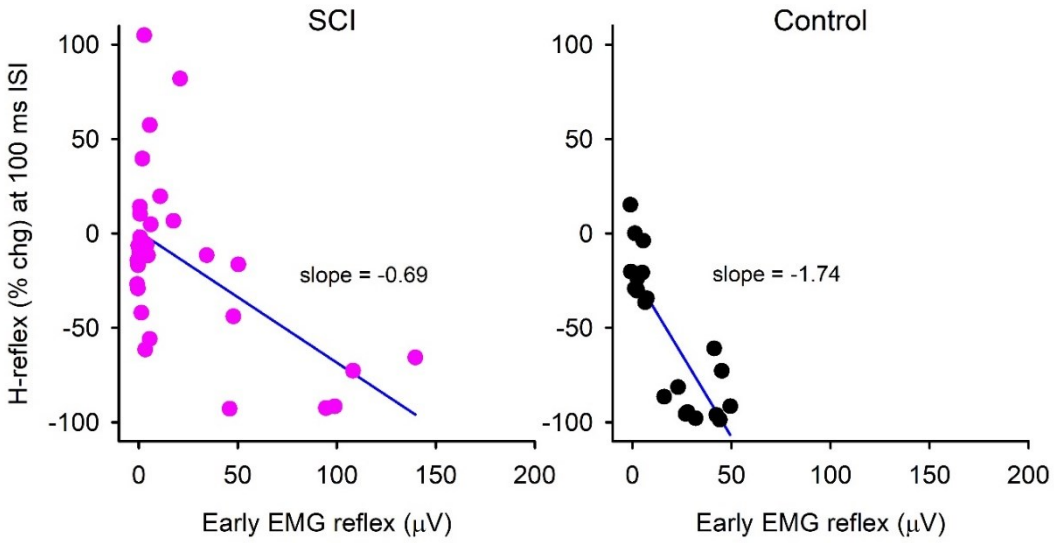

Figure 4.4. Relationship between conditioned H-reflex suppression and early reflex EMG. % change in the conditioned SOL H-reflex at the 100 ms ISI plotted against the resting soleus EMG 30-50 ms after the CPN stimulation for participants with SCI (left) and controls (right). There was a significant, negative correlation in both the SCI (r = -0.57, n = 34 data points from 20 participants, 6 early EMG points unavailable) and control (r = -0.84; n = 22 data points from 13 participants, 4 early EMG points unavailable) groups ($P < 0.001$, Pearson Product Moment Correlation). Data from the 1.0 and 1.5 x MT stimulation are combined.

Long-duration inhibition of H-reflexes by post activation depression

If the short duration inhibition of the soleus H-reflex in the control participants was mediated by post activation depression of the soleus Ia afferents, then the duration of this inhibition should last for several seconds. As previously demonstrated in Metz *et al*., 2022, H-reflexes were strongly suppressed by a 1.5 x MT CPN conditioning stimulation in controls out to 2500 ms (black, Fig. 4.5A). Interestingly, H-reflexes were also suppressed in the participants

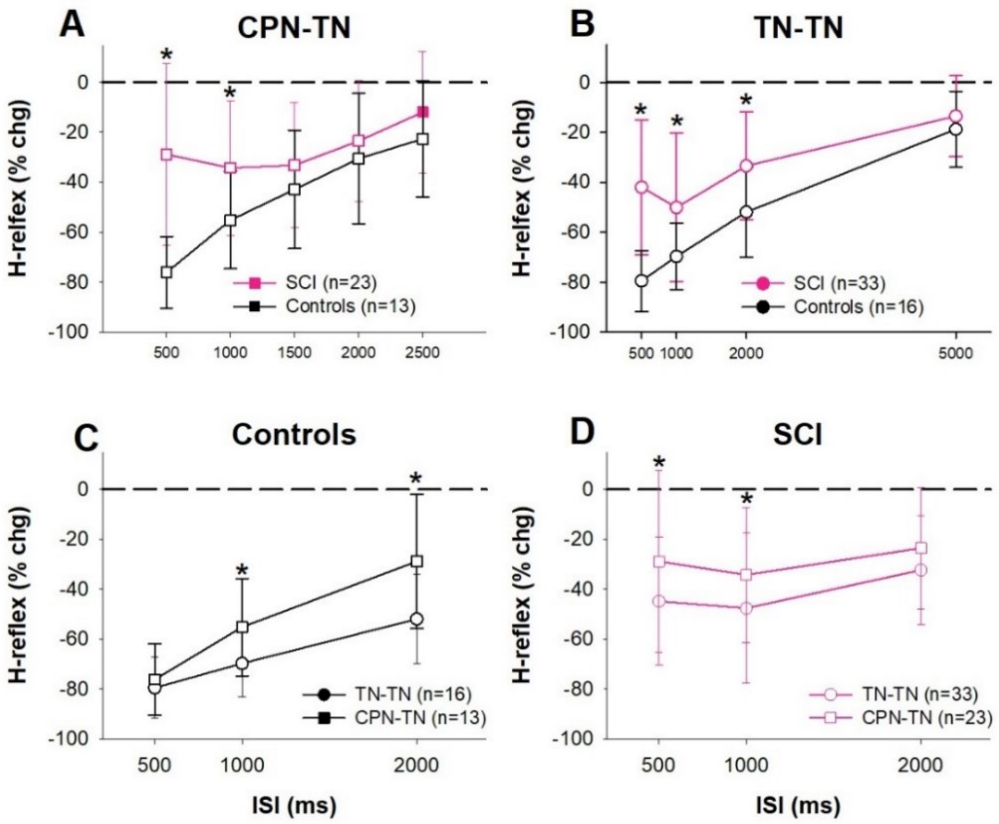

Figure 4.5: Long-lasting soleus H-reflex inhibition. A) Mean (±SD) % change of soleus H-reflexes from a 1.5 x MT CPN conditioning stimulation (CPN-TN) in the SCI (pink, n=23) and control (black, n=13) groups plotted as a function of ISI. There was an effect of ISI on the conditioned H-reflex in the SCI group ($F(22, 5) = 10.965$, $P < 0.001$, observed power = 1.00) and control group ($F(12, 5) = 55.697$, $P < 0.001$, observed power = 1.00, both one-way RM ANOVA) with the conditioned H-reflex smaller than a 0% change between 500 and 2000 ms in the SCI group and at all ISIs in the control group ($P < 0.05$, Tukey Test). The modulation of the conditioned H-reflex was different between the SCI and control groups across the different ISIs ($F(1, 34) = 6.978$, $P = 0.012$, observed power = 0.728), with greater H-reflex suppression in the control group at the 500 ($P < 0.001$) and 1000 ms ISI ($P = 0.020$, pairwise comparison with Bonferroni adjustment). **B)** Mean (±SD) % change of soleus H-reflex from repetitive TN stimulation (TN-TN or RDD) in the SCI (n=33) and control (n=16) group plotted as a function of ISI. There was an effect of ISI on the conditioned H-reflex in the SCI group ($F(32, 5) = 44.999$, $P < 0.001$, observed power = 1.000) and control group ($F(15, 4) = 200.877$, $P < 0.001$, observed power = 1.000) with conditioned H-reflexes smaller than a 0% change at all ISIs in both groups ($P < 0.05$, Tukey Test). The modulation of the conditioned H-reflex was different between the SCI and control groups across the different ISIs ($F(1,47) = 11.365$, $P = 0.002$, observed power = 0.910, mixed RM ANOVA), with greater H-reflex

suppression in the control group at the 500 ($P < 0.001$), 1000 ($P = 0.016$) and 2000 ms ISI ($P = 0.001$, pairwise comparison with Bonferroni adjustment). **C & D)** Same data as A and B but plotted to compare CPN conditioning and RDD within each group. **C)** In the control group, the H-reflex modulation across the tested ISIs was different between the CPN-TN and TN-TN conditions ($F(1, 27) = 5.246$, $P = 0.030$, observed power = 0.598, mixed RM ANOVA), with greater suppression in the TN-TN condition at 100 ms ($P = 0.025$) and 2000 ms ISI ($P = 0.015$, pairwise comparison with Bonferroni adjustment). **D)** In the SCI group, the H-reflex modulation across the tested ISIs was also different between the CPN-TN and TN-TN conditions ($F(1, 54) = 4.004$, $P = 0.05$, observed power = 0.502, mixed RM ANOVA), with greater H-reflex suppression in the TN-TN condition at the 500 ($P = 0.037$) and 1000 ms ISIs ($P = 0.047$, pairwise comparison with Bonferroni adjustment). White symbols mark H-reflexes that are significantly different than a 0% change. * indicates a significant difference between groups.

with SCI but only out to the 2000 ms ISI with less suppression compared to the control group at the 500 and 1000 ms ISIs (see statistics in legend). In line with the long-lasting H-reflex being suppressed by post activation depression in the soleus Ia afferents, a similar pattern of H-reflex suppression was produced during RDD when the soleus Ia afferents were directly activated by repeated TN stimulation at similar ISIs (Fig. 4.5B). Again, the amount of H-reflex suppression during RDD was less in participants with SCI at the 500, 1000 and 2000 ms ISIs compared to controls, consistent with previously published findings (Aymard *et al.*, 2000; Schindler-Ivens & Shields, 2000; Kumru *et al.*, 2015), but in contrast to Hofstoetter *et al*., 2019. In both the controls and participants with SCI, H-reflex suppression was larger during repeated TN stimulation (RDD) compared to the CPN conditioning (Figs. 4.5C and D).

Long-duration facilitation of H-reflexes during tonic PAD

When a conditioning afferent stimulation does not produce a PAD-evoked spike in the test Ia afferent, subsequent H-reflexes are facilitated rather than inhibited by PAD, potentially

due to the facilitation of sodium channels in the Ia afferent nodes and thus, action potential conduction (Hari *et al.*, 2021; Metz *et al.*, 2021; Metz *et al.*, 2022). As shown previously in controls (Metz *et al.*, 2021), a high frequency (200 Hz), long-duration (500 ms) of low-intensity (4 mA) stimulation to the cutaneous branch of the deep peroneal nerve (cDPN), that itself produces minor to no effects in the soleus EMG, can produce facilitation of soleus H-reflexes that lasts for minutes (black, Fig. 4.6A), with the H-reflex facilitated at many time points after the cDPN conditioning (open symbols in Fig. 4.6B, see legend for statistics). This long-lasting facilitation is thought to be mediated by the fast train of cDPN stimulation producing GABA spillover and activation of $\alpha 5GABA_A$ receptors and tonic PAD in the soleus Ia afferents. The same cDPN stimulation also produced an increase in the H-reflex across all time points in the participants with SCI but was smaller and with no time point having an H-reflex larger than a 0% change (pink Fig. 4.6Ai, all closed symbols in Fig. 4.6B). Likewise, post-hoc analysis revealed that the amount of H-reflex suppression was significantly smaller in the participants with SCI compared to controls at many time points over the first 1.5 minutes post-conditioning (* in Fig. 4.6B). As we discuss below, a lack of H-reflex facilitation by PAD networks may have occurred because Ia conduction in chronic SCI is already overly secure so that further enhancement by nodal facilitation from PAD has a smaller effect.

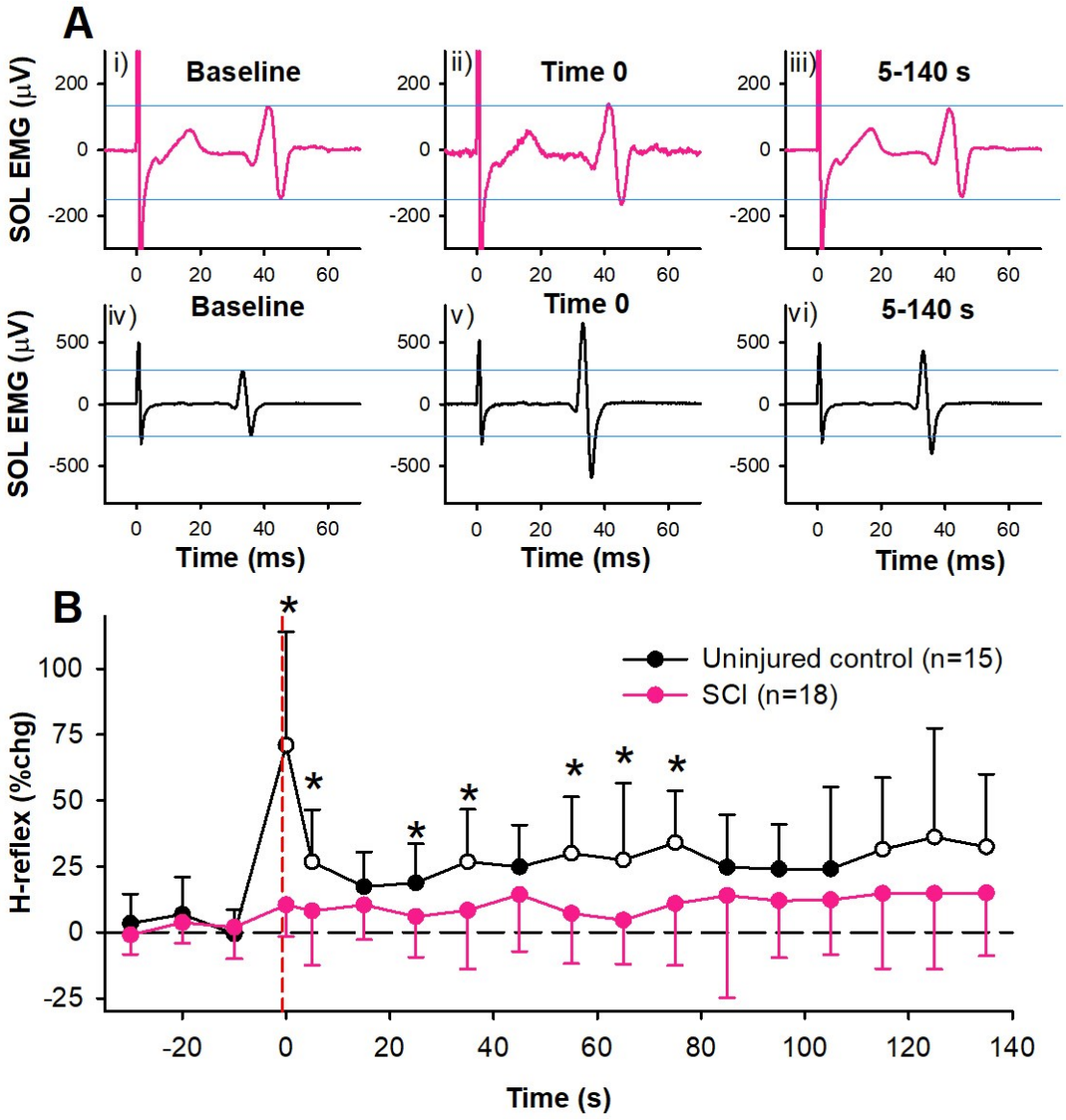

Figure 4.6: H-reflex facilitation during tonic PAD. A) Average soleus H-reflex (unrectified EMG) before (**i**, n = 7 H-reflexes), immediately after (**ii**, n = 1 H-reflex) and 5-140 seconds (**iii**, n = 27 H-reflexes) after a train (200 Hz, 500 ms, 4.0 mA) of cDPN stimulation in a participant with SCI (pink lines). Same data in iv, v and vii for a control (black lines) participant. Blue lines mark the peak-peak amplitude of the average baseline H-reflex. **B)** Average % soleus H-reflex compared to the average of 7 test H-reflexes immediately preceding the cDPN conditioning stimulation (vertical red dashed line) for the SCI (pink, n=18) and uninjured control (black, n=15) groups. In each participant, H-reflexes were averaged into 10-second bins (3 trials with 2 H's per bin = 6 H's per bin) and then averaged across participants. H-reflexes varied in the control group ($F(14, 18) = 9.416$, $P < 0.001$, observed power = 1.000) and SCI group ($F(17, 18) = 2.167$, $P = 0.004$, observed

power = 0.799) across the tested time points (one-way RM ANOVA). The increase in H-reflexes was greater than 0 % at multiple time points in the control group only (marked by open circles, $P < 0.05$, Tukey test). The H-reflex was different between the SCI and control group ($F(1,30) = 47.728$, $P = 0.007$, observed power = 0.807, mixed ANOVA) at multiple time points (marked by *, $P < 0.05$, multiple pairwise comparisons with Bonferroni adjustment). There was no increase in soleus EMG 30 to 50 ms after the cDPN stimulation in the control (0.3 ± 0.7 μV, $P = 0.33$) or SCI group (0.7 ± 2.3 μV, $P = 0.07$), not shown.

Discussion

Following SCI there are complex changes in spinal GABA neurons below the injury given their dependence on sensorimotor activity (Mende *et al.*, 2016). Although the number of GABA interneurons with axo-axonic connections to Ia afferents ($GABA_{axo}$) that release *synaptic* GABA (GAD2) does not appear to change after SCI, the number of their boutons innervating Ia afferent terminals appears to decrease (Kapitza *et al.*, 2012; Smith *et al.*, 2017; Khalki *et al.*, 2018), potentially from a lack of activity dependent release of BDNF and glutamate from sensory afferents (Mende *et al.*, 2016). This decrease in synaptic GABA to Ia afferent terminals, and the decreased excitability of phasic PAD measured in dorsal roots (Caron *et al.*, 2020), was thought to decrease presynaptic inhibition of the Ia afferent after SCI and the suppression of MSRs by PAD (Caron *et al.*, 2020). However, the recent finding that PAD does not produce presynaptic inhibition (Hari *et al.*, 2021) puts this mechanism into question and we propose here that the reduced suppression of H-reflexes is instead mediated by a reduced PAD-evoked post activation depression of the Ia-motoneuron synapse. Moreover, other studies report that after SCI there is an upregulation of the enzyme GAD67 (encoded by the GAD1 gene) that produces *extra-synaptic* GABA (Tillakaratne *et al.*, 2000; Russ *et al.*, 2013) and decreased RNA for the ventral GABA transporters (GAT1 and GAT3) (Tachibana *et al.*, 2002; Ryge *et al.*, 2010). These activity changes may culminate to increase the continual activation of extra-synaptic $\alpha5GABA_A$ receptors and tonic PAD in Ia afferents, to ultimately produce continual and secure action potential conduction after SCI (Lucas-Osma *et al.*, 2018; Hari *et al.*, 2021). As we discuss below, the reduced long-lasting facilitation of H-reflexes by cutaneous inputs that readily activate tonic PAD may be an indication that Ia afferent conduction is maximally facilitated after SCI and thus,

not as well modulated by descending, sensory and locomotor inputs to help control the properly timed activation of spinal networks during movement.

Suppression of H-reflexes by post activation depression of the Ia afferents mediating the H-reflex.

If suppression of the soleus H-reflex from flexor afferent conditioning is not produced by activation of $GABA_A$ receptors and PAD at the Ia afferent terminal, what then is mediating this inhibition in controls and why is it reduced following SCI? We have recently shown that suppression of monosynaptic reflexes (MSRs) in animals or H-reflexes in humans by a conditioning afferent stimulation is in large part due to post activation depression. Post-activation depression is produced by a prior activation of the same EPSP, where the first and second EPSPs are evoked by the same Ia afferent population. We demonstrated that a conditioning heteronymous or antagonist afferent stimulation could evoke a rapidly rising PAD in the test (agonist) Ia afferents that triggers orthodromic action potentials that travel down to the afferent terminal, as evidenced by their monosynaptic activation of the test motoneurons (Eccles *et al.*, 1961b; Duchen, 1986; Willis, 1999; Metz *et al.*, 2022). These PAD-evoked spike(s) activated in the Ia afferent terminal suppressed synaptic transmission via post activation depression and when these same afferents were subsequently activated by a direct stimulation to the test nerve, the size of the test MSRs or H-reflexes were reduced. Support for the suppression of the MSR or H-reflex being mediated by post-activation depression of the test Ia afferent terminal was demonstrated by its dependance on the presence of a PAD-evoked spike in the test Ia afferent or the resulting activation of a short-latency EPSP in the test

motoneurons and by the long duration suppression of the MSR or H-reflex, out to 2.5 seconds, which fits with the time course of post activation depression. Similar to these findings in rodents and uninjured control participants, in this study H-reflex suppression by antagonist afferent conditioning in participants with SCI was also related to an early reflex response in the test soleus muscle and the duration of this H-reflex suppression lasted for many seconds, suggesting that post activation depression also mediated the H-reflex suppression in chronic SCI, although to a lesser extent as discussed below.

Mechanisms producing post activation depression and its possible reduction in chronic SCI.

Although not well studied for Ia afferents in the spinal cord, there are three potential mechanisms that we know of for post activation depression of a repetitively activated Ia-motoneuron synapse. First, an action potential at the Ia afferent terminal may deplete transmitter packaging and release from the Ia synapse and account for the early period of H-reflex suppression (< 500 ms) given that the recovery time constant from maximal transmitter depletion is around 300-400 ms, as measured in the large glutaminergic synapses in the Calx of Held (Neher & Sakaba, 2001). It may be that after SCI, mechanisms involved in reducing transmitter packaging following the invasion of an action potential in the terminal are down regulated, although it is difficult to speculate without isolated recordings from spinal Ia afferent synapses. Secondly, the refractory period of the Ia afferent afterhyperpolarization (AHP) would also make it susceptible to failure for very fast repeated activation, but this likely only occurs for repetition rates near 10 ms, well short of the ISI intervals that produced H-reflex inhibition. Moreover, there was no H-reflex inhibition observed at the fast 3 ms ISI in both controls and participants with SCI, making AHP refractoriness an unlikely mechanism. Third, post activation depression

may be produced if the test afferents that were activated by the PAD-evoked spike in turn activated $GABA_{axo}$ interneurons that synapse back onto the terminals of the test afferents themselves (see Fig. 11 in Metz *et al*., 2022). A self-feedback release of GABA onto the same Ia afferent terminals would likely activate $GABA_B$ receptors that are present in large numbers compared to the $GABA_A$ receptors on the Ia afferent terminal (Hari *et al.*, 2021). Activation of $GABA_B$ receptors produces presynaptic inhibition of Ia afferents by inhibiting voltage dependent calcium channels on the presynaptic boutons to reduce the calcium-dependent exocytosis of neurotransmitter following the arrival of an action potential at the afferent terminal (Curtis & Lacey, 1994; Curtis *et al.*, 1997; Howell & Pugh, 2016). The time course of the $GABA_B$ receptor mediated inhibition, which can last for several seconds (Eccles *et al.*, 1961a; Kangrga *et al.*, 1991; Curtis & Lacey, 1994, 1998; Yang *et al.*, 2001), fits with the long-lasting duration of H-reflex suppression for both the antagonist (CPN) and direct (TN) conditioning of the soleus Ia afferents. Thus, activation of soleus Ia afferents, either from a PAD-evoked spike during CPN conditioning or from direct TN stimulation during RDD, could in theory activate $GABA_{axo}$ interneurons that project back onto the soleus afferent terminal to inhibit further neurotransmitter release, and H-reflex suppression, for several seconds. As mentioned above, projections of GABA neurons to Ia afferent terminals are reduced after SCI (Kapitza *et al.*, 2012; Khalki *et al.*, 2018), potentially resulting in a reduced activation of $GABA_B$ receptors to subsequently reduce post activation depression and suppression of H-reflexes. Interestingly, the $\alpha5$ $GABA_A$ receptor inverse agonist L655,708, which reduces PAD-evoked Ia spikes and likely the post activation depression they mediate (Metz *et al.*, 2022), also reduces RDD (Delgado-Lezama *et al.*, 2021). Likewise, application of the $GABA_B$ receptor antagonist CGP55845 also reduces post activation depression from RDD, potentially reducing the feedback activation of $GABA_B$ receptors on the

test Ia afferents (Fink, 2013). Further work examining this putative self-feedback GABA loop onto the Ia afferent terminal and its effects on conditioning MSRs and H-reflexes with and without SCI are needed.

In addition to the weaker post activation depression of the Ia-motoneuron synapse, a potentially larger direct excitation of the soleus motoneurons by the conditioning stimulation in participants with SCI, especially at the 1.5 x MT CPN intensity (Fig. 4.3Bii), may have further masked the weakened post activation depression of the Ia afferents to reduce overall H-reflex suppression at the earlier ISIs where postsynaptic effects could have an effect (< 500 ms). This larger postsynaptic activation may have come from a larger number of PAD-evoked soleus Ia spikes given that the number of dorsal root reflexes (DRRs) from GAD2 photoactivation appears to be increased in chronic SCI (Hari and Bennett personal communication). Alternatively, there may be a larger direct postsynaptic activation from the antagonist CPN conditioning stimulation due to reductions in reciprocal inhibition after SCI (Crone *et al.*, 1994; Crone *et al.*, 2003), enhanced sensory excitation of interneurons (Garcia-Ramirez *et al.*, 2014; Bellardita *et al.*, 2017) or reduced inhibitory currents in the MN (Norton *et al.*, 2008; Boulenguez *et al.*, 2010; Murray *et al.*, 2011). However, these postsynaptic effects cannot explain the reduced H-reflex suppression at the longer time points (> 500 ms) given that effects on the motoneuron from CPN or TN stimulation would have subsided by then.

Long-lasting facilitation of H-reflexes during tonic PAD

As described in the Introduction, when a conditioning stimulation does *not* produce PAD-evoked spikes in the test Ia afferents, conduction of Ia afferents is increased due to PAD depolarizing the afferent nodes and reducing downstream branchpoint failure (Lucas-Osma *et*

al., 2018; Hari *et al.*, 2021; Metz *et al.*, 2021). For example, a conditioning train of low-intensity, high frequency cutaneous stimulation can evoke a tonic PAD in Ia afferents that is mediated by extra-synaptic α5 $GABA_A$-receptors which lasts for several minutes (Lucas-Osma *et al.*, 2018; Hari *et al.*, 2021). As demonstrated in rodents and humans, this long-lasting PAD is reflected in the long-lasting facilitation of MSR and H-reflexes, respectively, and outlasts any direct depolarization of the motoneuron from the conditioning stimulation applied alone (Lucas-Osma *et al.*, 2018; Hari *et al.*, 2021; Metz *et al.*, 2021). However, we observed in this study that this long-lasting facilitation was reduced in participants with SCI compared to controls. This reduced facilitation may indicate that tonic PAD is reduced after SCI, potentially as a result of $GABA_{axo}$ interneuron loss within the dorsal horn that is related to the development of neuropathic pain after SCI (Meisner *et al.*, 2010). Alternatively, tonic PAD in Ia afferents may be constantly active after SCI to ensure secure conduction of sensory axons below the injury to facilitate activation of spinal circuits and motoneurons by sensory pathways and thus, not amenable to further facilitation. To support this idea, preliminary results suggest that like 5HT 2B/C receptors (Murray *et al.*, 2011), α5 $GABA_A$-receptors may become constitutively active after SCI to produce a basal level of tonic PAD [Hari and Bennett preliminary findings; see also (McCartney *et al.*, 2007; Wang *et al.*, 2008; O'Neill & Sylantyev, 2019)]. This was demonstrated by a larger hyperpolarization of Ia afferents following the application of the α5 $GABA_A$-receptor inverse agonist L655,708 in chronically injured mice compared to acutely injured mice. Likewise, there may be excessive extrasynaptic GABA due to an upregulation of the enzyme GAD67 (encoded by the GAD1 gene) (Tillakaratne *et al.*, 2000; Russ *et al.*, 2013) and/or decreased RNA for the ventral GABA transporters (GAT1 and GAT3) (Tachibana *et al.*, 2002; Ryge *et al.*, 2010) after chronic SCI. If Ia afferents after SCI have a basal level of α5 $GABA_A$-receptor activity and tonic

PAD, there may be little-to-no branch point failure and any further increase in extra-synaptic GABA by a cutaneous afferent stimulation train may not have any effect. Alternatively (or in addition), other forms of PAD activated by NMDA (Zimmerman *et al.*, 2019) or nicotinic receptors (Shreckengost *et al.*, 2010) that are less sensitive to cutaneous facilitation may predominate after SCI (Hari and Bennett preliminary findings).

Conclusion and functional implications

Previous studies examining presynaptic inhibition after neurotrauma have concluded that excessive activation of the spinal cord by Ia afferents in spasticity is produced by a reduction of $GABA_A$ receptor mediated PAD at the Ia afferent terminal including SCI (Ashby & Verrier, 1975; Mailis & Ashby, 1990; Roby-Brami & Bussel, 1990; Azouvi *et al.*, 1993; Calancie *et al.*, 1993; Faist *et al.*, 1994; Caron *et al.*, 2020), cerebral palsy (Mizuno *et al.*, 1971; Achache *et al.*, 2010), brain injury (Koelman *et al.*, 1993; Faist *et al.*, 1994), stroke (Milanov, 1992; Koelman *et al.*, 1993) and multiple sclerosis (Azouvi *et al.*, 1993; Koelman *et al.*, 1993; Nielsen *et al.*, 1995). Here we provide an alternative interpretation of the SCI data where reduced suppression of Ia afferent transmission by PAD is a result of reduced post activation depression, potentially mediated by a reduced feedback activation of $GABA_B$ receptors on the Ia afferent terminal (Lucas-Osma *et al.*, 2018; Hari *et al.*, 2021; Metz *et al.*, 2021; Metz *et al.*, 2022). Thus, further studies examining this potential feedback pathway and changes in GABAergic inputs to the Ia terminal and its density of $GABA_B$ receptors are needed to better understand the dysregulation of Ia afferent transmission after SCI.

Along with reduced post activation depression at the Ia afferent terminal, a large and continual activation of PAD that is less responsive to movement-initiated sensory, descending

and/or locomotor inputs would reduce the modulation of Ia afferent conduction and its properly timed facilitation of ongoing movement (Fink *et al.*, 2014; Mayer *et al.*, 2018). These are important considerations given that emerging techniques like epidural and transcutaneous spinal cord stimulation appear to rely on the phasic recruitment of sensory pathways to activate spinal networks involved in standing and walking (Harkema *et al.*, 2011; Gerasimenko *et al.*, 2015; Rowald *et al.*, 2022). Thus, treatments that reduce tonic PAD after SCI may help to restore modulated sensory feedback to facilitate movement. Reducing tonic PAD with the inverse agonist to the extrasynaptic $\alpha5$ $GABA_A$ receptor, L655,708, is a promising therapy because it would suppress tonic PAD and excessive Ia afferent conduction to reduce spasticity (Lucas-Osma *et al.*, 2018; Hari *et al.*, 2021) and at the same time, disinhibit postsynaptic neurons to facilitate spared motor pathways (Loeza-Alcocer *et al.*, 2013; Canto-Bustos *et al.*, 2017). In support of this the inverse agonist to the $\alpha5$ $GABA_A$ receptor, L655,708, has a dual effect in reducing extensor muscle spasms and promoting plantar stepping in both incomplete and completely injured rats and mice (Hari and Bennett preliminary results) and may hold promise in humans with SCI as previously tested for the neutral antagonist S44819 in human trials (Darmani *et al.*, 2016; Chabriat *et al.*, 2020).

References

Achache V, Roche N, Lamy JC, Boakye M, Lackmy A, Gastal A, Quentin V & Katz R. (2010). Transmission within several spinal pathways in adults with cerebral palsy. *Brain* **133,** 1470-1483.

Ashby P & Verrier M. (1975). Neurophysiological changes following spinal cord lesions in man. *Can J Neurol Sci* **2,** 91-100.

Aymard C, Katz R, Lafitte C, Lo E, Penicaud A, Pradat-Diehl P & Raoul S. (2000). Presynaptic inhibition and homosynaptic depression: a comparison between lower and upper limbs in normal human subjects and patients with hemiplegia. *Brain* **123 (Pt 8),** 1688-1702.

Azouvi P, Roby-Brami A, Biraben A, Thiebaut JB, Thurel C & Bussel B. (1993). Effect of intrathecal baclofen on the monosynaptic reflex in humans: evidence for a postsynaptic action. *J Neurol Neurosurg Psychiatry* **56,** 515-519.

Bellardita C, Caggiano V, Leiras R, Caldeira V, Fuchs A, Bouvier J, Low P & Kiehn O. (2017). Spatiotemporal correlation of spinal network dynamics underlying spasms in chronic spinalized mice. *Elife* **6**.

Boulenguez P, Liabeuf S, Bos R, Bras H, Jean-Xavier C, Brocard C, Stil A, Darbon P, Cattaert D, Delpire E, Marsala M & Vinay L. (2010). Down-regulation of the potassium-chloride cotransporter KCC2 contributes to spasticity after spinal cord injury. *Nat Med* **16,** 302-307.

Calancie B, Broton JG, Klose KJ, Traad M, Difini J & Ayyar DR. (1993). Evidence that alterations in presynaptic inhibition contribute to segmental hypo- and hyperexcitability after spinal cord injury in man. *Electroencephalogr Clin Neurophysiol* **89,** 177-186.

Canto-Bustos M, Loeza-Alcocer E, Cuellar CA, Osuna P, Elias-Vinas D, Granados-Soto V, Manjarrez E, Felix R & Delgado-Lezama R. (2017). Tonically Active alpha5GABAA Receptors Reduce Motoneuron Excitability and Decrease the Monosynaptic Reflex. *Front Cell Neurosci* **11,** 283.

Capaday C, Lavoie BA & Comeau F. (1995). Differential effects of a flexor nerve input on the human soleus H-reflex during standing versus walking. *Can J Physiol Pharmacol* **73,** 436-449.

Caron G, Bilchak JN & Cote MP. (2020). Direct evidence for decreased presynaptic inhibition evoked by PBSt group I muscle afferents after chronic SCI and recovery with step-training in rats. *J Physiol*.

Chabriat H, Bassetti CL, Marx U, Picarel-Blanchot F, Sors A, Gruget C, Saba B, Wattez M, Audoli ML & Hermann DM. (2020). Randomized Efficacy and Safety Trial with Oral S 44819 after Recent ischemic cerebral Event (RESTORE BRAIN study): a placebo controlled phase II study. *Trials* **21,** 136.

Crone C, Johnsen LL, Biering-Sorensen F & Nielsen JB. (2003). Appearance of reciprocal facilitation of ankle extensors from ankle flexors in patients with stroke or spinal cord injury. *Brain* **126,** 495-507.

Crone C, Nielsen J, Petersen N, Ballegaard M & Hultborn H. (1994). Disynaptic reciprocal inhibition of ankle extensors in spastic patients. *Brain* **117 (Pt 5),** 1161-1168.

Curtis DR, Gynther BD, Lacey G & Beattie DT. (1997). Baclofen: reduction of presynaptic calcium influx in the cat spinal cord in vivo. *Exp Brain Res* **113,** 520-533.

Curtis DR & Lacey G. (1994). GABA-B receptor-mediated spinal inhibition. *Neuroreport* **5,** 540-542.

Curtis DR & Lacey G. (1998). Prolonged GABA(B) receptor-mediated synaptic inhibition in the cat spinal cord: an in vivo study. *Exp Brain Res* **121,** 319-333.

Darmani G, Zipser CM, Bohmer GM, Deschet K, Muller-Dahlhaus F, Belardinelli P, Schwab M & Ziemann U. (2016). Effects of the Selective alpha5-GABAAR Antagonist S44819 on Excitability in the Human Brain: A TMS-EMG and TMS-EEG Phase I Study. *J Neurosci* **36,** 12312-12320.

Delgado-Lezama R, Bravo-Hernandez M, Franco-Enzastiga U, De la Luz-Cuellar YE, Alvarado-Cervantes NS, Raya-Tafolla G, Martinez-Zaldivar LA, Vargas-Parada A, Rodriguez-

Palma EJ, Vidal-Cantu GC, Guzman-Priego CG, Torres-Lopez JE, Murbartian J, Felix R & Granados-Soto V. (2021). The role of spinal cord extrasynaptic alpha5 GABAA receptors in chronic pain. *Physiol Rep* **9,** e14984.

Duchen MR. (1986). Excitation of mouse motoneurones by GABA-mediated primary afferent depolarization. *Brain Res* **379,** 182-187.

Eccles JC, Eccles RM & Magni F. (1961a). Central inhibitory action attributable to presynaptic depolarization produced by muscle afferent volleys. *J Physiol* **159,** 147-166.

Eccles JC, Kozak W & Magni F. (1961b). Dorsal root reflexes of muscle group I afferent fibres. *J Physiol* **159,** 128-146.

Eccles JC, Magni F & Willis WD. (1962). Depolarization of central terminals of Group I afferent fibres from muscle. *The Journal of physiology* **160,** 62-93.

El-Tohamy A & Sedgwick EM. (1983). Spinal inhibition in man: depression of the soleus H reflex by stimulation of the nerve to the antagonist muscle. *J Physiol* **337,** 497-508.

Faist M, Mazevet D, Dietz V & Pierrot-Deseilligny E. (1994). A quantitative assessment of presynaptic inhibition of Ia afferents in spastics. Differences in hemiplegics and paraplegics. *Brain* **117 (Pt 6),** 1449-1455.

Fink AJ. (2013). Exploring a behavioural role for presynaptic inhibition in spinal sensory-motor synapses. *PhD Thesis, Columbia University***,** 1-293.

Fink AJ, Croce KR, Huang ZJ, Abbott LF, Jessell TM & Azim E. (2014). Presynaptic inhibition of spinal sensory feedback ensures smooth movement. *Nature* **509,** 43-48.

Gallagher JP, Higashi H & Nishi S. (1978). Characterization and ionic basis of GABA-induced depolarizations recorded in vitro from cat primary afferent neurones. *The Journal of physiology* **275,** 263-282.

Garcia-Ramirez DL, Calvo JR, Hochman S & Quevedo JN. (2014). Serotonin, dopamine and noradrenaline adjust actions of myelinated afferents via modulation of presynaptic inhibition in the mouse spinal cord. *PLoS One* **9,** e89999.

Gerasimenko YP, Lu DC, Modaber M, Zdunowski S, Gad P, Sayenko DG, Morikawa E, Haakana P, Ferguson AR, Roy RR & Edgerton VR. (2015). Noninvasive Reactivation of Motor Descending Control after Paralysis. *J Neurotrauma* **32,** 1968-1980.

Grey MJ, Klinge K, Crone C, Lorentzen J, Biering-Sorensen F, Ravnborg M & Nielsen JB. (2008). Post-activation depression of soleus stretch reflexes in healthy and spastic humans. *Exp Brain Res* **185,** 189-197.

Hancock J, Knowles L & Gillies JD. (1973). Segmental reflex changes in acute and chronic spinal cats. *Proc Aust Assoc Neurol* **10,** 139-143.

Hari K, Lucas-Osma AM, Metz K, Lin S, Pardell N, Roszko D, Black S, Minarik A, Singla R, Stephens MJ, Fouad K, Jones KE, Gorassini M, Fenrich KK, Li Y & Bennett DJ. (2021). Nodal GABA facilitates axon spike transmission in the spinal cord. *BioRxiv*.

Harkema S, Gerasimenko Y, Hodes J, Burdick J, Angeli C, Chen Y, Ferreira C, Willhite A, Rejc E, Grossman RG & Edgerton VR. (2011). Effect of epidural stimulation of the lumbosacral spinal cord on voluntary movement, standing, and assisted stepping after motor complete paraplegia: a case study. *Lancet* **377,** 1938-1947.

Hofstoetter US, Freundl B, Binder H & Minassian K. (2019). Recovery cycles of posterior root-muscle reflexes evoked by transcutaneous spinal cord stimulation and of the H reflex in individuals with intact and injured spinal cord. *PLoS One* **14,** e0227057.

Howell RD & Pugh JR. (2016). Biphasic modulation of parallel fibre synaptic transmission by co-activation of presynaptic GABAA and GABAB receptors in mice. *J Physiol* **594,** 3651-3666.

Hultborn H. (2006). Spinal reflexes, mechanisms and concepts: from Eccles to Lundberg and beyond. *Prog Neurobiol* **78,** 215-232.

Hultborn H, Illert M, Nielsen J, Paul A, Ballegaard M & Wiese H. (1996). On the mechanism of the post-activation depression of the H-reflex in human subjects. *Experimental brain research* **108,** 450-462.

Kagamihara Y & Masakado Y. (2005). Excitability of spinal inhibitory circuits in patients with spasticity. *J Clin Neurophysiol* **22,** 136-147.

Kangrga I, Jiang MC & Randic M. (1991). Actions of (-)-baclofen on rat dorsal horn neurons. *Brain Res* **562,** 265-275.

Kapitza S, Zorner B, Weinmann O, Bolliger M, Filli L, Dietz V & Schwab ME. (2012). Tail spasms in rat spinal cord injury: changes in interneuronal connectivity. *Exp Neurol* **236,** 179-189.

Khalki L, Sadlaoud K, Lerond J, Coq JO, Brezun JM, Vinay L, Coulon P & Bras H. (2018). Changes in innervation of lumbar motoneurons and organization of premotor network following training of transected adult rats. *Exp Neurol* **299,** 1-14.

Knikou M & Mummidisetty CK. (2014). Locomotor training improves premotoneuronal control after chronic spinal cord injury. *J Neurophysiol* **111,** 2264-2275.

Koelman JH, Bour LJ, Hilgevoord AA, van Bruggen GJ & Ongerboer de Visser BW. (1993). Soleus H-reflex tests and clinical signs of the upper motor neuron syndrome. *J Neurol Neurosurg Psychiatry* **56,** 776-781.

Kumru H, Albu S, Valls-Sole J, Murillo N, Tormos JM & Vidal J. (2015). Influence of spinal cord lesion level and severity on H-reflex excitability and recovery curve. *Muscle Nerve* **52,** 616-622.

Loeza-Alcocer E, Canto-Bustos M, Aguilar J, Gonzalez-Ramirez R, Felix R & Delgado-Lezama R. (2013). alpha(5)GABA(A) receptors mediate primary afferent fiber tonic excitability in the turtle spinal cord. *J Neurophysiol* **110,** 2175-2184.

Lucas-Osma AM, Li Y, Lin S, Black S, Singla R, Fouad K, Fenrich KK & Bennett DJ. (2018). Extrasynaptic proportional, variant5GABAA receptors on proprioceptive afferents produce a tonic depolarization that modulates sodium channel function in the rat spinal cord. *J Neurophysiol*.

Mailis A & Ashby P. (1990). Alterations in group Ia projections to motoneurons following spinal lesions in humans. *J Neurophysiol* **64,** 637-647.

Mayer WP, Murray AJ, Brenner-Morton S, Jessell TM, Tourtellotte WG & Akay T. (2018). Role of muscle spindle feedback in regulating muscle activity strength during walking at different speed in mice. *J Neurophysiol* **120,** 2484-2497.

McCartney MR, Deeb TZ, Henderson TN & Hales TG. (2007). Tonically active GABAA receptors in hippocampal pyramidal neurons exhibit constitutive GABA-independent gating. *Mol Pharmacol* **71,** 539-548.

Meisner JG, Marsh AD & Marsh DR. (2010). Loss of GABAergic interneurons in laminae I-III of the spinal cord dorsal horn contributes to reduced GABAergic tone and neuropathic pain after spinal cord injury. *J Neurotrauma* **27,** 729-737.

Mende M, Fletcher EV, Belluardo JL, Pierce JP, Bommareddy PK, Weinrich JA, Kabir ZD, Schierberl KC, Pagiazitis JG, Mendelsohn AI, Francesconi A, Edwards RH, Milner TA, Rajadhyaksha AM, van Roessel PJ, Mentis GZ & Kaltschmidt JA. (2016). Sensory-Derived Glutamate Regulates Presynaptic Inhibitory Terminals in Mouse Spinal Cord. *Neuron* **90,** 1189-1202.

Metz K, Concha-Matos I, Hari K, Bseis O, Afsharipour B, Lin S, Li Y, Fenrich KF, Bennett DJ & Gorassini M. (2022). Post-activation depression produces extensor H-reflex suppresion following flexor afferent conditioning. *BioRxiv*.

Metz K, Concha-Matos I, Li Y, Afsharipour B, Thompson CK, Negro F, Bennett DJ & Gorassini M. (2021). Facilitation of sensory axon conduction to motoneurons during cortical or sensory evoked primary afferent depolarization (PAD) in humans. *BioRxiv*.

Milanov I. (1992). A comparative study of methods for estimation of presynaptic inhibition. *J Neurol* **239,** 287-292.

Mizuno Y, Tanaka R & Yanagisawa N. (1971). Reciprocal group I inhibition on triceps surae motoneurons in man. *J Neurophysiol* **34,** 1010-1017.

Murray KC, Stephens MJ, Ballou EW, Heckman CJ & Bennett DJ. (2011). Motoneuron excitability and muscle spasms are regulated by 5-HT2B and 5-HT2C receptor activity. *J Neurophysiol* **105,** 731-748.

Naftchi NE, Schlosser W & Horst WD. (1979). Correlation of changes in the GABA-ergic system with the development of spasticity in paraplegic cats. *Adv Exp Med Biol* **123,** 431-450.

Neher E & Sakaba T. (2001). Estimating transmitter release rates from postsynaptic current fluctuations. *J Neurosci* **21,** 9638-9654.

Nielsen J, Petersen N, Ballegaard M, Biering-Sorensen F & Kiehn O. (1993). H-reflexes are less depressed following muscle stretch in spastic spinal cord injured patients than in healthy subjects. *Experimental brain research* **97,** 173-176.

Nielsen J, Petersen N & Crone C. (1995). Changes in transmission across synapses of Ia afferents in spastic patients. *Brain* **118 (Pt 4),** 995-1004.

Norton JA, Bennett DJ, Knash ME, Murray KC & Gorassini MA. (2008). Changes in sensory-evoked synaptic activation of motoneurons after spinal cord injury in man. *Brain* **131,** 1478-1491.

O'Neill N & Sylantyev S. (2019). The Functional Role of Spontaneously Opening GABAA Receptors in Neural Transmission. *Front Mol Neurosci* **12,** 72.

Prochazka A. (2015). Sensory control of normal movement and of movement aided by neural prostheses. *J Anat* **227,** 167-177.

Quevedo J, Eguibar JR, Jimenez I, Schmidt RF & Rudomin P. (1993). Primary afferent depolarization of muscle afferents elicited by stimulation of joint afferents in cats with intact neuraxis and during reversible spinalization. *J Neurophysiol* **70,** 1899-1910.

Rabchevsky AG & Kitzman PH. (2011). Latest approaches for the treatment of spasticity and autonomic dysreflexia in chronic spinal cord injury. *Neurotherapeutics* **8,** 274-282.

Roby-Brami A & Bussel B. (1990). Effects of flexor reflex afferent stimulation on the soleus H reflex in patients with a complete spinal cord lesion: evidence for presynaptic inhibition of Ia transmission. *Exp Brain Res* **81,** 593-601.

Rothwell JC, Traub MM, Day BL, Obeso JA, Thomas PK & Marsden CD. (1982). Manual motor performance in a deafferented man. *Brain* **105 (Pt 3),** 515-542.

Rowald A, Komi S, Demesmaeker R, Baaklini E, Hernandez-Charpak SD, Paoles E, Montanaro H, Cassara A, Becce F, Lloyd B, Newton T, Ravier J, Kinany N, D'Ercole M, Paley A, Hankov N, Varescon C, McCracken L, Vat M, Caban M, Watrin A, Jacquet C, Bole-Feysot L, Harte C, Lorach H, Galvez A, Tschopp M, Herrmann N, Wacker M, Geernaert L, Fodor I, Radevich V, Van Den Keybus K, Eberle G, Pralong E, Roulet M, Ledoux JB, Fornari E, Mandija S, Mattera L, Martuzzi R, Nazarian B, Benkler S, Callegari S, Greiner N, Fuhrer B, Froeling M, Buse N, Denison T, Buschman R, Wende C, Ganty D, Bakker J, Delattre V, Lambert H, Minassian K, van den Berg CAT, Kavounoudias A, Micera S, Van De Ville D, Barraud Q, Kurt E, Kuster N, Neufeld E, Capogrosso M, Asboth L, Wagner FB, Bloch J & Courtine G. (2022). Activity-dependent spinal cord neuromodulation rapidly restores trunk and leg motor functions after complete paralysis. *Nat Med*.

Rudomin P & Schmidt RF. (1999). Presynaptic inhibition in the vertebrate spinal cord revisited. *Exp Brain Res* **129,** 1-37.

Russ JB, Verina T, Comer JD, Comi AM & Kaltschmidt JA. (2013). Corticospinal tract insult alters GABAergic circuitry in the mammalian spinal cord. *Front Neural Circuits* **7,** 150.

Ryge J, Winther O, Wienecke J, Sandelin A, Westerdahl AC, Hultborn H & Kiehn O. (2010). Transcriptional regulation of gene expression clusters in motor neurons following spinal cord injury. *BMC Genomics* **11,** 365.

Schindler-Ivens S & Shields RK. (2000). Low frequency depression of H-reflexes in humans with acute and chronic spinal-cord injury. *Exp Brain Res* **133,** 233-241.

Shreckengost J, Calvo J, Quevedo J & Hochman S. (2010). Bicuculline-sensitive primary afferent depolarization remains after greatly restricting synaptic transmission in the mammalian spinal cord. *J Neurosci* **30,** 5283-5288.

Silva NA, Sousa N, Reis RL & Salgado AJ. (2014). From basics to clinical: a comprehensive review on spinal cord injury. *Prog Neurobiol* **114,** 25-57.

Smith CC, Paton JFR, Chakrabarty S & Ichiyama RM. (2017). Descending Systems Direct Development of Key Spinal Motor Circuits. *J Neurosci* **37,** 6372-6387.

Tachibana T, Noguchi K & Ruda MA. (2002). Analysis of gene expression following spinal cord injury in rat using complementary DNA microarray. *Neurosci Lett* **327,** 133-137.

Thompson FJ, Reier PJ, Lucas CC & Parmer R. (1992). Altered patterns of reflex excitability subsequent to contusion injury of the rat spinal cord. *J Neurophysiol* **68,** 1473-1486.

Tillakaratne NJ, Mouria M, Ziv NB, Roy RR, Edgerton VR & Tobin AJ. (2000). Increased expression of glutamate decarboxylase (GAD(67)) in feline lumbar spinal cord after complete thoracic spinal cord transection. *J Neurosci Res* **60,** 219-230.

Wang L, Spary E, Deuchars J & Deuchars SA. (2008). Tonic GABAergic inhibition of sympathetic preganglionic neurons: a novel substrate for sympathetic control. *J Neurosci* **28,** 12445-12452.

Willis WD. (2006). John Eccles' studies of spinal cord presynaptic inhibition. *Prog Neurobiol* **78,** 189-214.

Willis WD, Jr. (1999). Dorsal root potentials and dorsal root reflexes: a double-edged sword. *Exp Brain Res* **124,** 395-421.

Yang K, Wang D & Li YQ. (2001). Distribution and depression of the GABA(B) receptor in the spinal dorsal horn of adult rat. *Brain Res Bull* **55,** 479-485.

Zimmerman AL, Kovatsis EM, Pozsgai RY, Tasnim A, Zhang Q & Ginty DD. (2019). Distinct Modes of Presynaptic Inhibition of Cutaneous Afferents and Their Functions in Behavior. *Neuron* **102,** 420-434 e428.

Chapter 5: Final discussion and conclusions

Considerations from previous work

It is likely that post-activation depression of Ia afferents contributed to H-reflex suppression observed in previous work that was often attributed to $GABA_A$ receptor mediated presynaptic inhibition, like those discussed in the introduction chapter of this thesis (Mizuno *et al.*, 1971; El-Tohamy & Sedgwick, 1983; Hultborn *et al.*, 1987a; Faist *et al.*, 1994; Capaday *et al.*, 1995). Interestingly, post-activation depression following successive activations of the same H-reflex is present even when the stimulation to produce the first H-reflex is subthreshold in the resting muscle EMG (Taborikova & Sax, 1969). Therefore, even low intensity electrical conditioning stimulation that does not evoke an excitatory response in the test muscle EMG could be contributing to successive post-activation of the H-reflex pathway. It is important that future studies work to differentiate the type of H-reflex suppression observed.

Many classical studies also assessed putative presynaptic inhibition using vibration of the *homonymous* muscle or tendon (Ashby & Verrier, 1975; Desmedt & Godaux, 1978; Milanov, 1992; Calancie *et al.*, 1993; Koelman *et al.*, 1993; Valls-Sole *et al.*, 1994; Pierrot-Deseilligny, 1997), which would inevitably lead to post-activation depression of the test afferents (Curtis & Eccles, 1960; Hultborn *et al.*, 1996a). Vibration of the homonymous tendon/muscle has since been disregarded as an effective way to measure presynaptic inhibition (Curtis & Eccles, 1960; Hultborn *et al.*, 1987a; Nielsen & Petersen, 1994; Nielsen *et al.*, 1995); however, studies using this method continue to be referenced for changes in supposed PAD-mediated presynaptic inhibition of Ia afferent terminals in various populations [see (De Gail *et al.*, 1966; Milanov, 1992; Calancie *et al.*, 1993) in (Stein, 1995)]. The results from many of these studies have helped guide treatment options for various populations living with movement disorders such as

spasticity, often with minimal clinical success. The work shown in this thesis presents a need to re-evaluate the findings regarding presynaptic inhibition in these patient populations, potentially uncovering new mechanisms involved and novel treatment avenues.

Weakness and additional considerations

Direct evidence for $GABA_A$ receptor mechanisms

In this thesis we examined pathways and mechanisms putatively involving the $GABA_A$ receptor in Ia afferents in humans. In humans, we did not directly antagonize the $GABA_A$ receptor and we were therefore unable to directly prove a role for it in the pathways we examined. However, our study draws many parallels from animal experiments using intracellular recordings and manipulation of receptors using light, drugs and electrical stimulation to directly test the various mechanisms and pathways involved (Lucas-Osma *et al.*, 2018b; Hari *et al.*, 2021). For example, the time course and frequency dependence of H-reflex modulation from various putative PAD-evoking conditioning stimulations had similarities to characteristics of PAD in animals.

Future studies using microneurography to measure antidromic spikes from PAD in humans, like in (Shefner *et al.*, 1992b), could provide more insight into mechanisms like post-activation depression from PAD-evoked spikes. Experiments using drugs to manipulate $GABA_A$ receptors in human participants, like the $\alpha5GABA_A$ receptor neutral antagonist S44819 used in clinical stroke trials (Darmani *et al.*, 2016; Chabriat *et al.*, 2020), could also provide insight into specific mechanisms involved in our experiments. However, these drugs would need to be very specific given that $GABA_A$ is widespread through the CNS and manipulation of these receptors can have sever adverse effects such as seizures (Treiman, 2001).

The challenges of understanding what receptors, pathways and mechanisms are involved in our human work, a limitation of all human work, highlights the importance of parallel animal and intracellular work. We had the unique opportunity to work closely with a laboratory performing intracellular recordings and immunolabelling in genetically modified mice and could compare our findings and protocols [many of the parallel animal findings have been published in (Lucas-Osma *et al.*, 2018b; Hari *et al.*, 2021)]. This partnership gave us invaluable insight into what mechanisms were potentially involved in our human findings.

Methodological considerations when sampling motor units (motoneurons)

It is difficult to decipher the exact mechanisms responsible for the H-reflex suppression and facilitation we observed but we were able to effectively dissociate presynaptic effects on the Ia afferent from the postsynaptic effects on the motoneurons using single motor unit analysis. Single motor unit recordings are extremely important for understanding effects at the motoneuron level but also present some limitations. The H-reflex is a summation of several motoneurons, whereas single motor unit recordings are based on only a few of the lowest threshold motoneurons. It is possible that the motoneurons involved in the H-reflex are different from those sampled to construct the peristimulus frequencygram (PSF) used to see the effect of a conditioning stimulation on the test motoneurons. Both the H-reflex and PSF would include low threshold motoneurons, so likely similar motoneurons types are being tested. The response of higher threshold single motor units, however, is still unknown. As techniques and technologies advance, such as electrode arrays for dissociating single motor units, we will hopefully be able to dissociate single motor unit firing properties from a wide variety of motoneuron types and muscles.

Factors other than direct motoneuron activation from the conditioning stimulation can also affect the motoneuron membrane potential. For example, the reduction in the soleus PSF from the TA tendon vibration (chapter 2) could be due to a decrease in the alpha-gamma loop since the motor units are recorded during a contraction. During a voluntary contraction, intrafusal muscle fibres contract with the extrafusal fibres, exciting Ia afferents that activate signal α-motoneurons which then helps to drive and maintain the contraction of the extrafusal muscle fibre, called the alpha-gamma loop (Taylor *et al.*, 2006; Li *et al.*, 2015). The conditioning vibration could be reducing transmission along the Ia afferents in this gamma loop, reducing the total input to the α-motoneurons and decreasing their firing rate. The contraction level needed to recruit a single motor unit is very small and alpha-gamma co-activation/the alpha-gamma loop is likely not a large driving force in maintain motoneuron firing (Taylor *et al.*, 2006); however, reduced alpha-gamma coactivation could still account for at least some of the reduction in the PSF that we observed.

We were also unable to record single motor units or EMG with a contraction from our participants with SCI, given that most participants were unable to elicit or maintain a voluntary contraction. In the future, recruiting participants with incomplete injury who can hold a voluntary contraction could allow for better analysis.

Interneuron effects

The H-reflex is mainly monosynaptic but contains oligosynaptic components as well (Jankowska *et al.*, 1981a; Burke *et al.*, 1983, 1984). Therefore, we could be recording changes from other afferent types and various interneurons along polysynaptic pathways (Jankowska, 1992). We used a relatively low-threshold H-reflex, to mainly activate Ia afferents with monosynaptic input to motoneurons, but we cannot know for certain if other afferent types were

activated by the peripheral nerve stimulation to activate the H-reflex and if any interneurons were involved in the pathway. Similarly, we cannot know for certain what afferent types our conditioning stimulation activated, with the higher intensity stimulation (i.e. 1.5 x MT CPN stimulation) likely activating mixed afferents. Although, PAD interneurons can be activated by a variety of afferent fibre types (Jankowska, 1992) and our stronger conditioning input likely activated mixed afferents that converge on PAD interneurons to produce a stronger PAD. In the future, it would be useful to use microneurography to provide more definitive evidence that the conditioning stimulation is producing dorsal root reflexes (as in (Shefner *et al.*, 1992b)) and thus directly activating PAD on the test Ia afferents, resulting in post-activation depression of subsequent activations.

With the above considerations taken into account, our study and many studies assessing putative presynaptic inhibition, mainly focus on afferent transmission along the monosynaptic Ia afferent – motoneuron pathway; however, monosynaptic inputs make up only a small percentage of the total input to motoneurons (Conradi, 1969; Jankowska, 1992). The relevance of interneuronal and polysynaptic pathways is especially important when assessing mechanisms involved in spasticity and hyperexcitability following injury.

Other contaminating effects

While a useful technique, using the H-reflex to assess afferent transmission along a monosynaptic pathway is far from perfect and many factors must be taken into account to effectively use the H-reflex (Voerman *et al.*, 2005). For example, small changes in sensory input from the position of the subject's head, limb and body can all affect the gain of the H-reflex (Traccis *et al.*, 1987; Goulart *et al.*, 2000; Voerman *et al.*, 2005). Muscle background activity, age, limb length and height can all also affect the gain and latency of the H-reflex (Braddom &

Johnson, 1974; Jankus *et al.*, 1994). Controlling for these factors is imperative for obtaining consistent results. Our participants were all seated in a similar reclined position and were asked to rest with no movement or talking during testing; however, there is always a margin for error.

It is also possible that muscle movement from the various nerve stimulations caused some of the responses we observed. For example, the long-lasting H-reflex inhibition (>2500 ms) from the strong (1.5 x MT) CPN conditioning stimulation could have been the result of a muscle twitch in the TA that caused the ankle to dorsiflex and stretch the SOL muscle (Nielsen *et al.*, 1995; Kohn *et al.*, 1997). A large muscle twitch in the antagonist muscle would rotate the joint and stretch the test muscle which would inevitably lead to post-activation depression (Kohn *et al.*, 1997). It is possible that even a small muscle twitch in the TA muscle causes enough movement, even with the ankle restrained, to stretch the soleus muscle/tendon and cause soleus muscle spindles to fire, thus causing post-activation depression of subsequent activations. As mentioned above, studies using microneurography are needed to decipher if the conditioning stimulation is evoking a dorsal root reflex in the test afferents, such as in (Shefner *et al.*, 1992b).

Clinical Importance and Future Directions

The proprioceptive feedback studied here is essential for normal functional movement (Rothwell *et al.*, 1982) and imperative for the initiation and maintenance of locomotor recovery following CNS injury (Takeoka *et al.*, 2014; Takeoka & Arber, 2019; Lalonde & Bui, 2021). While sensory transmission has been studied for many years (Mott & Sherrington, 1895), our understanding of how normal sensory transmission is processed and used by the CNS is quite limited. This understanding becomes even more limited when we consider sensory transmission

following CNS injury and how changes in sensory transmission are involved in the development of movement disorders such as spasticity.

In our study we did not use any measures to identify the severity or type (i.e. hyperreflexia, spasms, clonus, increased muscle tone) of spasticity in our SCI participants, so it is unknown how this affected our results. Many different mechanisms are involved in the development of spasticity and these mechanisms likely change based on the type of spasticity and injury (Nielsen *et al.*, 2007). One of the major challenges with human work is finding populations of people large enough with the same injury severity, level, type, age, rehabilitation and therapy regime, time since injury, medication and so on to decipher a specific mechanism. Even participants that have the same injury on paper can clinically present very differently.

The mechanisms involved in the development of spasticity after CNS injury remain relatively unclear making current treatment options generally unspecific, typically including a host of side-effects and reduce their therapeutic effect over time (Rabchevsky & Kitzman, 2011). The work presented here opens new avenues for exploring the mechanisms involved in spasticity, potentially leading to new treatment options. For example, suppressing extrasynaptic $GABA_A$ (α5) receptors (i.e. using the α5$GABA_A$ receptor neutral antagonist S44819 used in human stroke trials (Darmani *et al.*, 2016; Chabriat *et al.*, 2020)) could restore some natural branchpoint failure along Ia afferents, reducing aberrant afferent transmission while not dampening remaining useful motor function.

Many new rehabilitation techniques also involve electrical stimulation of sensory afferents or trans-spinal stimulation to enhance motor recovery and reduce spasticity; however, the mechanisms involved remain relatively unknown (Harkema, 2008; Courtine *et al.*, 2009;

Angeli *et al.*, 2018; Mekhael *et al.*, 2019). Our findings could provide insight into how these treatments work, allowing them to be adapted and become more therapeutically effective.

References

Angeli CA, Boakye M, Morton RA, Vogt J, Benton K, Chen Y, Ferreira CK & Harkema SJ. (2018). Recovery of Over-Ground Walking after Chronic Motor Complete Spinal Cord Injury. *N Engl J Med* **379,** 1244-1250.

Ashby P & Verrier M. (1975). Neurophysiological changes following spinal cord lesions in man. *Can J Neurol Sci* **2,** 91-100.

Braddom RL & Johnson EW. (1974). H reflex: review and classification with suggested clinical uses. *Arch Phys Med Rehabil* **55,** 412-417.

Burke D, Gandevia SC & McKeon B. (1983). The afferent volleys responsible for spinal proprioceptive reflexes in man. *J Physiol* **339,** 535-552.

Burke D, Gandevia SC & McKeon B. (1984). Monosynaptic and oligosynaptic contributions to human ankle jerk and H-reflex. *J Neurophysiol* **52,** 435-448.

Calancie B, Broton JG, Klose KJ, Traad M, Difini J & Ayyar DR. (1993). Evidence that alterations in presynaptic inhibition contribute to segmental hypo- and hyperexcitability after spinal cord injury in man. *Electroencephalogr Clin Neurophysiol* **89,** 177-186.

Capaday C, Lavoie BA & Comeau F. (1995). Differential effects of a flexor nerve input on the human soleus H-reflex during standing versus walking. *Can J Physiol Pharmacol* **73,** 436-449.

Chabriat H, Bassetti CL, Marx U, Picarel-Blanchot F, Sors A, Gruget C, Saba B, Wattez M, Audoli ML & Hermann DM. (2020). Randomized Efficacy and Safety Trial with Oral S 44819 after Recent ischemic cerebral Event (RESTORE BRAIN study): a placebo controlled phase II study. *Trials* **21,** 136.

Conradi S. (1969). Ultrastructure of dorsal root boutons on lumbosacral motoneurons of the adult cat, as revealed by dorsal root section. *Acta Physiol Scand Suppl* **332,** 85-115.

Courtine G, Gerasimenko Y, van den Brand R, Yew A, Musienko P, Zhong H, Song B, Ao Y, Ichiyama RM, Lavrov I, Roy RR, Sofroniew MV & Edgerton VR. (2009). Transformation of nonfunctional spinal circuits into functional states after the loss of brain input. *Nat Neurosci* **12,** 1333-1342.

Curtis DR & Eccles JC. (1960). Synaptic action during and after repetitive stimulation. *The Journal of physiology* **150,** 374-398.

Darmani G, Zipser CM, Bohmer GM, Deschet K, Muller-Dahlhaus F, Belardinelli P, Schwab M & Ziemann U. (2016). Effects of the Selective alpha5-GABAAR Antagonist S44819 on Excitability in the Human Brain: A TMS-EMG and TMS-EEG Phase I Study. *J Neurosci* **36,** 12312-12320.

De Gail P, Lance JW & Neilson PD. (1966). Differential effects on tonic and phasic reflex mechanisms produced by vibration of muscles in man. *J Neurol Neurosurg Psychiatry* **29,** 1-11.

Desmedt JE & Godaux E. (1978). Mechanism of the vibration paradox: excitatory and inhibitory effects of tendon vibration on single soleus muscle motor units in man. *J Physiol* **285,** 197-207.

El-Tohamy A & Sedgwick EM. (1983). Spinal inhibition in man: depression of the soleus H reflex by stimulation of the nerve to the antagonist muscle. *J Physiol* **337,** 497-508.

Faist M, Mazevet D, Dietz V & Pierrot-Deseilligny E. (1994). A quantitative assessment of presynaptic inhibition of Ia afferents in spastics. Differences in hemiplegics and paraplegics. *Brain* **117 (Pt 6),** 1449-1455.

Goulart F, Valls-Sole J & Alvarez R. (2000). Posture-related changes of soleus H-reflex excitability. *Muscle Nerve* **23,** 925-932.

Hari K, Lucas-Osma AM, Metz K, Lin S, Pardell N, Roszko D, Black S, Minarik A, Singla R, Stephens MJ, Fouad K, Jones KE, Gorassini M, Fenrich KK, Li Y & Bennett DJ. (2021). Nodal GABA facilitates axon spike transmission in the spinal cord. *BioRxiv*.

Harkema SJ. (2008). Plasticity of interneuronal networks of the functionally isolated human spinal cord. *Brain Res Rev* **57,** 255-264.

Hultborn H, Illert M, Nielsen J, Paul A, Ballegaard M & Wiese H. (1996). On the mechanism of the post-activation depression of the H-reflex in human subjects. *Experimental brain research* **108,** 450-462.

Hultborn H, Meunier S, Morin C & Pierrot-Deseilligny E. (1987). Assessing changes in presynaptic inhibition of I a fibres: a study in man and the cat. *J Physiol* **389,** 729-756.

Jankowska E. (1992). Interneuronal relay in spinal pathways from proprioceptors. *Prog Neurobiol* **38,** 335-378.

Jankowska E, McCrea D & Mackel R. (1981). Oligosynaptic excitation of motoneurones by impulses in group Ia muscle spindle afferents in the cat. *J Physiol* **316,** 411-425.

Jankus WR, Robinson LR & Little JW. (1994). Normal limits of side-to-side H-reflex amplitude variability. *Arch Phys Med Rehabil* **75,** 3-7.

Koelman JH, Bour LJ, Hilgevoord AA, van Bruggen GJ & Ongerboer de Visser BW. (1993). Soleus H-reflex tests and clinical signs of the upper motor neuron syndrome. *J Neurol Neurosurg Psychiatry* **56,** 776-781.

Kohn AF, Floeter MK & Hallett M. (1997). Presynaptic inhibition compared with homosynaptic depression as an explanation for soleus H-reflex depression in humans. *Exp Brain Res* **116,** 375-380.

Lalonde NR & Bui TV. (2021). Do spinal circuits still require gating of sensory information by presynaptic inhibition after spinal cord injury? *Current Opinion in Physiology* **19,** 113-118.

Li S, Zhuang C, Hao M, He X, Marquez JC, Niu CM & Lan N. (2015). Coordinated alpha and gamma control of muscles and spindles in movement and posture. *Front Comput Neurosci* **9,** 122.

Lucas-Osma AM, Li Y, Lin S, Black S, Singla R, Fouad K, Fenrich KK & Bennett DJ. (2018). Extrasynaptic proportional, variant5GABAA receptors on proprioceptive afferents produce a tonic depolarization that modulates sodium channel function in the rat spinal cord. *J Neurophysiol*.

Mekhael W, Begum S, Samaddar S, Hassan M, Toruno P, Ahmed M, Gorin A, Maisano M, Ayad M & Ahmed Z. (2019). Repeated anodal trans-spinal direct current stimulation results in long-term reduction of spasticity in mice with spinal cord injury. *The Journal of physiology* **597,** 2201-2223.

Milanov I. (1992). A comparative study of methods for estimation of presynaptic inhibition. *J Neurol* **239,** 287-292.

Mizuno Y, Tanaka R & Yanagisawa N. (1971). Reciprocal group I inhibition on triceps surae motoneurons in man. *J Neurophysiol* **34,** 1010-1017.

Mott FW & Sherrington CS. (1895). Experiments upon the influence of sensory nerves upon movements and nutrition of the limbs. *Proceedings of the Royal Society* **B,** 481-488.

Nielsen J & Petersen N. (1994). Is presynaptic inhibition distributed to corticospinal fibres in man? *J Physiol* **477,** 47-58.

Nielsen J, Petersen N & Crone C. (1995). Changes in transmission across synapses of Ia afferents in spastic patients. *Brain* **118 (Pt 4),** 995-1004.

Nielsen JB, Crone C & Hultborn H. (2007). The spinal pathophysiology of spasticity--from a basic science point of view. *Acta Physiol (Oxf)* **189,** 171-180.

Pierrot-Deseilligny E. (1997). Assessing changes in presynaptic inhibition of Ia afferents during movement in humans. *J Neurosci Methods* **74,** 189-199.

Rabchevsky AG & Kitzman PH. (2011). Latest approaches for the treatment of spasticity and autonomic dysreflexia in chronic spinal cord injury. *Neurotherapeutics* **8,** 274-282.

Rothwell JC, Traub MM, Day BL, Obeso JA, Thomas PK & Marsden CD. (1982). Manual motor performance in a deafferented man. *Brain* **105 (Pt 3),** 515-542.

Shefner JM, Buchthal F & Krarup C. (1992). Recurrent potentials in human peripheral sensory nerve: possible evidence of primary afferent depolarization of the spinal cord. *Muscle Nerve* **15,** 1354-1363.

Stein RB. (1995). Presynaptic inhibition in humans. *Prog Neurobiol* **47,** 533-544.

Taborikova H & Sax DS. (1969). Conditioning of H-reflexes by a preceding subthreshold H-reflex stimulus. *Brain* **92,** 203-212.

Takeoka A & Arber S. (2019). Functional Local Proprioceptive Feedback Circuits Initiate and Maintain Locomotor Recovery after Spinal Cord Injury. *Cell Rep* **27,** 71-85 e73.

Takeoka A, Vollenweider I, Courtine G & Arber S. (2014). Muscle spindle feedback directs locomotor recovery and circuit reorganization after spinal cord injury. *Cell* **159,** 1626-1639.

Taylor A, Durbaba R, Ellaway PH & Rawlinson S. (2006). Static and dynamic gamma-motor output to ankle flexor muscles during locomotion in the decerebrate cat. *J Physiol* **571,** 711-723.

Traccis S, Rosati G, Patraskakis S, Bissakou M, Sau GF & Aiello I. (1987). Influences of neck receptors on soleus motoneuron excitability in man. *Exp Neurol* **95,** 76-84.

Treiman DM. (2001). GABAergic mechanisms in epilepsy. *Epilepsia* **42 Suppl 3,** 8-12.

Valls-Sole J, Alvarez R & Tolosa ES. (1994). Responses of the soleus muscle to transcranial magnetic stimulation. *Electroencephalogr Clin Neurophysiol* **93,** 421-427.

Voerman GE, Gregoric M & Hermens HJ. (2005). Neurophysiological methods for the assessment of spasticity: the Hoffmann reflex, the tendon reflex, and the stretch reflex. *Disabil Rehabil* **27,** 33-68.

Bibliography

Achache V, Roche N, Lamy JC, Boakye M, Lackmy A, Gastal A, Quentin V & Katz R. (2010). Transmission within several spinal pathways in adults with cerebral palsy. *Brain* **133,** 1470-1483.

Adams MM & Hicks AL. (2005). Spasticity after spinal cord injury. *Spinal Cord* **43,** 577-586.

Afsharipour B, Manzur N, Duchcherer J, Fenrich KF, Thompson CK, Negro F, Quinlan KA, Bennett DJ & Gorassini MA. (2020). Estimation of self-sustained activity produced by persistent inward currents using firing rate profiles of multiple motor units in humans. *J Neurophysiol* **124,** 63-85.

Ahuja CS, Wilson JR, Nori S, Kotter MRN, Druschel C, Curt A & Fehlings MG. (2017). Traumatic spinal cord injury. *Nat Rev Dis Primers* **3,** 17018.

Aimonetti JM, Vedel JP, Schmied A & Pagni S. (2000). Distribution of presynaptic inhibition on type-identified motoneurones in the extensor carpi radialis pool in man. *The Journal of physiology* **522 Pt 1,** 125-135.

Aimonetti JM, Vedel JP, Schmied A & Pagni S. (2000). Mechanical cutaneous stimulation alters Ia presynaptic inhibition in human wrist extensor muscles: a single motor unit study. *The Journal of physiology* **522 Pt 1,** 137-145.

Akay T, Tourtellotte WG, Arber S & Jessell TM. (2014). Degradation of mouse locomotor pattern in the absence of proprioceptive sensory feedback. *Proc Natl Acad Sci U S A* **111,** 16877-16882.

Alvarez FJ, Taylor-Blake B, Fyffe RE, De Blas AL & Light AR. (1996). Distribution of immunoreactivity for the beta 2 and beta 3 subunits of the GABAA receptor in the mammalian spinal cord. *J Comp Neurol* **365,** 392-412.

Alvarez FJ. (1998). Anatomical basis for presynaptic inhibition of primary sensory fibers. In *Presynaptic Inhibition and Neuron Control*, ed. Rudmon P, Romo R & Mendell LM, pp. 13-41. Oxford University Press, New York.

Anderson KD. (2004). Targeting recovery: priorities of the spinal cord-injured population. *J Neurotrauma* **21,** 1371-1383.

Angeli CA, Boakye M, Morton RA, Vogt J, Benton K, Chen Y, Ferreira CK & Harkema SJ. (2018). Recovery of Over-Ground Walking after Chronic Motor Complete Spinal Cord Injury. *N Engl J Med* **379,** 1244-1250.

Ashby P & Verrier M. (1975). Neurophysiological changes following spinal cord lesions in man. *Can J Neurol Sci* **2,** 91-100.

Ashby P & Verrier M. (1976). Neurophysiologic changes in hemiplegia. Possible explanation for the initial disparity between muscle tone and tendon reflexes. *Neurology* **26,** 1145-1151.

Ashby P, Verrier M & Lightfoot E. (1974). Segmental reflex pathways in spinal shock and spinal spasticity in man. *J Neurol Neurosurg Psychiatry* **37,** 1352-1360.

Aymard C, Katz R, Lafitte C, Lo E, Penicaud A, Pradat-Diehl P & Raoul S. (2000). Presynaptic inhibition and homosynaptic depression: a comparison between lower and upper limbs in normal human subjects and patients with hemiplegia. *Brain* **123 (Pt 8),** 1688-1702.

Azouvi P, Roby-Brami A, Biraben A, Thiebaut JB, Thurel C & Bussel B. (1993). Effect of intrathecal baclofen on the monosynaptic reflex in humans: evidence for a postsynaptic action. *J Neurol Neurosurg Psychiatry* **56,** 515-519.

Baker LL & Chandler SH. (1987). Characterization of postsynaptic potentials evoked by sural nerve stimulation in hindlimb motoneurons from acute and chronic spinal cats. *Brain Res* **420,** 340-350.

Baker SN & Perez MA. (2017). Reticulospinal Contributions to Gross Hand Function after Human Spinal Cord Injury. *J Neurosci* **37,** 9778-9784.

Baker SN. (2011). The primate reticulospinal tract, hand function and functional recovery. *J Physiol* **589,** 5603-5612.

Ballermann M & Fouad K. (2006). Spontaneous locomotor recovery in spinal cord injured rats is accompanied by anatomical plasticity of reticulospinal fibers. *Eur J Neurosci* **23,** 1988-1996.

Behrman AL & Harkema SJ. (2000). Locomotor training after human spinal cord injury: a series of case studies. *Phys Ther* **80,** 688-700.

Bellardita C, Caggiano V, Leiras R, Caldeira V, Fuchs A, Bouvier J, Low P & Kiehn O. (2017). Spatiotemporal correlation of spinal network dynamics underlying spasms in chronic spinalized mice. *Elife* **6**.

Bennett DJ, Sanelli L, Cooke CL, Harvey PJ & Gorassini MA. (2004). Spastic long-lasting reflexes in the awake rat after sacral spinal cord injury. *J Neurophysiol* **91,** 2247-2258.

Berardelli A, Day BL, Marsden CD & Rothwell JC. (1987). Evidence favouring presynaptic inhibition between antagonist muscle afferents in the human forearm. *J Physiol* **391,** 71-83.

Betley JN, Wright CV, Kawaguchi Y, Erdelyi F, Szabo G, Jessell TM & Kaltschmidt JA. (2009). Stringent specificity in the construction of a GABAergic presynaptic inhibitory circuit. *Cell* **139,** 161-174.

Biering-Sorensen B, Kristensen IB, Kjaer M & Biering-Sorensen F. (2009). Muscle after spinal cord injury. *Muscle Nerve* **40,** 499-519.

Boulenguez P, Liabeuf S, Bos R, Bras H, Jean-Xavier C, Brocard C, Stil A, Darbon P, Cattaert D, Delpire E, Marsala M & Vinay L. (2010). Down-regulation of the potassium-chloride cotransporter KCC2 contributes to spasticity after spinal cord injury. *Nat Med* **16,** 302-307.

Braddom RL & Johnson EW. (1974). H reflex: review and classification with suggested clinical uses. *Arch Phys Med Rehabil* **55,** 412-417.

Burke D, Gandevia SC & McKeon B. (1983). The afferent volleys responsible for spinal proprioceptive reflexes in man. *J Physiol* **339,** 535-552.

Burke D, Gandevia SC & McKeon B. (1984). Monosynaptic and oligosynaptic contributions to human ankle jerk and H-reflex. *J Neurophysiol* **52,** 435-448.

Burke D, Gracies JM, Meunier S & Pierrot-Deseilligny E. (1992). Changes in presynaptic inhibition of afferents to propriospinal-like neurones in man during voluntary contractions. *J Physiol* **449,** 673-687.

Calancie B, Broton JG, Klose KJ, Traad M, Difini J & Ayyar DR. (1993). Evidence that alterations in presynaptic inhibition contribute to segmental hypo- and hyperexcitability after spinal cord injury in man. *Electroencephalogr Clin Neurophysiol* **89,** 177-186.

Canto-Bustos M, Loeza-Alcocer E, Cuellar CA, Osuna P, Elias-Vinas D, Granados-Soto V, Manjarrez E, Felix R & Delgado-Lezama R. (2017). Tonically Active alpha5GABAA Receptors Reduce Motoneuron Excitability and Decrease the Monosynaptic Reflex. *Front Cell Neurosci* **11,** 283.

Capaday C, Lavoie BA & Comeau F. (1995). Differential effects of a flexor nerve input on the human soleus H-reflex during standing versus walking. *Can J Physiol Pharmacol* **73,** 436-449.

Caron G, Bilchak JN & Cote MP. (2020). Direct evidence for decreased presynaptic inhibition evoked by PBSt group I muscle afferents after chronic SCI and recovery with step-training in rats. *J Physiol*.

Carpenter D, Lundberg A & Norrsell U. (1963). Primary Afferent Depolarization Evoked from the Sensorimotor Cortex. *Acta Physiol Scand* **59,** 126-142.

Cartlidge NE, Hudgson P & Weightman D. (1974). A comparison of baclofen and diazepam in the treatment of spasticity. *J Neurol Sci* **23,** 17-24.

Chabriat H, Bassetti CL, Marx U, Picarel-Blanchot F, Sors A, Gruget C, Saba B, Wattez M, Audoli ML & Hermann DM. (2020). Randomized Efficacy and Safety Trial with Oral S 44819 after Recent ischemic cerebral Event (RESTORE BRAIN study): a placebo controlled phase II study. *Trials* **21,** 136.

Chang E, Ghosh N, Yanni D, Lee S, Alexandru D & Mozaffar T. (2013). A Review of Spasticity Treatments: Pharmacological and Interventional Approaches. *Crit Rev Phys Rehabil Med* **25,** 11-22.

Chen Y, He Y & DeVivo MJ. (2016). Changing Demographics and Injury Profile of New Traumatic Spinal Cord Injuries in the United States, 1972-2014. *Arch Phys Med Rehabil* **97,** 1610-1619.

Choo AM, Liu J, Lam CK, Dvorak M, Tetzlaff W & Oxland TR. (2007). Contusion, dislocation, and distraction: primary hemorrhage and membrane permeability in distinct mechanisms of spinal cord injury. *J Neurosurg Spine* **6,** 255-266.

Clarkson AN, Huang BS, Macisaac SE, Mody I & Carmichael ST. (2010). Reducing excessive GABA-mediated tonic inhibition promotes functional recovery after stroke. *Nature* **468,** 305-309.

Conradi S. (1969). Ultrastructure of dorsal root boutons on lumbosacral motoneurons of the adult cat, as revealed by dorsal root section. *Acta Physiol Scand Suppl* **332,** 85-115.

Courtine G, Gerasimenko Y, van den Brand R, Yew A, Musienko P, Zhong H, Song B, Ao Y, Ichiyama RM, Lavrov I, Roy RR, Sofroniew MV & Edgerton VR. (2009).

Transformation of nonfunctional spinal circuits into functional states after the loss of brain input. *Nat Neurosci* **12,** 1333-1342.

Cramer SC, Lastra L, Lacourse MG & Cohen MJ. (2005). Brain motor system function after chronic, complete spinal cord injury. *Brain* **128,** 2941-2950.

Crone C & Nielsen J. (1989). Methodological implications of the post activation depression of the soleus H-reflex in man. *Experimental brain research* **78,** 28-32.

Crone C, Hultborn H, Mazieres L, Morin C, Nielsen J & Pierrot-Deseilligny E. (1990). Sensitivity of monosynaptic test reflexes to facilitation and inhibition as a function of the test reflex size: a study in man and the cat. *Exp Brain Res* **81,** 35-45.

Crone C, Johnsen LL, Biering-Sorensen F & Nielsen JB. (2003). Appearance of reciprocal facilitation of ankle extensors from ankle flexors in patients with stroke or spinal cord injury. *Brain* **126,** 495-507.

Crone C, Nielsen J, Petersen N, Ballegaard M & Hultborn H. (1994). Disynaptic reciprocal inhibition of ankle extensors in spastic patients. *Brain* **117 (Pt 5),** 1161-1168.

Crowe MJ, Bresnahan JC, Shuman SL, Masters JN & Beattie MS. (1997). Apoptosis and delayed degeneration after spinal cord injury in rats and monkeys. *Nat Med* **3,** 73-76.

Curtis DR & Eccles JC. (1960). Synaptic action during and after repetitive stimulation. *The Journal of physiology* **150,** 374-398.

Curtis DR & Lacey G. (1994). GABA-B receptor-mediated spinal inhibition. *Neuroreport* **5,** 540-542.

Curtis DR & Lacey G. (1998). Prolonged GABA(B) receptor-mediated synaptic inhibition in the cat spinal cord: an in vivo study. *Exp Brain Res* **121,** 319-333.

Curtis DR & Lodge D. (1982). The depolarization of feline ventral horn group Ia spinal afferent terminations by GABA. *Exp Brain Res* **46,** 215-233.

Curtis DR, Gynther BD, Lacey G & Beattie DT. (1997). Baclofen: reduction of presynaptic calcium influx in the cat spinal cord in vivo. *Exp Brain Res* **113,** 520-533.

Curtis DR. (1998). *Two types of inhibition in the spinal cord*. Oxford University Press, New York.

Cushing S, Bui T & Rose PK. (2005). Effect of nonlinear summation of synaptic currents on the input-output properties of spinal motoneurons. *J Neurophysiol* **94,** 3465-3478.

D'Amico JM, Condliffe EG, Martins KJ, Bennett DJ & Gorassini MA. (2014). Recovery of neuronal and network excitability after spinal cord injury and implications for spasticity. *Front Integr Neurosci* **8,** 36.

Darmani G, Zipser CM, Bohmer GM, Deschet K, Muller-Dahlhaus F, Belardinelli P, Schwab M & Ziemann U. (2016). Effects of the Selective alpha5-GABAAR Antagonist S44819 on Excitability in the Human Brain: A TMS-EMG and TMS-EEG Phase I Study. *J Neurosci* **36,** 12312-12320.

De Gail P, Lance JW & Neilson PD. (1966). Differential effects on tonic and phasic reflex mechanisms produced by vibration of muscles in man. *J Neurol Neurosurg Psychiatry* **29,** 1-11.

de Leon RD, Hodgson JA, Roy RR & Edgerton VR. (1998). Locomotor capacity attributable to step training versus spontaneous recovery after spinalization in adult cats. *J Neurophysiol* **79,** 1329-1340.

Delgado-Lezama R, Bravo-Hernandez M, Franco-Enzastiga U, De la Luz-Cuellar YE, Alvarado-Cervantes NS, Raya-Tafolla G, Martinez-Zaldivar LA, Vargas-Parada A, Rodriguez-Palma EJ, Vidal-Cantu GC, Guzman-Priego CG, Torres-Lopez JE, Murbartian J, Felix R & Granados-Soto V. (2021). The role of spinal cord extrasynaptic alpha5 GABAA receptors in chronic pain. *Physiol Rep* **9,** e14984.

Delgado-Lezama R, Loeza-Alcocer E, Andres C, Aguilar J, Guertin PA & Felix R. (2013). Extrasynaptic GABA(A) receptors in the brainstem and spinal cord: structure and function. *Curr Pharm Des* **19,** 4485-4497.

Delwaide PJ & Oliver E. (1988). Short-latency autogenic inhibition (IB inhibition) in human spasticity. *J Neurol Neurosurg Psychiatry* **51,** 1546-1550.

Desmedt JE & Godaux E. (1978). Mechanism of the vibration paradox: excitatory and inhibitory effects of tendon vibration on single soleus muscle motor units in man. *J Physiol* **285,** 197-207.

DeVivo MJ & Chen Y. (2011). Trends in new injuries, prevalent cases, and aging with spinal cord injury. *Arch Phys Med Rehabil* **92,** 332-338.

Devivo MJ. (2012). Epidemiology of traumatic spinal cord injury: trends and future implications. *Spinal Cord* **50,** 365-372.

Dietz V. (2000). Spastic movement disorder. *Spinal Cord* **38,** 389-393.

Drew GM, Siddall PJ & Duggan AW. (2001). Responses of spinal neurones to cutaneous and dorsal root stimuli in rats with mechanical allodynia after contusive spinal cord injury. *Brain Res* **893,** 59-69.

Duchen MR. (1986). Excitation of mouse motoneurones by GABA-mediated primary afferent depolarization. *Brain Res* **379,** 182-187.

Eccles JC & Rall W. (1951). Effects induced in a monosynaptic reflex path by its activation. *Journal of neurophysiology* **14,** 353-376.

Eccles JC, Eccles RM & Magni F. (1961a). Central inhibitory action attributable to presynaptic depolarization produced by muscle afferent volleys. *J Physiol* **159,** 147-166.

Eccles JC, Kozak W & Magni F. (1961b). Dorsal root reflexes of muscle group I afferent fibres. *J Physiol* **159,** 128-146.

Eccles JC, Magni F & Willis WD. (1962). Depolarization of central terminals of Group I afferent fibres from muscle. *The Journal of physiology* **160,** 62-93.

Eccles JC, Schmidt R & Willis WD. (1963). Pharmacological Studies on Presynaptic Inhibition. *J Physiol* **168,** 500-530.

Eccles JC, Schmidt RF & Willis WD. (1962c). Presynaptic inhibition of the spinal monosynaptic reflex pathway. *J Physiol* **161,** 282-297.

Edstrom L. (1970). Selective changes in the sizes of red and white muscle fibres in upper motor lesions and Parkinsonism. *J Neurol Sci* **11,** 537-550.

Eguibar JR, Quevedo J & Rudomin P. (1997). Selective cortical and segmental control of primary afferent depolarization of single muscle afferents in the cat spinal cord. *Experimental brain research* **113,** 411-430.

El-Tohamy A & Sedgwick EM. (1983). Spinal inhibition in man: depression of the soleus H reflex by stimulation of the nerve to the antagonist muscle. *J Physiol* **337,** 497-508.

Faist M, Dietz V & Pierrot-Deseilligny E. (1996). Modulation, probably presynaptic in origin, of monosynaptic Ia excitation during human gait. *Exp Brain Res* **109,** 441-449.

Faist M, Mazevet D, Dietz V & Pierrot-Deseilligny E. (1994). A quantitative assessment of presynaptic inhibition of Ia afferents in spastics. Differences in hemiplegics and paraplegics. *Brain* **117 (Pt 6),** 1449-1455.

Fedirchuk B, Wenner P, Whelan PJ, Ho S, Tabak J & O'Donovan MJ. (1999). Spontaneous network activity transiently depresses synaptic transmission in the embryonic chick spinal cord. *J Neurosci* **19,** 2102-2112.

Fink AJ, Croce KR, Huang ZJ, Abbott LF, Jessell TM & Azim E. (2014). Presynaptic inhibition of spinal sensory feedback ensures smooth movement. *Nature* **509,** 43-48.

Fink AJ. (2013). Exploring a behavioural role for presynaptic inhibition in spinal sensory-motor synapses. *PhD Thesis, Columbia University***,** 1-293.

Fisher MA. (1992). AAEM Minimonograph #13: H reflexes and F waves: physiology and clinical indications. *Muscle Nerve* **15,** 1223-1233.

Frank K & Fortes MGF. (1957). Presynaptic and postsynaptic inhibition of monosynaptic reflexes. . *Fed Proc* **16,** 39-40.

Frank K. (1959). Basic mechanisms of synaptic transmission in the central nervous system. *Inst Radio Eng Trans Med Electron* **ME-6,** 85-88.

Fung J & Barbeau H. (1994). Effects of conditioning cutaneomuscular stimulation on the soleus H-reflex in normal and spastic paretic subjects during walking and standing. *Journal of neurophysiology* **72,** 2090-2104.

Gallagher JP, Higashi H & Nishi S. (1978). Characterization and ionic basis of GABA-induced depolarizations recorded in vitro from cat primary afferent neurones. *The Journal of physiology* **275,** 263-282.

Garcia-Ramirez DL, Calvo JR, Hochman S & Quevedo JN. (2014). Serotonin, dopamine and noradrenaline adjust actions of myelinated afferents via modulation of presynaptic inhibition in the mouse spinal cord. *PLoS One* **9,** e89999.

Gerasimenko YP, Lu DC, Modaber M, Zdunowski S, Gad P, Sayenko DG, Morikawa E, Haakana P, Ferguson AR, Roy RR & Edgerton VR. (2015). Noninvasive Reactivation of Motor Descending Control after Paralysis. *J Neurotrauma* **32,** 1968-1980.

Gorassini MA, Knash ME, Harvey PJ, Bennett DJ & Yang JF. (2004). Role of motoneurons in the generation of muscle spasms after spinal cord injury. *Brain* **127,** 2247-2258.

Goulart F, Valls-Sole J & Alvarez R. (2000). Posture-related changes of soleus H-reflex excitability. *Muscle Nerve* **23,** 925-932.

Grey MJ, Klinge K, Crone C, Lorentzen J, Biering-Sorensen F, Ravnborg M & Nielsen JB. (2008). Post-activation depression of soleus stretch reflexes in healthy and spastic humans. *Exp Brain Res* **185,** 189-197.

Hancock J, Knowles L & Gillies JD. (1973). Segmental reflex changes in acute and chronic spinal cats. *Proc Aust Assoc Neurol* **10,** 139-143.

Hari K, Lucas-Osma AM, Metz K, Lin S, Pardell N, Roszko D, Black S, Minarik A, Singla R, Stephens MJ, Fouad K, Jones KE, Gorassini M, Fenrich KK, Li Y & Bennett DJ. (2021). Nodal GABA facilitates axon spike transmission in the spinal cord. *BioRxiv*.

Hari K, Lucas-Osma AM, Metz K, Lin S, Pardell N, Roszko D, Black S, Minarik A, Singla R, Stephens MJ, Fouad K, Jones KE, Gorassini M, Fenrich KK, Li Y & Bennett DJ. (2022). Nodal GABA facilitates axon spike transmission in the spinal cord. *Nature Neuroscience* In press.

Hari K, Lucas-Osma AM, Metz K, Lin S, Pardell N, Roszko D, Black S, Minarik A, Singla R, Stephens MJ, Fouad K, Jones KE, Gorassini M, Fenrich KK, Li Y & Bennett DJ. (2021). Nodal GABA facilitates axon spike transmission in the spinal cord. *BioRxiv*.

Harkema S, Gerasimenko Y, Hodes J, Burdick J, Angeli C, Chen Y, Ferreira C, Willhite A, Rejc E, Grossman RG & Edgerton VR. (2011). Effect of epidural stimulation of the lumbosacral spinal cord on voluntary movement, standing, and assisted stepping after motor complete paraplegia: a case study. *Lancet* **377,** 1938-1947.

Harkema SJ. (2008). Plasticity of interneuronal networks of the functionally isolated human spinal cord. *Brain Res Rev* **57,** 255-264.

Hayes ES & Carlton SM. (1992). Primary afferent interactions: analysis of calcitonin gene-related peptide-immunoreactive terminals in contact with unlabeled and GABA-immunoreactive profiles in the monkey dorsal horn. *Neuroscience* **47,** 873-896.

Heckmann CJ, Gorassini MA & Bennett DJ. (2005). Persistent inward currents in motoneuron dendrites: implications for motor output. *Muscle Nerve* **31,** 135-156.

Henneman E, Luscher HR & Mathis J. (1984). Simultaneously active and inactive synapses of single Ia fibres on cat spinal motoneurones. *The Journal of physiology* **352,** 147-161.

Hofstoetter US, Freundl B, Binder H & Minassian K. (2019). Recovery cycles of posterior root-muscle reflexes evoked by transcutaneous spinal cord stimulation and of the H reflex in individuals with intact and injured spinal cord. *PLoS One* **14,** e0227057.

Howell RD & Pugh JR. (2016). Biphasic modulation of parallel fibre synaptic transmission by co-activation of presynaptic GABAA and GABAB receptors in mice. *J Physiol* **594,** 3651-3666.

Howells J, Sangari S, Matamala JM, Kiernan MC, Marchand-Pauvert V & Burke D. (2020). Interrogating interneurone function using threshold tracking of the H reflex in healthy subjects and patients with motor neurone disease. *Clin Neurophysiol* **131,** 1986-1996.

Hughes DI, Mackie M, Nagy GG, Riddell JS, Maxwell DJ, Szabo G, Erdelyi F, Veress G, Szucs P, Antal M & Todd AJ. (2005). P boutons in lamina IX of the rodent spinal cord express high levels of glutamic acid decarboxylase-65 and originate from cells in deep medial dorsal horn. *Proc Natl Acad Sci U S A* **102,** 9038-9043.

Hultborn H, Illert M, Nielsen J, Paul A, Ballegaard M & Wiese H. (1996). On the mechanism of the post-activation depression of the H-reflex in human subjects. *Experimental brain research* **108,** 450-462.

Hultborn H, Meunier S, Morin C & Pierrot-Deseilligny E. (1987a). Assessing changes in presynaptic inhibition of I a fibres: a study in man and the cat. *J Physiol* **389,** 729-756.

Hultborn H, Meunier S, Pierrot-Deseilligny E & Shindo M. (1987b). Changes in presynaptic inhibition of Ia fibres at the onset of voluntary contraction in man. *J Physiol* **389,** 757-772.

Hultborn H. (2006). Spinal reflexes, mechanisms and concepts: from Eccles to Lundberg and beyond. *Prog Neurobiol* **78,** 215-232.

Iles JF & Pisini JV. (1992). Cortical modulation of transmission in spinal reflex pathways of man. *J Physiol* **455,** 425-446.

Iles JF & Roberts RC. (1987). Inhibition of monosynaptic reflexes in the human lower limb. *J Physiol* **385,** 69-87.

Iles JF. (1996). Evidence for cutaneous and corticospinal modulation of presynaptic inhibition of Ia afferents from the human lower limb. *J Physiol* **491 (Pt 1),** 197-207.

Jankowska E, McCrea D & Mackel R. (1981). Oligosynaptic excitation of motoneurones by impulses in group Ia muscle spindle afferents in the cat. *J Physiol* **316,** 411-425.

Jankowska E, McCrea D, Rudomin P & Sykova E. (1981). Observations on neuronal pathways subserving primary afferent depolarization. *J Neurophysiol* **46,** 506-516.

Jankowska E. (1992). Interneuronal relay in spinal pathways from proprioceptors. *Prog Neurobiol* **38,** 335-378.

Jankus WR, Robinson LR & Little JW. (1994). Normal limits of side-to-side H-reflex amplitude variability. *Arch Phys Med Rehabil* **75,** 3-7.

Kagamihara Y & Masakado Y. (2005). Excitability of spinal inhibitory circuits in patients with spasticity. *J Clin Neurophysiol* **22,** 136-147.

Kangrga I, Jiang MC & Randic M. (1991). Actions of (-)-baclofen on rat dorsal horn neurons. *Brain Res* **562,** 265-275.

Kapitza S, Zorner B, Weinmann O, Bolliger M, Filli L, Dietz V & Schwab ME. (2012). Tail spasms in rat spinal cord injury: changes in interneuronal connectivity. *Exp Neurol* **236,** 179-189.

Kapitza S, Zorner B, Weinmann O, Bolliger M, Filli L, Dietz V & Schwab ME. (2012). Tail spasms in rat spinal cord injury: changes in interneuronal connectivity. *Exp Neurol* **236,** 179-189.

Khalki L, Sadlaoud K, Lerond J, Coq JO, Brezun JM, Vinay L, Coulon P & Bras H. (2018). Changes in innervation of lumbar motoneurons and organization of premotor network following training of transected adult rats. *Exp Neurol* **299,** 1-14.

Khan AS, Patrick SK, Roy FD, Gorassini MA & Yang JF. (2016). Training-Specific Neural Plasticity in Spinal Reflexes after Incomplete Spinal Cord Injury. *Neural Plast* **2016,** 6718763.

Knikou M & Mummidisetty CK. (2014). Locomotor training improves premotoneuronal control after chronic spinal cord injury. *J Neurophysiol* **111,** 2264-2275.

Koelman JH, Bour LJ, Hilgevoord AA, van Bruggen GJ & Ongerboer de Visser BW. (1993). Soleus H-reflex tests and clinical signs of the upper motor neuron syndrome. *J Neurol Neurosurg Psychiatry* **56,** 776-781.

Koelman JH, Bour LJ, Hilgevoord AA, van Bruggen GJ & Ongerboer de Visser BW. (1993). Soleus H-reflex tests and clinical signs of the upper motor neuron syndrome. *J Neurol Neurosurg Psychiatry* **56,** 776-781.

Kohn AF, Floeter MK & Hallett M. (1997). Presynaptic inhibition compared with homosynaptic depression as an explanation for soleus H-reflex depression in humans. *Exp Brain Res* **116,** 375-380.

Krenz NR & Weaver LC. (1998). Sprouting of primary afferent fibers after spinal cord transection in the rat. *Neuroscience* **85,** 443-458.

Kumru H, Albu S, Valls-Sole J, Murillo N, Tormos JM & Vidal J. (2015). Influence of spinal cord lesion level and severity on H-reflex excitability and recovery curve. *Muscle Nerve* **52,** 616-622.

Lalonde NR & Bui TV. (2021). Do spinal circuits still require gating of sensory information by presynaptic inhibition after spinal cord injury? *Current Opinion in Physiology* **19,** 113-

Lee JK, Emch GS, Johnson CS & Wrathall JR. (2005). Effect of spinal cord injury severity on alterations of the H-reflex. *Exp Neurol* **196,** 430-440.

Leppanen L & Stys PK. (1997). Ion transport and membrane potential in CNS myelinated axons. II. Effects of metabolic inhibition. *J Neurophysiol* **78,** 2095-2107.

Levy RA & Anderson EG. (1972). The effect of the GABA antagonists bicuculline and picrotoxin on primary afferent terminal excitability. *Brain Res* **43,** 171-180.

Li S, Zhuang C, Hao M, He X, Marquez JC, Niu CM & Lan N. (2015). Coordinated alpha and gamma control of muscles and spindles in movement and posture. *Front Comput Neurosci* **9,** 122.

Li Y & Bennett DJ. (2003). Persistent sodium and calcium currents cause plateau potentials in motoneurons of chronic spinal rats. *J Neurophysiol* **90,** 857-869.

Li Y, Li X, Harvey PJ & Bennett DJ. (2004). Effects of baclofen on spinal reflexes and persistent inward currents in motoneurons of chronic spinal rats with spasticity. *J Neurophysiol* **92,** 2694-2703.

Lin S, Li Y, Lucas-Osma AM, Hari K, Stephens MJ, Singla R, Heckman CJ, Zhang Y, Fouad K, Fenrich KK & Bennett DJ. (2019). Locomotor-related V3 interneurons initiate and coordinate muscles spasms after spinal cord injury. *J Neurophysiol* **121,** 1352-1367.

Liu M, Wu W, Li H, Li S, Huang LT, Yang YQ, Sun Q, Wang CX, Yu Z & Hang CH. (2015). Necroptosis, a novel type of programmed cell death, contributes to early neural cells damage after spinal cord injury in adult mice. *J Spinal Cord Med* **38,** 745-753.

Liu Y, Latremoliere A, Li X, Zhang Z, Chen M, Wang X, Fang C, Zhu J, Alexandre C, Gao Z, Chen B, Ding X, Zhou JY, Zhang Y, Chen C, Wang KH, Woolf CJ & He Z. (2018). Touch and tactile neuropathic pain sensitivity are set by corticospinal projections. *Nature* **561,** 547-550.

Loeza-Alcocer E, Canto-Bustos M, Aguilar J, Gonzalez-Ramirez R, Felix R & Delgado-Lezama R. (2013). alpha(5)GABA(A) receptors mediate primary afferent fiber tonic excitability in the turtle spinal cord. *J Neurophysiol* **110,** 2175-2184.

Lucas-Osma AM, Li Y, Lin S, Black S, Singla R, Fouad K, Fenrich KK & Bennett DJ. (2018). Extrasynaptic proportional, variant5GABAA receptors on proprioceptive afferents produce a tonic depolarization that modulates sodium channel function in the rat spinal cord. *J Neurophysiol*.

Luscher HR, Ruenzel P, Fetz E & Henneman E. (1979). Postsynatpic population potentials recorded from ventral roots perfused with isotonic sucrose: connections of groups Ia and II spindle afferent fibers with large populations of motoneurons. *J Neurophysiol* **42,** 1146-1164.

Magladery JW, Teasdall RD, Park AM & Languth HW. (1952). Electrophysiological studies of reflex activity in patients with lesions of the nervous system. I. A comparison of spinal motoneurone excitability following afferent nerve volleys in normal persons and patients with upper motor neurone lesions. *Bull Johns Hopkins Hosp* **91,** 219-244; passim.

Mailis A & Ashby P. (1990). Alterations in group Ia projections to motoneurons following spinal lesions in humans. *J Neurophysiol* **64,** 637-647.

Martinez-Valdes E, Negro F, Laine CM, Falla D, Mayer F & Farina D. (2017). Tracking motor units longitudinally across experimental sessions with high-density surface electromyography. *J Physiol* **595,** 1479-1496.

Masland WS. (1972). Facilitation during the H-reflex recovery cycle. *Arch Neurol* **26,** 313-319.

Matthews PB. (1996). Relationship of firing intervals of human motor units to the trajectory of post-spike after-hyperpolarization and synaptic noise. *The Journal of physiology* **492 (Pt 2),** 597-628.

Matthews PB. (1996). Relationship of firing intervals of human motor units to the trajectory of post-spike after-hyperpolarization and synaptic noise. *J Physiol* **492 (Pt 2),** 597-628.

Mayer WP, Murray AJ, Brenner-Morton S, Jessell TM, Tourtellotte WG & Akay T. (2018). Role of muscle spindle feedback in regulating muscle activity strength during walking at different speed in mice. *J Neurophysiol* **120,** 2484-2497.

McCartney MR, Deeb TZ, Henderson TN & Hales TG. (2007). Tonically active GABAA receptors in hippocampal pyramidal neurons exhibit constitutive GABA-independent gating. *Mol Pharmacol* **71,** 539-548.

McCrea DA, Shefchyk SJ & Carlen PL. (1990). Large reductions in composite monosynaptic EPSP amplitude following conditioning stimulation are not accounted for by increased postsynaptic conductances in motoneurons. *Neurosci Lett* **109,** 117-122.

Meisner JG, Marsh AD & Marsh DR. (2010). Loss of GABAergic interneurons in laminae I-III of the spinal cord dorsal horn contributes to reduced GABAergic tone and neuropathic pain after spinal cord injury. *J Neurotrauma* **27,** 729-737.

Mekhael W, Begum S, Samaddar S, Hassan M, Toruno P, Ahmed M, Gorin A, Maisano M, Ayad M & Ahmed Z. (2019). Repeated anodal trans-spinal direct current stimulation results in long-term reduction of spasticity in mice with spinal cord injury. *The Journal of physiology* **597,** 2201-2223.

Mende M, Fletcher EV, Belluardo JL, Pierce JP, Bommareddy PK, Weinrich JA, Kabir ZD, Schierberl KC, Pagiazitis JG, Mendelsohn AI, Francesconi A, Edwards RH, Milner TA, Rajadhyaksha AM, van Roessel PJ, Mentis GZ & Kaltschmidt JA. (2016). Sensory-Derived Glutamate Regulates Presynaptic Inhibitory Terminals in Mouse Spinal Cord. *Neuron* **90,** 1189-1202.

Metz K, Concha Matos I, Li Y, Afsharipour B, Thompson CK, Negro F, Quinlan KA, Bennett DJ & Gorassini M. (2022). Facilitation of sensory axon conduction to motoneurons

during cortical or sensory evoked primary afferent depolarization (PAD) in humans. Submitted *J. Physiol.*

Metz K, Concha-Matos I, Hari K, Bseis O, Afsharipour B, Lin S, Li Y, Fenrich KF, Bennett DJ & Gorassini M. (2022). Post-activation depression produces extensor H-reflex suppresion following flexor afferent conditioning. *BioRxiv*.

Metz K, Concha-Matos I, Li Y, Afsharipour B, Thompson CK, Negro F, Bennett DJ & Gorassini M. (2021). Facilitation of sensory axon conduction to motoneurons during cortical or sensory evoked primary afferent depolarization (PAD) in humans. *BioRxiv*.

Meunier S & Pierrot-Deseilligny E. (1998). Cortical control of presynaptic inhibition of Ia afferents in humans. *Experimental brain research* **119,** 415-426.

Milanov I. (1992). A comparative study of methods for estimation of presynaptic inhibition. *J Neurol* **239,** 287-292.

Mirbagheri MM, Barbeau H, Ladouceur M & Kearney RE. (2001). Intrinsic and reflex stiffness in normal and spastic, spinal cord injured subjects. *Exp Brain Res* **141,** 446-459.

Misiaszek JE. (2003). The H-reflex as a tool in neurophysiology: its limitations and uses in understanding nervous system function. *Muscle Nerve* **28,** 144-160.

Mizuno Y, Tanaka R & Yanagisawa N. (1971). Reciprocal group I inhibition on triceps surae motoneurons in man. *J Neurophysiol* **34,** 1010-1017.

Morin C, Pierrot-Deseilligny E & Hultborn H. (1984). Evidence for presynaptic inhibition of muscle spindle Ia afferents in man. *Neurosci Lett* **44,** 137-142.

Mott FW & Sherrington CS. (1895). Experiments upon the influence of sensory nerves upon movements and nutrition of the limbs. *Proceedings of the Royal Society* **B,** 481-488.

Murray KC, Stephens MJ, Ballou EW, Heckman CJ & Bennett DJ. (2011a). Motoneuron excitability and muscle spasms are regulated by 5-HT2B and 5-HT2C receptor activity. *J Neurophysiol* **105,** 731-748.

Murray KC, Stephens MJ, Rank M, D'Amico J, Gorassini MA & Bennett DJ. (2011b). Polysynaptic excitatory postsynaptic potentials that trigger spasms after spinal cord injury in rats are inhibited by 5-HT1B and 5-HT1F receptors. *J Neurophysiol* **106,** 925-943.

Nacimiento W, Sappok T, Brook GA, Toth L, Schoen SW, Noth J & Kreutzberg GW. (1995). Structural changes of anterior horn neurons and their synaptic input caudal to a low

thoracic spinal cord hemisection in the adult rat: a light and electron microscopic study. *Acta Neuropathol* **90,** 552-564.

Naftchi NE, Schlosser W & Horst WD. (1979). Correlation of changes in the GABA-ergic system with the development of spasticity in paraplegic cats. *Adv Exp Med Biol* **123,** 431-450.

Nakashima K, Rothwell JC, Day BL, Thompson PD & Marsden CD. (1990). Cutaneous effects on presynaptic inhibition of flexor Ia afferents in the human forearm. *J Physiol* **426,** 369-380.

Negro F, Muceli S, Castronovo AM, Holobar A & Farina D. (2016). Multi-channel intramuscular and surface EMG decomposition by convolutive blind source separation. *J Neural Eng* **13,** 026027.

Neher E & Sakaba T. (2001). Estimating transmitter release rates from postsynaptic current fluctuations. *J Neurosci* **21,** 9638-9654.

Nicol MJ & Walmsley B. (1991). A serial section electron microscope study of an identified Ia afferent collateral in the cat spinal cord. *J Comp Neurol* **314,** 257-277.

Nielsen J & Kagamihara Y. (1993). The regulation of presynaptic inhibition during co-contraction of antagonistic muscles in man. *J Physiol* **464,** 575-593.

Nielsen J & Petersen N. (1994). Is presynaptic inhibition distributed to corticospinal fibres in man? *J Physiol* **477,** 47-58.

Nielsen J, Petersen N & Crone C. (1995). Changes in transmission across synapses of Ia afferents in spastic patients. *Brain* **118 (Pt 4),** 995-1004.

Nielsen J, Petersen N, Ballegaard M, Biering-Sorensen F & Kiehn O. (1993a). H-reflexes are less depressed following muscle stretch in spastic spinal cord injured patients than in healthy subjects. *Experimental brain research* **97,** 173-176.

Nielsen JB, Crone C & Hultborn H. (2007). The spinal pathophysiology of spasticity--from a basic science point of view. *Acta Physiol (Oxf)* **189,** 171-180.

Nielsen JB, Morita H, Wenzelburger R, Deuschl G, Gossard JP & Hultborn H. (2019). Recruitment gain of spinal motor neuron pools in cat and human. *Experimental brain research*.

Noonan VK, Fingas M, Farry A, Baxter D, Singh A, Fehlings MG & Dvorak MF. (2012). Incidence and prevalence of spinal cord injury in Canada: a national perspective. *Neuroepidemiology* **38,** 219-226.

Norton JA, Bennett DJ, Knash ME, Murray KC & Gorassini MA. (2008). Changes in sensory-evoked synaptic activation of motoneurons after spinal cord injury in man. *Brain* **131,** 1478-1491.

Ondarza AB, Ye Z & Hulsebosch CE. (2003). Direct evidence of primary afferent sprouting in distant segments following spinal cord injury in the rat: colocalization of GAP-43 and CGRP. *Exp Neurol* **184,** 373-380.

O'Neill N & Sylantyev S. (2019). The Functional Role of Spontaneously Opening GABAA Receptors in Neural Transmission. *Front Mol Neurosci* **12,** 72.

Oyinbo CA. (2011). Secondary injury mechanisms in traumatic spinal cord injury: a nugget of this multiply cascade. *Acta Neurobiol Exp (Wars)* **71,** 281-299.

Pierce JP & Mendell LM. (1993). Quantitative ultrastructure of Ia boutons in the ventral horn: scaling and positional relationships. *J Neurosci* **13,** 4748-4763.

Pierrot-Deseilligny E, Katz R & Morin C. (1979). Evidence of Ib inhibition in human subjects. *Brain Res* **166,** 176-179.

Pierrot-Deseilligny E. (1997). Assessing changes in presynaptic inhibition of Ia afferents during movement in humans. *J Neurosci Methods* **74,** 189-199.

Powers RK & Binder MD. (2001). Input-output functions of mammalian motoneurons. *Rev Physiol Biochem Pharmacol* **143,** 137-263.

Prochazka A. (2015). Sensory control of normal movement and of movement aided by neural prostheses. *J Anat* **227,** 167-177.

Quadri SA, Farooqui M, Ikram A, Zafar A, Khan MA, Suriya SS, Claus CF, Fiani B, Rahman M, Ramachandran A, Armstrong IIT, Taqi MA & Mortazavi MM. (2018). Recent update on basic mechanisms of spinal cord injury. *Neurosurg Rev*.

Quevedo J, Eguibar JR, Jimenez I, Schmidt RF & Rudomin P. (1993). Primary afferent depolarization of muscle afferents elicited by stimulation of joint afferents in cats with intact neuraxis and during reversible spinalization. *J Neurophysiol* **70,** 1899-1910.

Rabchevsky AG & Kitzman PH. (2011). Latest approaches for the treatment of spasticity and autonomic dysreflexia in chronic spinal cord injury. *Neurotherapeutics* **8,** 274-282.

Rank MM, Murray KC, Stephens MJ, D'Amico J, Gorassini MA & Bennett DJ. (2011). Adrenergic receptors modulate motoneuron excitability, sensory synaptic transmission and muscle spasms after chronic spinal cord injury. *J Neurophysiol* **105,** 410-422.

Robertson B & Taylor WR. (1986). Effects of gamma-aminobutyric acid and (-)-baclofen on calcium and potassium currents in cat dorsal root ganglion neurones in vitro. *Br J Pharmacol* **89,** 661-672.

Roby-Brami A & Bussel B. (1990). Effects of flexor reflex afferent stimulation on the soleus H reflex in patients with a complete spinal cord lesion: evidence for presynaptic inhibition of Ia transmission. *Exp Brain Res* **81,** 593-601.

Rossi A, Decchi B & Ginanneschi F. (1999). Presynaptic excitability changes of group Ia fibres to muscle nociceptive stimulation in humans. *Brain Res* **818,** 12-22.

Rossignol S, Drew T, Brustein E & Jiang W. (1999). Locomotor performance and adaptation after partial or complete spinal cord lesions in the cat. *Prog Brain Res* **123,** 349-365.

Rothwell JC, Traub MM, Day BL, Obeso JA, Thomas PK & Marsden CD. (1982). Manual motor performance in a deafferented man. *Brain* **105 (Pt 3),** 515-542.

Rowald A, Komi S, Demesmaeker R, Baaklini E, Hernandez-Charpak SD, Paoles E, Montanaro H, Cassara A, Becce F, Lloyd B, Newton T, Ravier J, Kinany N, D'Ercole M, Paley A, Hankov N, Varescon C, McCracken L, Vat M, Caban M, Watrin A, Jacquet C, Bole-Feysot L, Harte C, Lorach H, Galvez A, Tschopp M, Herrmann N, Wacker M, Geernaert L, Fodor I, Radevich V, Van Den Keybus K, Eberle G, Pralong E, Roulet M, Ledoux JB, Fornari E, Mandija S, Mattera L, Martuzzi R, Nazarian B, Benkler S, Callegari S, Greiner N, Fuhrer B, Froeling M, Buse N, Denison T, Buschman R, Wende C, Ganty D, Bakker J, Delattre V, Lambert H, Minassian K, van den Berg CAT, Kavounoudias A, Micera S, Van De Ville D, Barraud Q, Kurt E, Kuster N, Neufeld E, Capogrosso M, Asboth L, Wagner FB, Bloch J & Courtine G. (2022). Activity-dependent spinal cord neuromodulation rapidly restores trunk and leg motor functions after complete paralysis. *Nat Med*.

Rudomin P & Schmidt RF. (1999). Presynaptic inhibition in the vertebrate spinal cord revisited. *Exp Brain Res* **129,** 1-37.

Rudomin P, Jimenez I, Solodkin M & Duenas S. (1983). Sites of action of segmental and descending control of transmission on pathways mediating PAD of Ia- and Ib-afferent fibers in cat spinal cord. *Journal of neurophysiology* **50,** 743-769.

Rudomin P. (1990). Presynaptic inhibition of muscle spindle and tendon organ afferents in the mammalian spinal cord. *Trends Neurosci* **13,** 499-505.

Rudomin P. (1999). Presynaptic selection of afferent inflow in the spinal cord. *J Physiol Paris* **93,** 329-347.

Russ JB, Verina T, Comer JD, Comi AM & Kaltschmidt JA. (2013). Corticospinal tract insult alters GABAergic circuitry in the mammalian spinal cord. *Front Neural Circuits* **7,** 150.

Ryge J, Winther O, Wienecke J, Sandelin A, Westerdahl AC, Hultborn H & Kiehn O. (2010). Transcriptional regulation of gene expression clusters in motor neurons following spinal cord injury. *BMC Genomics* **11,** 365.

Salio C, Merighi A & Bardoni R. (2017). GABAB receptors-mediated tonic inhibition of glutamate release from Abeta fibers in rat laminae III/IV of the spinal cord dorsal horn. *Mol Pain* **13,** 1744806917710041.

Schanne FA, Kane AB, Young EE & Farber JL. (1979). Calcium dependence of toxic cell death: a final common pathway. *Science* **206,** 700-702.

Schindler-Ivens S & Shields RK. (2000). Low frequency depression of H-reflexes in humans with acute and chronic spinal-cord injury. *Exp Brain Res* **133,** 233-241.

Senter HJ & Venes JL. (1979). Loss of autoregulation and posttraumatic ischemia following experimental spinal cord trauma. *J Neurosurg* **50,** 198-206.

Shefner JM, Berman SA, Sarkarati M & Young RR. (1992a). Recurrent inhibition is increased in patients with spinal cord injury. *Neurology* **42,** 2162-2168.

Shefner JM, Buchthal F & Krarup C. (1992). Recurrent potentials in human peripheral sensory nerve: possible evidence of primary afferent depolarization of the spinal cord. *Muscle Nerve* **15,** 1354-1363.

Sherrington CS. (1908). On reciprocal innervation of antagonist muscles. Twelfth Note - Proprioceptive reflexes. *Proc R Soc Lond B Biol Sci* **80,** 552-564.

Shreckengost J, Calvo J, Quevedo J & Hochman S. (2010). Bicuculline-sensitive primary afferent depolarization remains after greatly restricting synaptic transmission in the mammalian spinal cord. *J Neurosci* **30,** 5283-5288.

Silva NA, Sousa N, Reis RL & Salgado AJ. (2014). From basics to clinical: a comprehensive review on spinal cord injury. *Prog Neurobiol* **114,** 25-57.

Simon CM, Sharif S, Tan RP & LaPlaca MC. (2009). Spinal cord contusion causes acute plasma membrane damage. *J Neurotrauma* **26,** 563-574.

Simon O & Yelnik AP. (2010). Managing spasticity with drugs. *Eur J Phys Rehabil Med* **46,** 401-410.

Smith CC, Paton JFR, Chakrabarty S & Ichiyama RM. (2017). Descending Systems Direct Development of Key Spinal Motor Circuits. *J Neurosci* **37,** 6372-6387.

Spaulding SJ, Hayes KC & Harburn KL. (1987). Periodicity in the Hoffmann reflex recovery curve. *Exp Neurol* **98,** 13-25.

Stein RB. (1995). Presynaptic inhibition in humans. *Prog Neurobiol* **47,** 533-544.

Stratten WP & Barnes CD. (1971). Diazepam and presynaptic inhibition. *Neuropharmacology* **10,** 685-696.

Stuart GJ & Redman SJ. (1992). The role of GABAA and GABAB receptors in presynaptic inhibition of Ia EPSPs in cat spinal motoneurones. *J Physiol* **447,** 675-692.

Taborikova H & Sax DS. (1969). Conditioning of H-reflexes by a preceding subthreshold H-reflex stimulus. *Brain* **92,** 203-212.

Tachibana T, Noguchi K & Ruda MA. (2002). Analysis of gene expression following spinal cord injury in rat using complementary DNA microarray. *Neurosci Lett* **327,** 133-137.

Takeoka A & Arber S. (2019). Functional Local Proprioceptive Feedback Circuits Initiate and Maintain Locomotor Recovery after Spinal Cord Injury. *Cell Rep* **27,** 71-85 e73.

Takeoka A, Vollenweider I, Courtine G & Arber S. (2014). Muscle spindle feedback directs locomotor recovery and circuit reorganization after spinal cord injury. *Cell* **159,** 1626-1639.

Taylor A, Durbaba R, Ellaway PH & Rawlinson S. (2006). Static and dynamic gamma-motor output to ankle flexor muscles during locomotion in the decerebrate cat. *J Physiol* **571,** 711-723.

Thompson FJ, Reier PJ, Lucas CC & Parmer R. (1992). Altered patterns of reflex excitability subsequent to contusion injury of the rat spinal cord. *J Neurophysiol* **68,** 1473-1486.

Tillakaratne NJ, Mouria M, Ziv NB, Roy RR, Edgerton VR & Tobin AJ. (2000). Increased expression of glutamate decarboxylase (GAD(67)) in feline lumbar spinal cord after complete thoracic spinal cord transection. *J Neurosci Res* **60,** 219-230.

Traccis S, Rosati G, Patraskakis S, Bissakou M, Sau GF & Aiello I. (1987). Influences of neck receptors on soleus motoneuron excitability in man. *Exp Neurol* **95,** 76-84.

Treiman DM. (2001). GABAergic mechanisms in epilepsy. *Epilepsia* **42 Suppl 3,** 8-12.

Trigo FF, Marty A & Stell BM. (2008). Axonal GABAA receptors. *Eur J Neurosci* **28,** 841-848.

Turker KS & Powers RK. (1999). Effects of large excitatory and inhibitory inputs on motoneuron discharge rate and probability. *J Neurophysiol* **82,** 829-840.

Ueno M, Nakamura Y, Li J, Gu Z, Niehaus J, Maezawa M, Crone SA, Goulding M, Baccei ML & Yoshida Y. (2018). Corticospinal Circuits from the Sensory and Motor Cortices Differentially Regulate Skilled Movements through Distinct Spinal Interneurons. *Cell Rep* **23,** 1286-1300 e1287.

Valls-Sole J, Alvarez R & Tolosa ES. (1994). Responses of the soleus muscle to transcranial magnetic stimulation. *Electroencephalogr Clin Neurophysiol* **93,** 421-427.

Vincent JA, Gabriel HM, Deardorff AS, Nardelli P, Fyffe REW, Burkholder T & Cope TC. (2017). Muscle proprioceptors in adult rat: mechanosensory signaling and synapse distribution in spinal cord. *J Neurophysiol* **118,** 2687-2701.

Voerman GE, Gregoric M & Hermens HJ. (2005). Neurophysiological methods for the assessment of spasticity: the Hoffmann reflex, the tendon reflex, and the stretch reflex. *Disabil Rehabil* **27,** 33-68.

Wall PD. (1958). Excitability changes in afferent fibre terminations and their relation to slow potentials. *J Physiol* **142,** i3-21.

Walmsley B, Graham B & Nicol MJ. (1995). Serial E-M and simulation study of presynaptic inhibition along a group Ia collateral in the spinal cord. *J Neurophysiol* **74,** 616-623.

Wang L, Spary E, Deuchars J & Deuchars SA. (2008). Tonic GABAergic inhibition of sympathetic preganglionic neurons: a novel substrate for sympathetic control. *J Neurosci* **28,** 12445-12452.

Wernig A, Muller S, Nanassy A & Cagol E. (1995). Laufband therapy based on 'rules of spinal locomotion' is effective in spinal cord injured persons. *Eur J Neurosci* **7,** 823-829.

Willis WD, Jr. (1999). Dorsal root potentials and dorsal root reflexes: a double-edged sword. *Exp Brain Res* **124,** 395-421.

Willis WD, Nunez R & Rudomin P. (1976). Excitability changes of terminal arborizations of single Ia and Ib afferent fibers produced by muscle and cutaneous conditioning volleys. *J Neurophysiol* **39,** 1150-1159.

Willis WD. (2006). John Eccles' studies of spinal cord presynaptic inhibition. *Prog Neurobiol* **78,** 189-214.

Yang K, Wang D & Li YQ. (2001). Distribution and depression of the GABA(B) receptor in the spinal dorsal horn of adult rat. *Brain Res Bull* **55,** 479-485.

Yavuz US, Negro F, Diedrichs R & Farina D. (2018). Reciprocal inhibition between motor neurons of the tibialis anterior and triceps surae in humans. *J Neurophysiol* **119,** 1699-1706.

Zbili M & Debanne D. (2019). Past and Future of Analog-Digital Modulation of Synaptic Transmission. *Front Cell Neurosci* **13,** 160.

Zehr EP & Stein RB. (1999). Interaction of the Jendrassik maneuver with segmental presynaptic inhibition. *Exp Brain Res* **124,** 474-480.

Zhang F, Vierock J, Yizhar O, Fenno LE, Tsunoda S, Kianianmomeni A, Prigge M, Berndt A, Cushman J, Polle J, Magnuson J, Hegemann P & Deisseroth K. (2011). The microbial opsin family of optogenetic tools. *Cell* **147,** 1446-1457.

Zimmerman AL, Kovatsis EM, Pozsgai RY, Tasnim A, Zhang Q & Ginty DD. (2019). Distinct Modes of Presynaptic Inhibition of Cutaneous Afferents and Their Functions in Behavior. *Neuron* **102,** 420-434 e428.

Zorrilla de San Martin J, Trigo FF & Kawaguchi SY. (2017). Axonal GABAA receptors depolarize presynaptic terminals and facilitate transmitter release in cerebellar Purkinje cells. *J Physiol* **595,** 7477-7493.

Appendix

GABA facilitates spike propagation through branch points of sensory axons in the spinal cord

Krishnapriya Hari[1,7], Ana M. Lucas-Osma[1,2,7], Krista Metz[1], Shihao Lin[1], Noah Pardell[1], David A. Roszko[1], Sophie Black[1], Anna Minarik[1], Rahul Singla[1], Marilee J. Stephens[1,3], Robert A. Pearce[4], Karim Fouad[1,2], Kelvin E. Jones[1,5], Monica A. Gorassini[1,3,8], Keith K. Fenrich[1,2,8], Yaqing Li[1,6,8] and David J. Bennett[1,2,8,9*]

[1]Neuroscience and Mental Health Institute, University of Alberta, Edmonton, AB, T6G 2R3, Canada.
[2]Faculty of Rehabilitation Medicine, University of Alberta, Edmonton, AB, T6G 2G4, Canada.
[3]Department of Biomedical Engineering, Faculty of Medicine and Dentistry, T6G 2V2, University of Alberta, Edmonton, AB, Canada. [4]Department of Anesthesiology, Wisconsin-Madison, Madison, Wisconsin, 53792, USA. [5]Faculty of Kinesiology, Sport and Recreation, University of Alberta, Edmonton, AB, T6G 2H9, Canada. [6]Present address: Department of Physiology, Emory University, Atlanta, GA, 30322, USA. [7]These authors contributed equally. [8]Senior authors. [9]Lead Contact.
*Corresponding author: bennettd@ualberta.ca

Abstract

Movement and posture depend on sensory feedback that is regulated by specialized GABAergic neurons ($GAD2^+$) that form axo-axonic contacts onto myelinated proprioceptive sensory axons and are thought to be inhibitory. However, we report here that activating $GAD2^+$ neurons directly with optogenetics or indirectly by cutaneous stimulation actually facilitates sensory feedback to motoneurons in rodents and humans. $GABA_A$ receptors located at or near nodes of Ranvier of sensory axons cause this facilitation, by preventing spike propagation failure at the many axon branch points, which is otherwise common without GABA. In contrast, $GABA_A$ receptors are generally lacking from axon terminals and so cannot inhibit transmitter release onto motoneurons, unlike $GABA_B$ receptors that cause presynaptic inhibition. GABAergic innervation near nodes and branch points allows individual branches to function autonomously, with $GAD2^+$ neurons regulating which branches conduct, adding a computational layer to the neuronal networks generating movement and likely generalizing to other CNS axons.

Main

The ease with which animals move defies the complexity of the underlying neuronal circuits, which include corticospinal tracts (CSTs) that coordinate skilled movement, spinal interneurons that form central patterns generators (CPGs) for walking, and motoneurons that ultimately drive the muscles(Goulding, 2009). Sensory feedback ensures the final precision of such motor acts, with proprioceptive feedback to motoneurons producing a major part of the muscle activity in routine movement and posture(Capaday & Stein, 1986; Bennett *et al.*, 1996), without which coordination is poor(Andrechek *et al.*, 2002). Proprioceptive sensory feedback is regulated by specialized GABAergic neurons ($GAD2^+$; abbreviated $GABA_{axo}$ neurons) that form axo-axonic connections onto the sensory axon terminals(Hughes *et al.*, 2005; Betley *et al.*, 2009; Fink *et al.*, 2014). These neurons are thought to produce presynaptic inhibition of sensory feedback to motoneurons(Eccles *et al.*, 1961a; Rudomin & Schmidt, 1999; Engelman & MacDermott, 2004) and possibly limit inappropriate sensory feedback(Bennett *et al.*, 1996; Fink *et al.*, 2014). However, during movement the CST, CPG and even sensory neurons all augment $GABA_{axo}$

neuron activity(Jankowska *et al.*, 1981b; Rossignol *et al.*, 1998; Rudomin & Schmidt, 1999; Lucas-Osma *et al.*, 2018a; Ueno *et al.*, 2018; Zimmerman *et al.*, 2019) right at a time when sensory feedback is known to be increased to ensure precision and postural stability(Capaday & Stein, 1986; Bennett *et al.*, 1996), raising the question of whether $GABA_{axo}$ neurons have a yet undescribed excitatory action.

The long-standing view that GABAergic neurons and associated axonal $GABA_A$ receptors produce presynaptic inhibition of proprioceptive sensory axon terminals in adult mammals actually lacks direct evidence. This is largely because of the difficulty in recording from these small terminals(Lucas-Osma *et al.*, 2018a) and the technical limitations of previously employed reduced spinal cord preparations (immature)(Fink, 2013a; Fink *et al.*, 2014) or anesthetized animals, since anesthetics themselves modulate $GABA_A$ receptors(Eccles *et al.*, 1961a; Stuart & Redman, 1992). Thus, in this paper we used optogenetic approaches to directly target $GABA_{axo}$ neurons in awake animals and in isolated whole adult spinal cord preparations. Surprisingly, we found that optogenetically activating these GABAergic neurons markedly facilitates sensory axon transmission to motoneurons via axonal $GABA_A$ receptors, throwing into doubt the concept of presynaptic inhibition mediated by $GABA_A$ receptors.

The mechanism by which $GABA_A$ receptors are theorized to produced presynaptic inhibition is rather counterintuitive and based on indirect evidence(Stuart & Redman, 1992; Rudomin & Schmidt, 1999). That is, sensory axons, like many other axons, have high intracellular chloride concentrations, leading to an outward chloride ion flow through activated $GABA_A$ receptors(Rudomin & Schmidt, 1999; Szabadics *et al.*, 2006; Bardoni *et al.*, 2013). Thus, $GABA_A$ receptors cause a depolarization of sensory axons (primary afferent depolarization, PAD)(Barron & Matthews, 1938; Rudomin & Schmidt, 1999; Trigo *et al.*, 2008; Howell & Pugh, 2016; Lucas-Osma *et al.*, 2018a), which is on face value excitatory, rather than inhibitory, sometimes even evoking axon spikes(Lucas-Osma *et al.*, 2018a). Nevertheless, PAD and associated $GABA_A$ receptors have variously been theorized to cause presynaptic inhibition by depolarization-dependent inactivation or shunting of sodium currents at the sensory axon terminals(Cattaert & El Manira, 1999; Trigo *et al.*, 2008). However, we do not even know if terminals of large myelinated proprioceptive sensory axons express $GABA_A$ receptors at all, despite their demonstrated innervation by $GABA_{axo}$ neurons(Betley *et al.*, 2009). These terminals

appear to lack the α5 subunit of extrasynaptic $GABA_A$ receptors(Lucas-Osma *et al.*, 2018a) and the more ubiquitous β2/3 subunits of $GABA_A$ receptors(Alvarez *et al.*, 1996), but this leaves open the possibility that they express other $GABA_A$ subunits or $GABA_B$ receptors. We thus examined this question here and found again that $GABA_A$ receptors are generally not at these axon terminals, but are instead near sodium channels (Na_V) of the nodes of Ranvier throughout the myelinated regions of the axon, spatially coincident with innervation by $GABA_{axo}$ neurons, consistent with earlier electron microscopy observations of GABAergic innervation of afferent nodes(Walmsley *et al.*, 1995) and imaging of α5 subunits(Lucas-Osma *et al.*, 2018a). What then is the function of such $GABA_A$ receptors near sodium channels?

An unexplored possibility is that the depolarizing action of $GABA_A$ receptors (and $GABA_{axo}$ neurons) near nodes aids sodium spike propagation between axon nodes. This has not previously been considered, as spikes are thought to securely propagate from node to node, at least in the orthodromic direction(Lucas-Osma *et al.*, 2018a). Myelinated proprioceptive axons branch extensively in the spinal cord(Lucas-Osma *et al.*, 2018a)(Fig. 1a) and each branch point poses a theoretical risk for spike propagation failure at downstream nodes(Goldstein & Rall, 1974; Debanne *et al.*, 2011). However, branch points are always located at nodes (Na_V)(Lucas-Osma *et al.*, 2018a), likely to minimize this failure. Nevertheless, indirect evidence has suggested that propagation failure can occur(Swadlow *et al.*, 1980; Henneman *et al.*, 1984a; Wall & McMahon, 1994; Burke & Glenn, 1996). Thus, in the present study we sought direct evidence of nodal spike failure near branch points and examined whether $GABA_A$ receptors near or at nodes facilitates afferent conduction by preventing this failure. We already know that PAD and $GABA_A$ receptors lower the threshold for initiating axon spikes by extracellular stimulation(Wall, 1958), and even initiate spikes(Lucas-Osma *et al.*, 2018a), but do not know whether they aid normal spike propagation. We found that spike propagation depends so heavily on GABA that blocking GABA action makes the majority of proprioceptive sensory axons fail to propagate spikes to motoneurons, and thus GABA near sodium channels provides a powerful mechanism to turn on specific nodes and branches to regulate sensory feedback.

Results

Nodal $GABA_A$ and terminal $GABA_B$ receptors.

To confirm and extend previous observations that $GABA_A$ receptors are near nodes of proprioceptive sensory axons (group Ia) rather than at ventral terminals(Alvarez *et al.*, 1996; Lucas-Osma *et al.*, 2018a), we immunolabelled the most common subunits of synaptic and extrasynaptic $GABA_A$ receptors expressed in these axons(Wu *et al.*, 2021a), both in rats with neurobiotin filled axons (Fig. 1) and $VGLUT1^{Cre/+}$ mice with axons labelled by a reporter gene (Extended Data Fig. 1). $GABA_A$ receptors containing α5, α1, α2 and γ2 subunits were expressed on these axons, especially near sodium channels (< 6 μm away; Fig. 1c-f, Extended Data Fig. 1). Specifically, $GABA_A$ receptors were in the plasma membrane on large myelinated 1st and 2nd order branches in the spinal cord at their nodes (identified by large sodium channel clusters, nearby paranodal Caspr, and/or axonal tapers; Fig. 1a-c,e; Extended Data Fig. 1a,c,f), and on short unmyelinated terminal branches in the dorsal and intermediate laminae (3rd order; Figs. 1a,e). The latter were near the nodes on 1st order branches (< 100 μm away) where they can influence these nodes, consistent with previous observations of axonal GABAergic contacts(Walmsley *et al.*, 1995; Watson & Bazzaz, 2001). In contrast, $GABA_A$ receptors were mostly absent from the long unmyelinated ventral terminal branches, where the axon boutons synapse onto motoneurons in the ventral horn (3rd order; Figs. 1a,d,e; Extended Data Fig. 1b,d,g,h), which also generally lacked sodium channels(Lucas-Osma *et al.*, 2018a). This left $GABA_A$ receptors on average far from the terminal boutons contacting motoneurons (~500 μm; Fig. 1f) relative to the axon space constant (λ_S ~90 μm), with the majority of receptors in dorsal and intermediate laminae. Nodes were widely spaced, as were branch points (~50 μm separation, Fig. 1g), but branch points were always near nodes (Na_V; Fig. 1c,g), the latter providing additional evidence for nodal $GABA_A$ receptors, since these receptors were near branch points (Fig 1f). Nodes sometimes occurred without branching (49%, as in Fig. 1b, rat). Overall, synaptic α1 and α2 and extrasynaptic α5 $GABA_A$ receptors were each expressed in about 30% of nodes, roughly equally distributed among branched and unbranched nodes (Fig 1h). Importantly, the majority of nodes were electrotonically close (< 90 μm, λ_S) to $GABA_A$ receptors on a neighboring node (96%) or bouton (80%) on the same axon, thus leaving little doubt that nodes are somehow influenced by $GABA_A$ receptors. While synaptic α1 and α2 $GABA_A$ receptors

were in single large clusters, extrasynaptic α5 $GABA_A$ receptors were in multiple smaller clusters, some in the membrane at the node (yellow arrows), and others in the cytoplasm near the node (grey arrows, Fig 1c and Extended Data Fig 1a), though all membrane receptors were at nodes. In contrast to $GABA_A$ receptors, $GABA_B$ receptors were found mostly on terminal branches in the ventral horn where boutons had dense receptor expression (Fig. 1d-f, Extended Data Fig. 1e,g,h), and not usually on larger myelinated ventral or dorsal branches, and thus absent from nodes (Figs. 1c,e,h; Extended Data Fig. 1e).

Propagation failure in dorsal horn axon branches.

Considering that $GABA_A$ receptors are expressed in large myelinated dorsal branches of proprioceptive axons, we next directly recorded from these branches in the dorsal horn of rat and mouse spinal cords (Figs. 2 and 3) to examine whether spike propagation depends on these receptors. When we stimulated the dorsal root (DR) containing the axon branch, an all-or-nothing spike was recorded in many branches (Figs. 2b, 3d) at the latency of the fastest afferent volley that arrived at the spinal cord (group Ia afferents; EC in Fig. 2b). However, in other axon branches this spike did not occur (~20%), but at the same latency there was a small all-or-nothing residual spike (*failure potential, FP;* Ia afferents). This FP was indicative of a spike activating a distant node, but failing to propagate further to the recording site, leaving only its passively attenuated potential, with smaller FPs reflecting more distal failure points in the spinal cord (Figs. 2c-g, 3e-f; typically a few nodes away). Failure never occurred in the DR itself (Fig. 2f). The failing branches with FPs were otherwise indistinguishable from non-failing axon branches, exhibiting full spikes (> 60 mV) with current injection pulses (directly evoking spike; or aiding DR spike, Fig. 2c*ii*, g), and low conductances and resting potentials (~ -65 mV, Fig. 2h), ruling out penetration injury. With high repetitive DR stimulation rates all branches (100%) exhibited propagation failure and an associated FP (Fig. 2e-g), again with the FP implying that the spike is reliably initiated in the DR, but incompletely propagates within the spinal cord.

Axon spike failure was voltage dependent: in branches with failing spikes (FPs) depolarizations that brought the axon closer to threshold enabled full DR-evoked spikes (via current injection, Fig. 2c*i*; or spontaneous depolarization, Fig. 2d). Also, in branches without spike failure at rest (secure spikes) a steady hyperpolarizing current induced spike failure (FP), with more branches

failing with increasing hyperpolarization (Extended Data Fig. 2). With increasing hyperpolarization, nodes failed progressively more distal to the electrode, causing abrupt drops in the overall spike amplitude with each failure and a characteristic delay in the nodal spike prior to failure, with spike attenuation consistent with λ_S being about two internodal distances (~90 μm; Extended Data Fig. 2a-d). Simulating spike propagation by applying a brief current pulse to mimic the current arriving from an upstream node (and FP) yielded similar results, with full spikes evoked at rest, but hyperpolarization leading to a spike delay and then failure (Extended Data Fig. 3). Large depolarizations inactivated spikes, though outside of the physiological range (> - 50 mV, Extended Data Fig. 3b-c).

Nodal spike facilitation by GABA.

Since sensory axons are tonically depolarized by spontaneous GABA activity(Lucas-Osma *et al.*, 2018a), we wondered whether this $GABA_A$ current aids propagation. Blocking extrasynaptic α5 $GABA_A$ receptors (with L655708) or all $GABA_A$ receptors (with gabazine) increased the incidence of spike failure (to ~45% and 65%, respectively; Fig. 2f) and sensitivity to hyperpolarization (Extended Data Fig. 2e-h), without altering overall spike properties (Fig. 2g), implying that spike propagation is highly dependent on $GABA_A$ receptors located near enough to nodes to influence sodium channels (within λ_S). Application of 5-HT to mimic natural brainstem-derived 5-HT also increased failure (Fig. 2f), likely via its indirect inhibition of $GABA_A$ receptor activity(Lucas-Osma *et al.*, 2019).

Nodal spike facilitation by $GABA_{axo}$ neuron activation.

To examine whether $GABA_{axo}$ neurons facilitate spike propagation, we expressed light-sensitive channelrhodopsin-2 (ChR2) in $GAD2^+$ neurons in adult $GAD2^{CreER/+}$;$R26^{LSL\text{-}ChR2\text{-}EYFP}$ mice (termed GAD2//ChR2-EYFP mice, Fig. 3). A brief light pulse (5 - 10 ms) produced a long-lasting depolarization and spiking in these $GABA_{axo}$ neurons (Fig. 3a), followed by a longer lasting $GABA_A$-mediated depolarization (PAD) of proprioceptive axons at a monosynaptic latency that was blocked by gabazine (Fig. 3a-b). In these mice, spikes in proprioceptive axons failed with a similar incidence as observed in rats (Figs. 3c-h), but the light-evoked PAD prevented this failure (Fig. 3e-g), similar to direct depolarization. Occasionally, spikes were only

partially rescued by PAD (< 60 mV spikes; Fig. 3g), suggestive of PAD restoring conduction in some, but not all, nodes. In branches with secure non-failing spikes, light had minor effects (Fig. 3d), but blocking $GABA_A$ receptors again increased the incidence of spike failure (Fig. 3h).

In GAD2//ChR2-EYFP or GAD2//ChR2-EYFP//tdTom mice the EYFP and tdTom reporters labelled GABAergic neurons (Fig. 3k; $VGAT^+$, $GAD2^+$ and $VGLUT1^-$) residing near the central canal and throughout much of the dorsal horn (Fig. 3i-o, Extended Data Fig 4). These neurons densely innervated the dorsal horn (Fig. 3j,l,n; Extended Data Fig. 4a), and less densely innervated both the ventral horn and dorsal columns with terminal boutons (Fig. 3l,m,o), allowing GABAergic innervation of sensory axons along their entire length. They made both synaptic and perisynaptic contacts along proprioceptive Ia sensory axons labelled either intracellularly with neurobiotin or peripherally with a viral vector, both at nodes and sensory axon terminals (Figs. 3k, and 1e, Extended Data Fig 4), confirming their identity as $GABA_{axo}$ neurons. Consistent with the $GABA_A$ receptor distribution, ~25% of nodes were directly innervated by GABAergic $GAD2^+$ neurons ($GABA_{axo}$ neurons; Extended Data Fig. 4). Furthermore, the majority of nodes were electrotonically close ($< \lambda_S$) to such GABAergic contacts on a neighbouring node or an unmyelinated branch on the same axon (98% or 77%, respectively; Extended Data Fig. 4). Also, most nodes (95%) had nearby $GABA_{axo}$ terminal boutons not contacting the axon (within 5 µm, $GAD2^+$ or $VGAT^+$; Extended Data Fig. 4), potentially providing extrasynaptic GABA.

Consistent with the predominantly dorsal $GAD2^+$ innervation of nodes (Fig 3) and lack of terminal $GABA_A$ receptors (Fig 1), PAD was evoked by light focused on the dorsal horn, but not on the ventral horn (Fig 3b, bottom). Furthermore, light-evoked PAD improved axon conductance even after silencing neuronal circuits with CNQX (50 µM, n = 11/11 axons in two mice, not shown, as in Fig 3e-g), indicating that nodal facilitation is caused directly by $GABA_A$ receptors on the axon near the intra-axonal recording site and its nearby nodes (within ~λ), and not via an indirect circuit. GABAergic neurons contacting ventral sensory terminals (previously termed GABApre neurons(Fink *et al.*, 2014)) are likely a subpopulation of the $GAD2^+$ neurons that contact nodes and all terminals ($GABA_{axo}$ neurons, Fig 3), since many $GAD2^+$ neurons are

located in superficial dorsal laminae (Fig 4l), unlike GABApre neurons located near the central canal(Fink *et al.*, 2014).

Computer simulations of branch point failure and rescue by GABA.

To establish that spike failure arises at the branch points where GABA can influence them, we generated a computer simulation of a proprioceptive sensory axon arbour in the spinal cord (Extended Data Fig. 5)(Walmsley *et al.*, 1995). With simulated DR stimulation, spike failure occurred distal to complex branch points (at nodes N2 and N3 in Extended Data Fig. 5a-b) that had associated increases in net conductance, which shunted the nodal currents. Simulated nodal $GABA_A$ receptor activation rescued these failed spikes, with increasing $GABA_A$ receptor activation (g_{GABA}) preventing more branch point failures (Extended Data Fig. 5c). Importantly, a single well placed GABA contact (at either N2 or N3, or on a nearby bouton) rescued conduction in an entire branch. In contrast, when we moved all these $GABA_A$ receptors to the ventral terminals, then their activation did not rescue failed spikes (Extended Data Fig. 5d). This is because $GABA_A$-induced depolarizations (PAD) were attenuated sharply with distance (λ_S ~90 μm); so only PAD generated near nodes, and not far away at ventral terminals, was visible at the dorsal columns (Extended Data Fig. 5a,g-h), in agreement with previous terminal recordings(Lucas-Osma *et al.*, 2018a).

Spike facilitation by sensory evoked $GABA_{axo}$ activity

We next examined whether natural activation of $GABA_{axo}$ neurons affects proprioceptive axon conduction (Fig 4). $GABA_{axo}$ neurons are indirectly activated by sensory activity via two variants of a trisynaptic circuit, where sensory axons drive excitatory neurons that activate $GABA_{axo}$ neurons and cause PAD: one driven by cutaneous afferents and the other by proprioceptive afferents (Extended Data Figs. 6 and 7)(Lucas-Osma *et al.*, 2018a). As expected, following DR stimulation these circuits caused fast synaptic and slower extrasynaptic $GABA_A$ receptor mediated depolarizations of proprioceptive axons (termed sensory-evoked phasic PAD and tonic PAD, respectively(Lucas-Osma *et al.*, 2018a)) that were blocked by $GABA_A$ receptor antagonists, and mimicked by optogenetic activation of $GABA_{axo}$ neurons (Fig. 4a-d).

Like with direct $GABA_{axo}$ activation, spike propagation failure was prevented by sensory-evoked phasic PAD, regardless of whether the failure was spontaneous (Figs. 4e-f,h), 5-HT-induced (Fig. 4h), or repetition-induced (Extended Data Fig. 7b-f). The latter is particularly important because sensory axons naturally fire at high rates, where they are vulnerable to spike failure (Fig. 2e-f). This action of phasic PAD was abolished by gabazine but not L655708, supporting a synaptic origin (Fig. 4h). Slow extrasynaptic GABAergic depolarization (tonic PAD; L655708-sensitive(Lucas-Osma *et al.*, 2018a)) further facilitated spike propagation (Fig. 4g), especially as it built up with repeated DR stimulation (at 1 Hz; Extended Data Fig. 5b). Cutaneous (Extended Data Fig. 6), proprioceptive (Extended Data Fig. 7) or mixed afferent (Fig. 4e-h) -evoked PAD all helped prevent spike failure.

In secure non-failing axon branches sensory-evoked PAD (or optogenetic $GABA_{axo}$ activation) sped up the spikes and lowered their threshold (rheobase current; Fig. 3d and Extended Data Fig. 8a-d), as predicted from computer simulations (Extended Data Fig. 5e). Importantly, spike height was only slightly reduced during PAD (~1% or 1 mV) indicating that $GABA_A$ receptor conductances have minimal shunting action on nearby spikes (Fig. 3 and Extend Data Fig. 8a-d).

Failure of axon conduction to motoneurons and rescue by PAD.

To quantify the overall failure of spikes to conduct from the DR to the sensory axon terminals we measured whether axon branches not conducting during failure were *not* refractory to subsequent stimulation with a microelectrode in the ventral horn (Extended Data Fig. 9). This method indicated that about 50 – 80% of sensory axons failed to conduct to their ventral terminals under resting conditions, especially in long axons, whereas sensory-evoked PAD decreased failure to < 30%. Similar conclusions were reached by directly recording the extracellular afferent volley in the ventral horn produced by the spikes propagating from a DR stimulation to the motoneurons, which was consistently increased by PAD (Extended Data Fig. 10).

Facilitation of sensory feedback to motoneurons by $GABA_A$ receptors.

To examine the functional role of GABA in regulating sensory feedback to motoneurons, we recorded monosynaptic excitatory postsynaptic potentials (EPSPs) from motoneurons in response to proprioceptive sensory axon stimulation (Fig. 5). This EPSP was inhibited by optogenetically silencing $GABA_{axo}$ neurons with light in mice expressing archaerhodopsin-3 (Arch3, induced in $GAD2^{CreER/+}$;$R26^{LSL\text{-}Arch3\text{-}GFP}$ mice; abbreviated GAD2//Arch3, Fig. 5a-b,d), consistent with a tonic $GABA_A$ receptor tone facilitating spike propagation in axons. Likewise, the EPSP was reduced when sensory axon conduction was reduced by blocking endogenous $GABA_A$ receptor tone with antagonists, despite increasing motoneuron and polysynaptic reflex excitability (the latter minimized with APV, Fig. 5c,d). $GABA_B$ antagonists slightly increased the EPSP, suggesting a tonic $GABA_B$-mediated presynaptic inhibition (Fig. 5d), though much smaller than the tonic $GABA_A$-mediated nodal facilitation that dominates when all GABA was reduced (in GAD2//Arch3 mice).

Consistent with $GABA_A$ receptors and PAD facilitating axon conduction, the monosynaptic EPSP was facilitated during, but not after, depolarizing proprioceptive axons (evoking PAD) with an optogenetic activation of $GABA_{axo}$ neurons in GAD2//ChR2 mice (10 ms *light conditioning stimulation*; Fig. 5e-f). The EPSP was also facilitated by naturally activating $GABA_{axo}$ neurons by a *sensory conditioning stimulation* (Extended Data Fig. 11), including with a conditioning stimulation of cutaneous and/or proprioceptive afferents (Extended Data Fig. 11a,b,e). The latter indicates that proprioceptive activity primes subsequent proprioceptive reflex transmission (*self-facilitation*). $GABA_A$ receptor antagonists (gabazine), but not $GABA_B$ antagonists (CGP55845), blocked the EPSP facilitation with sensory (Extended Data Fig. 11e) or light (Fig. 5f) conditioning.

The facilitation of the EPSP by conditioning-evoked PAD arose from axonal $GABA_A$ receptors, rather than from postsynaptic actions on the motoneurons, since it occurred with weak conditioning stimuli that produced only a transient background postsynaptic depolarization that terminated before the EPSP testing (at 60 ms; Figs. 5e, Extended Data Fig. 11b,g), followed by a slight hyperpolarization that if anything would reduce the EPSP (shunting the synaptic current, Extended Data Fig. 11h). Increasing the DR conditioning intensity produced large background

depolarizing conductances in the motoneurons during the EPSP testing, which led to postsynaptic inhibition of the EPSP (shunting inhibition; Extended Data Fig. 11d,g) and post activation depression, masking the effect of nodal facilitation. Importantly, sometimes PAD itself induced afferent spikes (Extended Data Fig. 8e; termed DRR spikes), and following these spikes, the EPSP was always smaller than when these spikes were not present (n = 8/8 mice, not shown). This is because these DRR spikes themselves triggered EPSPs, leading to a post activation depression, as noted by Eccles(Eccles *et al.*, 1961a), and thus we minimized DRR activity by keeping the conditioning-evoked PAD small.

Sensory conditioning was particularly effective when it was repeated to mimic natural firing, which increased tonic PAD for minutes (Fig. 5g). This facilitated the EPSP for ~3 min after a brief fast DR repetition (200 Hz, 0.5 s conditioning, Fig. 5i, Extended Data Fig. 11e, *Tonic*), and ~1 min after slower repetition (0.1 Hz, 2 min conditioning, Extended Data Fig. 11e, *After effect*), both long outlasting postsynaptic effects from each conditioning pulse (< 1 s). This was blocked by L655708 or gabazine (Extended Data Fig. 11e). Interestingly, optogenetic activation of $GABA_{axo}$ neurons did not produce a similar after effect, consistent with this tonic PAD and associated nodal facilitation being mediated by extrasynaptic GABA spillover from other sources of GABA(Lucas-Osma *et al.*, 2018a).

Increases in the probability of unitary EPSPs by nodal facilitation.

We often noticed large all-or-nothing EPSPs (unitary EPSPs) spontaneously fluctuating on and off during repeated EPSP testing, leading to discrete large changes in the total EPSP size and time course (Fig. 5j-k). We thought this might be due to spontaneous branch point failures, rather than quantal changes in transmitter release that produce much smaller fluctuations(Redman, 1990), as previously suggested(Henneman *et al.*, 1984a). Indeed, when we increased the axon conduction by activating the $GABA_{axo}$ neurons and PAD (via a cutaneous conditioning train) the *probability* of unitary EPSPs occurring increased (Fig. 5k-l), and this sometimes recruited further large unitary EPSPs (Fig. 5k). In contrast, the *size* of the underlying unitary EPSP was not increased by this conditioning (Fig. 5j-l), ruling out decreases in terminal presynaptic inhibition or postsynaptic inhibition contributing to the increased overall EPSP (Fig. 5i,l). The unitary EPSP actually decreased slightly, likely from $GABA_B$ receptors causing presynaptic inhibition.

In contrast, the increased unitary EPSP probability arose from $GABA_A$ receptors causing nodal facilitation.

Facilitation of sensory feedback to motoneurons by $GABA_{axo}$ neurons in awake mice.

To determine whether $GABA_{axo}$ neurons increase sensory feedback to motoneurons in *awake* mice we activated these neurons with light applied through a window chronically implanted over the spinal cord of GAD2//ChR2 mice (Fig. 6), and assessed the monosynaptic reflex (MSR) recorded in tail muscles in response to nerve stimulation (counterpart of EPSPs; Fig 6a-c). As expected, the MSR was facilitated by a conditioning light pulse, but only during, and not after, the expected time of phasic PAD induced on sensory axons (Fig. 6b-d,j). This light-induced *facilitation* occurred both at rest and when there was a background voluntary contraction, with the latter matched with and without light, again ruling out postsynaptic depolarization related differences in MSR (Fig. 6d). Light alone caused a brief pause in ongoing EMG (~30 ms post-light; Fig. 6b), indicative of postsynaptic inhibition, which masked nodal facilitation at short intervals.

Facilitation of sensory feedback to motoneurons during PAD in awake rat and humans.

When we evoked PAD by cutaneous sensory stimulation in awake rats (Extended Data Fig. 12) or humans (Extended Data Fig. 13) the MSR reflex recorded in the tail or lower leg (soleus) was again increased and L655708 sensitive, consistent with the increased EPSPs seen in rats in vitro (Fig 5). This generalizes our main finding to lumbar spinal circuits that control the leg. Importantly, the probability of a single motor unit (MU) contributing to the human MSR was increased by cutaneous conditioning (Extended Data Fig. 13f*i-ii*). This occurred without an increase in the estimated EPSP amplitude or rise time (PSF; see Methods; Extended Data Fig. 13F*iii*) or motoneuron depolarization prior to the MSR testing (Extended Data Fig. 13F*iv*), consistent with an increased probability of unitary EPSPs and decreased branch point failure, as in rats (Fig. 5).

Discussion

Following the pioneering studies of Eccles on inhibition of the monosynaptic connection from sensory axons to motoneurons(Eccles *et al.*, 1961a), the concept of presynaptic inhibition of axon terminals has stood as a cornerstone of our understanding of mammalian brain and spinal cord function(Engelman & MacDermott, 2004). While presynaptic inhibition has never been directly confirmed in these sensory axons, recordings from invertebrate sensory axons have established the idea that terminal $GABA_A$ receptor-mediated depolarizations (PAD) can cause conductance increases or sodium channel inactivation that inhibit transmitter release(Cattaert & El Manira, 1999; Trigo *et al.*, 2008). Thus, our finding that $GABA_A$ receptors are located too far (relative to the short λ_S) from the axon terminals to influence terminal depolarizations or cause presynaptic inhibition of transmitter release onto motoneurons had not been anticipated. However, in retrospect a lack of terminal $GABA_A$ receptors had previously been noted(Alvarez *et al.*, 1996; Lucas-Osma *et al.*, 2018a), as had a lack of ventral terminal depolarization during $GABA_{axo}$ neuron activity(Lucas-Osma *et al.*, 2018a) (Extended Data Table 1). Direct recordings from terminal boutons of other axon types in the mammalian brain, such as the Calyx of Held, have shown that terminal $GABA_A$ or glycine receptors sometimes cause presynaptic inhibition, and at other times facilitate transmitter release, depending on their action on terminal calcium and potassium channels(Trigo *et al.*, 2008; Howell & Pugh, 2016; Zbili & Debanne, 2019). However, these terminal actions of GABA are very different from the actions of GABA near the nodes that we have uncovered. That is, $GABA_A$ receptors or direct current injections near sodium channels help prevent conduction failure at nodes downstream to a branch point by depolarizing the failing nodes closer to spike threshold (nodal facilitation; summarized in Fig 7), similar to the relief from spike failure seen by depolarization in the leech(Swadlow *et al.*, 1980). Neuronal circuits that control $GABA_{axo}$ neurons help produce this PAD and associated nodal facilitation, as does tonic PAD produced by spillover of GABA from any source during repeated cutaneous stimulation(Lucas-Osma *et al.*, 2018a), ultimately inducing a tonic GABAergic facilitation of nodal conduction (ArchT and gabazine-sensitive). The profound inhibitory action of $GABA_A$ receptors antagonists or optogenetic inhibition of $GABA_{axo}$ neurons on PAD and sensory transmission demonstrates that without axonal GABA, and associated depolarizations, nodal spike transmission fails in many central branches of large myelinated proprioceptive

sensory axons, leaving large silent branches, depending on the branching structure (Extended Data Fig 5) and prior history of activity (firing frequency; see also(Swadlow *et al.*, 1980)). This inhibitory action is not due to $GABA_A$ receptor antagonists working on neuronal circuits that somehow indirectly affect PAD, because tonic PAD and nodal facilitation are resistant to blocking all circuit activity with TTX or CNQX, and blocked by subsequent application of these $GABA_A$ antagonists(Lucas-Osma *et al.*, 2018a).

Our computer simulations demonstrate that spike conduction failure is only initiated at particularly vulnerable branch points, as previously suggested(Swadlow *et al.*, 1980), and thus only nodes at or downstream of these failure points require GABAergic facilitation, consistent with the observation that $GABA_A$ receptors and GABAergic contacts ($VGAT^+$, $GAD2^+$) are only at or near a fraction of nodes (Fig 1)(Walmsley *et al.*, 1995). For this, $GABA_A$ receptors need only be within 90 μm of the node (λ_S), at another node or even on one of the short unmyelinated terminal branches in dorsal and intermediate regions connected to the node. Ultrastructural imaging of the spinal cord has demonstrated that $GABA_A$ receptors often lack presynaptic contacts(Alvarez *et al.*, 1996), consistent with many GABA receptors being activated extrasynaptically from spillover of nearby GABA, and accounting for the fewer number of nodes with GABAergic contacts than nodes with GABA receptors. Limitations in our confocal imaging leave many open questions for future study, including the precise spatial relation of GABA receptors to sodium channels, myelin and intracellular structures. We cannot rule out the possibility that the oligodendrocytes at the paranode influence GABAergic control of the axon, since they express GABA receptors and GABA(Serrano-Regal *et al.*, 2020), and $GABA_{axo}$ contacts sometimes straddle the paranodal myelin and the node, maybe forming a tripartite neuron-glia-axon arrangement. Nevertheless, our observations of GABA facilitating conduction to these dorsal branches can only be accounted for by nodal facilitation, regardless of the details of how GABA innervates these nodes or nearby branches. The concept of nodal facilitation that we describe here may generalize to other large central axons, such as pyramidal cells, that are innervated by GABAergic neurons, branch extensively (and so may fail), and have depolarizing actions of GABA(Szabadics *et al.*, 2006; Trigo *et al.*, 2008; Zorrilla de San Martin *et al.*, 2017; Burke & Bender, 2019), allowing selective recruitment of specific axon branches and functional pathways, especially for high frequency firing (as in Extended Data Fig. 7).

Sensory driven $GABA_{axo}$ circuits and associated PAD are experimentally convenient, since they allow us to estimate how sensory transmission to motoneurons is modulated with $GABA_{axo}$ neuron activity in humans. Specifically, the expected time-course of PAD evoked by cutaneous conditioning is associated with a potent reflex facilitation in humans and awake rodents. This suggests a substantial ongoing spike failure prior to facilitation that can be alleviated by $GABA_{axo}$ activity (PAD). Indeed, we found that during PAD the *probability* of EPSPs occurring (and MU firing) is increased without changing the EPSP *size*, as estimated by PSFs in humans. The latter rules out changes in presynaptic inhibition with PAD that *grades* the EPSP size, including ruling out previous arguments that MSR facilitation by cutaneous conditioning is due to a removal of presynaptic inhibition(Rudomin *et al.*, 1974; Aimonetti *et al.*, 2000b).

A pressing question that remains is how can nearly a century of research on sensory transmission and presynaptic inhibition be reconciled with GABA-mediated nodal facilitation and reflex facilitation (summarized in Extended Data Table 1)? Sensory axon conduction failure has repeatedly been noted from indirect observations(Swadlow *et al.*, 1980; Henneman *et al.*, 1984a; Wall & McMahon, 1994; Li *et al.*, 2020), but $GABA_A$ receptors and PAD were previously thought to cause, rather than prevent, conduction failure(Wall & McMahon, 1994), even though computer simulations showed physiological GABA levels unlikely to block spike propagation(Walmsley *et al.*, 1995), as we confirmed. Furthermore, the fundamental assumption that $GABA_A$ receptors cause presynaptic inhibition that reduces transmitter release from sensory axons was from the outset circumspect, based mainly on the observation that a conditioning stimulation on a flexor nerve caused an inhibition of the MSR evoked in extensor muscles that was somewhat correlated to the time-course of PAD caused by this conditioning in flexor afferents(Eccles *et al.*, 1961a). However, in retrospect this PAD is too brief to account for the much longer (up to 1 s) inhibition caused by this conditioning(Eccles *et al.*, 1961a; Curtis & Lacey, 1994; Rudomin & Schmidt, 1999), and $GABA_B$ receptor antagonists block much of this MSR inhibition(Curtis & Lacey, 1994; Fink, 2013a). This fits with $GABA_B$ receptors being at the terminals (Fig. 1) and being primarily responsible for presynaptic inhibition in proprioceptive axons, as in other neurons(Trigo *et al.*, 2008; Howell & Pugh, 2016), though further study of $GABA_B$ receptor function is now needed. This predominant $GABA_B$ receptor action in

proprioceptive axon terminals does not rule out $GABA_A$-mediated presynaptic inhibition in other sensory axons that have terminal $GABA_A$ receptor expression, such as cutaneous Aβ afferents(Lucas-Osma *et al.*, 2018a).

Anatomical studies suggest that $GABA_{axo}$ neuron activation is likely accompanied by some postsynaptic inhibition, since most $GABA_{axo}$ contacts on afferent terminals also contact motoneurons, in a triad(Pierce & Mendell, 1993; Hughes *et al.*, 2005). Indeed, we find that $GABA_{axo}$ neuron activation produces an inhibition of motoneurons (Fig. 6b) and associated MU firing that masks, and at times overwhelms, the facilitation of the MSR by $GABA_A$ receptors (as with muscle vibration; Extended Data Fig. 13), and thus is readily mistaken for presynaptic inhibition. The argument that presynaptic inhibition with conditioning should be evident from reductions in the EPSP without changing its time course(McCrea *et al.*, 1990) now seems untenable, especially as conditioned unitary EPSPs differ markedly in shape and conditioning increases the number of unitary EPSPs contributing to the EPSP, as different axon branches are recruited (Fig. 5k)(Henneman *et al.*, 1984a).

Early on Barron and Matthews(Barron & Matthews, 1938) and later others(Fink *et al.*, 2014; Lucas-Osma *et al.*, 2018a) established that sensory-evoked PAD (or light-evoked) excites axons by directly inducing spiking, including spikes in the sensory axons mediating the MSR itself, raising a further contradiction with presynaptic inhibition. While these PAD-triggered spikes only sometimes fully propagate antidromically out the DR(Beloozerova & Rossignol, 1999), they are more likely to conduct orthodromically(Lucas-Osma *et al.*, 2018a) where they activate the motoneurons(Eccles *et al.*, 1961a; Fink *et al.*, 2014), making these axons and their motoneuron synapse refractory to subsequent testing(Eccles *et al.*, 1961a). This contributes to a long-lasting *post activation depression* of the MSR pathway that is $GABA_A$-mediated (sensitive to $GABA_A$ antagonists, like PAD) and is thus readily mistaken for $GABA_A$-mediated presynaptic inhibition(Stuart & Redman, 1992; Fink, 2013a; Fink *et al.*, 2014). While such PAD-triggered spikes are fundamentally excitatory, it remains an open question as to the physiological role of their induced post activation depression.

Functionally, nodal facilitation and regulation of branch point failure by $GABA_{axo}$-driven $GABA_A$ receptors acts like a global switching system that recruits entire silent sensory or motor circuits. This system works in concert with terminal presynaptic inhibition (including $GABA_B$ receptor action) that locally fine tunes reflex gains to optimize the stability and compliance of the limbs(Bennett *et al.*, 1996; Fink *et al.*, 2014). The direct activation of $GABA_{axo}$ neurons and associated PAD by cortical (CST) and spinal (CPG) circuits(Rossignol *et al.*, 1998; Russ *et al.*, 2013; Ueno *et al.*, 2018), and inhibition by the brainstem (e.g. 5-HT)(Nelson *et al.*, 1979; Lucas-Osma *et al.*, 2019), suggests that nodal facilitation is under explicit central control during reaching and locomotion. The widespread action of PAD, occurring simultaneously over many spinal segments,(Rudomin & Schmidt, 1999; Lucas-Osma *et al.*, 2018a) implies that nodal facilitation acts over large regions of the spinal cord to ready sensory axons for action during cortical, spinal or sensory evoked activity, reminiscent of the Jendrassik maneuver(Zehr & Stein, 1999), ensuring that adequate sensory feedback aids postural stability and walking. More generally, our results imply that each axonal branch point has the capacity to function separately, depending on its GABAergic innervation, increasing the complexity of sensory processing in the spinal cord.

Methods

Adult mice, rats and humans used.

Recordings were made from large proprioceptive group Ia sensory afferents, GABAergic neurons, motoneurons and muscles in adult mice (2.5 – 6 months old, both female and male equally; strains detailed below) and rats (3 - 8 months old, female only, Sprague-Dawley). All experimental procedures were approved by the University of Alberta Animal Care and Use Committee, Health Sciences division. Recordings were also made from the soleus muscle of neurologically intact adult humans (female and male equally), aged 21 to 58, with written informed consent prior to participation. Experiments were approved by the Health Research Ethics Board of the University of Alberta (Protocols 00023530 and 00076790) and conformed to the Declaration of Helsinki. No effects of sex were noted and data from both sexes were combined for analysis.

Mice used for optogenetics and imaging.

We evaluated GABAergic neurons in a strain of mice with Cre expressed under the endogenous *Gad2* promotor region. *Gad2* encodes the Glutamate decarboxylase 2 enzyme GAD2 (also called GAD65), which is unique to axoaxonic contacting GABAergic neurons that project to the ventral horn, whereas all GABAergic neurons express GAD1(Betley *et al.*, 2009). These $GAD2^{+}$ neurons were activated or inhibit optogenetically using channelrhodopsin-2 (ChR2)(Zhang *et al.*, 2011; Pinol *et al.*, 2012) or archaerhodopsin-3 (Ach3)(Chow *et al.*, 2010; Kralj *et al.*, 2011), respectively. The following mouse strains were employed (Extended Data Table 2):
1) *Gad2*$^{tm1(cre/ERT2)Zjh}$ mice (abbreviated $Gad2^{CreER}$ mice; The Jackson Laboratory, Stock # 010702; $CreER^{T2}$ fusion protein expressed under control of the endogenous *Gad2* promotor)(Taniguchi *et al.*, 2011),
2) B6;129S-*Gt(ROSA)26Sor*$^{tm32(CAG-COP4*H134R/EYFP)Hze}$ mice (abbreviated $R26^{LSL\text{-}ChR2\text{-}EYFP}$ mice; The Jackson Laboratory, Stock # 012569; ChR2-EYFP fusion protein expressed under the R26::CAG promotor in cells that co-express Cre because a loxP-flanked STOP cassette, LSL, prevents transcription of the downstream ChR2-EYFP gene)(Madisen *et al.*, 2012),
3) B6.Cg-*Gt(ROSA)26Sor*$^{tm14(CAG-tdTomato)Hze}$ and B6.Cg-*Gt(ROSA)26Sor*$^{tm9(CAG-tdTomato)Hze}$ mice (abbreviated $R26^{LSL\text{-}tdTom}$ mice; The Jackson Laboratory, Stock # 007914 and #007909;

tdTomato fluorescent protein expressed under the R26::CAG promotor in cells that co-express Cre)(Madisen *et al.*, 2010),
4) B6;129S-*Gt(ROSA)26Sor*$^{tm35.1(CAG-aop3/GFP)Hze}$ mice (abbreviated R26$^{LSL\text{-}Arch3\text{-}GFP}$ mice; The Jackson Laboratory Stock # 012735; Arch3-GFP fusion protein expressed under the R26::CAG promotor in cells that co-express Cre)(Madisen *et al.*, 2012),
5) B6;129S-*Slc17a7*$^{tm1.1(cre)Hze}$ mice (abbreviated VGLUT1^{Cre} mice; The Jackson Laboratory, Stock # 023527; Cre protein expressed under control of the endogenous *Vglut1* promotor; spinal cords kindly donated by Dr. Francisco J. Alvarez)(Harris *et al.*, 2014) and
6) EIIa-cre x Gabra5-floxed in a C57BL/6 mouse background, with cre bred out to yield α5 $GABA_A$ receptor knockout mice (termed Gabra5 KO mice; produced by RA Pearce laboratory). Gabra5-floxed mice are specifically C57BL/6-Gabra5tm2.1Uru/J mice and possess loxP sites flanking exons 4-5 of the Gabra5 receptor subunit gene. EIIa-cre mice are specifically 6.FVB-Tg(EIIa-cre)C5379Lmgd/J (The Jackson Laboratory, Stock # 003724).

Heterozygous GAD2^{CreER} mice (i.e., GAD2$^{CreER/+}$ mice) were crossed with homozygous reporter strains to generate GAD2$^{CreER/+}$; R26$^{LSL\text{-}ChR2\text{-}EYFP}$, GAD2$^{CreER/+}$; R26$^{LSL\text{-}tdTom}$ and GAD2$^{CreER/+}$; R26$^{LSL\text{-}Arch3\text{-}GFP}$ mice that we abbreviate: GAD2//ChR2, GAD2//tdTom and GAD2//Arch3 mice. Offspring without the GAD2^{CreER} mutation, but with the effectors ChR2, Arch3 or tdTom were used as controls. We also used mice bred by crossing homozygous VGLUT1^{Cre} mice with R26$^{lsl\text{-}tdTom}$ reporter mice to obtain mice with VGLUT1 labelled sensory axons(Todd *et al.*, 2003).

CreER is an inducible form of Cre that requires tamoxifen to activate (Feil *et al.*, 1997), which we applied in adult mice to prevent developmental issues of earlier induction of Cre. Specifically, mice were injected at 4 - 6 weeks old with two doses of tamoxifen separated by two days, and studied > 1 month later, long after washout of tamoxifen. Each injection was 0.2 mg/g wt (i.p.) of tamoxifen dissolved in a corn oil delivery vehicle (Sigma C8267). These tamoxifen-treated mice were denoted GAD2//ChR2+ and GAD2//Arch3+, and non treated mice were used as controls and denoted GAD2//ChR2- and GAD2//Arch2-. For all mice, genotyping was performed according to the Jackson Laboratories protocols by PCR of ear biopsies using primers specific for the appropriate mutant and wild type alleles for each of the mouse lines (see Extended Data Table 2 for primer details).

Ex vivo recording from axons and motoneurons in whole adult spinal cords.

Mice or rats were anaesthetized with urethane (for mice 0.11 g/100 g, with a maximum dose of 0.065 g; and for rats 0.18 g/100 g, with a maximum dose of 0.45 g), a laminectomy was performed, and then the entire sacrocaudal spinal cord was rapidly removed and immersed in oxygenated modified artificial cerebrospinal fluid (mACSF), as detailed previously (Harvey *et al.*, 2006; Murray *et al.*, 2010; Murray *et al.*, 2011b). This preparation is particularly useful as the small sacrocaudal spinal cord is the only portion of the adult spinal cord that survives whole ex vivo, allowing axon conduction to be assessed along large distances. Furthermore, this segment of cord innervates the axial muscles of the tail that are readily assessable for reflex recording in awake animals, and has proven to be a useful model of motor function in normal and injured spinal cords, with very similar spinal circuitry, reflex and motoneuron properties to those seen in the hindlimb of other preparations, including having reciprocal inhibition, Ia afferent innervation of muscle spindles and monosynaptic reflexes(Bennett *et al.*, 1999; Bennett *et al.*, 2001; Li *et al.*, 2004a; Murray *et al.*, 2010). Interestingly, the rat motoneuron firing rates in the sacral region are more similar to those in human hindlimb motoneurons than the much higher firing rats seen in rat hindlimb motoneurons, and thus the sacral cord has proven to be a useful model of lumbar motoneuron function in humans(Heckmann *et al.*, 2005). Spinal roots were removed, except the sacral S3, S4 and caudal Ca1 ventral and dorsal roots on both sides of the cord. After 1.5 hours in the dissection chamber (at 20° C), the cord was transferred to a recording chamber containing normal ACSF (nACSF) maintained at 23 - 32°C, with a flow rate > 3 ml/min. A one-hour period in nACSF was given to wash out the residual anaesthetic prior to recording, at which time the nACSF was recycled in a closed system. The cord was secured onto tissue paper at the bottom of a rubber (Silguard) chamber by insect pins in connective tissue and cut root fragments. The dorsal surface of the cord was usually oriented upwards when making intracellular recording from afferents in the dorsal horn, whereas the cord was oriented with its left side upwards when making recordings from motoneurons or afferent terminals in the ventral horn. The laser beam used for optogenetics was focused vertically downward on the GAD2 neurons, as detailed below.

Optogenetic regulation of $GABA_{axo}$ neurons.

The GAD2//ChR2 or GAD2//Arch3 mice were used to optogenetically excite or inhibit GAD2+ neurons (with 447 nm D442001FX and 532 nM LRS-0532-GFM-00200-01 lasers from Laserglow Technologies, Toronto), respectively, using methods we previously described (Lin *et al.*, 2019). Light was derived from the laser passed through a fibre optic cable (MFP_200/220/900-0.22_2m_FC-ZF1.25 and MFP_200/240/3000-0.22_2m_FC-FC, Doric Lenses, Quebec City) and then a half cylindrical prism the length of about two spinal segments (8 mm; 3.9 mm focal length, Thor Labs, Newton, USA,), which collimated the light into a narrow long beam (200 µm wide and 8 mm long). This narrow beam was usually focused longitudinally on the left side of the spinal cord roughly at the level of the dorsal horn, to target the epicentre of $GABA_{axo}$ neurons, which are dorsally located (Fig. 3). ChR2 rapidly depolarizes neurons (Zhang *et al.*, 2011), and thus we used 5 – 10 ms light pulses to activate $GABA_{axo}$ neurons, as confirmed by direct recordings from these neuron (see below). Light was always kept at a minimal intensity, 1.1x T, where T is the threshold to evoke a light response in sensory axons, which made local heating from light unlikely. Arch3 is a proton pump that is activated by green light, leading to a hyperpolarization and slowly increased pH (over seconds), both of which inhibit the neurons (Zhang *et al.*, 2011; El-Gaby *et al.*, 2016). Thus, we used longer light pulses (~200 ms) to inhibit $GABA_{axo}$ neurons.

To directly confirm the presence of functional ChR2 expression in $GABA_{axo}$ neurons of GAD2//ChR2 mice we recorded from them with similar methods and intracellular electrodes used to record from motoneurons (see below). Electrodes were advanced into these cells through the dorsal horn (with the dorsal surface oriented upwards), and their identity established by a direct response to light activation of the ChR2 construct (5 – 10 ms light pulse, 447 nm), without a synaptic delay (<1 ms) and continued light response after blocking synaptic transmission.

Dorsal and ventral root stimulation.

Dorsal and ventral roots (DR and VR) were mounted on silver-silver chloride wires above the nASCF of the recording chamber and covered with grease (a 3:1 mixture of petroleum jelly and mineral oil) for monopolar stimulation (Li *et al.*, 2004a; Li *et al.*, 2017; Lucas-Osma *et al.*,

2018a). This grease was surrounded by a more viscous synthetic high vacuum grease to prevent oil leaking into the bath flow. Bipolar stimulation was also used at times to reduce the stimulus artifact during recording from ventral roots (detailed below). Roots were stimulated with a constant current stimulator (Isoflex, Israel) with short pulses (0.1 ms). Note that proprioceptive afferents are selectively activated by low intensity DR stimulation (1.1 – 1.5 x afferent volley threshold, T) and cutaneous afferents are additionally activated by higher intensity DR stimulation (2 – 3xT). DRs were dissected to be as long as possible, and the distal end of this root was stimulated, so it was ~20 mm way from the spinal cord. In this way the DR stimulation site itself (at wire, and threshold for stimulation) could not be affected by axonal depolarizations in the spinal cord, since dorsal root potentials from spinal events (PAD) are only observed very close to the cord (within a few mm, see below), and drop exponentially in size with distance(Lucas-Osma *et al.*, 2018a).

Intracellular recording from sensory axon branches in the dorsal horn.

Electrode preparation and amplifier. Recording from fine afferent collaterals in the spinal cord without damaging them or disturbing their intracellular milieu required specialized ultra-sharp intracellular electrodes modified from those we developed for motoneuron recording(Harvey *et al.*, 2006). That is, glass capillary tubes (1.5 mm and 0.86 mm outer and inner diameters, respectively; with filament; 603000 A-M Systems; Sequim, USA) were pulled with a Sutter P-87 puller (Flaming-Brown; Sutter Instrument, Novato, USA) set to make bee-stinger shaped electrodes with a short relatively wide final shaft (~1 mm) that tapered slowly from 30 to 3 µm over its length, and then abruptly tapered to a final tip over the final 20 µm length. The tip was subsequently bevelled to a < 100 nm hypodermic-shaped point, as verified with electron microscope images (Harvey et al. 2006). This very small tip and wide shaft gave a combination of ease of penetrating axons in dense adult connective tissue, and good current-passing capabilities to both control the potential and fill the axons with neurobiotin. Prior to beveling, electrodes were filled through their tips with 2 M K-acetate mixed with varying proportions of 2 M KCl (to make KCl concentrations ranging of 0, 100, 500, and 1000 mM) or 500 mM KCl in 0.1 Trizma buffer with 5 - 10% neurobiotin (Vector Labs, Birmingame, USA). Electrodes were then beveled from an initial resistance of 40 - 150 MΩ to 30 - 40 MΩ using a rotary beveller (Sutter BV-10). GABAergic chloride-mediated potentials (PAD) and their

reversal potentials were the same with different concentrations of KCl, without passing large amounts of negative current, as we have previously detailed(Lucas-Osma *et al.*, 2018a), indicating that the ultra-sharp tips impeded passive fluid exchange between the electrode and intracellular milieu, with in particular electrode Cl^- not affecting the axon; thus, recordings were mostly made with electrodes with 1 M K-acetate and 1 M KCl, when not filling cells with neurobiotin.

Intracellular recording and current injection were performed with an Axoclamp2B amplifier (Axon Inst. and Molecular Devices, San Jose, USA). Recordings were low pass filtered at 10 kHz and sampled at 30 kHz (Clampex and Clampfit; Molecular Devices, San Jose, USA). Sometimes recordings were made in discontinuous-single-electrode voltage-clamp (gain 0.8 – 2.5nA/mV; for Ca PICs) or discontinuous-current-clamp modes (switching rate 7 kHz), as indicated (the latter only when injecting current, for example during recording of input resistance or the voltage dependence of spikes).

Axon penetration. Electrodes were advanced into myelinated afferents of the sacrocaudal spinal cord with a stepper motor (Model 2662, Kopf, USA, 10 μm steps at maximal speed, 4 mm/s), usually at the boundary between the dorsal columns and dorsal horn gray matter, where axons bundle together densely, as they branch and descend to the ventral horn (Extended Data Fig 4A). Extracellular tissue (especially myelin in the white matter) often impeded and blocked the electrode tip following a forward step, as determined by an increase in resistance to small current pulses passed from the tip of the electrode (20 ms, -0.3 nA, 1 Hz), and this was cleared with a brief high frequency current (from capacitance overcompensation buzz) and moving backwards slowly, the latter which helped prevent tissue dimpling. Prior to penetrating afferents, we recorded the extracellular (EC) afferent volley following dorsal root (DR) stimulation (0.1 ms pulses, 3xT, T: afferent volley threshold, where T = ~3 uA, repeated at 1 Hz), to determine the minimum latency and threshold of afferents entering the spinal cord. The group Ia afferent volley occurs first with a latency of 0.5 - 1.0 ms, depending on the root length (which were kept as long as possible, 10 - 20 mm), corresponding to a conduction velocity of about 16 - 24 m/s, as previously described for in vitro conduction at 23 C (Li *et al.*, 2004b; Lucas-Osma *et al.*, 2018a). When a forward step penetrated an axon, small slow movements were made to stabilize the

recordings. Penetrations were usually in the myelinated portion of the axon between nodes, rather than at nodes, because the chance of penetrating a node is low since they only make up a small fraction of the total axon length (Fig. 1). The spikes from the two nodes adjacent to the electrode were readily detected separately when testing for the spike threshold with current injection pulses (20 ms; rheobase test), because just at threshold the current sometimes evoked a spike from just one node and not the other, which usually halved the total spike height, consistent with the penetration being about halfway between the two nodes separated by about a space constant distance.

Proprioceptive afferent identification. Upon penetration, afferents were identified with direct orthodromic spikes evoked from DR stimulation. We focused on the lowest threshold proprioceptive group Ia afferents, identified by their direct response to DR stimulation, very low threshold (< 1.5 x T, T: afferent volley threshold), short latency (group Ia latency, coincident with onset of afferent volley), and antidromic response to ventral horn afferent terminal microstimulation (~ 10 μA stimulation via tungsten microelectrode to activate Ia afferent terminals; tested in some afferents, detailed below)(Lucas-Osma *et al.*, 2018a). Post hoc these were confirmed to be large proprioceptive Ia afferents by their unique extensive terminal branching around motoneurons, unlike large cutaneous Aβ afferents that do not project to the ventral horn. Clean axon penetrations without injury occurred abruptly with a sharp pop detected on speakers attached to the recorded signal, the membrane potential settling rapidly to near – 70 mV, and > 70 mV spikes usually readily evoked by DR stimulation or brief current injection pulses (1 – 3 nA, 20 ms, 1 Hz). Sensory axons also had a characteristic >100 ms long depolarization following stimulation of a dorsal root (primary afferent depolarization, PAD, at 4 - 5 ms latency, detailed below) and short spike afterhyperpolarization (AHP ~ 10 ms), which further distinguished them from other axons or neurons. Injured axons had higher resting potentials (> - 60 mV), poor spikes (< 60 mV) and low resistance (to current pulse; R_m < 10 MΩ), and were discarded.

Quantification of spike conduction failure in the dorsal horn: failure potentials (FPs). Sometimes healthy intracellular penetrations were made into a sensory axon branch (e.g. < -60 mV rest, large PAD), but dorsal root stimulation did not evoke a full spike, even though a full >

60 mV spike could be readily evoked by intracellular current injection. Instead, DR stimulation evoked a partial spike at the latency and threshold of group Ia afferents, indicating that this was a branch of a Ia afferent that failed to fully conduct spikes to the electrode, with only the passively attenuated spike from the last node to spike prior to conduction failure recorded at the electrode (failure potential, FP; also referred to as electronic residue by Luscher(Luscher *et al.*, 1994a)). The size of the FP reflected how far away the spike failure occurred, with spatial attenuation corresponding to a space constant of about 90 μm (see Results), and so FPs became exponentially smaller with distance from failure and undetectable when many mm away (nodes separated by about 50 μm). Occasionally axons were penetrated with undetectable DR evoked spikes or FPs, but otherwise they had characteristics of a Ia afferent (PAD, R_m similar). These were likely afferents with FPs too distal to detect, but were usually excluded from the main analysis to avoid ambiguity, though this underestimates the incidence of failure. However, some of these axons exhibited short latency, low threshold DR spikes when depolarized by a prior DR stimulation (PAD) of an adjacent DR, in which case they were unequivocally Ia afferents and included in the analysis (Fig. 4f).

Both during extracellular and intracellular recording the group Ia afferent volley (small negative field) was observed as the first event after DR stimulation (the latter subthreshold to a spike), though this was usually small in relation to intracellular events and ignored. However, this was sometimes removed from the intracellular record by subtracting the extracellular potential recorded just outside the same axon to determine the actual transmembrane potential (Lucas-Osma *et al.*, 2018a). This was necessary to see the very smallest FPs following DR stimulation in some afferents, as the negative volley from other nearby afferents obscured the FPs.

After quantifying the axons spikes and conduction failures (FPs) under resting conditions, we then examined the changes in spike conduction with changes in membrane potential induced by either directly injecting current into axons or inducing GABA-mediated changes in membrane potential by pharmacological methods, optogenetic methods (activating ChR2 on $GABA_{axo}$ neurons to induce PAD) or more naturally evoking PAD with a DR stimulation.

Neurobiotin filling of axons. Some of the proprioceptive afferents that we recorded intracellularly were subsequently filled with neurobiotin by passing a very large positive 2 - 4 nA current with 90% duty cycle (900 ms on, 100 ms off) for 10 - 20 min. The identity of group Ia proprioceptive afferents were then confirmed anatomically by their unique extensive innervation of motoneurons(Lucas-Osma *et al.*, 2018a). Prior to penetrating and filling axons with neurobiotin filled electrodes, a small negative holding current was maintained on the electrodes to avoid spilling neurobiotin outside axons.

Quantification of spike conduction failure in the ventral horn

Wall's method. To measure whether spikes fail during propagation to their fine terminals in the ventral horn we examined whether failed axon segments were relatively less refractory to activation after spike conduction failure, using a double pulse method adapted from Wall(Wall & McMahon, 1994; Wall, 1998). The essence of the method is that after DR activation all nodes that generate spikes become relatively refractory for a few ms, whereas nodes that fail to spike are not refractory to activation. Thus, a microelectrode placed near these failing nodes more readily activates them if they fail rather than generate spikes with DR stimulation and orthodromic conduction. For this we placed a tungston microelectrode (12 MΩ, #575400, A-M Systems, Sequim, USA) in the ventral horn near the axons terminals on motoneurons, to activate the branches/nodes of the axon projecting to the motoneuron that may have failed (VH stimulation).

Spikes from VH or DR stimulation were recorded intracellularly in a proprioceptive Ia axon penetrated in the dorsal columns directly above the VH stimulation site or in an adjacent segment, with two combinations of double axon stimulations. First, we applied two rapidly repeated VH stimuli (VH doublet; two 0.1 ms pulses) at a ~4 ms interval to make the axon relatively refractory to stimulation and determine both the threshold current to activate the first spike (T_{VH1}, with VH1 stimulation) and the higher threshold current to overcome this the inactivation and generate a second spike (T_{VH2}, with VH2 stimulation). Second, we repeated this double spike activation, but with the first activation from a supra-threshold DR stimulation (at 1.5x DR threshold) and the second from a VH stimulation at the T_{VH2} intensity from B (DR-VH pair). In this case the VH stimulation readily activates the axon spike if the orthodromic DR

evoked spike does not propagate to the ventral horn, leaving the silent portion of the axon non refractory. Accordingly, we also determined the threshold current to activate the VH after the DH in this arrangement (termed $T_{DR,VH}$), which was lower than T_{VH2}. For comparison to the spike inactivation with VH doublets, we adjusted the DR-VH pair timing slightly so that the pairs of spikes (or expected spikes, at vertical lines) are separated by the same interval (~ 4 ms) when they reach the recording site, to compensate for DR conduction delays. The putative spike failure with DR stimulation happens at a node somewhere between the recording site and the VH, because we only studied axons that securely conducted single DR pulses to the recording site, and thus failure was not directly visible.

We quantified the spike failure based on the following considerations: If the DR-evoked spike entirely fails to propagate to the VH, then the threshold for subsequently activating the ventral horn ($T_{DR,VH}$) should be the same as the threshold without any prior activation ($T_{VH1} = T_{DR,VH}$), whereas if it does not fail, then the threshold for activating the ventral horn should be the same as with a VH doublet ($T_{VH2} = T_{DR,VH}$). In between these two extreme scenarios, the DR evoked spike may only partially fail to propagate spikes to the ventral horn (by only some of its branches failing or conducting only partially to the VH); in this case $T_{DR,VH}$ should be between T_{VH1} and T_{VH2}, with the difference $T_{VH2} - T_{VH1}$ representing the range of possible thresholds between full failure and full conduction. Thus, overall the failure was quantified as: $Conduction\ failure = (T_{VH2} - T_{DR,VH}) / (T_{VH2} - T_{VH1}) \times 100\%,$ which is 100% at full failure and 0% with no failure. This estimate is predicated on the assumption that the failed spikes are only relatively refractory to conduction and increased stimulation can overcome this failure, which is reasonable for the interspike intervals we used, and means that the computed % failure reflects the number of nodes that failed to spike, with more dorsal branch point failures giving more failed nodes. On the other hand, we used interspike intervals that were short enough for the DR stimulation not to evoke PAD that affected the subsequent spike threshold (~ 4 ms), in contrast to the longer intervals where PAD can help DR doublet firing (DR-DR in Extended Data Fig. 7, ~ 5 - 10 ms).

Extracellular recording from sensory axon terminals. To directly record spike conduction in proprioceptive afferent terminal branches in the VH we used our intracellular glass pipette electrode (~30 MΩ) positioned just outside these axons (extracellular, EC), to avoid penetration

injury in these fine axon branches. The DR was stimulated near threshold for spikes (1.1xT, T: afferent volley threshold) to evoke the EC response in a few single axons near the electrode, and many trials were averaged to remove noise from these small signals (20 – 50 trials at 3 s intervals). The EC field was multiphasic as previously described for other axons(Dudel, 1965; Hubbard *et al.*, 1969; Munson & Sypert, 1979a), with a small initial positive field resulting from passively conducted axial current from sodium spikes at distant nodes (closer to the DR; outward current at electrode), some of which fail to propagate spikes to the VH recording site, making this field a measure of conduction failure(Dudel, 1965; Hubbard *et al.*, 1969). Following this, a larger negative field arises, resulting from spikes arising at nodes near the electrode (inward current), making this negative field a measure of secure conduction. A relatively large stimulus artifact is present prior to these fields, due to the small size of the EC fields themselves, and we truncated this.

We conducted three control experiments to confirm the relation of these EC fields to spike conduction. First, in the dorsal horn where we can readily intracellularly record from large proprioceptive axon branches, we compared intracellular (IC) recordings from axons to EC recordings just outside the same axon, to confirm that the DR evoked spike (IC) arrives at about the time of the negative EC field. Second, we locally applied TTX to the DR near the recording site (10 µl bolus of 100 µM TTX over DR) which eliminated the negative field and left only the initial positive field, confirming that the positive field is from distal nodes upstream of the TTX block, and generated by passive axial current conduction. This is important, since some investigators have argued on theoretical grounds that the positive field can instead result from the closed-end electrical properties of axons at their terminals(Katz & Miledi, 1965), rather than spike failure, though others have refuted this(Dudel, 1965). Finally, we improved nodal spike conduction by reducing the divalent cations Mg^{++} and Ca^{++} in the bath medium, since divalent cations normally cause a gating or guarding action on the sodium channel, the latter by one charge binding to the membrane and the other raising the local extracellular positive charge, and overall raising the local voltage drop across the channel and its spike threshold(Armstrong & Cota, 1991). This decreased the failure-related initial positive field and increased the main EC negative field, indicating improved conduction, and again confirming the use of these fields as

measures of conduction, similar to previous conclusions for the motor endplate(Hubbard *et al.*, 1969) and mathematical consideration of axon cable properties (Stein, 1980).

To quantify the EC fields we estimated the overall conduction to the recording site as: *Conduction Index = nf / (nf + pf) x 100%*, where pf and nf are the positive and negative EC field amplitudes. This conduction index approaches 100% for full conduction (pf ~=0) and 0% for no conduction (*nf* = 0). The absolute EC field potential amplitudes are highly variable between different recordings sites, and thus are difficult to quantify across animals and sites, whereas this ratio of field amplitudes (nf / (nf + pf)) eliminates the variability, and can effectively be viewed as a normalization of the negative field (nf) by the total field peak-to-peak size (nf + pf).

Intracellular recording from motoneurons.

The same intracellular glass electrode, stepper motor and amplifier used for recording sensory axons were used for intracellular recording from motoneurons, except that the electrodes were bevelled to a lower resistance (30 MΩ). The electrode was advanced into motoneurons with fast 2 μm steps and brief high frequency currents (capacitance overcompensation) guided by audio feedback from a speaker. After penetration, motoneuron identification was made with antidromic ventral root stimulation, and noting ventral horn location, input resistance and time constant (> 6 ms for motoneurons)(Murray *et al.*, 2010). The monosynaptic excitatory postsynaptic potentials (EPSPs) and associated currents (EPSCs) were measured in motoneurons following stimulation of dorsal roots (at 1.1- 1.5 xT, 0.1 ms, 3 – 10 s trial intervals). These were identified as monosynaptic by their rapid onset (first component), lack of variability in latency (< 1 ms jitter), persistence at high rates (10 Hz) and appearance in isolation at the threshold for DR stimulation (< 1.1xT; T, Threshold for EPSP, which also equals afferent volley threshold), unlike polysynaptic EPSPs which varying in latency, disappear at high rates, and mostly need stronger DR stimulation to activate.

Dorsal and ventral root grease gap recording.

In addition to recording directly from single proprioceptive axons and motoneurons, we employed a grease gap method to record the composite intracellular response of many sensory

axons or motoneurons by recording from dorsal and ventral roots, respectively, as previously detailed for similar sucrose and grease gap methods, where a high impedance seal on the axon reduces extracellular currents, allowing the recording to reflect intracellular potentials(Luscher *et al.*, 1979; Stein, 1980; Leppanen & Stys, 1997a; Lucas-Osma *et al.*, 2018a). We mounted the freshly cut roots onto silver-silver chloride wires just above the bath, and covered them in grease over about a 2 mm length, as detailed above for monopolar recordings. Return and ground wires were in the bath and likewise made of silver-silver chloride. Specifically for sensory axons, we recorded from the central ends of dorsal roots cut within about 2 - 4 mm of their entry into the spinal cord, to give the compound potential from all afferents in the root (dorsal roots potential, DRP), which has previously been shown to correspond to PAD, though it is attenuated compared to the intracellular recordings of PAD(Lucas-Osma *et al.*, 2018a). The signal attenuation has two reasons. First the voltage PAD is attenuated along the length of nerve in the bath, as detailed in the next paragraph. Second, the grease does not completely remove the extracellular fluid around the nerve, even though we deliberately allowed the nerve to dry for a few seconds before greasing, and this causes a conductance that shunts or short circuits the recorded signal, reducing it by about half(Hubbard *et al.*, 1969; Leppanen & Stys, 1997a). For optogenetic experiments we additionally added silicon carbide powder (9 % wt, Tech-Met, Markham) to the grease to make it opaque to light and minimize light induced artifactual current in the silver-silver chloride recording wire during optogenetic activation of ChR2 (detailed below). Likewise, we covered our bath ground and recording return wires with a plastic shield to prevent stray light artifacts. The dorsal root recordings were amplified (2,000 times), high-pass filtered at 0.1 Hz to remove drift, low-pass filtered at 10 kHz, and sampled at 30 kHz (Axoscope 8; Axon Instruments/Molecular Devices, Burlingame, CA).

These grease gap recordings of PAD on sensory afferents reflect only the response of largest diameter axons in the dorsal root, mainly group I proprioceptive afferents, because of the following considerations. First, the largest axons in peripheral nerves have a nodal spacing of about 1 mm(Rushton, 1951; Arbuthnott *et al.*, 1980), and length constants λ_S are estimated to be similar, at about 1 – 2 times the nodal spacing(Blight, 1985), Further, in our recordings we were only able to get the grease to within about 2 mm of the spinal cord. Thus, the centrally generated signal (PAD) is attenuated exponentially with distance x along the axon length in the bath (x = 2

mm). This is proportional to exp(– x / λ_S) (see (Stein, 1980)), which is 1 / e^2 = 0.11 for x = 2 λ_S, as is approximately the case here. This makes a central PAD of about 4 mV appear as a ~0.4 mV potential on the root recording (DRP, 10 times smaller), as we previously reported(Lucas-Osma *et al.*, 2018a). Furthermore, the nodal spacing and λ_S decrease linearly with smaller axon diameters(Rushton, 1951; Stein, 1980), making the voltages recorded on the smaller afferents contribute to much less of the compound root potential (halving the diameter attenuates PAD instead by $1/e^4$ or 0.012, which is 99% attenuation). Finally, unmyelinated sensory axons attenuate voltages over a much shorter distance than myelinated axons, since that membrane resistance (Rm) drops markedly without myelin and λ_S is proportional to $\sqrt{Rm/Ri}$ (where Ri is axial resistance; Stein 1980). Thus, any centrally generated change in potential in these small axons is unlikely to contribute to the recorded signal 2 mm away.

The composite EPSPs in many motoneurons were likewise recorded from the central cut end of ventral roots mounted in grease (grease gap), which has also previously been shown to yield reliable estimates of the EPSPs, though again attenuated by the distance from the motoneurons(Fedirchuk *et al.*, 1999). The monosynaptic EPSPs were again identified as monosynaptic by their rapid onset (first component, ~1 ms after afferent volley arrives in the ventral horn; see below), lack of variability in latency (< 1 ms jitter), persistence at high rates (10 Hz) and appearance in isolation at the threshold (T) for evoking EPSPs with DR stimulation (< 1.1xT, T ~ afferent volley threshold), unlike polysynaptic reflexes which varying in latency, disappear at high rates, and mostly need stronger DR stimulation to activate.

Analysis of synaptic responses in sensory axons (PAD) and motoneurons (EPSPs).

When we recorded from sensory axons of an associated dorsal root (directly or via the dorsal roots) stimulation of an adjacent dorsal root (not containing the recorded axon; 0.1 ms, 1 – 3xT; T: threshold to evoke PAD or EPSPs, same as afferent volley threshold) evoked a characteristic large and long depolarization of the afferents, previously demonstrated to be mediated by GABAergic input onto the sensory axons(Lucas-Osma *et al.*, 2018a). This depolarization is termed primary afferent depolarization (PAD). PAD occurs at a minimal latency of 4 – 5 ms following the afferent volley, consistent with its minimally trisynaptic origin(Jankowska *et al.*,

1981b; Lucas-Osma *et al.*, 2018a), making it readily distinguishable from earlier events on the axon. PAD has a fast synaptic component evoked by a single DR stimulation (rising within 30 ms and decaying exponentially over < 100 ms; termed phasic PAD) and a slower longer lasting extrasynaptic component (starting at about 30 ms and lasting many seconds) that is enhanced by repeated DR stimulation (tonic PAD, especially with cutaneous stimulation)(Lucas-Osma *et al.*, 2018a). We used this sensory activation of PAD or direct optogenetic activation of PAD to examine the action of GABA on sensory axon spike transmission to motoneurons, usually evoking phasic PAD about 10 – 60 ms prior to spikes or associated EPSPs on motoneurons (during phasic PAD), though we also examined longer lasting effects of tonic PAD evoked by repeated DR stimulation. Sometimes PAD is so large that it directly evokes spikes on the afferents, and these travel out the dorsal root, and thus they have been termed dorsal root reflexes (DRRs)(Barron & Matthews, 1938; Lucas-Osma *et al.*, 2018a). We usually minimized these DRRs by keeping the DR stimulus that evokes PAD low (1.1 - 3.0 xT), though there were inevitably some DRRs, as they even occur in vivo in cats and humans(Eccles *et al.*, 1961a; Shefner *et al.*, 1992b; Beloozerova & Rossignol, 1999).

When we recorded from motoneurons (directly or via ventral roots) stimulation of proprioceptive afferents in a dorsal root (0.1 ms, 1.1-1.5xT, T: EPSP threshold, which is similar to afferent volley threshold) evoked a monosynaptic EPSP, and associated monosynaptic reflex (MSR, spikes from EPSP). This EPSP is depressed by fast repetition (rate depended depression, RDD) (Boulenguez *et al.*, 2010), and thus to study the EPSP we evoked it at long intervals (10 s, 0.1 Hz rate) where RDD was less. However, even with this slow repetition rate (0.1 Hz), at the start of testing the first EPSP was often not similar to the steady state EPSP after repeated testing. Thus, to avoid RDD we usually ran the 0.1 Hz EPSP testing continuously throughout the experiment, at least until a steady state response was reached (after 10 minutes). We then examined the action of activating (or inhibiting) $GABA_{axo}$ neurons on this steady state EPSP, by introducing light or sensory conditioning that activated these neurons at varying intervals (inter-stimulus intervals, ISIs) prior to each EPSP stimulation (control, GAD2//ChR2 mice and GAD2//Arch3 mice). We averaged the EPSP from ~10 trials (over 100 s) just before conditioning and then 10 trials during conditioning, and then computed the change in the peak size of the monosynaptic EPSP with conditioning from these averages. After conditioning was completed EPSP testing continued and

any residual changes in the EPSP was computed from the 10 trials following conditioning (after-effect). Finally, EPSP testing continued over many minutes after which the original steady state EPSP was established. The background motoneuron potential, membrane resistance (Rm) and time constant just prior to the EPSP was also assessed before and after conditioning to examine whether there were any postsynaptic changes that might contribute to changes in the EPSP with conditioning. Along with the VR recordings, we simultaneously recorded PAD from DRs by similar averaging methods (10 trials of conditioning), to establish the relation of changes in EPSPs with associated sensory axon depolarization PAD.

Drugs and solutions

Two kinds of artificial cerebrospinal fluid (ACSF) were used in these experiments: a modified ACSF (mACSF) in the dissection chamber prior to recording and a normal ACSF (nACSF) in the recording chamber. The mACSF was composed of (in mM) 118 NaCl, 24 NaHCO3, 1.5 CaCl2, 3 KCl, 5 MgCl2, 1.4 NaH2PO4, 1.3 MgSO4, 25 D-glucose, and 1 kynurenic acid. Normal ACSF was composed of (in mM) 122 NaCl, 24 NaHCO3, 2.5 CaCl2, 3 KCl, 1 MgCl2, and 12 D-glucose. Both types of ACSF were saturated with 95% O2-5% CO2 and maintained at pH 7.4. The drugs sometimes added to the ACSF were APV (NMDA receptor antagonist), CNQX (AMPA antagonist), gabazine ($GABA_A$ antagonist), bicuculline ($GABA_A$, antagonist), L655708 (α5 $GABA_A$, antagonist), CGP55845 ($GABA_B$ antagonist; all from Tocris, USA), 5-HT, kynurenic acid (all from Sigma-Aldrich, USA), and TTX (TTX-citrate; Toronto Research Chemicals, Toronto). Drugs were first dissolved as a 10 - 50 mM stock in water or DMSO before final dilution in ACSF. DMSO was necessary for dissolving gabazine, L655708, bicuculline and CGP55845, but was kept at a minimum (final DMSO concentration in ACSF < 0.04%), which by itself had no effect on reflexes or sensory axons in vehicle controls (not shown). L655708 was particularly difficult to dissolve and precipitated easily, especially after it had been exposed a few times to air; so immediately after purchase we dissolved the entire bottle and froze it at -40^{o}C in single use 5 - 20 µl aliquots, and upon use it was first diluted in 100 µl distilled water before dispersing it into ACSF.

Recording monosynaptic reflexes in awake mice and rats, and PAD activation.

Window implant over spinal cord. In GAD2//ChR2+ mice and control GAD2//ChR- mice a glass window was implanted over the exposed spinal cord to gain optical access to the sacrocaudal spinal cord, as described previously (Lin *et al.*, 2019). Briefly, mice were given Meloxicam (1 mg/kg, s.c.) and then anesthetized using ketamine hydrochloride (100 mg/kg, i.p.) and xylazine (10 mg/kg, i.p.). Using aseptic technique, a dorsal midline incision was made over the L2 to L5 vertebrae. Approximately 0.1 ml of Xylocaine (1%) was applied to the surgical area and then rinsed. The animals were suspended from a spinal-fork stereotaxic apparatus (Harvard Apparatus) and the muscles between the spinous and transverse processes were resected to expose the L2 to L5 vertebrae. The tips of modified staples were inserted along the lateral edge of the pedicles and below the lateral processes of L2 and L5, and glued in place using cyanoacrylate. A layer of cyanoacrylate was applied to all of the exposed tissue surrounding the exposed vertebrae followed by a layer of dental cement to cover the cyanoacrylate and to form a rigid ring around the exposed vertebrae. A modified paperclip was implanted in the layer of dental cement to serve as a holding point for surgery. A laminectomy was performed at L3 and L4 to expose the spinal cord caudal to the transection site. Approximately 0.1 ml of Xylocaine (1%) was applied directly to the spinal cord for 2 – 3 s, and then rinsed. A line of Kwik-Sil (World-Precision Instruments) was applied to the dura mater surface along the midline of the spinal cord and a glass window was immediately placed over the exposed spinal cord. The window was glued in place along the outer edges using cyanoacrylate followed by a ring of dental cement. Small nuts were mounted onto this ring to later bolt on a backpack to apply the laser light (on the day of experimentation). Saline (1 ml, s.c.) and buprenorphine (0.03 mg/kg, s.c.) was administered post-operatively, and analgesia was maintained with buprenorphine (0.03 mg/kg, s.c.) every 12 hours for two days. Experimentation started 1 week after the window implant when the mouse was fully recovered.

Percutaneous EMG wire implant and fibre optic cable attachment. On the day of experimentation, the mouse was briefly sedated with isoflurane (1.5 %) and fine stainless steel wires (AS 613, Cooner Wire, Chatsworth, USA) were percutaneously implanted in the tail for recording EMG and stimulating the caudal tail trunk nerve, as we previously detailed (wires de-insulated by 2 mm at their tip and inserted in the core of 27 gauge needle that was removed after

insertion)(Murray *et al.*, 2010). A pair of wires separated by 8 mm were inserted at base of the tail for recording EMG the tail muscles, and second pair of wires was inserted nearby for bipolar activation of the caudal trunk nerve to evoke reflexes. A fifth ground wire was implanted between the EMG and stimulation wires. Following this a backpack was bolted into the nuts imbedded in the dental cement ring around the window. This backpack held and aligned a light fibre optic cable that was focused on the centre of the S3 – S4 sacral spinal cord. The Cooner wires were secured to the skin with drops of cyanoacrylate and taped onto the backpack so that the mouse could not chew them. The isoflurane was removed, and the mouse quickly recovered from the anesthesia and was allowed to roam freely around an empty cage during recording, or was sometimes lightly restrained by hand or by a sling. The fibre optic cable was attached to a laser (447 nM, same above) and the Cooner wires attached to the same models of amplifiers and stimulators used for ex vivo monosynaptic testing detailed above.

MSR testing.

The monosynaptic reflex (MSR) was recorded in the tail EMG at ~6 ms latency after stimulating the caudal tail trunk nerve at a low intensity that just activated proprioceptive afferents (0.2 ms current pulses, 1.1 xT, T: Threshold to evoke MSR, which is near afferent threshold), usually near the threshold to activate motor axons and an associated M-wave (that arrived earlier). We studied the tail MSR reflex because our ex vivo recordings were made in the corresponding sacral spinal cord of adult mice and rats, which is the only portion of the spinal cord that survives whole ex vivo, due to its small diameter (Li *et al.*, 2004a). This reflex was verified to be of monosynaptic latency because it was the first reflex to arrive, had little onset jitter, and had the same latency as the F wave (not shown; the F wave is evoked by a strong stimulation of all motor axons, at 5xT, which causes a direct motoneuron response on the same axons, while the monosynaptic EPSP is blocked by collision at this intensity) (Stalberg *et al.*, 2019). The MSR also underwent rate dependent depression (RDD) with fast repeated stimulation and so was synaptic and not a direct muscle response (M-wave), which occurred earlier at sufficient intensity to recruit the motor axons (not shown).

Conditioning of the MSR by optogenetic activation of $GABA_{axo}$ neurons. As with in vitro EPSP testing, the MSR was tested repeatedly at long 5 – 10 s intervals until a steady state MSR

was achieved. Then testing continued but with a conditioning light pulse applied just prior to the MSR stimulation (40 – 120 ms), to examine the effect of PAD evoked during this time frame on sensory transmission to motoneurons. Background EMG just prior to MSR testing was assessed to estimate the postsynaptic activity on the motoneurons. The changes in MSR and background EMG with light were quantified by comparing the average response before and during the light application, computed from the mean rectified EMG at 6 – 11 ms after the nerve stimulation (MSR) and over 20 ms prior to the nerve stimulation (background just prior to the MSR, Bkg). Because awake mice spontaneously varied their EMG, we plotted the relation between the MSR and the background EMG, with as expected a positive linear relation between these two variables(Matthews, 1986), computed by fitting a regression line. In trials with conditioning light applied the same plot of EMG vs background EMG was made and a second regression line computed. The change in the MSR with conditioning at a fixed matched background EMG level was then computed for each mouse by measuring the difference between the regression line responses at the fixed background EMG. This ruled out changes in MSRs being due to postsynaptic changes. Two background levels were assessed: rest (0%) and 30% of maximum EMG, expressed as a percentage of the control pre-conditioning MSR. The change in background EMG with light was computed by comparing the EMG just prior to the light application (over 20 ms prior) to the EMG just prior to the MSR (over 20 ms prior, Bkg), and expressed as a percentage of the maximum EMG.

Cutaneous conditioning of the MSR in rats. A similar examination of how PAD affected the MSR was performed in rats with percutaneous tail EMG recording. However, in this case PAD was evoked by a cutaneous conditioning stimulation of the tip of the tail (0.2 ms pulses, 3xT, 40 – 120 ms prior to MSR testing) using an additional pair of fine Cooner wires implanted at the tip of the tail (separated by 8 mm). In rats the MSR latency is later than in mice due to the larger peripheral conduction time, ~12 ms (as again confirmed by a similar latency to the F wave). This MSR was thus quantified by averaging rectified EMG over a 12 – 20 ms window. Also, to confirm the $GABA_A$ receptor involvement in regulating the MSR, the antagonist L655708 was injected systemically (1 mg/kg i.p., dissolved in 50 µl DMSO and diluted in 900 µl saline). Again, the MSR was tested at matched background EMG levels before and after conditioning (or L655708 application) to rule out changes in postsynaptic inhibition.

Conditioning of the MSRs in humans

H-reflex as an estimate of the MSR. Participants were seated in a reclined, supine position on a padded table. The right leg was bent slightly to access the popliteal fossa and padded supports were added to facilitate complete relaxation of all leg muscles. A pair of Ag-AgCl electrodes (Kendall; Chicopee, MA, USA, 3.2 cm by 2.2 cm) was used to record surface EMG from the soleus muscle. The EMG signals were amplified by 1000 and band-pass filtered from 10 to 1000 Hz (Octopus, Bortec Technologies; Calgary, AB, Canada) and then digitized at a rate of 5000 Hz using Axoscope 10 hardware and software (Digidata 1400 Series, Axon Instruments, Union City, CA) (Murray *et al.*, 2010). The tibial nerve was stimulated with an Ag-AgCl electrode (Kendall; Chicopee, MA, USA, 2.2 cm by 2.2 cm) in the popliteal fossa using a constant current stimulator (1 ms rectangular pulse, Digitimer DS7A, Hertfordshire, UK) to evoke an H-reflex in the soleus muscle, an estimate of the MSR (Hultborn *et al.*, 1987a). Stimulation intensity was set to evoke a test (unconditioned) MSR below half maximum. MSRs recorded at rest were evoked every 5 seconds to minimize RDD (Hultborn *et al.*, 1996a) and at least 20 test MSRs were evoked before conditioning to establish a steady baseline because the tibial nerve stimulation itself can presumably also activate spinal GABAergic networks, as in rats. All MSR were recorded at rest, except when the motor unit firing probabilities were measured (see below).

Conditioning of the MSR. To condition the soleus MSR by cutaneous stimulation, the cutaneous medial branch of the deep peroneal (cDP) nerve was stimulated on the dorsal surface of the ankle using a bipolar arrangement (Ag-AgCl electrodes, Kendall; Chicopee, MA, USA, 2.2 cm by 2.2 cm), set at 1.0xT, where T is the threshold for cutaneous sensation. A brief burst (3 pulses, 200 Hz for 10 ms) of cDP stimuli was applied before evoking a MSR at various inter-stimulus intervals (ISIs; interval between tibial and cDP nerve stimuli) within the window expected for phasic PAD evoked by cutaneous stimuli, presented in random order at 0, 30, 60, 80, 100, 150 and 200 ms ISIs. Seven conditioned MSR at each ISI were measured consecutively and the average of these MSR (peak-to-peak) was used as an estimate of the conditioned MSR. This was compared to the average MSR without conditioning, computed from the 7 trials just prior to conditioning.

The cDP nerve was also stimulated with a 500 ms long train at 200 Hz to condition the MSR, and examine the effect of tonic PAD evoked by such long trains, as in rats. Following the application of at least 20 test MSRs (every 5 s), a single cDP train was applied 700 ms before the next MSR and following this the MSR continued to be evoked for another 90 to 120 s (time frame of tonic PAD). We also conditioned the soleus MSR with tibialis anterior (TA; antagonist muscle, flexor) tendon vibration (brief burst of 3 cycles of vibration at 200Hz) to preferentially activate Ia afferents, as has been done previously (Hultborn *et al.*, 1987a).

Motor unit recording to examine postsynaptic actions of conditioning. Surface electrodes were used to record single motor units in the soleus muscle during low level contractions by placing electrodes on or near the tendon or laterally on the border of the muscle as detailed previously (Matthews, 1996). Alternatively, single motor unit activity from the soleus muscle was also recorded using a high density surface EMG electrode (OT Bioelettronica, Torino, Italy, Semi-disposable adhesive matrix, 64 electrodes, 5x13, 8 mm inter-electrode distance) with 3 ground straps wrapped around the ankle, above and below the knee. Signals were amplified (150 times), filtered (10 to 900 Hz) and digitized (16 bit at 5120 Hz) using the Quattrocento Bioelectrical signal amplifier and OTBioLab+ v.1.2.3.0 software (OT Bioelettronica, Torino, Italy). The EMG signal was decomposed into single motor units using custom MatLab software as per (Negro *et al.*, 2016). Intramuscular EMG was used to record MUs in one participant as detailed previously (Norton *et al.*, 2008) to verify single motor unit identification from surface EMG.

To determine if there were any postsynaptic effects from the conditioning stimulation on the motoneurons activated during the MSR, we examined whether the cDP nerve stimulation produced any changes in the tonic firing rate of single motor units, which gives a more accurate estimate of membrane potential changes in motoneurons compared to compound EMG. Single motor units were activated in the soleus muscle by the participant holding a small voluntary contraction of around 5% of maximum. Both auditory and visual feedback were used to keep the firing rates of the units steady while the conditioning cutaneous was applied every 3 to 5 seconds. The instantaneous firing frequency profiles from many stimulation trials were superimposed and time-locked to the onset of the conditioning stimulation to produce a peri-stimulus frequencygram (PSF, dots in Extended Data Fig 13b*iii*), as previously detailed (Turker

& Powers, 2005; Norton *et al.*, 2008). A mean firing profile resulting from the conditioning stimulation (PSF) was produced by averaging the frequency values in 20 ms bins across time post conditioning (thick lines in Extended Data Fig 13b*iii* and c*iii*). To quantify if the conditioning stimulation changed the mean firing rate of the tonically firing motor units, the % change in the mean PSF rate was computed at the time when the H reflex was tested (vertical line in Extended Data Fig 13b*ii-iii*).

Unitary EPSP estimates from PSF. To more directly examine if the facilitation in MSR resulted from changes in transmission in Ia afferents after cutaneous afferent conditioning, we measured changes in the firing probability of single motor units (MUs) during the brief MSR time-course (typically 30 to 45 ms post tibial nerve stimulation) with and without cDP nerve conditioning. Soleus MSRs were as usual evoked by stimulating the tibial nerve, but while the participant held a small voluntary plantarflexion to activate tonic firing of a few single motor units. The size of the MSR was set to just above reflex threshold (when the M-wave was < 5% of maximum) so that single motor units at the time of the MSR could be distinguished from the compound potential from many units that make up the MSR (Nielsen *et al.*, 2019b). For a given trial run, test MSRs were evoked every 3-5 s for the first 100 s and then MSR testing continued for a further 100s, but with a cDP-conditioning train (50 ms, 200 Hz) applied 500 ms prior to each MSR testing stimulation. These repeated high frequency trains evoke a tonic PAD in rats that facilitates sensory conduction. A 500 ms ISI was used to ensure the firing rate of the motor unit returned to baseline before the MSR was evoked, and this is also outside of the range of phasic PAD. Approximately 40-50 usable test and conditioned firing rate profiles were produced for a single session where the motor units had a steady discharge rate before the cDP nerve stimulation. Sessions were repeated 3-6 times to obtain a sufficient number of frequency points to construct the PSF (~ 200 trials).

To estimate the EPSP profile and prior background motoneuron activity, motor unit (MU) firing was again used to construct a PSF, as detailed above, but this time locked to the tibial nerve stimulation used to evoke the MSR, so that we could estimate the motoneuron behaviour during the MSR (EPSP). When more than one MU was visible in the recordings firing from these units (usually 2 – 3) were combined into a single PSF. Overall this gave about of 100 – 600 MU MSR

test sweeps to generate each PSF. Firing frequency values were initially averaged in consecutive 20 ms bins to produce a mean PSF profile over time before the tibial nerve stimulation, for both unconditioned and conditioned MSR reflex trials. From this, the mean background firing rate within the 100 ms window immediately preceding the tibial stimulation was compared between the test and conditioned MSR trials to determine if the conditioning cDP nerve stimulation produced a change in firing rate, and thus post-synaptic effect, just before the conditioned MSR was evoked. Next, as an estimate of EPSP size, the mean firing rate during the MSR window was also measured, but computed with smaller PSF bins of 0.5 ms during the MSR. Finally, for each PSF generated with or without conditioning, the probability that a motor unit discharged during the MSR window (30 to 45 ms after the TN stimulation) was measured as the number of discharges during the time of the MSR window divided by the total number of tibial nerve test stimuli.

Temperature, latency and PAD considerations.

Large proprioceptive group Ia sensory afferents conduct in the peripheral tail nerve with a velocity of about 33 m/s (33 mm/ms) in mice (Walsh *et al.*, 2015). Motor axons are similar, though slightly slower (30 m/s)(Rasminsky *et al.*, 1978). Thus, in the awake mouse stimulation of Ia afferents in the mouse tail evokes spikes that take ~ 2 ms to conduct to the motoneurons in the spinal cord ~70 mm away. Following ~1 ms synaptic and spike initiation delay in motoneurons, spikes in the motor axons take a further ~2 ms to reach the muscles, after which the EMG is generated with a further 1 ms synaptic and spike initiation delay at the motor endplate to produce EMG. All told this gives a monosynaptic reflex latency of ~6 ms. The motor unit potentials within the EMG signal have a duration of about 3 – 5 ms, and thus we averaged rectified EMG over 6 – 11 ms to quantify the MSR. We have shown that similar considerations hold for the rat where tail nerve conduction velocities are similar, except the distance from the tail stimulation to the spinal cord is larger (150 mm), yielding a peripheral nerve conduction delay of ~10 ms and total MSR delay of ~12 ms (Bennett *et al.*, 2004). In humans the MSR latency is dominated by the nerve conduction latency (50 – 60 m/s) over a large distance (~800 mm), yielding MSR latencies of ~30 ms.

In our ex vivo whole adult spinal cord preparation the bath temperature was varied between 23 and 32ºC. All data displayed is from 23 – 24ºC, though we confirmed the main results (facilitation of sensory axon transmission to motoneuron by PAD) at 32ºC. The Q10 for peripheral nerve conduction (ratio of conduction velocities with a 10 ºC temperature rise) is about 1.3 (Leandri *et al.*, 2008), yielding a conduction in dorsal roots of about 20 m/s at 23 – 24 ºC, as we directly confirmed (not shown). Thus, when the DR is stimulated 20 mm from the cord the latency of spike arrival at the cord should be about 1 ms, which is consistent with the time of arrival of afferent volleys that were seen in the intracellular and extracellular recordings from sensory axons (e.g. Figs. 2b and 4e).

When we found that PAD evoked in sensory axons can prevent failure of spikes to propagate in the cord after DR stimulation, we worried that PAD somehow influenced the initiation of the spike by the dorsal root stimulation at the silver wire. However, we ruled this out by stimulating dorsal roots as far away from the spinal cord as possible (20 mm), where PAD has no effect, due to the exponential attenuation of its dorsal root potential with distance (see above), and found that PAD still facilitated sensory axon spike transmission to motoneurons. The added advantage of these long roots is that there is a clean 1 ms separation between the stimulus artifact and the afferent volley arriving at the spinal cord, allowing us to quantify small FPs and afferent volleys that are otherwise obscured by the artifact.

We did not consistently use high temperature ex vivo baths (32ºC) because the VR and DR responses to activation of DRs or PAD neurons are irreversibly reduced by prolonged periods at these temperatures, suggesting that the increased metabolic load and insufficient oxygen penetration deep in the tissue damages the cord at these temperatures. Importantly, others have reported that in sensory axons PAD-evoked spikes (DRRs) are eliminated in a warm bath and argued that this means they are not present in vivo, and not able to evoke a motoneuron response (Fink *et al.*, 2014), despite evidence to the contrary (Eccles *et al.*, 1961a; Beloozerova & Rossignol, 1999). However, we find that PAD itself is reduced in a warm bath by the above irreversible damage, and it is thus not big enough to evoke spikes in sensory axons; thus, this does not tell us whether these spikes should be present or not in vivo. Actually, in vivo we sometimes observed that with optogenetic activation of $GABA_{axo}$ neurons and associated PAD

there was a direct excitation of the motoneurons (seen in the EMG) at the latency expected for PAD evoked spikes (not shown). However, this was also at the latency of the postsynaptic inhibition produced by this same optogenetic stimulation, which often masked the excitation (Fig. 6). In retrospect, examining the $GABA_{axo}$ evoked motoneuron responses during optogenetic-evoked PAD (Fink et al.)(Fink, 2013a; Fink *et al.*, 2014), or sensory-evoked PAD(Stuart & Redman, 1992; Fink, 2013a), there is either outright excitation or an excitation riding on the postsynaptic IPSPs resulting from the activation of there $GABA_{axo}$ neurons. This is consistent with the PAD-evoked spike activating the monosynaptic pathway, which inhibits subsequently tested monosynaptic responses by post activation depression (see Discussion).

The latency of a single synapse in our ex vivo preparation at 23 – 24ºC was estimated from the difference between the time arrival of the sensory afferent volley at the motoneurons (terminal potential seen in intracellular and extracellular recordings) and the onset of the monosynaptic EPSP in motoneurons. This was consistently 1 – 1.2 ms (Fig. 5b and e). This is consistent with a Q10 of about 1.8 – 2.4 for synaptic transmission latency (Czeh & Dezso, 1982; Silver *et al.*, 1996), and 0.4 ms monsynaptic latency at body temperature (Munson & Sypert, 1979b; Lev-Tov *et al.*, 1983). Based on these considerations we confirm that the PAD evoked in sensory axons is monosynaptically produced by optogenetic activation of $GABA_{axo}$ neurons with light, since it follows ~1 ms after the first spike evoked in GABAaxo neurons by light (Fig. 3a). This first spike in $GABA_{axo}$ neurons itself takes 1 – 2 ms to arise and so the overall latency from light activation to PAD production can be 2 - 3 ms (Fig. 3f), as seen for IPSCs at this temperature in other preparations (Takahashi, 1992). With DRs stimulation PAD arises with a minimally 4 – 5 ms latency, which is consistent with a trisynaptic activation of the sensory axon, after taking into account time for spikes to arise in the interneurons involved (Fig. 4a,e).

Viral labelling of sensory afferents.

Large diameter peripheral afferents were labelled by viral injections, as previously detailed(Foust *et al.*, 2008; Li *et al.*, 2020), providing an additional method of examining central afferent projections in the spinal cord. Adeno-associated viral vectors (AAVs) with the transgene encoding the cytoplasmic fluorophore tdTom under the CAG promoter were injected IP into anesthetized P1-2 mice (AAV9-CAG-tdTom, 5.9×10^{12} vg/ml; 2-4 µl per injection; UNC Vector

Core). To improve transduction efficiencies, viral vectors were incubated with LAH4 peptide (200 μM) at 37 °C for ~45 min immediately prior to injection. Mice were perfused for immunolabelling > 60 days post injection (adult mice). This injection method yields a sparce Golgi-like labelling of about 5% of afferents in each spinal segment, without central labelling of other neurons (with the exception of one or two motoneurons labelled per spinal segment), allowing afferents to be traced to the motoneurons for morphological identification as Ia afferents.

Immunohistochemistry.

Tissue fixation and sectioning. After sensory axons were injected with neurobiotin ex vivo in mouse and rat sacrocaudal spinal cords, the cords were left in the recording chamber in oxygenated nACSF for an additional 4 – 6 hr to allow time for diffusion of the neurobiotin throughout the axon. Then the spinal cord was immersed in 4% paraformaldehyde (PFA; in phosphate buffer) for 20-22 hours at 4°C, cryoprotected in 30% sucrose in phosphate buffer for 24-48 hours. Alternatively, afferents were labelled genetically in VGLUT1$^{Cre/+}$; R26$^{lsl\text{-}tdTom}$ mice or by a AAV9-CAG-tdTom viral injection, which were euthanized with Euthanyl (BimedaMTC; 700 mg/kg) and perfused intracardially with 10 ml of saline for 3 – 4 min, followed by 40 ml of 4% paraformaldehyde (PFA; in 0.1 M phosphate buffer at room temperature), over 15 min (Gabra5-KO mice also fixed similarly). Then spinal cords of these mice were post-fixed in PFA for 1 hr at 4°C, and then cryoprotected in 30% sucrose in phosphate buffer (~48 hrs). Following cryoprotection all cords were embedded in OCT (Sakura Finetek, Torrance, CA, USA), frozen at -60C with 2-methylbutane, cut on a cryostat NX70 (Fisher Scientific) in sagittal or transverse 25 μm sections, and mounted on slides. Slides were frozen until further use.

Immunolabelling. The tissue sections on slides were first rinsed with phosphate buffered saline (PBS, 100 mM, 10 min) and then again with PBS containing 0.3% Triton X-100 (PBS-TX, 10 min rinses used for all PBS-TX rinses). For the sodium channel antibody, we additionally performed antigen retrieval by incubating slides three times for 10 min each with a solution of 0.2% sodium borohydride (NaBH4, Fisher, S678-10) in PB, followed by a PBS rinse (4x 5 min), because this antibody is sensitive to over-fixation. We verified that this sodium channel antibody labels axon nodes just as well in our tissue treated with the antigen retrieval, compared to in

control tissue that was only lightly fixed (PFA perfusion, followed by no postfixation, not shown). Next, for all tissue, nonspecific binding was blocked with a 1 h incubation in PBS-TX with 10% normal goat serum (NGS; S-1000, Vector Laboratories, Burlingame, USA) or normal donkey serum (NDS; ab7475, Abcam, Cambridge, UK). Sections were then incubated for at least 20 hours at room temperature with a combination of the following primary antibodies in PBS-TX with 2% NGS or NDS: rabbit anti-α_5 $GABA_A$ receptor subunit (1:200; TA338505, OriGene Tech., Rockville, USA; same antibody as SAB2100878, Sigma-Aldrich, St. Louis, USA; verified with Western blot and IHC(Loeza-Alcocer *et al.*, 2013; Bravo-Hernandez *et al.*, 2016), and knockout detailed below), rabbit anti-α1 $GABA_A$ receptor subunit (1:300; 06-868, Sigma-Aldrich, St. Louis, USA; verified by Western blot, IHC, and α1 $GABA_A$ knockout(Zhou *et al.*, 2013; Wu *et al.*, 2021b)), guinea pig anti-α2 $GABA_A$ receptor subunit (1:500; 224 104, Synaptic Systems, Goettingen, Germany; verified with Western blot, IHC, lack of labelling with loss of GABRA2 quantified with RT-qPCR(Zhou *et al.*, 2019), and labelling in HEK239 cells transfected with GABRA2 cDNA(Brown *et al.*, 2016)), chicken anti-γ2 $GABA_A$ receptor subunit (1:500; 224 006, Synaptic Systems, Goettingen, Germany; verified with Western blot, IHC and receptor colocalization with gephrine(Dzyubenko *et al.*, 2021)), rabbit anti-$GABA_{B1}$ receptor subunit (1:500; 322 102, Synaptic Systems, Goettingen, Germany), mouse anti-Neurofilament 200 (NF200) (1:2000; N0142, Sigma-Aldrich, St. Louis, USA), guinea pig anti-Neurofilament M (NFM, 1:500; 171 204, Synaptic Systems), guinea pig anti-VGLUT1 (1:1000; AB5905, Sigma-Aldrich, St. Louis, USA), rabbit anti-Caspr (1:500; ab34151, Abcam, Cambridge, UK), mouse anti-Caspr (1:500; K65/35, NeuroMab, Davis, USA), chicken anti-Myelin Basic Protein (MBP) (1:200; ab106583, Abcam, Cambridge, UK), guinea pig anti-GAD2/GAD65 (1:500; 198 104; Synaptic Systems); chicken anti-VGAT (1:500; 131 006, Synaptic Systems, Goettingen, Germany), rabbit anti-VGAT (1:500; AB5062P, Sigma-Aldrich, St. Louis, USA), rabbit anti-EYFP (1:500; orb256069, Biorbyt, Riverside, UK), goat anti-RFP (1:500; orb334992, Biorbyt, Riverside, UK), rabbit anti-RFP (1:500; PM005, MBL International, Woburn, USA), rabbit anti-GFP (1:500, A11122, ThermoFisher Scientific, Waltham, USA), and mouse anti-Pan Sodium Channel (1:500; S8809, Sigma-Aldrich, St. Louis, USA). The latter is a pan-sodium antibody, labelling an intracellular peptide sequence common to all known vertebrate sodium channels. Genetically expressed EYFP, tdTom (RFP) and GFP were amplified with the above antibodies, rather than rely on the endogenous fluorescence. When anti-mouse antibodies were applied in

mice tissue, the M.O.M (Mouse on Mouse) immunodetection kit was used (M.O.M; BMK-2201, Vector Laboratories, Burlingame, USA) prior to applying antibodies. This process included 1h incubation with a mouse Ig blocking reagent. Primary and secondary antibody solutions were diluted in a specific M.O.M diluent.

The following day, tissue was rinsed with PBS-TX (3x 10 min) and incubated with fluorescent secondary antibodies. The secondary antibodies used included: goat anti-rabbit Alexa Fluor 555 (1:200; A32732, ThermoFisher Scientific, Waltham, USA), goat anti-rabbit Alexa Fluor 647 (1:500, ab150079, Abcam, Cambridge, UK), goat ant-rabbit Pacific orange (1:500; P31584, ThermoFisher Scientific, Waltham, USA), goat anti-mouse Alexa Fluor 647 (1:500; A21235, ThermoFisher Scientific, Waltham, USA), goat anti-mouse Alexa Fluor 488 (1:500; A11001, ThermoFisher Scientific, Waltham, USA), goat anti-mouse Alexa Fluor 555 (1:500; A28180, ThermoFisher Scientific, Waltham, USA), goat anti-guinea pig Alexa Fluor 647 (1:500; A21450, ThermoFisher Scientific, Waltham, USA), goat anti-chicken Alexa Fluor 405 (1:200; ab175674, Abcam, Cambridge, UK), goat anti-chicken Alexa Fluor 647 (1:500; A21449, ThermoFisher Scientific, Waltham, USA), donkey anti-goat Alexa Fluor 555 (1:500; ab150130, Abcam, Cambridge, UK), donkey anti-rabbit Alexa Fluor 488 (1:500; A21206, ThermoFisher Scientific, Waltham, USA), Streptavidin-conjugated Alexa Fluor 488 (1:200; 016-540-084, Jackson immunoResearch, West Grove, USA) or Streptavidin-conjugated Cyanine Cy5 (1:200; 016-170-084, Jackson immunoResearch, West Grove, USA) in PBS-TX with 2% NGS or NDS, applied on slides for 2 h at room temperature. The latter streptavidin antibodies were used to label neurobiotin filled afferents. After rinsing with PBS-TX (2 times x 10 min/each) and PBS (2 times x 10 min/each), the slides were covered with Fluoromount-G (00-4958-02, ThermoFisher Scientific, Waltham, USA) and coverslips (#1.5, 0.175 mm, 12-544-E; Fisher Scientific, Pittsburg, USA).

Standard negative controls in which the primary antibody was either 1) omitted or 2) blocked with its antigen (quenching) were used to confirm the selectivity of the antibody staining, and no specific staining was observed in these controls. Previous tests detailed by the manufactures further demonstrate the antibody specificity, including quenching, immunoblots (Western blots), co-immunoprecipitation, and/or receptor knockout. Most antibodies had been previously tested

with quenching for selectivity, as detailed in the manufacture's literature and other publications (Lucas-Osma *et al.*, 2018a), but we verified this for the GABA receptors with quenching. For antibody quenching, the peptides used to generate the antibodies, including anti-α5 $GABA_A$ receptor subunit (AAP34984, Aviva Systems Biology, San Diego, USA), anti-α1 $GABA_A$ receptor subunit (224-2P, Synaptic Systems, Goettingen, Germany) and anti-γ2 $GABA_A$ receptor subunit (224-1P, Synaptic Systems, Goettingen, Germany), were mixed with the antibodies at a 10:1 ratio and incubated for 20 h and 4°C. This mixture was then used instead of the antibody in the above staining procedure. Control receptor knockout experiments were also performed on for the anti-α5 $GABA_A$ antibody, with this antibody producing no receptor labelling in brain tissue from α5 $GABA_A$ knockout mice (Gabra5 KO mice; Extended Data Fig. 14).

Confocal and epifluorescence microscopy

Image acquisition was performed by confocal (Leica TCS SP8 Confocal System) and epifluorescence (Leica DM 6000 B) microscopy for high magnification 3D reconstruction and low magnification imaging, respectively. All the confocal images were taken with a 63x (1.4 NA) oil immersion objective lens and 0.1 µm optical sections that were collected into a z-stack over 10–20 µm. Excitation and recording wavelengths were set to optimize the selectivity of imaging the fluorescent secondary antibodies. The same parameters of laser intensity, gain and pinhole size was used to take pictures for each animal, including the negative controls. Complete sagittal sections were imaged with an epifluorescence 10x objective lens using the Tilescan option in Leica Application Suite X software (Leica Microsystems CMS GmbH, Germany). Sequential low power images were used to reconstruct the afferent extent over the whole spinal cord, using CorelDraw (Ottawa, Canada), and to identify locations where confocal images were taken.

3D reconstruction of afferents and localization of GABA receptors.

The fluorescently labelled afferents (neurobiotin, tdTom), GABA receptors, VGLUT1, VGAT, NF200, Caspr, MBP and sodium channels were analyzed by 3D confocal reconstruction software in the Leica Application Suite X (Leica Microsystems CMS GmbH) (Lucas-Osma *et al.*, 2018a). To be very conservative in avoiding non-specific antibody staining, a threshold was set for each

fluorescence signal at a minimal level where no background staining was observed in control tissue with the primary antibody omitted, less 10%. Signals above this threshold were rendered in 3D for each antibody. Any GABA receptor, Caspr or Na_V expression within the volume of the neurobiotin filled axon (binary mask set by threshold) was labelled in 3D reconstructions (yellow, pink and white respectively in Fig. 1). Receptor density within the axon membrane surface area was quantified using the same Leica software. Receptors are usually cycled in and out of the membrane(Murray *et al.*, 2010) and so receptors within the axon cytoplasm provide additional evidence of the presence of axonal GABA receptors, distinct from receptors that may be in the postsynaptic contacts of the afferents. Thus, we also computed the receptor densities in the axon volume and found qualitatively the same distribution (at nodes and terminals) as with surface density calculations and thus only reported the surface membrane density. Receptor densities were measured for all orders of branch sizes (1^{st}, 2^{nd}, 3^{rd} etc.; see below), for both branches dorsal to the central canal (dorsal) and ventral to the central canal (ventral). Nodes were identified with dense bands of Caspr or Na channel labelling (and lack of MBP). Branch points were also identified. We also examined raw image stacks of the neurobiotin afferents and receptors, to confirm that the automatically 3D reconstructed and identified receptors labelled within the afferent (yellow) corresponded to manually identified receptors colocalized with neurobiotin (Fig. 1). This was repeated for a minimum of 10 examples for each condition, and in all cases the 3D identified and manually identified receptors and channels were identical. Many receptors and channels lay outside the afferent, and near the afferent these were difficult to manually identify without the 3D reconstruction software, making the 3D reconstruction the only practical method to fully quantify the receptors over the entire afferent. We also optimized the reconstruction of the neurobiotin filled afferents following the methods of Fenrich(Fenrich *et al.*, 2014), including brightening and widening the image edges slightly (1 voxel, 0.001 μm^3) when necessary to join broken segments of the afferent in the final afferent reconstruction, to account for the a priori knowledge that afferents are continuous and neurobiotin signals tend to be weaker at the membrane (image edges) and in fine processes. Finally, we also counted the proportion of nodes and ventral boutons innervating motoneurons that contain GABA receptors clusters, as an additional quantification of the receptor distribution. Limitations in the sensitivity of receptor antibody labeling leave open the possibility that we missed small quantities of receptors. Thus, while we find that most proprioceptive afferent terminal boutons lack $GABA_A$ receptors(Lucas-

Osma *et al.*, 2018a) (see Results) there may well still be small quantities of receptors. However, these receptors are unlikely to have much functional impact, since previous direct recording from ventral terminals boutons show little PAD at the time when PAD is observed in more dorsal portions of the same axons(Lucas-Osma *et al.*, 2018a).

GABA receptors usually occurred in the axons in distinct clusters. The distances from these receptor clusters to nodes or branch points was measured and average distances computed (from centers of clusters to centre of nodes), from high power confocal images evenly sampled across the axon arbour. Some nodes did not branch, so receptors at these nodes were fairly far from the nearest branch (~20 μm), making the average receptor to branch point distance larger than the receptor to node distance, the latter which were small because $GABA_A$ receptors were mainly only at nodes (see Results). The average distance between the receptor clusters and the nearest axon terminals on the motoneurons was also computed, but this was complicated by the very large distances often involved, forcing us to compute the distances from low power images and relate these to the high power images of receptors sampled relatively evenly along the axon arbour. For this distance calculation, to avoid sampling bias in the high power images, we only admitted images from axon branch segments (1^{st}, 2^{nd} and 3^{rd} order, detailed below) that had a receptor density within one standard deviation (SD) of the mean density in branch types with the highest density (1^{st} or 2^{nd} order ventral branches for $GABA_A$ receptors and 3^{rd} order ventral terminal branches for $GABA_B$ receptors; i.e. images from axons branches with density above the dashed confidence interval lines in Fig. 1e were included; this SD computed from densities of pooled axons from all rats, rather than single rat averages, to better reflect the axon density variability). This eliminated very large distances being included from branch segments with relatively insignificant receptor densities. We also confirmed these calculations by computing the weighted sum of all the receptor distances weighted by the sum of the receptor density for each branch type (and divided by the sum of all receptor densities), which further eliminated sampling bias. This gave similar average distance results to the above simpler analysis (not shown).

Sensory axon branch order terminology. The branches of proprioceptive axons were denoted as follows: dorsal column branches, 1^{st} order branches that arose of the dorsal column and project toward the motoneurons, 2^{nd} order branches that arose from the 1^{st} order branches, and 3^{rd} order branches that arose from the 2^{nd} order branches. Higher order branches occasionally arose

from the 3rd order branches, but these were collectively denoted 3rd order branches. First and second order branches were myelinated with large dense clusters of sodium channels at the nodes in the myelin gaps, which were characteristically widely spaced. As the second order branches thinned near the transition to 3rd order branches, they became unmyelinated, and at this point sodium channel clusters were smaller and more closely spaced (~6 μm apart, not shown). These thinned branches gave off 3rd order (and higher) unmyelinated terminal branches with chains of characteristic terminal boutons that terminated on motoneurons. The 1st order branches gave off 2nd order branches along most of their length as they traversed the cord from the dorsal columns to the motoneurons, but we separately quantified 1st, 2nd and 3rd order branches in more dorsal (including dorsal and intermediated laminae) and ventral (ventral laminae) regions of the cord.

Node identification. Nodes in myelinated axon segments nodes were identified either directly via direct Na channel clusters and paranodal Caspr, or indirectly by their characteristic paranodal taper. That is, in the paranodal region the neurobiotin filled portion of the axon tapered to a smaller diameter, likely because the Caspr and presumably other proteins displaced the cytoplasmic neurobiotin, which also made the intracellular neurobiotin label less dense (Fig. 1b, black regions in taper). Regardless of the details, this taper made nodes readily identifiable. This taper forces the axial current densities to increase at the nodes, presumably assisting spike initiation, and consistent with previous reconstructions of myelinated proprioceptive afferents (Nicol & Walmsley, 1991).

GAD2 neuron labelling. $GABA_{axo}$ neurons that express GAD2 were visualized by genetically tagging them with Cre-ER driven fluorescent reporters. Usually we used the ChR2-EYFP reporter to both insert ChR2 and label with EYFP. This ChR2 construct is membrane bound and so does not fill soma or large processes making cells sometimes hard to visualize. Thus, in some animals we additionally included the Cre driven tdTom reporter, which is a cytoplasmic reporter that fills the entire cell to help visualize the complete anatomy of the entire $GABA_{axo}$ neuron (Fig 3). In this case, GAD2 neurons should have both EYFP (green in Fig 3) and tdTom (red) reporter labelling. However, the balance of green and red expression intensity was variable, with some processes with more EYFP and others with more tdTom, leading to some axons more one color than the other. This was likely due to a number of factors. First, membrane bound fluorophores

are easier to see in small diameter axons or dendrites, because of a higher membrane-to-cytoplasm ratio, making red more visible in small axons. Second, variability in tissue penetration of the antibodies we used to amplify the reporter signals and more intense ChR2-EYFP labelling (green) in axons may have led to variable red and green intensity. Finally, genetic variability in the Cre-ER driven reporter expression, which only occurs transiently after the tamoxifen administration, may explain why a small proportion of neurons are either just green or just red, with one reporter not expressed by this transient Cre expression. Expression of only one reporter happened in only a small proportion of neurons, but when it did our double reporter method is an advantage in visualizing these neurons.

Computer simulations

All computer models and simulations were implemented in NEURON ver7.5 (Hines & Carnevale, 2001). The geometry and myelination pattern of the model were extracted from a previous study that used serial-section electron microscopy to generate about 15,000 photomicrographs to reconstruct a large myelinated proprioceptive Ia afferent collateral in the cat (Nicol and Walmsley, 1991)(Nicol & Walmsley, 1991). This structure was used in a prior modeling study (Walmsley *et al.*, 1995). Four classes of segment were defined in the model: myelinated internodes, nodes, unmyelinated bridges, and terminal boutons. Data from 18 of the 83 segments were missing from the original study. The missing data were estimated using mean values of the same segment class. The cable properties of the model were determined from diameter-dependent equations previously used for models of myelinated axons(McIntyre *et al.*, 2002) and included explicit representation of myelinated segments using the double cable approach(Stephanova & Bostock, 1995; McIntyre *et al.*, 2002; Cohen *et al.*, 2020). Hodgkin-Huxley style models of voltage gated sodium (transient and persistent) and potassium channels were adopted from a previous study, at 37ºC(McIntyre *et al.*, 2002). All three voltage-gated conductances were colocalized to unmyelinated nodes and segments throughout the modelled axon collateral. The density of sodium and potassium conductances was adjusted to match the size and shape of experimentally recorded action potentials. To be conservative, sodium channels were placed at each node and bouton ($gNa = 1\ S/cm^2$), even though bouton immunolabelling for these channels was not common in our terminal bouton imaging (Fig. 1), since disperse weak

sodium channel labelling may have been missed. Removing these bouton sodium channels did not qualitatively change our computer simulation results (not shown). Current clamp stimulation was applied to the middle of the first myelinated segment (pulse width 0.1 ms, amplitude 2 nA; near dorsal root) to initiate propagating action potentials in the model. Voltage at multiple sites of interest along the collateral was measured to assess propagation of action and graded potentials through branch points. Transient chloride conductance (i.e. $GABA_A$ receptors) was modeled using a double-exponential point process (Eq. 1); parameters were manually fit to experimental data. $GABA_A$ receptors were localized to nodes at branch points to match experimental data. The amplitude and time course of the modeled PAD (also termed PAD) was measured from the first myelinated internode segment, similar to the location of our intra-axonal recordings.

$$g(t) = g\_max * \beta * (e\text{^}((-t)/\tau\_decay\ ) - e\text{^}((-t)/\tau\_rise\ )\ ) \text{, where } \beta = 1/((e\text{^}((-\gamma)/\tau\_decay\ ) - e\text{^}((-\gamma)/\tau\_rise\ )\ )\ ) \text{, and } \gamma = (\tau\_rise * \tau\_decay)/(\tau\_decay - \tau\_rise\ ) * \log(\tau\_decay/\tau\_rise\ ) \quad (Eq.\ 1)$$

The parameters at all synapses were the same: time constant of rise (τ_{rise}) = 6ms, time constant of decay (τ_{decay}) = 50ms, default maximum conductance (g_{max}) = 1.5nS (varied depending on simulation, see figure legends), and chloride reversal potential (E_{Cl^-}) = -25mV (i.e. 55 mV positive to the resting potential to match our experimental data) (Lucas-Osma *et al.*, 2018a). Space constants (λ_S) were computed for each segment of the afferent, from subthreshold current injections (100 ms) on the distal end of each branch segment and fitting an exponential decay (with space constant λ_S) to the passive depolarization along its length, and then repeating this with current injected in the proximal end to get a second λS, and finally averaging these two space constants.

QUANTIFICATION AND STATISTICAL ANALYSIS

Data were analyzed in Clampfit 8.0 (Axon Instruments, USA) and Sigmaplot (Systat Software, USA). A Student's *t*-test or ANOVA (as appropriate) was used to test for statistical differences between variables, with a significance level of $P < 0.05$ (two tailed). Power of tests was

computed with $\alpha = 0.05$ to design experiments. A Kolmogorov-Smirnov test for normality was applied to the data set, with a $P < 0.05$ level set for significance. Most data sets were found to be normally distributed, as is required for a *t*-test. For those that were not normal a Wilcoxon Signed Rank Test was instead used with $P < 0.05$. Categorical data was instead analyzed using Chi-squared tests, with Yate's continuity correction used for 2×2 contingency tables and again significant difference set at $P < 0.05$. Effects in male and female animals were similar and grouped together in analysis. For in vivo experiments, a single data point is taken from the average response in each subject/animal and *n* values indicate subject number. Axons and motoneurons were recorded ex vivo from widely separated locations (one segment apart or contralateral) within the whole spinal cord, and are considered independent; so statistics were performed across all neurons (*n*) from all animals, though all main effects were confirmed to occur in each animal, and comparing across animal averages also showed significant changes (*n* animal numbers). Data are indicated as box plots representing the interquartile range and median (thin line) and error bars representing the 90^{th} and 10^{th} percentile, interpolated between nearest points (Cleveland method). Mean also shown as thick line in boxes.

Data availability

All data are available in the manuscript or the supplementary materials. Raw data are available upon request to the corresponding authors. This study did not generate data sets or new unique reagents.

Code availability

The computer code used to perform the axon simulations (Extended Data Fig. 5) are publicly available on the github repository: https://github.com/kelvinejones/noah-axon.git

Acknowledgements

We thank Leo Sanelli, Jennifer Duchcherer, Babak Afsharipour and Christopher K. Thompson for technical assistance, and Shawn Hochman, CJ Heckman, FJ Alvarez and Tia Bennett for discussions and editing the manuscript. VGLUT1^{Cre} mice cords were kindly donated by Dr. Francisco J. Alvarez. We thank Prof Uwe Rudolph (McLean Hospital, currently University of Illinois Urbana-Champaign) for providing Gabra5-floxed mice. This research was supported by the Canadian Institutes of Health Research (MOP 14697 and PJT 165823 D.J.B.) and the US National Institutes of Health (NIH, R01NS47567, D.J.B. and K.F.; R01GM118801, R.A.P.).

Author information

Contributions. K.H, and A.M.L-O. designed the study, carried out the animal experiments and analyzed data. K.M. and M.A.G. designed and performed the human experiments. N.P. and K.E.J. designed and performed the computer simulations. S.L., S.B., A.M., M.J.S. and R.S. assisted with animal electrophysiology. K.F. and A.M.L-O provided confocal microscopy. K.K.F, S.L., D.A.R. and K.H. developed the transgenic mice and performed the optogenetic experiments. R.A.P. developed transgenic mice used in immunohistochemical studies. Y.L. and D.J.B. conceived and designed the study, carried out experiments and analyzed data. D.J.B, K.H., and Y.L. wrote the paper, with editing from other authors. These authors contributed equally: Krishnapriya (Veni) Hari and Ana M. Lucas-Osma. These authors jointly supervised this work as senior authors: Yaqing Li, Keith K. Fenrich and David J. Bennett.

Corresponding author. David J. Bennett

Ethical declarations

All authors declare no competing interests.

References

Achache V, Roche N, Lamy JC, Boakye M, Lackmy A, Gastal A, Quentin V & Katz R. (2010). Transmission within several spinal pathways in adults with cerebral palsy. *Brain* **133,** 1470-1483.

Adams MM & Hicks AL. (2005). Spasticity after spinal cord injury. *Spinal Cord* **43,** 577-586.

Afsharipour B, Manzur N, Duchcherer J, Fenrich KF, Thompson CK, Negro F, Quinlan KA, Bennett DJ & Gorassini MA. (2020). Estimation of self-sustained activity produced by persistent inward currents using firing rate profiles of multiple motor units in humans. *J Neurophysiol* **124,** 63-85.

Ahuja CS, Wilson JR, Nori S, Kotter MRN, Druschel C, Curt A & Fehlings MG. (2017). Traumatic spinal cord injury. *Nat Rev Dis Primers* **3,** 17018.

Aimonetti JM, Vedel JP, Schmied A & Pagni S. (2000a). Distribution of presynaptic inhibition on type-identified motoneurones in the extensor carpi radialis pool in man. *The Journal of physiology* **522 Pt 1,** 125-135.

Aimonetti JM, Vedel JP, Schmied A & Pagni S. (2000b). Mechanical cutaneous stimulation alters Ia presynaptic inhibition in human wrist extensor muscles: a single motor unit study. *The Journal of physiology* **522 Pt 1,** 137-145.

Akay T, Tourtellotte WG, Arber S & Jessell TM. (2014). Degradation of mouse locomotor pattern in the absence of proprioceptive sensory feedback. *Proc Natl Acad Sci U S A* **111,** 16877-16882.

Alvarez FJ. (1998). Anatomical basis for presynaptic inhibition of primary sensory fibers. In *Presynaptic Inhibition and Neuron Control*, ed. Rudmon P, Romo R & Mendell LM, pp. 13-41. Oxford University Press, New York.

Alvarez FJ, Taylor-Blake B, Fyffe RE, De Blas AL & Light AR. (1996). Distribution of immunoreactivity for the beta 2 and beta 3 subunits of the GABAA receptor in the mammalian spinal cord. *J Comp Neurol* **365,** 392-412.

Anderson KD. (2004). Targeting recovery: priorities of the spinal cord-injured population. *J Neurotrauma* **21,** 1371-1383.

Andrechek ER, Hardy WR, Girgis-Gabardo AA, Perry RL, Butler R, Graham FL, Kahn RC, Rudnicki MA & Muller WJ. (2002). ErbB2 is required for muscle spindle and myoblast cell survival. *Mol Cell Biol* **22,** 4714-4722.

Angeli CA, Boakye M, Morton RA, Vogt J, Benton K, Chen Y, Ferreira CK & Harkema SJ. (2018). Recovery of Over-Ground Walking after Chronic Motor Complete Spinal Cord Injury. *N Engl J Med* **379,** 1244-1250.

Arbuthnott ER, Boyd IA & Kalu KU. (1980). Ultrastructural dimensions of myelinated peripheral nerve fibres in the cat and their relation to conduction velocity. *The Journal of physiology* **308,** 125-157.

Armstrong CM & Cota G. (1991). Calcium ion as a cofactor in Na channel gating. *Proceedings of the National Academy of Sciences of the United States of America* **88,** 6528-6531.

Ashby P & Verrier M. (1975). Neurophysiological changes following spinal cord lesions in man. *Can J Neurol Sci* **2,** 91-100.

Ashby P & Verrier M. (1976). Neurophysiologic changes in hemiplegia. Possible explanation for the initial disparity between muscle tone and tendon reflexes. *Neurology* **26,** 1145-1151.

Ashby P, Verrier M & Lightfoot E. (1974). Segmental reflex pathways in spinal shock and spinal spasticity in man. *J Neurol Neurosurg Psychiatry* **37,** 1352-1360.

Aymard C, Katz R, Lafitte C, Lo E, Penicaud A, Pradat-Diehl P & Raoul S. (2000). Presynaptic inhibition and homosynaptic depression: a comparison between lower and upper limbs in normal human subjects and patients with hemiplegia. *Brain* **123 (Pt 8),** 1688-1702.

Azouvi P, Roby-Brami A, Biraben A, Thiebaut JB, Thurel C & Bussel B. (1993). Effect of intrathecal baclofen on the monosynaptic reflex in humans: evidence for a postsynaptic action. *J Neurol Neurosurg Psychiatry* **56,** 515-519.

Baker LL & Chandler SH. (1987). Characterization of postsynaptic potentials evoked by sural nerve stimulation in hindlimb motoneurons from acute and chronic spinal cats. *Brain Res* **420,** 340-350.

Baker SN. (2011). The primate reticulospinal tract, hand function and functional recovery. *J Physiol* **589,** 5603-5612.

Baker SN & Perez MA. (2017). Reticulospinal Contributions to Gross Hand Function after Human Spinal Cord Injury. *J Neurosci* **37,** 9778-9784.

Ballermann M & Fouad K. (2006). Spontaneous locomotor recovery in spinal cord injured rats is accompanied by anatomical plasticity of reticulospinal fibers. *Eur J Neurosci* **23,** 1988-1996.

Bardoni R, Takazawa T, Tong CK, Choudhury P, Scherrer G & Macdermott AB. (2013). Pre- and postsynaptic inhibitory control in the spinal cord dorsal horn. *Annals of the New York Academy of Sciences* **1279,** 90-96.

Barron DH & Matthews BH. (1935). Intermittent conduction in the spinal cord. *J Physiol* **85,** 73-103.

Barron DH & Matthews BH. (1938). The interpretation of potential changes in the spinal cord. *The Journal of physiology* **92,** 276-321.

Behrman AL & Harkema SJ. (2000). Locomotor training after human spinal cord injury: a series of case studies. *Phys Ther* **80,** 688-700.

Bellardita C, Caggiano V, Leiras R, Caldeira V, Fuchs A, Bouvier J, Low P & Kiehn O. (2017). Spatiotemporal correlation of spinal network dynamics underlying spasms in chronic spinalized mice. *Elife* **6**.

Beloozerova I & Rossignol S. (1999). Antidromic discharges in dorsal roots of decerebrate cats. I. Studies at rest and during fictive locomotion. *Brain research* **846,** 87-105.

Bennett DJ, De Serres SJ & Stein RB. (1996). Gain of the triceps surae stretch reflex in decerebrate and spinal cats during postural and locomotor activities. *The Journal of physiology* **496 (Pt 3),** 837-850.

Bennett DJ, Gorassini M, Fouad K, Sanelli L, Han Y & Cheng J. (1999). Spasticity in rats with sacral spinal cord injury. *J Neurotrauma* **16,** 69-84.

Bennett DJ, Li Y, Harvey PJ & Gorassini M. (2001). Evidence for plateau potentials in tail motoneurons of awake chronic spinal rats with spasticity. *Journal of neurophysiology* **86,** 1972-1982.

Bennett DJ, Sanelli L, Cooke CL, Harvey PJ & Gorassini MA. (2004). Spastic long-lasting reflexes in the awake rat after sacral spinal cord injury. *J Neurophysiol* **91,** 2247-2258.

Berardelli A, Day BL, Marsden CD & Rothwell JC. (1987). Evidence favouring presynaptic inhibition between antagonist muscle afferents in the human forearm. *J Physiol* **391,** 71-83.

Betley JN, Wright CV, Kawaguchi Y, Erdelyi F, Szabo G, Jessell TM & Kaltschmidt JA. (2009). Stringent specificity in the construction of a GABAergic presynaptic inhibitory circuit. *Cell* **139,** 161-174.

Biering-Sorensen B, Kristensen IB, Kjaer M & Biering-Sorensen F. (2009). Muscle after spinal cord injury. *Muscle Nerve* **40,** 499-519.

Blight AR. (1985). Computer simulation of action potentials and afterpotentials in mammalian myelinated axons: the case for a lower resistance myelin sheath. *Neuroscience* **15,** 13-31.

Bos R, Brocard F & Vinay L. (2011). Primary afferent terminals acting as excitatory interneurons contribute to spontaneous motor activities in the immature spinal cord. *The Journal of neuroscience : the official journal of the Society for Neuroscience* **31,** 10184-10188.

Bostock H & Grafe P. (1985). Activity-dependent excitability changes in normal and demyelinated rat spinal root axons. *The Journal of physiology* **365,** 239-257.

Boulenguez P, Liabeuf S, Bos R, Bras H, Jean-Xavier C, Brocard C, Stil A, Darbon P, Cattaert D, Delpire E, Marsala M & Vinay L. (2010). Down-regulation of the potassium-chloride cotransporter KCC2 contributes to spasticity after spinal cord injury. *Nat Med* **16,** 302-307.

Boyden ES, Zhang F, Bamberg E, Nagel G & Deisseroth K. (2005). Millisecond-timescale, genetically targeted optical control of neural activity. *Nat Neurosci* **8,** 1263-1268.

Braddom RL & Johnson EW. (1974). H reflex: review and classification with suggested clinical uses. *Arch Phys Med Rehabil* **55,** 412-417.

Bravo-Hernandez M, Corleto JA, Barragan-Iglesias P, Gonzalez-Ramirez R, Pineda-Farias JB, Felix R, Calcutt NA, Delgado-Lezama R, Marsala M & Granados-Soto V. (2016). The alpha5 subunit containing GABAA receptors contribute to chronic pain. *Pain* **157,** 613-626.

Brown LE, Nicholson MW, Arama JE, Mercer A, Thomson AM & Jovanovic JN. (2016). gamma-Aminobutyric Acid Type A (GABAA) Receptor Subunits Play a Direct Structural Role in Synaptic Contact Formation via Their N-terminal Extracellular Domains. *J Biol Chem* **291,** 13926-13942.

Burke D, Gandevia SC & McKeon B. (1983). The afferent volleys responsible for spinal proprioceptive reflexes in man. *J Physiol* **339,** 535-552.

Burke D, Gandevia SC & McKeon B. (1984). Monosynaptic and oligosynaptic contributions to human ankle jerk and H-reflex. *J Neurophysiol* **52,** 435-448.

Burke D, Gracies JM, Meunier S & Pierrot-Deseilligny E. (1992). Changes in presynaptic inhibition of afferents to propriospinal-like neurones in man during voluntary contractions. *J Physiol* **449,** 673-687.

Burke KJ, Jr. & Bender KJ. (2019). Modulation of Ion Channels in the Axon: Mechanisms and Function. *Frontiers in cellular neuroscience* **13,** 221.

Burke RE & Glenn LL. (1996). Horseradish peroxidase study of the spatial and electrotonic distribution of group Ia synapses on type-identified ankle extensor motoneurons in the cat. *The Journal of comparative neurology* **372,** 465-485.

Calancie B, Broton JG, Klose KJ, Traad M, Difini J & Ayyar DR. (1993). Evidence that alterations in presynaptic inhibition contribute to segmental hypo- and hyperexcitability after spinal cord injury in man. *Electroencephalogr Clin Neurophysiol* **89,** 177-186.

Capaday C, Lavoie BA & Comeau F. (1995). Differential effects of a flexor nerve input on the human soleus H-reflex during standing versus walking. *Can J Physiol Pharmacol* **73,** 436-449.

Capaday C & Stein RB. (1986). Amplitude modulation of the soleus H-reflex in the human during walking and standing. *J Neurosci* **6,** 1308-1313.

Caron G, Bilchak JN & Cote MP. (2020). Direct evidence for decreased presynaptic inhibition evoked by PBSt group I muscle afferents after chronic SCI and recovery with step-training in rats. *J Physiol*.

Carpenter D, Lundberg A & Norrsell U. (1963). Primary Afferent Depolarization Evoked from the Sensorimotor Cortex. *Acta Physiol Scand* **59,** 126-142.

Cartlidge NE, Hudgson P & Weightman D. (1974). A comparison of baclofen and diazepam in the treatment of spasticity. *J Neurol Sci* **23,** 17-24.

Cattaert D & El Manira A. (1999). Shunting versus inactivation: analysis of presynaptic inhibitory mechanisms in primary afferents of the crayfish. *The Journal of neuroscience : the official journal of the Society for Neuroscience* **19,** 6079-6089.

Chabriat H, Bassetti CL, Marx U, Picarel-Blanchot F, Sors A, Gruget C, Saba B, Wattez M, Audoli ML & Hermann DM. (2020). Randomized Efficacy and Safety Trial with Oral S 44819 after Recent ischemic cerebral Event (RESTORE BRAIN study): a placebo controlled phase II study. *Trials* **21,** 136.

Chang E, Ghosh N, Yanni D, Lee S, Alexandru D & Mozaffar T. (2013). A Review of Spasticity Treatments: Pharmacological and Interventional Approaches. *Crit Rev Phys Rehabil Med* **25,** 11-22.

Chen Y, He Y & DeVivo MJ. (2016). Changing Demographics and Injury Profile of New Traumatic Spinal Cord Injuries in the United States, 1972-2014. *Arch Phys Med Rehabil* **97,** 1610-1619.

Choo AM, Liu J, Lam CK, Dvorak M, Tetzlaff W & Oxland TR. (2007). Contusion, dislocation, and distraction: primary hemorrhage and membrane permeability in distinct mechanisms of spinal cord injury. *J Neurosurg Spine* **6,** 255-266.

Chow BY, Han X, Dobry AS, Qian X, Chuong AS, Li M, Henninger MA, Belfort GM, Lin Y, Monahan PE & Boyden ES. (2010). High-performance genetically targetable optical neural silencing by light-driven proton pumps. *Nature* **463,** 98-102.

Chua HC & Chebib M. (2017). GABAA Receptors and the Diversity in their Structure and Pharmacology. *Adv Pharmacol* **79,** 1-34.

Chuang SH & Reddy DS. (2018). Genetic and Molecular Regulation of Extrasynaptic GABA-A Receptors in the Brain: Therapeutic Insights for Epilepsy. *J Pharmacol Exp Ther* **364,** 180-197.

Clarkson AN, Huang BS, Macisaac SE, Mody I & Carmichael ST. (2010). Reducing excessive GABA-mediated tonic inhibition promotes functional recovery after stroke. *Nature* **468,** 305-309.

Cohen CCH, Popovic MA, Klooster J, Weil MT, Mobius W, Nave KA & Kole MHP. (2020). Saltatory Conduction along Myelinated Axons Involves a Periaxonal Nanocircuit. *Cell* **180,** 311-322 e315.

Conradi S. (1969). Ultrastructure of dorsal root boutons on lumbosacral motoneurons of the adult cat, as revealed by dorsal root section. *Acta Physiol Scand Suppl* **332,** 85-115.

Courtine G, Gerasimenko Y, van den Brand R, Yew A, Musienko P, Zhong H, Song B, Ao Y, Ichiyama RM, Lavrov I, Roy RR, Sofroniew MV & Edgerton VR. (2009). Transformation of nonfunctional spinal circuits into functional states after the loss of brain input. *Nat Neurosci* **12,** 1333-1342.

Cramer SC, Lastra L, Lacourse MG & Cohen MJ. (2005). Brain motor system function after chronic, complete spinal cord injury. *Brain* **128,** 2941-2950.

Crone C, Hultborn H, Mazieres L, Morin C, Nielsen J & Pierrot-Deseilligny E. (1990). Sensitivity of monosynaptic test reflexes to facilitation and inhibition as a function of the test reflex size: a study in man and the cat. *Exp Brain Res* **81,** 35-45.

Crone C, Johnsen LL, Biering-Sorensen F & Nielsen JB. (2003). Appearance of reciprocal facilitation of ankle extensors from ankle flexors in patients with stroke or spinal cord injury. *Brain* **126,** 495-507.

Crone C & Nielsen J. (1989). Methodological implications of the post activation depression of the soleus H-reflex in man. *Experimental brain research* **78,** 28-32.

Crone C, Nielsen J, Petersen N, Ballegaard M & Hultborn H. (1994). Disynaptic reciprocal inhibition of ankle extensors in spastic patients. *Brain* **117 (Pt 5),** 1161-1168.

Crowe MJ, Bresnahan JC, Shuman SL, Masters JN & Beattie MS. (1997). Apoptosis and delayed degeneration after spinal cord injury in rats and monkeys. *Nat Med* **3,** 73-76.

Curtis DR. (1998a). *Two types of inhibition in the spinal cord*. Oxford University Press, New York.

Curtis DR. (1998b). Two types of inhibition in the spinal cord. . In *Presynaptic Inhibition and Neuron Control*, ed. Rudmon P, Romo R & Mendell LM, pp. 150-161. Oxford University Press, New York.

Curtis DR & Eccles JC. (1960). Synaptic action during and after repetitive stimulation. *The Journal of physiology* **150,** 374-398.

Curtis DR, Gynther BD, Lacey G & Beattie DT. (1997). Baclofen: reduction of presynaptic calcium influx in the cat spinal cord in vivo. *Exp Brain Res* **113,** 520-533.

Curtis DR & Lacey G. (1994). GABA-B receptor-mediated spinal inhibition. *Neuroreport* **5,** 540-542.

Curtis DR & Lacey G. (1998). Prolonged GABA(B) receptor-mediated synaptic inhibition in the cat spinal cord: an in vivo study. *Exp Brain Res* **121,** 319-333.

Curtis DR & Lodge D. (1982). The depolarization of feline ventral horn group Ia spinal afferent terminations by GABA. *Exp Brain Res* **46,** 215-233.

Cushing S, Bui T & Rose PK. (2005). Effect of nonlinear summation of synaptic currents on the input-output properties of spinal motoneurons. *J Neurophysiol* **94,** 3465-3478.

Czeh G & Dezso GT. (1982). Separation of temperature sensitive and temperature insensitive components of the postsynaptic potentials in the frog motoneurons. *Neuroscience* **7,** 2105-2115.

D'Amico JM, Condliffe EG, Martins KJ, Bennett DJ & Gorassini MA. (2014). Recovery of neuronal and network excitability after spinal cord injury and implications for spasticity. *Front Integr Neurosci* **8,** 36.

Darmani G, Zipser CM, Bohmer GM, Deschet K, Muller-Dahlhaus F, Belardinelli P, Schwab M & Ziemann U. (2016). Effects of the Selective alpha5-GABAAR Antagonist S44819 on Excitability in the Human Brain: A TMS-EMG and TMS-EEG Phase I Study. *J Neurosci* **36,** 12312-12320.

De Gail P, Lance JW & Neilson PD. (1966). Differential effects on tonic and phasic reflex mechanisms produced by vibration of muscles in man. *J Neurol Neurosurg Psychiatry* **29,** 1-11.

de Leon RD, Hodgson JA, Roy RR & Edgerton VR. (1998). Locomotor capacity attributable to step training versus spontaneous recovery after spinalization in adult cats. *J Neurophysiol* **79,** 1329-1340.

Debanne D, Campanac E, Bialowas A, Carlier E & Alcaraz G. (2011). Axon physiology. *Physiol Rev* **91,** 555-602.

Delgado-Lezama R, Loeza-Alcocer E, Andres C, Aguilar J, Guertin PA & Felix R. (2013). Extrasynaptic GABA(A) receptors in the brainstem and spinal cord: structure and function. *Curr Pharm Des* **19,** 4485-4497.

Delwaide PJ & Oliver E. (1988). Short-latency autogenic inhibition (IB inhibition) in human spasticity. *J Neurol Neurosurg Psychiatry* **51,** 1546-1550.

Desmedt JE & Godaux E. (1978). Mechanism of the vibration paradox: excitatory and inhibitory effects of tendon vibration on single soleus muscle motor units in man. *J Physiol* **285,** 197-207.

Devivo MJ. (2012). Epidemiology of traumatic spinal cord injury: trends and future implications. *Spinal Cord* **50,** 365-372.

DeVivo MJ & Chen Y. (2011). Trends in new injuries, prevalent cases, and aging with spinal cord injury. *Arch Phys Med Rehabil* **92,** 332-338.

Dietz V. (2000). Spastic movement disorder. *Spinal Cord* **38,** 389-393.

Drew GM, Siddall PJ & Duggan AW. (2001). Responses of spinal neurones to cutaneous and dorsal root stimuli in rats with mechanical allodynia after contusive spinal cord injury. *Brain Res* **893,** 59-69.

Duchen MR. (1986). Excitation of mouse motoneurones by GABA-mediated primary afferent depolarization. *Brain Res* **379,** 182-187.

Dudel J. (1965). The Mechanism of Presynaptic Inhibition at the Crayfish Neuromuscular Junction. *Pflugers Arch Gesamte Physiol Menschen Tiere* **284,** 66-80.

Dzyubenko E, Fleischer M, Manrique-Castano D, Borbor M, Kleinschnitz C, Faissner A & Hermann DM. (2021). Inhibitory control in neuronal networks relies on the extracellular matrix integrity. *Cell Mol Life Sci* **78,** 5647-5663.

Eccles JC, Eccles RM & Magni F. (1961a). Central inhibitory action attributable to presynaptic depolarization produced by muscle afferent volleys. *J Physiol* **159,** 147-166.

Eccles JC, Kozak W & Magni F. (1961b). Dorsal root reflexes of muscle group I afferent fibres. *J Physiol* **159,** 128-146.

Eccles JC & Krnjevic K. (1959). Potential changes recorded inside primary afferent fibres within the spinal cord. *The Journal of physiology* **149,** 250-273.

Eccles JC, Magni F & Willis WD. (1962a). Depolarization of central terminals of Group I afferent fibres from muscle. *J Physiol* **160,** 62-93.

Eccles JC, Magni F & Willis WD. (1962b). Depolarization of central terminals of Group I afferent fibres from muscle. *The Journal of physiology* **160,** 62-93.

Eccles JC & Rall W. (1951). Effects induced in a monosynaptic reflex path by its activation. *Journal of neurophysiology* **14,** 353-376.

Eccles JC, Schmidt R & Willis WD. (1963). Pharmacological Studies on Presynaptic Inhibition. *J Physiol* **168,** 500-530.

Eccles JC, Schmidt RF & Willis WD. (1962c). Presynaptic inhibition of the spinal monosynaptic reflex pathway. *J Physiol* **161,** 282-297.

Edstrom L. (1970). Selective changes in the sizes of red and white muscle fibres in upper motor lesions and Parkinsonism. *J Neurol Sci* **11,** 537-550.

Eguibar JR, Quevedo J & Rudomin P. (1997). Selective cortical and segmental control of primary afferent depolarization of single muscle afferents in the cat spinal cord. *Experimental brain research* **113,** 411-430.

El-Gaby M, Zhang Y, Wolf K, Schwiening CJ, Paulsen O & Shipton OA. (2016). Archaerhodopsin Selectively and Reversibly Silences Synaptic Transmission through Altered pH. *Cell Rep* **16,** 2259-2268.

El-Tohamy A & Sedgwick EM. (1983). Spinal inhibition in man: depression of the soleus H reflex by stimulation of the nerve to the antagonist muscle. *J Physiol* **337,** 497-508.

Engelman HS & MacDermott AB. (2004). Presynaptic ionotropic receptors and control of transmitter release. *Nature reviews Neuroscience* **5,** 135-145.

Esclapez M, Tillakaratne NJ, Kaufman DL, Tobin AJ & Houser CR. (1994). Comparative localization of two forms of glutamic acid decarboxylase and their mRNAs in rat brain supports the concept of functional differences between the forms. *The Journal of neuroscience : the official journal of the Society for Neuroscience* **14,** 1834-1855.

Faist M, Dietz V & Pierrot-Deseilligny E. (1996). Modulation, probably presynaptic in origin, of monosynaptic Ia excitation during human gait. *Exp Brain Res* **109,** 441-449.

Faist M, Mazevet D, Dietz V & Pierrot-Deseilligny E. (1994). A quantitative assessment of presynaptic inhibition of Ia afferents in spastics. Differences in hemiplegics and paraplegics. *Brain* **117 (Pt 6),** 1449-1455.

Fedirchuk B, Wenner P, Whelan PJ, Ho S, Tabak J & O'Donovan MJ. (1999). Spontaneous network activity transiently depresses synaptic transmission in the embryonic chick spinal cord. *J Neurosci* **19,** 2102-2112.

Feil R, Wagner J, Metzger D & Chambon P. (1997). Regulation of Cre recombinase activity by mutated estrogen receptor ligand-binding domains. *Biochem Biophys Res Commun* **237,** 752-757.

Fenrich KK, Zhao EY, Wei Y, Garg A & Rose PK. (2014). Isolating specific cell and tissue compartments from 3D images for quantitative regional distribution analysis using novel computer algorithms. *Journal of neuroscience methods* **226,** 42-56.

Fink AJ. (2013a). Exploring a behavioral role for presynaptic inhibition at spinal sensory-motor synapses. *PhD Thesis, Columbia University***,** 1-293.

Fink AJ. (2013b). Exploring a behavioural role for presynaptic inhibition in spinal sensory-motor synapses. *PhD Thesis, Columbia University***,** 1-293.

Fink AJ, Croce KR, Huang ZJ, Abbott LF, Jessell TM & Azim E. (2014). Presynaptic inhibition of spinal sensory feedback ensures smooth movement. *Nature* **509,** 43-48.

Fisher MA. (1992). AAEM Minimonograph #13: H reflexes and F waves: physiology and clinical indications. *Muscle Nerve* **15,** 1223-1233.

Foust KD, Poirier A, Pacak CA, Mandel RJ & Flotte TR. (2008). Neonatal intraperitoneal or intravenous injections of recombinant adeno-associated virus type 8 transduce dorsal root ganglia and lower motor neurons. *Hum Gene Ther* **19,** 61-70.

Frank K. (1959a). Basic mechanisms of synaptic transmission in the central nervous system. *Inst Radio Eng Trans Med Electron* **ME-6,** 85-88.

Frank K. (1959b). Basic mechanisms of synaptic transmission in the central nervous system. *Inst Radio Eng Trans Med Electron* **ME-6,** 85-88.

Frank K & Fortes MGF. (1957). Presynaptic and postsynaptic inhibition of monosynaptic reflexes. . *Fed Proc* **16,** 39-40.

Fung J & Barbeau H. (1994). Effects of conditioning cutaneomuscular stimulation on the soleus H-reflex in normal and spastic paretic subjects during walking and standing. *Journal of neurophysiology* **72,** 2090-2104.

Gallagher JP, Higashi H & Nishi S. (1978a). Characterization and ionic basis of GABA-induced depolarizations recorded in vitro from cat primary afferent neurones. *J Physiol* **275,** 263-282.

Gallagher JP, Higashi H & Nishi S. (1978b). Characterization and ionic basis of GABA-induced depolarizations recorded in vitro from cat primary afferent neurones. *The Journal of physiology* **275,** 263-282.

Gemes G, Koopmeiners A, Rigaud M, Lirk P, Sapunar D, Bangaru ML, Vilceanu D, Garrison SR, Ljubkovic M, Mueller SJ, Stucky CL & Hogan QH. (2013). Failure of action potential propagation in sensory neurons: mechanisms and loss of afferent filtering in C-type units after painful nerve injury. *The Journal of physiology* **591,** 1111-1131.

Goldstein SS & Rall W. (1974). Changes of action potential shape and velocity for changing core conductor geometry. *Biophysical journal* **14,** 731-757.

Gorassini MA, Knash ME, Harvey PJ, Bennett DJ & Yang JF. (2004). Role of motoneurons in the generation of muscle spasms after spinal cord injury. *Brain* **127,** 2247-2258.

Goulart F, Valls-Sole J & Alvarez R. (2000). Posture-related changes of soleus H-reflex excitability. *Muscle Nerve* **23,** 925-932.

Goulding M. (2009). Circuits controlling vertebrate locomotion: moving in a new direction. *Nature reviews Neuroscience* **10,** 507-518.

Graham B & Redman S. (1994). A simulation of action potentials in synaptic boutons during presynaptic inhibition. *Journal of neurophysiology* **71,** 538-549.

Grey MJ, Klinge K, Crone C, Lorentzen J, Biering-Sorensen F, Ravnborg M & Nielsen JB. (2008). Post-activation depression of soleus stretch reflexes in healthy and spastic humans. *Exp Brain Res* **185,** 189-197.

Hari K, Lucas-Osma AM, Metz K, Lin S, Pardell N, Roszko D, Black S, Minarik A, Singla R, Stephens MJ, Fouad K, Jones KE, Gorassini M, Fenrich KK, Li Y & Bennett DJ. (2021). Nodal GABA facilitates axon spike transmission in the spinal cord. *BioRxiv*.

Harkema SJ. (2008). Plasticity of interneuronal networks of the functionally isolated human spinal cord. *Brain Res Rev* **57,** 255-264.

Harris JA, Hirokawa KE, Sorensen SA, Gu H, Mills M, Ng LL, Bohn P, Mortrud M, Ouellette B, Kidney J, Smith KA, Dang C, Sunkin S, Bernard A, Oh SW, Madisen L & Zeng H. (2014). Anatomical characterization of Cre driver mice for neural circuit mapping and manipulation. *Front Neural Circuits* **8,** 76.

Harvey PJ, Li Y, Li X & Bennett DJ. (2006). Persistent sodium currents and repetitive firing in motoneurons of the sacrocaudal spinal cord of adult rats. *J Neurophysiol* **96,** 1141-1157.

Hayes ES & Carlton SM. (1992). Primary afferent interactions: analysis of calcitonin gene-related peptide-immunoreactive terminals in contact with unlabeled and GABA-immunoreactive profiles in the monkey dorsal horn. *Neuroscience* **47,** 873-896.

Heckmann CJ, Gorassini MA & Bennett DJ. (2005). Persistent inward currents in motoneuron dendrites: implications for motor output. *Muscle Nerve* **31,** 135-156.

Henneman E, Luscher HR & Mathis J. (1984a). Simultaneously active and inactive synapses of single Ia fibres on cat spinal motoneurones. *The Journal of physiology* **352,** 147-161.

Henneman E, Luscher HR & Mathis J. (1984b). Simultaneously active and inactive synapses of single Ia fibres on cat spinal motoneurones. *The Journal of physiology* **352,** 147-161.

Hines ML & Carnevale NT. (2001). NEURON: a tool for neuroscientists. *Neuroscientist* **7,** 123-135.

Hofstoetter US, Freundl B, Binder H & Minassian K. (2019). Recovery cycles of posterior root-muscle reflexes evoked by transcutaneous spinal cord stimulation and of the H reflex in individuals with intact and injured spinal cord. *PLoS One* **14,** e0227057.

Howell RD & Pugh JR. (2016). Biphasic modulation of parallel fibre synaptic transmission by co-activation of presynaptic GABAA and GABAB receptors in mice. *J Physiol* **594,** 3651-3666.

Howells J, Sangari S, Matamala JM, Kiernan MC, Marchand-Pauvert V & Burke D. (2020). Interrogating interneurone function using threshold tracking of the H reflex in healthy subjects and patients with motor neurone disease. *Clin Neurophysiol* **131,** 1986-1996.

Howland B, Lettvin JY, McCulloch WS, Pitts W & Wall PD. (1955). Reflex inhibition by dorsal root interaction. *Journal of neurophysiology* **18,** 1-17.

Hubbard JI, Llinas R & Quastel DMJ. (1969). *Electrophysiological Analysis of Synaptic Transmission*. Edward Arnold Ltd, London.

Hughes DI, Mackie M, Nagy GG, Riddell JS, Maxwell DJ, Szabo G, Erdelyi F, Veress G, Szucs P, Antal M & Todd AJ. (2005). P boutons in lamina IX of the rodent spinal cord express high levels of glutamic acid decarboxylase-65 and originate from cells in deep medial dorsal horn. *Proc Natl Acad Sci U S A* **102,** 9038-9043.

Hultborn H. (2006). Spinal reflexes, mechanisms and concepts: from Eccles to Lundberg and beyond. *Prog Neurobiol* **78,** 215-232.

Hultborn H, Illert M, Nielsen J, Paul A, Ballegaard M & Wiese H. (1996a). On the mechanism of the post-activation depression of the H-reflex in human subjects. *Experimental brain research* **108,** 450-462.

Hultborn H, Illert M, Nielsen J, Paul A, Ballegaard M & Wiese H. (1996b). On the mechanism of the post-activation depression of the H-reflex in human subjects. *Experimental brain research* **108,** 450-462.

Hultborn H, Meunier S, Morin C & Pierrot-Deseilligny E. (1987a). Assessing changes in presynaptic inhibition of I a fibres: a study in man and the cat. *J Physiol* **389,** 729-756.

Hultborn H, Meunier S, Pierrot-Deseilligny E & Shindo M. (1987b). Changes in presynaptic inhibition of Ia fibres at the onset of voluntary contraction in man. *J Physiol* **389,** 757-772.

Iles JF. (1996). Evidence for cutaneous and corticospinal modulation of presynaptic inhibition of Ia afferents from the human lower limb. *J Physiol* **491 (Pt 1),** 197-207.

Iles JF & Pisini JV. (1992). Cortical modulation of transmission in spinal reflex pathways of man. *J Physiol* **455,** 425-446.

Iles JF & Roberts RC. (1987). Inhibition of monosynaptic reflexes in the human lower limb. *J Physiol* **385,** 69-87.

Ishizuka N, Mannen H, Hongo T & Sasaki S. (1979). Trajectory of group Ia afferent fibers stained with horseradish peroxidase in the lumbosacral spinal cord of the cat: three dimensional reconstructions from serial sections. *The Journal of comparative neurology* **186,** 189-211.

Jankowska E. (1992). Interneuronal relay in spinal pathways from proprioceptors. *Prog Neurobiol* **38,** 335-378.

Jankowska E, McCrea D & Mackel R. (1981a). Oligosynaptic excitation of motoneurones by impulses in group Ia muscle spindle afferents in the cat. *J Physiol* **316,** 411-425.

Jankowska E, McCrea D, Rudomin P & Sykova E. (1981b). Observations on neuronal pathways subserving primary afferent depolarization. *J Neurophysiol* **46,** 506-516.

Jankowska E, McCrea D, Rudomin P & Sykova E. (1981c). Observations on neuronal pathways subserving primary afferent depolarization. *Journal of neurophysiology* **46,** 506-516.

Jankus WR, Robinson LR & Little JW. (1994). Normal limits of side-to-side H-reflex amplitude variability. *Arch Phys Med Rehabil* **75,** 3-7.

Kangrga I, Jiang MC & Randic M. (1991). Actions of (-)-baclofen on rat dorsal horn neurons. *Brain Res* **562,** 265-275.

Kapitza S, Zorner B, Weinmann O, Bolliger M, Filli L, Dietz V & Schwab ME. (2012). Tail spasms in rat spinal cord injury: changes in interneuronal connectivity. *Exp Neurol* **236,** 179-189.

Katz B & Miledi R. (1965). Propagation of Electric Activity in Motor Nerve Terminals. *Proc R Soc Lond B Biol Sci* **161,** 453-482.

Khalki L, Sadlaoud K, Lerond J, Coq JO, Brezun JM, Vinay L, Coulon P & Bras H. (2018). Changes in innervation of lumbar motoneurons and organization of premotor network following training of transected adult rats. *Exp Neurol* **299,** 1-14.

Khan AS, Patrick SK, Roy FD, Gorassini MA & Yang JF. (2016). Training-Specific Neural Plasticity in Spinal Reflexes after Incomplete Spinal Cord Injury. *Neural Plast* **2016,** 6718763.

Knikou M & Mummidisetty CK. (2014). Locomotor training improves premotoneuronal control after chronic spinal cord injury. *J Neurophysiol* **111,** 2264-2275.

Koelman JH, Bour LJ, Hilgevoord AA, van Bruggen GJ & Ongerboer de Visser BW. (1993). Soleus H-reflex tests and clinical signs of the upper motor neuron syndrome. *J Neurol Neurosurg Psychiatry* **56,** 776-781.

Kohn AF, Floeter MK & Hallett M. (1997). Presynaptic inhibition compared with homosynaptic depression as an explanation for soleus H-reflex depression in humans. *Exp Brain Res* **116,** 375-380.

Kralj JM, Douglass AD, Hochbaum DR, Maclaurin D & Cohen AE. (2011). Optical recording of action potentials in mammalian neurons using a microbial rhodopsin. *Nature methods* **9,** 90-95.

Krenz NR & Weaver LC. (1998). Sprouting of primary afferent fibers after spinal cord transection in the rat. *Neuroscience* **85,** 443-458.

Kumru H, Albu S, Valls-Sole J, Murillo N, Tormos JM & Vidal J. (2015). Influence of spinal cord lesion level and severity on H-reflex excitability and recovery curve. *Muscle Nerve* **52,** 616-622.

Lagrange AH, Hu N & Macdonald RL. (2018). GABA beyond the synapse: defining the subtype-specific pharmacodynamics of non-synaptic GABAA receptors. *The Journal of physiology* **596,** 4475-4495.

Lalonde NR & Bui TV. (2021). Do spinal circuits still require gating of sensory information by presynaptic inhibition after spinal cord injury? *Current Opinion in Physiology* **19,** 113-118.

Lalonde RL & Bui T. (2020). Do spinal circuits still require gating of sensory information by presynaptic inhibition after spinal cord injury? *Current Opinion in Physiol* **21,** 113-118.

Lamotte d'Incamps B, Destombes J, Thiesson D, Hellio R, Lasserre X, Kouchtir-Devanne N, Jami L & Zytnicki D. (1998). Indications for GABA-immunoreactive axo-axonic contacts on the intraspinal arborization of a Ib fiber in cat: a confocal microscope study. *The Journal of neuroscience : the official journal of the Society for Neuroscience* **18,** 10030-10036.

Leandri M, Leandri S & Lunardi G. (2008). Effect of temperature on sensory and motor conduction of the rat tail nerves. *Neurophysiol Clin* **38,** 297-304.

Lee JK, Emch GS, Johnson CS & Wrathall JR. (2005). Effect of spinal cord injury severity on alterations of the H-reflex. *Exp Neurol* **196,** 430-440.

Leppanen L & Stys PK. (1997a). Ion transport and membrane potential in CNS myelinated axons I. Normoxic conditions. *Journal of neurophysiology* **78,** 2086-2094.

Leppanen L & Stys PK. (1997b). Ion transport and membrane potential in CNS myelinated axons. II. Effects of metabolic inhibition. *J Neurophysiol* **78,** 2095-2107.

Lev-Tov A, Fleshman JW & Burke RE. (1983). Primary afferent depolarization and presynaptic inhibition of monosynaptic group Ia EPSPs during posttetanic potentiation. *Journal of neurophysiology* **50,** 413-427.

Lev-Tov A, Meyers DE & Burke RE. (1988). Activation of type B gamma-aminobutyric acid receptors in the intact mammalian spinal cord mimics the effects of reduced presynaptic Ca2+ influx. *Proceedings of the National Academy of Sciences of the United States of America* **85,** 5330-5334.

Levy RA & Anderson EG. (1972). The effect of the GABA antagonists bicuculline and picrotoxin on primary afferent terminal excitability. *Brain Res* **43,** 171-180.

Li S, Zhuang C, Hao M, He X, Marquez JC, Niu CM & Lan N. (2015). Coordinated alpha and gamma control of muscles and spindles in movement and posture. *Front Comput Neurosci* **9,** 122.

Li Y & Bennett DJ. (2003). Persistent sodium and calcium currents cause plateau potentials in motoneurons of chronic spinal rats. *J Neurophysiol* **90,** 857-869.

Li Y, Gorassini MA & Bennett DJ. (2004a). Role of persistent sodium and calcium currents in motoneuron firing and spasticity in chronic spinal rats. *Journal of neurophysiology* **91,** 767-783.

Li Y, Hari K, Lucas-Osma AM, Fenrich KK, Bennett DJ, Hammar I & Jankowska E. (2020). Branching points of primary afferent fibers are vital for the modulation of fiber excitability by epidural DC polarization and by GABA in the rat spinal cord. *Journal of neurophysiology* **124,** 49-62.

Li Y, Harvey PJ, Li X & Bennett DJ. (2004b). Spastic long-lasting reflexes of the chronic spinal rat studied in vitro. *Journal of neurophysiology* **91,** 2236-2246.

Li Y, Li X, Harvey PJ & Bennett DJ. (2004c). Effects of baclofen on spinal reflexes and persistent inward currents in motoneurons of chronic spinal rats with spasticity. *J Neurophysiol* **92,** 2694-2703.

Li Y, Lucas-Osma AM, Black S, Bandet MV, Stephens MJ, Vavrek R, Sanelli L, Fenrich KK, Di Narzo AF, Dracheva S, Winship IR, Fouad K & Bennett DJ. (2017). Pericytes impair capillary blood flow and motor function after chronic spinal cord injury. *Nature medicine* **23,** 733-741.

Lin S, Li Y, Lucas-Osma AM, Hari K, Stephens MJ, Singla R, Heckman CJ, Zhang Y, Fouad K, Fenrich KK & Bennett DJ. (2019). Locomotor-related V3 interneurons initiate and coordinate muscles spasms after spinal cord injury. *J Neurophysiol* **121,** 1352-1367.

Liu M, Wu W, Li H, Li S, Huang LT, Yang YQ, Sun Q, Wang CX, Yu Z & Hang CH. (2015). Necroptosis, a novel type of programmed cell death, contributes to early neural cells damage after spinal cord injury in adult mice. *J Spinal Cord Med* **38,** 745-753.

Liu Y, Latremoliere A, Li X, Zhang Z, Chen M, Wang X, Fang C, Zhu J, Alexandre C, Gao Z, Chen B, Ding X, Zhou JY, Zhang Y, Chen C, Wang KH, Woolf CJ & He Z. (2018). Touch and tactile neuropathic pain sensitivity are set by corticospinal projections. *Nature* **561,** 547-550.

Lloyd DP. (1949). Post-tetanic potentiation of response in monosynaptic reflex pathways of the spinal cord. *The Journal of general physiology* **33,** 147-170.

Loeza-Alcocer E, Canto-Bustos M, Aguilar J, Gonzalez-Ramirez R, Felix R & Delgado-Lezama R. (2013). alpha(5)GABA(A) receptors mediate primary afferent fiber tonic excitability in the turtle spinal cord. *J Neurophysiol* **110,** 2175-2184.

Lomeli J, Quevedo J, Linares P & Rudomin P. (1998). Local control of information flow in segmental and ascending collaterals of single afferents. *Nature* **395,** 600-604.

Lucas-Osma AM, Li Y, Lin S, Black S, Singla R, Fouad K, Fenrich KK & Bennett DJ. (2018a). Extrasynaptic alpha5GABAA receptors on proprioceptive afferents produce a tonic depolarization that

modulates sodium channel function in the rat spinal cord. *Journal of neurophysiology* **120,** 2953-2974.

Lucas-Osma AM, Li Y, Lin S, Black S, Singla R, Fouad K, Fenrich KK & Bennett DJ. (2018b). Extrasynaptic proportional, variant5GABAA receptors on proprioceptive afferents produce a tonic depolarization that modulates sodium channel function in the rat spinal cord. *J Neurophysiol*.

Lucas-Osma AM, Li Y, Murray K, Lin S, Black S, Stephens MJ, Ahn AH, Heckman CJ, Fenrich KK, Fouad K & Bennett DJ. (2019). 5-HT1D receptors inhibit the monosynaptic stretch reflex by modulating C-fiber activity. *Journal of neurophysiology* **121,** 1591-1608.

Luscher C, Streit J, Lipp P & Luscher HR. (1994a). Action potential propagation through embryonic dorsal root ganglion cells in culture. II. Decrease of conduction reliability during repetitive stimulation. *Journal of neurophysiology* **72,** 634-643.

Luscher C, Streit J, Quadroni R & Luscher HR. (1994b). Action potential propagation through embryonic dorsal root ganglion cells in culture. I. Influence of the cell morphology on propagation properties. *Journal of neurophysiology* **72,** 622-633.

Luscher HR, Ruenzel P, Fetz E & Henneman E. (1979). Postsynatpic population potentials recorded from ventral roots perfused with isotonic sucrose: connections of groups Ia and II spindle afferent fibers with large populations of motoneurons. *J Neurophysiol* **42,** 1146-1164.

Luscher HR, Ruenzel P & Henneman E. (1983). Composite EPSPs in motoneurons of different sizes before and during PTP: implications for transmission failure and its relief in Ia projections. *Journal of neurophysiology* **49,** 269-289.

Madisen L, Mao T, Koch H, Zhuo JM, Berenyi A, Fujisawa S, Hsu YW, Garcia AJ, 3rd, Gu X, Zanella S, Kidney J, Gu H, Mao Y, Hooks BM, Boyden ES, Buzsaki G, Ramirez JM, Jones AR, Svoboda K, Han X, Turner EE & Zeng H. (2012). A toolbox of Cre-dependent optogenetic transgenic mice for light-induced activation and silencing. *Nat Neurosci* **15,** 793-802.

Madisen L, Zwingman TA, Sunkin SM, Oh SW, Zariwala HA, Gu H, Ng LL, Palmiter RD, Hawrylycz MJ, Jones AR, Lein ES & Zeng H. (2010). A robust and high-throughput Cre reporting and characterization system for the whole mouse brain. *Nat Neurosci* **13,** 133-140.

Magladery JW, Teasdall RD, Park AM & Languth HW. (1952). Electrophysiological studies of reflex activity in patients with lesions of the nervous system. I. A comparison of spinal motoneurone excitability following afferent nerve volleys in normal persons and patients with upper motor neurone lesions. *Bull Johns Hopkins Hosp* **91,** 219-244; passim.

Mailis A & Ashby P. (1990). Alterations in group Ia projections to motoneurons following spinal lesions in humans. *J Neurophysiol* **64,** 637-647.

Martinez-Valdes E, Negro F, Laine CM, Falla D, Mayer F & Farina D. (2017). Tracking motor units longitudinally across experimental sessions with high-density surface electromyography. *J Physiol* **595,** 1479-1496.

Masland WS. (1972). Facilitation during the H-reflex recovery cycle. *Arch Neurol* **26,** 313-319.

Matthews PB. (1986). Observations on the automatic compensation of reflex gain on varying the pre-existing level of motor discharge in man. *The Journal of physiology* **374,** 73-90.

Matthews PB. (1996). Relationship of firing intervals of human motor units to the trajectory of post-spike after-hyperpolarization and synaptic noise. *The Journal of physiology* **492 (Pt 2),** 597-628.

McCrea DA, Shefchyk SJ & Carlen PL. (1990). Large reductions in composite monosynaptic EPSP amplitude following conditioning stimulation are not accounted for by increased postsynaptic conductances in motoneurons. *Neurosci Lett* **109,** 117-122.

McIntyre CC, Richardson AG & Grill WM. (2002). Modeling the excitability of mammalian nerve fibers: influence of afterpotentials on the recovery cycle. *Journal of neurophysiology* **87,** 995-1006.

Mekhael W, Begum S, Samaddar S, Hassan M, Toruno P, Ahmed M, Gorin A, Maisano M, Ayad M & Ahmed Z. (2019). Repeated anodal trans-spinal direct current stimulation results in long-term reduction of spasticity in mice with spinal cord injury. *The Journal of physiology* **597,** 2201-2223.

Mende M, Fletcher EV, Belluardo JL, Pierce JP, Bommareddy PK, Weinrich JA, Kabir ZD, Schierberl KC, Pagiazitis JG, Mendelsohn AI, Francesconi A, Edwards RH, Milner TA, Rajadhyaksha AM, van Roessel PJ, Mentis GZ & Kaltschmidt JA. (2016). Sensory-Derived Glutamate Regulates Presynaptic Inhibitory Terminals in Mouse Spinal Cord. *Neuron* **90,** 1189-1202.

Metz K, Concha-Matos I, Hari K, Bseis O, Afsharipour B, Lin S, Li Y, Fenrich KF, Bennett DJ & Gorassini M. (2022). Post-activation depression produces extensor H-reflex suppresion following flexor afferent conditioning. *BioRxiv*.

Metz K, Concha-Matos I, Li Y, Afsharipour B, Thompson CK, Negro F, Bennett DJ & Gorassini M. (2021). Facilitation of sensory axon conduction to motoneurons during cortical or sensory evoked primary afferent depolarization (PAD) in humans. *BioRxiv*.

Meunier S & Pierrot-Deseilligny E. (1998a). Cortical control of presynaptic inhibition of Ia afferents in humans. *Exp Brain Res* **119,** 415-426.

Meunier S & Pierrot-Deseilligny E. (1998b). Cortical control of presynaptic inhibition of Ia afferents in humans. *Experimental brain research* **119,** 415-426.

Milanov I. (1992). A comparative study of methods for estimation of presynaptic inhibition. *J Neurol* **239,** 287-292.

Mirbagheri MM, Barbeau H, Ladouceur M & Kearney RE. (2001). Intrinsic and reflex stiffness in normal and spastic, spinal cord injured subjects. *Exp Brain Res* **141,** 446-459.

Misiaszek JE. (2003). The H-reflex as a tool in neurophysiology: its limitations and uses in understanding nervous system function. *Muscle Nerve* **28,** 144-160.

Mizuno Y, Tanaka R & Yanagisawa N. (1971). Reciprocal group I inhibition on triceps surae motoneurons in man. *J Neurophysiol* **34,** 1010-1017.

Morin C, Pierrot-Deseilligny E & Hultborn H. (1984). Evidence for presynaptic inhibition of muscle spindle Ia afferents in man. *Neurosci Lett* **44,** 137-142.

Mott FW & Sherrington CS. (1895). Experiments upon the influence of sensory nerves upon movements and nutrition of the limbs. *Proceedings of the Royal Society* **B,** 481-488.

Munson JB & Sypert GW. (1979a). Properties of single central Ia afferent fibres projecting to motoneurones. *The Journal of physiology* **296,** 315-327.

Munson JB & Sypert GW. (1979b). Properties of single fibre excitatory post-synaptic potentials in triceps surae motoneurones. *The Journal of physiology* **296,** 329-342.

Murray KC, Nakae A, Stephens MJ, Rank M, D'Amico J, Harvey PJ, Li X, Harris RL, Ballou EW, Anelli R, Heckman CJ, Mashimo T, Vavrek R, Sanelli L, Gorassini MA, Bennett DJ & Fouad K. (2010). Recovery of motoneuron and locomotor function after spinal cord injury depends on constitutive activity in 5-HT2C receptors. *Nature medicine* **16,** 694-700.

Murray KC, Stephens MJ, Ballou EW, Heckman CJ & Bennett DJ. (2011a). Motoneuron excitability and muscle spasms are regulated by 5-HT2B and 5-HT2C receptor activity. *J Neurophysiol* **105,** 731-748.

Murray KC, Stephens MJ, Rank M, D'Amico J, Gorassini MA & Bennett DJ. (2011b). Polysynaptic excitatory postsynaptic potentials that trigger spasms after spinal cord injury in rats are inhibited by 5-HT1B and 5-HT1F receptors. *J Neurophysiol* **106,** 925-943.

Nacimiento W, Sappok T, Brook GA, Toth L, Schoen SW, Noth J & Kreutzberg GW. (1995). Structural changes of anterior horn neurons and their synaptic input caudal to a low thoracic spinal cord hemisection in the adult rat: a light and electron microscopic study. *Acta Neuropathol* **90,** 552-564.

Nakashima K, Rothwell JC, Day BL, Thompson PD & Marsden CD. (1990). Cutaneous effects on presynaptic inhibition of flexor Ia afferents in the human forearm. *J Physiol* **426,** 369-380.

Negro F, Muceli S, Castronovo AM, Holobar A & Farina D. (2016). Multi-channel intramuscular and surface EMG decomposition by convolutive blind source separation. *J Neural Eng* **13,** 026027.

Neher E & Sakaba T. (2001). Estimating transmitter release rates from postsynaptic current fluctuations. *J Neurosci* **21,** 9638-9654.

Nelson SG, Collatos TC, Niechaj A & Mendell LM. (1979). Immediate increase in Ia-motoneuron synaptic transmission caudal to spinal cord transection. *Journal of neurophysiology* **42,** 655-664.

Nicol MJ & Walmsley B. (1991). A serial section electron microscope study of an identified Ia afferent collateral in the cat spinal cord. *J Comp Neurol* **314,** 257-277.

Nielsen J & Kagamihara Y. (1993). The regulation of presynaptic inhibition during co-contraction of antagonistic muscles in man. *J Physiol* **464,** 575-593.

Nielsen J & Petersen N. (1994). Is presynaptic inhibition distributed to corticospinal fibres in man? *J Physiol* **477,** 47-58.

Nielsen J, Petersen N, Ballegaard M, Biering-Sorensen F & Kiehn O. (1993a). H-reflexes are less depressed following muscle stretch in spastic spinal cord injured patients than in healthy subjects. *Exp Brain Res* **97,** 173-176.

Nielsen J, Petersen N, Ballegaard M, Biering-Sorensen F & Kiehn O. (1993b). H-reflexes are less depressed following muscle stretch in spastic spinal cord injured patients than in healthy subjects. *Experimental brain research* **97,** 173-176.

Nielsen J, Petersen N & Crone C. (1995). Changes in transmission across synapses of Ia afferents in spastic patients. *Brain* **118 (Pt 4),** 995-1004.

Nielsen JB, Crone C & Hultborn H. (2007). The spinal pathophysiology of spasticity--from a basic science point of view. *Acta Physiol (Oxf)* **189,** 171-180.

Nielsen JB, Morita H, Wenzelburger R, Deuschl G, Gossard JP & Hultborn H. (2019a). Recruitment gain of spinal motor neuron pools in cat and human. *Experimental brain research*.

Nielsen JB, Morita H, Wenzelburger R, Deuschl G, Gossard JP & Hultborn H. (2019b). Recruitment gain of spinal motor neuron pools in cat and human. *Experimental brain research* **237,** 2897-2909.

Noonan VK, Fingas M, Farry A, Baxter D, Singh A, Fehlings MG & Dvorak MF. (2012). Incidence and prevalence of spinal cord injury in Canada: a national perspective. *Neuroepidemiology* **38,** 219-226.

Norton JA, Bennett DJ, Knash ME, Murray KC & Gorassini MA. (2008). Changes in sensory-evoked synaptic activation of motoneurons after spinal cord injury in man. *Brain* **131,** 1478-1491.

Olsen RW & Sieghart W. (2009). GABA A receptors: subtypes provide diversity of function and pharmacology. *Neuropharmacology* **56,** 141-148.

Ondarza AB, Ye Z & Hulsebosch CE. (2003). Direct evidence of primary afferent sprouting in distant segments following spinal cord injury in the rat: colocalization of GAP-43 and CGRP. *Exp Neurol* **184,** 373-380.

Oyinbo CA. (2011). Secondary injury mechanisms in traumatic spinal cord injury: a nugget of this multiply cascade. *Acta Neurobiol Exp (Wars)* **71,** 281-299.

Pan ZZ. (2012). Transcriptional control of Gad2. *Transcription* **3,** 68-72.

Paul J, Zeilhofer HU & Fritschy JM. (2012). Selective distribution of GABA(A) receptor subtypes in mouse spinal dorsal horn neurons and primary afferents. *The Journal of comparative neurology* **520,** 3895-3911.

Persohn E, Malherbe P & Richards JG. (1991). In situ hybridization histochemistry reveals a diversity of GABAA receptor subunit mRNAs in neurons of the rat spinal cord and dorsal root ganglia. *Neuroscience* **42,** 497-507.

Pierce JP & Mendell LM. (1993). Quantitative ultrastructure of Ia boutons in the ventral horn: scaling and positional relationships. *J Neurosci* **13,** 4748-4763.

Pierrot-Deseilligny E. (1997). Assessing changes in presynaptic inhibition of Ia afferents during movement in humans. *J Neurosci Methods* **74,** 189-199.

Pierrot-Deseilligny E, Katz R & Morin C. (1979). Evidence of Ib inhibition in human subjects. *Brain Res* **166,** 176-179.

Pinol RA, Bateman R & Mendelowitz D. (2012). Optogenetic approaches to characterize the long-range synaptic pathways from the hypothalamus to brain stem autonomic nuclei. *Journal of neuroscience methods* **210,** 238-246.

Powers RK & Binder MD. (2001). Input-output functions of mammalian motoneurons. *Rev Physiol Biochem Pharmacol* **143,** 137-263.

Prochazka A. (2015). Sensory control of normal movement and of movement aided by neural prostheses. *J Anat* **227,** 167-177.

Prochazka A & Gorassini M. (1998). Ensemble firing of muscle afferents recorded during normal locomotion in cats. *The Journal of physiology* **507 (Pt 1),** 293-304.

Quadri SA, Farooqui M, Ikram A, Zafar A, Khan MA, Suriya SS, Claus CF, Fiani B, Rahman M, Ramachandran A, Armstrong IIT, Taqi MA & Mortazavi MM. (2018). Recent update on basic mechanisms of spinal cord injury. *Neurosurg Rev*.

Rabchevsky AG & Kitzman PH. (2011). Latest approaches for the treatment of spasticity and autonomic dysreflexia in chronic spinal cord injury. *Neurotherapeutics* **8,** 274-282.

Rank MM, Murray KC, Stephens MJ, D'Amico J, Gorassini MA & Bennett DJ. (2011). Adrenergic receptors modulate motoneuron excitability, sensory synaptic transmission and muscle spasms after chronic spinal cord injury. *J Neurophysiol* **105,** 410-422.

Rasminsky M, Kearney RE, Aguayo AJ & Bray GM. (1978). Conduction of nervous impulses in spinal roots and peripheral nerves of dystrophic mice. *Brain research* **143,** 71-85.

Redman S. (1990). Quantal analysis of synaptic potentials in neurons of the central nervous system. *Physiol Rev* **70,** 165-198.

Redman SJ. (1998). The relative contributions of GABAA and GABAB receptors to presynaptic inhibition of group Ia EPSPs. In *Presynaptic Inhibition and Neuron Control*, ed. Rudmon P, Romo R & Mendell LM, pp. 162-177. Oxford University Press, New York.

Robertson B & Taylor WR. (1986). Effects of gamma-aminobutyric acid and (-)-baclofen on calcium and potassium currents in cat dorsal root ganglion neurones in vitro. *Br J Pharmacol* **89,** 661-672.

Roby-Brami A & Bussel B. (1990). Effects of flexor reflex afferent stimulation on the soleus H reflex in patients with a complete spinal cord lesion: evidence for presynaptic inhibition of Ia transmission. *Exp Brain Res* **81,** 593-601.

Rossi A, Decchi B & Ginanneschi F. (1999). Presynaptic excitability changes of group Ia fibres to muscle nociceptive stimulation in humans. *Brain Res* **818,** 12-22.

Rossignol S, Beloozerova I, Gossard JP & Dubuc R. (1998). Presynaptc mechanisms during locomotion. In *Presynaptic Inhibition and Neuron Control*, ed. Rudmon P, Romo R & Mendell LM, pp. 385-397. Oxford University Press, New York.

Rossignol S, Drew T, Brustein E & Jiang W. (1999). Locomotor performance and adaptation after partial or complete spinal cord lesions in the cat. *Prog Brain Res* **123,** 349-365.

Rothwell JC, Traub MM, Day BL, Obeso JA, Thomas PK & Marsden CD. (1982). Manual motor performance in a deafferented man. *Brain* **105 (Pt 3),** 515-542.

Rudomin P. (1990). Presynaptic inhibition of muscle spindle and tendon organ afferents in the mammalian spinal cord. *Trends Neurosci* **13,** 499-505.

Rudomin P. (1999). Presynaptic selection of afferent inflow in the spinal cord. *J Physiol Paris* **93,** 329-347.

Rudomin P, Jimenez I, Solodkin M & Duenas S. (1983). Sites of action of segmental and descending control of transmission on pathways mediating PAD of Ia- and Ib-afferent fibers in cat spinal cord. *Journal of neurophysiology* **50,** 743-769.

Rudomin P, Nunez R, Madrid J & Burke RE. (1974). Primary afferent hyperpolarization and presynaptic facilitation of Ia afferent terminals induced by large cutaneous fibers. *Journal of neurophysiology* **37,** 413-429.

Rudomin P & Schmidt RF. (1999). Presynaptic inhibition in the vertebrate spinal cord revisited. *Exp Brain Res* **129,** 1-37.

Rushton WA. (1951). A theory of the effects of fibre size in medullated nerve. *The Journal of physiology* **115,** 101-122.

Russ JB, Verina T, Comer JD, Comi AM & Kaltschmidt JA. (2013). Corticospinal tract insult alters GABAergic circuitry in the mammalian spinal cord. *Front Neural Circuits* **7,** 150.

Salio C, Merighi A & Bardoni R. (2017). GABAB receptors-mediated tonic inhibition of glutamate release from Abeta fibers in rat laminae III/IV of the spinal cord dorsal horn. *Mol Pain* **13,** 1744806917710041.

Schanne FA, Kane AB, Young EE & Farber JL. (1979). Calcium dependence of toxic cell death: a final common pathway. *Science* **206,** 700-702.

Schindler-Ivens S & Shields RK. (2000). Low frequency depression of H-reflexes in humans with acute and chronic spinal-cord injury. *Exp Brain Res* **133,** 233-241.

Segev I. (1990). Computer study of presynaptic inhibition controlling the spread of action potentials into axonal terminals. *Journal of neurophysiology* **63,** 987-998.

Senter HJ & Venes JL. (1979). Loss of autoregulation and posttraumatic ischemia following experimental spinal cord trauma. *J Neurosurg* **50,** 198-206.

Serrano-Regal MP, Luengas-Escuza I, Bayon-Cordero L, Ibarra-Aizpurua N, Alberdi E, Perez-Samartin A, Matute C & Sanchez-Gomez MV. (2020). Oligodendrocyte Differentiation and Myelination Is Potentiated via GABAB Receptor Activation. *Neuroscience* **439,** 163-180.

Shefner JM, Berman SA, Sarkarati M & Young RR. (1992a). Recurrent inhibition is increased in patients with spinal cord injury. *Neurology* **42,** 2162-2168.

Shefner JM, Buchthal F & Krarup C. (1992b). Recurrent potentials in human peripheral sensory nerve: possible evidence of primary afferent depolarization of the spinal cord. *Muscle Nerve* **15,** 1354-1363.

Sherrington CS. (1908). On reciprocal innervation of antagonist muscles. Twelfth Note - Proprioceptive reflexes. *Proc R Soc Lond B Biol Sci* **80,** 552-564.

Silva NA, Sousa N, Reis RL & Salgado AJ. (2014). From basics to clinical: a comprehensive review on spinal cord injury. *Prog Neurobiol* **114,** 25-57.

Silver RA, Cull-Candy SG & Takahashi T. (1996). Non-NMDA glutamate receptor occupancy and open probability at a rat cerebellar synapse with single and multiple release sites. *The Journal of physiology* **494 (Pt 1),** 231-250.

Simon CM, Sharif S, Tan RP & LaPlaca MC. (2009). Spinal cord contusion causes acute plasma membrane damage. *J Neurotrauma* **26,** 563-574.

Simon O & Yelnik AP. (2010). Managing spasticity with drugs. *Eur J Phys Rehabil Med* **46,** 401-410.

Spaulding SJ, Hayes KC & Harburn KL. (1987). Periodicity in the Hoffmann reflex recovery curve. *Exp Neurol* **98,** 13-25.

Stalberg E, van Dijk H, Falck B, Kimura J, Neuwirth C, Pitt M, Podnar S, Rubin DI, Rutkove S, Sanders DB, Sonoo M, Tankisi H & Zwarts M. (2019). Standards for quantification of EMG and neurography. *Clin Neurophysiol* **130,** 1688-1729.

Stein RB. (1980). *Nerve and Muscle : Membranes, Cells, and Systems*. Springer US, Boston, MA.

Stein RB. (1995). Presynaptic inhibition in humans. *Prog Neurobiol* **47,** 533-544.

Stephanova DI & Bostock H. (1995). A distributed-parameter model of the myelinated human motor nerve fibre: temporal and spatial distributions of action potentials and ionic currents. *Biol Cybern* **73,** 275-280.

Stratten WP & Barnes CD. (1971). Diazepam and presynaptic inhibition. *Neuropharmacology* **10,** 685-696.

Stuart GJ & Redman SJ. (1992). The role of GABAA and GABAB receptors in presynaptic inhibition of Ia EPSPs in cat spinal motoneurones. *J Physiol* **447,** 675-692.

Swadlow HA, Kocsis JD & Waxman SG. (1980). Modulation of impulse conduction along the axonal tree. *Annu Rev Biophys Bioeng* **9,** 143-179.

Sypert GW, Munson JB & Fleshman JW. (1980). Effect of presynaptic inhibition on axonal potentials, terminal potentials, focal synaptic potentials, and EPSPs in cat spinal cord. *Journal of neurophysiology* **44,** 792-803.

Szabadics J, Varga C, Molnar G, Olah S, Barzo P & Tamas G. (2006). Excitatory effect of GABAergic axo-axonic cells in cortical microcircuits. *Science* **311,** 233-235.

Taborikova H & Sax DS. (1969). Conditioning of H-reflexes by a preceding subthreshold H-reflex stimulus. *Brain* **92,** 203-212.

Takahashi T. (1992). The minimal inhibitory synaptic currents evoked in neonatal rat motoneurones. *The Journal of physiology* **450,** 593-611.

Takeoka A & Arber S. (2019). Functional Local Proprioceptive Feedback Circuits Initiate and Maintain Locomotor Recovery after Spinal Cord Injury. *Cell Rep* **27,** 71-85 e73.

Takeoka A, Vollenweider I, Courtine G & Arber S. (2014). Muscle spindle feedback directs locomotor recovery and circuit reorganization after spinal cord injury. *Cell* **159,** 1626-1639.

Taniguchi H, He M, Wu P, Kim S, Paik R, Sugino K, Kvitsiani D, Fu Y, Lu J, Lin Y, Miyoshi G, Shima Y, Fishell G, Nelson SB & Huang ZJ. (2011). A resource of Cre driver lines for genetic targeting of GABAergic neurons in cerebral cortex. *Neuron* **71,** 995-1013.

Taylor A, Durbaba R, Ellaway PH & Rawlinson S. (2006). Static and dynamic gamma-motor output to ankle flexor muscles during locomotion in the decerebrate cat. *J Physiol* **571,** 711-723.

Tillakaratne NJ, Mouria M, Ziv NB, Roy RR, Edgerton VR & Tobin AJ. (2000). Increased expression of glutamate decarboxylase (GAD(67)) in feline lumbar spinal cord after complete thoracic spinal cord transection. *J Neurosci Res* **60,** 219-230.

Todd AJ, Hughes DI, Polgar E, Nagy GG, Mackie M, Ottersen OP & Maxwell DJ. (2003). The expression of vesicular glutamate transporters VGLUT1 and VGLUT2 in neurochemically defined axonal populations in the rat spinal cord with emphasis on the dorsal horn. *The European journal of neuroscience* **17,** 13-27.

Traccis S, Rosati G, Patraskakis S, Bissakou M, Sau GF & Aiello I. (1987). Influences of neck receptors on soleus motoneuron excitability in man. *Exp Neurol* **95,** 76-84.

Treiman DM. (2001). GABAergic mechanisms in epilepsy. *Epilepsia* **42 Suppl 3,** 8-12.

Trigo FF, Marty A & Stell BM. (2008). Axonal GABAA receptors. *Eur J Neurosci* **28,** 841-848.

Turker KS & Powers RK. (1999). Effects of large excitatory and inhibitory inputs on motoneuron discharge rate and probability. *J Neurophysiol* **82,** 829-840.

Turker KS & Powers RK. (2005). Black box revisited: a technique for estimating postsynaptic potentials in neurons. *Trends Neurosci* **28,** 379-386.

Ueno M, Nakamura Y, Li J, Gu Z, Niehaus J, Maezawa M, Crone SA, Goulding M, Baccei ML & Yoshida Y. (2018). Corticospinal Circuits from the Sensory and Motor Cortices Differentially Regulate Skilled Movements through Distinct Spinal Interneurons. *Cell Rep* **23,** 1286-1300 e1287.

Valls-Sole J, Alvarez R & Tolosa ES. (1994). Responses of the soleus muscle to transcranial magnetic stimulation. *Electroencephalogr Clin Neurophysiol* **93,** 421-427.

Verdier D, Lund JP & Kolta A. (2004). Synaptic inputs to trigeminal primary afferent neurons cause firing and modulate intrinsic oscillatory activity. *Journal of neurophysiology* **92,** 2444-2455.

Vincent JA, Gabriel HM, Deardorff AS, Nardelli P, Fyffe REW, Burkholder T & Cope TC. (2017). Muscle proprioceptors in adult rat: mechanosensory signaling and synapse distribution in spinal cord. *J Neurophysiol* **118,** 2687-2701.

Voerman GE, Gregoric M & Hermens HJ. (2005). Neurophysiological methods for the assessment of spasticity: the Hoffmann reflex, the tendon reflex, and the stretch reflex. *Disabil Rehabil* **27,** 33-68.

Wall PD. (1958). Excitability changes in afferent fibre terminations and their relation to slow potentials. *J Physiol* **142,** i3-21.

Wall PD. (1998). Some unanswered questions about the mechanims and function of presynaptic inhibition. In *Presynaptic Inhibition and Neuron Control*, ed. Rudmon P, Romo R & Mendell LM, pp. 228-241. Oxford University Press, New York.

Wall PD & McMahon SB. (1994). Long range afferents in rat spinal cord. III. Failure of impulse transmission in axons and relief of the failure after rhizotomy of dorsal roots. *Philos Trans R Soc Lond B Biol Sci* **343,** 211-223.

Walmsley B, Graham B & Nicol MJ. (1995). Serial E-M and simulation study of presynaptic inhibition along a group Ia collateral in the spinal cord. *J Neurophysiol* **74,** 616-623.

Walsh ME, Sloane LB, Fischer KE, Austad SN, Richardson A & Van Remmen H. (2015). Use of Nerve Conduction Velocity to Assess Peripheral Nerve Health in Aging Mice. *J Gerontol A Biol Sci Med Sci* **70,** 1312-1319.

Watson AH & Bazzaz AA. (2001). GABA and glycine-like immunoreactivity at axoaxonic synapses on 1a muscle afferent terminals in the spinal cord of the rat. *The Journal of comparative neurology* **433,** 335-348.

Wernig A, Muller S, Nanassy A & Cagol E. (1995). Laufband therapy based on 'rules of spinal locomotion' is effective in spinal cord injured persons. *Eur J Neurosci* **7,** 823-829.

Willis WD. (2006). John Eccles' studies of spinal cord presynaptic inhibition. *Prog Neurobiol* **78,** 189-214.

Willis WD, Jr. (1999). Dorsal root potentials and dorsal root reflexes: a double-edged sword. *Exp Brain Res* **124,** 395-421.

Willis WD, Nunez R & Rudomin P. (1976). Excitability changes of terminal arborizations of single Ia and Ib afferent fibers produced by muscle and cutaneous conditioning volleys. *J Neurophysiol* **39,** 1150-1159.

Wu H, Petitpre C, Fontanet P, Sharma A, Bellardita C, Quadros RM, Jannig PR, Wang Y, Heimel JA, Cheung KKY, Wanderoy S, Xuan Y, Meletis K, Ruas J, Gurumurthy CB, Kiehn O, Hadjab S & Lallemend F. (2021a). Distinct subtypes of proprioceptive dorsal root ganglion neurons regulate adaptive proprioception in mice. *Nat Commun* **12,** 1026.

Wu K, Castellano D, Tian Q & Lu W. (2021b). Distinct regulation of tonic GABAergic inhibition by NMDA receptor subtypes. *Cell Rep* **37,** 109960.

Yavuz US, Negro F, Diedrichs R & Farina D. (2018). Reciprocal inhibition between motor neurons of the tibialis anterior and triceps surae in humans. *J Neurophysiol* **119,** 1699-1706.

Yavuz US, Negro F, Sebik O, Holobar A, Frommel C, Turker KS & Farina D. (2015). Estimating reflex responses in large populations of motor units by decomposition of the high-density surface electromyogram. *J Physiol* **593,** 4305-4318.

Zbili M & Debanne D. (2019). Past and Future of Analog-Digital Modulation of Synaptic Transmission. *Front Cell Neurosci* **13,** 160.

Zehr EP & Stein RB. (1999). Interaction of the Jendrassik maneuver with segmental presynaptic inhibition. *Exp Brain Res* **124,** 474-480.

Zhang F, Vierock J, Yizhar O, Fenno LE, Tsunoda S, Kianianmomeni A, Prigge M, Berndt A, Cushman J, Polle J, Magnuson J, Hegemann P & Deisseroth K. (2011). The microbial opsin family of optogenetic tools. *Cell* **147,** 1446-1457.

Zhou C, Huang Z, Ding L, Deel ME, Arain FM, Murray CR, Patel RS, Flanagan CD & Gallagher MJ. (2013). Altered cortical GABAA receptor composition, physiology, and endocytosis in a mouse model of a human genetic absence epilepsy syndrome. *J Biol Chem* **288,** 21458-21472.

Zhou W, He Y, Rehman AU, Kong Y, Hong S, Ding G, Yalamanchili HK, Wan YW, Paul B, Wang C, Gong Y, Zhou W, Liu H, Dean J, Scalais E, O'Driscoll M, Morton JEV, study DDD, Hou X, Wu Q, Tong Q, Liu Z, Liu P, Xu Y & Sun Z. (2019). Loss of function of NCOR1 and NCOR2 impairs memory through a novel GABAergic hypothalamus-CA3 projection. *Nat Neurosci* **22,** 205-217.

Zimmerman AL, Kovatsis EM, Pozsgai RY, Tasnim A, Zhang Q & Ginty DD. (2019). Distinct Modes of Presynaptic Inhibition of Cutaneous Afferents and Their Functions in Behavior. *Neuron* **102,** 420-434 e428.

Zorrilla de San Martin J, Trigo FF & Kawaguchi SY. (2017). Axonal GABAA receptors depolarize presynaptic terminals and facilitate transmitter release in cerebellar Purkinje cells. *J Physiol* **595,** 7477-7493.

Figure Legends (Appendix)

Fig. 1 | Nodal $GABA_A$ and terminal $GABA_B$ receptors in rats. a, Neurobiotin filled proprioceptive Ia axon in the sacrocaudal rat spinal cord (S4 and Ca1), reconstructed from fluorescent images (inset), with branching order indicated and different primary branches distinguished by color. Some ventral branches truncated for clarity (green). Axon diameter not to scale. Central canal: cc. Dorsal columns: dc. Dorsal and ventral horns: DH and VH. **b**, Node on axon branch in DH immunolabelled for sodium channels (Na_V), paranodal Caspr and myelin (MBP), shown with raw images (maximum projection of z-stack), with the paranodal taper indicated, and co-labelling within the axon rendered in 3D (bottom). 1st order branch in DH. **c-d**, α1 $GABA_A$, α5 $GABA_A$ and $GABA_B$ receptor immunolabelling in axon branches (raw maximum projection: top row, 3D reconstruction: bottom), with all receptors colocalized with the axon labelled yellow. Receptor clusters specifically in the axon membrane indicated with yellow arrows. Some α5 $GABA_A$ receptors are in axon cytoplasm (yellow with gray arrow) or in nearby neurons (red), and not in axon membrane. In (**c**) nodes identified by Na_V (or Caspr) and paranodal taper, and located at branch points (bp, 1st to 2nd bp in DH). Raw images for bottom left 3D image of (**c**) detailed in Extended Data Fig 1f. In (**d**) ventral terminal boutons identified by vesicular glutamate transporter 1 (VGLUT1) and adjacent to motoneurons. GABAergic contacts identified by vesicular inhibitory amino acid transporter (VGAT). **e**, Receptor densities on axon branches of varying order in dorsal (dorsal and intermediate laminae) and ventral regions. Box plots: median, thin line; mean, thick line; interquartile range, box; error bars detailed in Methods. Dashed lines: lower confidence interval, 1 SD below mean maximum density. *significantly more than ventral terminal (3rd order) receptor density, + ventral terminal receptor density significantly more than 1st and 2nd order branch densities, $P < 0.05$, $n = 5$ rats each, with 11, 17 and 12 independently filled and reconstructed axons for α1 $GABA_A$, α5 $GABA_A$ and $GABA_B$ receptors, respectively. **f**, Distances from GABA receptor clusters in the membrane to nodes (d_{RN}, Na_V), branch points (d_{RB}) or ventral terminals at motoneurons (d_{RT}). Distances to 1st and 2nd order dorsal and ventral nodes similar and pooled, as were branch points. *significantly less than d_{RT}. + significantly less than d_{RN} and d_{RB}; $n = 5$ rats, with 89, 36 and 70 clusters for α1 $GABA_A$, α5 $GABA_A$ and $GABA_B$, respectively. **g**, Distances between branch points (d_{BB}), nodes (Na_V clusters, d_{NN}), and branch points and their nearest node (d_{NB}) for 1st and

2^{nd} order branches. On dorsal columns d_{NN} = 243 ± 117 μm (not shown). *significantly larger than d_{NB}; *n* = 5 rats, same axons as (**e**), with 95 nodes and 57 bp. **h**, Proportion of nodes with GABA receptors, with and without (hashed) nearby branch points; n = 5 rats each, with 86, 75, 91, and 103 nodes for α5, α1, α2 $GABA_A$ and $GABA_B$ receptors, respectively.

Fig. 2 | Spike failure. a, Recording from ex vivo whole adult rat spinal cord. **b-d**, Intracellular recordings from proprioceptive axon branches in the dorsal horn (DH), with dorsal root (DR) stimulation (1.1x T, 0.1 ms; T: afferent volley spike threshold) evoking a spike in some branches (secure, **b**) and only a failed spike in others (failure potential, FPs; **c**, **d**), but depolarization restoring full spikes (black, **c** and **d**). Averages of 10 trials at 3 s intervals. Resting potential: thin line. EC: extracellular afferent volley. Axons from S4 sacral DR. **e**, Fast repeated DR stimulation induced failure in secure spikes (not failing on first stimulation, 1.1xT). Threshold interval (longest) for failure (FP, pink), and just prior to threshold (gold). **f**, Proportions of DH axon branches (or DR axons) failing to spike with DR stimulation under control resting conditions and with L655708 (0.3 μM), gabazine (50 μM; GBZ), 5-HT (10 μM) or fast repetition (doublet, **e**). *significantly more than control, χ-squared test, number of axons indicated in bars (*n* = 84, 47, 18, 46, 45 and 30, from 11 rats each condition). **g**, Summary of spike and FP heights in secure and failing branches. Box plots. *significantly smaller than secure spike, $P < 0.05$, for spikes in (**f**). **h**, Resting membrane potential and conductance for secure and failing branches, not significantly different, $P > 0.05$, for control axons in (**f**).

Fig. 3 | Nodal facilitation by $GABA_{axo}$ neurons. a, Intracellular recording from $GABA_{axo}$ neuron in ex vivo spinal cord of GAD2//ChR2-EYFP mouse, with ChR2 activated with a light pulse focused on the dorsal horn (5 ms, λ = 447nm laser, 0.7 mW/mm^2, 1.5x light threshold to evoke PAD, T) causing a long depolarization and asynchronous spiking (cell isolated in 50 μM gabazine). Average of 10 trials at 0.3 Hz, blue. Cell resting at -61mV. PAD from (**b)** also shown, grey. **b**, Intracellular recording from proprioceptive axon branch (in DH, sacral S3, resting at -71 mV; average of 10 trials at 0.3 Hz) with same dorsal light pulse (1.5xT) producing a long depolarization (PAD). Box plots summary. *significantly less with gabazine or omitting ChR2 (control mice) or focusing light on the ventral rather than dorsal horn (ventral light), *n* = 14 axons, from 5 mice each. **c-g**, DR stimulation at rest (1.1xT) evoked a secure spike in some axon

branches (**d**) and not others (**e, f**, FPs; DH S3 axons). Light evoked PAD (λ, 1.5xT, 10 ms prior) rescued most failed spikes (**e, f**) and sped up conduction in secure spikes (**d**). Box plots of FPs and spikes (**g**); *significant increase with light, n = 11 axons from (**b**); + significant reduction in light effect with 50 μM gabazine, n =11 axons from (**b**). **h**, Incidence of branches with failed DR-evoked spikes. *significant change with gabazine, χ-squared test, $P < 0.05$, for $n = 45$ control axons (Cntr) and $n = 27$ axons treated with gabazine. **i-o**, $GABA_{axo}$ neurons imaged in S3 sacral spinal cord of GAD2//ChR2-EYFP//tdTom mice (**j, l-o**; green/red, merge yellow; $n = 3$ mice) or GAD2//ChR2-EYFP mice (**k**, green, dorsal horn, $n = 5$ mice), shown with raw images (maximum projection). Innervation of reconstructed neurobiotin filled sensory axons (gold in **j** and **k**, as in Fig. 1) by $GABA_{axo}$ neurons (green; axon contacts labelled red in **k**) in dorsal horn. Nodes identified by Caspr and paranodal taper, sensory terminals by VGLUT1, $GABA_{axo}$ terminals by VGAT, and axonal $GABA_A$ receptors by the α5$GABA_A$ subunit. ChR2-EYFP is mainly expressed on plasma membranes(Boyden *et al.*, 2005), whereas tdTom is cytoplasmic, and so EYFP rings the tdTom labelling, especially evident on the soma and boutons (**j, l-o**). Regions in (**l**) expanded in (**m-o**).

Fig. 4 | Sensory driven nodal facilitation. a, Experimental setup to indirectly activate $GABA_{axo}$ neurons by DR stimulation (DR1) by trisynaptic PAD circuits (detailed in Extended Data Figs. 6-7) in ex vivo spinal cords of rats or GAD2//ChR2-EYFP mice. **b-c**, Depolarization (PAD) of a proprioceptive axon branch (**b**, intracellular in sacral S3 DH) or multiple axons in a DR (**c**, grease gap recording; sacral S3 DR; DR2) from stimulating the adjacent S4 DR (1.1 - 3xT, 0.1 ms pulse; DR1; T: afferent volley spike threshold) or applying a light pulse to activate $GABA_{axo}$ neurons (5 ms, 447nm, 0.7 mW/mm^2, as in Fig. 3b), both blocked by gabazine (50 μM), in GAD2//ChR2 mouse. Thin line resting potential. **d**, Summary box plots of peak phasic PAD evoked in axons by adjacent DR stimulation (DR1) or light, at rest (top, n = 16 axons from 6 rats or n = 14 axons from 5 mice, the latter from Fig. 3b) and with hyperpolarization (-10 mV, bottom, same rats and axons), and effects of applied gabazine (50 μM; n = 14 axons from 5 rats) or L655708 (0.3 μM; n = 14 axons from 5 rats). *significant difference from pre-drug (blue, lower plot), $P < 0.05$. **e-g**, DR axon branches (sacral S3 DH) exhibiting spike failure (FPs, magenta) following stimulating their DR (S3 DR, 1.2xT, 0.1 ms; DR2) in rats at rest. Spikes rescued by PAD evoked by prior conditioning of adjacent DR (S4 or contralateral S3 DR, at

3xT; DR1). Rescue occurred with fast synaptic depolarizations (phasic PAD; **e-f**) and tonic depolarizations (tonic PAD, **g**), both for local FPs (large, **e**) or distal FPs (small, **f-g**). **h**, FP or spike heights before and during DR evoked phasic PAD (n = 17 axons from 11 rats) as in **e-f**, and actions of L655708 (n = 12 axons from 5 rats, 0.3 μM), gabazine (n = 12 axons from 5 rats, 50 μM) and 5-HT (n = 12 axons from 5 rats, 10 μM). *significant increase in spike with PAD, $P < 0.05$.

Fig. 5 | Facilitation of monosynaptic sensory transmission by GABA. a, Ex vivo recording from motoneurons while illuminating $GABA_{axo}$ neurons with light λ. **b-d**, Composite monosynaptic EPSP from motoneuron pool (recorded in sacral S4 VR) evoked by a DR stimulation pulse alone (S4 DR, 0.1 ms, 1.1xT, magenta; T: EPSP threshold). Actions of optogenetic silencing $GABA_{axo}$ neurons with light (**a-b**, 532nm, 5 mW/mm^2, 80 ms, in n = 7 composite EPSPs from 4 GAD2//Arch3 mice), blocking $GABA_A$ receptors (**c**, with bicuculline or gabazine, 50 μM, with and without NMDA antagonist APV, 50 μM; n = 23 from 10 mice and 13 EPSPs from 5 mice, respectively; rats similar, not shown), or blocking $GABA_B$ receptors (**d**, CGP55845, 0.3 μM, n = 20 composite EPSPs in 20 mice). PAD shown for reference, recorded on S3 DR (**c,** top). Summary box plots of changes in EPSP and background postsynaptic activity (Bkg, over 10 ms prior to EPSP) with light or drugs, and with Arch3+ and Arch3- mice (**d**). * significant change, Δ, $P < 0.05$. GAD2//Arch3 mice are VGAT+, not shown. **e-f**, Composite EPSP (evoked in S4 or S3 motoneurons, as in **a-b**) before, during and post PAD (recorded simultaneously on S3 DR) evoked by light activation of $GABA_{axo}$ neurons (10 ms, 1.1xT, 447nm, 0.5 mW/mm^2, 60 ms and 140 ms pre EPSP, ISI) in GAD2//ChR2 mice. Box plots of changes in EPSP and Bkg (10 ms prior) with light in $ChR2^+$ mice without and with gabazine (50 μM, during PAD), and in $ChR2^-$ mice (60 ms ISI). * significant change, $P < 0.05$, for each n = 7 composite EPSPs from 7 mice each. **g**, Tonic PAD (L655708 sensitive) recorded in sacral S4 proprioceptive Ia axon in response to 0.5 s, 200 Hz DR stimulation train applied to the largely cutaneous Ca1 DR of caudal cord (3xT, DR2) in rat. **h-i**, Average EPSP in S4 motoneuron (intracellular recording, EPSP evoked by S4 DR stimulation at 3 s intervals used for average; DR1) before and during tonic PAD (**i**) evoked by the brief DR train of (**h)**, at matched postsynaptic potentials. **j-k**, Individual trials used to make EPSP averages in (**i**) (at 1 s intervals, **h**), with large all or nothing unitary EPSPs (thick lines unitary averages; dotted single occurrence

of Unit 3). Lowpass filtered at 3 kHz. **l**, Changes in unitary EPSP probability and size, and overall EPSP with tonic PAD. Box plots. * significant change, $P < 0.05$, $n = 18$ motoneurons from 5 rats.

Fig. 6 | Facilitation of reflexes in awake mice. a, Recording tail muscle EMG and evoking monosynaptic reflexes (MSR) with tail nerve stimulation (1.1xT, 0.2 Hz; T: reflex threshold), while activating $GABA_{axo}$ neurons (PAD) with light (λ = 447 nm, 10 ms pulse, 1.5xT, 5 mW/mm^2) in GAD2//ChR2 mice. **b-c**, Effect of light pulse λ on active background EMG (Active Bkg condition in **b**) and the MSR evoked 60 ms later, the latter expanded in (**c**). MSR tested with (**c**, top; Active Bkg, 30% max) and without (**c**, bottom; Rest) background EMG. Thin black lines in (**b)** are individual trial examples at 10 s intervals (0.1 Hz); thick lines: averages. **d**, Changes in MSR with light activation of $GABA_{axo}$ neurons at matched postsynaptic background (Bkg measured over 20 ms prior to MSR; lack of change in Bkg). Measured in active and resting (no Bkg) states, in ChR2+ and ChR2- mice (rest only), and during (60 ms ISI) and post PAD (200ms ISI at rest only). ISI: interstimulus interval. Box plots. * significant change, $P < 0.05$, $n = 5$ mice each.

Fig. 7 | Graphical summary of nodal facilitation. a, Spike propagation (green arrows) in myelinated proprioceptive afferents is facilitated by $GABA_A$ receptors at or near nodes, depolarizing axons closer to spike threshold via outward chloride currents. GABAergic neurons ($GABA_{axo}$) provide synaptic or perisynaptic innervation of nodes and nearby afferent boutons, and optogenetic or endogenous activation of these neurons increases sensory transmission to motoneurons. **b**, Without this $GABA_A$ receptor activity, spikes fail to propagate into some of the branches of proprioceptive sensory axons in the spinal cord, due to branch point failure. Failure is initiated when a parent branch, p, cannot provide enough current to drive the daughter branches, d, with at least one of the daughters failing, especially if that branch has further branch points, producing a large conductive load. Overall, nodal facilitation by $GABA_{axo}$ neurons allows selective regulation of conduction in individual branches, increasing the computational complexity of sensory circuits.

Supplementary information (Appendix)

GABA facilitates spike propagation through branch points of sensory axons in the spinal cord

Krishnapriya Hari[1,7], Ana M. Lucas-Osma[1,2,7], Krista Metz[1], Shihao Lin[1], Noah Pardell[1], David A. Roszko[1], Sophie Black[1], Anna Minarik[1], Rahul Singla[1], Marilee J. Stephens[1,3], Robert A. Pearce[4], Karim Fouad[1,2], Kelvin E. Jones[1,5], Monica A. Gorassini[1,3,8], Keith K. Fenrich[1,2,8], Yaqing Li[1,6,8] and David J. Bennett[1,2,8,9*]

[1]Neuroscience and Mental Health Institute, University of Alberta, Edmonton, AB, T6G 2R3, Canada. [2]Faculty of Rehabilitation Medicine, University of Alberta, Edmonton, AB, T6G 2G4, Canada. [3]Department of Biomedical Engineering, Faculty of Medicine and Dentistry, T6G 2V2, University of Alberta, Edmonton, AB, Canada. [4]Department of Anesthesiology, Wisconsin-Madison, Madison, Wisconsin, 53792, USA. [5]Faculty of Kinesiology, Sport and Recreation, University of Alberta, Edmonton, AB, T6G 2H9, Canada. [6]Present address: Department of Physiology, Emory University, Atlanta, GA, 30322, USA. [7]These authors contributed equally. [8]Senior authors. [9]Lead Contact.

*Corresponding author: bennettd@ualberta.ca

Extended Data Fig. 1 | Nodal and not terminal $GABA_A$ receptors in mice and rats.
a-b, In the sacrocaudal spinal cord of mice we examined the distribution of $GABA_A$ receptor subunits on nodes and terminals of sensory axons, including extrasynaptic α5 subunits, synaptic α1 and α2 subunits, and ubiquitous γ2 subunits (e.g. forming the common α1βγ2 or α5βγ2 receptors, though less common extrasynaptic α1βδ have been reported)(Olsen & Sieghart, 2009; Chua & Chebib, 2017; Chuang & Reddy, 2018; Lagrange *et al.*, 2018). We genetically labelled primary sensory axons by their expression of the vesicular glutamate transporter VGLUT1 with a reporter in $VGLUT1^{Cre/+}$; $R26^{LSL\text{-}tdTom}$ mice (tdTom reporter displayed as green, for consistency with Fig. 1). VGLUT1 is mainly only expressed in sensory axons(Todd *et al.*, 2003), especially ventral proprioceptive afferents, as other afferents do not reach the ventral horn(Lucas-Osma *et al.*, 2018a). Axons were reconstructed in 3D as detailed in Fig. 1. 3D reconstructed nodes of Ranvier on myelinated 2nd order ventral branches are shown identified by paranodal Capsr immunolabelling (**a**, bottom), along with raw confocal image stacks (maximum projection from z-stack) prior to 3D reconstruction (**a**, top; receptors red). As in rats, nodes were often near branch points (green arrow). Terminal boutons from the ventral horn are likewise shown with raw and 3D rendered images (**b**). GABA receptors colocalized with the axon are labelled yellow in the 3D reconstructions. Receptor clusters specifically in the plasma membrane are indicated by yellow arrows in (**a**). Similar to rats, the α5, α1, and γ2 $GABA_A$ receptor subunits were found on large axon branches (1st and 2nd order) in the dorsal, intermediate, and ventral cord, near nodes (**a**), but not on ventral horn terminal boutons (**b**, 3rd order). As also seen in rats (Fig 1e), synaptic $GABA_A$ receptors were usually in single large membrane bound clusters at nodes, whereas extrasynaptic α5 receptors were often broken up into multiple clusters, with the largest clusters in the membrane (yellow arrows), and smaller cytoplasmic clusters several µm from the edge of the node under the paranodal Caspr (grey arrows; Fig 1f). Cytoplasmic α5 receptors have been reported previously(Wu *et al.*, 2021b). Many receptors were in neighboring neurons (red arrows), and in our previous publication(Lucas-Osma *et al.*, 2018a) these and cytoplasmic axon receptors may have been mistaken for nodal receptors in the axon membrane, though this is corrected here with evaluation of higher resolution confocal images. The presence of these α5, α1, and γ2 $GABA_A$ subunits is consistent with their mRNA previously reported in the dorsal root ganglion(Persohn *et al.*, 1991). Also, the finding of α1 subunits on these axons is consistent with the recent observation that α1 is only on myelinated sensory axons, rather than unmyelinated C fibres(Paul *et al.*, 2012). **c**, Synaptic α2 $GABA_A$ receptor labelling in mouse and rat axons (rat axon labelled as in Fig 1) with nodes labelled with both antibodies to sodium channels Na_V and Caspr, to confirm the relation of receptors to the node and paranodal region. Receptors are often at the transition between the node and paranodal Caspr, as here. Putative GABAergic synaptic contact labelled with VGAT. **d**, Ventral terminal boutons in $VGLUT1^{Cre/+}$; $R26^{LSL\text{-}tdTom}$ mouse (with reporter labelling the complete axon, green) immunolabelled with VGLUT1 to verify that these are afferent terminals, which have vesicular $VGLUT1^+$ protein expression. Immunolabelling for γ2 $GABA_A$ receptors again showed that terminals lacked this ubiquitous subunit that makes up most $GABA_A$ receptors. **e**, Immunolabelling for $GABA_B$ receptors on 3D reconstructed sensory axons, with same format and mice of (**a**-**b**). $GABA_B$ receptors were generally absent from nodes identified by paranodal Caspr, but present on ventral terminal boutons, as in rats (Fig. 1). Similar results (**a- e**) were obtained from n = 5 mice. **f**, Synaptic α1 $GABA_A$ receptor labelling at a rat Ia afferent node labelled with both antibodies to sodium channels Na_V and Caspr, to confirm the relation of receptors to the node and paranodal region in rat, like in mouse (**c,** same node as in left of Fig 1c, but Na_V and raw images included). Putative GABAergic synaptic contact labelled with VGAT, where left red arrow shows GABAA receptor contacting VGAT at edge of node. VGAT is near, but does not contact Caspr (in 3D view), but may well contact the paranodal myelin loops, since oligodendrocytes express GABA receptors(Serrano-Regal *et al.*, 2020). Node is at dorsal 2nd order axon branch point. **g-h**, Box plots of the proportion of ventral terminal boutons with GABA receptors in both mice (**g ,**$VGLUT1^+$) and rats (**h**), again showing that few boutons contain $GABA_A$ receptors, whereas many contain $GABA_B$ receptors. * significantly more $GABA_B$ than $GABA_A$ receptors, n = 5 animals per condition, with 70 - 120 terminals examined per animal and receptor.

Extended Data Fig. 2 | Voltage dependence of nodal spike propagation failure following dorsal root stimulation. **a-d**, Intracellular recording from proprioceptive Ia afferent branches in the rat dorsal horn with secure spikes at rest, evoked by DR stimulation (1.1xT, 0.1 ms; T: afferent volley spike threshold; sacral S4 DR; **a, d**). Spike failure was induced by increasing hyperpolarization (failure near rest in **d**, but not **a**), with a delay and then abrupt loss of height, reflecting failure of successively further away nodes (**a, d**). Of the two local nodes adjacent to the electrode, one failed first with hyperpolarization, leaving the attenuated spike from the other node (local FP, about 1 λ_S away), which eventually failed as well with further hyperpolarization, leaving a much smaller FP from more distal nodes (distal FP). Spike failure in a node was always proceeded by a delay in the nodal spike. Estimated contributions from local nodes (**b-c**) were computed by subtraction from traces in (**d**). Spike attenuation was down to about 1/e by the second failure, consistent with the space constant λ_S being two internodal distances (**c**), or about 90 µm. Note that due to attenuation of injected current with distance, larger hyperpolarizations were needed to stop spikes with more distal vulnerable nodes (secure spikes), as observed by smaller distal FPs (**a** verses **d**), and some axon spikes could not be stopped (not shown; Spike only, quantified in **e**). Data collected in discontinuous current clamp (DCC) mode so electrode rectification during the injected hyperpolarizing current did not affect potential (DCC switching rate 7 kHz, low pass filtered at 3 kHz to remove switching artifact, which also removed stimulus artifact). **e**, Distribution of spiking in branches with full spikes only, one local nodal spike (local FP), or a distal nodal spike (distant FP) remaining after maximal hyperpolarization, and * significant change when blocking α5 $GABA_A$ receptors with L655708 (0.1 - 0.3 µM) using χ-squared test, $P < 0.05$; $n = 68$ control and $n = 47$ L655708 treated axon branches from 7 rats. **f**, Box plots of spike or FP heights and delays in branches and rats indicated in (**e**), measured just prior to spike failure (or at maximal hyperpolarization for secure spikes) and after failure (for local and distal FPs, as induced in **a-d**). Delay measured relative to peak of spike at rest. + FP significantly different than spike at rest, $P < 0.05$. **g**, Box plots of the hyperpolarization needed to induce failure, in axon branches and rats from (**e**). * significant change with L655708, $P < 0.05$. **h**, Incidence of failure at varying potentials (% of total spikes from **e**). * significantly more failure with L655708, χ-squared test, $P < 0.05$. Note that secure spikes in rats and mice are not overall different when measure by spike height at rest (Figs. 2g and 3g). However, the spike height shown here in (**f**) is the height while the cell is hyperpolarized far from rest, and so is much larger than at rest, since spikes generally overshoot to near the reversal potential for sodium, and so spike heights while hyperpolarizing are not comparable to the spikes at rest in mice or rats (measured from holding potential to peak). Thus, during hyperpolarization the nodes produce larger overall spikes, including FPs from local nodes (**a-f**). Also, during hyperpolarization from current injection, the two adjacent nodes to the electrode fail, unlike during natural failures, and thus when one nodes fails the spike only halves in height, leaving the spike from the second adjacent node (**a-b**). Thus, these local FPs are large in relation to the FPs from distal nodes with natural failure (Fig 2).

Extended Data Fig. 3 | Voltage dependence of spike failure with simulated nodal currents.
Simulating spike propagation failure in a proprioceptive axon by applying a brief intracellular current injection to mimic the current arriving from an upstream node (and FP), yielded full spikes evoked at rest, but nearby nodal spikes delayed and then failing as the membrane was held progressively more hyperpolarized with a steady bias current. Also, large steady depolarizations inactivated these spikes, though well outside of the physiological range (> -50 mV). **a**, Intracellular recording from proprioceptive Ia afferent branch in the rat dorsal horn (sacral S4 axon). A brief current injection pulse (0.5 ms) was applied to simulate the current arriving from distal nodes during normal axon spike conduction, and repeated at 1s intervals. During these pulses the membrane was held at varying potentials for 1 – 2 s with steady current injection, with numbers and colours denoting a given holding potential (in DCC mode). At the most hyperpolarized levels spikes failed to be evoked and only the passive response is seen, like a FP (blue, 1). As the potential was depolarized to near the axon's resting potential (-67 mV) partial spikes occurred (green, 2 and 3), likely from a single adjacent node activating, and then delayed broad spikes occurred, as both adjacent nodes were activated. At more depolarized levels the spikes arose more rapidly and increased in height to full secure spikes (4). **b**, In the same axon as (**a**), at holding potentials well above those seen physiologically (near -50 mV, lower plots) spikes started to exhibit sodium channel inactivation and failure, with a decrease in spike height and delay (7 – 8) and eventually full failure (shown in **c**). Adjacent nodes started failing at slightly different times with different delays, broadening the spike and eventually separating into two distinct nodal spikes (8*). **c**, Spike heights plotted as a function of holding potential, including those spikes illustrated in (**a** and **b**), with spike number-labels indicated. Left grey line indicates passive leak current response, and shows deviation from passive response near rest. Shaded green region shows all or nothing failure or spikes near the resting potential. Middle grey line shows a region of secure spikes with relatively invariant spikes. Right grey line shows spike inactivation with large depolarizations and outright failure near - 50 mV. Note the split vertical axis. Similar voltage dependence of spike failure occurred for n = 5/5 axons showed similar results, from 4 rats. This demonstrates two modes of spike failure: 1) spikes that fail at rest or at hyperpolarized potentials and 2) spikes that fail with large depolarizations above rest. The latter is likely not physiological, since even the largest PAD that we have observed (5 – 10 mV; Fig. 4d) does not depolarize axons to -50 mV, since axons rest near -70 mV, and PAD is only large at hyperpolarized levels (Fig. 4d) and decreases steeply as the potential approaches the reversal potential for chloride (-15 mV)(Lucas-Osma *et al.*, 2018a). **d**, Schematic of recording arrangement and relation to adjacent nodes for data in (**e**) and (**f**). **e**, Expansion of responses 1 (blue) and 3 (pink) from (**a**), and difference (cyan) to show the first local nodal spike height at threshold, recorded at electrode. Active nodes from schematic in (**d**) shown with shaded boxes. **f**, Spikes near sodium inactivation from (**b**) (7 and 8), with differences indicating local nodal spikes (grey: 7 - 8, and cyan: 7 – 7', both truncated to only show estimated nodal spike). Nodes likely arranged as in (**d**).

Extended Data Fig. 4 | GABAergic innervation of nodes and nearby boutons in viral vector labelled proprioceptive afferents. a, Sensory afferents labelled in the spinal cord and DR of adult GAD2//ChR2-EYFP mouse (GAD2-EYFP) by a peripheral adeno-associated virus (AAV9-tdTom); confocal image of a transverse spinal cord section. Large myelinated proprioceptive Ia afferents were identified by characteristic extensive ventral horn branching and innervation of motoneurons (as in Fig 1a). These Ia afferents left the dorsal columns in bundles that were readily traced to the ventral horn in serial sections, with an S-shaped projection path from the dorsal columns to the motoneurons (as in Fig 3j)(Ishizuka *et al.*, 1979). The relatively sparce afferent labelling helped facilitate this tracing of afferent innervation. The peripheral AAV9-tdTom injection occasionally also labelled one motoneuron in a transverse (lower white arrow), though this only occurred a couple times per spinal cord segment, making them possible to distinguished from afferents elsewhere. No other central neurons were labelled, indicated that the viral vector only affected peripheral sensory and motor axons, as we previously found(Li *et al.*, 2020). $EYFP^+$ cells ($GABA_{axo}$ neurons) were only in the dorsal and intermediate laminae (GAD2-$EYFP^+$), with projections into the ventral horn and dorsal columns along the entire path of the Ia afferent bundles, as detailed in Fig 3. The approximate regions where images in (**b-h**) were taken are indicated in (**a**), but in different transverse sections, oriented similarly. **b**, $GABA_{axo}$ neurons formed a dense plexus that wound around Ia afferents as they branched out of the dorsal columns into the grey matter (at dashed line). **c**, Main 1^{st} order myelinated branch of a Ia afferent in intermediate laminae with three nodes at branch points labelled with axonal caspr, approximate myelin regions marked with white lines, and $GABA_{axo}$ neurons seen wrapping the axon (top images). Node 1 had a GAD2-EYFP+ contact that had presynaptic GAD2 labelled with an antibody (GAD2-Ab, cyan; yellow marks contact of afferent, GAD2-EYFP and GAD2-Ab computed in 3D), whereas Nodes 2 and 3 lacked contacts, though the short branch arising off of Node 3 had a nearby unmyelinated terminal branch with a $GAD2^+$ contact. GAD2 (GAD65) is known to be closely associated with GABAergic terminals and vesicular GABA and highly enriched in terminals compared to elsewhere in neurons(Esclapez *et al.*, 1994; Hughes *et al.*, 2005; Betley *et al.*, 2009; Pan, 2012), and thus the GAD2-Ab provides a presynaptic contact label, consistent with the intense GAD2-Ab labelling we observed in GAD2-EYFP boutons (also $bassoon^+$, not shown), and similar to the GAD65-intense boutons on afferents previously detailed(Hughes *et al.*, 2005). Expanded view of Node 1 shown at bottom left, where *all* caspr labelling is displayed, including in overlapping nearby axons, whereas in other images only the axonal caspr in the 3D volume of the afferent is shown for clarity, together with raw images from other antibodies. Expanded view of Node 1 contact shown on bottom right, where all GAD2-ab labelling is shown, whereas in other images only GAD2-Ab in the GAD2-EYFP neuron volume is shown. Not all GAD2-Ab was in GAD2-$EYFP^+$ neurons, likely due to variability in tamoxifen induced cre or transport of EYFP in GAD2//Ch2R-EYFP mice. **d**, Nodal contact in the ventral horn, shown with similar format to (**c**), with again a $GABA_{axo}$ neuron wrapping around the axon and specifically making a contact at the node (yellow; EYFP+, GAD2-Ab^+). White lines: estimated myelin regions. 1^{st} order afferent. **e**, Two nodes on two 1^{st} order Ia afferent branches in the dorsal horn plexus of (**b**), again delineated by paranodal caspr, one of which had a $GABA_{axo}$ neuron contact (GAD2-EYFP, marked yellow again) with presynaptic GAD2-Ab (cyan, shown in 3D volume of $GABA_{axo}$ neuron) and the other did not. **f-g**, Nodes from 1^{st} order Ia afferent branches, identified by paranodal Caspr, in control wild-type mice, and so lacking EYFP, but inhibitory innervation examined with VGAT or GAD2 antibodies. In (**f**) the node had a direct $VGAT^+$ contact and nearby contacts on the small unmyelinated branch arising from the node (contacts computed in 3D labelled yellow). In (**g**) the node lacked a direct GABAergic contact, but had a nearby GAD2-Ab^+ contact on a bouton of a short unmyelinated branch arising from the node. **h**, Complex node in intermediate laminae with enlarged inter-myelin region and two unmyelinated branches, one with a GAD2-Ab^+ contact on the neck of the branch, and the other with contacts on nearby boutons (not shown, above top of image). Same format as (**d-e**). Similar to enlarged nodal boutons of Walmsley(Walmsley *et al.*, 1995). **i**, Quantification of the fraction of total nodes with direct synaptic GABAergic contacts (nodal contacts, GAD2-Ab^+, ~25%), nearby contacts at a node or unmyelinated terminal branch/bouton on the same axon (within λ_S = 90 μm; 98 - 77%; as in **c**) and putative extrasynaptic innervation (within 5 μm, ~95%) from $GABA_{axo}$ neurons, with presynaptic GABA inferred from GAD2-Ab immunolabelling, in 3 mice from n = 43 - 53 nodes each on 1^{st} and 2^{nd} order branches of Ia afferents. $VGAT^+$ contacts on or near nodes occurred with similar incidence (28% of nodes had synaptic contacts, from n = 50 nodes, not shown). Similar incidence of contacts occurred in rat afferents labelled with neurobiotin (not shown). Synaptic contacts occurred at unbranched or branched nodes, as did extrasynaptic innervation, with about half the nodes branched overall. Synaptic contacts that occurred on short unmyelinated afferent terminal branches arising from the node usually occurred at a bouton and are labelled as: Nearby bouton. Synaptic $GAD2^+$ contacts occurred most frequently at or near complex branch points where a parent branch split into large daughter branches (**d**) or the daughter branches had large boutons (**g-h**), which theoretically increased the local conductance and probability of spike failure downstream to the branch point (as in Extended Data Fig. 5).

Extended Data Fig. 5 | Computer simulation of branch point failure and rescue by GABA.
a, Model of a 3D reconstructed proprioceptive afferent, drawn to scale, except myelinated branch lengths all shortened an order of magnitude. Double line segments are myelinated (white) and the rest unmyelinated. Adapted from anatomical studies of Walmsley(Walmsley *et al.*, 1995). Nodes are indicated with a green dot, and ventrally projecting terminal boutons indicated with a yellow dot. As in our axons of Fig. 1, branch points were always at nodes. $GABA_A$ receptors of equal conductance (nS) were placed at each node and associated branch points, and total dorsal columns (dc) depolarization from phasically activating these receptors is shown in inset. The branch lengths (L) and computed space constants (λ_S) are indicated in gray boxes for each segment of the afferent, the latter computed from subthreshold current injections into each segment. From left to right the gray boxes are for segments spanning from the dorsal columns (dc) to N0, N0 to N1, N1 to N5, N1 to N4, N4 to B2 and N5 to B1. Average space constant was λ_S = 91 μm, similar to in other axons(Zorrilla de San Martin *et al.*, 2017). **b**, Responses to simulated dorsal root (DR) stimulation (0.1 ms pulse, 2 nA, at black arrows) computed at various downstream branch points (nodes) and terminal boutons in the spinal cord, with resting potential indicated by thin dashed line (-82 mV). A sodium spike propagated to the branch point at node N1, but failed to invade into the downstream branches, leaving nodes N2 and N3 with only a passive depolarization from the N1 spike (failure potential, FP). Further downstream nodes and terminals experienced vary little depolarization during this failure (N5, B1 and B2). In this case the GABA conductance was set to zero (g_{GABA} = 0, control), simulating a lack of GABA tone. Note that only the nodes beyond the parent branch at node N1 failed due to the conductance increases in large daughter branches to nodes N2 and N3 that drew more current than node N1 could provide (shunting conductances). Node 3 is particularly interesting as it does not itself branch, though a neighbouring node has a small branch, both contributing to the overall conductance and related failure, and Node 2 has two adjacent branches contributing to its conductance. Other branch points with relatively smaller conductance increases (N0, simpler branching) did not fail to conduct spikes. Generally speaking, if the upstream node of a parent branch cannot provide enough current to activate the nodes of its daughter branches then spikes fail, and this is especially likely with multiple sequential branch points, like in N1 – N2. However, failure even occurs at daughter nodes than themselves lack branches (N3), so GABA receptors are useful in aiding spikes at unbranched nodes. **c**, As seen experimentally, nodal $GABA_A$ receptor activation to produce PAD prior to the DR stimulation (~ 10 ms prior; as in Fig. 4f) rescued spikes from failing to propagate. That is, with $GABA_A$ receptors placed just at nodes and associated branch points a weak phasic activation of these receptors (conductance g_{GABA} = 0.6 - 1.5 μS per node shown) rescued conduction down the branch to node N2, with full nodal spikes seen at the distal node N4 and the terminal bouton B2 (DR stimulation at peak of PAD, detailed in (**g**) with black arrows indicating DR stimulation timing). A larger GABA receptor activation (2.4 nS) additionally rescued spike conduction down the branch to node N3, with full spike conduction to the distal node N5 and the terminal bouton B1. Note that increasing GABA conductance sped up the arrival of distal spikes (e.g. at N4 and B2), by up to 1 ms, suggesting substantial variation in sensory transmission times induced by GABA, as we see experimentally. Also note that this nodal GABA depolarized the nodes (N1 – N3) relative to rest (thin dashed line), thus assisting spike initiation. In contrast, nodal GABA did not depolarize the terminal boutons (B1 and B2), consistent with our recent direct recordings from terminals(Lucas-Osma *et al.*, 2018a). Sensitivity analysis revealed similar results with a wide range of sodium channel and GABA receptor conductances, though increasing sodium conductance sufficiently prevented failure all together (not shown, but like in Extended Data Fig. 10f). Interestingly, when we put GABA receptors only at node N2 (or at the unmyelinated bouton immediately above N2) then the spike propagating though N2 to the terminal bouton B2 was rescued with the same GABA conductance (0.6 μS, not shown), as in the main simulation (**c**). Likewise with GABA receptors only at node N3 and nowhere else, then the spike was rescued at that node N3 (at 2.4 μS; not shown). **d**, When instead we removed all nodal GABA receptors and instead place them on terminal boutons (near B1 and B2, yellow, with equivalent total conductance, 2.4 μS condition), then activating them did not rescue the spike propagation failure, since the associated depolarization of nodes is too attenuated at the failure point (N1-N3; no change from resting potential). The GABA receptors did depolarize the terminal boutons (B1 and B2, thick dashed lines) substantially relative to the resting potential (thin dashed lines), but this depolarization was sharply attenuated in more proximal nodes (N1-3). **e**, Reduction of spike height (shunt) and speeding of spike onset with increasing GABA conductance at a non-failing node (N1; model with nodal and not terminal bouton GABA conductances, **c**), consistent with actual recordings from axons in Fig. 3d and Extended Data Fig. 8a. **f-h**, PAD recorded at the dorsal columns (dc) during conditions in (**b**-**d**), respectively, as experimentally recorded dorsal PAD. A phasic GABA induced depolarization (PAD) was generated by changing GABA conductances, g_{GABA}, as detailed in Methods, and GABA receptor location varied as in (**c-d**). DRs were stimulated at the peak of this PAD in (**c-d**). Note that nodal (**g**) but not terminal (**h**) $GABA_A$ receptors caused a visible depolarization (PAD) at the dc, due to less electrotonic attenuation over a shorter distance to the dc.

Extended Data Fig. 6 | Cutaneous driven trisynaptic circuits mediating PAD and assisting repetitive firing. **a**, Cutaneous driven dorsal trisynaptic circuit mediating PAD. A minimally trisynaptic circuit is classically known to depolarize afferents via $GABA_{axo}$ neurons. This circuit involves sensory afferents activating excitatory intermediary neurons (glutamatergic) that in turn activate $GABA_{axo}$ neurons that return to innervate sensory axons(Jankowska *et al.*, 1981b; Lalonde & Bui, 2020). Even though $GABA_{axo}$ neurons are small(Betley *et al.*, 2009) this circuit influences afferents over widespread regions of the spinal cord(Lucas-Osma *et al.*, 2018a). Specifically, the activation of a small group of sensory axons in just one DR or nerve causes this trisynaptic circuit to produce a widespread activation of many axons across the spinal cord, even many segments away and across the midline(Lucas-Osma *et al.*, 2018a). This allowed us to activate PAD from adjacent roots without directly activating an axon in a particular root, as detailed in Fig. 4 and the rest of this figure. One variant of this classic trisynaptic circuit specifically involves cutaneous stimulation activating dorsal intermediary neurons(Jankowska *et al.*, 1981b; Zimmerman *et al.*, 2019) that activates $GABA_{axo}$ neurons (likely dI4 neurons(Lalonde & Bui, 2020)) that in turn innervate cutaneous afferents, which we term the cutaneous dorsal circuit. While this cutaneous dorsal circuit also synaptically innervates some proprioceptive afferents(Rudomin, 1999) (**a**), its main action on proprioceptive afferents is to produce a pronounced extrasynaptic spillover of GABA that depolarizes these afferents tonically via α5 $GABA_A$ receptors (termed: tonic PAD, L655708 sensitive), especially with repetitive cutaneous nerve stimulation (1 - 200 Hz) that leads to minutes of depolarization(Lucas-Osma *et al.*, 2018a), and we see similar tonic PAD here (detailed next). **b**, Intracellular recording from a proprioceptive axon branch in rat dorsal horn (sacral S4 axon, DR2). The axon branch spontaneously exhibited spike propagation failure when its was stimulated alone (denoted DR2 stimulation, repeated at 1 Hz, 1.1xT, 0.1 ms; T: afferent volley spike threshold), with only a small failure potential (FP) visible (lower pink traces). Activation of a largely cutaneous DR (caudal Ca1 DR, innervating the tip of the tail, stimulation at intensity for cutaneous afferents, 3xT, 0.1 ms; denoted DR1) evoked a slowly rising tonic PAD when repeated at 1 Hz (blue). When the axon stimulation (DR2 stimulation) was combined with the repeated cutaneous stimulation (DR1, 60 ms prior to each DR2 stimulation) the slowly building PAD prevented spike failure (black spikes), and this outlasted the cutaneous stimulation (after effect). Similar results obtained in n = 20/20 axons tested from 10 rats.

Extended Data Fig. 7 | Proprioceptive driven trisynaptic circuit for PAD enabling high frequency spike transmission.
a, Proprioceptive driven ventral trisynaptic circuit mediating PAD. Another variant of the classic trisynaptic circuit involves proprioceptive afferents activating excitatory intermediary neurons (glutamatergic) that then activate $GABA_{axo}$ neurons that innervate these same afferents, including ventral terminal regions of the afferents(Jankowska *et al.*, 1981b; Lucas-Osma *et al.*, 2018a; Lalonde & Bui, 2020). This circuit is more ventrally located compared to the cutaneous dorsal PAD circuit(Jankowska *et al.*, 1981b), and thus, we term it the proprioceptive ventral PAD circuit. It likely involves $GABA_{axo}$ neurons that are from the dIL_A population(Lalonde & Bui, 2020). Importantly, the circuit is recurrent, with proprioceptive afferents causing self-facilitation of themselves (via homonymous PAD). It produces a fast phasic axon depolarization (phasic PAD, fast synaptic; Fig. 4c), as well as a slower tonic depolarization (tonic PAD, Fig. 4c, likely from extrasynaptic GABA spillover), as detailed previously(Lucas-Osma *et al.*, 2018a). Since proprioceptive sensory axons naturally fire at high rates(Prochazka & Gorassini, 1998) where they are vulnerable to spike failure (Fig. 2e-f), we examined the action of self-facilitation by GABA on this failure. **b-f**, During rapid repetitive stimulation of a DR to evoke spikes in a proprioceptive axon there was an inevitable activation of PAD from low threshold proprioceptive axons (homonymous PAD, **b**). This PAD helped spikes fire at high physiological rates of up to 200-300 Hz (5 – 3 ms intervals) before spike inactivation and failure occurred because, in absence of PAD, isolated repetitive activation of the axon with intracellular current pulses (IC) led to failure at much lower firing rates (~100 Hz; longer spike intervals; **b, e**), even after just two stimuli (doublets; **c, e**). Additional PAD evoked by simultaneous stimulation of an adjacent DR (2xT; T, spike threshold observed from afferent volley) reduced failure from fast repeated IC stimuli (**b, f**), repeated DR stimuli (doublet, **c, d, f**) or hybrid IC-DR stimulation pairs (**f**). Legend details are as follows: **b**, Intracellular recording from proprioceptive axon in rat dorsal horn (sacral S4 axon) with spikes securely evoked by fast repeated DR stimulation (top, 1.1xT, 0.1 ms, sacral S4 DR, denoted DR2; resting potential -68 mV), but spikes failing intermittently with repeated intracellular current injection (IC) at the same rate (bottom green), due to sodium channel inactivation. The reason that spike failure does not occur with the fast DR stimulation is that it is accompanied by a build up of tonic PAD (from self-activation) that helps prevent failure, because adding to the IC stimulation a simultaneous conditioning stimulation of other proprioceptive afferents in an adjacent DR (DR1 stim at 1.5xT, 0.1 ms, S3 DR) prevents spike failure (black trace, bottom), via the proprioceptive ventral circuit (**a**). This DR1 conditioning stimulation does not directly activate spikes in the axon, but it causes a fast depolarization (phasic PAD) that rapidly helps spikes (as early as 6 - 10 ms later), and a building tonic depolarization (tonic PAD) with repetition that further helps later spikes in the stimulation train (DR1 stimulation alone blue, middle trace). Similar results obtained in n = 7/7 axons from 4 rats. Likely similar tonic PAD and associated increased spike conduction helps explain post-tetanic potentiation of the monosynaptic EPSP, as previously suggested(Luscher *et al.*, 1983). **c**, Repeated DR stimulation at higher rates eventually causes spike failure in proprioceptive axons (sodium spike relatively refractory), as shown in the top panel where a double stimulation (doublet, S4 DR, denoted DR2-DR2, 1.1xT, 0.1 ms, resting at -75 mV) exhibits failure on the second spike (with large FP indicated, magenta). However, additional PAD provided by stimulating an adjacent DR (DR1; 1.5xT, group I intensity, 0.1 ms) about 10 ms earlier helps prevent this spike failure (black trace; blue trace: PAD alone). When the same axon was stimulated slightly slower (with a longer doublet interval, second plot, DR-DR) failure did not occur, which we designate the failure interval threshold, which is quantified in (**e**). The self-activated PAD caused by the first DR stimulation in this doublet helped prevent failure in second DR stimulation because replacing the first DR stimulation with an intracellular stimulation (IC, 2 nA) to activate the spike leads to failure of the second spike evoked by the DR stimulation at much longer intervals (lower trace, IC-DR). **d**, Another example of a failed doublet spike (DR2-DR2 stim, 1.1xT, 0.1 ms) that was rescued by PAD evoked by adjacent DR stimulation (DR1 1.5xT, 0.1 ms, resting at -78 mV), as in the top plots of (**c**), except that in this case the failure is at a more distal node, since the FP is small. **e**, Failure interval threshold (minimum firing interval prior to failure, or maximal firing rate) with DR doublets (DR-DR), IC doublets (IC-IC) or IC-DR pair stimulation. Note the shorter intervals possible with the PAD evoked by the first stimulation (DR-DR). * significantly longer than minimum DR doublet interval (DR-DR), n = 18 axons each condition from 5 rats, $P < 0.05$. **f**, Quantification of the FP heights that were induced by a fast doublet (DR-DR or IC-IC; n = 14 axons each from 5 rats, at failure threshold interval) or IC and DR stimulation (IC-DR; n = 11 axons from 5 rats), and the rescue of spikes by PAD evoked by adjacent DR stimulation for each condition. * significant increase in height with PAD, $P < 0.05$.

Extended Data Fig. 8 | Other excitatory actions of $GABA_A$ receptors on proprioceptive axons.
a, Intracellular recording from a rat sacral S3 proprioceptive Ia afferent branch in the dorsal horn with a secure spike evoked by S3 DR stimulation at rest (DR2, 1.1xT, 0.1 ms, - 60 mV rest, rat; T: spike threshold in afferent volley). Sensory-evoked PAD initiated by stimulating an adjacent DR (DR1; S4 DR; 2xT, 0.1 ms pulse, as in Fig. 4) 10 ms prior to the DR2 stimulation only moderately influenced the spike (DR1 stimulation time not shown). It sped up the spike latency and rise time, reduced the fall time and slightly reduced the spike height. Hyperpolarization induced spike failure (lower trace), as in Extend Data Fig. 2a. **b**, Summary box plots of change in spike peak latency (advance) and height with prior sensory PAD activation as in (**a**). *significant change, $P < 0.05$, $n = 26$ axons, from 9 rats. **c**, Intracellular recording from an S3 proprioceptive Ia afferent branch in the dorsal horn with a brief current injection pulse just subthreshold to initiating a spike (near rheobase, bottom trace) at rest, only initiating a passive response with a small failed spike (middle trace). However, prior activation of PAD by stimulating an adjacent DR (DR1 as in A; S4 DR, 2xT, 0.1ms top trace) allowed the same current pulse to evoke a spike (above rheobase). The passive response to the current injection (double blue arrow; resistance R = V/I) was decreased during the PAD, corresponding to an increase in conductance, that contributed to a shunt (reduction) of the currents generating the spike, though this only caused about a 1% drop in spike height (1 mV; **b**). DCC recording mode, as in Extend Data Fig. 2a-d. **d**, Summary box plots of rheobase (current threshold from **c**) before and during PAD, and change in shunt (conductance = 1/R) with PAD, as in (**c**). * significant change with PAD, $P < 0.05$, $n = 37$ axons from 11 rats. **e**, By itself sensory evoked PAD sometimes initiated a spike on its rising phase, when the DR stimulation was large enough, demonstrating a direct excitatory action of $GABA_A$ receptors, as previously reported(Lucas-Osma *et al.*, 2018a). These spikes propagate antidromically toward the DR; and are thus termed dorsal root reflexes (DRR). Example shown of intracellular recording from rat sacral S3 proprioceptive afferent branch in the dorsal horn, with PAD produced by a DR1 stimulation (S4 DR stimulation 3.5xT, 0.1 ms) evoking a spike that propagates out the DR (DRR). These DRR occurred in n = 11/120 axons from 15 rats (9% incidence). These PAD evoked spikes occur with a variable latency of 10 – 30 ms(Lucas-Osma *et al.*, 2018a) and thus make axons refractory for about 30 ms after the DR stimulation(Eccles *et al.*, 1962a). PAD evokes spikes with a high incidence (79%)(Lucas-Osma *et al.*, 2018a), but these spikes fail to propagate antidomically, yielding the 9% incidence we see. However, these spikes are more likely to travel othodromically (up to 79% incidence) and evoke EPSPs in motoneurons via the monosynaptic pathway(Eccles *et al.*, 1961a), and thus also produce a post activation depression of the EPSPs for many seconds. We thus kept the PAD low when examining the effects of PAD on EPSPs, to avoid these spikes and their subsequent inhibitory action (in Figs. 5 – 6).

Extended Data Fig. 9 | Estimating the overall spike conduction failure from the dorsal root to the motoneurons.
a, Experimental setup to indirectly measure sensory axon conduction failure following DR stimulation, by examining whether failed axon segments are relatively less refractory to activation after failure, using a double pulse method adapted from Wall(Wall & McMahon, 1994). A tungsten microelectrode (12 MΩ) was placed in the ventral horn (VH) near the sensory axon terminals on motoneurons (S3 or S4 VH), to activate the branches/nodes of the axon projecting to the motoneuron that may have failed (VH stimulation). Spikes from VH or DR stimulation were recorded intracellularly in a proprioceptive axon penetrated in the dorsal columns. **b**, *VH threshold in refractory period*. Rapidly repeated VH stimulation (VH doublet; two 0.1 ms pulses) at an interval short enough to produce spike inactivation on the second stimulation (4 ms), with stimulus current adjusted to threshold for inactivation, T_{VH2}. This T_{VH2} (~15 uA) was always higher than the threshold VH stimulation for evoking a spike with the first stimulation, T_{VH1} (~10 uA, not shown). Recorded in sacral S4 afferent resting at -72 mV, with doublets repeated at 3 s intervals to determine current thresholds. **c**, *VH threshold after DR stimulation*. Similar repeated activation of the axon in (**b**), but with the first activation from a DR stimulation (at 1.5x DR threshold) and the second from VH stimulation at the T_{VH2} intensity from (**b**). In this case the VH stimulation readily activated the axon spike, likely because the DR-evoked spike did not propagate to the VH, leaving the silent portion of the axon non refractory. Thus, this VH stimulation evoked spikes with a lower current than T_{VH2}, with this lower threshold denoted $T_{DR,VH}$ (~ 12 μA, not shown). This DR – VH stimulation interval was deliberately set too short for the involvement of PAD (which rises in > 4 ms; Fig. 4).
d, Computation of spike failure based on changes in VH stimulation thresholds. If the DR-evoked spike entirely fails to propagate to the VH, then the threshold for subsequently activating the VH ($T_{DR,VH}$) should be the same as the threshold without any prior activation ($T_{VH1} = T_{DR,VH}$), whereas if it does not fail then the threshold for activating the VH should be the same as with a VH doublet ($T_{VH2} = T_{DR,VH}$). In between these two extreme scenarios, the DR evoked spike may only partially fail to propagate spikes to the VH; in this case $T_{DR,VH}$ should be between T_{VH1} and T_{VH2}, with the difference $T_{VH2} - T_{VH1}$ representing the range of possible thresholds between full failure and conduction. Overall the % conduction failure can be thus quantified as: $(T_{VH2} - T_{DR,VH})/(T_{VH2} - T_{VH1}) * 100\%$, which is 100% at full failure and 0% with no failure. **e**, Average spike conduction failure to the VH in proprioceptive axons, and decrease following a DR conditioning stimulation that depolarized the axon (PAD). Box plots of failure estimated as in (**b-d**). Prior DR conditioning to produce PAD (via adjacent S4 or Ca1 DR stimulation at 3xT) reduced the failure estimated 20 ms later by the paired-pulse conduction testing (repeating DR – VH stimulations of **b-d**). DR conditioning itself lowered the thresholds for VH activation, as previously reported (not shown)(Wall, 1958). We studied two lengths of axons: long axons (intersegmental, n = 11 axons, from 5 rats) with the VH stimulation one segment away from the recording site, and short axons (segmental, n = 12, from 5 rats) with the VH stimulation near the recording site, in the same segment. + significantly less failure with PAD and * significantly less failure with short compared to long axons, $P < 0.05$.

Extended Data Fig. 10 | Axonal spike conduction estimated from extracellular recordings.
a, Experimental setup to directly record spike conduction failure in proprioceptive axon terminals in the ventral horn (VH) following DR stimulation. Extracellular (EC) recordings from axon terminals in VH, with glass electrode positioned just outside these axons, and for comparison EC recording in the dorsal horn (DH). **b**, EC field recorded in VH after DR stimulation (S4 DR, 1.1xT; T: afferent volley threshold), with a relatively large initial positive field (magenta arrows, pf) resulting from passively conducted axial current from sodium spikes at distant nodes (closer to the DR; outward current at electrode), some of which fail to propagate spikes to the VH recording site; thus, this field is a measure of conduction failure, as demonstrated in (**c-f**) below. Following this, a negative field arises (blue arrow, nf), resulting from spikes arising at nodes near the electrode (inward current); thus, this field is a measure of secure conduction. Reducing conduction failure by depolarizing the axon (+PAD) with a prior conditioning stimulation of an adjacent DR (Ca1, 2xT, 30 ms prior), decreased the positive field (pf) and increased the negative field (nf), consistent with increased conduction to the terminals, and in retrospect the same as Sypert et al. (1980)(Sypert *et al.*, 1980) saw in cat (their Fig. 4). Large stimulus artifacts prior to these fields are truncated. **c**, Control recordings from proprioceptive axons in dorsal horn (DH) to confirm the relation of the EC negative field (nf) to spike conduction. Intracellular (IC) recording from axon (sacral S4, resting at -64 mV) and EC recording just outside the same axon, showing the DR evoked spike (IC) arriving at about the time of the negative EC field (nf). There is likely little spike failure in this axon or nearby axons, due to the very small initial positive field (pf). EC fields are larger in DH compared to VH (G, 10x), and thus the artifact is relatively smaller. **d**, Locally blocking nodes with TTX to confirm the relation of the positive EC field to spike failure. EC recording from proprioceptive axon in the dorsal horn (S4), with an initial positive field (pf) followed by a negative field (nf), indicative of mixed failure and conduction. A local puff of TTX (10 µl of 100 µM) on the DR just adjacent to the recording site to transiently block DR conduction eliminated the negative field (nf) and broadened the positive field (pf), consistent with distal nodes upstream of the TTX block generating the positive field via passive axial current conduction, and closer nodes not spiking. Recordings were in the presence of synaptic blockade (with glutamate receptor blockers, kynurenic acid, CNQX and APV, at doses of 1000, 100 and 50 µM respectively), to prevent TTX spillover having an indirect action by blocking neuronal circuit activity, including $GABA_{axo}$ neuron activity. This synaptic blockade itself contributed to some spike failure, consistent with a block of $GABA_{axo}$ neuron activity, as there was a more prominent positive field (pf) compared to without blockade in (**c**). **e**, EC field recorded from terminals of proprioceptive axons in the ventral horn near motoneurons (S4), in the presence of an excitatory synaptic block that largely eliminates most neuronal circuit behaviour (with kynurenic acid, CNQX and APV, as in **d**). In this synaptic block negative fields were generally absent (nf = 0), and only prominent positive fields (pf) occurred (as with TTX block), suggesting that conduction to the VH often completely failed when circuit behavior is blocked, which likely indirectly reduces $GABA_{axo}$ neuronal circuit activity and its associated facilitation of nodal conduction. **f**, Rescue of spike conduction to the ventral horn by increasing sodium channel excitability by reducing the divalent cations Mg++ and Ca ++ in the bath medium(Armstrong & Cota, 1991). Same EC field recording as in **e**, but with divalent cations reduced (Mg^{++}, 0 mM; Ca^{++}, 0.1 mM). The positive field was largely eliminated (pf = 0) and replaced by a negative field (nf), consistent with elimination of conduction failure, and proving that the positive field is not a trivial property of axon terminals(Dudel, 1965; Katz & Miledi, 1965; Sypert *et al.*, 1980). **g**, Conduction index computed from positive (pf) and negative (nf) field amplitudes as: nf / (nf + pf) x 100%, which approaches 100% for full conduction (pf ~0; as in **c**) and 0% for no conduction (nf = 0; as in **e**). **h-i**, Summary of conduction index estimated from EC field potentials, shown with box plots. Without drugs present in the recording chamber, the axon conduction from the DR to the dorsal horn was about 70% (**h**, n = 17 axon fields, from 10 rats), consistent with Fig. 2, whereas conduction from the DR to the VH was only about 50% (**i**, n = 11, from 5 rats), suggesting substantial failure at the many branch points in the axon projections from the dorsal horn to the motoneurons. Increasing $GABA_{axo}$ neuron activity with DR conditioning (PAD, 30 – 60 ms prior) increased conduction (+GABA, in both the DH and VH, n = 5 and 9 from 5 rats, as in **b**), whereas decreasing GABA and all circuit activity in a synaptic blockade decreased conduction (-GABA, in both DH and VH, n = 5 and 6 from 5 rats, as in **d-e**). TTX (n = 5 from same rats, **h**) or removal of divalent cations (Mg^{++} and Ca^{++}, -Divalent, n = 5 from same rats in synaptic block, **i**) reduced or increased conduction, respectively (as in **d** and **f**). * significant difference from control pre-drug or pre-conditioning, $P < 0.05$.

Extended Data Fig. 11 | Sensory evoked facilitation of monosynaptic EPSPs by $GABA_A$ receptors.
a, Whole spinal cord ex vivo preparation for intracellular recording of EPSPs from motoneurons while stimulating dorsal roots (DRs). **b**, Monosynaptic EPSP in an S4 motoneuron evoked by a proprioceptive group I stimulation of the S4 DR (1.1xT, denoted DR2, lower traces; resting potential -75 mV: black line; T: EPSP threshold, similar current to afferent volley threshold), alone (pink) and 60 ms after (blue) a conditioning stimulation of cutaneous afferents in rat to evoked PAD (stimulation of the largely cutaneous Ca1 DR, 2.5xT; denoted DR1). Averages of 10 trials each at 10 s intervals. PAD evoked by the same cutaneous conditioning stimulation in a proprioceptive S4 DR afferent is shown for reference (top, recorded separately, as in Fig. 4b). **c**, EPSPs from (**b**) on expanded time scale. **d**, Similar to (**b**), but stronger conditioning stimulation (DR1, 3xT) evoking background postsynaptic activity (blue, Bkg) that lasted longer than 60 ms, and slightly inhibited the EPSP, likely from increased postsynaptic conductances shunting the EPSP (postsynaptic inhibition; light pink: overlay of EPSP alone) and masking nodal facilitation. **e**, Summary box plots of facilitation of EPSPs during phasic PAD evoked by either proprioceptive conditioning (S3 or contralateral S4 DR stimulation, 1.1xT, n = 11 motoneurons EPSPs in 5 mice, blue) or cutaneous conditioning (Ca1 DR stimulation, 2-3xT, in rats, n = 42 motoneurons/EPSPs in 10 rats, pink), and action of $GABA_A$ and $GABA_B$ antagonists (gabazine 50 μM, CGP55845 0.3 μM and L655708 0.3 μM grey, n = 5, 7, 9 EPSPs respectively in same animals, with again mice proprioceptive conditioning and rats cutaneous). EPSPs evoked in S3 and S4 motoneurons by DR2 (S3 or S4) stimulation at 1.1T, as in (**b**). Facilitation measured 60 ms post conditioning during phasic PAD (phasic condition indicated) and when postsynaptic actions of conditioning (Bkg) were minimal (as in **b**). After conditioning was completed EPSP testing continued and revealed a residual facilitation that lasted for 10 - 100 s (After effect, green, n = 9 EPSPs in 5 mice), due to a build up of tonic PAD, after which the EPSP returned to baseline (not shown), similar to post-tetanic potentiation(Luscher *et al.*, 1983). Also, a brief high frequency cutaneous stimulation train (200 Hz, 0.5 s, 2.5xT) that led to a very long lasting depolarization of proprioceptive axons (Tonic PAD, example in Fig. 5g) caused a facilitation of the monosynaptic EPSP that lasted for minutes (average shown, tonic cutaneous condition), and this was blocked by L655708 (in rats, n =5 EPSPs in 4 rats). * P < 0.05: significant change with conditioning. + P < 0.05: significant change with antagonist. Raw data points shown to indicate occasional inhibition of the MSR by conditioning, but overall facilitation. ChR2 activation of GABAaxo neurons lacked these long tonic PAD-mediated after effects on the EPSP facilitation (Fig. 5e-f, Post), suggesting an additional source of GABA mediating after effects. **f**, Summary box plots of change in EPSP induced by cutaneous DR (DR1) conditioning (and associated phasic PAD) 60 ms prior to evoking the EPSP, with varying EPSP stimulation intensity. When the DR that evoked the test EPSP (DR2) was stimulated at an intensity that produced less than half the maximal EPSP height (1.1xT, ~ 30% max EPSP, n =42, same data as in **e**) the facilitation of EPSP by conditioning was larger than when this DR2 stimulation was increased to produce a test EPSP near maximal (1.5xT, prior to conditioning, n = 18 EPSPs from same rats as in **e**). *P < 0.05: significant change with conditioning. This is likely because the stronger test stimulation reduced the headroom for increasing EPSPs by recruiting more proprioceptive axons, and increased self-facilitation prior to conditioning, the latter during repeated testing used to obtain EPSP averages. **g**, Summary of cutaneous facilitation of EPSPs from (**f**) (evoked by DR2 at 1.1xT), but separated into trials without (as in (**b**), n = 31 EPSPs, in 10 rats) and with (as in (**d**), n = 11 EPSPs in 10 rats) large background postsynaptic changes induced by conditioning that lasted up to and during the EPSP testing (at 60 ms post conditioning, Bkg). *P < 0.05: significant change with conditioning evoked PAD. + P < 0.05: significant reduction facilitation with increased background activity (Bkg). **h**, Remote postsynaptic inhibition from conditioning. Long lasting changes in intrinsic proprieties of motoneurons (S4 and S3) following a mixed proprioceptive and cutaneous conditioning DR stimulation (on S3 or contralateral S4 DR, 2.5xT, DR1) that only produced a transient postsynaptic depolarization that ended prior to EPSP testing (as in B), including a reduction in time constant (τ) and slight hyperpolarization of potential (V_m), both measured at the time of EPSP testing (measured at 60 ms post conditioning, but in trials without EPSP testing; n = 15 motoneurons in 5 rats). At this time, there was little change in somatic membrane resistance (Rm) with conditioning, suggesting that conditioning induced postsynaptic activity at a remote location in distal dendrites of the motoneuron. Indeed, when we voltage clamped the membrane potential during monosynaptic testing (DR2 at 1.1-1.5xT) to directly measure the synaptic current (EPSC) and minimize that inhibitory action of postsynaptic conductance increases, we found that the conditioning stimulation (DR1) produced a larger facilitation of the monosynaptic EPSC than the EPSP measured in current clamp in the same motoneurons (same n = 15 motoneurons). These results are consistent with the facilitation of the EPSP being masked by postsynaptic inhibition from increases in remote dendritic postsynaptic conductances triggered by the conditioning stimulation. *P < 0.05: significant change with conditioning.

Extended Data Fig. 12 | Facilitation of reflexes in awake rats | a-c, MSR recorded as in Fig 6, but in rat and with PAD instead activated with cutaneous conditioning (tip of tail, 0.2 ms, 2xT, 60 ms prior, 0.1 Hz repetition), at matched active Bkg EMG. * significant change with conditioning, $P < 0.05$, $n = 8$ rats (**c**). **d**, Decrease in MSR with L655708 (1 mg/kg i.p.) at matched Bkg EMG. Box plot. * significant change, $P < 0.05$, $n = 5$ rats. **e**, Typical MSR amplitude before, during and after conditioning as in (**a-c**) with after effect. **f**, Typical change in MSR with cutaneous conditioning as in (**a-c**) when the ISI is increased, compared to PAD (from Fig. 4). (**e,f**) similar results in $n = 5/5$ rats. **Summary of findings in awake rats**: Increasing $GABA_{axo}$ neuron activity with a brief cutaneous stimulation (**a**) increased the MSR (**b-c**) during a period consistent with nodal facilitation by PAD (30 – 200 ms post stimulation; **f**). We again kept the conditioning stimulation small enough to not change the background (**b**) to rule out postsynaptic actions. Blocking $GABA_A$ receptor tone (with L655708) decreased the MSR, at matched levels of background EMG (**d**), suggesting a spontaneous tonic PAD facilitating the MSR. Repeated cutaneous conditioning stimulation (trains) to induce a buildup in this tonic PAD caused an associated buildup of the MSR that outlasted the conditioning and its postsynaptic actions by many seconds (after effect; **e**).

Extended Data Fig. 13 | Facilitation of reflexes in humans.
a, To estimate the role of $GABA_{axo}$ neurons in humans we employed the sensory-evoked depolarization of proprioceptive axons by $GABA_{axo}$ neurons (sensory-evoked PAD; Fig. 4), which is known to occur in humans(Shefner *et al.*, 1992b). For this we recorded the MSR in the soleus muscle in response to tibial nerve stimulation. **b,** MSR in soleus EMG evoked by a tibial nerve pulse (1.1xT, 0.2 Hz, **b***i*), and phasic facilitation of the MSR following a brief conditioning of the cutaneous branch of the deep peroneal nerve (cDP nerve) at varying intervals (ISIs, **b***ii*, 1.0xT, perception threshold T, at rest), and lack of changes in background (Bkg) motor unit (MU) activity or EMG evoked by conditioning alone (**b***iii*, peri-stimulus frequencygram, PSF; with weak contraction). **c**, Same as (**b**), but with proprioceptive conditioning evoked by a brief tibial anterior (TA) muscle tendon vibration, which alone inhibited MU activity (postsynaptic inhibition, PSF Bkg, **c***iii*). **d**, Summary box plots of changes in MSR and postsynaptic (MU) activity with brief conditioning (cDP, n = 14 subjects; or TA vibration, n = 6 subjects; as in **b-c**) and long cutaneous conditioning trains (**e**, n = 14 subjects). * significant change with conditioning, $P < 0.05$. **e**, Tonic increase in MSR (tonic facilitation) after 0.5 s cutaneous conditioning train (cDP, 1.1xT, 200 Hz) at rest (**e***i-ii*), without prolonged changes in MU activity induced by conditioning alone (**e***iii*, PSF in weak contraction). MSR evoked by tibial stimulation every 5 s, with averages from repeated conditioning shown in (**e***ii*). * significant change in MSR, P < 0.05, n = 5 subjects. **f,** Overlay of all MU firing rates (PSF) with repeated MSR testing (at 5 s intervals) during ongoing weak contraction, and effect of the 0.5 s cutaneous conditioning train (**f***i*). Summary box plots of increased probability of MU firing during MSR (**f***ii*), without changing estimated EPSP size (**f***iii*, PSF thin line; thick line unitary EPSP shape from Fig. 5j) or background MU firing (Bkg, **f***iv*). * significant change with conditioning, $P < 0.05$, n = 10 subjects. **Summary of findings in humans**: Increasing $GABA_{axo}$ neuron activity with a brief cutaneous stimulation increased the MSR (**a, b***i***, d**) during a period consistent with nodal facilitation by PAD (30 – 200 ms post stimulation; **b***ii*). We again kept the conditioning stimulation small enough to not change the background EMG or single motor unit (MU) firing (**b*iii***) to rule out postsynaptic actions. When we instead increased PAD by a proprioceptive conditioning (via muscle TA vibration) the soleus MSR was inhibited (for up to 200 ms; **c***i*-**c***ii*), as previously reported(Hultborn *et al.*, 1987a). However, the vibration alone inhibited the ongoing MU discharge (**c***iii*), implying that this MSR inhibition was caused in part by postsynaptic inhibition, rather than PAD-mediated presynaptic inhibition(Hultborn *et al.*, 1987a). Repeated cutaneous conditioning stimulation (trains) to induce a buildup in this tonic PAD caused an associated buildup of the MSR that outlasted the conditioning and its postsynaptic actions by many seconds (after effect; **d,e**). Finally, the probability of a single MU contributing to the MSR was increased by cutaneous conditioning (**f***i-ii*), without increasing the estimated EPSP amplitude or rise time (PSF; see Methods; **f***iii*) or changing in the MU firing prior to the MSR testing (**f***iv*; motoneuron not depolarized closer to threshold), consistent with decreased branch point failure (Fig. 5).

Extended Data Fig. 14 | Lack of α5 $GABA_A$ receptor immunolabelling after receptor knockout, verifying antibody selectivity. a, Immunolabelling of α5 $GABA_A$ receptors with antibody to rabbit anti-α5 $GABA_A$ receptor subunit (1:200; TA338505, OriGene Tech), as used in Fig 1 and Extended Data Fig 1. Images taken in hippocampal region of wildtype adult mouse brain where neuronal α5 $GABA_A$ receptors are highly enriched. **b**, Lack of α5 $GABA_A$ receptor immunolabelling in α5 $GABA_A$ receptor knockout mouse (Gabra5 KO), from same region. **c-d**, Primary antibody omission controls in wild type and Gabra5 KO mice, respectively, where sections were processed as in (**a**) and (**b**), but no rabbit anti-α5 $GABA_A$ receptor antibody applied. Tissue sections in (**a**) and (**b**) were processed for immunolabelled side-by-side on the same slide, and images were obtained with identical confocal microscope settings and displayed at the same brightness as in antibody omission controls of (**c**) and (**d**) where no labelling was observed.

Extended Data Table 1. Chronological list of evidence contradicting the classical concept of presynaptic inhibition of transmitter release from proprioceptive sensory axon terminals on motoneurons.

Date	Contradictions in classic view of terminal presynaptic inhibition mediated by terminal $GABA_A$ receptors and PAD	Resolution of contradictions
1938	*Primary afferent depolarization (PAD) directly evokes spikes in sensory axons, producing excitation rather than presynaptic inhibition.* Barron and Matthews (1938)(Barron & Matthews, 1938) discovered that sensory nerve conditioning evokes a long depolarization in many other sensory afferents (primary afferent depolarization, PAD), which we now know is mostly $GABA_A$ mediated(Rudomin, 1999). They and others noted that sometimes this PAD was large enough to directly induce axon spiking, even in vivo(Beloozerova & Rossignol, 1999), including spikes in the sensory axons mediating the MSR itself, raising a contradiction with the notion of GABA mediated presynaptic inhibition(Lucas-Osma *et al.*, 2018a). While these PAD-triggered spikes do not fully propagate antidromically out the DRs in many axons (they fail en route), they are actually initiated in most axons and more likely to conduct orthodromically(Lucas-Osma *et al.*, 2018a), making most axons and their motoneuron synapse refractory to subsequent testing (*post activation depression*). Indeed, numerous groups have shown that these spikes directly activate the MSR pathway(Eccles *et al.*, 1961a; Duchen, 1986; Bos *et al.*, 2011; Fink *et al.*, 2014). Thus, these PAD-evoked spikes must inhibit afferent transmission in the MSR pathway by making axons refractory and producing post activation depression of their terminal synapse, even in humans where PAD evoked spikes occur(Shefner *et al.*, 1992b). This indirect inhibition is $GABA_A$ mediated and thus readily mistaken for presynaptic inhibition (sensitive to $GABA_A$ antagonists)(Curtis, 1998b; Redman, 1998), even though the PAD-evoked spike is fundamentally excitatory. Even Eccles noted this issue, and showed that just the refractory period alone in the sensory axon inhibits the MSR(Eccles *et al.*, 1961a).	*Post activation depression from PAD evoked spikes inhibits the MSR and masks facilitation of the MSR by nodal facilitation.* We find that facilitation of the MSR by conditioning evoked PAD is always reduced when it is associated with a large enough conditioning stimulation to evoke spikes in sensory afferents, which likely results from post activation depression of axon transmission. This likely explains why Fink et al.(Fink, 2013a; Fink *et al.*, 2014) recently saw inhibition of the MSR with optogenetic or sensory activation of $GABA_{axo}$ neurons (see Fig 4.12c in Fink(Fink, 2013a) for PAD evoked EPSC inhibiting the MSR). When looking for MSR facilitation, avoiding these spikes and post activation depression requires using weak conditioning stimuli, unlike previous studies(Eccles *et al.*, 1961a; Stuart & Redman, 1992).
1949	*Post-tetanic potentiation (PTP) of the MSR increases sensory nerve conduction, but its mechanisms have remained elusive.* Lloyd (1949)(Lloyd, 1949) concluded that increasing conduction along sensory axons (not just terminals) contributed to the minutes of facilitation of the MSR seen after a high frequency nerve stimulation train (PTP). However, he supposed this might be due to hyperpolarization of the sensory axons, even though we now know that such trains depolarize axons via tonic PAD(Lucas-Osma *et al.*, 2018a). The tonic PAD from these bursts must overwhelm the hyperpolarization driven by Na-K pump activity(Bostock & Grafe, 1985). Lloyd also concluded that PTP only occurred when the same nerve is used for the train (tetanus) as for testing the MSR.	*Repetitive nerve stimulation produces a tonic $GABA_A$ mediated depolarization (PAD) of axons that facilitates nodal conduction, and increases the MSR.* This PAD likely contributes to PTP, and is largest when the same nerve is tetanized, compared to other nerves, explaining why Lloyd missed the subtler facilitation from other nerves.
1958	*PAD is associated with a lowering of the threshold for activating spikes.* Early on Wall (1958)(Wall, 1958) noted that a conditioning nerve stimulation that depolarized sensory axons (PAD) was associated with a lower threshold to extracellularly activate these axons. Subsequently this was assumed to be due to the action of terminal $GABA_A$ receptors and presynaptic inhibition, and spike threshold changes were used to estimate the size of PAD(Lomeli *et al.*, 1998; Rudomin, 1999).	*PAD lowers the spike threshold via $GABA_A$ receptors at or near nodes assisting the sodium spike.* This is not related to presynaptic inhibition, but can still be used to estimate PAD as Rudomin and others have done.
1957 - 1994	*PAD is not correlated with inhibition of the monosynaptic reflex (MSR)*. Shortly after Frank and Fortes discovered that the leg extensor muscle MSR is inhibited by a conditioning of a flexor nerve in cats (PBST; like Fig. 6)(Frank & Fortes, 1957; Frank, 1959a), Eccles proposed the concept of presynaptic inhibition mediated by this conditioning depolarizing of the proprioceptive sensory axon terminals in the MSR pathway (PAD), simply because the MSR inhibition and PAD are somewhat correlated in time(Eccles *et al.*, 1961a). However, in retrospect PAD is far too brief to account for the much longer inhibition caused by this conditioning(Eccles *et al.*, 1962a; Curtis & Lacey, 1994), and some flexor nerve conditioning (a single PBST pulse) inhibits the MSR (Fig. 1 of Eccles, 1961(Eccles *et al.*, 1961a)), even though it	*PAD is correlated with nodal spike facilitation and facilitation of the MSR.* PAD causes facilitation of the MSR, explaining this correlation. When PAD is large and evokes axonal spikes, these cause post activation depression (detailed above) that should also be correlated with PAD, but is not due to presynaptic inhibition. Also,

	does not cause PAD in the extensor proprioceptors of the MSR at all(Eccles & Krnjevic, 1959).	barbiturates used by Eccles and others potentiated $GABA_A$ receptor currents.
1959 - 1993	*Postsynaptic inhibition inevitably accounts for part of the inhibition of the MSR by flexor nerve conditioning*. In his initial short report Frank (1959)(Frank, 1959a) correctly suggested that the early inhibition of the MSR by flexor nerve conditioning might be partly postsynaptic (rather than presynaptic), on motoneuron distal dendrites. Others dismissed postsynaptic inhibition because the decay times of the EPSP does not always change when the EPSP is reduced by conditioning, which they proposed indicated that there was no postsynaptic change in conductance in distal dendrites (McCrea *et al.*, 1990; Rudomin, 1999). However, this method is likely not very sensitive, due to variability in unitary EPSP time course. Also, anatomically ~70% of $GABA_{axo}$ contacts on afferent terminals also contact motoneurons (in a triad), so postsynaptic inhibition is likely inevitable(Pierce & Mendell, 1993; Hughes *et al.*, 2005).	*Postsynaptic inhibition masks facilitation of the MSR by nodal facilitation.* We find evidence for long lasting postsynaptic inhibition on distal motoneuron dendrites during nerve conditioning stimulation (including postsynaptic reductions in Tau, Vm and unitary EPSP heights and single MU firing). Crucially, minimizing postsynaptic inhibition requires using a small conditioning stimulation when looking for MSR facilitation, unlike previous studies (Stuart & Redman, 1992).
1961 - 2014	*Self-facilitation during repeated MSR testing reduces the possibility of observing facilitation with subsequent conditioning stimuli, leaving only inhibitory actions of conditioning.* Eccles and others knew that the same proprioceptive nerve stimulation that activates the MSR also depolarizes these proprioceptive afferents (PAD self-activation)(Eccles *et al.*, 1961a). Thus, just the act of repeatedly testing the MSR to find the average MSR prior to conditioning pre-activates PAD and produces self-facilitation of the MSR, reducing the headroom to observe changes in the MSR following a separate nerve conditioning stimulation that produces PAD. However, at the time it was not known that repeated nerve stimulation causes a tonic buildup of GABA and a tonic PAD that alters sensory transmission and MSR even at long repetition intervals of many seconds. Thus, Eccles and others used short test intervals (1 s) and strong maximal MSR test stimuli (Eccles *et al.*, 1961a; Stuart & Redman, 1992; Fink *et al.*, 2014), presumably assuming that there would be no interaction between test stimuli, which is not the case. In retrospect, these short test intervals and strong test stimuli must have preactivated tonic GABA, leaving little headroom to observe facilitation of the MSR (facilitation), and leaving mainly only inhibitory action possible.	*Self-facilitation masks facilitation of the MSR by a conditioning stimulation.* To observe facilitation of the MSR by a conditioning stimuli that produces a PAD it is important to use long test intervals (5 - 10 s) and small MSR test intensities (1.1xT) to minimize self activation of a tonic PAD prior to conditioning. While experimentally troublesome, self facilitation during repetitive activation is actually one of the main functions of PAD, allowing sensory axons to faithfully transmit spikes to motoneurons at high frequencies that would otherwise produce sodium spike inactivation.
1980	*Sensory axon terminal potentials at motoneurons are consistent with spike failure.* Early efforts to examine how spikes propagated to sensory axon terminals employed extracellular recordings (EC) near the motoneurons, called terminal potentials (Sypert et al. 1980)(Sypert *et al.*, 1980). However, unlike EC recordings from near conducting axons (Fig. 2b), these terminal potentials lacked much of the obvious negative field associated with the action potential, and instead had a prominent positive field, followed by a smaller negative field (Extended Data Fig. 10 and Sypert(Sypert *et al.*, 1980)). This positive field has been shown in other axons to be indicative of spike propagation failure and result from the passive axonal current caused by the last non-failing node, similar to a FP, as demonstrated in motor axon recording(Dudel, 1965; Hubbard *et al.*, 1969). Indeed, we found that even dorsal horn recordings could exhibit this positive field if the nearby dorsal root conduction is blocked with a microinjection of TTX (Extended Data Fig. 10d). Sypert(Sypert *et al.*, 1980) went on to show that with PAD evoked by nerve conditioning this positive terminal potential field was decreased, and incorrectly interpreted this as evidence for decreased spike conduction and thus supposed it was due to presynaptic inhibition.	*Positive terminal potential fields are decreased with PAD, indicative of decreased conduction failure, consistent with Sypert(Sypert et al., 1980).* There is a small negative field that follows the positive field in terminal potential recordings, representing spikes that actually reach the terminals. We quantified negative field and found it to increase with PAD, consistent again with increased spikes conducting to motoneurons (Extended Data Fig. 10). Blocking activity in the spinal cord with glutamate antagonists, which would include blocking $GABA_{axo}$ circuit activity, decreased this negative field.
1988 - 1998	*$GABA_B$ receptors cause presynaptic inhibition and related RDD.* Decades, after Eccles popularized the notion of $GABA_A$ mediated presynaptic inhibition, Curtis (1998)(Curtis & Lacey, 1994; Curtis, 1998b) concluded that the late part of the inhibition of the MSR by flexor nerve conditioning is instead $GABA_B$ receptor mediated, since it is reduced by the $GABA_B$ antagonist CGP55845 (as Fink also showed(Fink, 2013a)), and as is RDD(Lev-Tov *et al.*, 1988). RDD is a rate dependent depression in the MSR during repeated testing. We suggest that RDD is	*$GABA_B$ mediated presynaptic inhibition masks facilitation of the MSR by $GABA_A$ receptors. $GABA_B$ receptors* are located on the terminals, and produce presynaptic inhibition (Fig. 5) and RDD (Bennett and Hari, unpublished results), which are reduced by $GABA_B$

	partly mediated by a build up of GABA released by GABAergic neurons onto the terminals during this repeated MSR testing, though activity dependent homosynaptic depression likely also contributes(Hultborn *et al.*, 1996b).	antagonists (CGP55845) or silencing $GABA_{axo}$ neurons.
1990 - 1998	*$GABA_A$ receptors have direct postsynaptic inhibitory effects on many spinal neurons, making the actions of $GABA_A$ antagonists difficult to attribute to presynaptic inhibition*. By the 1990s Redman and others tried to confirm the role of $GABA_A$ receptors in presynaptic inhibition by locally applying the $GABA_A$ antagonists bicuculline to the spinal cord, and indeed found this drug or other antagonists reduced the inhibition of the MSR by flexor nerve conditioning (Eccles *et al.*, 1963; Stuart & Redman, 1992; Curtis & Lacey, 1994; Curtis, 1998b). However, we now know that this is indirectly due to bicuculline causing a widespread disinhibition of the spinal cord (including loss of post activation depression, detailed above) that leads to a convulsive spinal cord with very long lasting polysynaptic reflexes evoked by the nerve conditioning or the MSR testing itself, making pre and postsynaptic actions hard to distinguish. Further, we know that $GABA_A$ receptors mediate dorsal root reflexes and associated post activation depression of the MSR (see above point), and thus bicuculline and picrotoxin likely reduce the inhibition of the MSR via reducing post activation depression (see above), rather than changing presynaptic inhibition.	*$GABA_A$ receptor antagonists reduce the MSR, by reducing nodal facilitation.* Postsynaptic $GABA_A$ receptors have potent inhibitory actions on many spinal neurons involved in polysynaptic reflexes. However, minimizing these polysynaptic reflexes (by using weak test stimuli and blocking NMDA receptors, Fig 5c) reveals a direct inhibition of the MSR by $GABA_A$ antagonists, as does optogenetically silencing $GABA_{axo}$ neuron, consistent with $GABA_A$ receptors facilitating rather than inhibiting sensory transmission.
1990 - 1995	*PAD recorded in the dorsal roots cannot arise from terminal GABA receptors, due to spatial attenuation on the axon.* With advent of detailed anatomical and computer models of sensory axons(Segev, 1990; Graham & Redman, 1994; Walmsley *et al.*, 1995) it became clear that signals like spikes or PAD are attenuated over short distances in axons, < 200 µm. This implies that PAD recorded on or near the DR is unlikely to bare any relation to terminal presynaptic inhibition, despite claims to the contrary(Eccles *et al.*, 1963; Hultborn *et al.*, 1987a; Rudomin, 1999; Fink *et al.*, 2014).	*Space constant λ_S of sensory axons is about 90 µm.* Thus, the PAD recorded in the dorsal root must arise from GABA receptors at or near nodes, and not bear any relation to GABA action at the terminals 1000 µm away.
1994 - 1999	*Shunting inhibition produced by axon terminal $GABA_A$ receptors is not adequate to produce presynaptic inhibition of the MSR*. Numerous invertebrate studies proposed that the conductance from $GABA_A$ receptors in terminals caused a reduction in spike height via its shunting action that contributed to presynaptic inhibition with nerve conditioning(Cattaert & El Manira, 1999). However, the effects of conditioning on spikes was small and terminals were not actually recorded from. Subsequently modelling considerations led to the conclusion that shunting inhibition is not adequate to produce presynaptic inhibition and calcium was somehow involved(Graham & Redman, 1994), possibly further implicating $GABA_B$ receptors, as we see. Considering our estimated space constant λ_S of ~90 µm, the small shunting inhibition of the spike height (1 mV) we observe is very unlikely to prevent the spike produced at a given node from activating a downstream neighbouring node, since nodes are ~50 µm apart, leading to only about a 50% reduction in spike height at the downstream node (to ~40 mV, unless of course the node is failing), which is well above that needed to initiate a full nodal spike. Thus, spike propagation is very unlikely to be blocked by shunting inhibition. Also, terminal boutons are mostly on unmyelinated axons without sodium channels (passive, 3rd order), and so a 1% reduction in the spike arising from the last/closest node on the 2nd order branch will have little effect on the terminal depolarization (1%), ruling out substantial shunting inhibition of transmitter release from the terminal.	*$GABA_A$ receptors only slightly decrease spikes by shunting conductances, and otherwise assist nodal spike conduction in proprioceptive axons.* In non-failing secure spikes in sensory axons $GABA_A$ receptors lower the threshold for spike activation (rheobase) and speed the spikes, the latter by decreasing the time constant of the axon (RC). They do decrease the spike, but only by about 1%, consistent with shunting being unlikely to inhibit spike transmission to motoneurons. However, this does not rule out densely expressed $GABA_A$ receptors causing shunting and presynaptic inhibition in cutaneous afferents, as previously suggested(Wall, 1998; Verdier *et al.*, 2004; Lucas-Osma *et al.*, 2018a).
1994 - 1998	*Sodium spike inactivation from axon terminal $GABA_A$ receptor depolarization is not adequate to produce presynaptic inhibition.* Early poor quality recordings from sensory axons (resting near -50 mV from penetration injury)(Luscher *et al.*, 1994b) led to the prevailing view that spike failure with depolarization (PAD) was much more common than we now find with better recordings (resting near -70 mV, Extended Data Fig. 3b). Further, Redman later questioned this view, and it seems unlikely for the MSR pathway(Stuart & Redman, 1992; Redman, 1998).	*Physiological PAD depolarizations do not block proprioceptive sensory axons spikes, and instead prevent them from failing in the MSR pathway.* However, this does not rule out $GABA_A$ receptors causing spike inactivation in other axons(Lucas-Osma *et al.*, 2018a).
1995 - 1998	*Physiological $GABA_A$ receptor activation is unlikely to produce branch point failure in the sensory axons of the MSR pathway.* Over the years sensory axon conduction failure has been occasionally noted from indirect observations(Barron &	*$GABA_A$ receptors help prevent branch point failure and thus facilitate sensory transmission in the MSR.* Computer

	Matthews, 1935; Howland *et al.*, 1955; Swadlow *et al.*, 1980; Luscher *et al.*, 1983; Henneman *et al.*, 1984a; Wall, 1998; Gemes *et al.*, 2013; Li *et al.*, 2020). Wall and others(Walmsley *et al.*, 1995; Wall, 1998; Verdier *et al.*, 2004) questioned whether this failure could be increased by GABA. However, Wall thought GABA should inhibit rather than assist spikes by inactivating sodium channels. However, Wall was misled by two issues. First, at the time low quality recordings from sensory axons may have led to the misconception that spike failure with physiological depolarizations (like PAD) was common(Luscher *et al.*, 1994b), unlike what we observe. To be fair, Wall was studying cutaneous, as well as proprioceptive, afferents, which are more densely innervated by GABA receptors(Lucas-Osma *et al.*, 2018a), making spike inactivation by PAD more likely(Wall, 1998). Second, by this time $GABA_A$ and associated PAD had been firmly entrenched as synonymous with presynaptic inhibition.	simulations by Walmsley and others (Graham & Redman, 1994; Walmsley *et al.*, 1995) have led to the conclusion that physiological $GABA_A$ receptor conductances cannot stop spikes from propagating past a node. Instead, we report here that they help prevent spike failure near branch points, including in our computer simulations.
1996 - 2018	*Lack of $GABA_A$ receptors on proprioceptive Ia axon terminals*. Extrasynaptic α5 $GABA_A$ receptors are lacking at most proprioceptive axon terminals in the ventral horn(Lucas-Osma *et al.*, 2018a). Synaptic $GABA_A$ receptors also appear to be lacking from these terminals, though only indirectly studied(Alvarez *et al.*, 1996; Betley *et al.*, 2009; Fink *et al.*, 2014). $GABA_B$ receptor immunolabelling had not been investigated in these Ia afferents, though is has in others (Aβ)(Salio *et al.*, 2017).	*$GABA_A$ receptors are mostly at nodes, whereas $GABA_B$ receptors are at terminals in large proprioceptive afferents*.
2005 - 2014	*GABAergic innervation of axons.* Recently, GAD2 expressing GABAergic neurons were identified that make axoaxonic connections onto presynaptic terminals of proprioceptive axons(Hughes *et al.*, 2005; Betley *et al.*, 2009; Fink *et al.*, 2014) (termed $GABA_{axo}$ here). Previously, Walsmley found GABAergic P-boutons contacting nodes of these axons. Subsequently, Kolta and Zytnicki again found GABAergic contacts near branch points of mammalian afferents(Lamotte d'Incamps *et al.*, 1998; Verdier *et al.*, 2004), as did Cattaert in crayfish(Cattaert & El Manira, 1999).	*A key role of $GABA_{axo}$ neurons is to innervate proprioceptive afferent nodes via $GABA_A$ receptors and ventral terminals via $GABA_B$ receptors, producing nodal facilitation and presynaptic inhibition, respectively*.
2018	*$GABA_{axo}$ neuron activation by sensory conditioning does not depolarize proprioceptive axon terminals*. Direct recordings from the fine terminals of proprioceptive afferents reveal that during sensory conditioning the terminal is not depolarized during the long PAD recorded on dorsal roots(Lucas-Osma *et al.*, 2018a).	*$GABA_{axo}$ neuron activation depolarizes nodes*. Dorsally located nodes produce the PAD recorded in dorsal roots.

Extended Data Table 2. Resources used in Methods.

REAGENT or RESOURCE	SOURCE	IDENTIFIER
Antibodies		
Rabbit anti-α_5 $GABA_A$ receptor subunit	OriGene Tech.	TA338505
Rabbit anti- α_1 $GABA_A$ receptor subunit	Sigma-Aldrich	06-868
Guinea pig anti-α_2 $GABA_A$ receptor subunit	Synaptic Systems	224 104
Chicken anti-γ_2 $GABA_A$ receptor subunit	Synaptic Systems	224 006
Rabbit anti-$GABA_{B1}$ receptor subunit	Synaptic Systems	322 102
Mouse anti-NF200 (Neurofilament 200)	Sigma-Aldrich	N0142
Guinea pig anti-VGLUT1 (Vesicular glutamate transporter 1)	Sigma-Aldrich	AB5905
Rabbit anti-Caspr (Contactin associated protein)	Abcam	ab34151
Mouse anti-Caspr (Contactin associated protein)	NeuroMab	K65/35
Chicken anti-MBP (Myelin basic protein)	Abcam	ab106583
Chicken anti-VGAT (Vesicular inhibitory amino acid transporter)	Synaptic Systems	131 006
Rabbit anti-VGAT	Sigma-Aldrich	AB5062P
Rabbit anti-EYFP (Enhanced yellow fluorescent protein)	Biorbyt	orb256069
Goat anti-RFP (Red fluorescent protein; binds tdTom)	Biorbyt	orb334992
Rabbit anti-RFP (Red fluorescent protein; binds tdTom)	MBL Int.	PM005
Rabbit anti-GFP (Green fluorescent protein)	ThermoFisher Sc.	A11122
Mouse anti-Pan Sodium Channel (binds all Na_V types)	Sigma-Aldrich	S8809
Goat anti-rabbit Alexa Fluor 555	ThermoFisher Sc.	A32732
Goat anti-rabbit Alexa Fluor 647	Abcam	ab150079
Goat anti-rabbit Pacific orange	ThermoFisher Sc.	P31584
Goat anti-mouse Alexa Fluor 647	ThermoFisher Sc.	A21235
Goat anti-mouse Alexa Fluor 488	ThermoFisher Sc.	A11001
Goat anti-mouse Alexa Fluor 555	ThermoFisher Sc.	A28180
Goat anti-guinea pig Alexa Fluor 647	ThermoFisher Sc.	A21450
Goat anti-chicken Alexa Fluor 405	Abcam	ab175674
Donkey anti-goat Alexa Fluor 555	Abcam	ab150130
Donkey anti-rabbit Alexa Fluor 488	ThermoFisher Sc.	A21206
Streptavidin-conjugated Alexa Fluor 488	Jackson immunoR.	016-540-084
Streptavidin-conjugated Cyanine Cy5	Jackson immunoR.	016-170-084
Guinea pig anti-GAD2/GAD65	Synaptic Systems	198 104
Guinea pig anti-Neurofilament M (NFM),	Synaptic Systems	171 204
Chemicals, Peptides, and Recombinant Proteins		
M.O.M (Mouse on Mouse Immunodetection Kit)	Vector	BMK-2202
Experimental Models: Organisms/Strains		
$Gad2^{CreER}$ mouse: *$Gad2^{tm1(cre/ERT2)Zjh}$*/J	The Jackson Laboratory	Stock# 010702
$Vglut1^{cre}$ mouse: B6;129S-*$Slc17a7^{tm1.1(cre)Hze}$*/J	The Jackson Laboratory	Stock# 023527
$R26^{LSL\text{-}ChR2\text{-}EYFP}$ mouse: B6;129S-*$Gt(ROSA)26Sor^{tm32(CAG\text{-}COP4*H134R/EYFP)Hze}$*/J	The Jackson Laboratory	Stock# 012569
$R26^{LSL\text{-}Arch3\text{-}GFP}$ mouse: B6;129S-*$Gt(ROSA)26Sor^{tm35.1(CAG\text{-}aop3/GFP)Hze}$*/J	The Jackson Laboratory	Stock# 012735

R26$^{LSL\text{-}tdTom}$ mouse crossed with Gad2^{CreER} mice: B6.Cg-*Gt(ROSA)26Sor$^{tm14(CAG\text{-}tdTomato)Hze}$*/J	The Jackson Laboratory	Stock# 007914
R26$^{LSL\text{-}tdTom}$ mouse crossed with Vglut1^{Cre} mice: B6.Cg-*Gt(ROSA)26Sor$^{tm9(CAG\text{-}tdTomato)Hze}$*/J	The Jackson Laboratory	Stock# 007909
EIIa-cre mice crossed with Gabra5-floxed mice	Dr. Pearce	
Oligonucleotides		
5' -> ACG TTT CCT GTC CCT GTG TG -> 3' Common for Gad2^{CreER} mice	Integrated DNA technologies	11400
5' -> AGG CAA ATT TTG GTG TAC GG -> 3' Mutant for Gad2^{CreER} mice	Integrated DNA technologies	oIMR9074
5' -> CAG ACG CTG CAG TCT TTC AG -> 3' Wild type for Gad2^{CreER} mice	Integrated DNA technologies	oIMR3346
5' -> ACA TGG TCC TGC TGG AGT TC -> 3' Mutant Forward for ChR2 mice	Integrated DNA technologies	oIMR9102
5' -> GGC ATT AAA GCA GCG TAT CC -> 3' Mutant Reverse for ChR2 mice	Integrated DNA technologies	oIMR9103
5' -> AAG GGA GCT GCA GTG GAG TA -> 3' Wild type Forward for ChR2 mice	Integrated DNA technologies	oIMR9020
5' -> CCG AAA ATC TGT GGG AAG TC -> 3' Wild type Reverse for ChR2 mice	Integrated DNA technologies	oIMR9021
5' -> CTG TTC CTG TAC GGC ATG G -> 3' Mutant Forward for both tdTom mouse strains	Integrated DNA technologies	oIMR9105
5' -> GGC ATT AAA GCA GCG TAT CC -> 3' Mutant Reverse for both tdTom mouse strains	Integrated DNA technologies	oIMR9103
5' -> AAG GGA GCT GCA GTG GAG TA -> 3' Wild type Forward for both tdTom mouse strains	Integrated DNA technologies	oIMR9020
5' -> CCG AAA ATC TGT GGG AAG TC -> 3' Wild type Reverse for both tdTom mouse strains	Integrated DNA technologies	oIMR9021
5' -> CTT CTC GCT AAG GTG GAT CG -> 3' Mutant Forward for Arch3 mice	Integrated DNA technologies	12178
5' -> CAC CAA GAC CAG AGC TGT CA -> 3' Mutant Reverse for Arch3 mice	Integrated DNA technologies	12179
5' -> TCC CAA AGT CGC TCT GAG TT -> 3' Wild type Forward for Arch3 mice	Integrated DNA technologies	oIMR8713
5' -> CTT TAA GCC TGC CCA GAA GA -> 3' Wild type Reverse for Arch3 mice	Integrated DNA technologies	12177

5’ -> ATG AGC GAG GAG AAG TGT GG -> 3’ Common for VGLUT1^{cre} mice	Integrated DNA technologies	17904
5’ -> CCC TAG GAA TGC TCG TCA AG -> 3’ Mutant reverse for VGLUT1^{cre} mice	Integrated DNA technologies	12231
5’ -> GTG GAA GTC CTG GAA ACT GC -> 3’ Wild type reverse for VGLUT1^{cre} mice	Integrated DNA technologies	17905
Software and Algorithms		
Leica Application Suite X software	Leica Microsystems	
Clampfit 8.0	Axon Instruments	

Figures (Appendix)

Figure 1

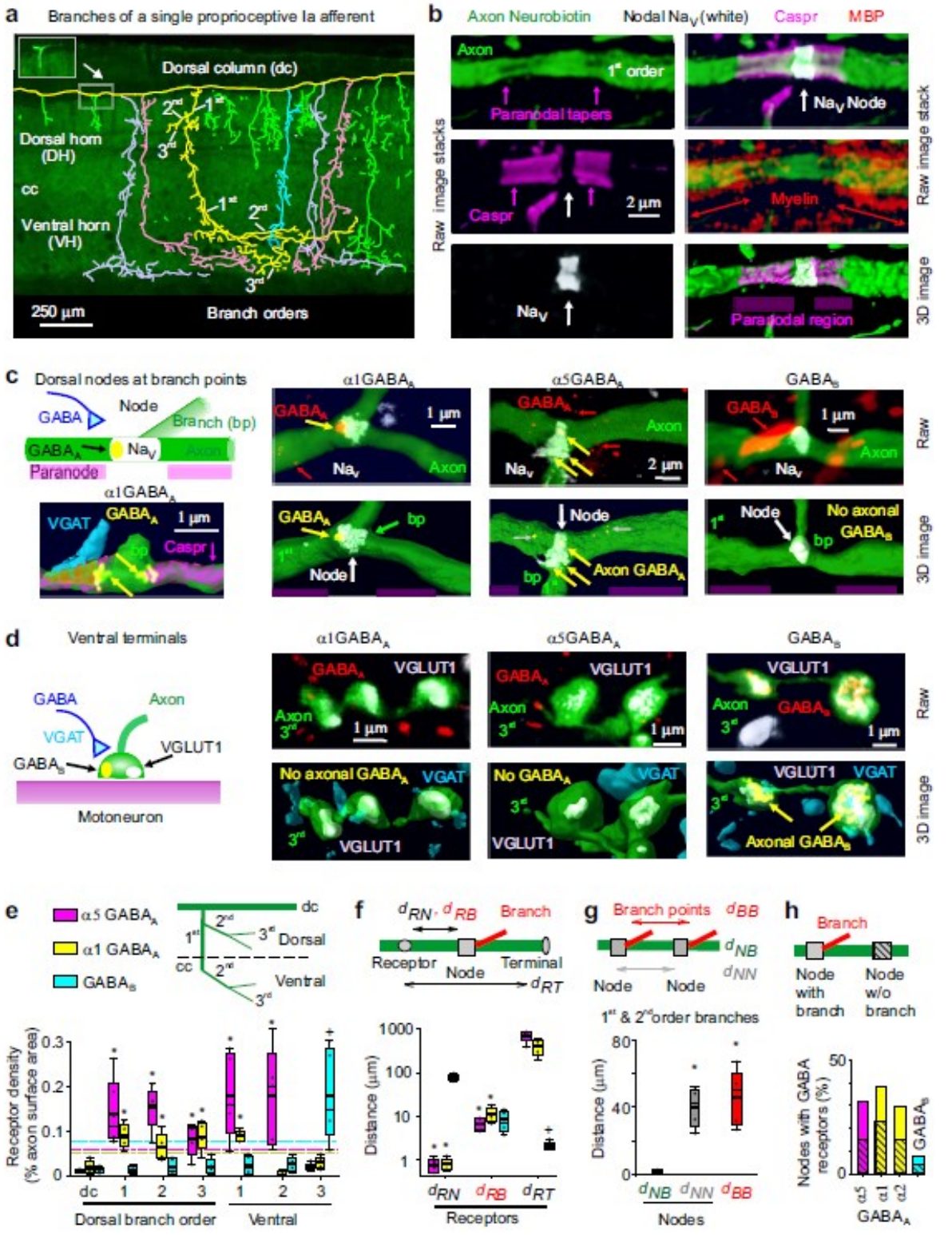

Figure 2

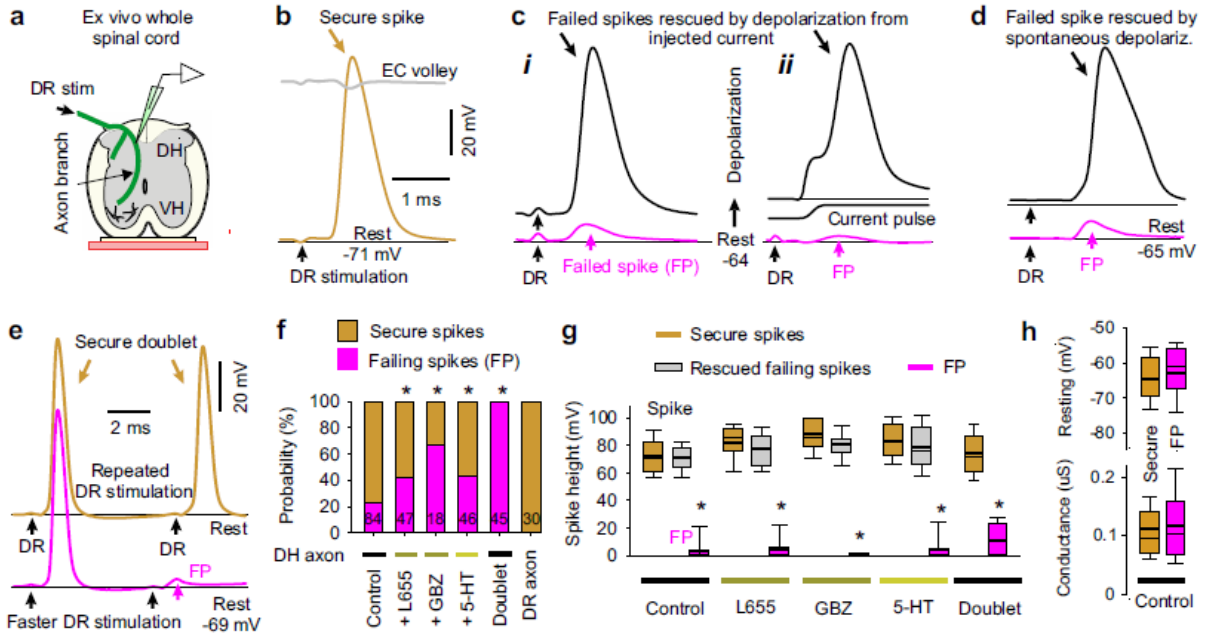
a
Ex vivo whole spinal cord
DR stim
Axon branch
DH
VH
b
Secure spike
EC volley
20 mV
1 ms
Rest
-71 mV
DR stimulation
c
Failed spikes rescued by depolarization from injected current
i
ii
Depolarization
Rest
-64
Current pulse
DR
Failed spike (FP)
DR
FP
d
Failed spike rescued by spontaneous depolariz.
Rest
-65 mV
DR
FP
e
Secure doublet
20 mV
2 ms
Repeated DR stimulation
Rest
DR
DR
FP
Faster DR stimulation
Rest
-69 mV
f
Secure spikes
Failing spikes (FP)
Probability (%)
100
80
60
40
20
0
84
47
18
46
45
30
DH axon
Control
+ L655
+ GBZ
+ 5-HT
Doublet
DR axon
g
Secure spikes
Rescued failing spikes
FP
Spike
Spike height (mV)
100
80
60
40
20
0
FP
Control
L655
GBZ
5-HT
Doublet
h
Resting (mV)
-50
-60
-70
-80
Secure
FP
Conductance (uS)
0.2
0.1
0
Control

Figure 3

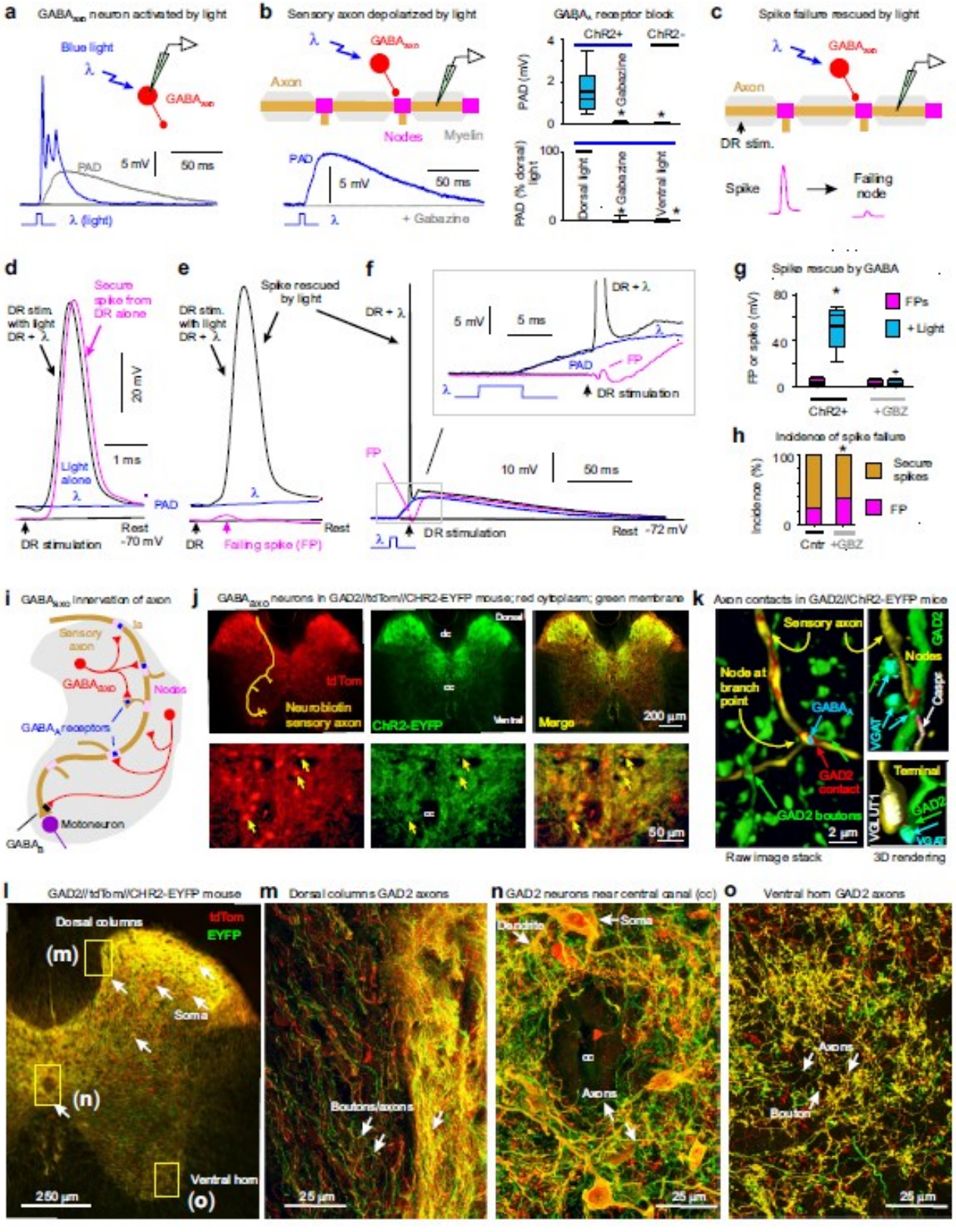
a
GABAaxo neuron activated by light
Blue light
λ
GABAaxo
PAD
5 mV
50 ms
λ (light)
b
Sensory axon depolarized by light
λ
GABAaxo
Axon
Nodes
Myelin
PAD
5 mV
50 ms
λ
+ Gabazine
GABAA receptor block
ChR2+
ChR2-
PAD (mV)
4
2
0
+ Gabazine
PAD (% dorsal light)
100
0
Dorsal light
+ Gabazine
Ventral light
c
Spike failure rescued by light
λ
GABAaxo
Axon
DR stim.
Spike
Failing node
d
DR stim. with light DR + λ
Secure spike from DR alone
20 mV
1 ms
Light alone
λ
PAD
DR stimulation
Rest -70 mV
e
DR stim. with light DR + λ
Spike rescued by light
λ
DR
Failing spike (FP)
Rest
f
DR + λ
5 mV
5 ms
DR + λ
λ
PAD
FP
λ
DR stimulation
FP
10 mV
50 ms
λ
DR stimulation
Rest -72 mV
g
Spike rescue by GABA
FP or spike (mV)
80
40
0
FPs
+ Light
ChR2+
+GBZ
h
Incidence of spike failure
Incidence (%)
100
0
Secure spikes
FP
Cntr
+GBZ
i
GABAaxo innervation of axon
Sensory axon
Ia
GABAaxo
Nodes
GABAA receptors
Motoneuron
GABAB
j
GABAaxo neurons in GAD2/tdTom/ChR2-EYFP mouse; red cytoplasm; green membrane
tdTom
Neurobiotin sensory axon
Dorsal
dc
cc
ChR2-EYFP
Ventral
Merge
200 µm
50 µm
k
Axon contacts in GAD2/ChR2-EYFP mice
Sensory axon
Node at branch point
GABAA
GAD2 contact
GAD2 boutons
2 µm
Raw image stack
GAD2
Nodes
Caspr
VGAT
Terminal
VGLUT1
GAD2
VGAT
3D rendering
l
GAD2/tdTom/ChR2-EYFP mouse
Dorsal columns
tdTom
EYFP
(m)
Soma
(n)
Ventral horn
(o)
250 µm
m
Dorsal columns GAD2 axons
Boutons/axons
25 µm
n
GAD2 neurons near central canal (cc)
Dendrite
Soma
cc
Axons
25 µm
o
Ventral horn GAD2 axons
Axons
Bouton
25 µm

Figure 4

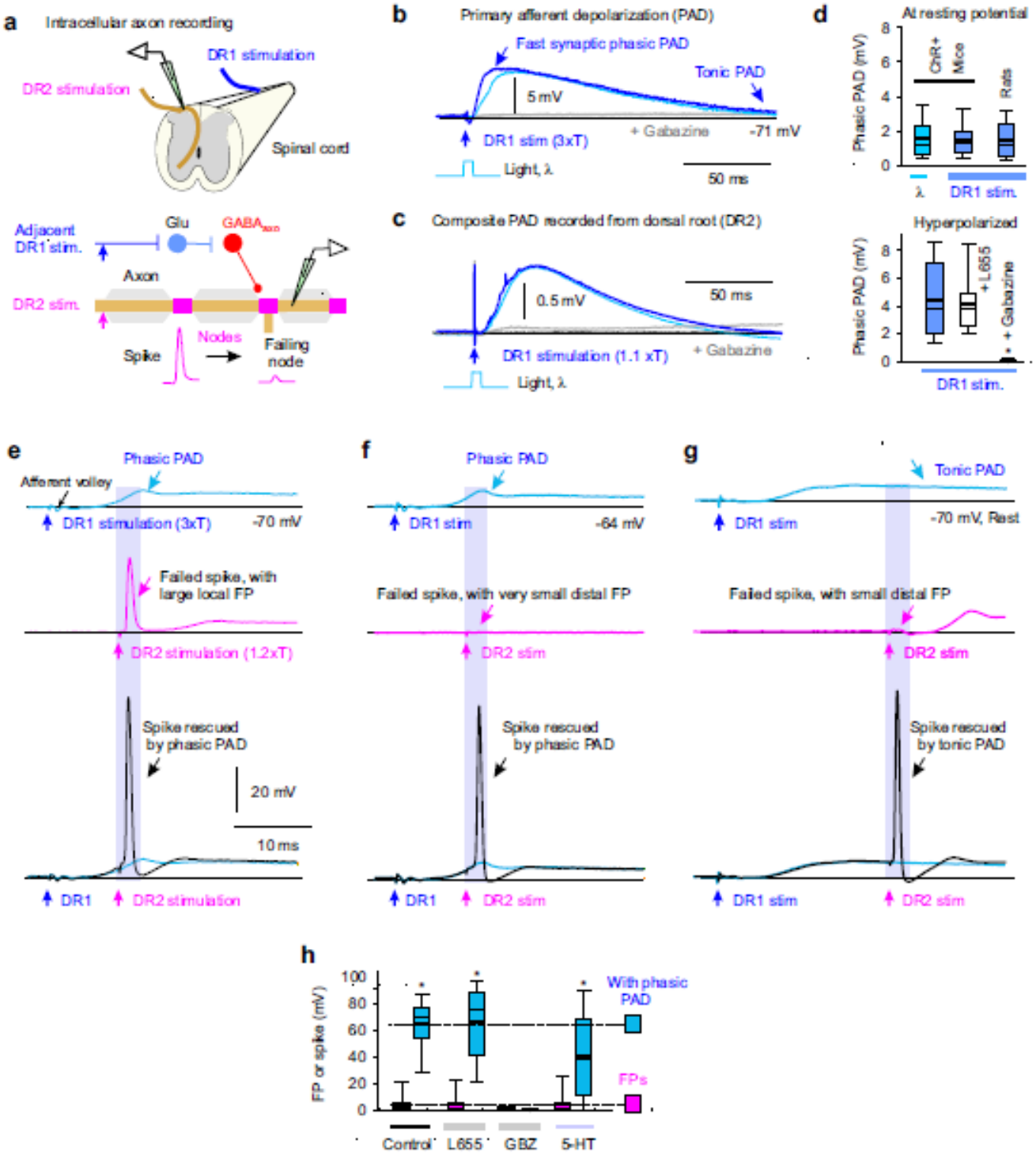
a
Intracellular axon recording
DR1 stimulation
DR2 stimulation
Spinal cord
Adjacent DR1 stim.
Glu
GABA axo
Axon
DR2 stim.
Spike
Nodes
Failing node
b
Primary afferent depolarization (PAD)
Fast synaptic phasic PAD
Tonic PAD
5 mV
+ Gabazine
-71 mV
DR1 stim (3xT)
Light, λ
50 ms
c
Composite PAD recorded from dorsal root (DR2)
0.5 mV
50 ms
DR1 stimulation (1.1 xT)
+ Gabazine
Light, λ
d
At resting potential
Phasic PAD (mV)
ChR+ Mice
Rats
λ
DR1 stim.
Hyperpolarized
+ L655
+ + Gabazine
DR1 stim.
e
Phasic PAD
Afferent volley
DR1 stimulation (3xT)
-70 mV
Failed spike, with large local FP
DR2 stimulation (1.2xT)
Spike rescued by phasic PAD
20 mV
10 ms
DR1
DR2 stimulation
f
Phasic PAD
DR1 stim
-64 mV
Failed spike, with very small distal FP
DR2 stim
Spike rescued by phasic PAD
DR1
DR2 stim
g
Tonic PAD
DR1 stim
-70 mV, Rest
Failed spike, with small distal FP
DR2 stim
Spike rescued by tonic PAD
DR1 stim
DR2 stim
h
FP or spike (mV)
With phasic PAD
FPs
Control
L655
GBZ
5-HT

Figure 5

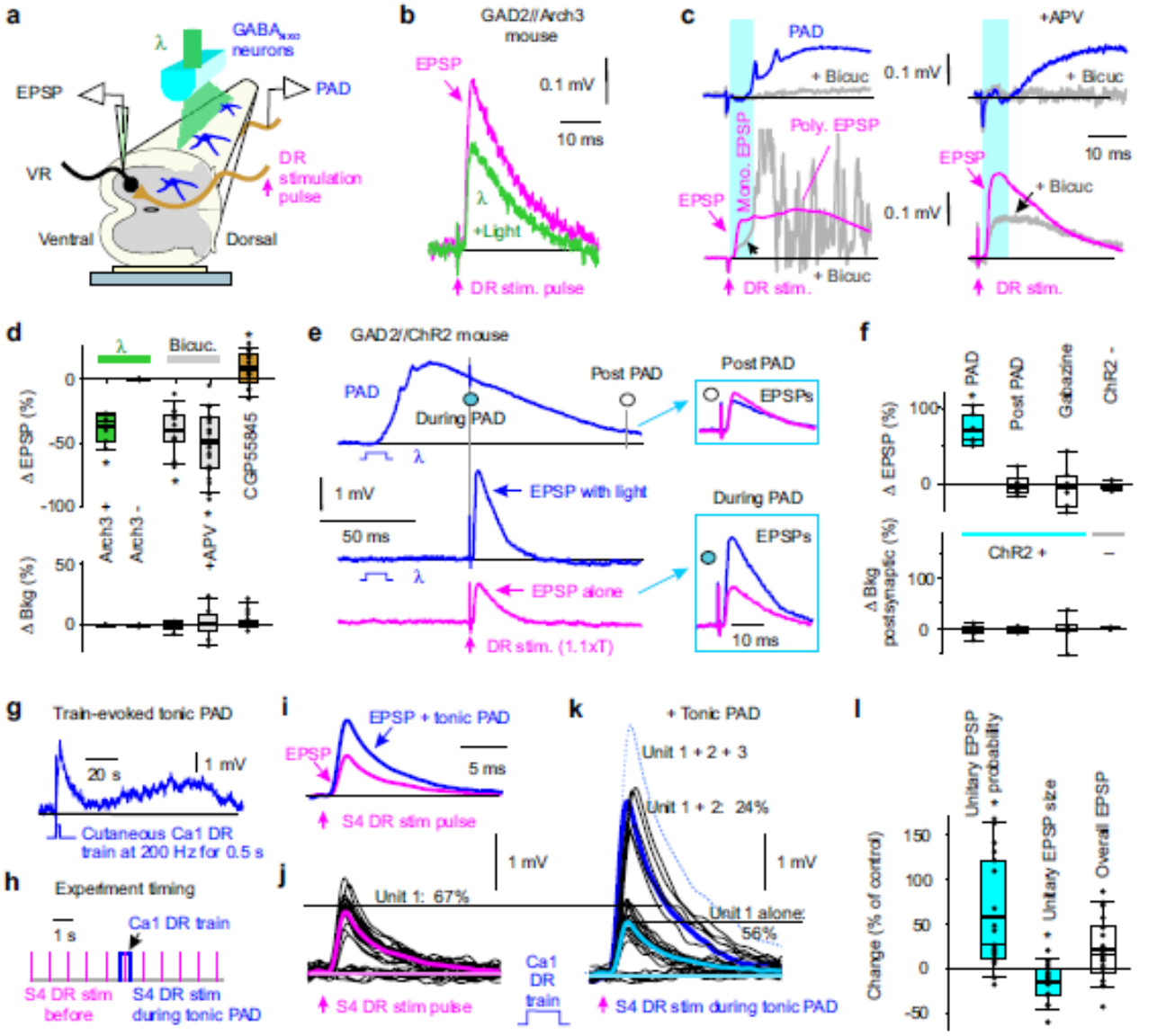
a
GABA$_{A,\infty}$ neurons
λ
EPSP
PAD
VR
DR stimulation pulse
Ventral
Dorsal
b
GAD2//Arch3 mouse
EPSP
0.1 mV
10 ms
λ
+Light
DR stim. pulse
c
PAD
+ Bicuc
0.1 mV
+APV
Poly. EPSP
Mono. EPSP
EPSP
DR stim.
d
λ
Bicuc.
Δ EPSP (%)
Δ Bkg (%)
Arch3 +
Arch3 -
+APV +
CGP55845
e
GAD2/ChR2 mouse
PAD
During PAD
Post PAD
EPSPs
1 mV
50 ms
EPSP with light
EPSP alone
DR stim. (1.1xT)
10 ms
f
+ PAD
Post PAD
Gabazine
ChR2 -
Δ EPSP (%)
ChR2 +
Δ Bkg postsynaptic (%)
g
Train-evoked tonic PAD
20 s
1 mV
Cutaneous Ca1 DR train at 200 Hz for 0.5 s
h
Experiment timing
1 s
Ca1 DR train
S4 DR stim before
S4 DR stim during tonic PAD
i
EPSP + tonic PAD
EPSP
5 ms
S4 DR stim pulse
j
1 mV
Unit 1: 67%
S4 DR stim pulse
Ca1 DR train
k
+ Tonic PAD
Unit 1 + 2 + 3
Unit 1 + 2: 24%
1 mV
Unit 1 alone: 56%
S4 DR stim during tonic PAD
l
Unitary EPSP + probability
Unitary EPSP size
Overall EPSP
Change (% of control)

Figure 6

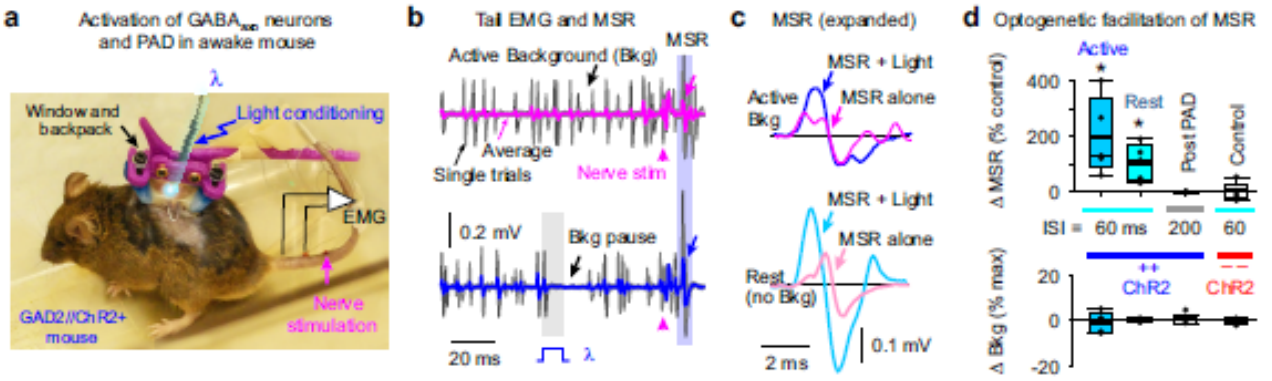
a
Activation of GABA$_{axo}$ neurons and PAD in awake mouse
λ
Window and backpack
Light conditioning
EMG
Nerve stimulation
GAD2/ChR2+ mouse
b
Tail EMG and MSR
MSR
Active Background (Bkg)
Average
Single trials
Nerve stim
0.2 mV
Bkg pause
20 ms
λ
c
MSR (expanded)
MSR + Light
Active Bkg
MSR alone
MSR + Light
Rest (no Bkg)
MSR alone
2 ms
0.1 mV
d
Optogenetic facilitation of MSR
Active
Rest
Post PAD
Control
Δ MSR (% control)
400
200
0
ISI = 60 ms 200 60
++
ChR2
ChR2
Δ Bkg (% max)
20
0
-20

Figure 7

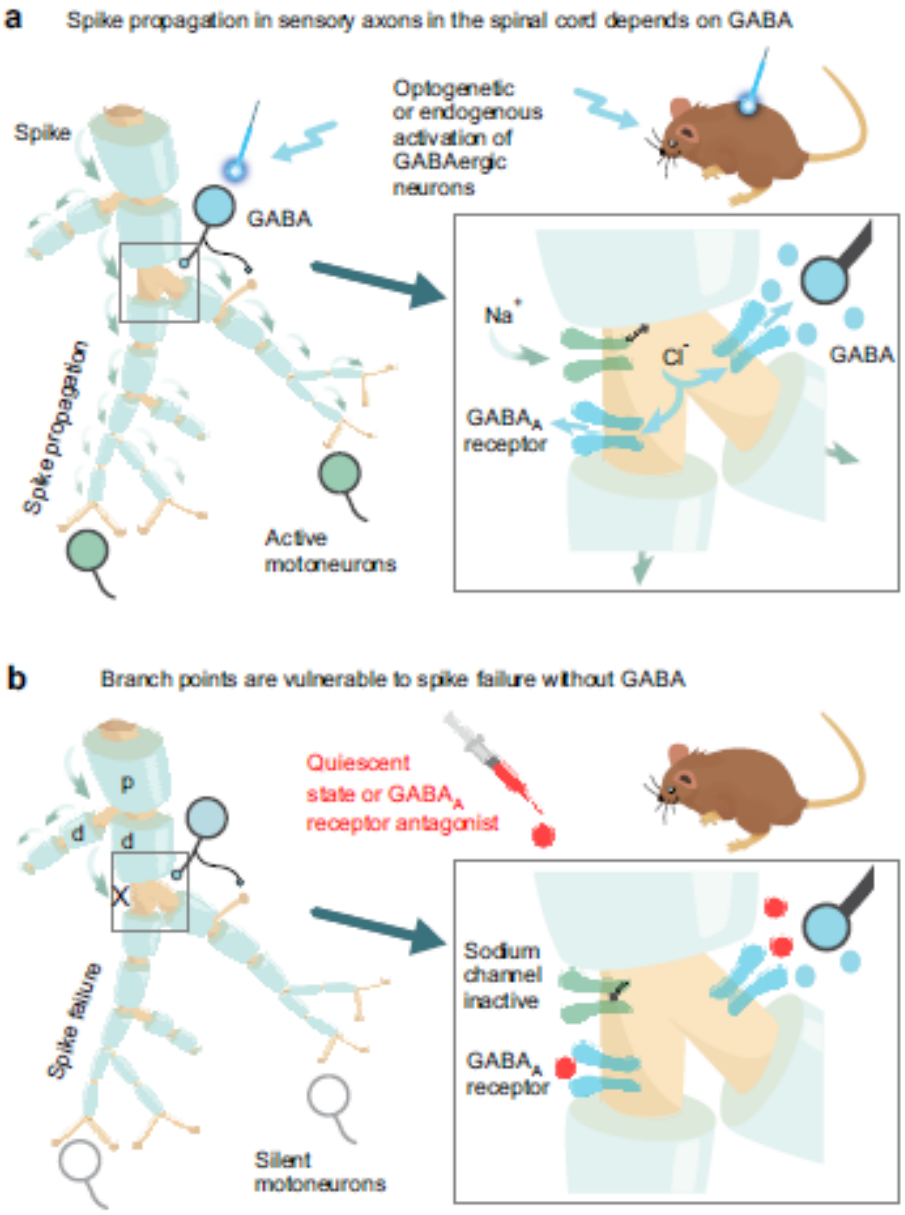
a
Spike propagation in sensory axons in the spinal cord depends on GABA
Spike
GABA
Optogenetic or endogenous activation of GABAergic neurons
Spike propagation
Active motoneurons
Na+
Cl-
GABA
GABAA receptor
b
Branch points are vulnerable to spike failure without GABA
p
d
d
X
Spike failure
Silent motoneurons
Quiescent state or GABAA receptor antagonist
Sodium channel inactive
GABAA receptor

Extended Data Fig. 1

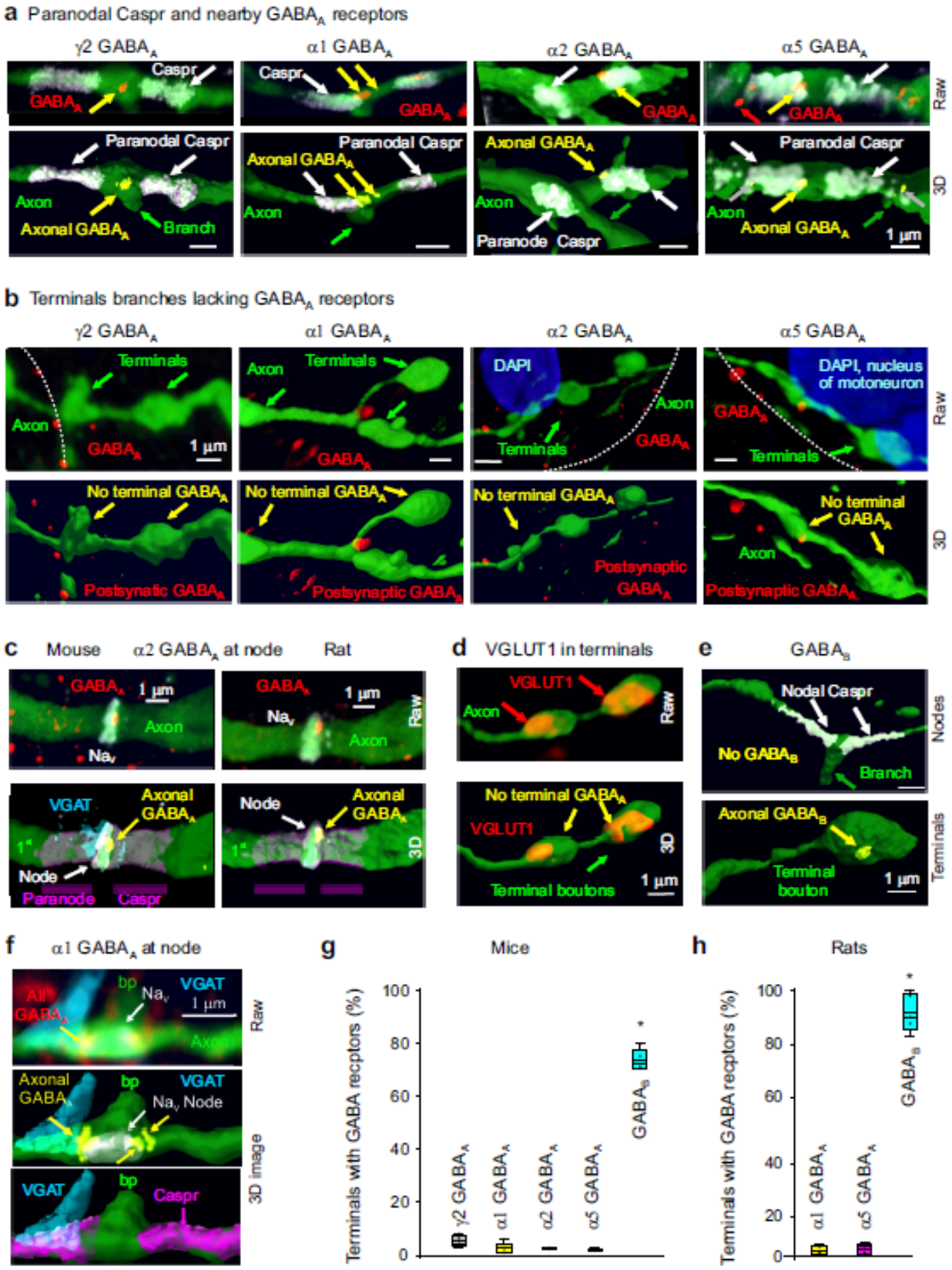

Extended Data Fig. 2

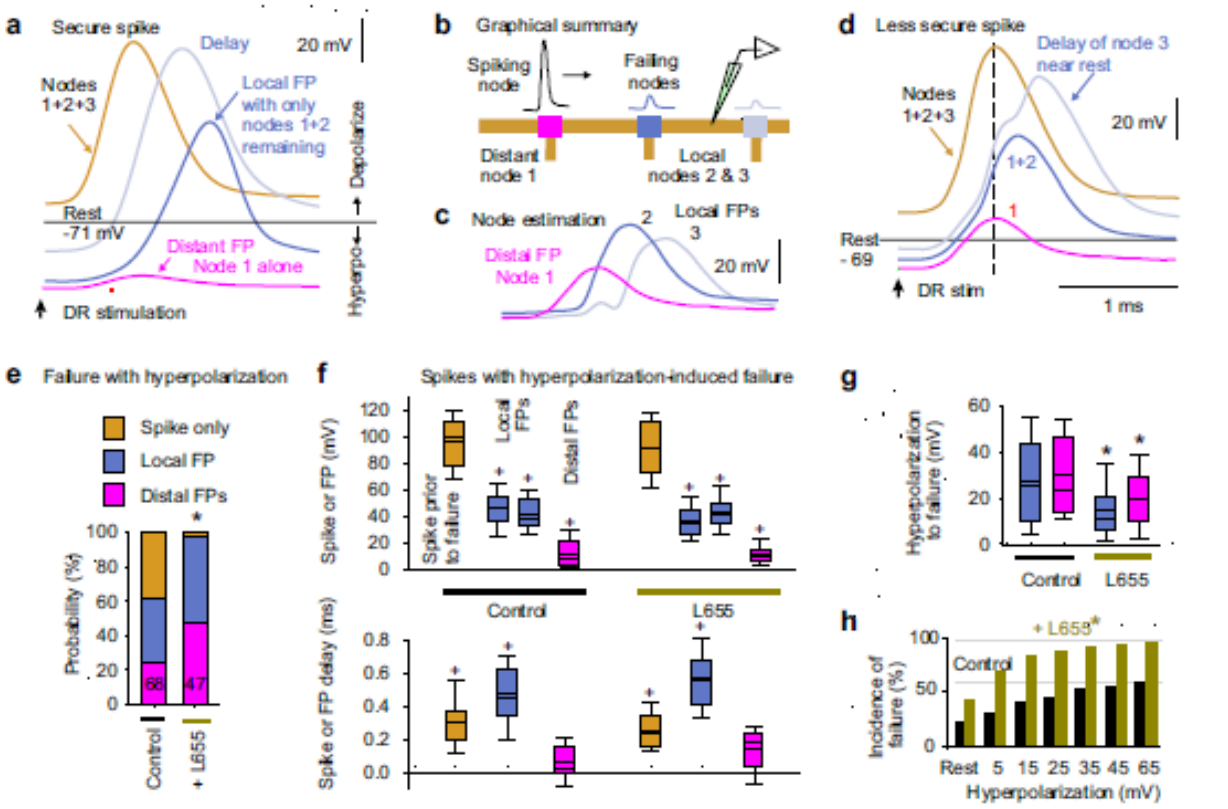

Extended Data Fig. 3

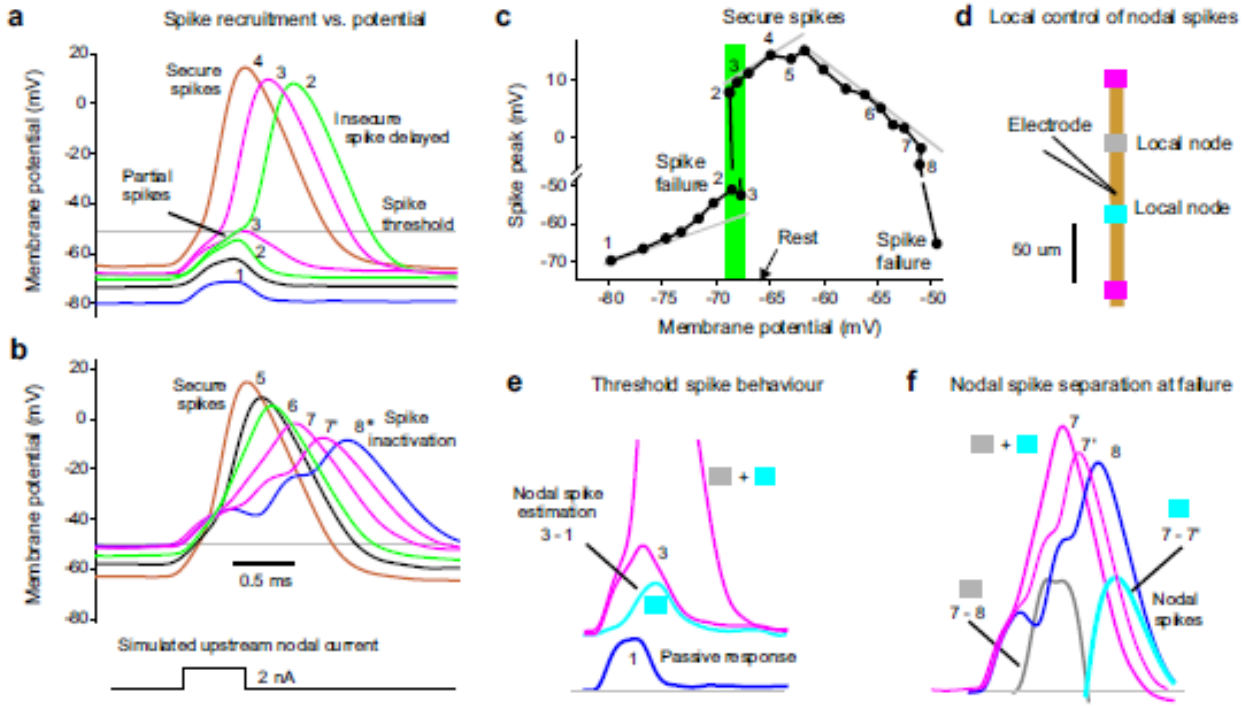

Extended Data Fig. 4

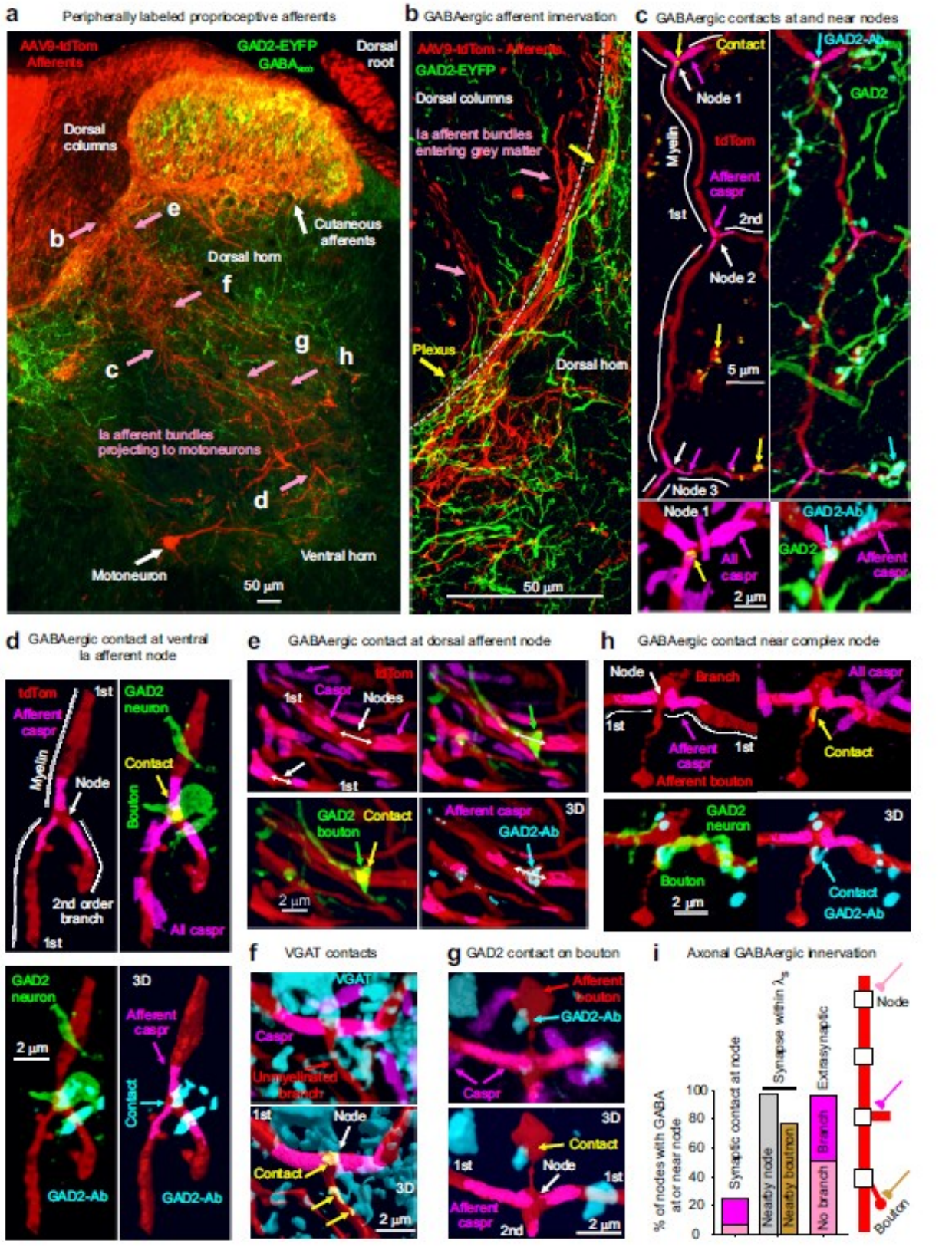

Extended Data Fig. 5

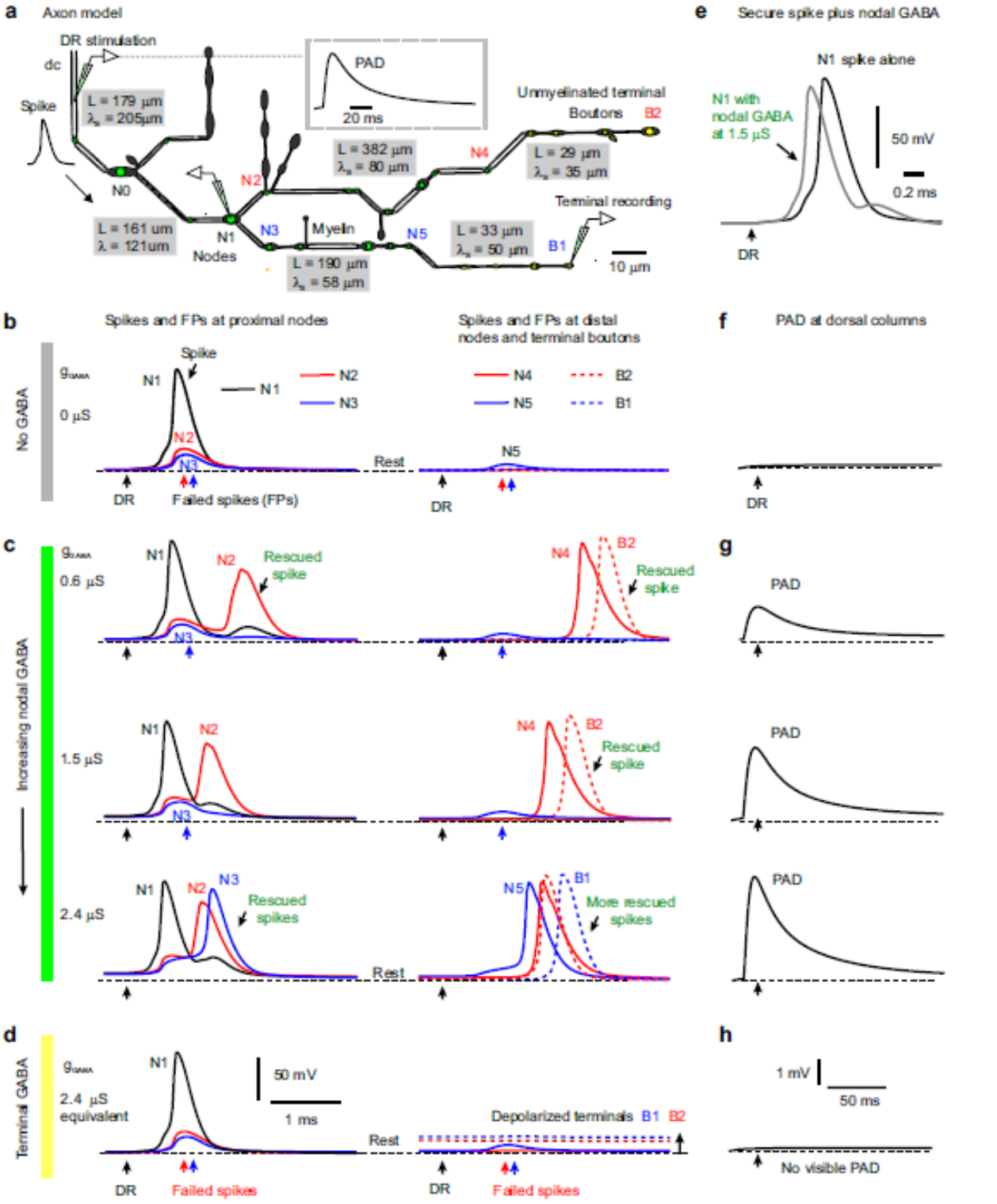

Extended Data Fig. 6

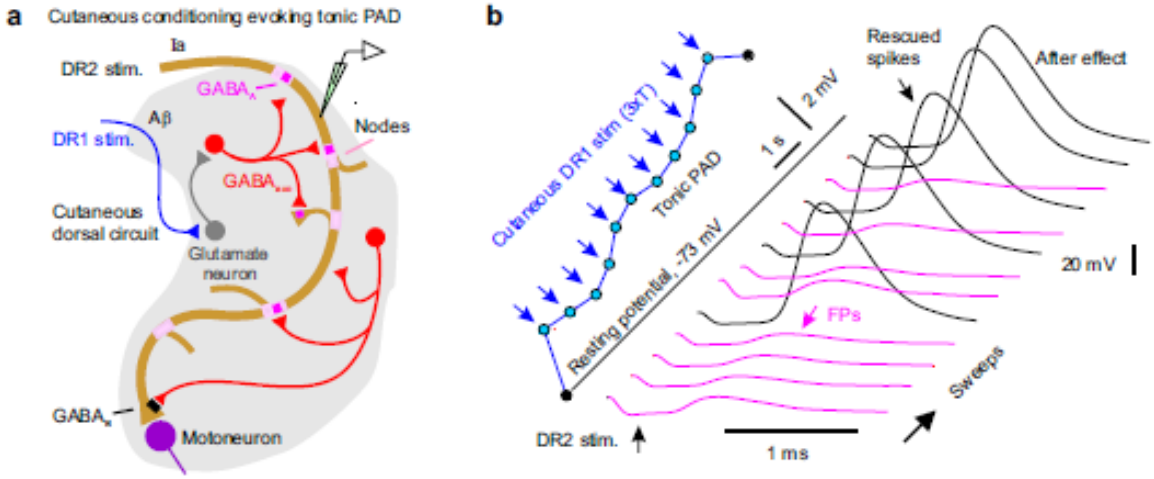

Extended Data Fig. 7

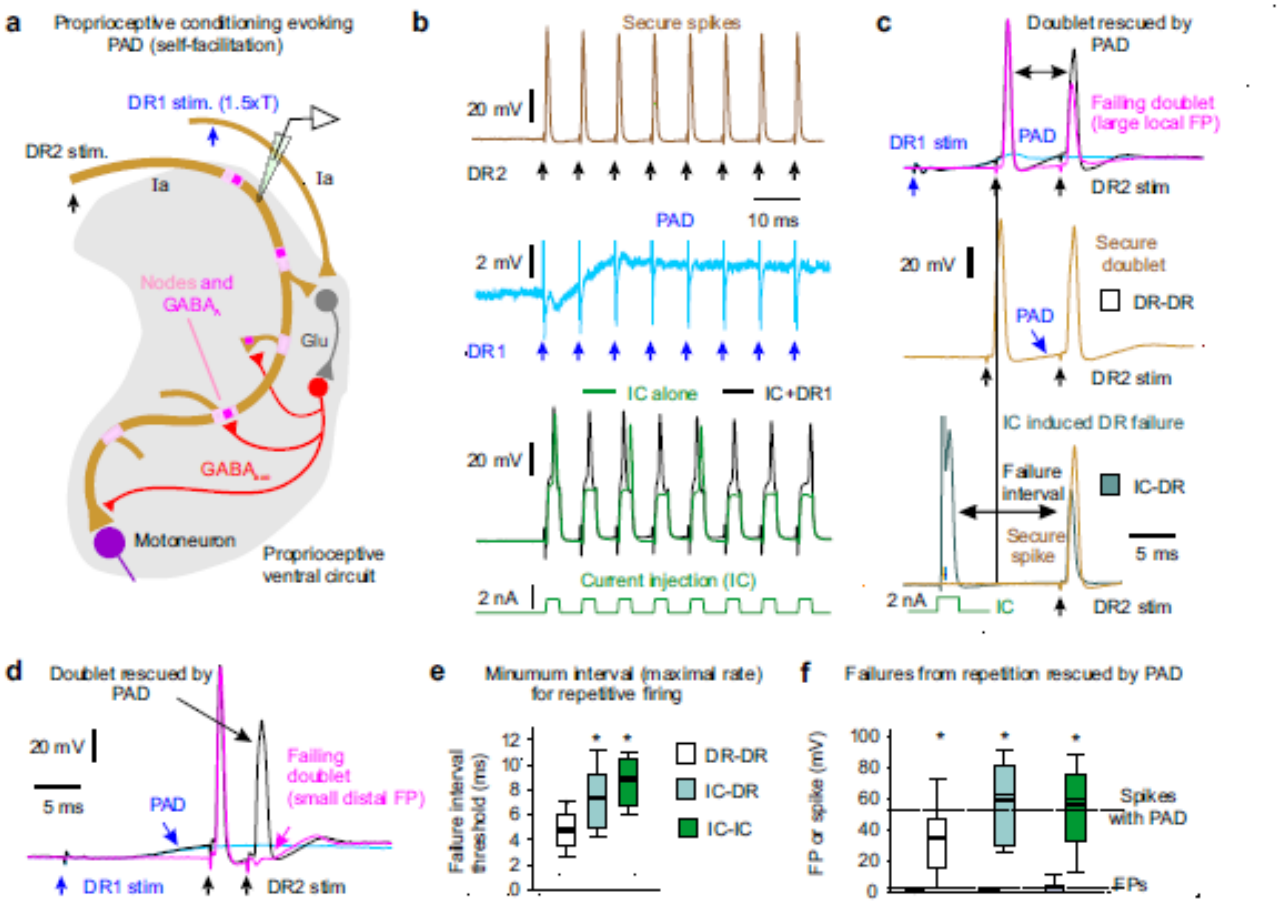

Extended Data Fig. 8

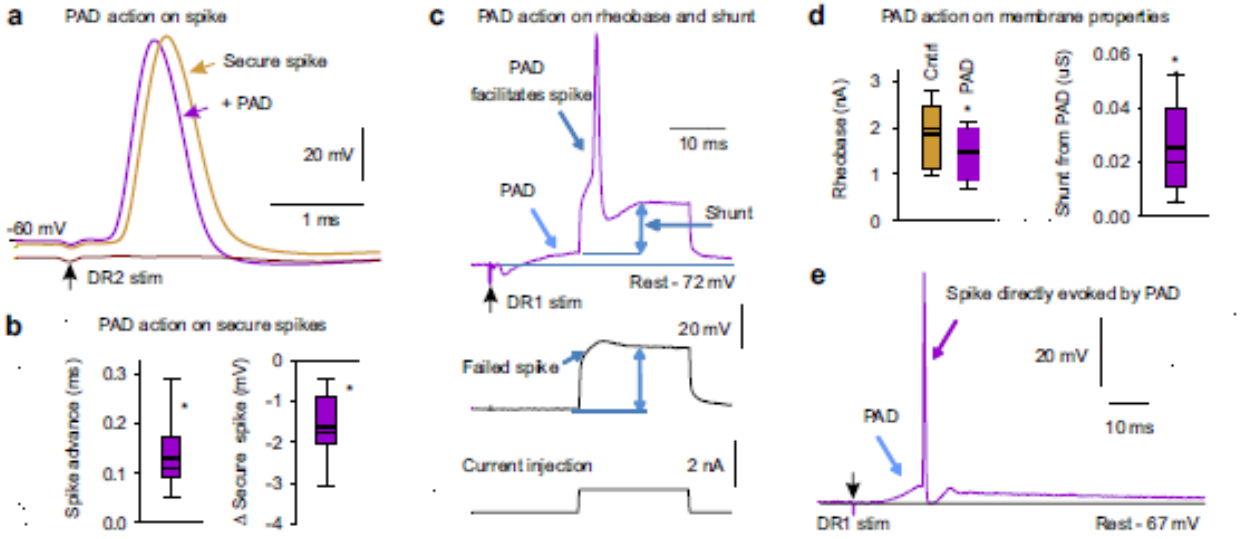

Extended Data Fig. 9

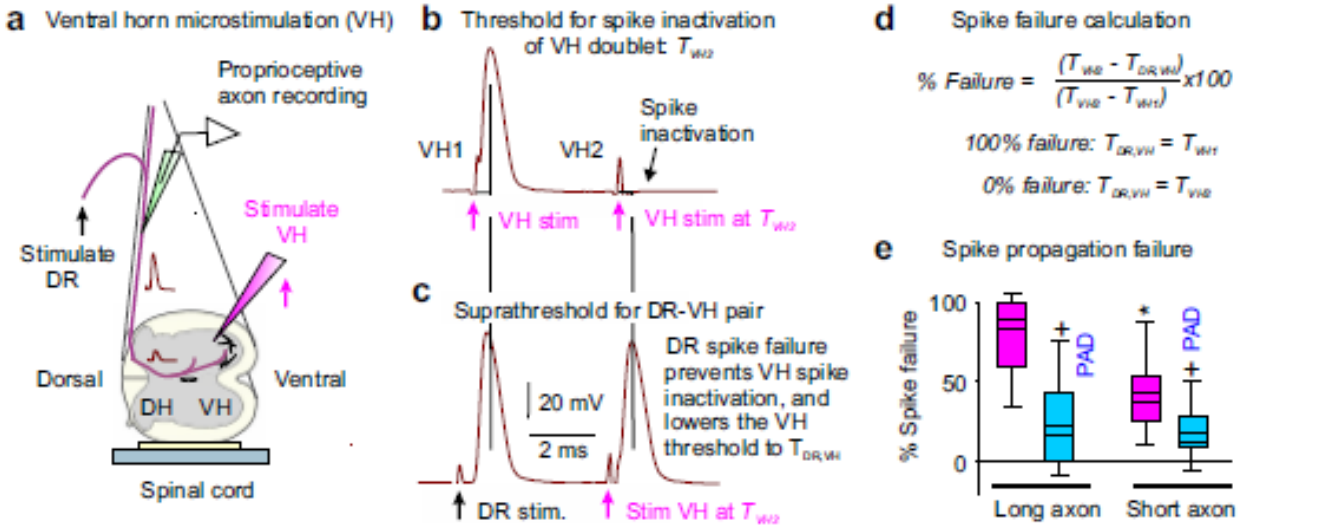

Extended Data Fig. 10

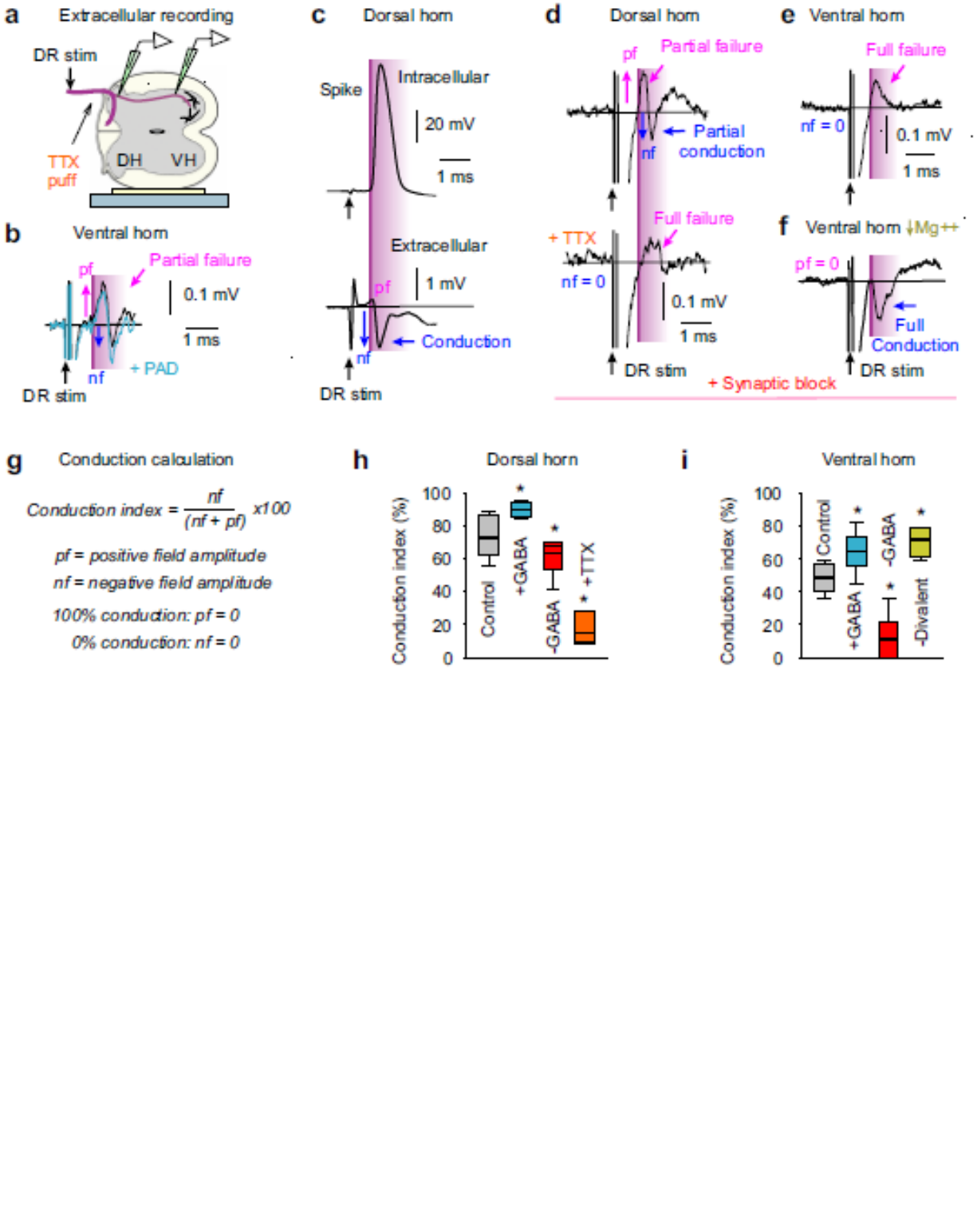

Extended Data Fig. 11

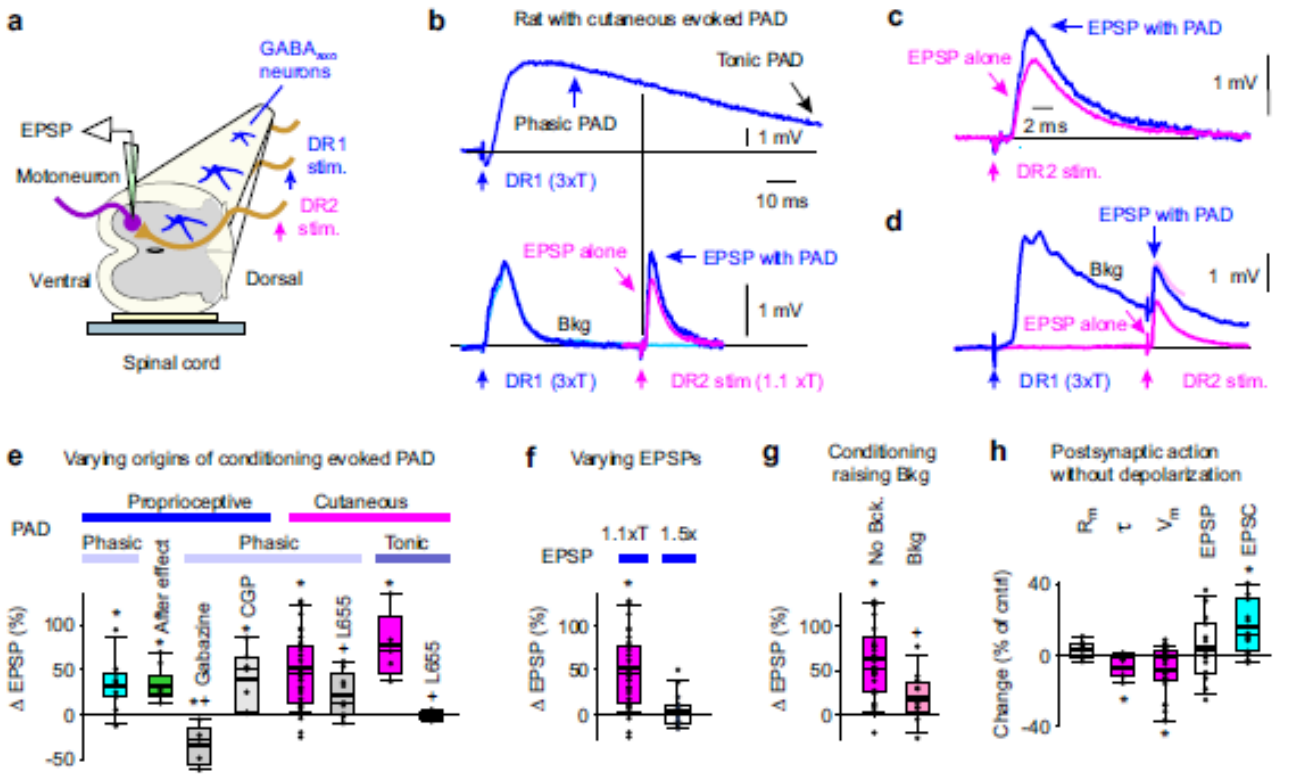

Extended Data Figure 12

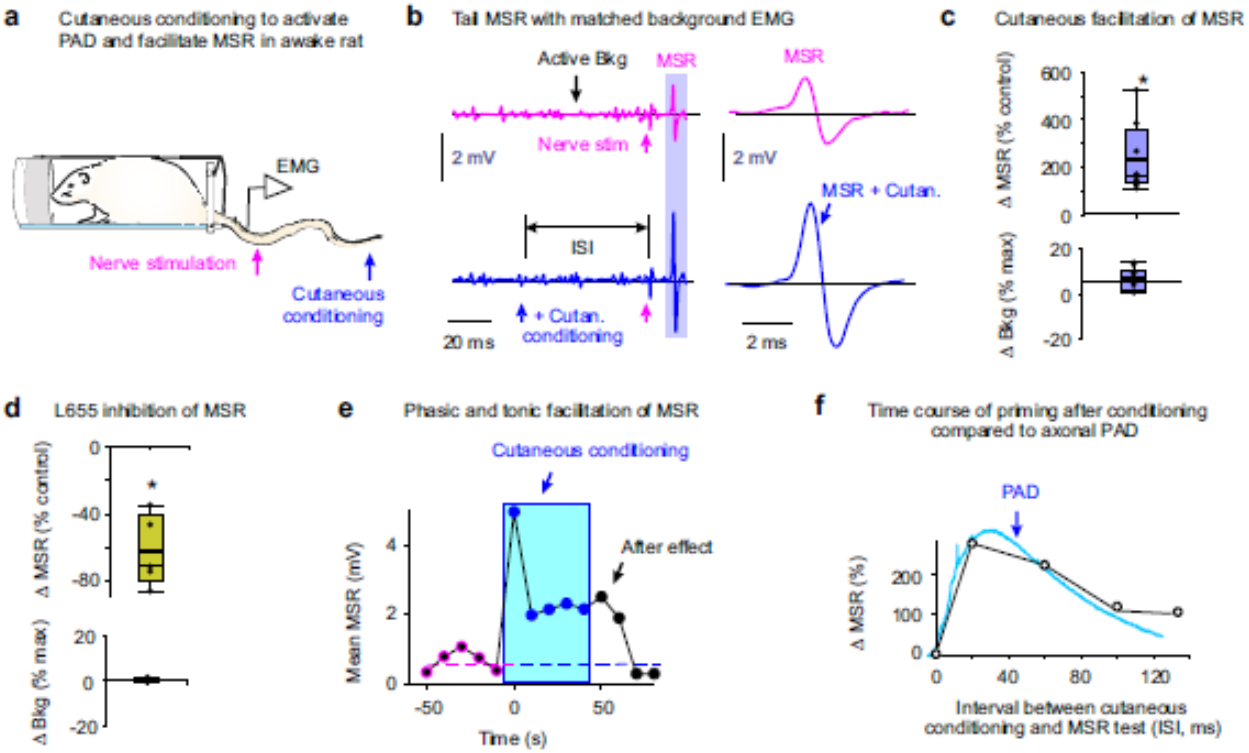

Extended Data Figure 13

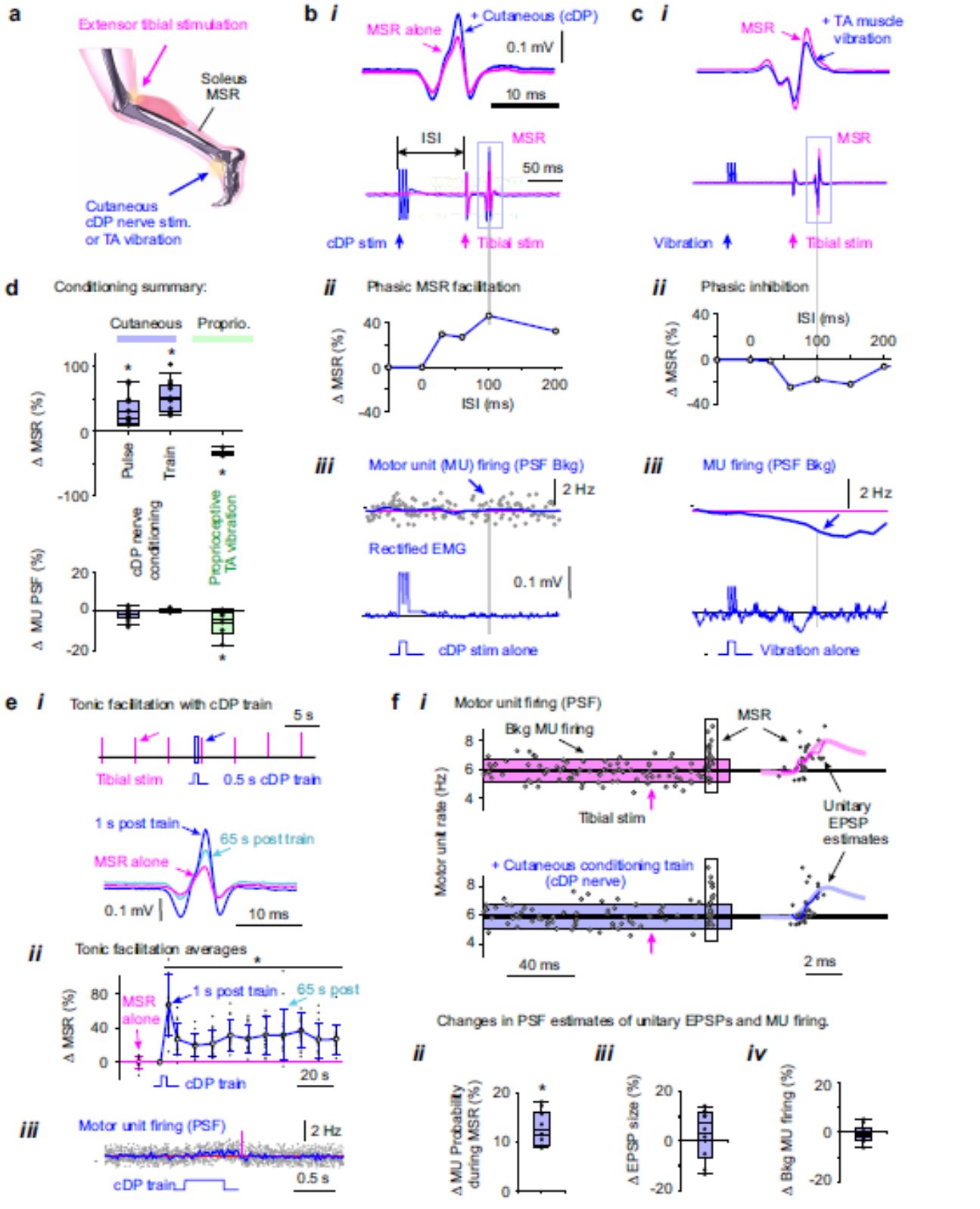

Extended Data Fig. 14